Investigating the expression of P2 purinergic receptors in sympathetic ganglia and perivascular nerves of arteries

Dalyan Eldaly

A Thesis Presented for the Degree of Doctor of Philosophy at the University of East Anglia

Faculty of Science, School of Biological Sciences

July 2022

In the name of God, the most Beneficent, the most Merciful

Declaration

I verify that the work presented in this thesis submitted by me for the degree of Doctor of Philosophy is my original work except where due reference is made to other authors. I also declare that it has not been previously submitted by me for a degree at University of East Anglia or any other university.

In line with the regulations for the degree of Doctor of Philosophy, I have submitted a thesis that has a word count of approximately 85300 words, including footnotes and references, but excluding appendix and supplementary of approximately 2100 words.

Abstract

Hypertension, also known as high blood pressure, is a serious medical condition that can increase the risk of several diseases including heart failure, stroke, and chronic kidney disease. It is a major cause of premature death worldwide, affecting up to one in every four men and one in every five women. One of the factors that play a role in hypertension progression is blood vessel innervation via perivascular sympathetic nerves. The importance of ATP released from sympathetic nerves as an extracellular signalling molecule is now well known and evidence is accumulating that ATP, and other nucleotides (ADP, UTP and UDP) play key roles in cardiovascular physiology and pathology via P2X (ion channel) and P2Y (G protein-coupled) receptors. Pre-junctional nerve terminals are equipped with a number of auto- and/or heteroreceptors, including ionotropic P2X and metabotropic P2Y receptors. Pre-junctional purinergic receptors serve as modulation sites of neurotransmitter release via ATP and other nucleotides released by neuronal activity and pathological signals. However, very little is currently known about the expression of P2 receptors in sympathetic post-ganglionic nerves that innervate blood tissues, where they have a potential pre-junctional role in regulating neurotransmission. This project aimed to characterise the P2 receptor profiles in mouse superior cervical ganglion and perivascular nerve terminals of the superior mesenteric artery and carotid artery. In addition, we aimed to investigate the expression and function of P2 receptors in human SH-SY5Y cells and *in vitro* differentiated SH-SY5Y cells as a model of adrenergic sympathetic neurons. RT-PCR revealed the presence of mRNA in all P2 receptors was expressed in superior cervical ganglion. However, some receptors (P2X2, P2X3, P2X5, P2X6, P2Y1, P2Y4 and P2Y12) were expressed in the superior cervical ganglion, but not expressed in the superior mesenteric artery and carotid artery. We suggest that receptor subtypes detected in sympathetic ganglia but not arteries could be expressed by sympathetic post-ganglionic nerves that innervate arteries and could serve as auto- and/or heteroreceptors to modulate neurotransmitters release. We confirmed the expression of all P2X (with the exception of P2X5 and P2X6) and P2Y1 at the protein level by immunohistochemistry, and we found these receptors colocalised with the general marker of neurons (PGP9.5), the adrenergic sympathetic marker tyrosine hydroxylase in superior cervical ganglion and perivascular nerves within the adventitia of the arteries. Moreover, it was determined in this project that the P2X agonist (BzATP) promoted intracellular calcium responses in differentiated SH-SY5Y cells are principally mediated by P2X7 receptors. The data outlined that P2X7 receptors are functionally active in differentiated SH-SY5Y cells and may be a novel and interesting drug target for modulating neurotransmission and thus may have potential therapeutic applications in vascular diseases including hypertension. Further research is required to fully investigate the

physiological roles of all of the P2 receptor subtypes expressed in sympathetic ganglia and pre-junctional sympathetic nerve terminals of arteries.

Contents

Declaration **3**

Abstract **4**

List of Figures **11**

List of Tables **16**

Abbreviation **18**

Acknowledgements **21**

Chapter 1: Introduction **22**

1.1 Hypertension 22

1.2 The vascular system 23

1.3 Purinergic signalling and purine receptors 24

1.3.1 P1 receptors 27

1.3.2 P2X receptors 27

1.3.2.1 Distribution of P2X receptors 29

1.3.3 P2Y receptors 30

1.3.3.1 Distribution of P2Y receptors 32

1.4 Regulation of vascular tone (hypertension) by P2 purinergic receptors 38

1.5 Purinergic signalling in the nervous system 42

1.6 Purinergic neurotransmission in the perivascular nervous system- innervation of blood vessels 46

1.6.1 The autonomic nervous system 47

1.6.1.1 Sympathetic nerves in the regulation of vascular tone 50

1.6.1.2 Parasympathetic nerves 56

1.6.2 Sensory-Motor Nerves 57

1.6.3 Non-adrenergic non-cholinergic nerves 59

1.7 Non-neuronal sources of purines 59

1.8 The effects of blood vessels on the autonomic nervous system 62

1.9 Control of vascular tone by perivascular nerves, smooth muscle cells and endothelial cells 63

1.10 Pre-junctional modulation of perivascular neurotransmission by purines - purines as pre-junctional neuromodulators 65

1.10.1 Facilitatory pre-junctional purinergic receptors 66

1.10.2 Inhibitory pre-junctional purinergic receptors 67

1.11 Calcium signalling 68

1.11.1 ON mechanisms 68

1.11.2 OFF mechanisms 69

1.12 Pharmacology 72

1.12.1 Non-selective P2 receptor agonists 72

1.12.2 Non-selective P2 receptor antagonists 72

1.12.3 P2 receptor agonists used in the project 73
1.12.3.1 ATP and α,β-methyleneATP 73
1.12.3.2 BzATP 73
1.12.3.3 Carbachol 74
1.12.4. P2 receptor antagonists used in the project 74
1.12.4.1. A438079 or 3-[[5-(2,3- dichlorophenyl)-1H-tetrazol-1-yl]methyl]pyridine 74
1.13 Project aims 77
Impact of COVID-19 on PhD work 78
Chapter 2: Materials and Methods 79
2.1 Materials 79
2.2 Animals 79
2.3 Dissection of mice 79
2.4 Transgenic mice (NPY-hrGFP) 83
2.5 Cell culture 86
2.6 Differentiation of SH-SY5Y human cells to adrenergic neurons 86
2.7 Cell passage 91
2.8 Measurements of intracellular free Ca^{2+} concentrations 91
2.9 Reverse transcription-polymerase chain reaction (RT-PCR) 98
2.9.1 Total RNA extraction 98
2.9.2 Elimination of genomic DNA using DNase1 and total RNA quantification 100
2.9.3 Complementary DNA (cDNA) synthesis 102
2.9.4 RT-PCR 102
2.9.4.1 Agarose gel electrophoresis 105
2.9.4.2 Primer design 105
2.10 Whole-mount preparations for immunohistochemistry 114
2.11 Cryostat sectioning for immunohistochemistry 119
2.12 Immunocytochemistry 121
2.13 Microscopy 122
2.13.1 Confocal microscopy 122
2.13.2 Apotome microscopy 122
2.14 Western Blot 123
2.14.1 Protein extraction 123
2.14.2 BCA protein assay 125
2.14.3 SDS polyacrylamide gel electrophoresis (SDS-PAGE) and gel transfer 127
2.14.4 Blocking, antibody staining and imaging 133
2.14.5 Calculation of molecular weight of proteins 140
2.15 Statistical analysis 143

Chapter 3: Expression of P2 purinergic receptor mRNA transcripts in mouse superior cervical ganglion, superior mesenteric arteries and carotid artery 144

3.1 Introduction 144

3.2 Aim 146

3.3 Results 147

3.3.1 Comparison of mRNA expression of neuronal and vascular markers in mouse superior cervical ganglion, superior mesenteric artery and carotid artery 147

3.3.2 Comparison of mRNA expression of P2X receptor subtypes in mouse superior cervical ganglion, superior mesenteric artery and carotid artery 153

3.3.3 Comparison of mRNA expression of P2Y receptor subtypes in mouse superior cervical ganglion, superior mesenteric artery and carotid artery 159

3.4 Discussion 163

3.4.1 Expression of neuronal and vascular markers in mouse superior cervical ganglion, superior mesenteric artery and carotid artery 163

3.4.2 Expression of P2X and P2Y receptors in mouse superior cervical ganglion, superior mesenteric artery and carotid artery 166

3.4.2.1 Expression of P2X and P2Y receptor mRNA transcripts in mouse superior mesenteric artery and carotid artery 166

3.4.2.2 Expression of P2X and P2Y receptor mRNA transcripts in mouse superior cervical ganglion 169

3.5 Summary 172

Chapter 4: Protein expression of P2 purinergic receptors on sympathetic neurons in mouse superior cervical ganglion and pre-junctional sympathetic nerves in superior mesenteric artery and carotid artery 173

4.1 Introduction 173

4.2 Aim 178

4.3 Results 180

4.3.1 Protein expression of P2 purinergic receptors in the mouse superior cervical ganglion (coexpression of PGP9.5 with P2 receptors) 180

4.3.2 Protein expression of P2 purinergic receptors in the mouse superior cervical ganglion (coexpression of TH with P2 receptors) 192

4.3.3 Protein expression of P2 purinergic receptors in the mouse superior cervical ganglion (coexpression of VNUT with P2 receptors) 203

4.3.4 Expression of P2 purinergic receptor in pre-junctional nerves in the mouse superior mesenteric and carotid arteries 210

4.3.5 Mouse superior cervical ganglion neurons and P2-positive neurons have vasomotor activity by expressing NPY. 224

4.3.6 Expression of total protein of P2 purinergic receptors in mouse superior cervical ganglion, superior mesenteric artery and carotid artery 236

4.4 Discussion 239

4.4.1. Expression of P2 purinergic receptors at the protein level in mouse sympathetic superior cervical ganglion 239

4.4.2 Mouse superior cervical ganglion neurons are capable of vesicular storage of ATP and possible exocytosis release by expressing VNUT 241
4.4.3. Sympathetic innervation of mouse mesenteric and carotid arteries, and the expression of purinergic receptors in perivascular nerves of the superior mesenteric and carotid arteries..... 243
4.4.4 P2 purinergic receptors were positive for NPY in mouse superior cervical ganglion neurons and in perivascular nerves of superior mesenteric artery but not carotid artery 249
4.5 Summary 253
Chapter 5: The expression and function of P2 purinergic receptors in the SH-SY5Y neuroblastoma cell line 255
5.1 Introduction 255
5.2 Aim 256
5.3 Results 258
5.3.1 Differentiation of SH-SY5Y cells to a neuronal phenotype 258
5.3.2 Comparison of the mRNA expression of P2X and P2Y receptor subtypes in undifferentiated and differentiated SH-SY5Y cells 261
5.3.3 Protein expression of P2 purinergic receptors in undifferentiated and differentiated SH-SY5Y cells 267
5.3.4 Expression of total protein of P2 receptors in undifferentiated and differentiated SH-SY5Y cells 277
5.3.5 Nucleotide-evoked calcium responses in undifferentiated and differentiated SH-SY5Y cells 279
5.3.6 P2X7 receptor was involved in nucleotide-evoked calcium responses in undifferentiated and differentiated SH-SY5Y cells..... 280
5.4 Discussion 296
5.4.1 Differentiation of SH-SY5Y cells into an adrenergic neuron phenotype 296
5.4.2 The expression of P2 receptors in undifferentiated and differentiated SH-SY5Y cells.... 298
5.4.3 P2X7 receptor activation elicits intracellular calcium responses in undifferentiated and differentiated SH-SY5Y cells 299
5.5 Summary 302
Chapter 6 303
6.1 Key findings 303
6.1.1 mRNA expression of neuronal and vascular markers in mouse superior cervical ganglion, superior mesenteric artery and carotid artery 303
6.1.2 mRNA expression of P2X and P2Y receptor subtypes in mouse superior cervical ganglion, superior mesenteric artery and carotid artery 303
6.1.3 Protein expression of P2 purinergic receptors on sympathetic neurons in mouse superior cervical ganglion and pre-junctional sympathetic nerves in superior mesenteric arteries and carotid arteries 304
6.1.4 Expression of P2X and P2Y receptors in human undifferentiated SH-SY5Y and differentiated cells 310
6.1.5 Nucleotide-evoked calcium responses in undifferentiated and differentiated SH-SY5Y cells 310
6.2 Future work 312

6.3 Conclusion 313

Appendix 314

References 316

Supplementary 316

S.1 Nucleotide and amino acid sequences of the mouse P2X2 gene including the DNA and cDNA. 352

S2. Multiple sequence alignment of the different P2X2 transcripts and the DNA sequence..... 356

S.3 Nucleotide and amino acid sequences of the mouse P2X6 gene including the DNA, cDNA and non-sense-mediated decay RNA. 363

S4. Nucleotide and amino acid sequences of the P2X3 gene including the DNA, cDNA and non-sense-mediated decay RNA. 369

List of Figures

Chapter 1

Figure 1.1 The activation of purinergic receptors by extracellular signalling mediated by purine nucleotides and nucleosides.

Figure 1.2 Structure of P2 receptors.

Figure 1.3 Crystal structure of P2X4 receptor.

Figure 1.4 Purinergic receptors in regulation of blood pressure.

Figure 1.5 Control of vascular tone in blood vessels via P2 purinergic receptors.

Figure 1.6 Mechanisms of ATP release, storage, degradation and reception.

Figure1.7 Organisation of the sympathetic and parasympathetic nervous system.

Figure 1.8 The roles of the perivascular nervous system.

Figure 1.9 Non-neuronal sources of purines.

Figure 1.10 Cross-section of a blood vessel showing local purinergic control mechanisms.

Figure 1.11 Calcium wave signalling in neurons.

Figure 1.12 Chemical structures of P2X receptor agonists.

Figure 1.13 Chemical structures of P2X7 receptor antagonist (A438079).

Chapter 2

Figure 2.1 Mouse tissues used throughout research.

Figure 2.2 Reporter genes are used to study the regulatory sequences of genes of interest.

Figure 2.3 Several methods used to differentiate SH-SY5Y cells into various types of functional neurons.

Figure 2.4 Fura-2 acetoxyethyl (AM) ester.

Figure 2.5 An example of an experimental setup of nucleotide-evoked intracellular calcium responses.

Figure 2.6 Total RNA extraction protocol.

Figure 2.7 Elimination of genomic DNA using DNase1 and total RNA quantification.

Figure 2.8 cDNA synthesis and RT-PCR.

Figure 2.9 Immunohistochemistry using cryosectioning.

Figure 2.10 BSA standards curve plotted against absorbance to quantify unknown protein concentrations.

Figure 2.11 Protein migration and separation in SDS-PAGE.

Figure 2.12 Western blot to detect specific protein molecules from a mixture of proteins.

Chapter 3

Figure 3.1 Expression of mRNA transcripts for neuronal and vascular markers in the mouse brain.
Figure 3.2 Expression of mRNA transcripts for neuronal and vascular markers in the mouse superior cervical ganglion, superior mesenteric artery and carotid artery.
Figure 3.3 Expression of mRNA transcripts for P2X receptors in the mouse brain.
Figure 3.4 Expression of mRNA transcripts for P2X receptors in the mouse superior cervical ganglion, superior mesenteric artery and carotid artery.
Figure 3.5 Expression of mRNA transcripts for P2Y receptors in the mouse brain.
Figure 3.6 Expression of mRNA transcripts for P2Y receptors in the mouse superior cervical ganglion, superior mesenteric artery and carotid artery.

Chapter 4

Figure 4.1 Vesicular storage and release of ATP from neurons and purinergic chemical transmission.
Figure 4.2 Coexpression of PGP 9.5 with P2X1 receptor in mouse superior cervical ganglion neurons.
Figure 4.3 Coexpression of PGP 9.5 with P2X2 receptor in mouse superior cervical ganglion neurons.
Figure 4.4 Coexpression of PGP 9.5 with P2X3 receptor in mouse superior cervical ganglion neurons.
Figure 4.5 Coexpression of PGP 9.5 with P2X4 receptor in mouse superior cervical ganglion neurons.
Figure 4.6 Coexpression of PGP 9.5 with P2X6 receptor in mouse superior cervical ganglion neurons.
Figure 4.7 Coexpression of PGP 9.5 with P2X7 receptor in mouse superior cervical ganglion neurons.
Figure 4.8 Coexpression of PGP 9.5 with P2Y1 receptor in mouse superior cervical ganglion neurons.
Figure 4.9 Control double immunofluorescence labelling for PGP9.5 and P2 receptors in mouse superior cervical ganglion neurons.
Figure 4.10 The percentage of PGP9.5-positive neurons expressing P2 receptors in the mouse superior cervical ganglion.
Figure 4.11 Coexpression of TH with PGP9.5 in mouse superior cervical ganglion neurons.
Figure 4.12 Coexpression of TH with P2X1 receptor in mouse superior cervical ganglion neurons.
Figure 4.13 Coexpression of TH with P2X2 receptor in mouse superior cervical ganglion neurons.
Figure 4.14 Coexpression of TH with P2X3 receptor in mouse superior cervical ganglion neurons.
Figure 4.15 Coexpression of TH with P2X4 receptor in mouse superior cervical ganglion neurons.
Figure 4.16 Coexpression of TH with P2X7 receptor in mouse superior cervical ganglion neurons.

Figure 4.17 Coexpression of TH with P2Y1 receptor in mouse superior cervical ganglion neurons.
Figure 4.18 Control double immunofluorescence labelling for TH and P2 receptors in superior cervical ganglion neurons.
Figure 4.19 The percentage of TH-positive neurons expressing P2 receptors in mouse superior cervical ganglion.
Figure 4.20 Coexpression of VNUT with PGP9.5 in mouse superior cervical ganglion neurons.
Figure 4.21 Coexpression of VNUT with P2X2 receptor in mouse superior cervical ganglion neurons.
Figure 4.22 Coexpression of VNUT with P2X3 receptor in mouse superior cervical ganglion neurons.
Figure 4.23 Coexpression of VNUT with P2Y1 receptor in mouse superior cervical ganglion neurons.
Figure 4.24 Control double immunofluorescence labelling for vesicular nucleotide transporter (VNUT) with P2 receptors in mouse superior cervical ganglion neurons.
Figure 4.25 The percentage of P2-positive neurons which are capable of vesicular storage of ATP (positive for VNUT) in mouse superior cervical ganglion.
Figure 4.26 Coexpression of PGP9.5 and TH in whole-mount preparations of mouse superior mesenteric and carotid arteries.
Figure 4.27 Coexpression of P2X1 and PGP9.5 in whole-mount preparations of mouse superior mesenteric and carotid arteries.
Figure 4.28 Coexpression of P2X2 and PGP9.5 in whole-mount preparations of mouse superior mesenteric and carotid arteries.
Figure 4.29 Coexpression of P2X3 and PGP9.5 in whole-mount preparations of mouse superior mesenteric and carotid arteries.
Figure 4.30 Coexpression of P2X4 and PGP9.5 in whole-mount preparations of mouse superior mesenteric and carotid arteries.
Figure 4.31 Coexpression of P2X6 and PGP9.5 in whole-mount preparations of mouse superior mesenteric and carotid arteries.
Figure 4.32 Coexpression of P2X7 and PGP9.5 in whole-mount preparations of mouse superior mesenteric and carotid arteries.
Figure 4.33 Coexpression of P2Y1 and PGP9.5 in whole-mount preparations of mouse superior mesenteric and carotid arteries.
Figure 4.34 Control double immunofluorescence labelling of PGP9.5 and P2 receptors in mouse superior mesenteric artery and carotid artery.
Figure 4.35 Control double immunofluorescence labelling of TH and PGP9.5 receptor in mouse superior mesenteric artery and carotid artery.
Figure 4.36 Immunofluorescence of cryostat sections of mouse superior mesenteric artery and carotid artery labelled with P2X2, P2X3, P2X7 and P2Y1.
Figure 4.37 Control immunofluorescence of cryostat sections of mouse superior mesenteric artery and carotid artery labelling of P2X, P2X3 and P2Y1 receptors.
Figure 4.38 Immunofluorescence labelling for PGP 9.5 in superior cervical ganglion isolated from transgenic mice (NPY-hrGFP).

Figure 4.39 Immunofluorescence labelling for P2X2 in superior cervical ganglion isolated from transgenic mice (NPY-hrGFP).
Figure 4.40 Immunofluorescence labelling for P2X3 in superior cervical ganglion isolated from transgenic mice (NPY-hrGFP).
Figure 4.41 Immunofluorescence labelling for P2Y1 in superior cervical ganglion isolated from transgenic mice (NPY-hrGFP).
Figure 4.42 Control Immunofluorescence labelling for PGP9.5 and P2 receptor in superior cervical ganglion isolated from transgenic mice (NPY-hrGFP).
Figure 4.43 The percentage of P2-positive neurons have vasomotor activity (positive for NPY) in mouse superior cervical ganglion.
Figure 4.44 Immunofluorescence of whole-mount preparations of transgenic GFP-NPY mouse superior mesenteric artery and carotid artery labelled with P2X2.
Figure 4.45 Immunofluorescence of whole-mount preparations of transgenic GFP-NPY mouse superior mesenteric artery and carotid artery labelled with P2X3.
Figure 4.46 Immunofluorescence of whole-mount preparations of transgenic GFP-NPY mouse superior mesenteric artery and carotid artery labelled with P2Y1.
Figure 4.47 Control immunofluorescence of whole-mount preparations of transgenic GFP-NPY mouse superior mesenteric artery and carotid artery labelled with P2X2, P2X3 and P2Y1.
Figure 4.48 Western blotting of P2 receptors in the mouse brain, superior cervical ganglion, superior mesenteric artery and carotid artery.
Figure 4.49 Anatomy of the common carotid artery, carotid sinus, carotid body and superior cervical ganglion.

Chapter 5

Figure 5.1 Retinoic acid-induced differentiated SH-SY5Y cells.
Figure 5.2 NPY expression in undifferentiated and differentiated SH-SY5Y cells.
Figure 5.3 Expression of mRNA transcripts for P2X receptors in the human brain, undifferentiated and differentiated SH-SY5Y cells.
Figure 5.4 Expression of mRNA transcripts for P2Y receptors in the human brain, undifferentiated and differentiated SH-SY5Y cells.
Figure 5.5 Colocalisation of PGP 9.5 with P2X2 receptor in undifferentiated and differentiated SH-SY5Y cells.
Figure 5.6 Colocalisation of PGP 9.5 with P2X3 receptor in undifferentiated and differentiated SH-SY5Y cells.
Figure 5.7 Colocalisation of PGP 9.5 with P2X7 receptor in undifferentiated and differentiated SH-SY5Y cells.
Figure 5.8 Control double immunofluorescence labelling for PGP9.5 and P2 receptors in undifferentiated SH-SY5Y cells and differentiated SH-SY5Y cells.
Figure 5.9 Colocalisation of TH with P2X2 receptor in undifferentiated and differentiated SH-SY5Y cells.
Figure 5.10 Colocalisation of TH with P2X3 receptor in undifferentiated and differentiated SH-SY5Y cells.
Figure 5.11 Colocalisation of TH with P2X7 receptor in undifferentiated and differentiated SH-SY5Y cells.

Figure 5.12 Control double immunofluorescence labelling for TH and P2 receptors in undifferentiated SH-SY5Y cells and differentiated SH-SY5Y cells.
Figure 5.13 Western blot analysis of P2X2, P2X3 and P2X7 receptor expression in undifferentiated and differentiated SH-SY5Y cells.
Figure 5.14 ATP elicited intracellular calcium responses in undifferentiated SH-SY5Y cells.
Figure 5.15 ATP elicited intracellular calcium responses in differentiated SH-SY5Y cells.
Figure 5.16 ATP elicited intracellular calcium responses in undifferentiated and differentiated SH-SY5Y cells.
Figure 5.17 α,β-Me-ATP elicited intracellular calcium responses in undifferentiated SH-SY5Y cells.
Figure 5.18 α,β-Me-ATP did not significantly elicit intracellular calcium responses in differentiated SH-SY5Y cells.
Figure 5.19 α,β-Me-ATP elicited intracellular calcium responses in undifferentiated SH-SY5Y cells but not in SH-SY5Y cells.
Figure 5.20 BzATP (target P2X7) elicited intracellular calcium responses in undifferentiated SH-SY5Y cells.
Figure 5.21 Selective antagonism of P2X7 receptors had an inhibitory effect on the BzATP-evoked calcium response in undifferentiated SH-SY5Y cells.
Figure 5.22 BzATP (target P2X7) elicited intracellular calcium responses in differentiated SH-SY5Y cells.
Figure 5.23 Selective antagonism of P2X7 receptors had an inhibitory effect on the BzATP-evoked calcium response in differentiated SH-SY5Y cells.
Figure 5.24 BzATP (target P2X7) elicited intracellular calcium responses in undifferentiated SH-SY5Y cells and differentiated SH-SY5Y cells.
Figure 5.25 Carbachol elicited intracellular calcium responses in undifferentiated SH-SY5Y cells and differentiated SH-SY5Y cells.
Figure 5.26 The representative trace of carbachol-evoked intracellular calcium responses in undifferentiated SH-SY5Y cells and differentiated SH-SY5Y cells.

Appendix

Figure A.1 Western blotting of P2X3 and P2Y1 receptors in the mouse brain and superior cervical ganglion.

List of Tables

Chapter 1

Table 1.1 Characteristics of P2X receptors.

Table 1.2 Characteristics of P2Y receptors.

Table 1.3 P2Y receptor agonist preferences and G-protein coupling.

Table 1.4 ATP as a cotransmitter in peripheral and central nervous systems.

Chapter 2

Table 2.1 The components of Hank's balanced salt solution.

Table 2.2 PCR programmes for genotyping of NPY-hrGFP.

Table 2.3 Culture media components.

Table 2.4 Differentiation media components.

Table 2.5 Salt buffered solution and loading buffer components.

Table 2.6 Receptor ligands used in measurements of intracellular free calcium experiment.

Table 2.7 Cycling conditions used in the RT-PCR reactions.

Table 2.8 Primer sequences for mouse P2X receptors.

Table 2.9 Primer sequences for mouse P2Y receptors.

Table 2.10 Primer sequences for mouse markers of neurons, smooth muscle cells and endothelial cells.

Table 2.11 Primer sequences for human P2X receptors.

Table 2.12 Primer sequences for human P2Y receptors.

Table 2.13 Blocking buffer used for immunohistochemistry experiments.

Table 2.14 Primary antibodies used for immunofluorescence experiments.

Table 2.15 Secondary antibodies used for immunofluorescence experiments.

Table 2.16 RIPA buffer used to prepare whole cell lysates.

Table 2.17 Polyacrylamide gel (separating gel- stacking gel) components.

Table 2.18 Preparation of separating (resolving) buffer and stacking buffer.

Table 2.19 Preparation of running buffer (10X) and transfer buffer (10X).

Table 2.20 Preparation of running buffer (1X) and transfer buffer (1X).

Table 2.21 Preparation of blocking buffer used in Western blot.

Table 2.22 Preparation of washing buffer used in Western blot.

Table 2.23 Primary antibodies used in Western blot.

Table 2.24 Secondary antibodies used in Western blot.

Table 2.25 The expected molecular weight of mouse P2 proteins studied in this project.

Table 2.26 The expected molecular weight of human P2 proteins studied in this project.

Chapter 3

Table 3.1 An overview of mRNA expression for neuronal and vascular markers in the mouse brain, superior cervical ganglion, superior mesenteric artery and carotid artery.

Table 3.2 An overview of mRNA expression for P2X receptors in the mouse brain, superior cervical ganglion, superior mesenteric artery and carotid artery.

Table 3.3 An overview of mRNA expression for P2Y receptors in the mouse brain, superior cervical ganglion, superior mesenteric artery and carotid artery.

Chapter 5

Table 5.1 An overview of mRNA expression for P2X receptors in the human brain, undifferentiated, and differentiated SH-SY5Y cells.

Table 5.2 An overview of mRNA expression for P2Y receptors in the human brain, undifferentiated, and differentiated SH-SY5Y cells.

Table 5.3 Characteristics of the calcium responses evoked by maximal concentrations of nucleotides in undifferentiated and differentiated SH-SY5Y cells. Mean ± SEM.

Chapter 6

Table 6.1 An overview of mRNA and protein expression for P2 receptors in the mouse superior cervical ganglion, superior mesenteric artery and carotid artery.

Abbreviation

AC	Adenylate cyclase
ACh	Acetylcholine
ADP	Adenosine diphosphate
AMP	Adenosine monophosphate
APS	Ammonium persulfate
ATP	Adenosine triphosphate
BCA	Bicinchoninic acid
BDNF	Brain-derived neurotrophic factor
BSA	Bovine serum albumin
BzATP	2'(3')-O-(4-benzoyl)adenosine triphosphate
CA	Carotid artery
Ca^{2+}	Calcium ions
cAMP	Cyclic adenosine monophosphate
CB	Carotid body
cDNA	Complementary DNA
CGRP	Calcitonin gene-related peptide
Cl^-	Chloride ions
CRLR	Calcitonin receptor-like receptor
DAG	Diacylglycerol
db-cAMP	Dibutyryl-cAMP
DMEM	Dulbecco's Modified Eagles medium
DMSO	Dimethylsulfoxide
dNTPs	2'-deoxynucleoside 5'-triphosphates
DTT	Dithiothreitol
EC_{50}	Concentration of an agonist giving half-maximal response
ECL	Enhanced chemiluminescence
EDHF	Endothelium-derived hyperpolarizing factor
ECs	Endothelial cells
eNOS	Endothelial nitric oxide synthase

FBS	Foetal bovine serum
F_{ratio}	Fluorescence ratio
Fura-2 AM	Fura-2 acetoxyethyl (AM) ester
GAPDH	Glyceraldehyde 3-phosphate dehydrogenase
GTP	Guanosine triphosphate
HBSS	Hank's balanced salt solution
HEPES	Hydroxyethyl piperazineethanesulfonic acid
hrGFP	Humanised Renilla green fluorescent protein
HRP	Horse radish peroxidase
IHC	Immunohistochemistry
IP3	Inositol 1,4,5-trisphosphate
K^+	Potassium ions
mRNA	messenger ribonucleic acid
NA	Noradrenaline
Na^+	Sodium ions
nNOS	Neuronal nitric oxide synthase
NO	Nitric oxide
NP40	Nonyl phenoxypolyethoxylethanol
NPY	Neuropeptide Y
OCT	Optimal cutting temperature
PBS	Phosphate buffered saline
PCR	Polymerase chain reaction
PFA	Paraformaldehyde
PGI2	Prostacyclin
PGP9.5	Protein gene product 9.5
PLC	Phospholipase C
PMA	Phorbol esters
PVDF	Polyvinylidene difluoride
RA	Retinoic acid
RAMP1	Receptor activity modifying protein

RIPA	Radioimmunoprecipitation assay
RT	Room temperature
RT-PCR	Reverse transcription-polymerase chain reaction
SBS	Salt buffered solution
SCG	Superior cervical ganglion
SDS	Sodium dodecyl sulfate
SERCA	Smooth endoplasmic reticular Ca2+ ATPase
SMA	Superior mesenteric artery
SMCs	Smooth muscle cells
SP	Substance P
TAE	Tris-acetate-EDTA
TEMED	Tetramethylethylenediamine
TH	Tyrosine hydroxylase
TM	Transmembrane
Tm	Typical melting temperature
UDP	Uridine diphosphate
UDP-Glu	Uridine diphosphate glucose
UTP	Uridine triphosphate
VAChT	Vesicular acetylcholine transporter
VGCC	Voltage-gated calcium channels
VNUT	Vesicular nucleotide transporter
vWF	von Willebrand Factor
α,β-meATP	α,βmethylene ATP
α-SMA	α-smooth muscle actin

Acknowledgements

I would like to acknowledge and give my warmest thanks to my supervisors Professor Samuel Fountain and Dr Derek Warren, for their endless guidance and support. In particular, I would like to thank Sam who made this work possible. His guidance and advice carried me through all the stages of my project. Thanks Sam for believing in me and for choosing me to pursue this project. I would have been completely lost without your help and guidance over the past four years. I would also like to thank my incredible parents (Tawfik and Ahed) for all their support in each part of my life. In addition, I would also like to thank my eight siblings (Nermin, Nivin, Yousef, Nadin, Nouran, Ahmad, Najwan and Mahmoud) for their unfailing support. I would like to thank Enana Alassaf for all her support since I moved to the UK and during my PhD, without her, I wouldn't be able to do this. I also want to extend a special thank you to Dr Stefan Bidula for all of his help in the lab and for putting up with my constant stream of questions.

In addition, I would also like to express my profound gratitude to all the members, past and present, of Fountain Lab, namely Dr Maria Gonzalez-Montelongo, Dr Neville Ngum, Dr Seema Ali, Jessica Meades, Anna Fortuny, Sonia Paz, Michelle Fletcher and Kayleigh Goddard. It was my privilege to work with them all. I want to say a huge thank you for all of their support and for generally making my PhD an incredible experience.

Furthermore, I would like to thank the UEA University of Sanctuary for funding my project. I would like to thank the UEA Sanctuary Liaison Officer, Madeleine Dutton and the Academic Lead for University of Sanctuary, Sophie North for all their support. Most importantly, I would like to thank all the microbiology laboratory team at the Norfolk Norwich University Hospital for their continuous support whilst writing up my PhD thesis. In addition, I would like to thank my friends Mohammad Hazam and Radwan Shaban for their support through the difficult times during my PhD. They were there when I needed them the most. Finally, I would like to express my deepest appreciation to my friend Olena Boiarovska (Бояровська Олена) for the support that she has given me over the preparing for my viva. Despite all the difficulties and suffering that she experienced in her country Ukraine, she has been a great source of comfort, support and inspiration since I met her. I want to say a huge thank you for Olena.

Chapter 1: Introduction

1.1 Hypertension

Hypertension is when there is abnormally high blood pressure in the arteries — the blood vessels that carry blood from the heart to the rest of the body. As a result, the flow of blood and oxygen to the heart and other organs is reduced. Hypertension is the leading cause of morbidity and mortality globally among all cardiovascular diseases. Hypertension is a major risk factor for a number of conditions, such as heart failure, stroke, chronic kidney disease, coronary artery disease, peripheral arterial disease, and vascular dementia. In 2020, 1.28 billion adults were diagnosed with hypertension, which made the health condition an issue of global concern. The pathophysiology of hypertension is complicated. It includes the multi-interaction of the sympathetic nervous system, the renin-angiotensin-aldosterone system, sodium homeostasis regulation, endothelium, and the immune system. Despite the availability of multiple antihypertensive drugs such as β-receptor blockers, angiotensin II receptor blockers, and angiotensin-converting enzyme inhibitors, approximately 1 in 5 adults (21%) are diagnosed with uncontrolled hypertension and these drugs are associated with side effects such as intolerance and poor efficacy (Li et al., 2022; Roth et al., 2018). Given the enormous number of people who have uncontrolled hypertension and the complexity of pathogenesis, developing new antihypertensive agents to provide more choices for those people is important. In human and other different models, hypertension is modulated by the sympathetic nervous system, including sympathetic innervation density, proportion of sympathetic neurotransmitters and sympathetic activity. For instance, it has been demonstrated in the tail arteries of spontaneously hypertensive rats that adenosine triphosphate (ATP) is increased during hypertension and it is considered the predominant perivascular sympathetic neurotransmitter (Pakdeechote et al., 2007; Shen et al., 2009). Purinergic receptors are implicated in several diseases, with cardiovascular diseases being the most common — as it is known that P2 receptors are mostly expressed on blood vessels. Recent studies showed that purinergic signalling in hypertension is mediated through the sympathetic nervous system, neurons in the brain stem, the endothelium, the carotid body, the renin-angiotensin system, sodium excretion, epithelial sodium channel activity, renal autoregulation and the immunological system (Li et al., 2022). Moreover, functional studies showed a rise in excitatory junction potentials facilitated by P2X receptors in mesenteric arteries of spontaneously hypertensive rats (Brock & Van Helden, 1995). Studies *in vivo* using hypertension models reported that the induction of carotid sinus baroreceptors by constant electrical stimulation can decrease the sympathetic outflow leading

to low blood pressure (Bisognano et al., 2011). Thus, expanding our understanding of these neurotransmitters and their purinergic receptors could help in controlling the high blood pressure that occurs in hypertension. This suggests that purinergic signalling has shown great therapeutic potential for hypertension.

1.2 The vascular system

The vascular system is comprised of a vast network of vessels including arteries, capillaries and veins. These vessels are responsible for the transport of nutrients throughout the body via the bloodstream, which maintains homeostasis. Three layers surround the entire vasculature. First, the internal layer, the tunica intima, is comprised of endothelial cells which play a role in modulating blood flow proportion. Second, the tunica media is the middle layer and is primarily made of smooth muscle cells which encircles endothelial cells and contributes to constriction and dilation of blood vessels. Finally, the outer layer is termed the tunica adventitia and contains a meshwork of perivascular nerves (Burnstock, 2009). Small arteries and arterioles contribute considerably to the control of blood pressure, as they are implicated for over 45% of the peripheral resistance to blood flow through the blood vessels. Vascular homeostasis is primarily determined by healthy endothelial cells, e.g., dysfunctional endothelial cells are a key factor in atherosclerosis progression. Several risk factors can impair the endothelium function, such as heart failure, hypertension, and diabetes. (Sheng & Zhu, 2018; Barton & Haudenschild, 2001). In addition, the autonomic nervous system is involved in the performance of the endothelial cells, e.g., perivascular nerves release neurotransmitters, via autonomic neuroeffector junctions, which act at endothelial receptors and modulate endothelial function (Burnstock, 2008). Due to the differential function of these vessels, it is suggested that they have alternate P2 purinergic receptors facilitated properties depending on the size of the arteries (Sheng & Zhu, 2018; Lewis et al., 1998). Purinergic signalling pathways play a vital role in vascular tone modulation and blood pressure modulation. ATP is coreleased with noradrenaline (NA) from perivascular sympathetic nerves leading to vasoconstriction via P2X1 receptors. ATP is released from the endothelium as a result of unstable blood flow or hypoxia and acts on endothelial P2X and P2Y receptors to induce nitric oxide (NO) and endothelium-derived hyperpolarizing factor (EDHF), causing vasodilation (Burnstock & Ralevic, 2014). Control of the vascular tone was known to be associated with antagonistic perivascular sympathetic noradrenergic constrictor nerves and parasympathetic cholinergic dilator nerves. However, recently it was demonstrated that vascular tone is a balance between cotransmitters released from perivascular nerves within the adventitia and numerous elements

released from the endothelium as a result of changes in blood flow, shear stress and hypoxia (Burnstock, 2017; Burnstock, 2009). One of the important factors involved in control of vascular tone is purine signalling pathways. Purinergic signalling can contribute in the short-term control of vascular tone in addition to its role in cell proliferation, migration and death in the long-term control of vascular remodelling by both ATP and its breakdown product, such as adenosine diphosphate (ADP), adenosine monophosphate (AMP) and adenosine (Burnstock, 2009). Although the role of purinergic signalling is clear, further investigation is required to discover the purinergic mechanisms in perivascular nerves in diverse blood vessels and different organisms related to the specific physiologic roles of the particular vessel. Additionally, the role of pre-junctional purinergic receptors requires further investigation. These regulatory mechanisms are important in pathological conditions, including hypertension, atherosclerosis, vascular pain, diabetes and restenosis.

1.3 Purinergic signalling and purine receptors

In the early 1970s, ATP was recognised as a transmitter in non-adrenergic, non-cholinergic nerves supplying the gut and bladder by Professor Geoffrey Burnstock (Burnstock, 1972). Despite earlier evidence in support of the hypothesis, there was initially much opposition to the idea, and it took another 20 years for purinergic signalling to be widely recognised by the scientific community (Burnstock, 2014). It is well known now that ATP is a cotransmitter in the central and peripheral nervous systems (Verkhratsky et al., 2020). Purinergic signalling is implicated in a wide range of physiological processes, including smooth muscle contraction, immune responses, embryonic development, and maintaining homeostasis, and it is now known that autocrine/paracrine signalling via extracellular nucleosides and nucleotides is one of the most common cell signalling mechanisms (Yegutkin 2014). Purinergic signalling is the activation of purinergic receptors by extracellular signalling mediated by purine nucleotides and nucleosides (Figure 1.1). These extracellular mediators include purine nucleoside (adenosine), nucleotides (ATP, ADP, AMP) and pyrimidine nucleotides including uridine diphosphate (UDP), uridine triphosphate (UTP) and uridine diphosphate glucose (UDP-Glu) — all of which are main extracellular messengers in the central nervous system and peripheral nervous system, regulating cell function (Jacobson, 2002). In 1987, it was demonstrated the receptors for adenosine (P1) receptors and ATP for (P2) receptors. Purine receptors are divided into two main types: P1 receptors which recognise adenosine, and P2 receptors which recognise purine and pyrimidine nucleotides such as ATP, ADP, UTP, UDP and UTP-Glu (Ralevic, 2009). Nineteen different purinergic receptors have

been cloned and the molecular and pharmacological properties of the homomeric and heteromeric receptors characterised. Depending on the mechanism of action, pharmacology and molecular cloning, P2 receptors are categorised into two groups: ionotropic P2X receptors, which are ligand-gated ion channels induced via extracellular nucleotides ATP which play a vital role in the control of arterial tone and blood pressure, and metabotropic P2Y receptors which are coupled to G proteins (Gitterman & Evans, 2000). Extracellular ligands including nucleotides and nucleosides are released from various cell types which are linked to the regulating of vascular tone. These ligands can act at P1 and P2 receptors located on endothelial cells, smooth muscle cells and perivascular nerves mediating vasomotor and trophic responses (Ralevic & Dunn, 2015; Burnstock, 2012). Purinergic receptor activation results in a variety of significant cellular signalling pathways, as evidenced by publications revealing short-term signalling in neurosecretion, neuromodulation, and neurotransmission. Furthermore, their activation also mediated long-term signalling involved in cell proliferation, differentiation and death (Verkhratsky et al., 2020). Purinergic receptors can be found in all types of oligodendrocytes, e.g., in all regions of perivascular nerves, neuronal cell bodies and terminals, satellite glia and Schwann cells. Both families of P1 and P2 receptors are mainly expressed on blood vessels, being located on perivascular nerves, vascular smooth muscle, and the endothelium. Arteries are innervated by autonomic nerves (mostly sympathetic) and sensory-motor neurons. These perivascular neurons located within the adventitia of arteries release neurotransmitters that influence arterial tone by controlling the activity of the purinergic receptors on arterial smooth muscle and endothelium. Pharmacological manipulation of perivascular nerve activity has the potential to modulate arterial tone and alter blood pressure (Ralevic, 2009; Burnstock & Knight, 2004).

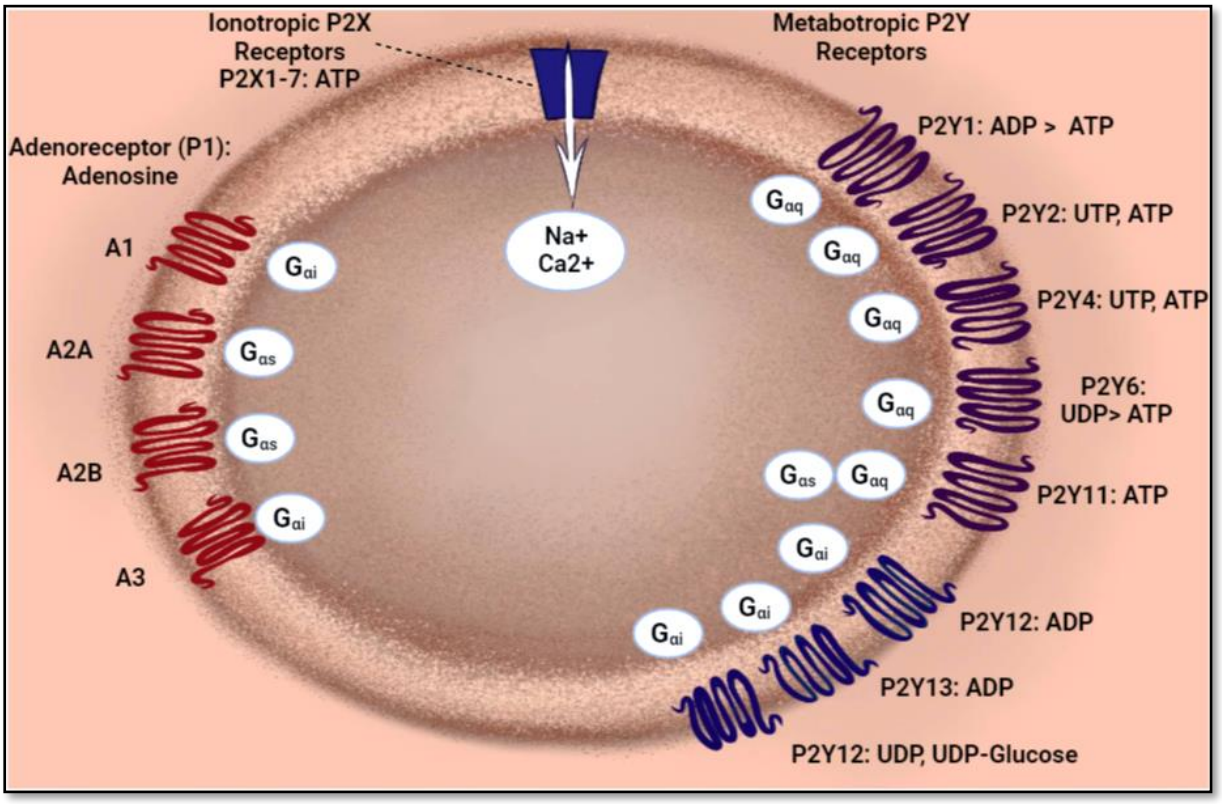

Figure 1.1: The activation of purinergic receptors by extracellular signalling mediated by purine nucleotides and nucleosides. Endogenous agonist selectivities for cell surface receptors for adenosine (P1 receptors) and purine nucleotides and UDP-sugars (P2 receptors). P2X1-7 receptors are ionotropic receptors which can form heteromeric receptors (e.g., P2X2/3). The G protein coupling of adenosine/P1 receptors and P2Y receptors is shown. Adapted from (Ralevic & Dunn, 2015).

1.3.1 P1 receptors

P1 receptors are G protein-coupled and have seven putative transmembrane domains with the NH_2 terminus located on the extracellular side and the COOH terminus located on the cytoplasmic side of the membrane. P1 receptors are divided into four subfamilies: A1, A2A, A2B and A3 (Ralevic, 2009; Ralevic & Burnstock, 1998). All four adenosine receptor subtypes are located in smooth muscle cells and endothelial cells of blood vessels and have a vital role in controlling arterial tone and cell proliferation. A1 and A3 receptors couple to the $G_{\alpha i}$ family of G proteins which inhibit the production of cyclic adenosine monophosphate (cAMP) and a decrease in the concentration of intracellular cAMP, while A2A and A2B couple to $G_{\alpha s}$ of G proteins and induce cAMP production (Abbracchio et al., 2009; Ralevic, 2009; Burnstock & King, 2002). A1 and A2A receptors have a high affinity for adenosine, while A2B and A3 receptors have relatively lesser affinity for the agonist (Fredholm et al., 2011). Although the preferred endogenous ligand of P1 purinergic receptors is the nucleoside, adenosine, A1 and A3 are also activated by inosine, a product formed from the deamination of adenosine by the enzyme adenosine deaminase (Jin et al., 1997; Fredholm et al., 2001, 2011). P1 receptors share between 31-40 % of the sequence homology with the largest homology seen between A2A and A2B approximately 46% (Piirainen et al., 2011). A1 receptors are widely distributed in the central nervous system, skeletal muscle, adrenal glands, and adipose tissue, while A2A receptors are widely found in heart, immune cells, spleen and platelets (Fredholm et al., 2011). A2B receptors are widely expressed in the brain and A3 receptors are ubiquitously distributed in rat testes, mast cells and at low levels found in the brain (Dixon et al., 1996). In addition, Inhibitory A1 receptors are present on sensory and sympathetic neurons, and excitatory A2A receptors are expressed on sympathetic nerves (Ralevic & Dunn, 2015). Adenosine release plays several important roles in the central nervous system, including its role in neural development, neuron-glia signalling and modulation of neural and glial functions. Moreover, adenosine exerts an essential role in the regulation of innate and adaptive immune systems. Adenosine dysregulation is implicated in several diseases such as epilepsy, psychiatric conditions and neurodegenerative disorders (Abbracchio et al., 2009; Boison, 2008).

1.3.2 P2X receptors

P2X receptors are cationic ligand-gated non-selective ion channels permeable to sodium (Na^+), potassium (K^+) and calcium (Ca^{2+}), and in exceptional circumstances, chloride (Cl^-) ions, that open within milliseconds upon activated by extracellular nucleotides ATP. In molecular architecture, they form a unique structural family. The receptor is a trimer, the

binding of ATP between subunits causes them to flex together within the ectodomain and separate in the membrane-spanning region to open a central channel (North, 2016). Up to this date, seven different subunits of P2X receptors are identified (P2X1-7), encoded by seven different genes, that share 40–50% sequence homology at the amino acid level. The length of the receptors ranges from 384 to 595 amino acids across the subtypes (North, 2002). As shown in Figure 1.2, each subunit has two transmembrane domains (TM1 and TM2), a large glycosylated extracellular loop (ectodomain) containing ten-conserved cysteine residues, and an intracellular carboxyl and amino terminus; at least three individual subunits are used to form trimers P2X receptors. While TM1 is responsible for channel gating, TM2 is responsible for lining of the ion conducting pore in the membrane, joined by a large extracellular loop. The ectodomain allows for the formation of disulphide bridges and forms the ATP-binding domain. The NH_2 terminal contains a consensus site for phosphorylation by protein kinase C and may be implicated in controlling P2X receptor currents (Kawate et al., 2009; Abbracchio et al., 2006; Roberts et al., 2006, Evans, 2002). Although the COOH terminus differs significantly between P2X isoforms, the remaining sequence shares 40– 55% of pairwise identity (North, 2002). The variety of P2X receptors phenotype is divided into homomeric and heteromeric according to the assembly of individual subunits; seven heteromeric (P2X1/2, P2X1/4, P2X1/5, P2X2/3, P2X2/6, P2X4/6 and P2X4/7) and six homomeric (P2X1–P2X5 and P2X7, P2X6 subunits probably do not oligomerise) channels have been revealed which must bind to three molecules of ATP in order to open (Abbracchio et al., 2009; Guo et al., 2007; Bean, 1990). P2X receptors gating is made up of three stages. First, the activation phase, which is a rapid rising phase of inward current induced by the application of agonists. Second, the desensitisation phase, which is a decay phase during the presence of agonists. Third, the deactivation phase which is a quick decay phase following the removal of agonists. The key differences between receptor isoforms rely on their agonist sensitivity and activation and deactivation rates (Coddou et al., 2011). P2X2 and P2X4 have been demonstrated to be slowly activating and desensitizing, whilst P2X1 and P2X3 are rapidly activating and desensitising (North, 2016). The P2X receptors play important roles in many physiological processes such as nerve transmission, arterial tone, pain sensation, and immune response. Agonist binding of P2X receptors leads to a structural change, which includes introducing a pore between the subunits and making the diffusion of cations such as Na^+, Ca^{2+}, and K^+ through the cell membrane (Li et al., 2010). It is demonstrated that P2X receptors respond differently to ATP concentrations and its analogue α,βmethylene ATP (α,β-meATP); P2X7 receptors are activated by 100–1000 μM ATP while P2X1-6 receptors have an EC_{50} of ~1– 10 μM (Abbracchio et al., 2009) and these receptors have variable rates of current decay. Thus, The P2X7 receptors have

an extra characteristic of being able to form membrane pores following prolonged stimulation to a high concentration of agonist allowing for molecules with large molecular weight to pass the membrane (Ralevic, 2009). Moreover, recombinant P2X receptors are controlled by protons, Ca^{2+} and zinc (Roberts et al., 2006). P2X2, P2X4, and P2X7 receptors may also go through a second permeability stage, allowing larger cations to pass through (Surprenant et al., 1996; Khakh et al., 1999). The crystal structure of zebrafish P2X4 and the location of its ATP binding sites were recently determined (Figure 1.3), leading to the hypothesis that ATP molecules sequentially activate homotrimers, with the first ATP molecule binding causing a conformational change that impacts the binding of subsequent ATP molecules. (Kawate et al., 2009; Browne and North, 2013). Similar to G-protein-coupled receptors, P2X receptors become desensitised by prolonged agonist application, causing a closure of the receptor pore. Relying on their sensitivity to desensitisation, P2X receptors are either slow-desensitising (P2X2, P2X4, P2X5, and P2X7) or fast-(P2X1 and P2X3) (Khakh et al., 2001; Jarvis and Khakh, 2009).

1.3.2.1 Distribution of P2X receptors

P2X receptors are widely distributed through the human body (Table 1.1). These receptors are expressed in several tissues such as blood vessels including arteries, veins and the nervous system including perivascular nerves (Gitterman & Evans, 2000; Abbracchio et al., 2006; Burnstock, 2007). The receptors, which are also found in the cardiovascular system, cardiac, skeletal, immune and inflammatory cells and in smooth muscle, are of great therapeutic interest and are increasingly being targeted by pharmaceutical companies (Syed et al., 2012). P2X1 receptors are widely expressed with prominent expression in vascular smooth muscle cells, platelets, megakaryocytes, and skeletal muscle (Brass et al., 2012). The P2X2 receptors are mostly expressed in the peripheral nervous system and the central nervous system with predominant expression in mesenteric ganglia neurons, dorsal ganglia neurons, astrocytes, and taste buds, and play a vital role in synaptic transmission, pain, and taste perception (Brass et al., 2012). Homomeric P2X3 and heteromeric P2X2/P2X3 receptors are mainly present on sensory neurons in trigeminal, nodose, and dorsal root ganglion. P2X4 receptors are widely expressed in many neuronal and non-neuronal tissues including rat brain, heart, spinal cord, lungs, and kidneys (Gever et al., 2006). Due to the lack of highly specific antagonists, the role of P2X4 receptors remains exclusive. It has been reported recently the role of P2X4 receptors in chronic inflammation and neuropathic pain by the spinal cord microglia (Brass et al., 2012). The P2X1 and P2X1/4 receptors are considered as the core functional P2X receptors present

in smooth muscle cells of the blood vessels and have a high sensitivity to α,β-meATP, causing rapid depolarisation and vasoconstriction (Gitterman & Evans, 2000; Ralevic & Dunn, 2015; Harhun et al., 2010). It has been demonstrated by immunohistochemical studies that P2X4, P2X5 and P2X6 were expressed on airway epithelial cells (Hargitai et al., 2010). P2X7 receptors are reported to be expressed in several tissues in the body including lungs, salivary glands, retinas, astroglia, microglia, lymphocytes, macrophage, neurons and osteoblasts. By using the reverse transcription-polymerase chain reaction (RT-PCR) and the Western blot, the expression of the new variant of P2X7 was confirmed in various tissues in mice, including the brain, lungs, spleen and salivary glands (Brass et al., 2012). In the vascular smooth muscle cells of blood vessels, P2X7 receptors also could be expressed (Ralevic & Dunn, 2015). The expression of P2X7 in neurons remains controversial. One of the main reasons for this argument is that P2X7 immunoreactivity is still present in brain preparations originating from P2X7 KO mice (Sánchez et al., 2005). Many studies demonstrated that homomeric P2X2 and P2X3 and heteromeric P2X2/3 receptors are abundantly expressed and predominant in the peripheral sensory nerve cells (Todd et al., 2006; Burnstock, 2007). Furthermore, previous studies showed that P2X receptors are expressed in both pre-synaptic and post-synaptic ganglia of sympathetic and parasympathetic nerves. Thus, the P2X receptors are involved in the regulation of neurotransmitter release during fast transmission (Abbracchio et al., 2009). Nevertheless, the functional expression of P2X receptors and their role in the sympathetic neural control of vascular resistance requires further investigation. In this project, the expression of P2 receptors in the pre-junctional nerve terminal of blood vessels was further investigated.

1.3.3 P2Y receptors

A huge variety of cellular processes such as arterial tone, platelet aggregation, inflammation and endothelial cell hydration can also be controlled by P2Y receptors, metabotropic G-protein-coupled receptors (Table 1.3). P2Y receptors include eight subunits that share 21– 48 % sequence homology with the greatest similarity observed between P2Y12 and P2Y13. P2Y receptors can form homodimers or heterodimers with other P2Y receptors or with other transmitter receptors such as A1 adenosine receptors. P2Y receptors can be activated by various purine and pyrimidine nucleotides such as ATP, ADP, UTP, UDP and UDP-Glu (Ecke et al., 2008; Fischer& Krugel, 2007; Abbracchio et al., 2006; Yoshioka et al., 2002). They have seven transmembrane-spanning domains, extracellular NH_2- and intracellular COOH-termini, and structural variability in the intracellular loops and C termini, all of which

alter the degree of coupling to $G_{\alpha q}$, $G_{\alpha s}$, or $G_{\alpha i}$ proteins (Figure 1.2). The existence of amino acids is important for ligand, phylogenetic similarity, selectivity of G-protein coupling and secondary messenger systems (Abbracchio et al 2006; Ralevic, 2009). P2Y receptors are divided into two subfamilies: P2Y1, P2Y2, P2Y4, P2Y6 and P2Y11 subfamilies, and P2Y12, P2Y13 and P2Y14 subfamilies. P2Y receptors of the first group are activated by $G_{\alpha q}$ leading to activate phospholipase C/inositol triphosphate and endoplasmic reticulum Ca^{2+}-release pathway or affect the adenylate cyclase, which in turn results in the alteration of cAMP levels. Furthermore, the activation of the first group of P2Y receptors by nucleotides promotes the dissociation of heterotrimeric G protein, e.g., separation of $G_{\beta\gamma}$ dimer from the G_{α} subunit. This causes the $G_{\alpha q}$ subunit to activate phospholipase C, which then hydrolyses phosphatidylinositol bisphosphate to inositol triphosphate. The inositol triphosphate then acts on its receptor (inositol triphosphate receptors) at the endoplasmic reticulum which then leads to the release of Ca^{2+} from the endoplasmic reticulum into cytosol. (Abbracchio et al 2006; Ralevic, 2009; Von Kügelgen & Hoffmann, 2016). P2Y receptors of the second group couple to $G_{\alpha i}$ and which leads to inhibiting adenylyl cyclase leading to a decreased cAMP accumulation and modulating ion channels. P2Y11 receptors couple to both $G_{\alpha s}$ and $G_{\alpha q}$ proteins to activate phospholipase C and adenylyl cyclase (Abbracchio et al 2006: Ralevic et al., 2015; Burnstock, 1997). P2Y receptors can be also divided into different groups according to their adenine-nucleotide (P2Y1, P2Y11, P2Y12 and P2Y13 receptors) and uracil nucleotide (P2Y2, P2Y4, P2Y6 and P2Y14 receptors) preferences (Von Kügelgen, 2006) or both such as P2Y2 receptors (Parravicini et al., 2008). As shown in (Table 1.2), unlike P2X receptors, which are only activated by ATP, P2Y receptors can be activated by both purine and pyrimidine nucleotides, dependent on the receptor subtype. Briefly, P2Y1, P2Y12, and P2Y13 receptors are all preferentially activated by ADP. P2Y2 and P2Y4 are both UTP receptors, whereas P2Y6 and P2Y14 receptors are activated by UDP. Additionally, P2Y receptors can be activated by sugar nucleotides (P2Y14 is a receptor for UDP-Glu), ADP and cysteinyl leukotriene E4 such as P2Y12 receptors (Parravicini et al., 2008). Some P2Y receptors such as P2Y11 might be activated by ATP resulting in an increase in cAMP, inositol triphosphate and cytosolic Ca^{2+}, while activation by UTP activates Ca^{2+} mobilisation without increasing in cAMP and inositol triphosphate (White et al., 2003). Furthermore, in some conditions, P2Y receptors could have direct interactions with other proteins without G protein facilitation (Abbracchio et al., 2009). The P2Y11 receptor may also contribute to activate adenylyl cyclase via $G_{\alpha s}$. Free ATP can mediate the activation of most P2Y receptors (P2Y1, P2Y2, P2Y4, P2Y6, P2Y11) while ADP can contribute to the activation of P2Y1, P2Y12 and P2Y13 receptors. P2Y14 receptors are expressed via acting at UDP and UDP-Glu, whereas ATP is a decreased efficacy agonist (Abbracchio et al., 2009).

1.3.3.1 Distribution of P2Y receptors

Several cellular functions are mediated by P2Y receptors in various tissues and organs (Table 1.2) such as the nervous system (in both glia and neurons), vascular tissue, kidneys, eyes, epithelia of the airway, the immune and inflammatory cells and the gastrointestinal tract (Brass et al., 2012: Parravicini et al., 2008). It has been suggested that these receptors are fundamental elements in many physiological processes, including vasodilation, neuromodulation, inflammation, and cell migration (Gitterman & Evans, 2000). Various subtypes of P2Y receptors are expressed by vascular smooth muscle, it has been demonstrated that P2Y2 receptors induced vasoconstriction in rat cerebral parenchymal arterioles (Burnstock, 2017). The activation of P2Y1 which acts at vasculature endothelium is mediated by ATP and ADP leading to vasorelaxation (Webb et al., 1993; Burnstock, 1997). In addition, the activation of P2Y receptors on smooth muscle cells following perivascular nerve stimulation can mediate vasoconstriction of coronary arteries, e.g., P2Y2, P2Y4 and P2Y6 receptors act at smooth muscle and activated by uridine nucleotides leading to vasoconstriction (Gitterman & Evans, 2000; Westcott & Segal, 2013). Functional P2Y1 and P2Y2 receptors are mainly expressed in endothelial cells, with some blood vessels expressing P2Y4, P2Y6 and P2Y14 receptors (Burnstock and Ralevic, 2014; Chambers et al., 2000). The binding of ATP released from endothelial cells to P2Y receptors during shear stress promotes phospholipase C activation and this leads to Ca^{2+} release and endothelial NO synthase activation resulting in smooth muscle cells dilation by NO production (Burnstock, 2012). However, it remains unclear whether the ATP released from perivascular nerves can reach endothelial cells to activate P2Y receptors (Westcott & Segal, 2013). In turn, these novel results can be utilised to develop more selective therapies which can be used for treating vascular diseases. It has been evidenced that there is expression of facilitatory P2X and inhibitory P2Y receptors on sympathetic nerves, however, further investigations are required to identify what P2 receptors are expressed in the perivascular nerve terminal of blood vessels. In this project, by using RT-PCR technique, the expression of both P2X and P2Y receptors was investigated using two different types of blood vessels and sympathetic ganglia. Then, immunohistochemical studies were performed to identify what P2 receptors are expressed in the perivascular nerve terminal of the blood vessels.

Table 1.1: Characteristics of P2X receptors. Adapted from (Layhadi, 2017; Burnstock & Knight, 2004).

P2XR subtype	Primary distribution	Downstream signalling pathway	Agonist(s)	Antagonists
P2X1	Smooth muscle, platelets, cerebellum, dorsal horn spinal neurons	Intrinsic ion channel	ATP = α,β-meATP = 2-meSATP	MRS2220, MRS2159, NF449, NF279, Ro-0437626, Suramin, PPADS, TNP-ATP
P2X2	Smooth muscle, central CNS, retina, chromaffin cells, autonomic and sensory ganglia		ATP ≥ ATPγS ≥ 2- meSATP > α,β-meATP	RB-2, NF279, NF770, NF776, NF778, PSB-12011, PSB-10211, Suramin, PPADS, TNP-ATP
P2X3	Sensory neurons and sympathetic neurons		2-meSATP ≥ ATP ≥ α,β-meATP	A-317491, NF023, NF279, NF449, RO-85, MRS2159, MRS2257, Suramin, PPADS, TNP-ATP
P2X4	CNS, immune cells, testes, colon		ATP > α,β-meATP > BzATP	5-BDBD, BBG, Paroxetine, PSB12062, BX430, Suramin, PPADS, TNP-ATP
P2X5	Skin, gut, bladder, spinal cord		ATP > 2-meSATP > ATPγS	BBG, Suramin, PPADS, TNPATP
P2X6	CNS		ATP > 2-meSATP Does not function as homomultimer	TNP-ATP, PPADS
P2X7	Immune cells, pancreas, skin		ATP > BzATP	MRS2159, KN-62, BBG, suramin, A438079, AZ11645373, PPADS

Table 1.2: Characteristics of P2Y receptors. Adapted from (Layhadi, 2017; Burnstock & Knight, 2004).

P2YR subtype	Primary distribution	Downstream signalling pathway	Agonist(s)	Antagonists
P2Y1	Epithelial and endothelial cells, platelets, immune cells, brain	GPCR: Gaq - PLCb activation, ↑[Ca^{2+}]i	2-MeSADP > 2- MeSATP = ADP > ATP	MRS2279, MRS2179, MRS2500
P2Y2	Epithelial and endothelial cells, immune cells	GPCR: Gaq and Gai - PLCb activation, ↑[Ca2+]i	UTP = ATP	Suramin, ARC118925XX
P2Y4	Endothelial cells, placenta	GPCR: Gaq - PLCb activation, ↑[Ca2+]i	UTP ≥ ATP	ATP (human), Reactive blue 2, PPADS
P2Y6	Epithelial cells, placenta, T cells, thymus	GPCR: Gaq - PLCb activation, ↑[Ca^{2+}]i	UDP > UTP >> ATP	MRS2578, Reactive blue 2, PPADS, suramin
P2Y11	Spleen, intestins, granulocytes	GPCR: Gaq and Gas - PLCb activation, AC activation, ↑[Ca^{2+}]i	AR-C67085MX > Bz-ATP ≥ ATP	Suramin, Reactive Blue 2, NF340, NF157
P2Y12	Platelets, glial and microglial cells of the brain	GPCR: Gai - inhibition of AC	ADP = 2-MeSADP	PSB-0739, Ticagrelor, Clopidogrel, ARC69931MX
P2Y13	Immune cells, pancreas, skin	GPCR: Gaq and Gai - inhibition of AC, PLCb activation	ADP = 2-MeSADP > ATP = 2-MeSATP	ARC-69931MX, ARC67085MX, MRS-2211
P2Y14	Adipose tissue, stomach, intestine, brain, mast cells	GPCR: Gai - inhibition of AC	UDP-glucose = UDP	N/A

Table 1.3: P2Y receptor agonist preferences and G-protein coupling. Table adapted from (Ali, 2019; Jacobson et al., 2012).

Receptor subtype	G-protein coupling	Preferred agonists (pEC_{50}, human)
P2Y1	$G_{\alpha q}$	ADP (5.90)
P2Y2	$G_{\alpha q}$, $G_{\alpha i}$	ATP (7.07) = UTP (8.10)
P2Y4	$G_{\alpha q}$, $G_{\alpha i}$	UTP (5.60)
P2Y6	$G_{\alpha q}$	UDP (6.52)
P2Y11	$G_{\alpha q}$, $G_{\alpha s}$	ATP (4.77)
P2Y12	$G_{\alpha i}$	ADP (7.22)
P2Y13	$G_{\alpha i}$	ADP (7.94)
P2Y14	$G_{\alpha i}$	UDP (6.80), UDP-glucose (6.45)

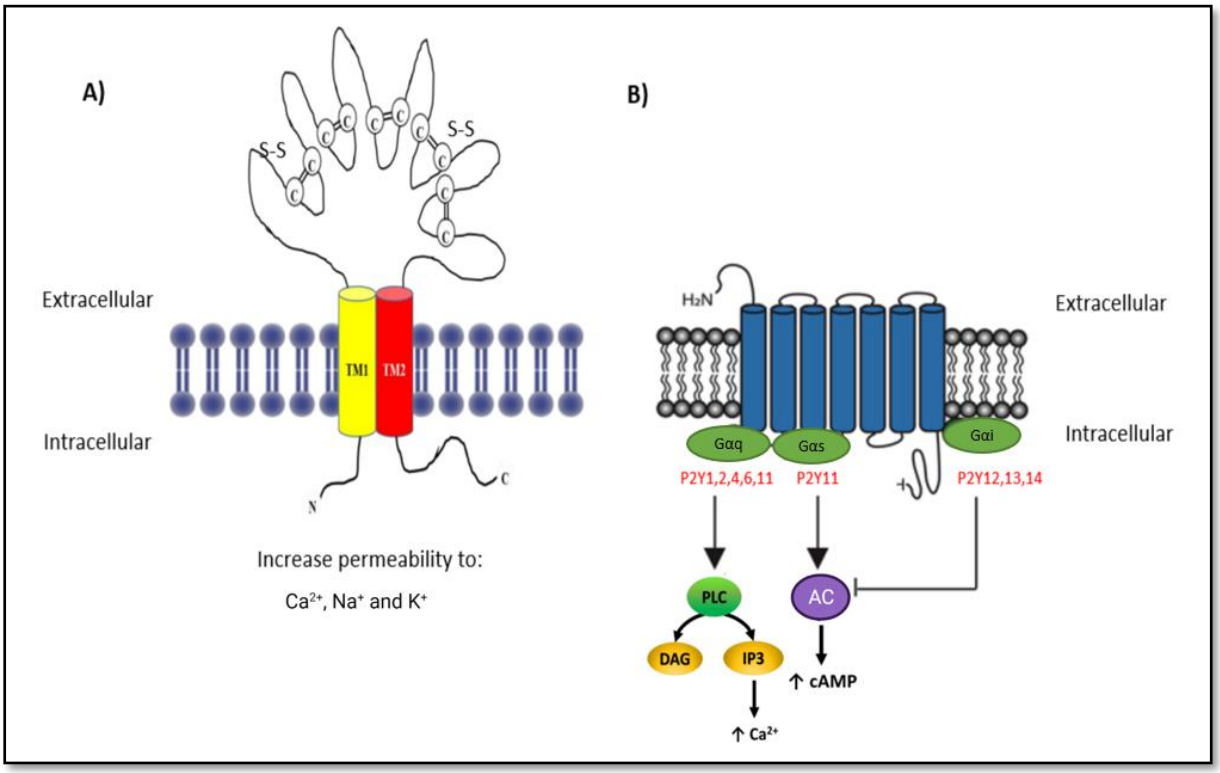

Figure 1.2: Structure of P2 receptors. **(A)** Each subunit of P2X receptor has two transmembrane domains (TM1 and TM2) which traverse the lipid bilayer of the plasma membrane and are connected by a long extracellular loop consisting of 10 cysteine residues that keep the extracellular structure stable via disulphide bridges. Both N- and C- termini are located intracellularly. Agonist binding of P2X receptors leads to a shape change, introducing a pore between the subunits and making diffusion of cations such as Na^+, Ca^{2+}, and K^+ through the cell membrane**. (B)** Illustration of G-protein coupled P2Y receptors. P2Y1,2,4,6 are coupled to $G_{\alpha q}$ subunit, thus the activation of these receptors activates phospholipase C, which produces diacylglycerol and inositol triphosphate. Inositol triphosphate then binds to its receptors on the surface of the endoplasmic reticulum to promote Ca^{2+} release from the endoplasmic reticulum into the cytosol. P2Y12,13,14 are coupled to $G_{\alpha i}$ subunit inhibiting adenylyl cyclase and preventing accumulation of cyclic AMP. P2Y11 is coupled to both $G_{\alpha q}$, $G_{\alpha s}$, subunits activating Ca^{2+} mobilization, and activating adenylate cyclase respectively. Adenylate cyclase then leads to an accumulation of intracellular cyclic AMP. PLC, phospholipase C; AC, adenylate cyclase; DAG, diacylglycerol; IP3, inositol triphosphate, cAMP, cyclic adenosine monophosphate.

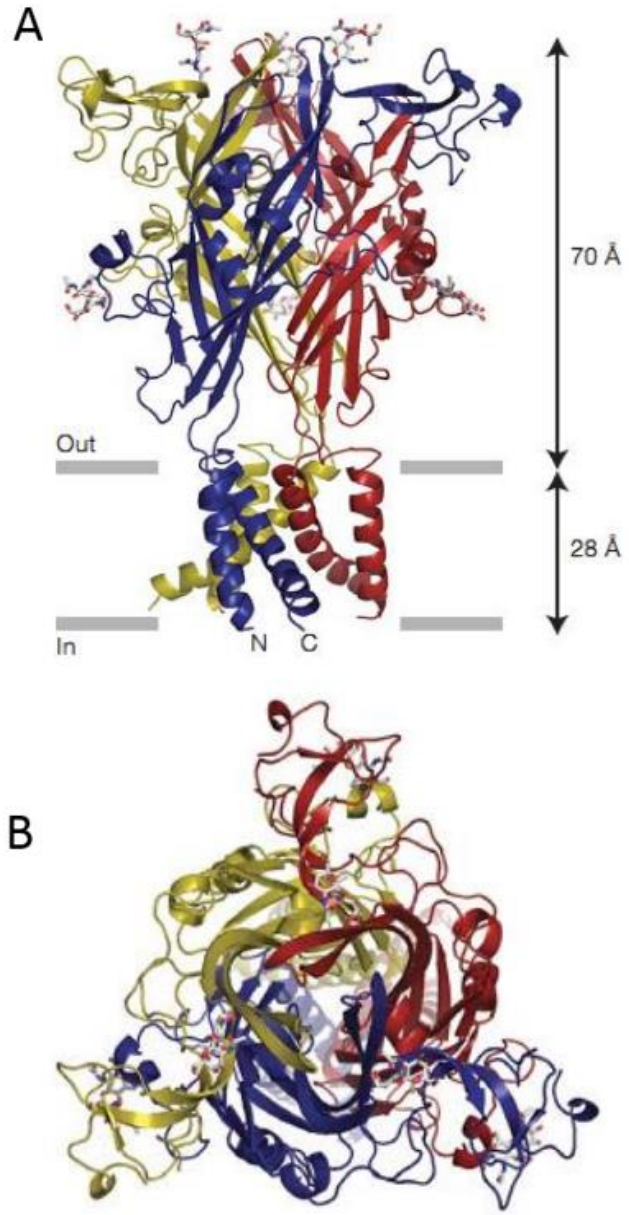

Figure 1.3: Crystal structure of P2X4 receptor. **(A)** Stereoview of homotrimeric zebrafish P2X4 receptor viewed parallel to the membrane. **(B)** Stereoview of homotrimeric zebrafish P2X4 receptor parallel to the molecular three-fold axis from the extracellular side of the membrane. Each trimer subunit is depicted in different colours (red, blue, and yellow). Adapted from (Kawate et al., 2009).

1.4 Regulation of vascular tone (hypertension) by P2 purinergic receptors

P2 receptors play a vital role in regulating of hypertension by acting on blood vessels and the central nervous system and contributing in renal autoregulation. Purinergic signalling influences hypertension in nine ways: sympathetic nerve activities, endothelial cells, neurons in the brain stem, renin-angiotensin system, carotid body, inflammation (Burnstock, 2017) sodium excretion, epithelial sodium channel activity and renal autoregulation, which have been associated with blood volume (Li et al., 2022) (Figure 1.4). Sympathetic nerve activity and the renin-angiotensin system directly affect blood pressure by influencing peripheral resistance, blood volume, and cardiac output (Li et al., 2022). Purinergic signalling events can contribute in short-term control of vascular tone via ATP released from sympathetic neurons, sensory-motor nerves and endothelial cells in the local blood vessels (Li et al., 2022, Burnstock, 1999, 2009). Perivascular sympathetic nerves release ATP as a contransmittter with NA and neuropeptide Y (NPY) which binds to vascular smooth muscle P2X1 receptors. As a result of this activation, rapid responses occur, including Ca^{2+} entry directly into the cell through the P2X channel or via voltage-gated Ca^{2+} channels which are opened in response to the P2X receptor, mediating membrane depolarisation and causing vasoconstriction (Ralevic, 2012) (Figure 1.5). Many blood vessels can be innervated by sensory-motor nerves, unmyelinated C-fibre and myelinated Aδ-fibre primary afferents which have a dual sensory (or afferent – carry signal to the CNS) and motor (or efferent- carries information from the CNS to the effector) function (Ralevic, & Dunn, 2015). ATP could be released from sensory-motor nerves "during axon reflex' activity" with calcitonin gene-related peptide (CGRP) and substance P (SP), and acts at the smooth muscle P2Y receptors leading to either vasoconstriction or vasodilation of blood vessels (Burnstock, 2006, 2009) (Figure 1.5). The expression of P2X receptors acting on smooth muscle cells can also promote vasorelaxation, however, the mechanisms are unclear (Westcott & Segal, 2013). Another way of contributing to purinergic signalling in hypertension is by the endothelium; ATP could be released from endothelial cells and erythrocytes during shear stress and hypoxia to act on its endothelia P2 receptors largely P2X4 via ATP (Li et al., 2022), P2Y1 via ADP (Motte et al., 1995), P2Y2 via ATP and UTP (Ralevic & Burnstock, 1998). The activation of these receptors leads to produce NO and EDHF, mediating vasodilation and a decrease in blood pressure (Burnstock, 1999, Burnstock, 2009 Burnstock, 2017; Wang et al., 2015) (Figure 1.5). Vasocontractile actions induced following ATP release could lead to a constant constriction of large cerebral vessels, mainly via P2Y receptors or short-term constriction through P2X receptors (Sprague et al., 2003, Burnstock, 2009). Other subtypes of P2Y receptors could be expressed on the endothelium including P2Y4 and P2Y6 according to Ralevic, (2001), and P2Y11 in human mammary arteries and umbilical veins

according to Wang et al., (2002). P2Y6 receptors have high levels of expression in mouse resistance arteries compared with P2Y6-deficient mice which had lower blood pressure. In *in vitro* studies in the rat model, P2Y6 receptors are activated via UDP and UTP were responsible for arterial contraction (Li et al., 2022; Kauffenstein et al., 2016). The P2Y11 receptor is closely associated with inflammation and may have therapeutic potential in immune system-related hypertension. (Yamamoto et al., 2006). It has been reported in rat mesenteric artery that the activation of P2X1 mediated endothelial-dependent vasorelaxation independently of NO which had no influence on dilation once blocked by the NO synthesis inhibitor (Harrington & Mitchell, 2004).

P2Y1 receptors within the central nervous system and peripheral nerves were involved in blood pressure regulation. The inhibition of P2Y1 receptors in C1 neurons — in the rostral ventrolateral medulla — promoted a reduction in peripheral chemoreceptor-mediated phrenic nerve activity, sympathetic nerve activity, and blood pressure (Wenker et al., 2013). In this case, we can speculate that P2X receptors play biphasic vasomotor effects, e.g., the activation of P2X receptors placed on mesenteric artery endothelial cells was associated with a transient vasoconstriction followed by continued vasorelaxation. Another example is in the rat femoral artery, where there was ATP-induced vasodilation via endothelial P2X or vasoconstriction via P2X receptors on smooth muscle cells (Westcott & Segal, 2013). Moreover, the activation of vascular smooth muscle P1 receptors (mostly A2 receptors) via adenosine, which is produced after the breakdown of ATP release from nerves and endothelial cells, leads to vasodilatation via producing NO in the endothelium (Burnstock, 2009). P2X3 receptors placed on the carotid body are the most promising novel therapeutic target for hypertension (Li et al., 2022).

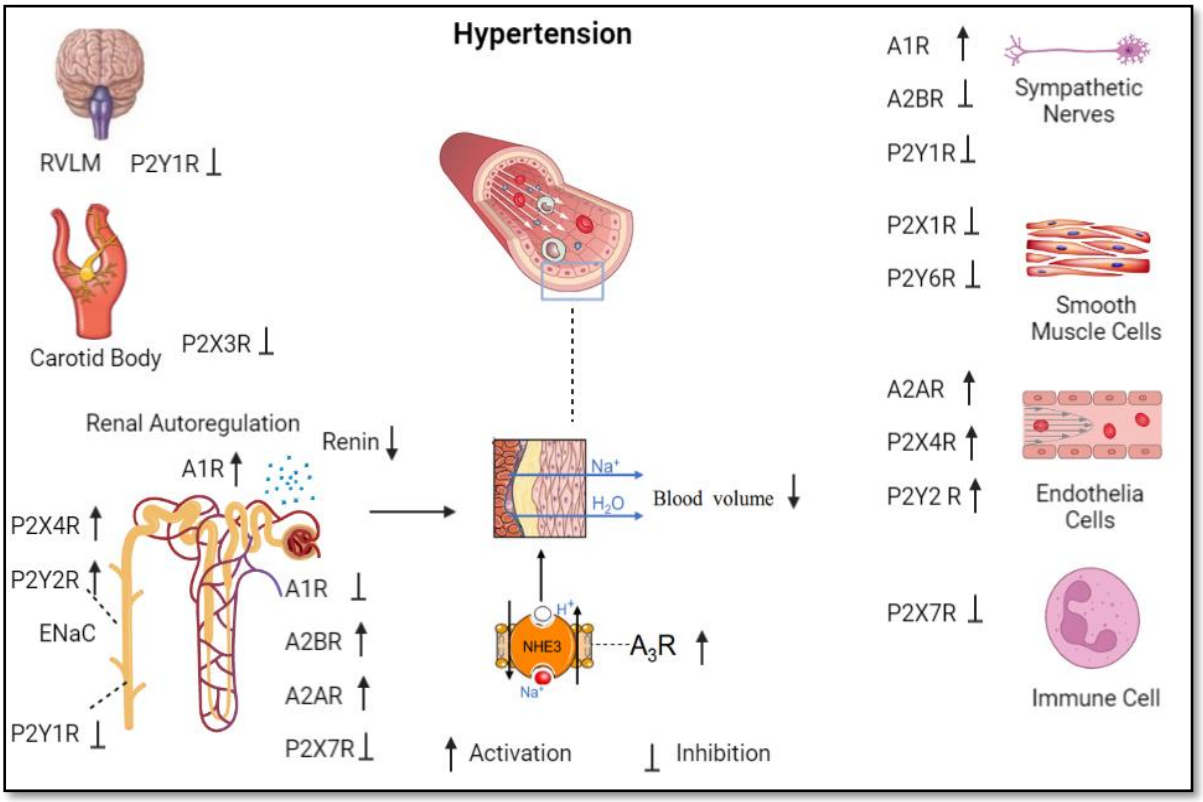

Figure 1.4: Purinergic receptors in regulation of blood pressure. Activation or inhibition of purinergic receptors can induce hypertension in nine different pathways, including sympathetic nerve activities, epithelial sodium channel, activity renin-angiotensin system, the endothelium, sodium excretion, renal autoregulation, neurons in the brain stem, carotid body and inflammation. The activation of A1 receptors promotes renin release. A1, A2B, A3, P2X4, P2Y1, and P2Y2 receptors facilitate sodium excretion. P2Y1 receptors are involved in neurogenic hypertension. P2X3 receptors located on the carotid body are the novel therapeutic target for hypertension. A2A, P2X4, and P2Y2 act at the endothelium of blood vessels, P2X1 and P2X6 receptors act at the smooth muscle cells, all play a vital role in the regulation of vascular tone. RVLM, rostral ventrolateral medulla; ENaC, epithelial sodium channel. Adapted from (Li et al., 2022).

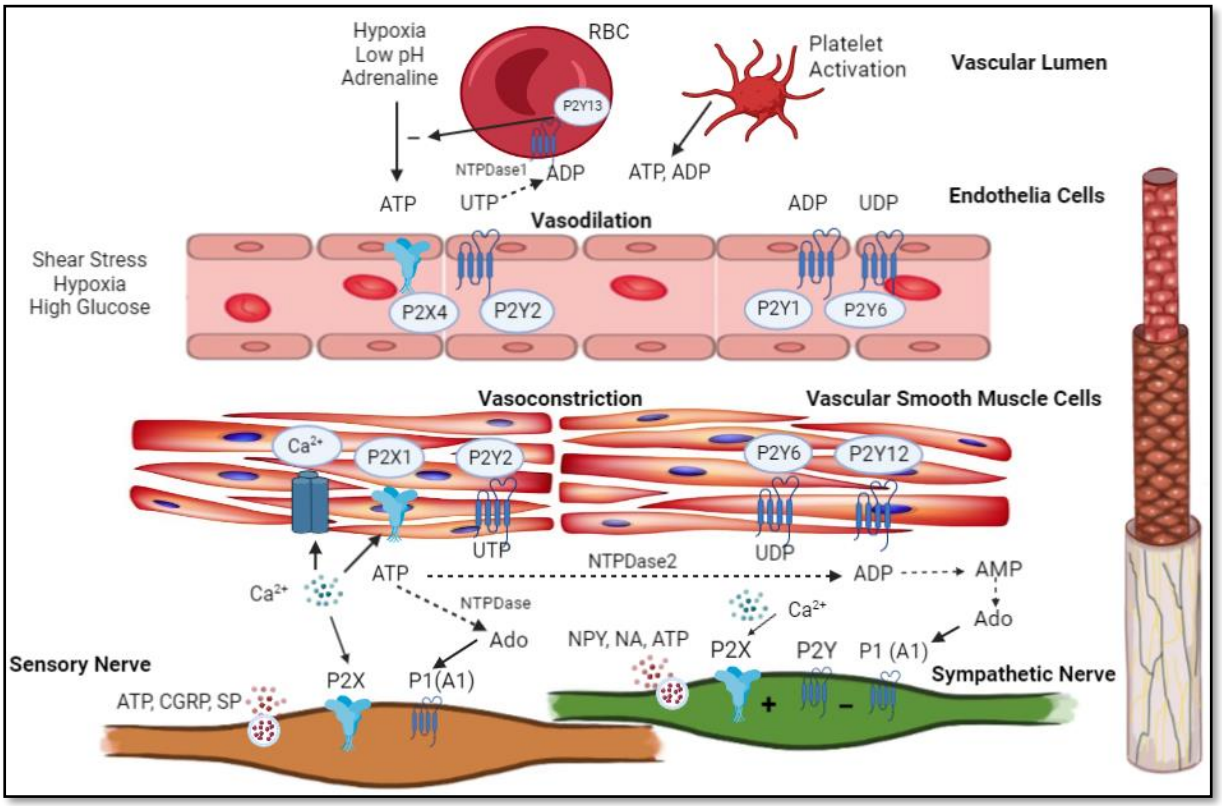

Figure 1.5. Control of vascular tone in blood vessels via P2 purinergic receptors. Perivascular nerves are located in the adventitial layer. Several different neurotransmitters are released from varicosities along the axons of efferent sympathetic and sensory nerves. In addition, it contains various receptors that play an important role in the pre-junctional regulation of neurotransmitters release. ATP is coreleased with NA and NPY as cotransmitters from perivascular sympathetic nerves within the adventitia. ATP could bind to various subtypes of P2 receptors (mainly P2X1) in smooth muscle including P2X1, P2Y2 and P2Y6. As a result of this activation, Ca^{2+} enters the cells resulting in depolarisation/excitatory junction potentials opening of voltage-gated Ca^{2+} channels, and further Ca^{2+}entry and depolarisation causing vasoconstriction. ATP could be released from sensory-motor neurons with CGRP and SP and acts at smooth muscle P2Y receptors leading to either vasoconstriction or vasodilation of blood vessels. ATP and UTP might be released from the endothelium, platelets and red blood cells during shear stress and hypoxia to act on P2Y1, P2Y2 and sometimes P2Y4, P2Y11 and P2X4 receptors resulting in vasodilation by NO, EDHF and prostaglandins. P2X and P2Y receptors can be found on sympathetic nerves modulating neurotransmitters release. Adenosine is produced when ATP and ADP are hydrolysed via ectonucleotidases (E-NTPDases and E-NPPs) to AMP, which is further hydrolysed by ecto-50-nucleotidase to adenosine. EC, endothelial cells; VSMC, vascular smooth muscle cells; Ado, adenosine; RBC, red blood cells. Adapted from (Erlinge & Burnstock, 2008; Westcott & Segal, 2013).

1.5 Purinergic signalling in the nervous system

ATP was known as a neurotransmitter coreleased from sympathetic nerves, parasympathetic nerves and sensory-motor and enteric nerves (Burnstock, 2007) (Table 1.4). It is currently recognized that ATP acts as either a sole cotransmitter in the central nervous system and peripheral nervous system including sympathetic ganglia and at the sympathoeffector junction (Boehm, 1999). In the central nervous system, ATP increased the central sympathetic drive, leading to increased systemic blood pressure (Li et al., 2022). In 1987, receptors for adenosine (P1) and ATP (P2) were identified. Subsequently, in 1992, interest in purinergic receptors was increased after they have been shown in different regions in the brain and spinal cord, being located in neurons and glia. Our understanding of purinergic neurotransmission has critically expanded in recent years through the cloning and characterisation of P2 receptors for ATP and related pyrimidine nucleotides. ATP was recognised as an excitatory transmitter or cotransmitter in the central and peripheral nervous system (Abbracchio et al., 2009; Burnstock, 2007). It is clear now that ATP has a vital role in cell proliferation, growth and development, and in disease and cytotoxicity (Zimmermann, 2006).

Nucleotides such as ATP, ADP and others are stored in and released from secretory and synaptic vesicles (Figure 1.6). It was demonstrated that Cl^--dependent vesicular nucleotide transporter (VNUT) can mediate ATP accumulation in vesicles (Sawada et al., 2008). VNUT, which is mainly expressed in the brain being allocated to chromaffin granules and astrocyte subpopulation, preferentially stores ATP, ADP and guanosine triphosphate (GTP) (Abbracchio et al., 2009). It is still unclear whether VNUT is colocalised with other vesicular neurotransmitter transporters and whether VNUT is correlated with synaptic vesicles. ATP is found in different concentrations in each synaptic and/or secretory vesicle and could be stored or coreleased with other neurotransmitters such as NA, g-aminobutyric acid (GABA), and glutamate (Pankratov et al., 2007). Exocytosis is one of the methods by which ATP is released from nerves, endocrine cells and platelets (Yegutkin 2014). There is compelling proof for ATP release from exocytotic neuronal vesicles. Recent research suggests that astrocytes release ATP via vesicles, which may involve lysosomes (Abbracchio et al., 2009). Additional nucleotide release mechanisms have been discovered, such as ATP-binding cassette transporters, connexin or pannexin hemichannels, plasmalemmal voltage-dependent anion channels, and P2X7 receptors (Abbracchio et al., 2009) (Figure 1.6). The release of ATP and other nucleotides is followed by rapid enzymatic degradation via ectonucleotidases. This process is functionally important as ATP metabolites function as physiological ligands for various

purinergic receptors such as adenosine A1 receptors. There are several types of ectonucleotidase families including E-NPPs (ectonucleotide pyrophosphatase and/or phosphodiesterases), E-NTPDases (ectonucleoside triphosphate diphosphohydrolases), ecto-5'-nucleotidase and alkaline phosphatases (Figures 1.5 & 1.6). For example, adenosine is produced when ATP and ADP are hydrolysed by E-NTPDases and E-NPPs to AMP, which is further hydrolysed by ecto-50-nucleotidase to adenosine. Furthermore, Adenosine can be released directly from subpopulations of neurons and/or astrocytes (Abbracchio et al., 2009; Zimmermann, 2006). The impact of ATP on blood pressure is a complex mechanism that primarily involves the activation of P2X and P2Y receptors in the central nervous system, peripheral sympathetic systems, endothelium and smooth muscle cells, and their interaction.

Table 1.4: ATP as a cotransmitter in peripheral and central nervous systems.

Neuron type	Co-transmitters
Peripheral nervous system	
Sympathetic nerves	ATP + NA + NPY
Parasympathetic nerves	ATP + ACh + VIP
Sensory-motor	ATP + CGRP + SP
NANC enteric nerves	ATP + NO + VIP
Motor nerves (in early development)	ATP + ACh
Central nervous system	
Cortex, caudate nucleus	ATP + ACh
Hypothalamus, locus ceruleus	ATP + NA
Hypothalamus, dorsal horn, retina	ATP + GABA
Mesolimbic system	ATP + DA
Hippocampus, dorsal horn	ATP + glutamate

ACh, acetylcholine; ATP, adenosine 5'-triphosphate; CGRP, calcitonin gene-related peptide; DA, dopamine; GABA, g-aminobutyric acid; NA, noradrenaline; NANC, non-adrenergic, non-cholinergic; NO, nitric oxide; NPY, neuropeptide Y; SP, substance P; VIP, vasoactive intestinal peptide. Adapted from (Abbracchio et al., 2009).

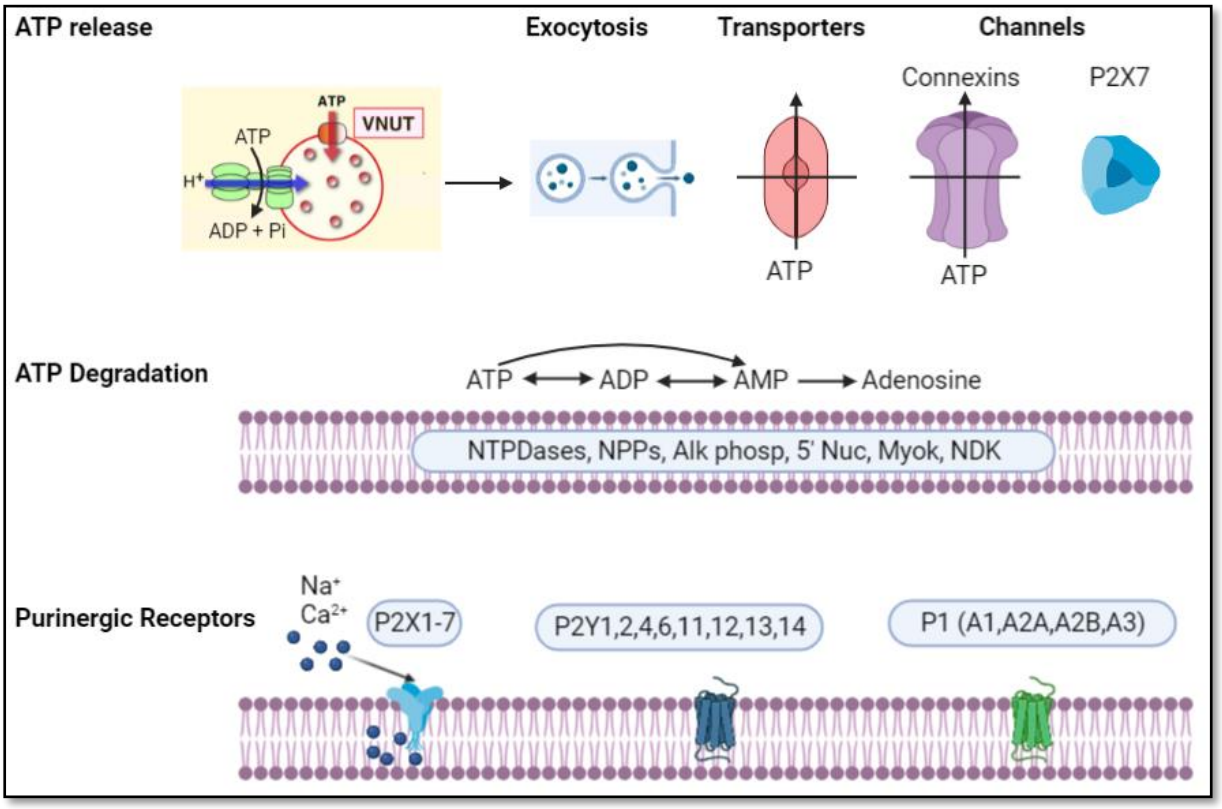

Figure 1.6: Mechanisms of ATP release, storage, degradation and reception. Nucleotides such as ATP, ADP and others are stored in and released from secretory and synaptic vesicles vesicular nucleotide transporters can mediate ATP accumulation in vesicles. Exocytosis is one of the methods by which ATP is released from nerves, endocrine cells and platelets. Extracellular ligands including nucleotides and nucleosides are released from various cell types and act at P1 and P2 mediating various functional responses. The release of ATP and other nucleotides is followed by rapid enzymatic degradation via ectonucleotidases such as E-NPPs, E-NTPDases, ecto-5'-nucleotidase and alkaline phosphatases. Adenosine is produced when ATP and ADP are hydrolysed by E-NTPDases and E-NPPs to AMP, which is further hydrolysed by ecto-50-nucleotidase to adenosine. Alk Phos, alkaline phosphatase; Myok, myokinase (adenylate kinase); NDK, nucleoside diphosphate kinase; NPPs, nucleotide pyrophosphatase and/or phosphodiesterases; 5`-Nuc, 5`-nucleotidase; VNUT, vesicular nucleotide transporter. Adapted from (Abbracchio et al., 2009).

1.6 Purinergic neurotransmission in the perivascular nervous system- innervation of blood vessels

Resistance vessels, such as the mesenteric arteries, are recognized to be innervated by several perivascular nerves, such as sympathetic nerves, non-cholinergic non-adrenergic nerves including CGRPergic nerves and NO nerves (Yokomizo et al., 2015). Histochemical and immunostaining studies helped to investigate the existence of perivascular nerves in several different tissues in addition to using specific neuronal markers to detect innervation sources (Westcott & Segal, 2013). The proportion and distribution of perivascular nerves can differ depending on the organism's species, vascular bed and blood vessel diameter. It has been reported in a previous study that the density of NPY, TH, CGRP, and SP-like immunoreactive nerves was significantly lower in the first branches than the second and third branches of mesenteric arteries, and there was a negative relationship between nerve density and arterial diameter, except for TH- like immunoreactive nerves. In all branches of the arteries, the density of NPY and TH- like immunoreactive was greater than CGRP- (with the exception of like immunoreactive nerves in the 1st branch), SP, or nNOS- like immunoreactive nerves. These findings suggest that vasoconstrictor nerves containing NPY, TH, and vasodilator CGRP nerves innervate each branch of the mesenteric arteries. They also speculate that the high density of perivascular nerves in the second and third branches may play an important role in the maintenance of vascular tone and regulation of organ and tissue blood flow (Yokomizo et al., 2015). However, the different populations of perivascular nerves in various diameter of small artery have not been fully investigated. The different populations of perivascular nerves in different diameters of small arteries have not been widely researched. Most investigations were not able to quantify nerve density because of the difficulties of quantitative comparisons resulting from variances in immunological markers, sample preparation and analytical techniques between laboratories. Recently, the relationship between the blood vessels and the perivascular autonomic nerves is more understood. It is clear now that neurotransmitters released from perivascular autonomic nerves can regulate vasoconstriction and thus arterial tone and blood pressure. However, how these elements affect, and which receptors are involved are still being investigated. Vasoactive neurotransmitters, such as ATP, NA and NPY, are released from varicosities of stimulated perivascular autonomic nerves and interact with vascular cells at relative junctions causing vasocontractile responses. In contrast, neuromodulators such as acetylcholine (ACh) and CGRP can mediate vasorelaxation (Sheng & Zhu, 2018; Burnstock, 2008).

1.6.1 The autonomic nervous system

It is known that the peripheral nervous system consists of the autonomic nervous system and the sensory nervous system. Perivascular nerves release adrenergic, cholinergic, peptidergic, purinergic, and nitrergic neurotransmitters, which promote constriction or dilation by their influences on smooth muscle cells, endothelial cells, and other perivascular nerve functions (Westcott & Segal, 2013). The autonomic nervous system has two main divisions: sympathetic nerves (adrenergic fibres), which release sympathetic neurotransmitters (which can mediate vasoconstriction) such as ATP, NA and NPY, and parasympathetic nerves (cholinergic fibres) which release neurotransmitters (which function as vasodilators) such as ACh, NO and vasoactive intestinal peptide (Figure 1.7). Thus, both arms of the autonomic nervous system including sympathetic nerves and parasympathetic nerves work antagonistically, synergistically, or independently and play an important role in the maintenance of physiological homeostasis and the regulation of responses to shear stress (Sheng & Zhu, 2018; Kenney & Ganta, 2011). The sensory nervous system releases neurotransmitters such as CGRP, SP and neurokinin-A and the activation of these nerves causes vasodilation (Sheng & Zhu, 2018). Perivascular nerves are located in the adventitial layer of blood vessels and do not make direct contact with smooth muscle cells or endothelial cells (Westcott & Segal, 2013) (Figure 1.5). These vessels are innervated by both the sympathetic and parasympathetic arms of the autonomic nervous system via neurotransmitters released from varicosities. These neurotransmitters released are involved in the vasoconstriction and vasodilation of blood vessels, allowing for the modulation of arterial tone and blood pressure (Sheng & Zhu, 2018),

Pre-synaptic receptors (in the context of neuron-neuron neurotransmission in the synaptic cleft) are located on, in or near the pre-synaptic axon nerve terminals and serve as sensors of the amount of neurotransmitters in the synaptic cleft. High levels of neurotransmitters in the synaptic cleft will activate the inhibitory pre-synaptic receptors, inhibiting further neurotransmitter release. In contrast, low levels of neurotransmitters in the synaptic cleft will activate the facilitatory pre-synaptic receptors, enhancing neurotransmitter release. Thus, pre-synaptic receptors play a role in maintaining homeostasis in neuronal transmission by fine-tuning of neurotransmitter release from the pre-synaptic nerve terminals (Miller, 1998; Nishanthi & Vimal 2017). Depending on the location and the neurotransmitter that is modulated by these receptors, there are two types of pre-synaptic receptors. Autoreceptors are pre-synaptic nerve terminal receptors that, when activated, elicit or inhibit the release of their own neurotransmitters. They modulate their own neurotransmission by

mediating negative or positive feedback loops, and this is termed homotropic interaction. The activation of adrenergic α2 autoreceptors on the pre-synaptic nerve terminal of adrenergic neurons, for example, inhibits NA release (Nishanthi & Vimal 2017). On the contrary, heteroreceptors are those receptors located on the pre-synaptic nerve terminals, which, on activation by transmitters released from other neurons in the vicinity, elicit or inhibit the release of neurotransmitters from the nerve terminals on which they are situated. These heteroreceptors are not activated by the neurotransmitters released from the nerve terminals on which they are placed. For example, activation of adrenergic α2 heteroreceptors placed on the pre-synaptic nerve terminals of cholinergic neurons inhibits the release of ACh from these nerve terminals, and this is called heterotropic interaction (Nishanthi & Vimal 2017). P2X receptors have been found on pre-synaptic nerve terminals, and their activation can modulate the release of neurotransmitters. Moreover, ATP has been demonstrated to be present at the synapse under investigation and to be released as a cotransmitter when stimulated. The remaining P2X receptor criteria have yet to be fulfilled (MacDermott et al, 1999). In our project, we investigated the expression of P2 receptors which could be present on pre-junctional nerve terminals (in the context of neurotransmission between sympathetic nerve and effectors, e.g., blood vessel). It is postulated that there are many more pre-junctional receptors yet to be uncovered, and their physiological roles have yet to be identified and utilized as targets for drug discovery. By providing a fine-tuning mechanism these receptors also offer attractive sites for pharmacotherapy in cardiovascular diseases.

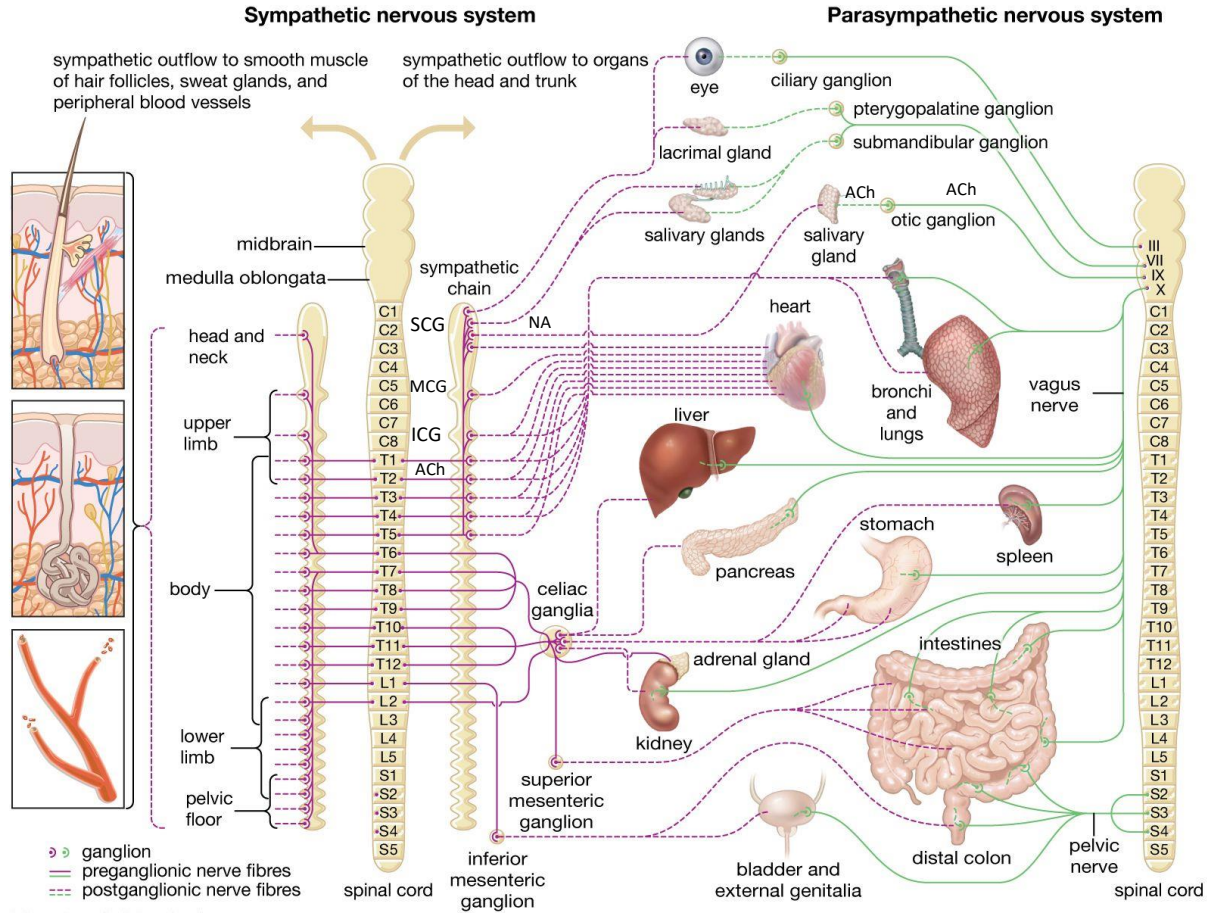

Figure1.7: Organisation of the sympathetic and parasympathetic nervous system. The autonomic nervous system includes two antagonistic groups of nerves, the sympathetic and parasympathetic nervous systems. The sympathetic nervous system uses spinal nerves to link the brain via pre-ganglionic efferent axons and the internal organs via post-ganglionic efferent axons. When stimulated, these nerves release neurotransmitters such as NA ans ACh preparing the organism for stress by increasing the heart rate, increasing blood flow to the muscles, and decreasing blood flow to the skin. The parasympathetic nerve fibres are the cranial nerves, primarily the vagus nerve, and the lumbar spinal nerves, once they are stimulated, these nerves increase digestive secretions and reduce the heartbeat. SCG, Superior cervical ganglion; MCG, Middle cervical ganglion; ICG, Interior cervical ganglion (stellate ganglion). Adapted from (Britannica, 2022).

1.6.1.1 Sympathetic nerves in the regulation of vascular tone

The sympathetic nerves are mostly adrenergic and originate from the thoracolumbar segments of the spinal cord, where they project to a variety of target organs, including smooth muscle. The pre-ganglionic neurons release ACh which acts at nicotinic receptors present on post-ganglionic neurons. The post-ganglionic neurons are placed at the adventitial layer, where activation of the nerves leads to neurotransmitter release from vesicles within the nerve varicosities (Kawasaki et al., 1988) (Figure 1.7). Perivascular sympathetic nerves are involved in the innervation of most blood vessels and immunolabelling techniques for tyrosine hydroxylase (TH) or NPY have been used to identify their reaction and thus their presence. These nerves innervate small and medium arteries, whereas the innervation is lower in large arteries (Sheng & Zhu, 2018; Ralevic and Dunn, 2015). Elements of the vascular system, including major arteries and arterioles are innervated via sympathetic nerves, however, other blood vessels such as collecting veins, venules and capillaries are infrequently innervated (Sheng & Zhu, 2018; Ruffolo et al., 1991). Sympathetic nerves which innervate blood vessels arise from the autonomic ganglion via post-ganglionic axon, with their cell bodies placed in the ganglia (McLachlan, 2003) (Figure 1.7). The perivascular sympathetic nerves allow organisms to respond in a suitable approach to destabilisations in either internal or external circumstances (Sheng & Zhu, 2018). The regulation of the sympathetic nervous system is an important factor in the control of vascular tone and blood pressure and plays a critical function in vascular homeostasis. Several elements can promote the activation of sympathetic nerves such as shear stress, haemorrhage, hypertension, trauma and pain that induce vascular resistance (Sheng & Zhu, 2018). The primary activation of sympathetic nerves is to regulate the vascular tone as the blockage of sympathetic ganglion was shown to cause a decrease in blood pressure (King et al., 2007). In addition, defected sympathetic nerve stimulation results in vasoconstriction and a fall in blood flow via α-adrenoreceptors (Navar, 2014; Sheng & Zhu, 2018). Clinical studies and experimental methods demonstrated that renal sympathetic nerves play a significant role in the intricate pathogenesis of hypertension. In addition, perivascular sympathetic nerves are associated with several physiological and pathological processes such as oxidative stress, leukocyte activation, inflammation and increased chemokines and cytokines activity (Navar, 2014; Sheng & Zhu, 2018).

ATP

The level of ATP and NA release as functional cotransmitters from sympathetic nerves could be affected by various factors including the type of species, age, blood vessel tone and size, stimulation time (the condition of the experiment) and diseases (Pakdeechote et al., 2007; Ralevic, 2009). The following mechanisms could allow ATP to enter the extracellular space: (1) vesicular exocytosis, (2) release through channels and membrane pores, (3) cytolytic release, and (4) carrier-mediated release. Vesicular exocytosis is one of the main mechanisms for neurotransmitters and neuromodulators to enter the extracellular space, and it is thought to be an extracellular Ca^{2+} -dependent process. Indeed, ATP is taken up and stored in synaptic vesicles of nerve terminals (Sperlagh et al., 2007). ATP acts at post-junctional P2X receptors (mostly P2X1) and this leads to activate L-type voltage-dependent Ca^{2+} channels. This process includes rapid responses involving Ca^{2+} entry directly through the P2X cation channels, membrane depolarisation (excitatory junction potentials), and Ca^{2+} influx through voltage-activated Ca^{2+}channels causing smooth muscle vasoconstriction (Sheng & Zhu, 2018; Ralevic and Dunn, 2015). Electrophysiology studies showed that electrical stimulation of perivascular nerves promotes excitatory junction potentials and slow membrane depolarisation of smooth muscle cells, however, these effects were eliminated by tetrodotoxin (TTX; Na^{+} channel blocker and blocker of nerve action potential) and guanethidine (sympathetic nerve blocker) showing that sympathetic nerves are implicated in vasocontractile responses (Ralevic, 2009). Immunoreactivity studies presented that P2X1 expression is higher in medium and small arteries than in large arteries which associates positively with the density of different sizes of blood vessels innervation (Ralevic & Dunn, 2015; Lewis & Evans, 2001). Generally, it was shown in human saphenous and renal veins, and rabbit saphenous veins that contractile P2X receptors are expressed in arteries and veins, however other studies demonstrated that P2Y receptors can be more essential than P2X1 receptors in veins. That was supported by studies in the guinea pig portal vein which suggested that the sympathetic neurogenic contraction is facilitated in part via NA and in another part by UTP (but not ATP) involving P2Y receptors (Ralevic & Dunn, 2015). The abundance of P2 receptor expression, the robust release of ATP in almost all parts of the central nervous system and peripheral nervous system suggesting that ATP plays an important role as a neuromodulator rather than a traditional transmitter (Sperlágh et al., 2007). Furthermore, ATP could be acting on pre-junctional P2 receptors as a neuromodulator. ATP can modulate neurotransmitter release by inhibiting pre-junctional A1 adenosine receptors when degraded to adenosine via ectonucleotidases (Ralevic, 2009; Ralevic & Dunn, 2015; Ralevic, 2009) **(**Figure 1.8**)**. Moreover, it has been reported that ATP induces the release of NA in an entirely Ca^{2+}-dependent manner in rat superior cervical ganglion. This

ATP-induced Ca^{2+} release was ~ 50% lower when either Ca^{2+} or Na^{+} channels were inhibited, suggesting that ATP receptors themselves, such as P2X receptors, mediated Ca^{2+}- dependent transmitter release (Boehm, 1999). Furthermore, a study in an axonal preparation obtained from ganglia removed from explant culture, showed that ATP elicited intraaxonal Ca^{2+} led to an increase in NA release. These responses were not changed when Ca^{2+} channels were blocked by cadmium (II) ion (Cd^{2+}), indicating that ATP receptors are present at pre-junctional sites and directly mediate transmembrane Ca^{2+} entry (Boehm, 1999). Although it has been recognized that ATP and NA are stored in the same sympathetic vesicles, this does not indicate that the elements have mutual functional roles. Other studies showed that there are independent vesicular stores of ATP and NA in perivascular nerves (Ralevic & Dunn, 2015). ATP mediates the initial transient phase of vasoconstriction, whilst NA mediates the secondary slowly and more sustained phase. ATP released from sympathetic nerves is quantified by using radiolabelled purines, and more lately by ATP biosensors (Ralevic & Dunn, 2015). Other studies showed that these neurotransmitters have vasomotor roles on various post-junctional receptors which may be suppressed using selective antagonists. α,β-meATP, which is a compound commonly used in studies of ATP cotransmission (selective P2 receptor desensitiser), is a stable analogue of ATP and acts as a selective agonist at both P2X1 and P2X3 receptors (Ralevic, 2009). Desensitisation is a loss of receptor responsiveness caused by the constant presence of agonist. Ionotropic receptor desensitisation includes structural and functional changes in membrane residing receptors. The rate of desensitisation and recovery varies greatly within the P2X receptor family (Giniatullin & Nistri, 2013). Following sympathetic nerve stimulation, excitatory junction potentials appeared and vasoconstriction is partially blocked by α,β-meATP and the P2 receptor antagonist (suramin), whereas the remaining effects might be blocked via α-adrenoceptor antagonists (such as prazosin). This result suggested the involvement of ATP and NA via both P2X1 receptors and α-adrenoceptor respectively (Ralevic, 2009; Burnstock, 2017; Burnstock & Warland, 1987). The release of ATP as a sympathetic neurotransmitter is predominant during short stimulation of perivascular nerves (during stress), while prolonged stimulation (during activities) induces NA release as a result of the contribution of diverse sympathetic vesicles colonies including different levels of NA and ATP (Ralevic, 2009; Burnstock, 2017). A previous study in rat mesenteric arteries reported that ATP release was increased as a result of neurally triggered contractions when vessels diameters decrease (Gitterman & Evans, 2000), Other studies considered ATP as the only factor of the contractile responses in jejunal branches of the rabbit mesenteric artery and guinea pig submucosal arterioles, with the contribution of NA being to act as a pre-junctional

neuromodulator via α_2- adrenoceptors, resulting in decreased neurotransmitters release (Ralevic, 2009) **(**Figure 1.8**)**.

The relationship between arterial tone and the levels of ATP and NA coreleased from sympathetic nerves has become clearer. It was shown that during an increase in blood pressure to physiological values (from 30 mmHg to 90 mmHg), there was a rise in ATP levels as a prevalent functional transmitter (Ralevic, 2009; Rummery et al., 2007). Conversely, during decreased vessel tone in rat mesenteric arteries, it was noticed that the neurotransmitters release from sympathetic nerves were missing (Pakdeechote et al., 2007). This evidence helped to expand our understanding of functional purinergic neurotransmitters *in vivo* in both normal conditions and in cases of hypertension. It has been shown that there are pre-junctional neurotransmitters, such as adenosine, angiotensin II and CGRP, which can mediate ATP and NA release (Ralevic, 2009). Furthermore, vasoconstriction can be induced as a result of the activation of P2X1 receptors via ATP and the activation of adenosine receptors via NA in a manner termed post-junctional synergism (Ralevic, 2009; Ralevic & Burnstock,1990). The vascular endothelial cells can respond to sympathetic neurotransmitters released directly or indirectly. Previous studies have reported that in large and small hamster mesenteric arteries and as a result of nerve stimulation, excitatory junction potentials were mediated via P2X receptors (Ralevic & Dunn, 2015). Moreover, exogenous ATP induced-hyperpolarisation was eliminated following endothelium deletion by P2Y antagonism (Westcott and Segal, 2013). Other data indicated that ATP release from perivascular nerves stimulated endothelial P2Y2-like receptors in the small (but not large) mesenteric arteries and that leads to stimulating EDHF release (Westcott & Segal, 2013). These results could indicate the communication between the endothelial cells and perivascular nerves including purine and endothelial P2Y receptors.

NA

NA is released mainly from sympathetic nerve terminals and binds to adrenergic receptors, including α1, α2, β1, and β2 adrenoceptors, leading to vasoconstriction and increased blood pressure (Schuller, 2007; Guyenet, 2006). Activation of smooth muscle α1-adrenergic receptors induces the contraction of smooth muscle cells by increasing intracellular Ca^{2+} levels while stimulation of smooth muscle α2-adrenergic receptors contributes to vasorelaxation via NO release (Guimarães, & Moura, 2001). In addition, the α2-adrenergic receptor-induced endothelial-dependent relaxation can abolish the α1-adrenergic receptor-induced vasoconstriction on smooth muscle cells (Sheng & Zhu, 2018). Previous studies reported that despite β-adrenergic receptors have little effect on the vascular resistance, these receptors have a vital role in regulating the cardiac output and heart rate, e.g., stimulation of the adrenergic

nerve fibres can decrease the cardiac functions with the defective β1- and β2-adrenergic receptors in animal models (Sheng & Zhu, 2018). However, other studies showed that activation of β-adrenergic receptors on smooth muscle cells results in vasorelaxant effects via activating adenylate cyclase and increases the cAMP level (Guimarães, & Moura, 2001).

NPY

NPY is predominantly distributed in the central nervous system and the perivascular nervous system, colocalised and coreleased from sympathetic varicosities with NA and ATP mediating cardiovascular system innervation, but acts mostly as a neuromodulator, enhancing post-junctional effects and acting pre-junctionally to decrease sympathetic neurotransmitters release (Ralevic, 2009; Ralevic & Dunn, 2015: Lundberg, 1996) (Figure 1.8). In the cerebral vasculature, the innervation of blood vessels by NPY leads to smooth muscle cells constriction, while NA promoted potently vasoconstriction in rabbit blood vessels (Sheng & Zhu, 2018). Moreover, NPY release contributes to endothelial cells constriction and smooth muscle cells proliferation (Taylor et al., 2007). It has been reported that NPY has a vital role in raising leukocyte adhesion to endothelial cells and NPY antagonist has been reported to have anti-inflammatory influences on acute and chronic arthritis (Claxson et al., 1990; Sung et al., 1991).

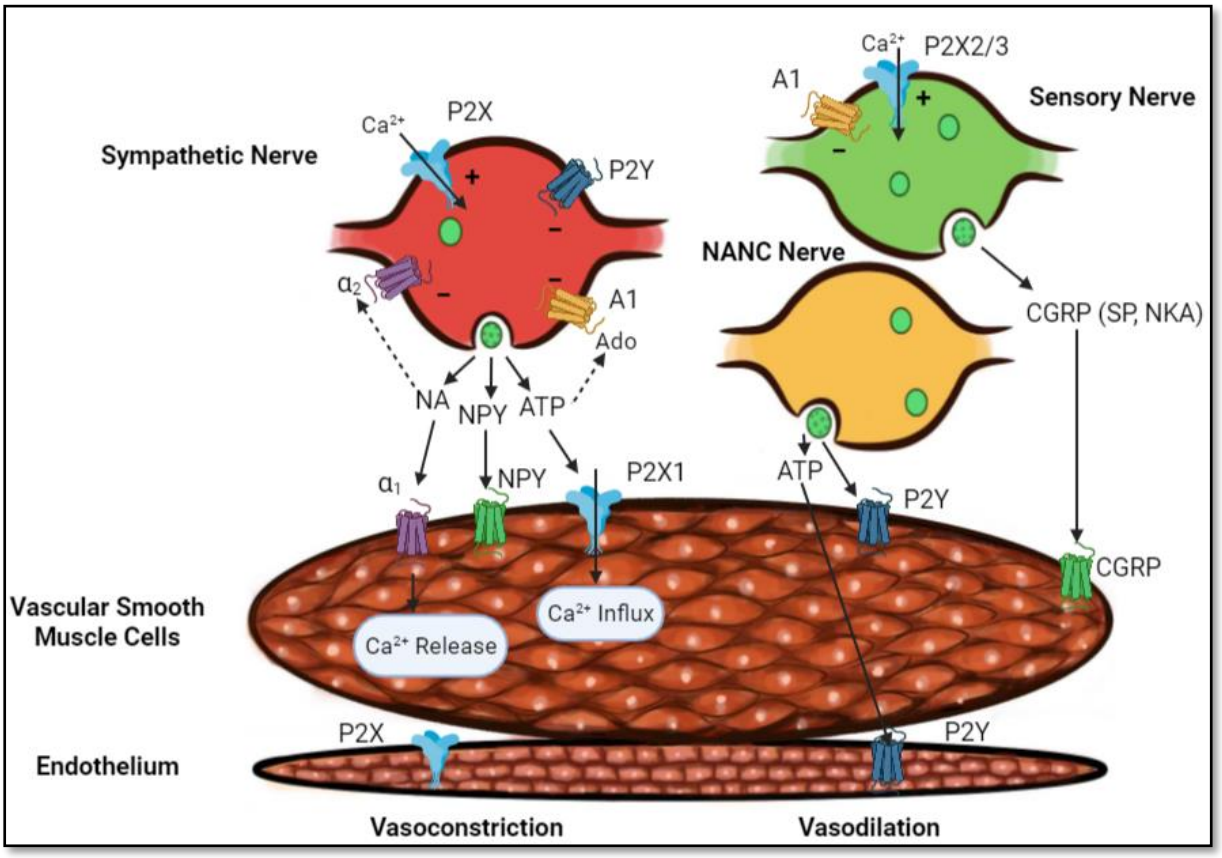

Figure 1.8: **The roles of the perivascular nervous system**. Purines (nucleotides) are stored in varicosities and released as neurotransmitters and neuromodulators from sympathetic nerves, nonadrenergic non-cholinergic nerves and sensory nerves. ATP is coreleased with NA and NPY from sympathetic nerves and binds to P2X1 receptors on smooth muscle inducing Ca^{2+} influx and vasoconstriction. Neurotransmitters release can be modulated by facilitatory P2X receptors or inhibitory P2Y receptors at sympathetic nerves and by facilitatory P2X and inhibitory A1 adenosine receptors at sensory nerves. Adenosine, which results from ATP degradation, can prevent the release of sympathetic neurotransmitters by pre-junctional adenosine A1 receptors. In addition, sympathetic neurotransmitters release can be inhibited via NA, by 2-adrenoceptors, and NPY, by Y2 receptors (not shown). ATP is released from nonadrenergic non-cholinergic nerves causing vasodilation by P2Y receptors on the smooth muscle or endothelium. NA, noradrenaline; ATP, adenosine triphosphate; Ach, acetylcholine; CGRP, calcitonin gene-related peptide; NPY, neuropeptide Y; NO, nitric oxide; NANC, nonadrenergic non-cholinergic nerves. Adapted from (Ralevic, 2009; Sheng & Zhu, 2018).

1.6.1.2 Parasympathetic nerves

As mentioned above, the autonomic nervous system has two main divisions including sympathetic nerves and parasympathetic nerves, parasympathetic nerves release ACh, and vasoactive intestinal peptide (used as a marker for parasympathetic nerves) and NO as neurotransmitters. Parasympathetic nerves originated in the central nervous system with most cell bodies placed in the ganglia (Hamel, 2006). The presence and functional effects of parasympathetic nerves are poorly-known relative to those of sympathetic or sensory nerves because of the difficulties in performing immunological experiments on parasympathetic innervation (Hill et al., 2001; Miao & Lee, 1990). Numerous tissues are innervated by parasympathetic nerves which play a significant role in different physiological and pathological processes, e.g., gastrointestinal peristalsis and digestion, inflammation, heart rate and immune responses (Sheng & Zhu, 2018). Most blood vessels apart from those in salivary glands and some cerebral blood vessels are not innervated via parasympathetic nerves (Ralevic, 2009; Ralevic & Dunn, 2015; Burnstock, 2017). The release of ATP from parasympathetic nerves has not been demonstrated yet. It has been reported that the stimulation of parasympathetic nerves in the brain induces vasorelaxation and raises cerebral blood flow. However, the functional roles of parasympathetic nerves in other vessels are not clear (Westcott & Segal, 2013). The Vagus nerve is the main parasympathetic nerve of the autonomic nervous system and expands throughout the body. It arises from the medulla oblongata of the brainstem and exits the cranium through the jugular foramen. The bilateral vagus nerves, which are accompanied by carotid arteries, have numerous branches in the neck, chest and abdomen, and respectively connect to the pharyngeal plexus, cardiac plexus, pulmonary plexus, oesophagal plexus, hepatic plexus, and abdominal plexus to control the functions of organs. The right and left vagal nerves are involved in regulating the heart rate by innervating the sinoatrial node and the atrioventricular node, respectively (Sheng & Zhu, 2018; Puledda & Goadsby, 2016). Vagus nerves include sensory afferent neurons and motor efferent neurons. The afferent nerves represent 70-80% of vagus nerve fibres and deliver a signal of tissue status to the brain while the efferent neurons integrate information sent to the central nervous system and regulate the peripheral effectors. Furthermore, the vagus nerves can also regulate the immune, endocrine, respiratory and cardiovascular systems and play an important role in inflammation, hemorrhagic, ischemia, shock, sepsis, epilepsy, and migraine (Sheng & Zhu, 2018; Tracey, 2007).

ACh

ACh is the first detected neurotransmitter released from perivascular nerves and promotes the contraction of smooth muscle cells. ACh acts on the acetylcholine receptors which are divided into two families. The nicotinic acetylcholine receptors include five subtypes: α (including ten subunits α1- α10), β (including four subunits β1-β4), γ, δ and ε. Five subunits are required to form each nicotinic acetylcholine receptor, while α7-α9 contributes to form functional nicotinic acetylcholine receptors as homooligomers (Sheng & Zhu, 2018). The muscarinic acetylcholine receptors consist of five related G protein-coupled receptors (M1 to M5): M1, M3 and M5 are coupled to the $G_{\alpha q}$ family of G proteins, while M2 and M4 are coupled to the G proteins of the $G_{\alpha i}$ family. The muscarinic acetylcholine receptors have an important role in controlling several essential physiological functions including smooth muscle cell constriction and heart rate (Fredriksson et al., 2003). As I mentioned previously, the vagus nerve is the main parasympathetic nerve regulating the pro-inflammatory cytokines formation (via nicotinic acetylcholine receptors) and cholinergic anti-inflammatory pathways and the inflammatory effects (Pavlov & Tracey, 2012). The cholinergic nerve fibres are involved in the innervation of various tissues including the endothelium and smooth muscle cells of blood vessels. It has been reported that the endothelial M3 receptors regulate arterial NO release which leads to relaxant responses. Adversely, the stimulation of M2 and M3 receptors via ACh in smooth muscle cells prevents the NO release leading to vasoconstriction (Bolton & Lim, 1991).

1.6.2 Sensory-Motor Nerves

The second part of the peripheral nervous system is the sensory (trigeminal) nervous system; these nerves release neurotransmitters, such as CGRP, SP and neurokinin-A from their peripheral endings causing efferent/motor responses which can innervate blood vessels (Ralevic, 2009). CGRP and SP can evoke vasorelaxation to contribute to vascular tone regulation. As a result, sensory-motor nerves introduce a neurogenic counterpart for vasocontractile sympathetic nerves (Ralevic & Dunn, 2015). The presence of sensory nerves has been widely described in various vascular beds in many animal species and humans (Hodges et al., 2009). Sensory-motor nerves innervate several blood vessels including unmyelinated C-fibre and myelinated Aδ-fibre primary afferents which have a double motor (or efferent) and sensory (or afferent) role (Burnstock, 2017). Sensory-motor nerves transfer information about environmental changes to the central nervous system, which induces autonomic evasion or compensatory reactions (Ralevic & Dunn, 2015). Several physiological

processes are mediated by neurotransmitters which are released from the sensory-motor nerves. Actions induced from this include contraction of smooth muscle and heart muscle, regulation of tissue growth and immune responses (Ralevic, 2009). Furthermore, it has been reported that in rabbit ear arteries, sensory-motor nerves can release ATP following antidromic induction which leads to vasorelaxation (Ralevic, 2009; Westcott & Segal, 2013; Burnstock, 2017). In rabbit small mesenteric arteries, neurogenic dilation was suppressed by capsaicin proposing the contribution of sensory nerves and was suggested to include the endothelial cells and ATP, which may be released from the sensory nerves, even though the study was not excluded other possible ATP sources such as the endothelial cells (Ralevic & Dunn, 2015).

CGRP

The main sensory-motor neurotransmitter is CGRP, while SP and ATP are released as cotransmitters. CGRP is synthesized in both central and peripheral sensory neurons, transported along axons and stored in vesicles with SP and ATP (Westcott & Segal, 2013). It has been shown that CGRP exists in perivascular nerves of human coronary arteries and veins and acts as an uncommon receptor mediating vasorelaxation (Opgaard et al., 1995). Following CGRP release, it binds to its G protein-coupled receptors CGRP1 and CGRP2 to mediate the vasorelaxant responses by hyperpolarisation of smooth muscle cells. CGRP1 receptors are mostly distributed in the cardiovascular system and have their selective antagonist, whereas the CGRP2 has a deficiency of selectivity for their ligands and further studies are required to understand more about their receptors and their ligands (Brain & Grant., 2004). Three elements are implicated for a functional CGRP receptor: a single membrane-spanning receptor activity modifying protein (RAMP1), calcitonin receptor-like receptor (CRLR) protein and other receptor component protein. It has been reported that the endothelial cells expressed the CRLR, RAMP1 protein components and the functional CGRP receptors. Furthermore, in rat mesenteric resistance arteries, perivascular release CGRP which acts on its endothelial CGRP1 receptors mediating vasodilatory responses (Sheng & Zhu, 2018; Hagner et al., 2001). Other studies showed that in pulmonary arteries, internal mammary arteries and thoracic aorta, CGRP stimulate vasodilation mediated by NO release, an endothelium-derived relaxing factor and a cAMP-dependent manner (Sheng & Zhu, 2018). However, other studies showed that CGRP does not have a significant role in the controlling of blood pressure in physiological conditions, while CGRP levels are changed in vascular disorders, such as Raynaud's disease and migraine (Brain & Grant., 2004).

SP

SP is a neurokinin which is synthesized in dorsal root ganglia, transported along axons and located in vesicles within sensory nerve terminals (White al., 1985). Following the release of SP, it binds to post-junctional G-protein coupled tachykinin (NK) receptors placed on endothelial cells to apply its effects, including an increase in Ca^{2+} to activate endothelial nitric oxide synthase (eNOS), increases vascular permeability, NO-dependent vasorelaxation and vasomotor control until it is broken down enzymatically (Brain & Grant, 2004; White al., 1985; Westcott & Segal, 2013). Nevertheless, the physiological function of SP in vascular resistance is controversial.

1.6.3 Non-adrenergic non-cholinergic nerves

Studies showed that ATP is a neurotransmitter released from non-adrenergic non-cholinergic nerves, and it contributes to neurogenic vasodilation in chicken anterior mesenteric arteries, guinea pig pulmonary artery and lamb small coronary arteries. In lamb small coronary arteries and guinea pig pulmonary arteries, ATP acts at P2Y receptors mediating vasorelaxant responses independently of the endothelium. While in chicken anterior mesenteric arteries, ATP released from perivascular neurons acts on endothelial P2Y1 receptors that lead to EDHF release resulting in circular smooth muscle hyperpolarisation (Ralevic, 2009). Moreover, it has been determined in the rabbit portal vein that ATP is a cotransmitter with NO released from non-adrenergic non-cholinergic nerves and this corelease causes vasorelaxation. This result was confirmed by a P2 receptor antagonist, suramin, and a NO synthase inhibitor which led to reduced non-adrenergic non-cholinergic neurogenic relaxant responses in the rabbit portal vein (Ralevic & Dunn, 2015; Brizzolara et al., 1993; Ralevic, 2009). It has been reported that the removal of endothelial cells did not affect neurogenic responses, and reduced responses to ATP and that indicates to vasodilation effects by P2Y receptors could be present on the smooth muscle cells (Ralevic & Dunn, 2015).

1.7 Non-neuronal sources of purines

Purines and pyrimidines are not only released from perivascular nerves but there are also other sources of purines which are related to purinergic receptor expression on blood vessels, mostly the endothelium, smooth muscle, erythrocytes, platelets and other non-neuronal cells (Emerson & Segal, 2000) (Figure 1.9). The physiological mechanisms of purine release play an important role in blood vessel tone (Ralevic, 2009). The most important source of nucleotides is the endothelium which can release ATP and UTP during stress conditions and

hypoxia (Milner et al., 1990; Bodin et al., 1992). The acting of ATP and UTP at endothelial P2 receptors play a role in the induction of vasorelaxant responses, mostly by NO and EDHF, which increases oxygen transport to the tissue (Buxton et al.,2001; Yang et al., 1994). Another source of purines is smooth muscle cells which can release ATP after the action of NA at post-junctional adrenoceptors (Sedaa et al., 1990). Moreover, in smooth muscle cells, ATP itself can release ATP via P2X receptor activation (Von Kügelgen & Starke, 1991). Erythrocytes release ATP during hypoxia, stress and decreased PH. In addition, they are likely a source of ADP and adenosine following the breaking down of ATP (Sprague et al., 1996). Platelets are considered as a store of high levels of ATP, ADP and UTP, and thus these nucleotides are released from the platelets during pathophysiological processes such as aggregation (damage to the integrity of the endothelium) leading to activate P2 receptor on smooth muscle cells, resulting in vasoconstriction (Ralevic, 2009; Goetz et al., 1971).

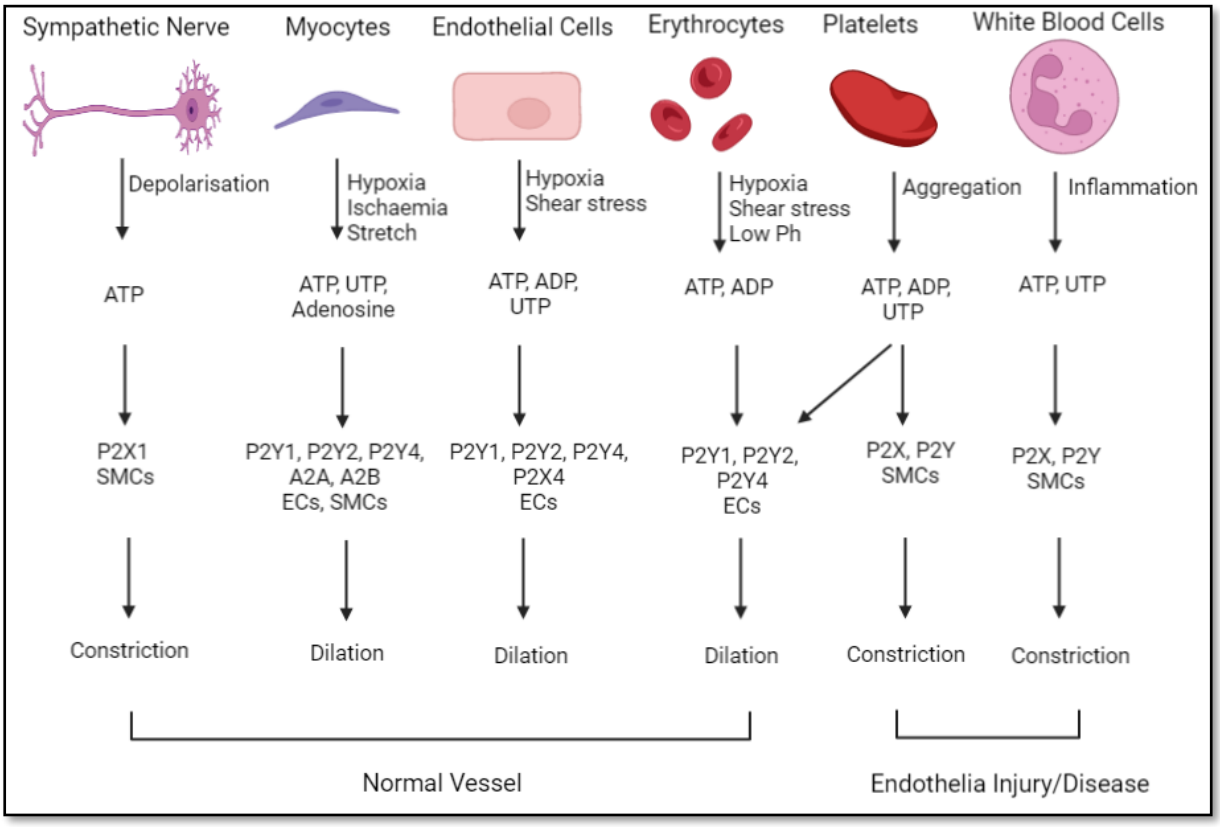

Figure 1.9: **Non-neuronal sources of purines**. In healthy blood vessels, ATP released from sympathetic nerves causes vasoconstriction. Purines and pyrimidines released from the endothelium, myocytes, and erythrocytes result in vasodilation. Nucleotides released from aggregating platelets lead to endothelium-dependent vasodilatation. However, in vascular diseases, white blood cells and platelets attach to dysfunctional endothelial cells or the underlying smooth muscle leading to nucleotides release which can help in a change in the balance of vasoconstriction. SMCs, Smooth muscle cells; ECs, Endothelial cells. Adapted from (Burnstock & Ralevic, 2014).

1.8 The roles of blood vessels in the autonomic nervous system

Endothelial cells are located in the internal layer of blood vessels and play a critical role in maintaining the structural and functional integrity of blood vessels. This includes regulation of the arterial tone and blood pressure and modulating the effects of the perivascular nervous system on vascular tone by vasoactive effectors (Sheng & Zhu, 2018). These factors such as NO which is an endothelium-derived relaxing factor that arises from L-arginine via endothelial NO synthase, based on cofactors such as tetrahydrobiopterin (Forstermann & Munzel, 2006). In addition, endothelin is released from the endothelium, resulting in mammalian vasculature contractile responses (Davenport et al., 2016). Dysfunctional endothelial cells are associated with diseases and processes such as the progression of atherogenesis and the autonomic nervous system activity via modulating the release of neurotransmitter, reuptake, or receptor sensitivity (Neunteufl et al., 1997; Sheng & Zhu, 2018). In healthy conditions, the autonomic nervous system and the endothelium work collectively to control arterial tone and blood pressure. Various factors are released from endothelial cells mediating constriction and vasodilation, altering autonomic nervous system activity and modulating end organ vessel responses. A previous study indicated that vasoconstrictive effects caused by α2-adrenergic nerves were abrogated via NO released from the endothelial cells (Sheng & Zhu, 2018). It has been reported that vasoconstriction induced via neurogenic NA is suppressed by the endothelium in the presence of shear stress in rabbit carotid arteries. However, this suppression is reduced by a guanylate cyclase inhibitor. That indicated that NO could inhibit both the central the peripheral cardiac system including vascular sympathetic activity (Sheng & Zhu, 2018). Furthermore, autonomic nervous responses could also be affected by endothelial contraction factors such as endothelin which can induce the smooth muscle cells sensitivity to NA leading to vasoconstriction and high blood pressure (Sheng & Zhu, 2018). Dysfunctional endothelium leads to several pathological conditions in the autonomic nervous system. It has been reported that the dysfunctional endothelium is implicated in decreasing sympathetic activity (e.g, regulates involuntary physiologic processes including heart rate, blood pressure) and the reuptake of NA into the sympathetic nerves to counteract the vasoconstriction factors in rabbit aorta (Sobey et al., 1994). A clinical study showed that the high level of plasma von Willebrand Factor (vWF), reflecting the damage of endothelial cells, can indicate a decrease in autonomic activity. Moreover, studies in young diabetic patients reported that defective endothelial cells could be implicated in peripheral neuropathy (Plater et al., 1996). Furthermore, endothelial dysfunction is involved in inflammation as a result of altering in neurotransmitters release from the autonomic nervous system (Conti et al., 2014).

1.9 Control of vascular tone by perivascular nerves, smooth muscle cells and endothelial cells

For many decades, the control of vascular tone was attributed to antagonistic sympathetic noradrenergic constrictor nerves and parasympathetic cholinergic dilator nerves. However, recently it has been clear that there are other factors can control and modulate vascular tone including neurotransmitters released from perivascular nerves and endothelial cells (Burnstock & Ralevic, 2014). ATP released from sympathetic nerves mediates vasocontractile responses by P2X1 receptors. It has been reported using the expression of mRNA, antibody detection and other functional studies that both P2X and P2Y receptors are expressed on vascular smooth muscle cells which control vascular tone. It was confirmed in mesenteric arteries of P2X1- defective mice that the P2X1 receptor contributes to vasoconstriction following ATP release (Vial & Evans, 2002). Both P2X and P2Y receptors are expressed on vascular endothelial cells which are considered as a source of purines. The main function of endothelial cells is their role in vasorelaxation to counterbalance vasoconstriction mediated via ATP coreleased with NA from perivascular sympathetic nerves (Burnstock & Ralevic, 2014). Moreover, nucleotides and nucleosides released from myocytes and blood cells act at P2 receptors on the endothelium. The predominant purine receptors expressed on animal and human endothelial cells are A2A and A2B adenosine receptors and P2Y1, P2Y2, and P2X4 nucleotide receptors (Burnstock & Ralevic, 2014). NO, EDHF and prostacyclin (PGI2) are released from the endothelium following the activation via purines resulting in vasodilation (Kelm et al., 1991). Activated platelets and endothelial cells release ATP, ADP and UTP. In the healthy endothelium of blood vessels, platelet aggregation is inhibited causing these nucleotides to act at endothelial P2Y receptors to release NO and EDHF, promoting vasorelaxation. However, in the case of dysfunctional endothelium or damage, platelet aggregation and accumulation of leukocytes can happen, leading to these elements bind to vascular smooth muscle P2 receptors causing vasoconstriction and smooth muscle proliferation (Burnstock & Ralevic, 2014) (Figure 1.10).

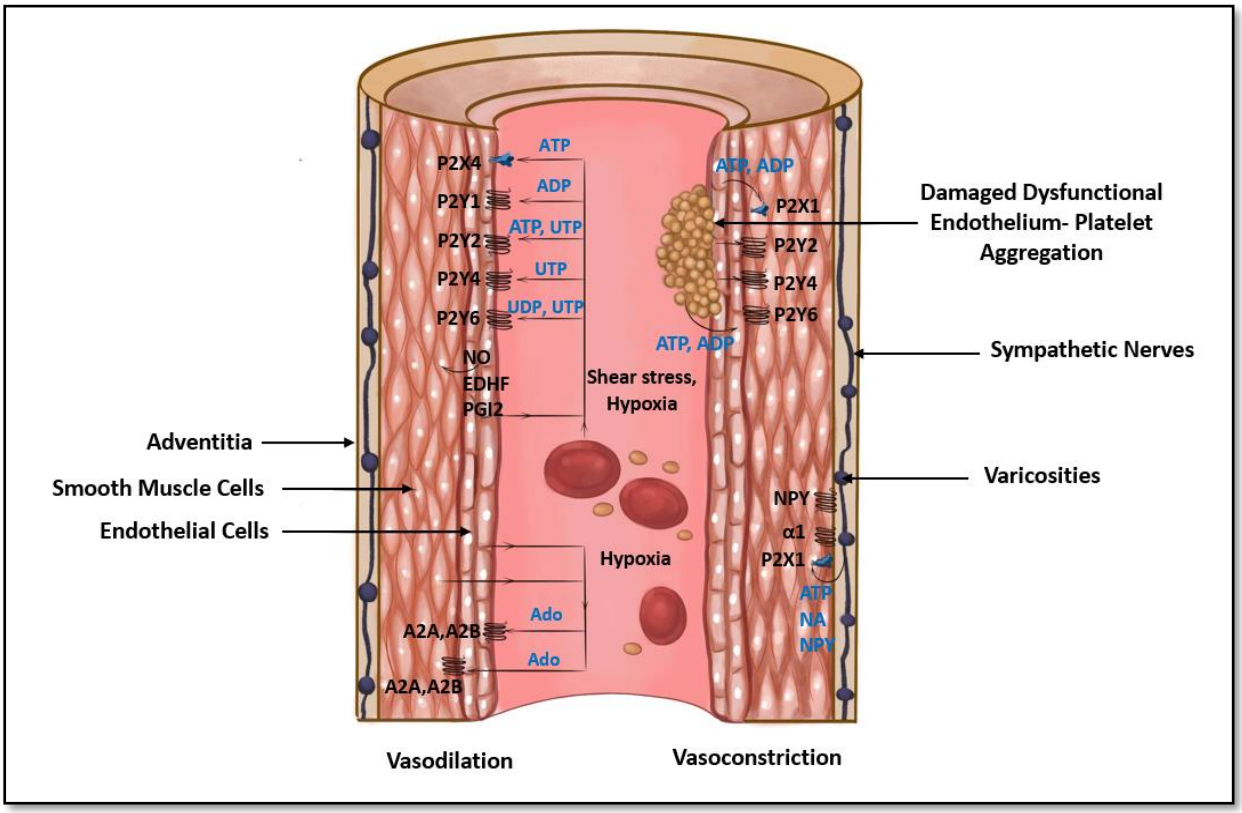

Figure 1.10: Cross-section of a blood vessel showing local purinergic control mechanisms. Left wall of blood vessel: purinergic vasorelaxant responses mainly involve the endothelium and the release of endothelium-derived relaxant factors including NO, EDHF, and PGI2, all of which suppress platelet aggregation. Smooth muscle and endothelium both have A2A and A2B receptors that act as vasorelaxants. The endothelium and erythrocytes are physiological sources of adenosine and nucleotides, while shear stress and hypoxia are known stimulants. Right wall of blood vessel: smooth muscle P2Y and P2X1 receptors are involved in purinergic vasoconstriction. When the endothelium is damaged/dysfunctional, platelets aggregate at the site of injury and produce ADP and ATP, which may elicit vasoconstriction via P2Y and P2X1 receptors expressed on the underlying vascular smooth muscle, emphasises the relevance of the endothelium. Perivascular sympathetic neurons in the adventitia produce ATP as a cotransmitter with NA and NPY to induce vasoconstriction via smooth muscle P2X1 receptors. NA's vasocontractile effects are mediated primarily through smooth muscle α1-adrenoceptors, although NPY also exerts post-junctional effects in some arteries via smooth muscle NPY receptors. Adapting from (Ralevic & Dunn, 2015).

1.10 Pre-junctional modulation of perivascular neurotransmission by purines - purines as pre-junctional neuromodulators

When nerves are electrically stimulated, NA and ATP are released from the nerve terminals, where they can act on receptors on the nerve terminal or on smooth muscle cells located pre-junctionally or post-junctionally (Brock and Cunnane, 1999). The activation of pre-junctional α2-adrenergic receptors has also been shown to inhibit further neurotransmitter release from the nerve terminals (Brock and Cunnane, 1999). Pre-junctional neurotransmitters released from perivascular nerves (autonomic and sensory) can be modulated by several factors. For instance, adenosine acts on pre-junctional A1 receptors of perivascular nerves and leads to inhibit the release of neurotransmitters. Upon activation of pre-junctional A1 adenosine receptors on sympathetic nerves by adenosine, the release of pre-junctional neurotransmitters could be reduced (Ralevic & Dunn, 2015). Contrastingly, in some blood vessels "such as the renal vasculature", A1 receptors are not expressed on the sympathetic nerves while expressed on smooth muscle cells mediating contractile responses (Jackson et al., 2012). Moreover, it has been shown in the rat mesenteric arterial bed that sensory-motor nerves express pre-junctional A1 adenosine receptors which can cause inhibition of the neurogenic vasorelaxant responses when activated (Rubino et al., 1993). Furthermore, the activation of pre-junctional receptors for NA (α2-adrenoceptors) and NPY present on sympathetic nerves leads to the inhibition of neurotransmitter release (Ralevic & Dunn, 2015). Pre-junctional nerve terminals are equipped with a number of auto- and/or heteroreceptors, including ionotropic P2X and metabotropic P2Y receptors. P2 receptors could function as modulation sites of transmitter release by ATP and other nucleotides released via neuronal activity and pathological signals (Sperlagh et al., 2007). It has been shown that ATP can directly modulate (inhibit or promote) the release of neurotransmitters by several actions on the pre-junctional P2 receptors (facilitatory P2X receptors and inhibitory P2Y receptors). Interestingly, ATP released from sympathetic nerves can activate directly inhibitory P2 receptors (P2Y-like) in the rat tail artery and kidney; as a result, they might behave as autoreceptors to prevent the ATP release, and coreleased NA and NPY (Ralevic & Dunn, 2015; Sperlágh et al., 2007). However, it is still little is known about the role of P2 receptors located on pe-junctional terminal of perivascular nerves and more studies are required to know more about pre-junctional P2 purinergic receptors in modulating neurotransmitters in diverse blood vessels and different organisms related to the specific physiologic roles of the particular vessel.

P2X and P2Y receptor subunits are found throughout the nervous system and play a variety of roles, including quick synaptic transmission, long-term plasticity, and trophic

changes that are critical for development, neuron-glia connections, and neuroimmunomodulation. Moreover, ATP could modify pre-junctional and post-junctional transmission, both in a positive and negative route by P2X and P2Y receptors activation, respectively (Sperlágh et al., 2007). The pre-junctional nerve terminal is a vital regulatory region where the efficacy of synaptic transmission could be modulated. While pre-junctional ionotropic receptors could elicit synaptic transmission, pre-junctional metabotropic receptors convey negative feedback regulation of transmitter release. Interestingly, the activation of ligand-gated ion channels followed by a high level of permeability of intracellular Ca^{2+} can directly stimulate transmitter release triggered by the Ca^{2+} influx through the receptor-ion channel complex (McGehee & Role, 1996; Sperlágh et al., 2007). The activation of various isoforms of receptors introduces a fine-tuning mechanism by which different neurotransmitters and modulators can impact the activity of each other. Pre-junctional receptors that control transmitter release also offer attractive target sites for existing and future pharmacotherapy.

1.10.1 Facilitatory pre-junctional purinergic receptors

Neurons within sympathetic ganglia possess various types of ligand-gated ion channels, e.g., P2X receptors, as confirmed by several techniques including RT-PCR, immunocytochemistry, autoradiography, and functional studies such as electrophysiological recordings. Because P2X receptors have relatively high Ca^{2+} permeability, they can initiate neurotransmitter release via Ca^{2+} influx through the receptor-ion channel complex or facilitate Ca^{2+}-dependent neurotransmitter release, if they are located near the release sites. It was observed that ATP elicited the release of tritiated NA from rat superior cervical ganglion neurons in the cell culture. This ATP-induced release was mediated by action potential propagation from neuronal somata down to the axon terminals. This confirmed that axon terminals of post-ganglionic sympathetic neurons possess P2X auto- and/or heteroreceptors which elicit neurotransmitter release (Boehm & Kubista 2002). Several studies demonstrated that pre-junctional P2 receptors could play a role in modulating neurotransmitter release. It was reported that the activation of ionotropic P2X receptors in sympathetic nerve terminals directly triggers NA release induced by nerve stimulation via a direct Ca^{2+} influx through the receptor-ion channel complex (Boehm & Kubista, 2002). P2X1, P2X3, or P2X2/P2X3 receptors were identified as facilitatory P2X receptors involved in the modulation of NA outflow in the rat vas deferens (Queiroz et al., 2003). Electrophysiological studies in the chicken ciliary ganglion and mouse motor nerve terminals confirmed that the P2 receptor facilitated ACh release (Sun & Stanley, 1996; Hong & Chang, 1998). For example, P2X7 receptors are inserted into the

membrane of mouse motor neuron terminals, and their activation causes vesicular exocytosis (Moores et al., 2005). Other subunit compositions of P2X receptors have not been reported at the neuromuscular junction, and it is also unknown whether such facilitatory receptors exist on the terminals of central cholinergic neurons. ATP could play a role in an increase in NA release following perivascular nerve stimulation in rabbit ear arteries (Miyahara & Suzuki, 1987). In sensory ganglion neurons (such as dorsal root ganglion and trigeminal neurons), P2X2/3 heteromeric receptors and/or P2X3 homomeric receptors have been presented to be involved in depolarising currents responses and that lead to elicit the release of glutamate and peptide. However, ATP and its analogues did not induce peripheral terminals of capsaicin-sensitive sensory-motor nerves in rat mesenteric arteries (Ralevic, 2001). The role of pre-junctional P2 receptors on perivascular nerves in controlling neurotransmitters release is still unclear and requires further investigation.

1.10.2 Inhibitory pre-junctional purinergic receptors

In addition to facilitatory modulation, P2 purinergic receptors can also contribute in the inhibitory modulation of neurotransmitters release, and the metabotropic P2Y receptors are supposed to play a key role in these actions. Adenosine acts on pre-junctional A1 adenosine receptors which are functionally expressed on sympathetic nerves, and upon activation results in a decrease in ATP release, in addition to the cotransmitters NA and NPY. It was reported that soluble ectonucleotidases are released together with ATP and NA which suggested another level of control to this feedback mechanism (Ralevic, 2009; Todorov et al., 1997). The pre-junctional release of neurotransmitters from sympathetic nerves could be also inhibitory modulated by pre-junctional α2- adrenoceptors which are activated via NA and NPY (Ralevic, 2009). P2 receptors (P2Y-like) act as autoreceptors on post-ganglionic sympathetic nerves and activated via ATP to eliminate NA release, in addition to their role in feedback suppression of coreleased NPY and ATP (Ralevic, 2009; von Kügelgen et al., 1989). It was recently identified in the mouse neuromuscular junction that pre-junctional P2Y receptors are involved in the inhibition of spontaneous ACh release, suggesting that the activation of P2Y receptors is coupled to $G_{\alpha i}$ proteins and modulates pre-synaptic Ca^{2+} channels related to tonic secretion of ACh (De Lorenzo et al, 2006). More studies are required to investigate more about which subtypes of pre-junctional P2 receptors are involved in this mechanism (Figure 1.8).

1.11 Calcium signalling

As an intracellular second messenger, calcium ions (Ca^{2+}) play an important role in many aspects of cellular processes, including cell differentiation, migration, death, and neurotransmission. Cells use much of their energy to control changes in Ca^{2+} concentration with a gradient maintained between their extracellular (~1 µM) and intracellular (~100 nM free) concentrations. Cellular processes controlled by Ca^{2+} are initiated by a simple rise in cytosolic levels of Ca^{2+} ($[Ca^{2+}]i$) from 100 nM (under resting conditions) to approximately 1 µM as a result of the application of external stimuli such as hormones, agonists and neurotransmitters to initiate various signalling pathways (Berridge et al., 2000). All P2X subtypes are permeable to Ca^{2+}; the ratio of Ca^{2+} to monovalent cations permeability varies between 1 and >5–10 for various P2X receptors (Abbrocchino et al., 2009). Ca^{2+} can enter the cell through voltage-gated Ca^{2+} channels and other ionotropic receptors. Moreover, intracellular Ca^{2+} can be released from intracellular stores following the activation of receptor tyrosine kinases and $G_{\alpha q}$-coupled receptors. Furthermore, Initial increases in Ca^{2+} via entry from the extracellular space elicit additional release from the endoplasmic reticulum via Ca^{2+} -sensitive ryanodine receptor (RyR) located on the surface of the endoplasmic reticulum (Clapham, 2007). Receptor tyrosine kinases and Gq-coupled receptors can activate phospholipase C, which cleaves phosphatidylinositol bisphosphate into inositol triphosphate and diacylglycerol. That is followed by the binding of inositol triphosphate to inositol triphosphate receptors expressed on the endoplasmic reticulum and triggers a conformational change causing Ca^{2+} to flow out of the endoplasmic reticulum and into the cytoplasm, thus enhancing intracellular Ca^{2+} (Figure 1.11). Three methods are involved in controlling the Ca^{2+} concentration gradient in cells: chelation, compartmentalization and extrusion. In addition, an array of channels, pumps and cytosolic buffers are implicated in controlling Ca^{2+} levels within a cell (Layhadi, 2017). However, in order to control the occurrence and magnitude of physiological events that are triggered by Ca^{2+}, its release and influx must be time-dependently regulated. A sophisticated cell-specific Ca^{2+}-signalling toolkit is responsible for this, which is consist of a complex network of Ca^{2+} channels, organelles, Ca^{2+} pumps, and signalling components that continually develop depending on the conditions (Berridge et al., 2000).

1.11.1 ON mechanisms

ON mechanisms allow Ca^{2+} signals to be produced either by allowing Ca^{2+} to be released from internal stores or Ca^{2+} influx from the extracellular space. The ON mechanisms allow Ca^{2+} influx include the receptor-operated, voltage-operated, and store-operated channels

placed in the plasm membrane (Figure 1.11). Internal stores, which have high levels of Ca^{2+} concentrations, include the endoplasmic reticulum, sarcoendoplasmic reticulum (muscle cells), mitochondria, and acidic organelles such as acidocalcisomes, lysosomes, and the Golgi apparatus (Berridge, 2002; Berridge et al., 2000). Examples of plasma membrane receptor-operated Ca^{2+} channels include the nicotinic acetylcholine receptor and the P2X purinergic receptors, which can increase cytosolic Ca^{2+} either by inducing Ca^{2+} release via the activation of phospholipase C or by allowing Ca^{2+} influx through transient receptor potential channels and store-operated Ca^{2+} channels (Berridge, 2002; Bootman et al., 2001; Hofmann, et al., 1999). Furthermore, electrical excitation causes membrane depolarisation leading to Ca^{+} influx through cell surface voltage-operated Ca^{2+} channels including Cav1 (L-type), Cav2 (N-, P/Q- and R-type), and Cav3 (T-type) channels (Catterall, 2000; Clapham, 2007). The most well-known Ca^{2+} channels are L-type channels, which are found in excitable cells and non-excitable cells, such as immune cells, where they regulate Ca^{2+} signalling, cell activation and survival (Suzuki et al., 2010). Voltage-operated Ca^{2+} channels allow an increase in Ca^{2+} directly via allowing Ca^{2+} entry, or indirectly by triggering the Ca^{2+}- induced-Ca^{2+}- release through inositol triphosphate receptors and ryanodine receptors (Berridge et al., 2000). Many cell types generate Ca^{2+} signals from internal storage (intracellular organelles) such as the endoplasmic reticulum, mitochondria, lysosomes and Golgi apparatus. The store-operated Ca^{2+} channels are auto-regulatory plasma membrane channels that open in response to internal store depletion (Putney, 2005; Murchison and Griffith, 2000; Vanoevelen et al., 2005).

1.11.2 OFF mechanisms

Ca^{2+} is rapidly eliminated from the cytosol after completing its signalling tasks to avoid Ca^{2+} overload, which can induce cell necrosis and apoptosis (Berridge, et al., 2000, 2003; Hajnóczky et al., 2003). The Ca^{2+} signalling toolkit has equipped itself with a number of sophisticated OFF mechanisms which work collectively to return Ca^{2+} to resting levels (100 nM). Various Ca^{2+} pumps, exchangers, and buffers are components of this system that promote Ca^{2+} extrusion or sequestration. The Ca^{2+} -signalling toolkit includes a number of pumps that eliminate Ca^{2+} from the cytosol either by extruding it from the cell or by sequestering it into intracellular organelles. Individual pumps' contributions are determined by Ca^{2+}, with higher-affinity systems clearing lower-concentration Ca^{2+} and lower-affinity mechanisms clearing higher-concentration Ca^{2+} (Berridge et al., 2003; Murchison and Griffith, 2000). Because of the potentially cytotoxic properties of high cytoplasmic Ca^{2+} levels, stimulus-induced augmented Ca^{2+} levels are quickly reduced by the extrusion of Ca^{2+} out of the cell via the

plasma membrane Ca^{2+} ATPases (PMCA) transporters or into the endoplasmic reticulum cellular Ca^{2+} stores via smooth endoplasmic reticular Ca^{2+} ATPase (SERCA) transporters. In addition, Na^{+}/Ca^{2+} exchangers and Ca^{2+} -activated K^{+} (or Cl^{-}) channels may also help to lower intracellular Ca^{2+} concentrations to baseline levels (Clapham, 2007) (Figure 1.11).

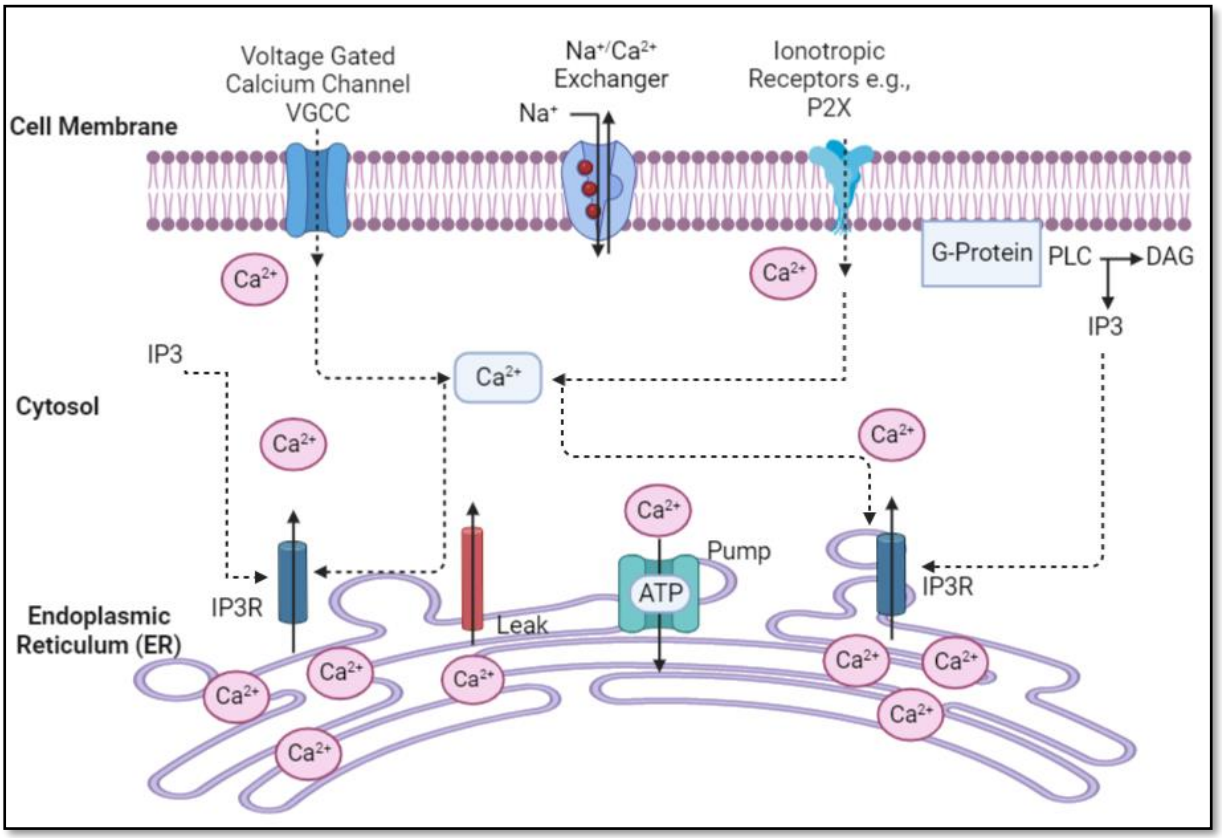

Figure 1.11: Calcium wave signalling in neurons. When a post-synaptic neuron is electrically stimulated by neurotransmitters at the receptors, its voltage-gated Ca^{2+} channels in the plasma membrane open, allowing Ca^{2+} to enter the cytosol. G-proteins are a group of proteins that are involved in signal transmission from outside stimuli to inside the cell, and they function as molecular switches. The G-protein activates the phospholipase C enzyme, resulting in the production of two second messengers: di-glyceride, which remains in the membrane, and inositol triphosphate, which diffuses through the cell's cytoplasm and acts at inositol triphosphate receptors. When both Ca^{2+} and inositol triphosphate activate an inositol triphosphate receptor channel, it opens, allowing $Ca^{2+}$to flow quickly from the endoplasmic reticulum to the cytoplasm. Na^{+}/Ca^{2+} exchangers and Ca^{2+}-activated K^{+} (or Cl^{-}) channels can help to reduce intracellular Ca^{2+}. DAG, di-glyceride; PLC, phospholipase C; VGCC, voltage-gated calcium channels; IP3, inositol triphosphate. Adapted from (Patoary et al., 2017).

1.12 Pharmacology

The main agonist for all homomeric and heteromeric P2X receptors is ATP, although activation is achieved in a receptor-specific manner with EC_{50} values ranging from nanomolar to submillimolar concentrations (Coddou et al., 2011). When P2X receptors were first discovered, there were few selective agonists and no useful antagonists available. Then, nonselective antagonists, such as suramin and pyridoxalphosphate-6-azophenyl-2',4'-disulfonic acid (PPADS), were identified later. Numerous effective and subtype-selective antagonists have been developed since then, notably in the last decade. These antagonists include NF449 and RO-1 at P2X1 receptors; PSB-1011 at P2X2 receptors; A317491, compound A, RO-3, and AF-353 at P2X3 and P2X2/3 receptors; 5-BDBD at P2X4 receptors; and A740003, A438079, A804598, GSK314181A, AZ10606120, AZ11645373, AZD-9056, CE-224535, and EVT-401 at P2X7 receptors. The therapeutic use of these products is now being investigated in a variety of diseases, including P2X1 for thrombosis; P2X3, P2X2/3, P2X4 and P2X7 for chronic neuropathic and inflammatory pain; P2X1, P2X3 and P2X2/3 for dysfunctional urinary bladder; P2X7 for rheumatoid arthritis, osteoarthritis and depression (Syed et al., 2012).

1.12.1 Non-selective P2 receptor agonists

The agonist potency profile of the nucleotides; α,β-methyleneATP, 2-methylthioATP (2-meSATP), and ATP was originally used to be agonists of the P2X receptors. Although with widely varying potency, ATP was revealed to be an agonist at all P2X receptor subtypes, and 2-meSATP is also active at all isoforms (Syed et al., 2012; King, 2001; Gever et al., 2006). Whilst α,β-meATP was identified to be an agonist exclusively at homomeric P2X1 and P2X3 receptors, as well as heteromeric P2X4/6 receptors and P2X1/5 receptors (Torres et al., 1998), and latterly, it was documented that α,β-meATP showed agonist activity at P2X5, P2X6 and P2X4 in a species-dependent manner (Syed et al., 2012). BzATP (2,3 -O-[4-benzoylbenzoyl]ATP) is usually referred to as a selective agonist for P2X7 receptors (Syed et al., 2012), but it also showed an agonist activity at P2X1, P2Y11 receptors and an antagonist at P2Y1 and P2Y12 receptors (Abbracchio, 2006).

1.12.2 Non-selective P2 receptor antagonists

There were no antagonists available when P2X receptors were initially characterised in 1985. Subsequently, suramin and PPADS have been demonstrated to block P2X receptors, but

with limited efficacy and subtype selectivity. Except for the P2X7 receptor, where hundreds of micromolar suramin is required, suramin antagonises most homomeric P2X subtypes at low micromolar concentrations, whilst P2X4 is insensitive. PPADS has a similar potency as suramin, or is somewhat more potent, however, the P2X7 receptor is substantially less responsive, and the P2X4 receptor is insensitive. (Syed et al., 2012; King, 2001; Gever et al., 2006; Jarvis & Khakh, 2009). Suramin and PPADS are both antagonists for certain P2Y receptor isoforms (Abbracchio, 2006).

1.12.3 P2 receptor agonists used in the project

1.12.3.1 ATP and α,β-methyleneATP

As it is mentioned previously, ATP is an agonist of all homomeric and heteromeric P2X receptors. While α,β-meATP, which possesses a methylene group, replaced oxygen atoms in the phosphodiester bridge between the phosphate moieties of ATP (Figure 1.12), it was identified to be an agonist exclusively at homomeric P2X1 and P2X3 receptors, as well as heteromeric P2X4/6 receptors and P2X1/5 receptors (Joseph et al., 2004). This resulted in desensitisation of the receptors due to the slowly degradable nature of α,β me-ATP (Kasakov and Burnstock, 1983). The α,β-meATP is also a P2X7 agonist, however, like ADP and UTP, α,β-meATP lacks the potential to promote Barium (Ba^{2+}) ion influx. (Chen et al., 2018). According to some reports, α,β-me ATP can activate P2Y11 receptors, which are not expressed on the endothelium and do not affect vasomotor responses (Harrington & Mitchell, 2005).

1.12.3.2 BzATP

The P2X7 receptor is widely expressed in the glial cells of the central nervous system and the peripheral nervous system, including microglia, astrocytes, oligodendrocytes, and Schwann cells, as well as in cells of the immune system, such as monocytes, macrophages, lymphocytes, dendritic cells, and mast cells. Several genetic studies have shown that P2X7 receptor has been associated to night-time diastolic blood pressure (Li et al 2022). In Dahl salt-sensitive rats, P2X7 receptors may play a role in the vicious cycle of salt-sensitive hypertension and renal damage. Blocking P2X7 receptors *in vivo* has the potential to prevent and improve salt-sensitive hypertension and renal damage (Ji et al., 2012). Higher concentrations of ATP (EC_{50} 100 µmol·L-1) are required to activate P2X7 receptors compared with other P2X receptors, and BzATP is approximately 30 times more potent than ATP, which is usually referred to as the most potent and more specific endogenous P2X7 agonist (Chen et al., 2018)

(Figure 1.12). However, other P2X receptors could be activated by BzATP such as P2X1 (Syed et al., 2012). At the rat receptor and In ‘‘normal’’ divalent concentrations (2 mM Ca^{2+}, 1 mM Mg^{2+}), The EC_{50} for ATP and BzATP are roughly 300 µM and 8 µM, respectively; higher concentrations are needed to activate the human P2X7 receptor (North & Surprenant, 2000).

1.12.3.3 Carbachol

Carbachol is a non-selective muscarinic and nicotinic receptor agonist which causes an increase in intracellular free Ca^{2+}. It has been reported that the application of carbachol to cultured human granulosa-lutein cells elicited extracellular Ca^{2+} influx via voltage-dependent Ca^{2+} channels as well as Ca^{2+} release from intracellular stores (Mayerhofer et al., 1992). Carbachol was prepared and used in this project as a control to ensure the cells were functioning correctly.

1.12.4. P2 receptor antagonists used in the project

1.12.4.1. A438079 or 3-[[5-(2,3- dichlorophenyl)-1H-tetrazol-1-yl]methyl]pyridine

In 2006, Abbot Laboratories identified two new selective and competitive antagonists of P2X7 antagonists, the disubstituted tetrazolylmethylpyridine, A438079 (Figure 1.13) and the disubstituted cyanoguanidine derivative, A740003 (Syed et al., 2012; Honore et al., 2006; Nelson et al., 2006). A438079 is active in the mid to high nanomolar range and is roughly three times more potent at the human homolog than the rat homolog, with little or no action at the other P2X subtypes examined. Moreover, It was reported that A438079 is effective at slightly higher concentrations, at the mouse P2X7 receptor. In addition, both compounds prevented the pore formation and secretion of interleukin-1β induced by the activation of BzATP of native P2X7 receptors in human THP-1 cells (Syed et al., 2012; Donnelly-Roberts et al., 2009).

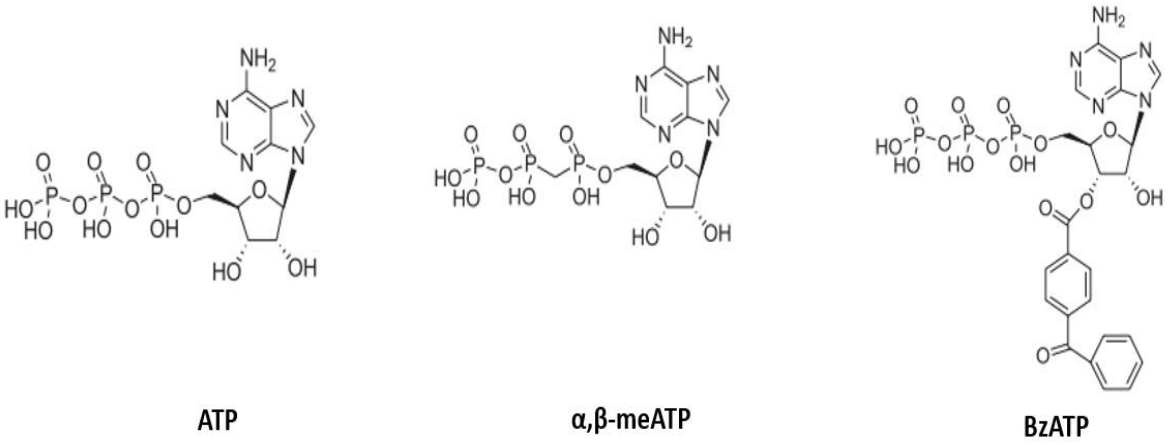

Figure 1.12: Chemical structures of P2X receptor agonists.

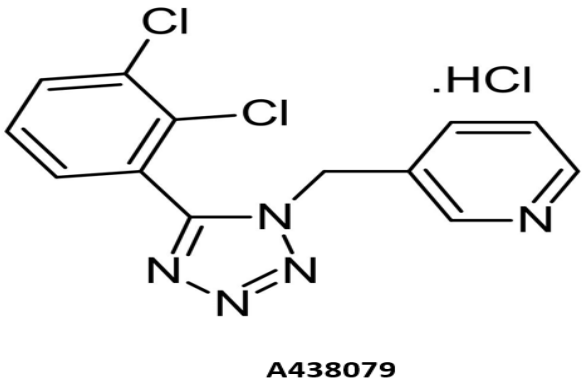

Figure 1.13: Chemical structures of P2X7 receptor antagonist (A438079).

1.13 Project aims

It is apparent from the current literature that hypertension is a serious medical condition that increases the risk of developing heart, brain, kidney, and other diseases. P2 Purinergic receptors play a vital role in regulating hypertension by acting on blood vessels and the central nervous system. There is a clear understanding to what the role of P2 receptors is in smooth muscle cells and endothelial cells in blood vessels. However, the role of P2 receptors located on pre-junctional perivascular nerve terminal of blood vessels is poorly understood, and more studies are required to understand the roles of pre-junctional P2 receptors in modulating neurotransmitters in diverse blood vessels. Pharmacological manipulation of perivascular nerve activity has the potential to modulate arterial tone and alter blood pressure. Thus, expanding our understanding of these pre-junctional purinergic receptors could help in controlling the high blood pressure that occurs in hypertension. That suggested that modulating purinergic signalling has shown great therapeutic potential in the treatment of hypertension. Therefore, this project hopes to study the expression of P2 receptors on pre-junctional perivascular nerve terminal of blood vessels. Then we aimed to study the contribution of P2 receptors toward nucleotides-evoked Ca^{2+} response using a model of adrenergic neurons. To achieve this, three key aims were set during this project:

1) Chapter 3 investigated the expression of P2 purinergic receptors, including all P2X and P2Y receptors in mouse arteries (including superior mesenteric artery and carotid artery) and associated sympathetic ganglia (superior cervical ganglion) of mice at the mRNA level using non-quantitative RT-PCR. This will help to determine whether receptors could be expressed on pre-junctional nerves. This is different from previous studies which were done on rat arteries.

2) Chapter 4 aimed to gain both a qualitative and quantitative understanding of the P2 purinergic receptors present on the pre-junctional terminal of sympathetic nerves, focussing specifically on their expression at the protein level in the cell bodies of the superior cervical ganglion and the pre-junctional terminal of sympathetic efferent nerves in superior mesenteric arteries and carotid artery using immunohistochemistry. Colocalisation experiments of P2 receptors with different markers including PGP9.5, TH, NPY and VNUT were involved in this study.

3) Chapter 3 aimed to identify and characterize the contribution of P2 activation toward intracellular Ca^{2+} response in human SH-SY5Y cells and in *in vitro* differentiated SH-SY5Y cells.

Impact of COVID-19 on PhD work

The PhD laboratory work started in October 2018 and continued until October 2021. The Covid-19 pandemic affected the progression of the PhD program which started in the beginning of 2020. I was unable to pursue my PhD work for six months in this time due to a national lockdown and laboratory closures. The laboratory opened again in late July 2020, however the pandemic caused rapid and unprecedented changes to how universities operated, for example, the number of PhD students that could access the laboratory at one time was limited due to social distancing requirements. This reduced the time in which I could perform my work. The COVID-19 pandemic had a significant impact on my doctoral studies and research experience. The necessary public health measures put in place impacted my research in many ways as well as limited laboratory access, I had to work in isolation without a research community and my access to resources was limited. All safety procedures were followed throughout my project to minimize the risk of infection, including wearing face masks, maintaining two-metre distances from colleagues where possible, and consistently checking for COVID-19 symptoms. In January 2022 tested positive for COVID-19, my symptoms during this time further impacted my work as I was unable to focus on my writing and work to the best of my ability for 10 days. The molecular experience I gained during my PhD performing PCR meant I was able to help the NHS team perform thousands of COVID-19 tests daily to help combat the pandemic. I was passionate when during this time knowing my work was assisting with the effort to overcome the pandemic. I worked 20 hours a week in Norwich and Norfolk University Hospital alongside doing my experiments in the laboratory and writing my thesis. As well as the practical implications, the pandemic also impacted my emotional wellbeing. The extra work and pressure of completing my PhD on time lead to times of exhaustion and low morale. After the restrictions were eased, I needed to work very hard to finish my PhD on time with no extension. After finishing my shifts in the hospital I would go to the research laboratory and stay late doing experiments and had little time to relax in between. Despite all the difficulties I faced, my determination and hardworking attitude meant I was able to achieve the aims of my project as planned at the beginning of the project.

Chapter 2: Materials and Methods

2.1 Materials

Most of the chemical reagents utilised throughout this project were obtained from Sigma Aldrich and Thermo Fisher Scientific. The instances where materials from other suppliers were used are noted within the text. A comprehensive list of all materials including buffers, primers, antibodies, agonists, and antagonists used throughout the study are presented in tables. All the infographics in this chapter were created using BioRender (BioRender, 2021), unless otherwise stated. Water used to prepare buffers and to dissolve products was deionised water, apart from in polymerase chain reaction (PCR) experiments where Nuclease-Free Water (Sigma-Aldrich) and sterile tips were used.

2.2 Animals

Mice used throughout the experiments were used in accordance with the UK Home Office regulations and the European Legal Framework for the Protection used for Scientific purposes (European Directive 86/609/EEC). Mice were housed in the Disease Modelling Unit at University of East Anglia at a controlled ambient temperature of 22°C with 50±10% relative humidity and a 12-h light/12-h dark cycle (lights on at 8:00 a.m.).

2.3 Dissection of mice

Mice were bred from a pure C57BL6 background. Adult male mice (25-30g) aged 15-20 weeks were killed by CO_2 asphyxia and death was confirmed by cervical dislocation. Superior mesenteric arteries (a part of a network of vascular beds that regulate vascular resistance) of different diameters (first order [300 – 400 µm] and second order [250–300 µm]), carotid arteries, superior cervical ganglions and brain were removed (Figure 2.1). To isolate the superior mesenteric arteries, the body was laid on its back on a dissecting board and stretch it flat by applying a needle in each limb. The belly was then .on its back on a dissecting board and stretch it flat by applying a needle in each limb (see Fig. 5b). Wipe the belly was wiped with 70% ethanol. The abdominal skin was open down to the pelvis by inserting one tip of the scissors between the skin and the abdominal wall. The peritoneum was removed to free the intestine. Then, the intestine was pushed downward to get free access to the duodenum and cut it below the stomach. The intestine and mesentery were

then pulled out from the abdominal cavity and placed into a physiological salt solution (Hank's balanced salt solution, HBSS) minus Ca^{2+} and Mg^{2+} (Table 2.1) at room temperature (RT) to be cleared of fat, blood and connective tissue. The duodenal is pinned using stainless steel insect pins on elastomer-coated cell culture plate filled with HBSS. The mesentery was unfolded in a wheel shape by inserting more pins, approximately at each bend of the intestine. Once a wheel is complete, carefully remove out excess of tissues (fat and connective tissue) around the mesenteric using microscissors. The mesenteric arteries were then cut off and placed into HBSS solution for furthers experiments or stored at -80 until used (Figure 2.1).

To isolate the common carotid artery and the superior cervical ganglion, the chest and the neck were opened to expose the right and left carotid arteries using dissecting scissors and curved forceps. Then, clear fat and nearby tissue were removed using curved forceps and fine tweezers until the full length of both carotids from the aorta to the common carotid bifurcation can be visualized. The common carotid artery with right and left bifurcations were cut and placed into a physiological HBSS solutions to be cleared of fat, blood and connective tissue. The superior cervical ganglion located between the two bifurcations were isolated. The isolated tissues were placed into HBSS solution for furthers experiments or stored at -80 until used (Figure 2.1).

Table 2.1: The components of Hank's balanced salt solution.

Hank's balanced salt solution	
Component	**Concentration**
NaCl	137 mM
KCl	8.4 mM
KH_2PO_4	0.44 mM
Na_2HPO_4	0.27 mM
D-(+)-Glucose	5.6 mM
Hydroxyethyl piperazineethanesulfonic acid (HEPES)	10 mM
Water	Up to a volume of 1 Litre
pH = 7.0	

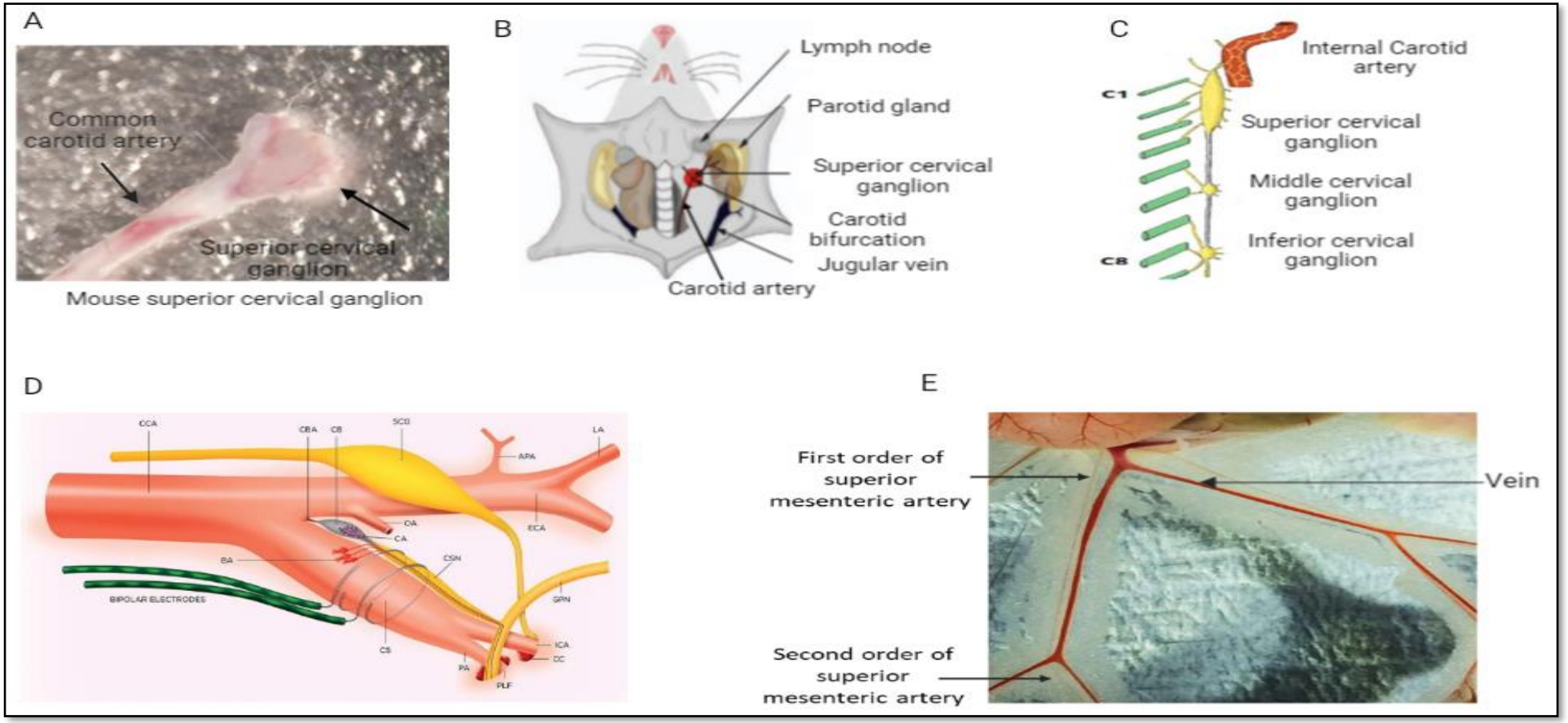

Figure 2.1: **Mouse tissues used throughout research. (A)** Mouse superior cervical ganglion. **(B)** The location of both carotid artery and superior cervical ganglion in the mouse neck. **(C)** Superior cervical ganglion is located posteriorly to the carotid artery, and anterior to the C1-4 vertebrae. **(D)** The difference in location between the superior cervical ganglion and carotid body. **(E)** The first and second order of superior mesenteric arteries. CA, carotid artery; SCG, superior cervical ganglion; CB, carotid body. Images C and D adapted from (Teachmeanatomy, 2022).

2.4 Transgenic mice (NPY-hrGFP)

NPY-hrGFP transgenic reporter mice (Jackson Laboratory, #006417) were kindly donated by Mohammad Hajihosseini (University of East Anglia). These transgenic mice promote the expression of bright humanised Renilla green fluorescent protein (hrGFP) under the control of the NPY promoter (Van den Pol et al., 2009) (Figure 2.2). The NPY-hrGFP mice were used in this project to investigate NPY-positive neurons and would tell us which neurons had vasomotor activities which were able to innervate target tissues including blood vessels, as many neurons in the superior cervical ganglion would lack vasomotor activity. This approach is especially effective for NPY neurons, which despite their large number in some tissues such as brain, NPY neurons are not identifiable (Van den Pol et al., 2009). The DNA from the transgenic mice (NPY-hrGFP) was subjected to PCR for genotyping and that is confirmed by the previous PhD student (Dr Estella Perez Ez) using the attached PCR conditions (Table 2.2). If a mouse was carrying the transgene, it would show a 400 base pair band. As a control, we always detected a 500 base pair wild-type band, unless the mouse was homozygous for NPY, in which case only the 400 base pair band was detected.

Table 2.2: PCR programmes for genotyping of NPY-hrGFP.

PCR programmes for genotyping of NPY-hrGFP		
Temperature (°C)	**Duration (seconds)**	**Cycle repeat**
94	120	1
94 61 68	30 30 160	10
94 61 68	30 30 160 (+ 40s each cycle)	17
68	420	1
6	600	1

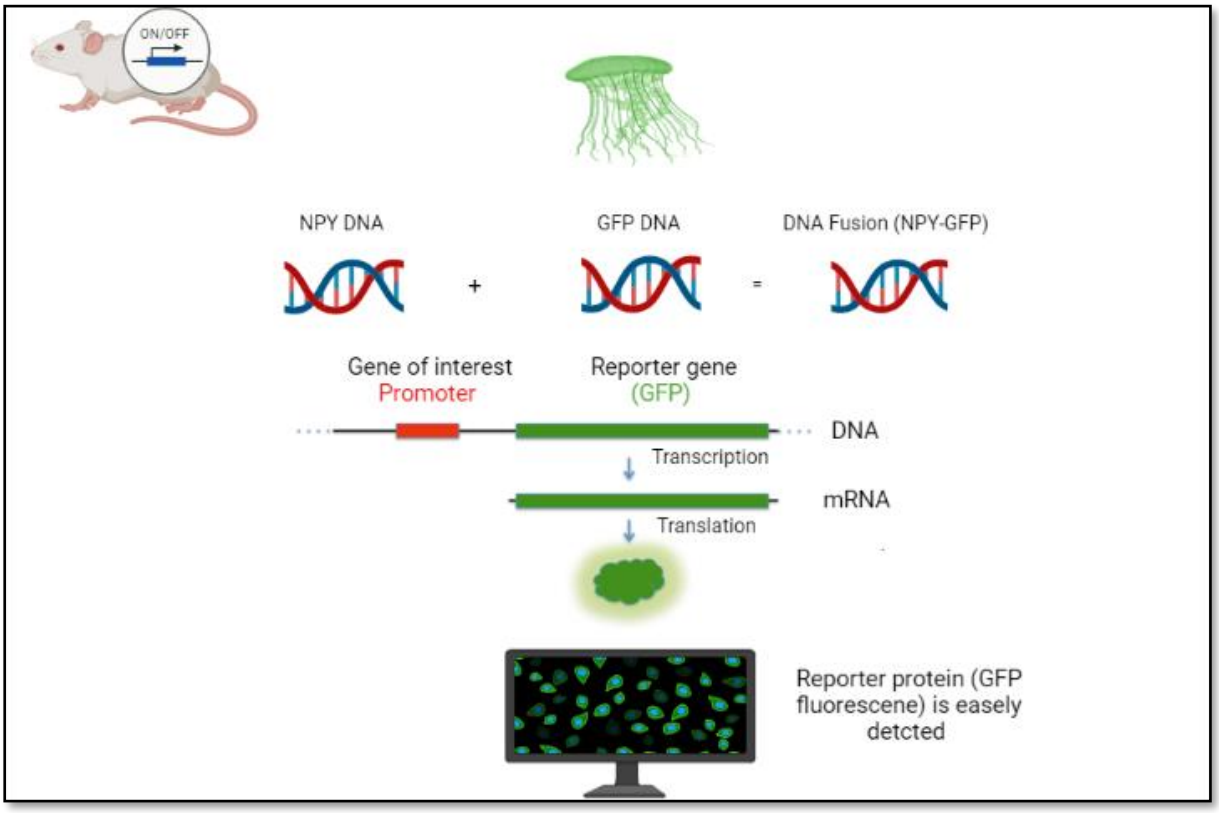

Figure 2.2: Reporter genes are used to study the regulatory sequences of genes of interest. Inserting a reporter gene (GFP from jellyfish) under control promoter of the gene of interest (NPY) results in a readily detectable fluorescent reporter protein, indicating that the functional promoter gene of interest has been detected. Red box, promoter of the gene of interest; green box, reporter gene; the initial of transcription and the translation stop are indicated. GFP, Green Fluorescent Protein.

2.5 Cell culture

The human SH-SY5Y neuroblastoma cell line (Supplied by European Collection of Authenticated Cell Cultures [ECACC] operated by Public Health England, Cat No 94030304 was used in this project as a neuronal cell model. SH-SY5Y is a human-derived cell line which was established in 1970 from a metastatic bone tumour that contains both neuroblast-like and epithelial-like cells (Shipley et al., 2016). The original cell line, called SK-N-SH, isolated from a metastatic bone tumour biopsy taken from a four-year-old female suffering from neuroblastoma (Biedler et al., 1973). The SH-SY5Y cells were maintained in Dulbecco's Modified Eagles medium (DMEM) supplemented with Foetal Bovine Serum (FBS) 10% (v/v) and 1% (v/v) solution containing 50 IU/ml penicillin and 50 µg/ml streptomycin (Gibco). This mixture will be referred to throughout this project as culture media (Table 2.3). The cells were maintained in uncoated tissue culture flasks (T75, T25) or multi-well plates (Thermo Fisher Scientific) in a saturated humidified incubator at 37^{o}C in the presence of 5% CO_2. The culture media was replaced every third day until a confluent monolayer was apparent.

2.6 Differentiation of SH-SY5Y human cells to adrenergic neurons

The undifferentiated SH-SY5Y cell line, a subline of the SK-N-SH cell line, was generated from a malignant neuroblastoma and contains many characteristics of mature dopaminergic and adrenergic neurons. They express markers of immature neurons, including NA and NPY production and depolarisation-evoked NA release (Schneider et al., 2017; Kovalevich & Langford, 2013; Xicoy et al, 2017). The expression of dopaminergic neuronal markers, muscarinic and nicotinic receptors has been reported in both undifferentiated and differentiated SH-SY5Y. Differentiated SH-SY5Y cells could be induced to acquire an adrenergic phenotype (Agholme et al., 2010). The SH-SY5Y human cells can be differentiated to a more mature neuron-like phenotype (various types of functional neurons) which is characterized by neuronal markers such as TH and NPY (Shipley et al., 2016). SH-SY5Y can be differentiated to mature human neurons, or specific neuron subtypes such as adrenergic, cholinergic, and dopaminergic neurons using a variety of differentiating agents, including all-trans-retinoic acid, phorbol esters, and particular neurotrophins such as brain-derived neurotrophic factor (Shipley et al., 2016) (Figure 2.3). To differentiate SH-SY5Y cells, an early passage (P13–19) of the cells was seeded in culture media in a saturated humidified incubator at 37^{o}C in the presence of 5% CO_2 until cells had reached 70-80% confluency. Cells were counted using haemocytometer and the appropriate numbers of cells were seeded in a suitable

flask/plate based on the experiment. One day after seeding, differentiation was induced by replacing the culture media with serum-free Neurobasal-A Medium (Thermo Fisher Scientific) supplemented with 10 μM of retinoic acid, 2% (v/v) B-27 Supplement (50X), 50 IU/ml penicillin and 50 μg/ml streptomycin (Gibco) (this mixture will be referred throughout this project as differentiation media) (Table 2.4). Cells were ready to be used in experiments 5 days after incubation at 37ºC and 5% CO_2.

Table 2.3: Culture media components.

Culture media components		
	Component	Concentration
Dulbecco′s Modified Eagle′s Medium - High Glucose DMEM (Sigma-Aldrich)	Glucose	4.5 g/l
	L-glutamine	0.6 g/l
	$NaHCO_3$	3.7 g/l
	Phenol red	0.015 g/l
	Amino Acids	-
	Vitamins	-
Foetal bovine serum (GE Healthcare)		10% (v/v)
Penicillin (Gibco)		50 IU/ml
Streptomycin (Gibco)		50 µg/ml

Table 2.4: Differentiation media components.

Differentiation media components		
Neurobasal-A Medium serum free (Thermo Fisher Scientific)	D-Glucose	4.5 g/l
	HEPES	2.6 g/l
	Sodium Pyruvate	0.025 g/l
	Phenol red	0.0081 g/l
	Amino Acids	-
	Vitamins	-
B-27 Supplement (50X), serum free (Thermo Fisher Scientific)	Vitamins and Proteins	2% (v/v)
All-trans-retinoic acid (Sigma- Aldrich)	Vitamin A acid	10 µM
Penicillin (Gibco)		50 IU/ml
Streptomycin (Gibco)		50 µg/ml

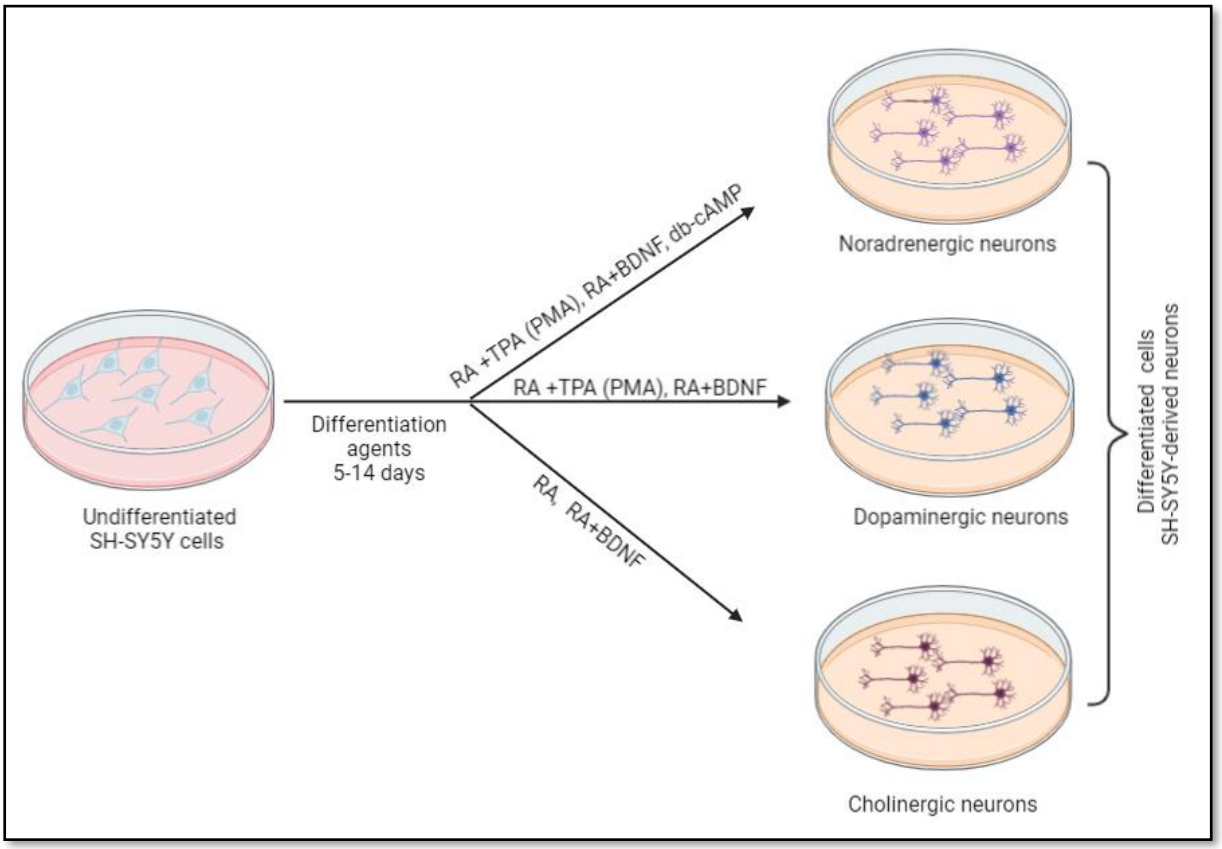

Figure 2.3: Several methods used to differentiate SH-SY5Y cells into various types of functional neurons. Different mechanisms can be exploited to induce differentiation of specific neuronal subtypes such as adrenergic, cholinergic, and dopaminergic neurons. Primarily, noradrenergic neurons are induced after the treatment of undifferentiated SH-SY5Y cells with retinoic acid, brain-derived neurotrophic factor, and phorbol esters or db-cAMP. Undifferentiated SH-SY5Y cells are differentiated to dopaminergic neurons after treatment with retinoic acid and brain-derived neurotrophic factor or phorbol esters and retinoic acid. Cholinergic neurons are induced via differentiation with retinoic acid or with retinoic acid and brain-derived neurotrophic factor (Bell & Zempel, 2021). The incubation time of undifferentiated SH-SY5Y cells with the differentiation agents varies but are usually between 5 and 14 days. RA, retinoic acid; BDNF, brain-derived neurotrophic factor; PMA (TPA), phorbol esters; db-cAMP, dibutyryl-cAMP.

2.7 Cell passage

SH-SY5Y cells are adherent and were cultured at 37°C and 5% CO_2 until cells had reached 70-80% confluency. Cells were passaged by rinsing cells twice with 10 ml warm phosphate buffered saline (PBS) prior to incubation with 2 ml 0.05% trypsin solution at 37°C for 2-3 minutes. To detach the adherent cells, gentle agitation was applied to the flask and the enzymatic reaction was terminated by diluting trypsin with the culture media to a final volume 5 ml. Cells were then centrifuged at 1200 rpm for 5 minutes at RT and the supernatant was aspirated. The cell pellet was re-suspended with the appropriate volume of culture media to be used for experiments or further seeding (1:1 split ratio). Cells were discarded at p20.

2.8 Measurements of intracellular free Ca^{2+} concentrations

Changes in intracellular Ca^{2+} mobilisation upon purinergic receptor activation were performed using the fluorescent Ca^{2+} indicator dye, Fura-2 acetoxyethyl (AM) ester (Abcam) (Grynkiewicz et al., 1985). Fura-2 AM, is a membrane-permeable Ca^{2+} ion indicator and can cross the cell membrane to the cytoplasm due to the acetoxymethyl moiety. The AM moiety allow fura-2 to traverse the cell membrane to the cytosol, where the AM group is cleaved by cellular esterases, which prevents fura-2 from leaving the cell. In the cytoplasm, Fura-2 is able to bind with the free intracellular Ca^{2+} (Hirst et al., 1999; Tsien, 1981) (Figure 2.4). The peak excitation wavelength of Fura-2 differs depending on its Ca^{2+} binding status, ranging from 335 nm in Ca^{2+}-bound states to 362 nm in Ca^{2+}-free states. However, the emission wavelength is constant (510 nm). The fluorescence ratio (340/380) can be calculated by measuring fluorescence at 510 nm with two excitation wavelengths, 340 nm and 380 nm, respectively. Calculating a ratio reduces the impact of photobleaching and neutralises variables such as cell thickness and local Fura-2 concentrations, improving the accuracy and reproducibility of results.

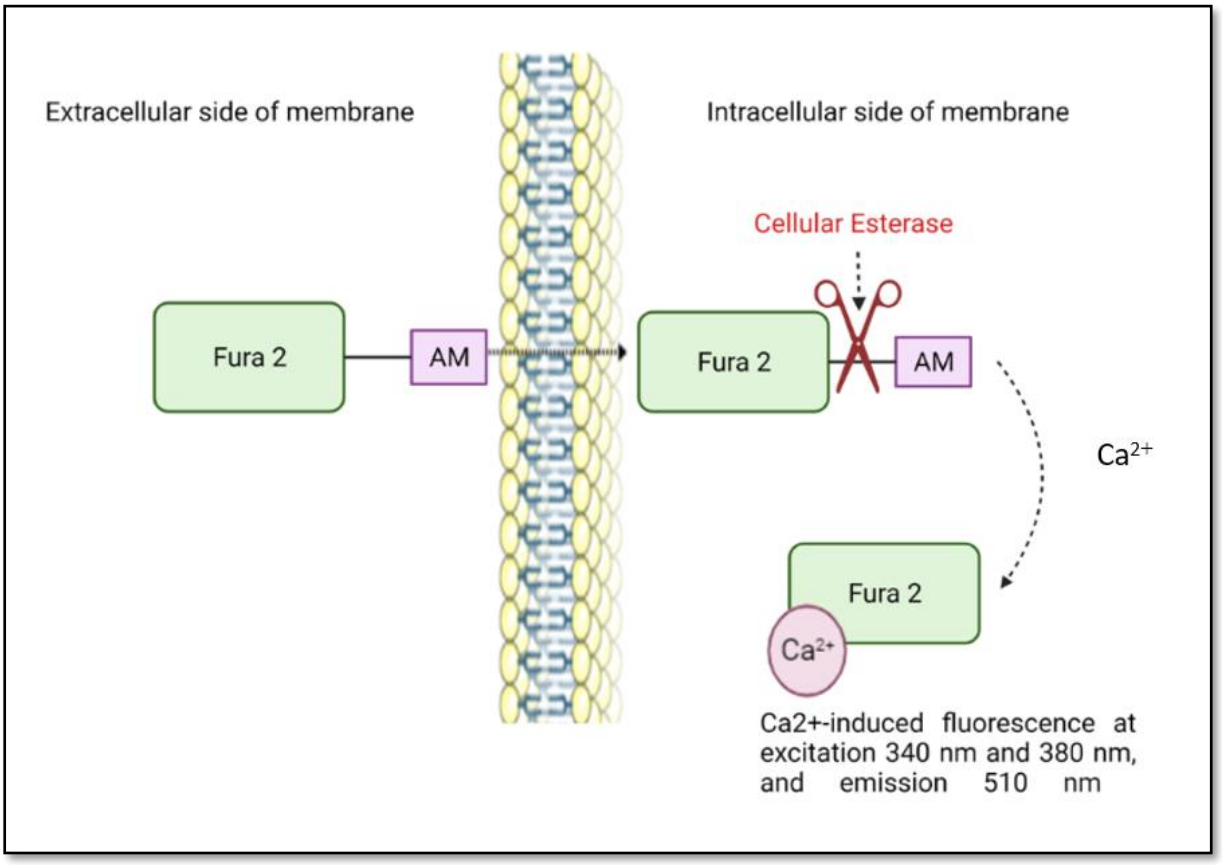

Figure 2.4: Fura-2 acetoxyethyl (AM) ester. Fura-2 AM is a membrane-permeable indicator, The AM moiety allows Fura-2 to traverse the cell membrane to the cytosol, where the AM group is cleaved by cellular esterases. Measurement of Ca^{2+}-induced fluorescence at both 340 nm and 380 nm allows for the quantification of Ca^{2+} based on 340/380 ratios.

To measure intracellular free Ca^{2+} concentrations following purinergic receptor activation, undifferentiated SH-SY5Y and differentiated SH-SY5 cells were seeded at a density of 3.5 x 10^4 cells/well in a 96-well plate in 200 µl cell culture media (Table 2.3) and incubated at 37ºC in 5% CO_2 for 24 hours. The next day, the culture media was removed and the cells were washed with warm salt buffered solution (SBS) (Table 2.5). Cells were then loaded with 2µg/ml Fura-2 AM in loading buffer (Table 2.5) for 1 hour at 37ºC, protected from light. The Fura-2 loading buffer was then removed and the cells were washed twice with 200 µl SBS, before finally adding 200 µl SBS to each of the experimental wells. In some instances, the cells were incubated for an additional 30 minutes with the P2X7 antagonist A438079 (10 µM; Tocris) (Nelson et al., 2006). During the incubation, ATP disodium salt (Abcam), α, β, me-ATP (Sigma -Aldrich) or BzATP (Abcam) solution was prepared (10 mM stock solution). Further dilutions were prepared at 5X the required concentration in SBS into 6 different concentrations, 0.3-2,000 µM for ATP, 1-1000 µM for α, β, me-ATP, and 1-300 µM for BzATP (Table 2.6, Figure 2.5). Carbachol (100 µM), a non-selective muscarinic and nicotinic receptor agonist which causes an increase in intracellular free Ca^{2+}, was prepared and used as a control to ensure the cells were functioning correctly.

An example of the 96 well plate containing P2 receptor agonists (drug plate) can be found in (Figure 2.5) and (Table 2.6). A FlexStation III microplate reader (Molecular Devices) was used to auto-inject agonists (final ATP concentrations were one fifth of the diluted concentrations prepared) from the drug plate onto the cells at 37ºC. The FlexStation III recorded fluorescence every three seconds to allow for Ca^{2+} quantification based on the 340/380 ratios. SoftMax Pro 5.4.5 software (Molecular Devices) was used to analyse data, including the F_{ratio} values at each time point, peak F_{ratio} (the maximum peak recorded after a drug was added), and the area under the curve. The data was used to plot a concentration-response relationship curve in which, the EC_{50} value could be determined. The EC_{50} value is the concentration of ATP that causes 50% activation, for example, half of the maximum response recorded, at the P2 receptor. All data was analysed using GraphPad software. All concentration response data was normalised to the maximal response, and all antagonist data was normalised to the vehicle controls DMSO 0.5% v/v.

Dose-response curves were fitted using a modified Hill equation via the following formula:

$$y = A1 + \frac{A2 - A1}{1 + 10^{(Logx0 - x)p}}$$

Where;

A1 = The bottom asymptote (minimum response on the y axis)

A2 = The top asymptote (maximum response on the y axis)

Logx0= The centre of curve (EC_{50})

P= The hill slope

The EC_{50} values were the value of Logx0, as the value represented the centre of the curve, which also corresponded to the half of maximal response concentration. To get the x value (concentration of ATP in log10) at any magnitude of response, the above equation was rearranged and y was substituted accordingly, and the value was base-10 anti-logged to get a value in molar.

$$x = -1\left(\frac{\sqrt[10]{\frac{A2 - A1}{y - A1} - 1}}{p} + Logx0\right)$$

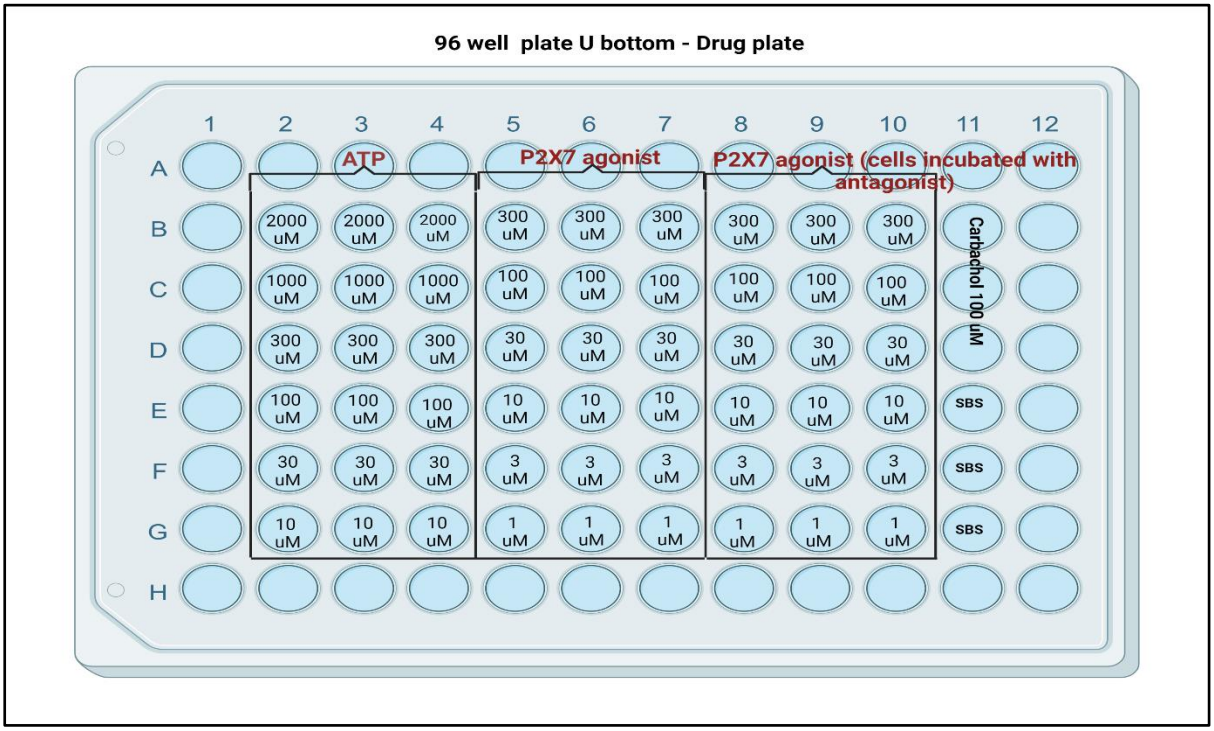

Figure 2.5: An example of an experimental setup of nucleotide-evoked intracellular calcium responses. Different P2 ligands including ATP, BzATP, and carbachol at various concentrations were loaded in 96 well U-bottom plate to be inserted into a FlexStation III microplate reader for Ca^{2+} quantification based on 340/380 ratios.

Table 2.5: Salt buffered solution and loading buffer components.

Salt buffered solution (SBS) components	
Component	Concentration
NaCl	130 mM
KCL	5 mM
$MgCl_2$	1.2 mM
$CaCl_2$	1.5 mM
D-(+)-Glucose	8 mM
HEPES	10 mM
pH = 7.4	
Storage at 4^{o}C for ≈ 14 days	
Loading buffer	
SBS	
Pluronic	0.01% (w/v)
Storage at 4^{o}C for ≈ 14 days	

HEPES, hydroxyethyl piperazineethanesulfonic acid; SBS, salt buffered solution,

Table 2.6: Receptor ligands used in measurements of intracellular free calcium experiment.

Compounds (modulator and antagonist) used in the project				
Agonist	**Target**	**Supplier**	**Concentration**	**Vehicle**
ATP	P2X, P2Y2, P2Y11	Abcam (Ab120385)	0.3 µM -2000 µM (Burnstock, 2007)	Water, dilutions in SBS
α, β-Me-ATP	P2X	Tocris (3209)	1 µM -1000 µM (Vial & Evans, 2002)	Water, dilutions in SBS
BzATP	P2X P2Y11	SA (B6396)	1 µM -300 µM (Zhang et al., 2005; Supłat-Wypych et al., 2010)	Water, dilutions in SBS
Carbachol	Muscarinic and Nicotinic receptors	SA (PHR1511)	100 µM (Larsson et al., 1998)	Water, dilutions in SBS
Antagonist	Target	Supplier	Concentration	
A438079	P2X7	Abcam (ab120413)	10 µM (Nelson et al., 2006)	DMSO

DMSO: Dimethylsulfoxide, SA: (Sigma- Aldrich), BzATP : 2'(3')-O-(4-benzoyl)adenosine triphosphate.

2.9 Reverse transcription-polymerase chain reaction (RT-PCR)

2.9.1 Total RNA extraction

In order to investigate the expression of P2 receptors; mouse brains, superior mesenteric arteries, carotid arteries and superior cervical ganglions tissues were dissected and placed in HBSS. Total RNA was extracted from all four tissues according to the TriReagent protocol (Sigma-Aldrich, Merck, UK), with the addition of Amplification Grade DNase I and DNase reaction buffer (Recombinant DNase I [rDNase I]) (Thermo Fisher Scientific) to remove DNA from total RNA. In brief, the tools and the work area were cleaned with RNaseZap (Invitrogen). RNaseZAP is a purifying agent used for eliminating RNase contamination from, e.g., surfaces and pipettors. Each tissue was transferred into an Eppendorf tube and 1 ml of Tri-reagent was added into each tube. Using clean plastic sticks, the tissues were macerated and incubated at RT for 5-10 minutes. Then, 100 µl 1-bromo-3-chloropropane was added to induce complete separation of the homogenate into aqueous and organic phases. The samples were vortexed for 10 seconds and allowed to stand at RT for 15 minutes, followed by centrifugation at 12,000 rpm for 20 minutes at 4°C. Centrifugation produced the formation of three phases, which include a lower red organic phase containing protein, a cloudy interphase containing denatured proteins and genomic DNA, and an upper aqueous clear phase containing RNA. After the top aqueous phase was transferred gently into a clean tube, the RNA was precipitated using 100 ul of 100% isopropanol and allowed to stand at RT for 10 minutes. The samples were then centrifuged at 12,000 rpm for 20 minutes at 4°C. The supernatant was removed, and the RNA pellet was washed with 1 ml ice-cold 75% (v/v) ethanol and centrifuged again as above. The supernatant was then removed, and the remaining RNA pellet was air-dried in an MSC hood for 30 minutes. The RNA pellet was then dissolved in 10-20 µl nuclease-free water and heated at 65°C for 5 minutes to ensure the complete dissolution of the RNA. In the case of the SH-SY5Y cells, the cells were seeded in a T25 flask and incubated in a humidified incubator at 37^{o}C in the presence of 5% CO_2. When a given cell line reached ~80% confluence (equating to roughly 1x10^{6} cells), cells were washed and pelleted prior to lysis with 1 ml of TRI-reagent and transferred to an Eppendorf tube. After which, the RNA extraction protocol described above commenced (Figure 2.6).

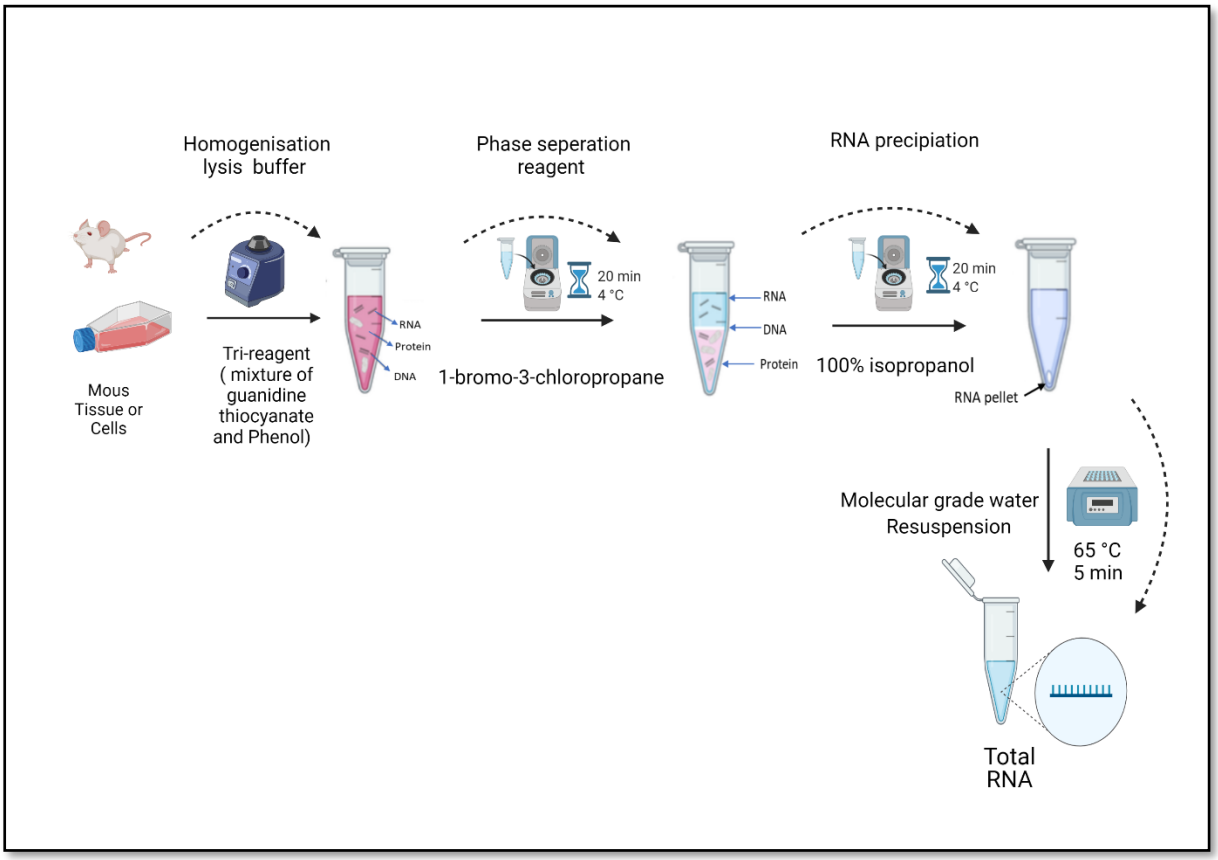

Figure 2.6: Total RNA extraction protocol. To obtain a cell/tissue lysate for RNA extraction, the tissue and cells were incubated with Tri-reagent, then the separation agent was added followed by centrifugation at 12,000 rpm at 4^{o}C for 20 minutes. The RNA phase was transferred into a fresh Eppendorf and isopropanol was added to produce an RNA pellet which was washed with cold 75% ethanol and centrifuged again. The pellet was left to air-dry and rehydration of RNA was achieved through the addition of 10-20 µl of nuclease-free water followed by heating at 65^{o}C for 5 minutes.

2.9.2 Elimination of genomic DNA using DNase1 and total RNA quantification

To remove potential contamination of genomic DNA and remove divalent cations which limit RNA degradation from the RNA preparations, the RNA was treated with a DNA-freeTM DNA kit (Thermo Fisher Scientific – Ambion, UK). Briefly, 0.1 volume of 10X DNase I buffer and 1 µl of rDNase were added to the total RNA of each sample, vortexed, and then incubated for 30 minutes at 37°C. The mixture was then incubated with 0.1 volume of DNase inactivation reagent for 2 minutes at RT. Afterwards, the mixture was centrifuged at 10,000 rpm for 1.5 mins and the supernatant containing RNA was transferred carefully into a fresh Eppendorf tube. Finally, the purity and quantity of RNA was assessed using a Nanodrop 2000 (Thermo Fisher Scientific). The absorbance was read at $A_{260\ nm}$ and $A_{280\ nm}$, with the ratio of the absorbance at 260 and 280 nm ($A_{260/280}$) being used to assess the purity of nucleic acids 260/280, A ratio of ~2.0 is generally accepted as "pure" for RNA. RNA was stored at -80°C for long-term storage until required (Figure 2.7).

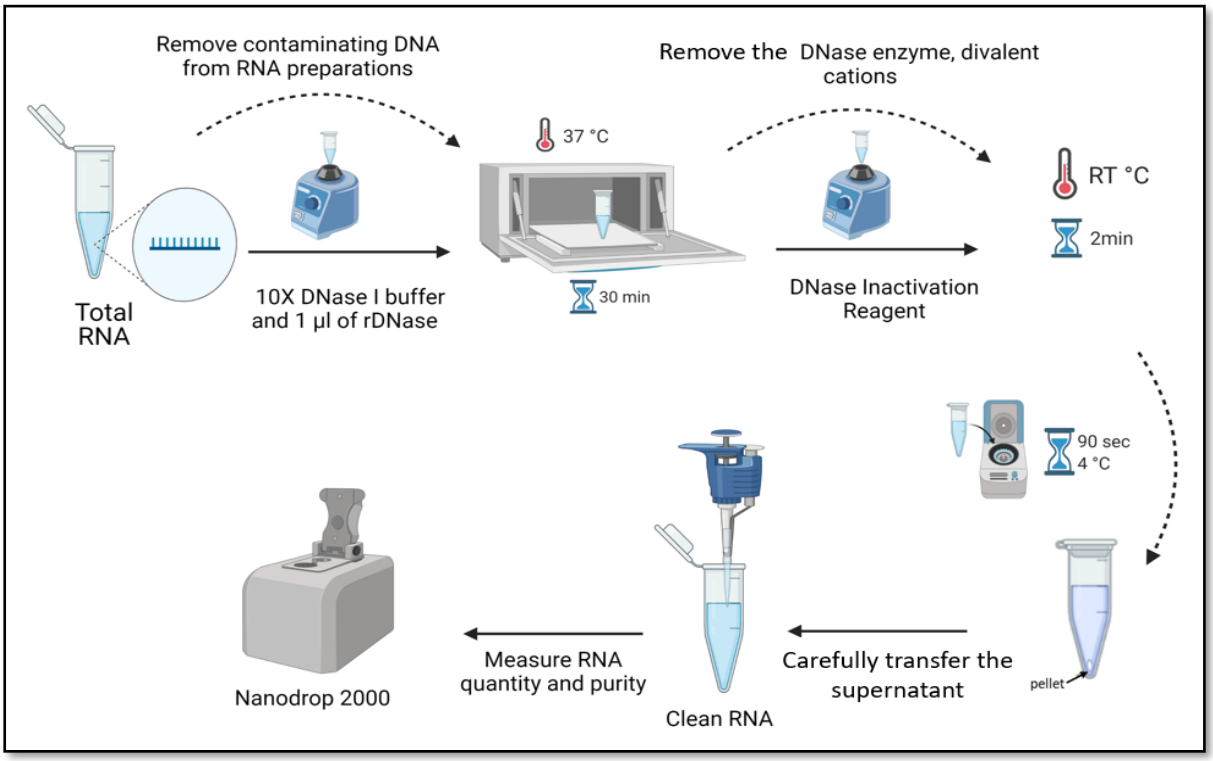

Figure 2.7: Elimination of genomic DNA using DNase1 and total RNA quantification. Cleaning of genomic DNA was achieved by using the Ambion® DNA-free™ Kit as described above. Total RNA concentration was quantified by adding 1 µl of the RNA sample to the NanoDrop. The absorbance was read at A_{260} (nm) and A_{280} (nm), with the ratio of the absorbance at 260 and 280 nm ($A_{260/280}$).

2.9.3 Complementary DNA (cDNA) synthesis

Reverse transcriptase is required for the conversion of messenger RNA (mRNA) to complementary DNA (cDNA) to enable amplification via PCR. Therefore, cDNA was synthesized by incubating 0.5 µg of the previously extracted total RNA of each sample, with 100 ng of random hexamer primers (Bioline, UK), consisting of a mixture of oligonucleotides representing all possible hexamer sequences, giving random coverage to all regions of the RNA to generate cDNA. Water was then added to achieve a total volume of 11 µl, then the mixture was heated for 10 minutes at 70^{o}C. The samples were then incubated with Superscript reverse transcriptase III (Invitrogen, UK) following the manufacturer's instructions. Briefly, each sample was treated with 4 µl of 5X first strand buffer (Invitrogen), 2 µl (0.1 M) Dithiothreitol (DTT) (Invitrogen), 1 µl (200 U) Superscript III reverse transcriptase enzyme (Invitrogen), 0.5 µl (10 mM) 2'-deoxynucleoside 5'-triphosphates (dNTPs) (Bioline) and 0.75 µl (30 U) RNasin ribonuclease inhibitor (Promega) to limit RNA degradation and improve total cDNA quality. Nuclease-free water was added to achieve a total volume of 20µl. Reactions were then incubated at 42^{o}C in a heat block for 1 hour followed by heat inactivation at 70^{o}C for 10 minutes. cDNA samples were stored at -20^{o}C until required. Representative control experiments without reverse transcriptase were performed to ensure that any PCR amplicon was derived from synthesized cDNA rather than genomic DNA. Mouse brain and commercial human brain mRNA (Thermo Fisher Scientific available from Ambion®) was transcribed to cDNA as a positive control for the gene of interest (Figure 2.8).

2.9.4 RT-PCR

RT-PCR reactions were performed in an Applied Biosystems Veriti Thermal Cycler PCR machine (Thermo Scientific, UK). Primers and PCR conditions used within this study can be found in (Table 2.7). The amplification reactions were prepared in a PCR tube containing 1µg cDNA (± reverse transcriptase), 25µl ReadyMix™ Taq PCR (Sigma-Aldrich, Merck, UK), 1µl forward and reverse primers (at a final concentration of 0.2µM) and nuclease-free water to a final volume of 50 µl. Once each sample reaction was thermally cycled, the resulting PCR reactions were stored at 4°C short term or at -20^{o}C long term. To investigate human P2Y11, 25µl OneTaq® 2X Master Mix with Standard Buffer (New England BioLabs) was used instead of the Master Mix used for other P2 receptors (Figure 2.8).

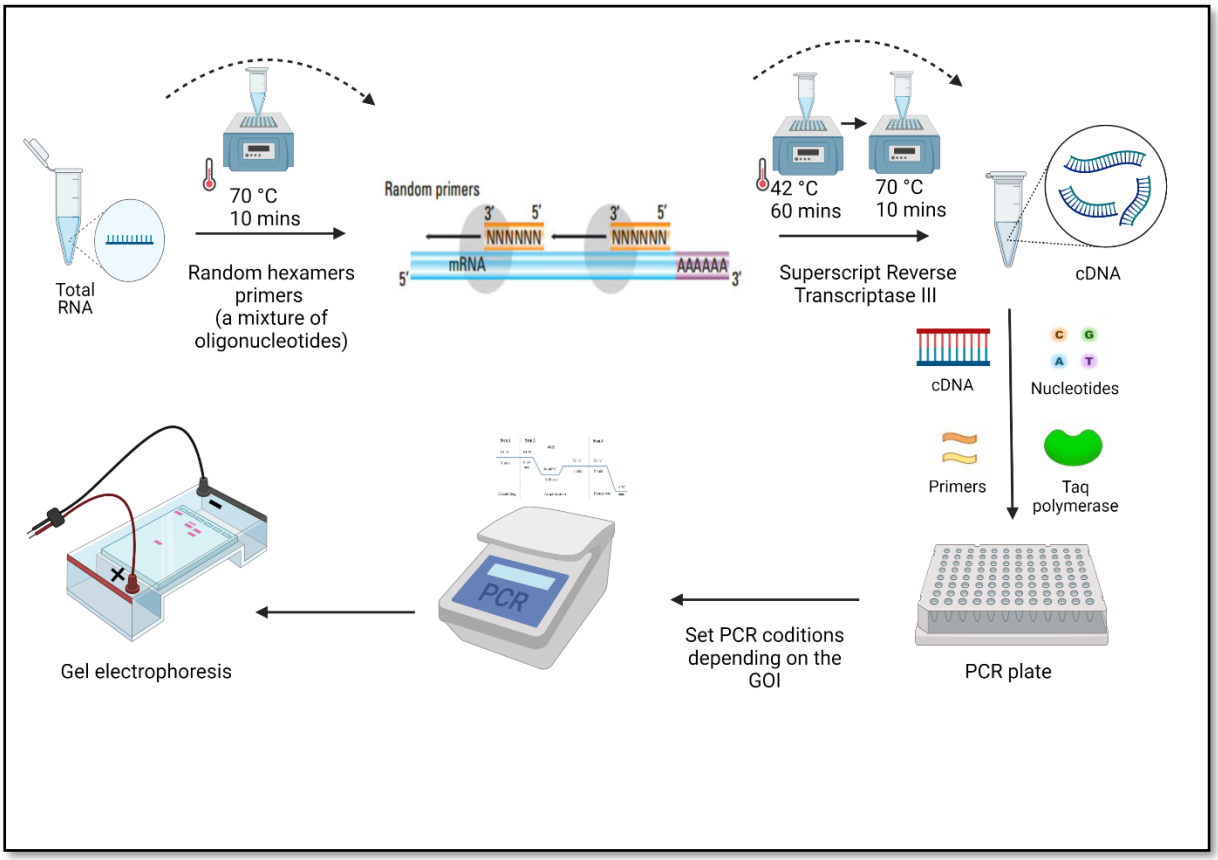

Figure 2.8: cDNA synthesis and RT-PCR. cDNA synthesis was achieved by the addition of random hexamer primers, followed by treating samples with Superscript reverse transcriptase III as per manufacturer instructions. PCR reactions were performed using the PCR cycles shown in (Table 2.7) and DNA fragments were separated using a 1.5% agarose gel. GOI, gene of interest

Table 2.7: Cycling conditions used in the RT-PCR reactions.

The PCR conditions were employed for each gene of interest				
Step		**Temperature ºC**	**Duration (mins)**	**Cycles**
Initial Denaturation		94 ºC	1	1
Amplification	Denaturation	94 ºC	0.5	40X
	Annealing	50-60 ºC	0.5	
	Elongation	72 ºC	1	
Final Elongation		72 ºC	5	1

2.9.4.1 Agarose gel electrophoresis

Agarose gel electrophoresis is a widely used technique for separating DNA fragments according to their size and charge allowing visualization on a gel by adding ethidium bromide. Ethidium bromide is a DNA intercalator, introducing itself between the base pairs in the double helix. To achieve this, a 1.5% (w/v) agarose gel was prepared by dissolving agarose (Thermo Fisher Scientific) in 150 ml of water. This solution was heated in a microwave to ensure that the agarose was fully dissolved. Following cooling, 3 ml of 50X Tris-acetate-EDTA (TAE) buffer (Thermo Fisher Scientific) was added. Then, 0.5 µg/ml ethidium bromide was added to the mixture to visualize the DNA under ultraviolet (UV) light. Using a gel mould with 20 wells comb, the agarose- ethidium bromide mixture was slowly poured into the mould.

The gel was left to solidify at RT for 30 mins. Twenty-five µl of PCR products for each gene of interest were then mixed with 5 µl of 6X gel loading dye (New England Biolabs) at a ratio of 5:1 (total volume 30 µl) followed by centrifugation. When the agarose gel was set, the multi-well comb was removed and the gel was placed in an electrophoresis tank containing 1X TAE buffer. The PCR reactions for each gene of interest (30 µl) were loaded alongside 6 µl Quick-Load® 100 bp DNA Ladder (New England BioLabs, UK). Electrophoresis was conducted at 100 V until the dye line was approximately 75-80% of the way down the gel. Based on gel concentration and voltage, a typical run time was approximately 60 to 90 mins. Once the gel electrophoresis run was finished, the DNA fragments were observed under UV illumination using a ChemiDoc™ XRS visualizer (Bio-Rad) (Figure 2.8). At least five separate RT-PCR experiments using five different mice were performed to investigate the expression of each P2 receptor. GADPH and β-actin were used as a house-keeping gene.

2.9.4.2 Primer design

Tables 2.8-2.12 contains the primer sequences that were used during the PhD. Primers were designed using the Primer Designing Tool on the NCBI website, or designed manually by previous PhD students, Dr Hinnah Campwala and Dr Seema Ali. All primers were purchased in a lyophilised from Thermo Fisher Scientific, apart from human P2X4 primers which were obtained from Merck. Primers were diluted to 10 µM working solutions after being reconstituted to 100 µM stocks in nuclease-free water. Both the 100 µM stocks and 10 µM of the prepared primers were stored at -20^{o}C. Some considerations were taken when the primers were designed, according to Thermo Fisher Scientific, are;

- In order to improve binding, the GC content of a primer should be between 40 and 60%, with the 3' of the primer terminating in G or C.
- Placed on the coding DNA sequence of the gene of interest.
- Limited cross homology with other genes.
- A suitable length for PCR primers is usually between 18 and 30 bases in length.
- The typical melting temperature (Tm) of the primers is between 60-65 ^{o}C and within 5°C of each other.
- Repeats of four or more nucleotides of the same base should be avoided.
- Primer pairs should not have complementary regions.
- Targets all variants of selected gene.
- Recommended product size is ≥ 200 bp where possible.

Table 2.8: Primer sequences for mouse P2X receptors.

Primer sequences for mouse P2X receptors				
Gene	**GenBank N (Accession)**	**Primers Sequence (5'>3')**	**Product size**	**Annealing Temp ºC**
P2X1	NM_008771.3	F: CTGGGGAGGGTGAACGTGA R: GCAGTCACAGGCCAAAAGTG	505	52.5
P2X2	NM_153400.4	F: CGGGGTGGGCTCCTTTCTGT R: GGACATGGTTACTGAAGAGCG	499	52.5
P2X3	NM_145526.2	F: AGCTGGTGAGCTGGGATAGA R: AACCCACCCCACAAAGTAGG	533	52.5
P2X4	NM_011026.3	F:TCACCCTCTTGGTAAAGAACAAC R: CACGGTCGCCACCCCTA	500	52.5
P2X5	NM_033321.3	F: CCTGAAGGGCGGTGTGATAG R: ATCTGTTCCCTGCCAAGAGC	647	55
P2X6	NM_011028.2	F: CAGGCCAAGAACTTCACACTC R: GGGGCTCTTGCCTCTTCATATT	566	55
P2X7	NM_011027.3	F: GCTCCTAGGTGAGGGTTTGC R: GGCAAGATGTTTCTCGTGGT	712	52.5

Table 2.9: Primer sequences for mouse P2Y receptors.

Primer sequences for mouse P2Y receptors				
Gene	**GenBank N (Accession)**	**Primers sequence (5'>3')**	**Product size**	**Annealing Temp ºC)**
P2Y1	NM_008772.5	F: TTATGTCAGCGTGCTGGTGT R: AGGGATGTCTTGTGACCATGT	668	58
P2Y2	NM_008773.4	F: TCTAGAGCGTGATCTCGGAGT R: TAAATGGCCAGTGGTCACCC	516	58
P2Y4	NM_020621.4	F:AGCCCAAGTTCTGGAGATGGTG R: GGTGGTTCCATTGGCATTGG	492	60
P2Y6	NM_183168.2	F: TTGCATGAGACAGACTCTCCG R: CACGACTCCACACACTACCC	500	52.5
P2Y12	NM_027571.4	F:ACCCTACAGAAACACTCAAGGC R: CAGGGTGTAGGGAATCCGTG	978	52.5
P2Y13	NM_028808.3	F: AAACAAAGCTGATGCTCGGGA R: TGTGACTGACCACCTGATGC	591	52.5
P2Y14	NM_001287123.1	F: GCTGACTTTCTCATGGGCCT R: AGGGGATTCTGGCAATGTGG	571	52.5

Table 2.10: Primer sequences for mouse markers of neurons, smooth muscle cells and endothelial cells.

Primer sequences for markers of mouse neurons, endothelial cells and smooth muscle cells				
Gene	**GenBank N (Accession)**	**Primers sequence (5'>3')**	**Product size**	**Annealing Temp ^{o}C**
PGP9.5	NM_011670.2	F: TCCCCCGAAGATAGAGCCAA R: CACATCCAGGGCCGTAACTT	555	53
VAChT	NM_003055.3	F: GTGCGCCACGTATCAGTCTA R: GGGTCACGGAGAAGGGATTC	527	53
TH	NM_009377.2	F: GCCGTCTCAGAGCAGGATAC R: TGGGTAGCATAGAGGCCCTT	692	53
CGRP	NM_001033954.3	F: GCTCACCAGGAAGGCATCAT R: GAAGGCTTCAGAGCCCACAT	375	53
SP	NM_009311.3	F: CAAGGAGAGCAAAGAGCGCC R: TGAGAGAGACGCACAGGAGT	808	53
nNOS	NM_008712.3	F: TCCTAACTGGATCCTCCCGC R: TTCACGAAGGCAGTGGACTC	537	53
α-SMA	NM_007392.3	F: CCTGAAGAGCATCCGACACT R: GCTGTTATAGGTGGTTTCGTGG	552	52.5
vWF	NM_011708.4	F: CGTTATAACAGCTGTGCGCC R: CGGATGCGCTTCTGAGAGAT	512	52.5

Gene	GenBank N (Accession)	Primers sequence (5'>3')	Product size	Annealing Temp ºC
GAPDH	NM_001289726.1	F: ACAGTCCATGCCATCACTGCC R: GCCTGCTTCACCACCTTCTTG	266	52.5

PGP9.5, protein gene product 9.5; VAChT, vesicular acetylcholine transporter; TH tyrosine hydroxylase; CGRP, calcitonin gene-related peptide; SP, substance P; nNOS, neuronal nitric oxide synthase; α-SMA, α-smooth muscle actin; vWF, von Willebrand factor; GAPDH, glyceraldehyde 3-phosphate dehydrogenase.

Table 2.11: Primer sequences for human P2X receptors.

Primer sequences for human P2X receptors				
Gene	**GenBank N (Accession)**	**Primers sequence (5'>3')**	**Product size**	**Annealing Temp**
P2X1	NM_002558.2	F: GCTTTCCACGCTTCAAGGTC R: GAGGTGACGGTAGTTGGTCC	341	60
P2X2	NM_170682.2	F: GCACAGACGGGTACCTGAAG R: GGAGTACTTGGGGTTGCACT	200	60
P2X3	NM_002559	F: TGTATCAGACAGCCAGTGCG R: CGGATGCCAAAAGCCTTCAG	564	60
P2X4	NM_002560.3	F: TTACGACCAAGGTCAAGGGC R: CCTGTTGAGACTCCGTTGCT	250	55
P2X5	NM_002561.3	F: GCAATGTGATGGACGTCAAGG R: GTACCCGGAGGAGACAGACT	263	55
P2X6	NM_005446.3	F: GACTTCGTGAAGCCACCTCA R: TTGTGGTTCATAGCGGCAGT	405	55
P2X7	NM_002562.5	F: CGGTTGTGTCCCGAGTATCC R: AATGCCCATTATTCCGCCCT	414	55

Table 2.12: Primer sequences for human P2Y receptors.

Primer sequences for human P2Y receptors				
Gene	**GenBank N (Accession)**	**Primers sequence (5'>3')**	**Product size**	**Annealing Temp**
P2Y1	NM_002563	F: GTTCAATTTGGCTCTGGCCG R: TTTTGTTTTTGCGGACCCCG	326	55
P2Y2	NM_002564.2	F: CCGCACCCTCTACTACTCCT R: TCAGTTCTGTCGGATCTGCG	243	55
P2Y4	NM_002565	F: CCCCAACCCTATGGCTCTTC R: TGGTCAAACTCTTCAGGCCG	427	55
P2Y6	NM_183168.2	F: GCTCTCACTGTCATCGGCTT R: TCTGCCATTTGGCTGTGAGT	391	55
P2Y11	NM_176798	F: CATGGCAGCCAACGTCTCG R: CAGGCTATACGCTCTGTAGGC	622	60
P2Y12	NM_022788	F: ACTGGGAACAGGACCACTGA R: CAGAATTGGGGCACTCAGC	698	55
P2Y13	NM_176894	F: TTCCCAGCCCTCTACACAGT R: GGCCCCTTTAAGGAAGCACA	461	55
P2Y14	NM_001081455	F: CGGAAGTGGCACAAAGCATC R: CCCTAAAACGGCTGGCATAGA	370	55

Gene	GenBank N (Accession)	Primers sequence (5'>3')	Product size	Annealing
β-actin	NM_001101.5	F: CACAGAGCCTCGCCTTTGCC R: CGATGCCGTGCTCGATGGGG	282	55

2.10 Whole-mount preparations for immunohistochemistry

To confirm the expression of the candidate P2 receptors on the perivascular nerves of the mouse blood vessels including superior mesenteric artery and carotid artery, colocalisation of the candidate P2 receptors and neuronal markers (such PGP9.5 and TH) were visualised using whole-mount preparations of superior mesenteric artery and carotid artery. In addition, studies exploring the colocalisation of the P2 receptors and VNUT or NPY were performed. To perform these colocalisation experiments, superior mesenteric artery (1^{st} order [300 - 400 µm] in diameter) and carotid arteries were isolated from male mice and immediately placed in cold HBSS to remove excess blood, and arteries were further cleaned of excess fat and connective tissue. The tissues were then fixed in 4% paraformaldehyde (PFA) diluted in PBS for 30 minutes. After fixation, the tissues were washed repeatedly in PBS 3 times for 5 minutes with gentle agitation. The specimens were incubated for 1 hour at RT in a blocking buffer (Table 2.13) of PBS containing 8% bovine serum albumin (BSA) and 10% normal goat serum (Fisher Scientific) to block endogenous peroxidase activity and nonspecific binding of antibodies, and 0.5% Triton X-100 for permeabilization. Thorough washing via PBS/Triton 0.5% three times for 5 minutes after blocking was performed to remove excess protein which could inhibit detection of the target antigen. The tissues were then incubated overnight at 4°C with the appropriate polyclonal primary antibodies diluted in the blocking buffer (Table 2.14). Control samples were incubated without primary antibodies as a negative control for non-specific secondary antibody staining. For immunofluorescence staining, the samples were then incubated for 1 hour at RT with secondary antibodies diluted in blocking buffer (Table 2.15). Afterwards, the tissues were thoroughly washed in PBS/ Triton 0.5% and the samples were mounted on slides with 20 µl of VectaMount™ Permanent Mounting Medium (Vector Laboratories, UK) and coverslips added. The slides were air-dried at RT, protected from light. Colocalisation experiments achieved in this project were performed at least three independent times.

Table 2.13: Blocking buffer used for immunohistochemistry experiments.

Blocking buffer components		
Components	**Concentration (Whole mount preparations)**	**Concentration (Frozen sections and cells)**
PBS 1X	-	-
Triton X-100	0.5% (v/v)	0.1% (v/v)
Normal goat serum	10% (v/v)	10% (v/v)
BSA	8% (w/v)	1% (w/v)
Storage at -20°C for ~ 6 months		

BSA, bovine serum albumin.

Table 2.14: Primary antibodies used for immunofluorescence experiments.

Primary antibodies used for immunofluorescence experiments				
Antibody	**Clonality**	**Company**	**Code number**	**Dilution**
Primary antibodies				
Rabbit anti-P2X1 (KO Validated)	Polyclonal H, M, R	Alomone	APR-001	1:200 (Vial & Evans, 2000)
Rabbit anti-P2X2 (KO Validated)	Polyclonal H, M, R	Alomone	APR-003	1:200 (Vial & Evans, 2000)
Rabbit anti-P2X3	Polyclonal H, M	Thermo Fisher Scientific (Invitrogen)	PA5-30894	1:100
Rabbit anti-P2X4 (KO Validated)	Polyclonal H, M, R	Alomone	APR-003	1:200 (Vial & Evans, 2000)
Rabbit anti-P2X6	Polyclonal H, M, R	Alomone	APR-013	1:200 (Antonio et al., 2009)
Rabbit anti-P2X7 (KO Validated)	Polyclonal H, M, R	Alomone	APR-004	1:200 (Antonio et al., 2009)
Rabbit anti-P2Y1	Polyclonal H, M, R	Aviva System Biology	OAAN02379	1:500

Antibody	Clonality	Company	Code number	Dilution
Sheep anti- TH	Polyclonal H, M, R	Thermo Fisher Scientific (Invitrogen)	PA1-4679	1:500 (Calkoen et al., 2015)
Chicken anti- TH	Polyclonal H, M, R	Abcam	ab76442	1:500 (Liu et al., 2021)
Sheep anti-NPY	Polyclonal H, M, Rb	Abcam	ab6173	1:200
Guinea pig anti-PGP9.5	Polyclonal H, M, R	Abcam	Ab10410	1:500 Danilova et al., (2019)
Rabbit anti-PGP9.5	Polyclonal H, M, R	Abcam	ab27053	1:1000
Guinea pig anti-VNUT	Polyclonal M, R	Sigma-Aldrich	ABN83	1:1000 (Stamboulian et al., 2010)

H, human; M, mouse; R, rat.

Table 2.15: Secondary antibodies used for immunofluorescence experiments.

Secondary antibodies used for immunofluorescence experiments				
Antibody	**Clonality**	**Company**	**Code number**	**Dilution**
Secondary antibodies				
Goat Anti-Guinea pig IgG H&L (Alexa Fluor® 647)	Polyclonal Guinea pig	Abcam	ab150187	1:500 (Chinen et al., 2020)
Goat Anti-Guinea pig IgG H&L (Alexa Fluor® 488)	Polyclonal Guinea pig	Abcam	ab150185	1:500 (Guo et al., 2021)
Donkey Anti-Rabbit IgG H&L (Alexa Fluor® 488)	Polyclonal Rabbit	Abcam	ab150073	1:500 (Rudnitskaya et al., 2020)
Donkey Anti-Rabbit IgG H&L (Alexa Fluor® 647)	Polyclonal Rabbit	Abcam	ab150075	1:500 (Liu et al., 2021)
Goat Anti-Chicken IgY H&L (Alexa Fluor® 647)	Polyclonal Chicken	Abcam	ab150171	1:400 (Balashova et al., 2019)
Goat Anti-Chicken IgY H&L (Alexa Fluor® 488)	Polyclonal Chicken	Abcam	ab150173	1:500 (Mizuno et al., (2020)
Donkey Anti-Sheep IgG H&L (Alexa Fluor® 647)	Polyclonal Sheep	Abcam	ab150179	1:200 (Ouyang et al., 2021)

2.11 Cryostat sectioning for immunohistochemistry

Superior cervical ganglion, superior mesenteric arteries (the1storder [300 – 400 µm] in diameter) and carotid arteries were dissected from male mice and immediately placed in cold HBSS to remove excess blood, prior to removal of excess fat and connective tissue. The tissues were then fixed in 4% PFA diluted in PBS for 30 minutes. After fixation, the tissues were washed twice for five minutes in PBS. To displace the water from the tissues, the tissues were saturated with 30% sucrose in PBS overnight at 4^{o}C or until the tissues were sunken. Next, the tissues were placed in a base mould and covered with optimal cutting temperature (OCT) compound (Agar Scientific) on dry ice. The mould was then stored at -80 until required. Afterwards, 10µm sections were acquired using a Microm HM-560 cryostat (Thermo Scientific, UK). The sections were mounted onto coverslips and placed into a 12 well-plate prior to air-drying for 10 minutes or storage at -80 C until required. The sections were then washed with warm PBS (37^{o}C) to remove the OCT. The sections were permeabilised and non-specific binding was blocked by incubating for 1 hour RT in a blocking solution of PBS containing 1% BSA, 10% normal goat serum (Fisher Scientific) and 0.1% Triton X-100 (Table 2.13). Following three 5-minute washes in PBS/Triton 0.1%, the sections were incubated overnight at 4°C with polyclonal primary antibodies (Table 2.14) diluted in blocking buffer. Some sections were incubated without primary antibodies as a negative control for non-specific secondary antibody staining. In the case of using blocking antigen as a negative control, the primary antibody was pre-incubated with its blocking peptide (1:1 in mg/ml) for 1 hour at RT. Then, the sections were incubated for 1 hour at RT with secondary antibodies (Table 2.15) diluted in the blocking buffer. Thereafter, the tissues were thoroughly washed in PBS/T 0.1% and the samples were mounted on slides with Fluoroshield Mounting Medium with DAPI (Abcam). This mounting media prevents photobleaching while DAPI was used to detect nuclear staining. The slides were air-dried at RT and protected from light (Figure 2.9). At least five independent experiments in triplicate were performed.

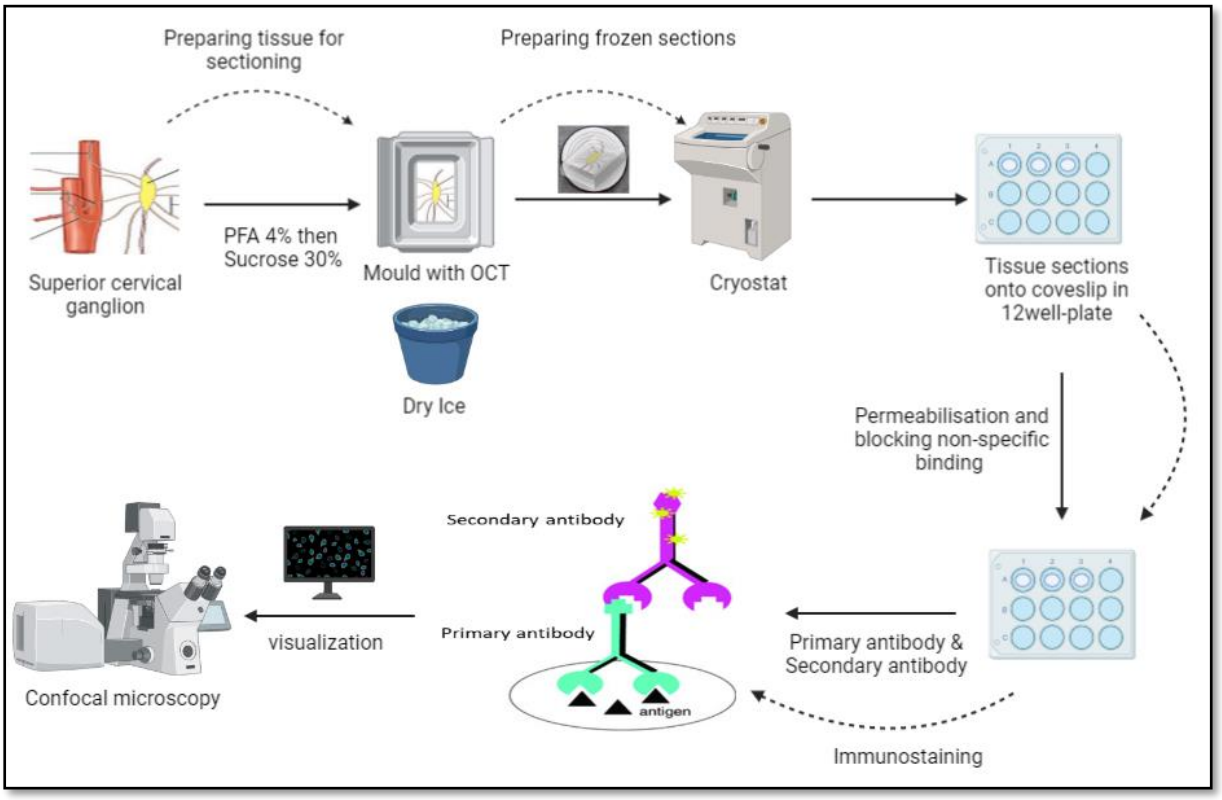

Figure 2.9: Immunohistochemistry using cryosectioning. Superior cervical ganglion was removed from mouse and fixed with 4% PFA followed by saturation with 30% sucrose. The tissue was then sectioned using the cryostat and placed onto coverslips before being allowed to dry. The sections were permeabilized and blocked in the appropriate permeabilization/blocking buffer. Then, the sections were immunostained with the primary antibody overnight, followed by the secondary antibody. Finally, the sections were visualised using confocal microscopy.

2.12 Immunocytochemistry

To confirm the SH-SY5Y cells were differentiated to neurons and to confirm the expression of candidate P2 receptors on human undifferentiated SH-SY5Y cells and differentiated SH-SY5Y cells, immunocytochemistry was performed. To achieve this, human SH-SY5Y cells (35000/well) were seeded onto Poly-D-lysine hydrobromide coated-coverslips (0.1mg/ml) (Sigma-Aldrich) in a 24 well-plate and incubated with 400 µl/ culture media (Table 2.3) at 37^{o}C in the presence of 5% CO_2 for 48 hours. In the case of differentiated SH-SY5Ycells, the culture media was replaced after 48 hours of seeding cells with the differentiation media (Table 2.4) and incubated at 37^{o}C in the presence of 5% CO_2 for 5 days. The culture or differentiating media was then gently aspirated off and the cells washed with PBS twice. This was followed by fixation with 4% PFA for 15 minutes. Following washing with PBS, the cells were permeabilised and non-specific binding was blocked by incubating the cells in a blocking buffer consisting of 10% normal goat serum, 1% bovine serum albumin and 0.1 % Triton X-100 in PBS (Table 2.13). This was typically performed for 1 hour at RT with gentle agitation. The cells were then incubated with the respective primary antibodies diluted in the blocking buffer overnight at 4^{o}C. As a negative control for non-specific secondary antibody binding, the cells were incubated without primary antibodies. The following day, the excess primary antibody was removed, cells were washed with PBS, and the cells were incubated with the appropriate secondary antibodies diluted in blocking buffer for 1 hour. Finally, the cells were mounted onto glass slides using Fluoroshield Mounting Medium with DAPI (Abcam) and images were taken using confocal microscopy. At least three separate experiments in triplicate were performed.

2.13 Microscopy

2.13.1 Confocal microscopy

Tissues were visualised at the Henry Welcome Laboratory for Cell Imaging, using Laser-scanning confocal microscope Zeiss LSM510 META (Zeiss), equipped with an excitation filter system of Alexa Fluor 458/488 nm and Alexa Fluor 647. Images were captured using an objective magnification of 10-20X, with serial z-stacks taking 7-10 optical sections at 10 µm each. Images for each sample were standardized to corresponding negative controls (as prepared above in section (2.10). These 7-10 optical images of the sections were scaled and overlapped together using Image J software.

2.13.2 Apotome microscopy

Images were captured as a single section (10 µm thickness) under 10X and 20X objectives. Images were merged, scaled and the cell bodies of neurons were counted using ImageJ Fiji. The presented images of superior cervical ganglion sections in this thesis were acquired by confocal microscopy. Data analysis was performed on all fluorescent images acquired, using the Zeiss Apotome Imager M2 microscope (Axiovert 200M) equipped with a Zeiss AxioCam HRm and the Axiovision 4.8 software.

2.14 Western Blot

2.14.1 Protein extraction

Western blots were performed to confirm the protein expression of the genes of interest and to confirm the antibodies used in immunofluorescence experiments were specific for the protein of interest.

In the case of the SH-SY5Y cells, the cells were seeded onto a 6-well plate in a humidified incubator at 37ºC in the presence of 5% CO_2. Once a cell line reached about 80% confluence, the cells were washed with cold PBS and scraped off the 6-well plate using 50 µl/well of cold radioimmunoprecipitation assay (RIPA) buffer (Table 2.16) containing protease inhibitor (Complete-EDTA; Roche), transferred into 1.5ml Eppendorf and kept on ice for 30 mins. The cells were then homogenised for 20 seconds twice using a homogenizer (BioSpec Products Mini-BeadBeater) followed by centrifugation at 12,000 rpm for 20 minutes at 4ºC. The supernatant containing the whole cell extract was then gently transferred into a fresh Eppendorf and protein concentration was measured using Pierce™ BCA Protein Assay Kit (Thermo Fisher Scientific). Mouse tissues (superior cervical ganglion, superior mesenteric artery and carotid artery) were lysed with 250 µl of cold RIPA buffer containing protease inhibitor and the same protocol was followed. Mouse brain was used as a positive control for mouse P2 receptors (Figure 2.12).

Table 2.16: RIPA buffer used to prepare whole cell lysates.

RIPA buffer components	
Component	Concentration
Tris-HCl	50 mM
NaCl	150 mM
NP40	1% (v/v)
Sodium deoxycholate	0.5% (w/v)
SDS	0.1% (v/v)
H2O	Up to 100 ml
pH = 7.6	
Storage at 4°C for ~ 6 months	

NP40, nonyl phenoxypolyethoxylethanol; SDS, sodium dodecyl sulfate.

2.14.2 BCA protein assay

To determine concentrations of unknown protein in the samples, serial dilutions of BSA were prepared. Briefly, a 1 ml ampule of 2 mg/ml Albumin Standard was diluted with water into clean Eppendorfs. The bicinchoninic acid (BCA) working reagent was then prepared by mixing 50 parts of BCA Reagent A with 1 part of BCA Reagent B (e.g., 10 ml of A + 0.2 ml of B). In a 96 well-plate, 25 µl of each BSA dilution and 25µl of the total extracted protein were loaded into the wells. Next, 200 µl of the working reagent was added to each well and the plate was mixed gently on a plate shaker for 30 seconds. The plate was then covered and incubated at 37^{o}C for 30 minutes. The absorbance was then measured at 562 nm on a FlexStation III microplate reader (Molecular Devices). Finally, a standard curve was used to determine the protein concentration of each unknown sample (Figure 2.10, 2.12).

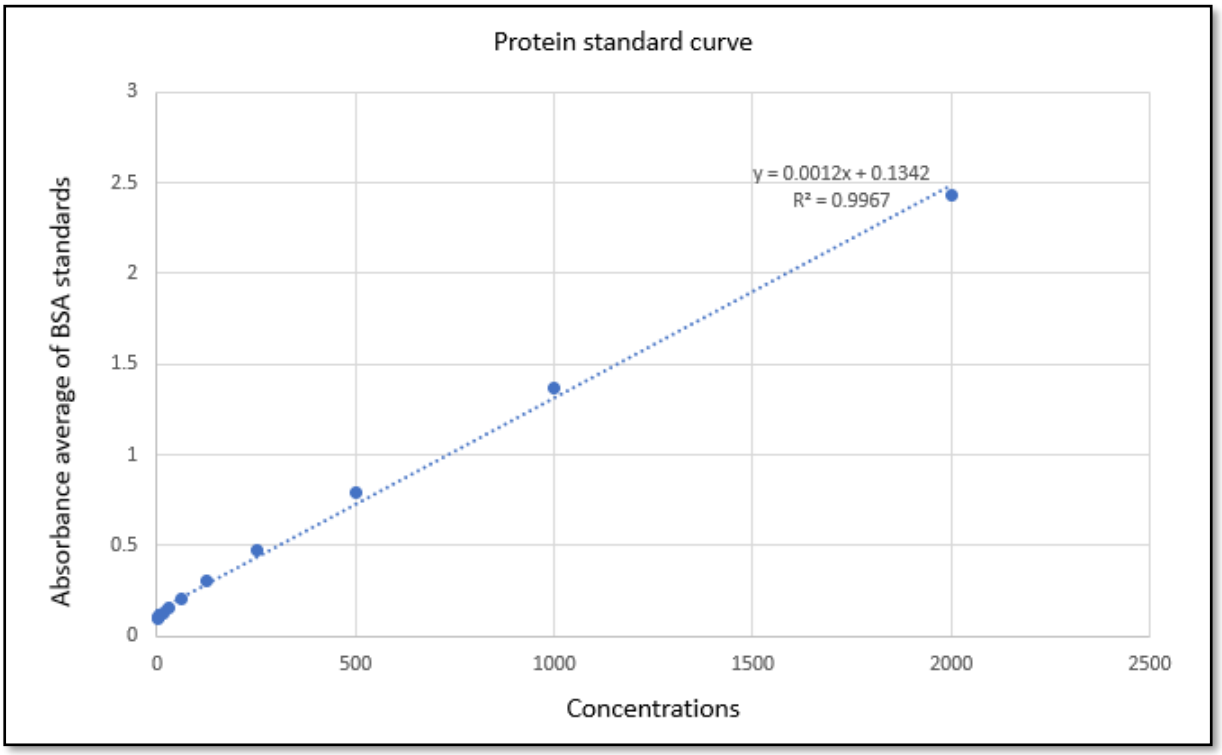

Figure 2.10: **BSA standards curve plotted against absorbance to quantify unknown protein concentrations**. This standard curve of protein concentration vs absorbance was used to determine unknown protein concentrations. R^2 =0.9967; coefficient of the slope b= 0.0012, and intercept = 0.1342 was used to calculate protein concentration in µg/ml. Where y is absorbance and x is concentration. In a standard reaction, 25 µl of each BSA concentration and unknown sample were mixed with 200 µl of the BCA working reagent and then incubated at 37ºC for 30 minutes. The absorbance was then measured at 562 nm. The calibration curve is needed to calculate sample concentration.

2.14.3 SDS polyacrylamide gel electrophoresis (SDS-PAGE) and gel transfer

The SDS polyacrylamide gel composed of a 10% separating (resolving) gel and a 5% stacking gel (Tables 2.17 & 2.18), was prepared to separate and identify specific proteins (P2X or P2Y), depending on the molecular weight and charge, from a complex mixture of total proteins extracted from cells or tissues. Next, 30 μg of total protein from cell lysates or tissue homogenates were boiled for 5 minutes at 95^{o}C with 7.5 μl of NuPAGE LDS sample buffer 4X (Thermo Fisher Scientific), 3 μl of NuPAGE™ sample reducing Agent (dithiothreitol, DTT) 10X (Thermo Fisher Scientific) and water to achieve a total volume of 30 μl. The samples were then centrifuged to remove condensation. The 10% SDS-polyacrylamide gel was prepared the day before and stored at 4^{o}C. The gel was run in an electrophoresis tank filled with running buffer (1X) at 100 V for 90-120 minutes (Figure 2.12, Tables 2.19 & 2.20).

The gel containing the separated proteins, was then transferred to a polyvinylidene difluoride (PVDF) membrane and activated with methanol for 1-2 minutes. To transfer the protein to the PVDF membrane, the cassette was prepared using a “sandwich” of sponge, filter papers, PVDF membrane and the gel, taking care to remove all bubbles. Next, the cassette was placed into an electrophoresis tank where the gel sits at the negative end and the membrane at the positive end (Figure 2.11). The electrophoresis tank was filled with transfer buffer (1X) (Table 2.19, 2.20) an electrical current was passed through for 60 minutes at 100 V. Once transfer had finished, transfer of proteins to the membrane was validated via Ponceau S staining before the blocking step (Figure 2.12).

Table 2.17: Polyacrylamide gel (separating gel- stacking gel) components.

Polyacrylamide gel components		
Component	**Separating gel 10%**	**Stacking gel 5%**
	Volume (10 ml)	**Volume (5 ml)**
Separating or Stacking Buffer (4X)	2.5 ml (Separating buffer)	1.25 ml (Stacking buffer)
Acrylamide 30% (37.5.1) (Bio-Rad)	3.3 ml	0.833 ml
H_2O	4 ml	2.862 ml
APS 10%	150 µl	50 µl
TEMED (Sigma-Aldrich)	50 µl	6 µl
Storage at 4 ^{o}C for ~ 1 -2 days		

APS, ammonium persulfate; TEMED, tetramethylethylenediamine.

Table 2.18: Preparation of separating (resolving) buffer and stacking buffer.

Separating (resolving) buffer (4X) components		
Component	**Concentration**	**Mass**
Tris Base	0.5 M	90.85 g
SDS	0.4% (w/v)	20 g
H_2O	Up to 500 ml	
pH = 8.8		
Storage at RT for ~ 1 year		
Stacking buffer (4X) components		
Component	**Concentration**	**Mass**
Tris Base	0.5 M	30.30 g
SDS	0.4% (w/v)	20 g
H_2O	Up to 500 ml	
pH = 6.8		
Storage at RT for ~ 1 year		

SDS, sodium dodecyl sulfate.

Table 2.19: Preparation of running buffer (10X) and transfer buffer (10X).

Running buffer (10X) components		
Component	**Concentration**	**Mass**
Tris Base	25 mM	30 g
SDS	0.1% (w/v)	10 g
Glycine	192 mM	144 g
H_2O	Up to 1000 ml	
Storage at RT for ~ 1 year		
Transfer buffer (10X) components		
Component	**Concentration**	**Mass**
Tris Base	15 mM	18.1 g
Glycine	120 mM	90 g
H_2O	Up to 1000 ml	
Storage at 4^oC for ~ 1 year		

SDS, sodium dodecyl sulfate.

Table 2.20: Preparation of running buffer (1X) and transfer buffer (1X).

Running and transfer buffer (1X) components		
	Running buffer (1X)	**Transfer buffer (1X)**
Component	**Volume (1000 ml)**	**Volume (1000 ml)**
Running or Transfer Buffer (10X)	100 ml (Running Buffer 10X)	100 ml (Transfer Buffer 10X)
Methanol (100%)	-	200 ml
H_2O	900 ml	700 ml
Prepared before use		

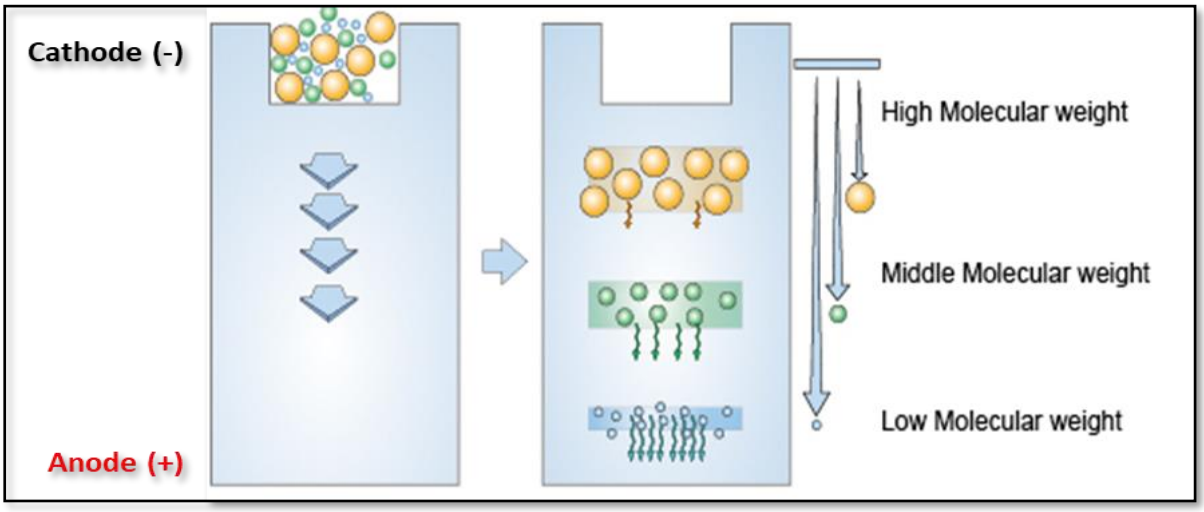

Figure 2.11. Protein migration and separation in SDS-PAGE. Proteins were separated under electric fields based on different molecular weights. High molecular weight proteins migrate from the negative (cathode) to the positive anode slower than proteins with lower molecular weight. Adapted from (The Basis of Western Blot - Creative Diagnostics, 2021).

2.14.4 Blocking, antibody staining and imaging

Protein transfer was checked by Ponceau staining. The membrane was washed gently with water and then blocked with 5% blocking buffer (Table 2.21) for 1 h at RT. The blocking buffer was then removed and washed with washing buffer twice (PBS/ Triton 0.1%) (Table 2.22). Immunoblotting was performed by incubating the membrane overnight with the appropriate dilutions of primary antibodies in the blocking buffer (Table 2.23). The following day, the membrane was washed with washing buffer for 5 minutes three times, then the membrane was incubated with the appropriate dilutions of secondary antibodies conjugated with horseradish peroxidase (HRP) in the blocking buffer at RT for 1 h (Table 2.24). Finally, the membranes were washed, and protein bands were visualized after incubation with the Pierce™ enhanced chemiluminescence Western blotting substrate (Thermo Fisher Scientific) (Figure 2.12). Images of the membranes were taken using a Las-3000 camera (Fujifilm, Japan), and analysed using BioImage software (Bio-Rad). All the buffers, primary antibodies and secondary antibodies used in Western blot experiments are in the attached table below. β-actin was used as a loading control. Some of the antibodies from Alomone came with a blocking peptide (the original antigen used for immunization during the generation of the polyclonal antibody). In this instance, this was used as a negative control to confirm that the primary antibody bound the target protein. In this case, the primary body was pre-incubated with its blocking peptide (1:1) for 1 hour at RT. Following incubation with the blocking peptide, the mixture was added to the samples and no band was detected.

Table 2.21: Preparation of blocking buffer used in Western blot.

Blocking buffer components	
Component	**Volume (50 ml)**
Milk 5% (w/v)	2.5 g
PBS / Triton X-100 [0.1% (v/v)]	Up to 50 ml
Storage at 4^{o}C for ~ 1 week	

Table 2.22: Preparation of washing buffer used in Western blot.

Washing buffer components	
Component	**Volume (1000 ml)**
PBS 1%	10 tablets
Triton X-100 [0.1% (v/v)]	1 ml
H_2O	Up to 1000 ml
pH = 7.3-7.5	
Storage at RT for ~ 1 year	

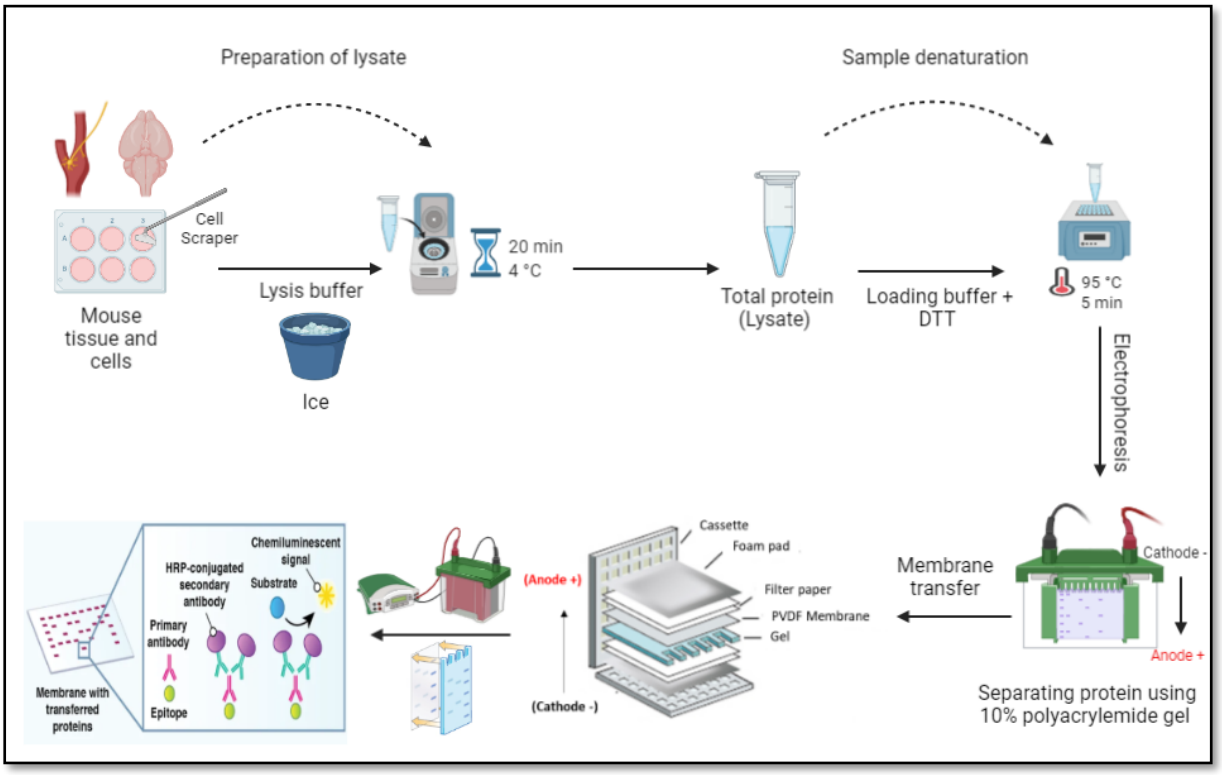

Figure 2.12: Western blot to detect specific protein molecules from a mixture of proteins. Mouse tissues or human cells were homogenized in lysis buffer. Lysates were acquired by centrifugation and protein concentration was quantified using a BCA protein assay kit. Proteins were separated via SDS-PAGE and transferred to a PVDF membrane. The membrane was then blocked with 5% milk in PBS/0.1% Triton for 1 hour at RT then incubated with the appropriate primary antibodies overnight. After three washes in PBS/Triton 0.1 %, the membrane was then incubated with HRP-conjugated secondary antibody for 1 hour at RT and visualized with an entry-level peroxidase substrate for enhanced.

Table 2.23: Primary antibodies used in Western blot.

Primary antibodies used in Western blot					
Antibody	**Predicted size in kDa**	**Clonality**	**Company**	**Code number**	**Dilution**
Primary antibody					
Rabbit anti-P2X1 (KO Validated)	55	Polyclonal H, M, R	Alomone	APR-001	1:1000 (Seref-Ferlengez et al., 2016)
Rabbit anti-P2X2 (KO Validated)	45-55	Polyclonal H, M, R	Alomone	APR-003	1:2000 (Rivera et al., 2007)
Rabbit anti-P2X3	44	Polyclonal H, M	Fisher Scientific (Invitrogen)	PA5-30894	1:500
Rabbit anti-P2X3	44	Polyclonal H, M, R	Alomone	APR-016	1:1000 (Seref-Ferlengez et al., 2016)
Rabbit anti-P2X3	44	Polyclonal H, M, R	Abcam	ab10269	1:500 (Sun et al., 2021)
Rabbit anti-P2X4 (KO Validated)	50	Polyclonal H, M, R	Alomone	APR-003	1:500 (Toulme et al., 2010)

Antibody	Predicted size in kDa	Clonality	Company	Code number	Dilution
Rabbit anti-P2X6	40	Polyclonal H, M, R	Alomone	APR-0013	1:500 (Toulme et al., 2010)
Rabbit anti-P2X7 (KO Validated)	69	Polyclonal H, M, R	Alomone	APR-004	1:2500 (Toulme et al., 2010)
Rabbit anti-P2Y1	42	Polyclonal H, M, R	Aviva System Biology	OAAN02379	1:500
Rabbit anti-P2Y1	42	Polyclonal H, M, R	Alomone	APR-009	1:1000 (Seref-Ferlengez et al., 2016)
Mouse Anti-β-Actin−Peroxidase	42	Monoclonal	Sigma-Aldrich	A3854	1:2000

H, human; M, mouse; R, rat.

Table 2.24: Secondary antibodies used in Western blot.

Secondary antibodies used in Western blot					
Antibody	**Predicted size in kDa**	**Clonality**	**Company**	**Code number**	**Dilution**
Goat anti-Rabbit IgG (H+L), HRP	-	Polyclonal	Thermo Fisher Scientific (Invitrogen)	A16096	1:5000 (Kim et al., 2016)

2.14.5 Calculation of molecular weight of proteins

Accurate prediction of protein molecular weight can be made based on the known molecular weights and composition of amino acids in a given linear chain sequence (Labs, J. 2021). To determine the molecular weight of each gene of interest (P2 receptors), the Ensembl website was used to search the gene of interest for specific species. Then, all transcripts (splice variants) of the gene of interest were shown in a table and by pressing export data the peptide sequence was generated for each transcript with protein coding. Then, each sequence of peptide was copied and pasted in Protein Molecular Weight – Bioinformatics website to calculate the expected molecular weight (Tables 2.25 & 2.26).

Table 2.25: The expected molecular weight of mouse P2 proteins studied in this project.

Mouse P2 proteins molecular weight					
Gene	**Transcripts (splice variants)**	**Protein coding**	**Molecular weight (kDa)**	**No protein**	**Nonsense-mediated decay**
P2X1	3	2	44.86 - 41.75	1	-
P2X2	6	5	46.73 - 44.39 53.95 - 55.05 43.96	1	-
P2X3	5	3	34.33 – 44.44 41.79	2	-
P2X4	9	4	43.5 – 40.31 38.14 – 41.33	4	1
P2X6	3	2	39.96	-	1
P2X7	8	5	68.4 – 49.38 50.69 – 17.2 67.78	3	-
P2Y1	3	3	42.22	-	-

Table 2.26: The expected molecular weight of human P2 proteins studied in this project.

Human P2 proteins molecular weight					
Gene	**Transcripts (splice variants)**	**Protein coding**	**Molecular weight (kDa)**	**No protein**	**Nonsense-mediated decay**
P2X2	8	8	51.76 – 54.52 49.27 – 41.26 43.73 – 41.38 44.85 – 38.92	-	-
P2X3	3	1	44.29	1	1
P2X7	13	1	68.46	1	11

2.15 Statistical analysis

All data were analysed using GraphPad Prism (v. 6) or Excel (Microsoft Corporation, USA). Data were first assessed for normality using a Shapiro-Wilk test. Statistical analysis between paired data was performed by means of Student's paired t-tests while unpaired data was performed by means of Student's unpaired t-tests statistical analysis. Experiments involving more than two treatment groups (e.g., nucleotide-evoked Ca^{2+} responses experiments) were compared by a one-way ANOVA followed by Tukey's multiple comparison test to determine which means amongst a set of means differ from the rest and to make confidence intervals for all pairwise differences between factor level means while controlling the family error rate to a level you specify (GraphPad Prism 6). Significance was only considered for p-values of 0.05 and under (*$p<0.05$, **$p<0.01$, ***$p<0.001$, ****$p<0.0001$). Data was represented as mean ±SEM (standard error of the mean) indicates how different the population mean is likely to be from a sample mean. n representing the number of experiments or replicates.

Chapter 3: Expression of P2 purinergic receptor mRNA transcripts in mouse superior cervical ganglion, superior mesenteric arteries and carotid artery

3.1 Introduction

Arterial tone determines local blood flow, total peripheral resistance to blood flow and systemic blood pressure. Arteries are innervated by autonomic nerves (mostly sympathetic) and sensory-motor neurons. These perivascular neurons located within the adventitia of arteries release neurotransmitters that can influence arterial tone by engaging purinergic receptors on arterial smooth muscle and the endothelium (Ralevic, 2009). Purinergic receptors could be expressed on perivascular nerves of blood vessels and play a significant role in modulating neurotransmitters release following ATP release (Sperlágh et al., 2007). The role of pre-junctional P2 receptors on perivascular nerves in controlling neurotransmitters release is still unclear and requires further investigation. Pharmacological manipulation of perivascular nerve activity has the potential to modulate arterial tone and alter blood pressure.

The superior cervical ganglion, originates from the neural crest cells, is involved in the autonomic nervous system, explicitly with sympathetic efferent innervation, providing innervation to the head and neck region (Maningat & Munakomi, 2021). The cervical sympathetic trunk, which is located on the prevertebral fascia medial to the carotid sheath, contains three interconnected ganglia: the stellate, middle cervical, and superior cervical ganglia (Yokota et al., 2018). The superior cervical ganglion is elongated and cylindric and the largest ganglion of the cervical sympathetic trunk, located at the level of C1-C2 vertebra lying anteromedial or medial to their respective internal carotid arteries (Maningat & Munakomi, 2021) (Figure 2.1). The cell bodies of post-ganglionic sympathetic neurons and small intensely fluorescent cells in superior cervical ganglion obtain their pre-ganglionic innervation from thoracic spinal cord (T1–T4) nerves that course within the ipsilateral cervical sympathetic chains (Getsy et al., 2004). The superior cervical ganglion regulates the sympathetic tone of the vasculature of the head and neck, pupillary diameter, salivation, and pineal biochemistry. The internal carotid nerve runs parallel to the internal carotid artery, eventually producing a plexus of nerves that innervate the internal carotid artery, pterygopalatine artery, critical eye structures, and induces sympathetic innervation to the head and blood vessels in the heart (Maningat & Munakomi, 2021; Loesch et al., 2010). Thus, the superior cervical ganglion has been involved in the pathogenesis of several cardiovascular diseases and neuropathies including Horner's syndrome, stroke, and epilepsy (Loesch et al., 2010). The external carotid network of nerves innervates the smooth muscle of arteries via the common and external

carotid arteries, with some fibres also innervating the sweat glands of the face via the internal maxillary artery (Maningat & Munakomi, 2021). Finally, it was reported that superior cervical ganglion includes several types of cells including glial cells, Schwann cells, small intensely fluorescent cells (interneurons of the sympathetic ganglia originating from the neural crest), fibroblasts, and mast (Fioretto et al., 2011). The external and internal carotid nerves are the two primary trunks that arise from the superior cervical ganglion and carry the majority of post-ganglionic nerves (Getsy et al., 2004).

The carotid arteries are two large blood vessels which emerge from the distal segment of the third aortic arch and carry oxygenated blood to the brain. The baroreceptors of the common carotid artery play a role in blood pressure regulation via the cranial nerves. The carotid sinus densely innervates several types of receptors that play an important role in the control of blood pressure. The baroreceptors send signals to the brain and the signals are interpreted as an increase in blood pressure. The brain then sends signals to other organs of the body such as the blood vessels, heart and kidneys to decrease blood pressure. The heart and blood vessels receive efferent signals from the carotid baroreceptors via parasympathetic and sympathetic nerves. This process is called carotid sinus baroreflex which induces appropriate changes to the heart rate and blood pressure to keep them within acceptable physiological limits (Andani & Khan, 2020). The cell bodies of pre-ganglionic neurons are located within the lateral grey horn of the first thoracic segment of the spinal cord. Pre-ganglionic fibres relay in the superior cervical ganglion whilst post-ganglionic fibres leave the ganglions to innervate the internal carotid artery (Freddo & Chaum, 2017).

Small arteries and arterioles are known to contribute significantly to systemic blood pressure by accounting for roughly 45% of peripheral resistance to blood flow through the vasculature. The superior mesenteric artery is the main artery of the abdomen. It arises from the abdominal aorta and supplies arterial blood to the organs of the midgut. The superior mesenteric artery then gives rise to various branches that supply the small intestines, caecum, and both the ascending and part of the transverse colon. Moreover, superior mesenteric arteries are a part of a network of vascular beds that regulate vascular resistance. Perivascular nerves such as sympathetic adrenergic nerves, and non-adrenergic non-cholinergic nerves (including CGRPergic nerves) are known to be involved in the innervation of resistance vessels, such as the mesenteric artery (Yokomizo et al., 2015). It was reported that perivascular nerves innervate the rat mesenteric arteries, which play an important role in maintaining vascular tone and regulating organ and tissue blood flow. Post-ganglionic adrenergic neurons are the most important efferent neural pathway to blood arteries, with a few exceptions (Yokomizo et al.,

2015). The mesenteric artery is another vessel where there is a major ATP contribution to sympathetic cotransmission.

Both families of P2X and P2Y receptors are widely expressed in all regions of the perivascular nervous system, in neuronal cell bodies and terminals, in satellite glial cells and Schwann cells, and in blood vessels including perivascular nerves, smooth muscle cells and endothelial cells (Todd et al., 2006; Burnstock, 2007; Ralevic, 2009). In efferent autonomic nerves, P2 receptors may serve as auto- and/or heteroreceptors, regulating the release of NA, ATP and NPY from synaptic varicosities. In afferent sensory neurons, P2 receptors on sensory termini may be activated by nucleotides released by the artery (Ralevic, 2009). However, very little is known about the expression pattern of P2 receptors on particular nerve subtypes and purinergic autoregulation in the control of vascular tone.

3.2 Aim

In this chapter, I aimed to investigate the expression of purinergic receptors, including all P2X and P2Y receptors in arteries and associated sympathetic ganglia, including superior mesenteric artery and carotid artery, of mice. To fully characterise the profile of P2 purinergic receptors expressed in the superior mesenteric artery and carotid artery, mRNA transcript expression was explored using non-quantitative RT-PCR. In addition, by exploring the expression of P2X and P2Y receptors in the mouse superior cervical ganglion, this will help to determine whether receptors could be expressed on pre-junctional nerves. Thus, the expression of these receptors on perivascular nerves of vasculature can lead to using P2 receptors, which could serve as auto- and/ or heteroreceptors, as potential targets for the development of drugs to treat cardiovascular diseases such as hypertension.

3.3 Results

3.3.1 Comparison of mRNA expression of neuronal and vascular markers in mouse superior cervical ganglion, superior mesenteric artery and carotid artery

In this study, RT-PCR was performed to investigate the expression of various neuronal and vascular markers in the mouse superior cervical ganglion, superior mesenteric artery and carotid artery. To address this aim, the specificity and functionality of all primers were first tested in mouse brain mRNA of the same mouse. Following the validation of primers, the samples were tested for neuronal markers in order to determine which type of perivascular nerves were predominant. The expression of mRNA transcripts PGP 9.5, a cytoplasmic protein present in neurons and neuroendocrine cells, was used to distinguish between distinct neuronal populations and subtypes (Lundberg et al., 1988). VAChT, which is a protein that is required for cholinergic neurotransmission, was used in this study as a marker of cholinergic nerves. TH is locally synthesized in the cell body then delivered to the axon or pre-synaptic nerve terminal and was measured as a marker of adrenergic sympathetic neurons. TH is involved in the biosynthetic pathway of catecholamines including dopamine, NA, and adrenaline (Gervasi et al., 2016). CGRP, a common neurotransmitter of sensory neurons, was used as a marker of sensory neurons or non-adrenergic non-cholinergic neurons. SP, a neurotransmitter of primary sensory afferent neurons within the superficial dorsal horn of the spinal cord, was used as a marker of sensory neurons. nNOS, the enzyme responsible for the synthesis of NO by neurons, is primarily expressed by subpopulations of GABAergic interneurons and has an important role in the physiologic local human microvascular tone regulation (Melikian et al., 2009). Other vascular markers were used to confirm the existence of smooth muscle and endothelial cells in the studied tissues. α-SMA was measured as it is present in high concentrations in vascular smooth muscle cells (Skalli et al., 1989). vWF, synthesized by endothelial cells and megakaryocytes throughout the body, is commonly used as a marker of endothelial cells in blood vessels, although little is known about the expression and regulation of this haemostatic factor in endothelial cells in different vascular beds *in vivo* (Yamamoto et al., 1998).

As can be seen in Table 3.1 and Figure 3.1, all of the markers mentioned above were detected in the mouse brain at the expected sizes (555 bp [PGP 9.5], 527 bp [VAChT], 692 bp [TH], 375 bp [CGRP], 808 bp [SP], 537 bp [nNOS], 552 bp [α-SMA], and 512 bp [vWF]). In addition, nNOS mRNA showed another PCR amplificon of a lower molecular weight which could be a second variant of nNOS, but it was not detected via BLAST. A previous study has identified two nNOS proteins and transcripts in the rat kidney ; nNOSα and nNOSβ (Smith et al., 2009). The GAPDH mRNA amplification product of the housekeeping gene showed a

specific amplified band with an expected fragment size of 266 bp. These results supported the use of these primers for further studies. The superior cervical ganglion expressed PGP 9.5, TH, CGRP, α-SMA and vWF but VAChT, SP and nNOS were not expressed (Figure 3.2.A). These results indicated that the superior cervical ganglion has mostly sympathetic properties and could express sensory neurons. Although, a faint band was observed for CGRP compared to the very bright band detected with TH. Superior mesenteric artery and carotid artery had a similar expression pattern, however, CGRP was not detected in the carotid artery (Figures 3.2.B & 3.2.C). These results suggested that although the arteries were mostly innervated by sympathetic nerves, however further investigations were required to confirm whether these blood vessels were innervated via sensory nerves. Both tissues (superior mesenteric artery and carotid artery) strongly expressed α-SMA and vWF as markers of the presence of smooth muscle cells and endothelial cells respectively. VAChT was absent in the three tissues studied, suggesting the absence of cholinergic properties in these tissues. Perivascular cholinergic axons may originate from intrinsic enteric neurons in the submucosal or myenteric plexus, or from sacral parasympathetic efferent pathways (De Fontgalland et al., 2008). This suggested that enteric cholinergic neurons may not contributed to innervation of mesenteric arteries and carotid arteries in mice. A previous immunohistochemistry study in the limb muscle vasculature in rats and mice reported that the innervation of vasculature is sympathetic innervation, by showing immunoreactivity for TH and the peptide transmitters, NPY and infrequently vasoactive intestinal peptide. In contrast, VAChT and acetylcholinesterase activity was absent. Neuron cell bodies in sympathetic ganglion also did not show immunoreactivity for cholinergic markers, while TH was found (Guidry & Landis, 2000). Previous immunohistochemical studies in human mesenteric and submucosal arteries and veins demonstrated that the perivascular plexus of these vessels containing high levels of TH and NPY, accounting for more than 85% on all vessels (De Fontgalland et al., 2008). In addition, it was observed that nerve fibres that have been observed on mesenteric blood vessels of the guinea pig contain sympathetic perivascular nerve fibres, labelled by TH and NPY (Smyth et al., 2000). VAChT immunoreactivity was observed infrequently in low levels between the blood vessels (De Fontgalland et al., 2008). Our results are consistent with those of previous studies. Perivascular sensory nerves, in addition to endothelial cells, are involved in the modulation of vasomotor tone through the production of CGRP and SP. Sensory nerves, which are activated during inflammation, are also involved in the innervation of resistance vessels vasodilator by the release of CGRP. Immunohistochemically studies in rat mesenteric arteries showed NPY, TH, nNOS, CGRP, and SP nerves formed a plexus around outside of all branches of mesenteric arteries (Yokomizo et al., 2015). In human mesenteric arteries, exogenous

application of CGRP promotes potent vasodilation. however, another study reported the lack of CGRP in humans indicating that the functional significance of exogenous CGRP induced vasodilation requires further investigation. It has been reported previously that rat mesenteric resistance arteries are densely innervated by both sympathetic adrenergic nerves and capsaicin-sensitive sensory nerves, which mainly possess CGRP containing (CGRPergic) nerve fibres. Moreover, it has been demonstrated that CGRPergic nerves inhibit adrenergic nerve-mediated vasoconstriction by CGRP release, and oppositely, adrenergic nerves pre-synaptically prevent the neurogenic release of CGRP from the nerve to decrease CGRPergic nerve function (Hobara et al., 2006).

Table 3.1: An overview of mRNA expression for neuronal and vascular markers in the mouse brain, superior cervical ganglion, superior mesenteric artery and carotid artery.

Receptor	Tissue	Expression	Tissue	Expression	Tissue	Expression	Tissue	Expression
PGP9.5	Brain	+	Superior cervical ganglion	+	Superior mesenteric artery	+	Carotid artery	+
VAChT		+		-		-		-
TH		+		+		+		+
CGRP		+		+		+		-
SP		+		-		-		-
nNOS		+		-		-		-
α-SMA		+		+		+		+
vWF		+		+		+		+

A (+) sign indicates that the gene was expressed and a (–) sign indicates that the gene was not expressed. The results shown are representative from five independent experiments using five different mice.

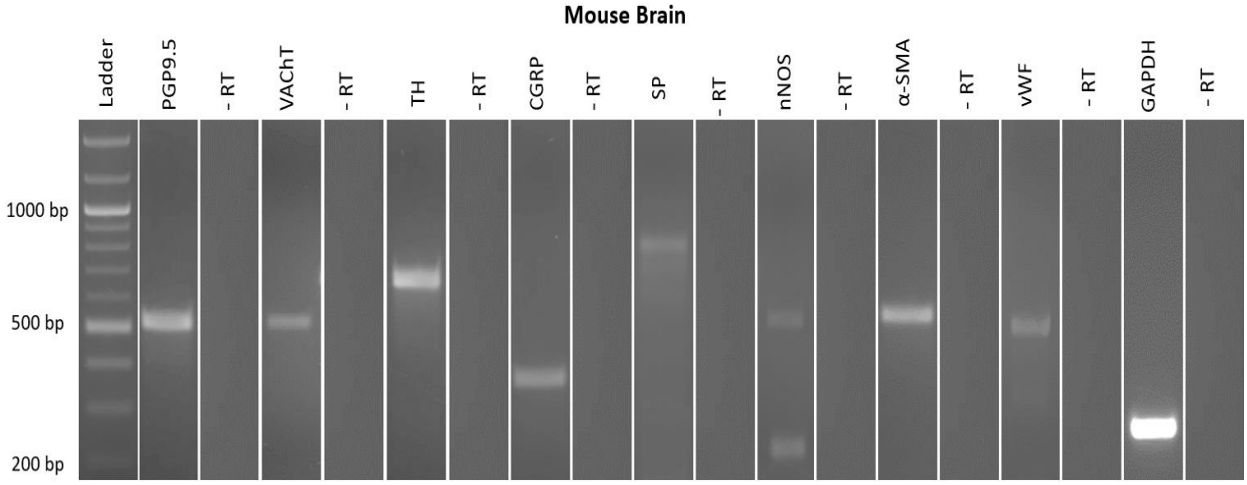

Figure 3.1: Expression of mRNA transcripts for neuronal and vascular markers in the mouse brain. All the markers were expressed in the brain of the expected sizes; PGP9.5 (555 bp), VAChT (527 bp), TH (692 bp), CGRP (375 bp), SP (808 bp), α-SMA (552 bp) and vWF (512 bp). Two bands for nNOS mRNA were observed in the brain only, one band was detected at the expected size (537 bp) and another lower band at (215 bp). GAPDH mRNA (housekeeping gene) were detected with an expected fragment size of 266 bp. No bands were present in the absence of reverse transcriptase showing there was no DNA contamination of the samples. - RT indicates the no reverse transcriptase control samples. The results shown are representative from five independent experiments using five different mice.

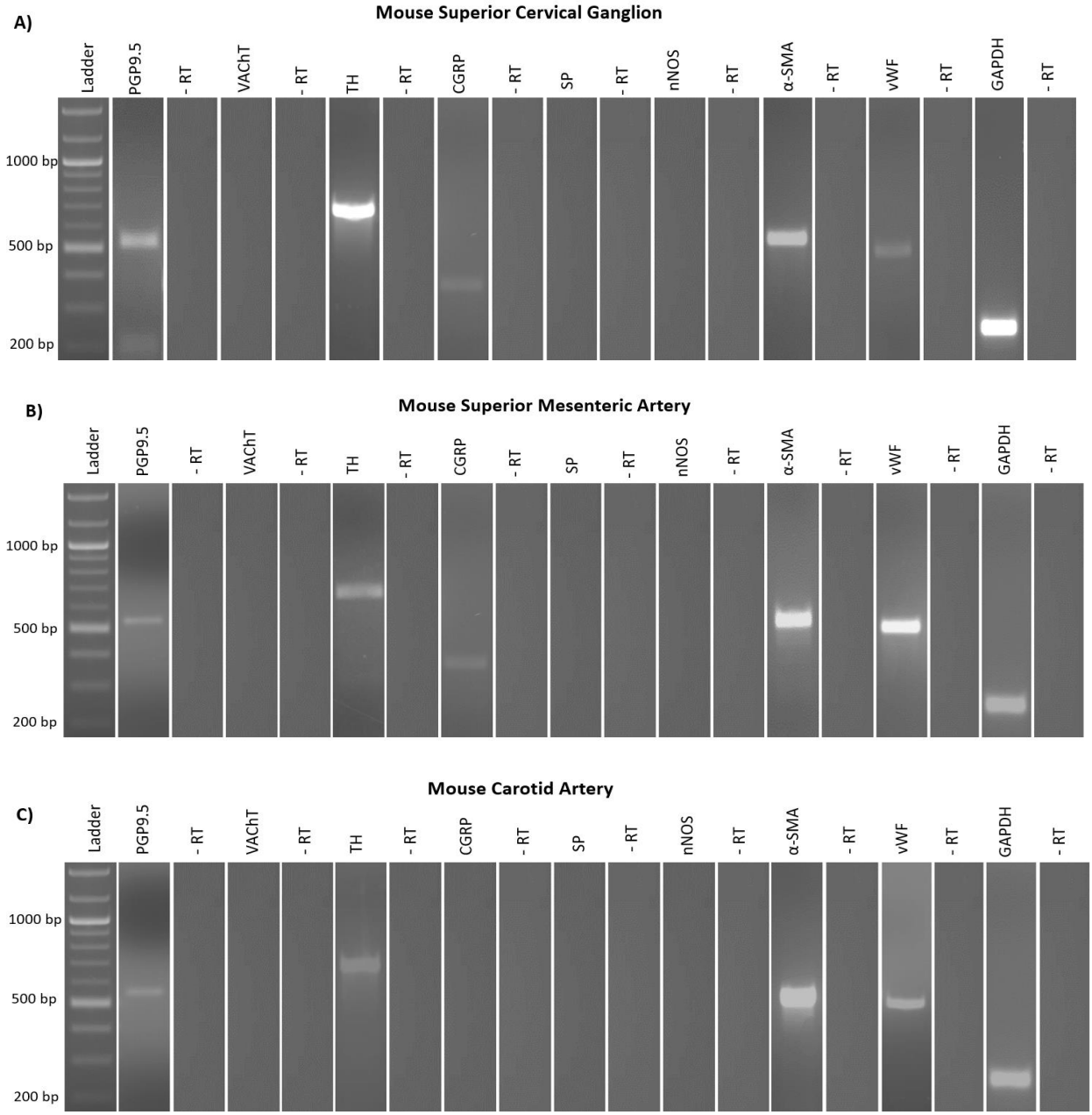

Figure 3.2: Expression of mRNA transcripts for neuronal and vascular markers in the mouse superior cervical ganglion, superior mesenteric artery and carotid artery. PGP9.5 (555 bp), TH (692 bp), α-SMA (552 bp) and vWF (512 bp) mRNAs were expressed in all tissues studied; superior cervical ganglion **(A)**, superior mesenteric artery **(B)** and carotid artery **(C)** at the expected sizes. VAChT and SP mRNAs were not expressed in all tissues studied. CGRP mRNA was expressed at 375 bp in the superior cervical ganglion, and in superior mesenteric artery, however, no band was present in the carotid artery. GAPDH mRNA (housekeeping gene) were detected in the tissues with an expected fragment size of 266 bp. No bands were present in the absence of reverse transcriptase showing there was no DNA contamination of the samples. The results shown are representative from five independent experiments using five different mice.

3.3.2 Comparison of mRNA expression of P2X receptor subtypes in mouse superior cervical ganglion, superior mesenteric artery and carotid artery

For the RT-PCR experiments, mRNA was used which was isolated from the superior mesenteric artery, carotid artery and superior cervical ganglion of mice. To address this aim, the specificity and functionality of all primers (Table 2.8) were first tested in mouse brain mRNA of the same mouse. Following the validation of primers, the expression of mRNA transcripts for P2X and P2Y receptors in superior cervical ganglion, superior mesenteric artery and carotid artery, were examined. Representative control experiments without reverse transcriptase (-RT) were performed to ensure that any PCR amplicon was derived from synthesized cDNA rather than genomic DNA. Genes with a band of the expected product size (bp) were deemed to be present (expressed), whereas genes were considered absent (not expressed) when they did not show a band. Tables 3.2 and Figures 3.3-3.6 give a summary of the results obtained for this study.

Using the primers in Table 2.8, The GAPDH mRNA of the housekeeping gene showed a specific amplified band with an expected fragment size of 266 bp in all tissues. The negative control (-RT) of mRNA transcripts for GADPH, mRNA did not have specific amplification bands. This indicated that the obtained bands were from synthesized cDNA rather than genomic DNA. All confirmed the ability of the use of cDNA synthesized from total RNA in this project to investigate the expression of P2 purinergic receptors. The mRNA transcripts for P2X1, P2X3, P2X4, P2X6 and P2X7 receptors were repeatedly expressed in the mouse brain but P2X5 was detected only once out of 5 experiments. Conversely, according to Sperlagh et al., (2007), P2X5 subtype has the most restricted localization in the brain, despite it shows strong expression in certain areas such as the nucleus tractus solitarii. Although several primers and various conditions were explored, P2X2 receptor mRNA was not detected in the mouse brain (Figure 3.3). Table 3.2 summarises the expression of P2X receptors in the mouse brain, superior cervical ganglion, superior mesenteric and carotid artery. In the superior cervical ganglion, amplified PCR products of the expected sizes were obtained for all P2X1-7 receptors at the expected product sizes; P2X1 (505 bp), P2X2 (499 bp), P2X3 (533 bp), P2X4 (500 bp), P2X5 (647 bp), P2X6 (566 bp) and P2X7 (712 bp). As mRNA for P2X2 was detected in the superior cervical ganglion but not the brain, this confirmed the specificity of these primers (Figure 3.4.A). It was also shown that P2X2 and P2X6 primers produced other PCR amplificon of a lower molecular weight in addition to the expected product for P2X2 and P2X6. A similar PCR amplicon for P2X6 was also detected in the mouse brain. It could be that these are alternative splice variants for P2X2 and P2X6. An analysis of these primers using BLAST

identified the second and third amplicons for P2X2, but it was not able to identify the alternative product produced during the amplification of P2X6, however, it was previously reported that alternative splicing of P2X6 receptor subtypes was detected during postnatal development of mouse brain (Da Silva et al., 2007). Regarding P2X2 and according to the attached supplementary (S.1 & S.2), the forward primer was designed on a splicing site which means that part of the premier is on exon 9 and the second part is on exon 10, thus the forward primer can not anneal to the DNA. According to P2X2 sequencing data the PCR product size is expected to be at 292 bp for (112478.8), 229 bp for (200037.5) and 499 bp for (195985.5). But (199165.5) has intron similar to the DNA (no splicing site at the primers annealing region), thus the primers can not be annealed. The expression of the second splice variant of the P2X2 receptor indicates a potential physiological role for this splice variant.

In mouse mesenteric artery (Figure 3.4.B) and carotid artery (Figure 3.4.C), P2X1, P2X4 and P2X7 mRNA revealed specific bands of the same size as the amplified target fragments. However, mRNA for P2X2, P2X3, P2X5 and P2X6 were not detected. The negative control (-RT) of mRNA transcripts for P2X1-7 receptors, mRNA did not have specific amplification bands in the corresponding lanes, indicating the obtained bands for expressed P2X receptors were synthesized cDNA rather than genomic DNA. A previous study demonstrated that P2X1 and P2X4 receptors are the major P2X receptors expressed in vascular smooth muscle cells. P2X7 receptors may also be expressed, while there was no expression or a little expression of P2X2, P2X3, P2X5 and P2X6 receptors (Ralevic & Dunn, 2015). Our findings consistent with earlier studies show that the mouse superior cervical ganglion and individual neurons may express multiple P2X receptors (Calvert & Evans, 2004). These results suggest that P2X1, P2X4 and P2X7 could be expressed on the layers of the blood vessels including perivascular nerves, smooth muscle cells and endothelial cells. It was previously reported that elements of the vascular system including major arteries and arterioles are innervated via sympathetic nerves (Sheng & Zhu, 2018; Ruffolo et al., 1991). Perivascular sympathetic nerves arise from post-ganglionic efferent axons and (form a plexus within the adventitia), with their cell bodies placed in the paravertebral ganglia (McLachlan, 2003). In addition, perivascular nerves are located in the adventitial layer of blood vessels and do not make direct contact with smooth muscle cells or endothelial cells (Westcott & Segal, 2013). Moreover, it was previously reported that P2-purinergic receptors activated via ATP occur not only on effector cells but can also occur on the post-ganglionic sympathetic neurons themselves. Post-ganglionic sympathetic neurons possess both excitatory and inhibitory P2-receptors. The receptors mediate rapid increases in intracellular Ca^{2+} levels leading to NA release. These receptors are most likely to be to belong to the neuronal types of P2X purinergic

receptors located on the sympathetic nerve cell bodies or their dendrites (Von Kügelgen et al., 1996). Taken together, we hypothesised that P2X2, P2X3, P2X5 and P2X6 could be expressed and serve as auto- and/or heteroreceptors on the perivascular nerves within the adventitia of the blood vessels but they were not derived from the perivascular nerves layer when RT-PCR was performed. Further investigations using immunohistochemical experiments were required to explore the colocalisation of P2X with neuronal markers such as PGP9.5 and TH to confirm the presence of these receptors on perivascular verves in the blood vessels.

Table 3.2: An overview of mRNA expression for P2X receptors in the mouse brain, superior cervical ganglion, superior mesenteric artery and carotid artery.

Receptor	Tissue	Expression	Tissue	Expression	Tissue	Expression	Tissue	Expression
P2X1	Brain	+	Superior cervical ganglion	+	Superior mesenteric artery	+	Carotid artery	+
P2X2		-		+		-		-
P2X3		+		+		-		-
P2X4		+		+		+		+
P2X5		+		+		-		-
P2X6		+		+		-		-
P2X7		+		+		+		+
GAPDH		+		+		+		+

A (+) sign indicates that the gene was detected and a (–) sign indicates that the gene was not detected. The results shown are representative from five independent experiments using five different mice.

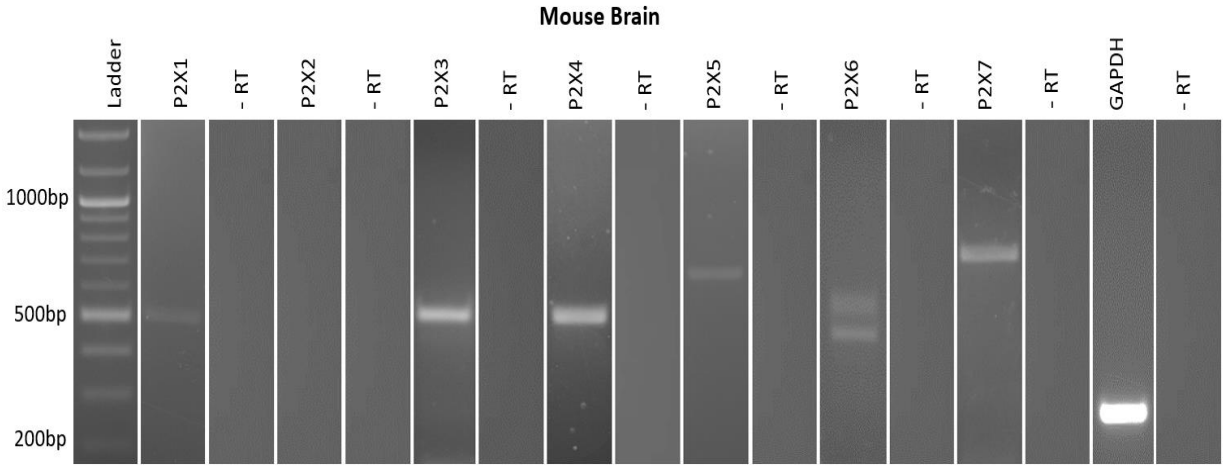

Figure 3.3: Expression of mRNA transcripts for P2X receptors in the mouse brain. mRNAs for all P2X receptors (except of P2X2) were found in the human brain. Two bands for P2X6 mRNA were observed in the brain, it could be that these are alternative splice variants. GAPDH mRNA (housekeeping gene) were detected. No bands were present in the absence of reverse transcriptase showing there was no DNA contamination of the samples. Expression was detected at 505 bp (P2X1), 533 bp (P2X3), 500 bp (P2X4), 647 bp (P2X5), 566 bp (P2X6), 712 bp (P2X7) and 266 bp (GAPDH). -RT indicates the no reverse transcriptase control samples. The results shown are representative from five independent experiments using five different mice.

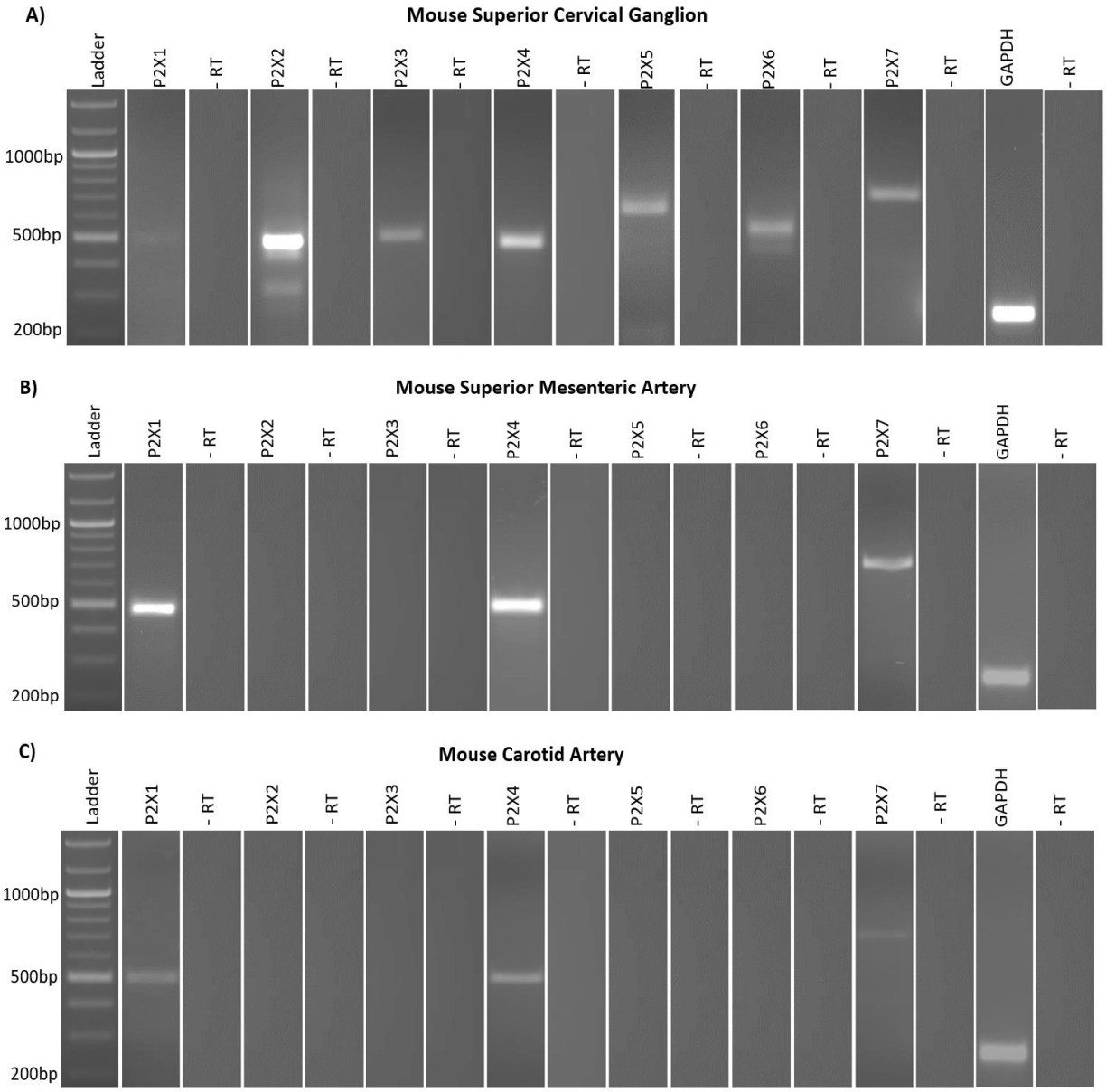

Figure 3.4: Expression of mRNA transcripts for P2X receptors in the mouse superior cervical ganglion, superior mesenteric artery and carotid artery. (A) mRNAs were found for all P2X receptors in the cervical ganglion, with two bands detected for P2X2 and P2X6. (**B)** mRNAs were found for P2X1, P2X4 and P2X7 receptors in the superior mesenteric artery. (**C)** The carotid artery expressed P2X1, P2X4 and P2X7. P2X2, P2X3, P2X5 and P2X6 receptors were not expressed in both the superior mesenteric artery and carotid artery. GAPDH mRNA (housekeeping gene) were detected in all tissues studied. No bands were present in the absence of reverse transcriptase showing there was no DNA contamination of the samples. Expression was detected at 505 bp (P2X1), 499 bp (P2X2), 533 bp (P2X3), 500 bp (P2X4), 647 bp (P2X5), 566 bp (P2X6), 712 bp (P2X7) and 266 bp (GAPDH). - RT indicates the no reverse transcriptase control samples. The results shown are representative from five independent experiments using five different mice.

3.3.3 Comparison of mRNA expression of P2Y receptor subtypes in mouse superior cervical ganglion, superior mesenteric artery and carotid artery

P2Y receptors, like P1 and P2X receptors, are widely distributed throughout the body and are involved in a wide range of cellular functions, including platelet aggregation, inflammation, and endothelial cell hydration (Boeynaems et al., 2012). Furthermore, arterial tone can also be controlled by P2Y receptors following activation by ATP or ADP. P2Y receptors include eight subunits and could form homodimers or heterodimers with other P2Y receptors or with other transmitter receptors such as A1 adenosine receptors (Ecke et al., 2008; Fischer& Krugel, 2007; Abbracchio et al., 2006; Yoshioka et al., 2002).

As shown in (Table 3.3, Figures 3.5 & 3.6) by using the primers in Table 2.9, The GAPDH mRNA of the housekeeping gene showed a specific amplified band with an expected fragment size of 266 bp in all tissues studied. Additionally, mRNA for all P2Y isoforms (except P2Y12) was found in the brain (Figure 3.5), whilst mRNA for all P2Yreceptors was identified in the superior cervical ganglion (Figure 3.6.A). Bands were detected at 668 bp (P2Y1), 615 bp (P2Y2), 490 bp (P2Y4), 500 bp (P2Y6), 978 bp (P2Y12), 591 bp (P2Y13), and 571 bp (P2Y14). The P2Y4 was detected faintly and only once out of 5 experiments in the mouse superior cervical ganglion. The mouse P2Y11 receptor is not present in mice, and primers for human P2Y11 did not detect murine P2Y11 (Calvert et al., 2004). In mouse superior mesenteric artery, PCR products for P2Y1 (faint band), P2Y2, P2Y6, P2Y13 and P2Y14 receptors were amplified (Figure 3.6.B). Additionally, P2Y2, P2Y6, P2Y13 and P2Y14 could be expressed in the carotid artery, but not P2Y1 receptors (Figure 3.6.C). No bands were amplified in the absence of reverse transcriptase, indicating that the obtained bands were from synthesized cDNA rather than genomic DNA. A previous study showed that P2Y1, P2Y2 and P2Y6 receptors could be expressed in the superior mesenteric artery (Calvert et al., 2004). Other studies in the medium mesenteric arteries from mouse demonstrated mRNA expression for P2Y1, P2Y2 and P2Y6 receptors, but P2Y4 receptor mRNA was not detected (Vial & Evans, 2002). Our results indicated that P2Y1, P2Y4, and P2Y12 could be expressed on the perivascular nerves of the adventitia of the blood vessels (superior mesenteric artery and carotid artery) but they were not derived from the layer through RT-PCR. Again, to confirm whether the protein is expressed, further investigations using immunohistochemical experiments are required to detect colocalisation of P2Y receptors with PGP9.5 and TH.

Table 3.3: An overview of mRNA expression for P2Y receptors in the mouse brain, superior cervical ganglion, superior mesenteric artery and carotid artery.

Receptor	Tissue	Expression	Tissue	Expression	Tissue	Expression	Tissue	Expression
P2Y1	Brain	+	Superior cervical anglion	+	Superior mesenteric artery	+	Carotid artery	-
P2Y2		+		+		+		+
P2Y4		+		+		-		-
P2Y6		+		+		+		+
P2Y12		-		+		-		-
P2Y13		+		+		+		+
P2Y14		+		+		+		+
P2Y11	Not found in mouse							

A (+) sign indicates that the gene was detected and a (–) sign indicates that the gene was not detected. The results shown are representative from five independent experiments using five different mice.

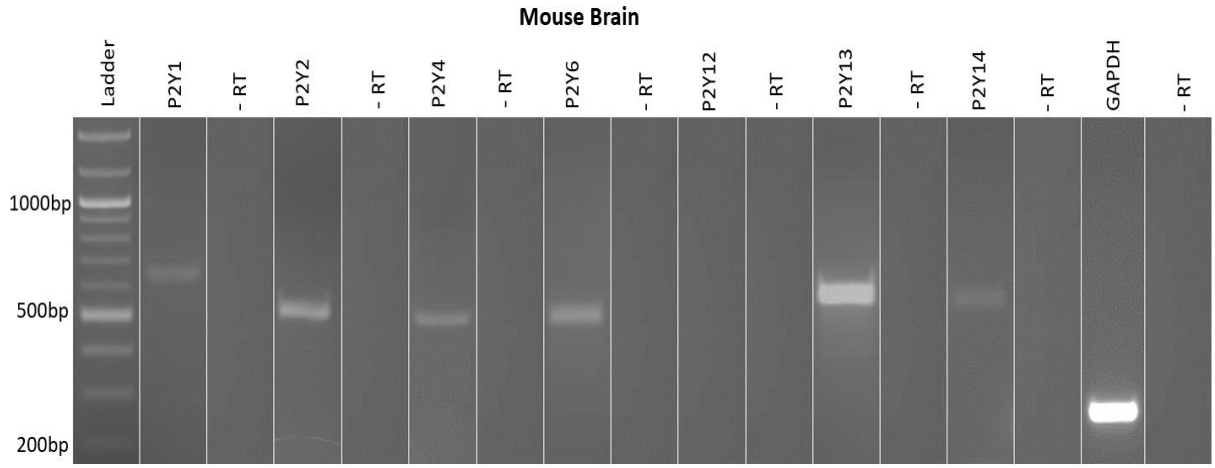

Figure 3.5: Expression of mRNA transcripts for P2Y receptors in the mouse brain. The mRNAs were found for all P2Y receptors except P2Y12 receptor was absent. GAPDH mRNA (housekeeping gene) was found with an expected fragment size. No bands were present in the absence of reverse transcriptase showing there was no DNA contamination of the samples. Expression was detected at 668 bp (P2Y1), 615 bp (P2Y2), 490 bp (P2Y4), 500 bp (P2Y6), 978 bp (P2Y12), 591 bp (P2Y13), and 571 bp (P2Y14) and 266 bp (GAPDH). - RT indicates the no reverse transcriptase control samples. The results shown are representative from five independent experiments using five different mice.

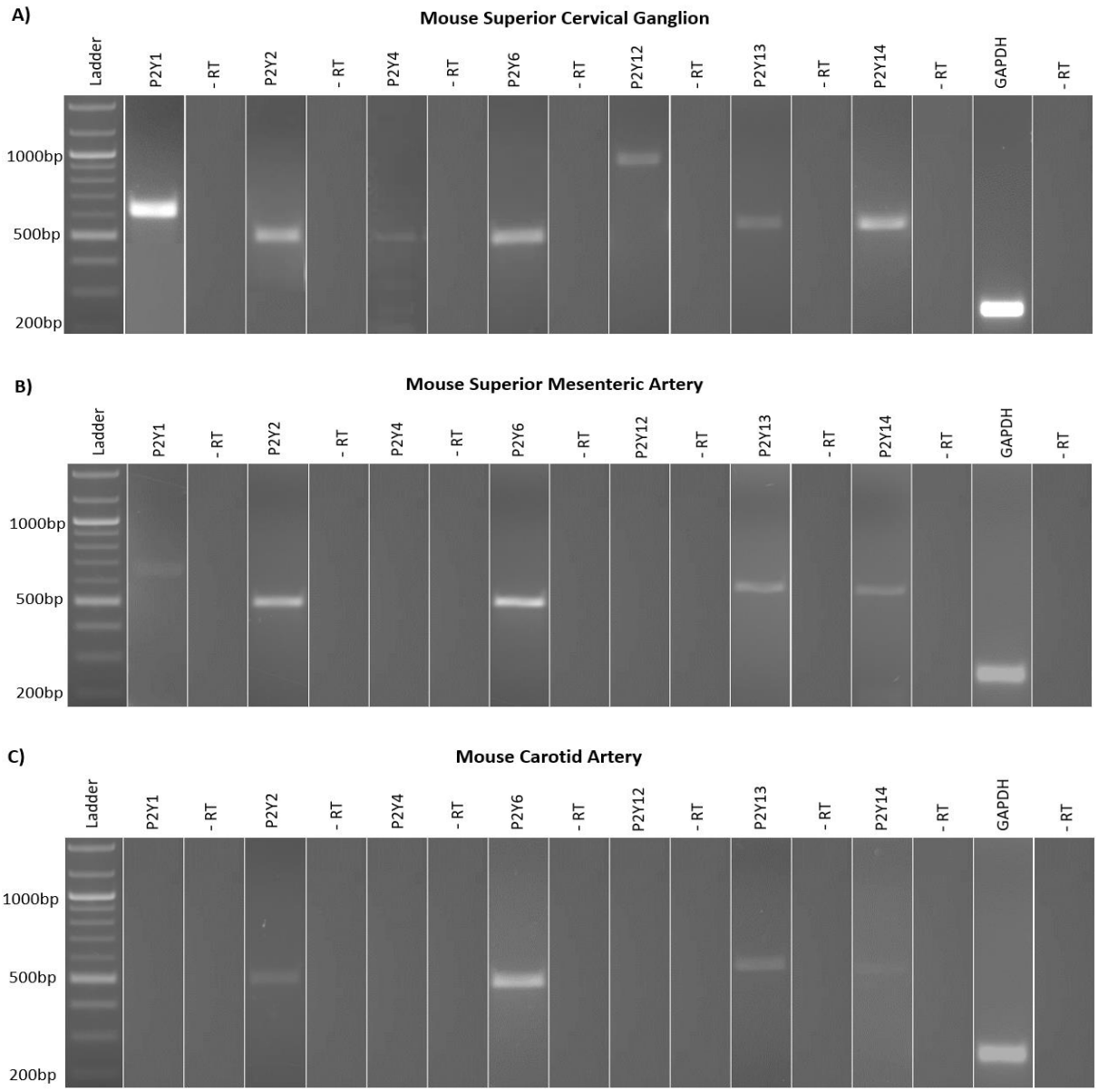

Figure 3.6: Expression of mRNA transcripts for P2Y receptors in the mouse superior cervical ganglion, superior mesenteric artery and carotid artery. (A) mRNAs were found for all P2Y receptors in the cervical ganglion. (**B)** mRNAs were found for P2Y1 (faint band), P2Y2, P2Y6, P2Y13 and P2Y14 receptors in the superior mesenteric artery. (**C)** The carotid artery expressed P2Y2, P2Y6, P2Y13 and P2Y14 receptors. P2Y4 and P2Y12 receptors were not expressed in both the superior mesenteric artery and carotid artery. GAPDH mRNA (housekeeping gene) were detected in all tissues studied. No bands were present in the absence of reverse transcriptase showing there was no DNA contamination of the samples. Expression was detected at 668 bp (P2Y1), 615 bp (P2Y2), 490 bp (P2Y4), 500 bp (P2Y6), 978 bp (P2Y12), 591 bp (P2Y13), and 571 bp (P2Y14) and 266 bp (GAPDH). - RT indicates the no reverse transcriptase control samples. The results shown are representative from five independent experiments using five different mice.

3.4 Discussion

3.4.1 Expression of neuronal and vascular markers in mouse superior cervical ganglion, superior mesenteric artery and carotid artery

Resistance vessels, such as mesenteric arteries, are known to be innervated by several perivascular nerves, including sympathetic adrenergic nerves, and non-adrenergic non-cholinergic nerves such as CGRPergic nerves (Yokomizo et al, 2015). Signal transduction pathways are activated when neurotransmitters bind to adrenergic, cholinergic and purinergic receptors, resulting in the observed changes in vascular function. Vascular factors, such as endothelium-derived relaxing factor NO, and constriction factor endothelin, play an essential role in the autonomic nervous system in physiologic conditions (Sheng, Y., & Zhu, L. (2018). Thus, autonomic nervous system dysfunction may be a risk factor for vascular diseases such as hypertension, heart failure, and diabetes mellitus. Thus, understanding the relationship between the autonomic nervous system and vascular system may deliver new and effective therapeutic strategies for vascular diseases.

In this part of project, the distribution pattern of perivascular nerves in some branches of the mouse superior mesenteric artery, carotid artery and superior cervical ganglion, were studied by RT-PCT using specific primers of some neuronal markers and vascular markers. Our findings showed that the superior mesenteric artery, carotid artery and superior cervical ganglion had expression of PGP9.5 (a general marker of neurons, including glial cells), TH (very bright band in the superior cervical ganglion), vWF and α-SMA. CGRP mRNA was weakly detected in the superior cervical ganglion with a very faint band observed in the superior mesenteric artery, but no band was detected in the carotid artery. While SP and VAChT were absent in all tissues. SP and AChT mRNA were detected in the mouse brain, which confirmed the efficiency of the primers. Our results indicated the presence of neurons in the arterial tissues. These neurons could be mostly sympathetic generated from sympathetic post-ganglion. However, further immunohistochemical studies are required to confirm the presence of PGP9.5 and TH protein and the absence of parasympathetic phenotype in the tissues. The results showed that the tissues could also be innervated by sensory nerves due to the presence of CGRP. Immunohistochemical studies could confirm that as well. It was previously observed that sympathetic vasoconstrictor NPY and non-adrenergic non-cholinergic nerves vasodilator CGRP nerves innervated rat mesenteric arteries, contributing to vascular tone modulation. A previous study (Yokomizo et al, 2015) using Immunohistochemistry showed immunopositive nerves of TH, CGRP, SP, NPY and nNOS in the first (1st), second (2nd), and third (3rd) branches of rat mesenteric arteries were almost the same, indicating no

change in the importance of the different nerve populations in regulating vascular tone. However, the innervation pattern of these non-adrenergic non-cholinergic perivascular nerves requires further investigations in small arteries. Furthermore, this previous study reported using double immunostaining studies that adrenergic TH nerves were shown to be in close contact to vasodilator nerves such as nNOS, CGRP, and SP nerves. This finding strongly indicated that the axo-axonal interaction between vasoconstrictor and vasodilator neurons regulated vascular tone (Yokomizo et al, 2015). The common carotid artery was sparsely innervated by CGRP immunoreactive nerve fibres (Mulderry et al., 1985). A study using the hamster carotid artery showed endothelial cells labelled for eNOS and smooth muscle cells labelled for nNOS (Segal et al., 1999). The studies using human mesenteric vessels revealed abnormalities in the perivascular innervation of patients with inflammatory bowel disease, with both sympathetic nerve density in arteries and veins and CGRP nerve density in veins significantly increased, implying a role in the pathogenesis and/or development of inflammatory bowel disease (Birch et al., 2008). The superior mesenteric artery from rats was highly innervated by SP, while the carotid artery had no SP-containing fibres. SP caused veins to constrict but had no effect on arteries, although there was a dose-dependent relaxation of the carotid artery. That suggested that these nerves do not subserve a vasomotor function. Moreover, the reduction of SP immunoreactivity from nerves in arteries and veins by capsaicin could suggest that SP-containing vascular nerves are primarily sensory in nature (Barja et al., 1983). According to Takaki et al., (2015) and Heym et al., (1993), the rat sympathetic ganglion, which contains small intensely fluorescent cells and sympathetic ganglionic cells, showed immunopositive stained for TH, and VAChT. A study on mouse intrinsic cardiac ganglia showed intense immunoreactivity of PGP 9.5, TH, choline acetyltransferase which is required for ACh synthesis, and VAChT (Hoard et al., 2008). It was previously reported that the glial cells in superior cervical ganglion showed muscarinic ACh receptors, which enable them to communicate chemically with the sympathetic neurons. That confirmed once elevation of intracellular Ca^{2+} was observed following the application of 0.01-2 mM ACh (Feldman-Goriachnik et al., 2018), and this is inconsistent with our current study. Immunohistochemical analysis of a previous study showed differences in the expression of vWF in different murine tissues (brain, heart, aorta, gut) and in different types of blood vessels of the same tissues (Yamamoto et al., 1998). In human mesenteric arteries and veins, nerves immunoreactive to PGP9.5, TH, CGRP and NPY were present. However, the artery was not shown to have nerves immunoreactive to NO synthase or choline acetyltransferase (Birch et al., 2008). The constriction was demonstrated to be mediated by sympathetic nerves, with NA, ATP, and NPY acting as co-transmitters. This is common in many mammalian vessels (Birch et al., 2008).

There is additional evidence that sensory innervation of blood arteries influences endothelial expression of vasoactive elements. Sensory deprivation causes sympathetic vasoconstriction in the rat mesenteric arteries, which is assumed to be caused by long-term trophic alterations in the vessels (Milner & Burnstock, 1996; Ralevic et al., 1995). A previous immunohistochemical study in mesenteric perivascular nerves using confocal microscopy documented the presence of TH, CGRP and NPY-immunoreactive nerve fibres, however, they did not reveal any immunoreactivity for nNOS or choline acetyltransferase. These results corroborate with the ones found in the current study (De Fontgalland et al., 2008; Birch et al., 2008). A previous study in mouse superior cervical ganglion determined the presence of CGRP during prenatal and postnatal development (Mitsuoka et al., 2018). In addition, CGRP has been reported to be found in the human, rat and cat superior cervical ganglion, supporting our observations regarding the expression of CGRP in the mouse superior cervical ganglion (Baffi et al., 1992). However, Tajti et al., (1999), reported that CGRP1 mRNA was absent in the human superior cervical ganglion via RT-PCR. While others documented that most human superior cervical ganglionic cells showed immunopositivity for TH, dopamine β-hydroxylase, CGRP, NPY and vasoactive intestinal polypeptide (Baffi et al., 1992). Radioimmunoassay has revealed the presence of SP in the superior cervical ganglion and submaxillary glands of rats (Robinson et al., 1980). It was demonstrated that NA and NPY containing cell bodies were present in high numbers (75% of all cells were positive) in the human superior cervical ganglion and distributed homogeneously throughout the ganglion and showed colocalisation. A low number of the superior cervical ganglion cell bodies were vasoactive intestinal polypeptide-immunoreactive (less than 5%) but none of them showed nNOS, CGRP or SP (Tajti et al., 199). These results suggested that multiple neurotransmitters may be employed by the post-ganglionic cells of the superior cervical ganglion. In contrast to our result, Ito et al., (2005) showed the presence of VAChT, a reliable marker for the pre-ganglionic terminal, and nNOS in mouse superior cervical ganglion. Our RT-PCR study showed expression of vWF which indicated the presence of endothelial cells in the mouse superior cervical ganglion. This was supported by a study in the rat superior cervical ganglion which reported that the majority of blood vessels in the superior cervical ganglion have a continuous endothelium with tight junctions; features associated with the blood-brain barrier of the central nervous system and perivascular nervous system. It is suggested that these vessels provide a barrier role between the capillary circulation and the superior cervical ganglion (Depace, 1982). Immunoreactivity to vWF was not detected in the mouse ligated carotid artery at 1 day after ligation. However, at day 3, a dense staining was detected in regions of the intima or intimal lesions. There was immunoreactivity to α-SMA in the medial layer of artery walls and fibrous tissue (Chang et al.,

2017). The cultured cells of the mouse and rat superior mesenteric artery retain expression of α-SMA and physiological responses to agonists and that support the positive band of α-SMA in the superior mesenteric artery shown in this project (Golovina & Blaustein, 2006).

3.4.2 Expression of P2X and P2Y receptors in mouse superior cervical ganglion, superior mesenteric artery and carotid artery

It is known that extracellular ATP released from perivascular nerves on blood vessels acts on purinergic receptors which are located on vascular smooth muscle and the endothelium. In addition, ATP, released from damaged tissues during trauma, shock or ischaemia can affect cardiovascular physiology. Moreover, purinergic receptors facilitated contractile responses have been characterized in different arteries from mouse, e.g., superior mesenteric artery. Previous studies have identified many P2X subtypes in the heart and the question arises as to the relationship between the purinergic receptors and the perivascular nerves that innervate the vascular system (Hansen et al., 1999). Furthermore, P2Y receptors are associated with various cellular functions in several different tissues such as the perivascular nerves, vascular tissue, gastrointestinal tract, eye, kidney, immune system, brain and inflammatory cells (Brass et al., 2012).

The present study demonstrated the mRNA expression of all P2X and P2Y receptors in mouse superior mesenteric artery, carotid artery, and superior cervical ganglion freshly isolated from wild-type C57BL6 mice. This data provides the foundations for further immunohistochemical analyses in these tissues and studies exploring the potential role of these receptors in vasorelaxation and contractility in response to nucleotides. In the following section, we will discuss many examples of the expression of the P2 receptors on both superior mesenteric artery and carotid artery, as well as vascular tissue and superior cervical ganglion in several organisms.

3.4.2.1 Expression of P2X and P2Y receptor mRNA transcripts in mouse superior mesenteric artery and carotid artery

Purine and pyrimidine nucleotides are produced from many sources and modulate arterial tone by acting on P2 receptors. ATP, which is co-compartmentalised and released with NA from sympathetic neurons, mediates vasoconstriction via P2X receptors in arteries (Vial & Evans, 2002). ATP is also released by the endothelium and blood cells, as well as by local tissue damage, where it can promote vasoconstriction by stimulating P2X and P2Y receptors. Endothelial cells and platelets produce the pyrimidines UTP and UDP, which can cause

prolonged vasoconstriction by activating pyrimidine-sensitive P2Y receptors (Vial & Evans, 2002; Ralevic and Burnstock, 1998). P2Y receptors are also involved in the control of vascular tone. P2Y1 receptors are found on endothelial cells and can mediate vasodilation following stimulation via ADP and ATP, while P2Y2, P2Y4 and P2Y6 activated by uridine nucleotides, and expressed on smooth muscle cells where they mediate vasoconstriction (Gitterman & Evans, 2000). Our results (Tables 3.2 & 3.3 and Figures 3.4 & 3.6) showed that P2X1, P2X4, P2X7, and all P2Y receptors, except P2Y4 and P2Y12, were present in mouse superior mesenteric artery, including endothelial cells, smooth muscle cells and perivascular nerves. The mRNA for these receptors were expressed on several different tissues, but not all. Some studies proposed there are many factors behind these differences in expression. These factors included the species, age, blood vessel size and whether any disease was present (Ralevic, 2012; Ralevic, 2009). A large amount of experimental data have confirmed the expression of P2X1, P2X4 and P2X7 in arterial tissues being mostly located on smooth muscle cells and the endothelium. In addition, it is well known that these receptors have roles in blood pressure regulation and vascular remodelling, except P2X7 which is still under investigation. For example, it is well known that the P2X1 receptor and P2X1/4 receptors are considered the core functional P2X receptors present in smooth muscle cells and have a high sensitivity to α,β-meATP, causing rapid depolarisation and vasoconstriction (Gitterman & Evans, 2000; Ralevic & Dunn, 2015; Harhun et al., 2010). It has been demonstrated that P2X4 receptors participate in mediating vasorelaxation in response to ATP produced by the endothelium in response to shear stress (Ralevic, 2012). According to previous studies, P2X1, P2Y1, P2Y2 and P2Y6 receptors are highly expressed on the vascular smooth muscle layer of the mouse, however, the P2Y4 receptor was not detected by RT-PCR (Vial & Evans, 2002). The same study confirmed the expression of P2X1 by performing functional experiments using superior mesenteric artery from P2X1 receptor-deficient mice. They showed that these P2X1-deficient mice did not have responses to α,β meATP (10 μM) or ATP (100 μM), which should evoke maximal transient vasoconstrictive responses in wild-type mice. In addition, by stimulating P2X1-deficient mice with ADP (1 mM), an agonist at P2Y1, P2Y12, and P2Y13 receptors, it was reported that these P2Y receptors were not involved in regulating the tone of medium mesenteric arteries. Other P2X receptors including P2X2, P2X4 and P2X5 have been shown to be expressed in rat coronary arteries, aorta and myocardium from numerous heart sites but these receptors were not expressed in the rat superior mesenteric artery (Vial & Evans, 2002; Nori et al., 1998). Immunohistochemical analyses in rat superior mesenteric artery reported that the P2X1 receptor isoform was expressed in all vessel sizes, while the P2X4 receptor was detected in the smooth muscle cells of large and medium sizes (Gitterman & Evans, 2000). The same study

demonstrated that P2X5 was weakly detectable in all sizes of arteries and P2X7 receptors were weakly expressed on the smooth muscle layer of large arteries and in the external non-smooth muscle layers of medium arteries. P2X2, P2X3 and P2X6 receptors subunits had immunoreactivity below the limit of detection in all rat arteries (Gitterman & Evans, 2000). Li et al., (2020) showed the expression of P2X1, P2X4 and P2X7 in various arterial tissues of rat (including mesenteric artery and internal carotid artery, pulmonary artery, thoracic aorta and tail artery). Whilst P2X2, P2X3, P2X5 and P2X6 receptors were not detected in these tissues. This is consistent with the results reported in our present study in mouse superior mesenteric artery and carotid artery (Figures 3.4 & 3.6). Moreover, using real-time fluorescent quantitative PCR, it was reported that the expression level of P2X1 and P2X4 receptor isoforms were similar in all arterial tissues, including superior mesenteric artery and carotid artery, except the tail artery where the expression of P2X1 receptor was increased. P2X7 receptor mRNA expression was higher in the mesenteric artery compared to the carotid artery and other arterial tissues (Li et al., 2020) and this is in agreement with the faint band for P2X7 detected in the mouse carotid artery in our study. Wang et al., (2018) showed that mRNA expression for P2X1, P2X4 and P2X7 receptors was high in the mesenteric artery from Wistar-Kayto rats. It is well known that the P2X1 receptor is the most important subtype responsible for inducing vascular smooth muscle contraction and it is expressed in the mesenteric artery, pulmonary artery, and thoracic artery of the rat (Li et al., 2012). Furthermore, it is widely established that the P2X4 receptor is the most dominant receptor in the human umbilical vein, thoracic aorta, pulmonary artery, and skin microvascular endothelial cells. It is also known that the endothelial P2X4 mediates Ca^{2+} influx and involves blood pressure regulation and vascular remodelling via NO and EDHF release (Bernier et al. 2018; Yamamoto et al. 2006). Yamamoto et al., (2006) reported that P2X4-deficient had smaller carotid artery diameters compared to WT mice. Additionally, the wall was thicker and the role of P2X4 in modulating vascular structure was suggested to be through endothelial production of NO. P2X7 mRNA was present in the adventitial layer of rat mesenteric artery, human thoracic aorta and umbilical vein endothelial cells (Lewis and Evans, 2001; Bernier et al., 2018). However, the effect of the P2X7 receptor on vascular function is still unclear (Li et al., 2020). Past studies confirmed that P2Y1 protein is expressed in the rat superior mesenteric artery and suggested that vasodilatation mediated by the P2Y1 receptor is reduced in superior mesenteric artery from type 1 diabetic rats. This impairment is caused by a decrease in P2Y1 receptor-mediated NO signalling rather than a decrease in P2Y1-receptor expression (Ishida et al., 2013). Studies using RT-PCR demonstrated that P2Y1, P2Y2 and P2Y6 were expressed in mesenteric arteries of mouse (Vial & Evans, 2002). It was also reported that transient constriction of mouse mesenteric artery

evoked by ATP and UTP, respectively, are mostly facilitated by P2X1 and P2Y6 receptors (Koltsova et al., 2009). By using the mouse genome genetics website (to determine the predicted receptor expression), our results are compatible with the predicted suggestions. The likelihood of P2X2, P2X3, P2X5, and P2Y12 being expressed in the mouse arteries was small, while the presence of these receptors in the perivascular nerves was higher. However, the probability of P2X6, P2Y4 and P2Y11 was non-existent in both the arterial tissues and perivascular nerves. However, the expression and the functional role of the receptors on both mouse superior mesenteric artery and carotid artery at the pre-junctional site or the perivascular nerves within the adventitia was still unclear. These receptors could be expressed on the pre-junctional nerve terminal of the blood vessels and serve as auto- and/or heteroreceptors. Pre-junctional receptors could be able to regulate the release of various neurotransmitters via feedback loops, making them a useful therapeutic target.

3.4.2.2 Expression of P2X and P2Y receptor mRNA transcripts in mouse superior cervical ganglion

The superior cervical ganglion has been employed as a model of peripheral sympathetic ganglions. These ganglia receive innervation from the spinal cord and send projections to the lacrimal gland, salivary gland and dilator pupillae muscles in the eye. The sympathetic nerves are mostly adrenergic and originate in the thoracolumbar segments of the spinal cord, where they project to a variety of target organs, including smooth muscle through sympathetic ganglions (Stevenson, 2015). ACh is released by pre-ganglionic neurons and binds to nicotinic receptors on post-ganglionic neurons. The post-ganglionic neurons end at the adventitial-medial border, where nerve activation results in the release of neurotransmitters (NA and ATP) from vesicles contained within the nerve varicosities. When neurons are electrically stimulated, NA and ATP are released from the nerve terminals, where they can act on receptors placed pre-junctionally, on the nerve terminal, or post-junctionally, on smooth muscle cells and endothelial cells (Stevenson, 2015). Post-junctional P2X and P2Y receptors can be activated by ATP, while post-junctional α1- and α2- adrenergic receptors can be activated via NA to cause vessel constriction (Brock & Cunnane, 1999). P2 receptors have also been shown to exist pre-junctionally and activation of these receptors could modulate (inhibit or facilitate) further neurotransmitter release from the nerve terminals. However, further investigation is required, which is the main aim of our project. In addition, differences in the regulation of sympathetic neural activity may contribute to the various roles played by arteries and veins in the control of blood flow and volume distribution. Therefore, research into the characterisation of vascular

sympathetic neurotransmission and which P2 receptors are expressed on pre-junctional sites is critical, as it may aid in the development of new therapeutic options for cardiovascular disorders that are characterised by elevated sympathetic nerve activity. For example, pre-junctional P2X3 and P2X2/3 receptors on cardiac sympathetic neurons may increase sympathetic neurotransmission via positive feedback (Ralevic, 2012). Furthermore, P2X2 and P2X3-immunoreactive nerve fibre terminals were also located widely in the carotid sinus, aortic arch, atrium, vena cava, ventricles and ganglionic neurons. It has been suggested that extracellular ATP activating homomeric P2X2 and P2X3 receptors and heteromeric P2X2/3 receptors within these tissues is complex in its regulation of systematic circulation blood pressure (Gitterman & Evans, 2000).

Our finding in this project using RT-PCR to characterise the expression of all P2 receptors subunits in mouse superior cervical ganglion suggested that all P2X1-7 and P2Y receptors mRNA are present in mouse superior cervical ganglion. Our hypothesis was, these receptors (especially P2X2, P2X3, P2X5, P2X6, P2Y1, P2Y4 and P2Y12 as they are not found on arterial smooth muscle and the endothelium) could be present as pre-junctional receptors on innervated blood vessels by sympathetic nerves via post-ganglionic axon. These pre-junctional receptors could serve as auto- and/or heteroreceptors and could be able to regulate the release of neurotransmitters so being able to modulate these signals has therapeutic applications in the treatment of vascular diseases, e.g., hypertension. The original mRNA extraction was achieved on entire superior cervical ganglion, which would have contained small intensely fluorescent cells (derived from the neural crest) and sympathetic ganglionic neural cells, glial cells, and blood vessels (Takaki et al., 2015; to Calvert, 2003). Thus, immunohistochemical experiments are required to confirm the presence of these receptors using subtype selective protein antibodies for each candidate P2 protein in colocalisation with neuronal markers.

According to Calvert, 2003 (Calvert, 2003), P2X1, P2X2, P2X3, P2X4 and P2X5 mRNAs were present in whole mouse superior cervical ganglion, with limited detection of both P2X6 and P2X7. One band was detected for P2X2, although the murine P2X2 receptor has splice variants. Other previous RT-PCR studies on splice variants of the P2X2 receptor using total RNA extracted from the cerebellum of neonatal (5-day-old) Sprague-Dawley rats produced two different sized products for P2X2. The experiment was repeated with a different primer set and showed the same results, suggesting that alternative splicing has the potential to produce an alternative naturally occurring variety of the P2X2 receptor (Calvert, 2003; Brändle et al., 1997; Simon et al., 1997). RT-PCR showed the presence of mRNA for all P2X receptors, suggesting the possibility of multiple subunit expression within the mouse superior cervical

ganglion (Calvert & Evans, 2004). This is compatible with our present results in this study. P2Y receptor isoforms were investigated previously in whole superior cervical ganglion from mice. The results showed positive bands of the expected product sizes for P2Y1, P2Y2, P2Y6, P2Y12 and P2Y13. However, the P2Y4 mRNA amplification product was not detected (Calvert, 2003). Although, the primers used were for amplification of P2Y4 receptors from genomic DNA (Vial et al., 2002). This is in close agreement with the current study except P2Y4 receptor which was detected in the mouse superior cervical ganglion in our study.

As it is mentioned above, in addition to neural cells, the superior cervical ganglion includes other components such as small intensely fluorescent cells, glial cells and blood vessels which could be included in the total RNA. Previous studies performing RT-PCR on neural cell cultures found mRNA for all the seven P2X receptors, but a decrease in P2X1 mRNA expression. This could be due to a decrease in the starting material utilised for mRNA extraction, or the existence of blood arteries in the whole tissue, which have significant P2X1 subunit expression in the smooth muscle and could have contributed a large amount of transcript to the whole tissue extractions (Calvert, 2003). This indicated that potentially all of the P2X receptors could be expressed by superior cervical ganglion neurons. However, these cultures would contain some glial cells as well as neurons. According to Calvert et al., (2004), P2Y subtype-selective primers amplified products belonging to P2Y1, P2Y2 and P2Y6 receptors, but not the P2Y4 receptor from the superior cervical ganglion (neuronal cell culture), in RT–PCR investigations.

Similar investigations have been conducted on this tissue in rats, and the results presented here are largely consistent with them. Xiang et al (1998) demonstrated by using immunoreactive experiments the expression of all P2X receptors except for P2X5 in the rat superior cervical ganglion. Furthermore, a previous study in rat superior cervical ganglion showed immunoreactivity for P2X1, P2X3, P2X4 and P2X5 (Li et al., 2000). According to Molliver et al., (2002), an in-situ hybridisation study for P2Y2 receptors in rat superior cervical ganglion presented low or no hybridisation, which suggested that there is maybe negligible (or very low) expression of P2Y2 receptors in the rat superior cervical ganglion. Previous combination studies of RT-PCR and Northern blot in the rat superior cervical ganglion demonstrated that P2Y1, P2Y2 and P2Y6 were all expressed at postnatal days 1. However, low expression levels were detected by RT-PCR for the P2Y4 receptor (Vartian et al., 2001) which is in close agreement with our current study.

3.5 Summary

This is the first study in which mouse superior cervical ganglion, superior mesenteric artery and carotid artery tissues have been examined for all P2 receptor expression. We found many of these receptors (P2X1, P2X4, P2X7, P2Y2, P2Y6, P2Y13 and P2Y14) were expressed in all the tissues. However, some receptors (P2X2, P2X3, P2X5, P2X6, P2Y1, P2Y4 and P2Y12) were expressed in the superior cervical ganglion but not expressed in the superior mesenteric artery (faint band for P2Y4) and carotid artery. We suggest that receptor subtypes detected in sympathetic ganglia but not arteries could be expressed by sympathetic post-ganglionic nerves that innervate arteries. Here they could serve as pre-junctional, regulating the release of NA, ATP or NPY from sympathetic varicosities. Our hypothesis is that pre-junctional receptors could be involved in the regulated release of neurotransmitters, so being able to modulate these signals has therapeutic applications in the treatment of vascular diseases such as hypertension. In the next chapter, we will use immunohistochemical studies to determine which P2X and P2Y receptors are expressed in the mouse superior cervical ganglion and pre-junctional sympathetic nerves of the superior mesenteric artery and carotid artery. The immunohistochemical studies will confirm whether these receptors, which are expressed in the superior cervical ganglion but not in arterial tissues, are present in perivascular nerves of arteries.

Chapter 4: Protein expression of P2 purinergic receptors on sympathetic neurons in mouse superior cervical ganglion and pre-junctional sympathetic nerves in superior mesenteric artery and carotid artery

4.1 Introduction

Neurons that innervate blood vessels possess a role in modulating their contractility via the surrounding smooth muscle cells and endothelial cells. The contractions of these muscles are controlled in part through signals received when neurotransmitters released by sympathetic neurons bind and activate their respective receptors on the smooth muscle cells and endothelial cells. This topic has clinical relevance as the constriction of blood vessels increases blood pressure and local tissue perfusion. Therefore, being able to modulate these signals has therapeutic applications in the treatment of hypertension. Myogenic constriction of blood vessels is generally thought to occur when the vascular smooth muscle membrane is stretched, causing it to depolarise, which causes an increase in the influx of Ca^{2+} through voltage-gated ion channels, which results in the contraction of the vascular smooth muscle (Kaley, 2000). This contractile mechanism is controlled by both external queues from the perivascular nerves and autoregulation via signals from the endothelial cells (Burnstock & Ralevic, 2014). The input from the perivascular nerves allows for the homeostasis of vascular tone due to the opposing signals of the sympathetic and parasympathetic branches of the autonomic nervous system. The majority of blood vessels are not innervated by the parasympathetic nervous system. However, some blood vessels can be innervated by parasympathetic nerves such as cardiac vessels. This nervous control tends to affect vascular resistance on the systemic level (Sheng & Zhu, 2018). Endothelial cells can modify the control of vascular tone on a more local level, often as a result of variations in blood flow, which is detected through shear stress or hypoxia (Burnstock & Ralevic, 2014). One class of receptors vital for the regulation of vascular tone at several levels are the purinergic receptors. These receptors are activated by the binding of extracellular ATP and its breakdown products. Purinergic signalling is required for control of vascular tone both autologously via the endothelial cells and the exogenous signals from the autonomic nervous system (Burnstock, 2018, Sheng & Zhu, 2018).

One type of the key receptors for the regulation and control of neurotransmission are pre-synaptic receptors (in the context of neuron-neuron neurotransmission in the synaptic cleft) which could serve as auto- and/or heteroreceptors playing a role in modulating neurotransmitters release. (Starke et al., 1989). These receptors sense the number of

neurotransmitters in the synaptic cleft and as a response, regulate any further release and that allows for fine-tuning of neurotransmitters release. Once the receptors are activated, they operate negative or positive feedback loops to inhibit or stimulate neurotransmission release, respectively, which play important physiological roles. (Nishanthi & Vimal, 2017). It has been suggested that these auto- and heteroreceptors act by changing the levels of Ca^{2+} entry into the varicosities, thus influencing neurotransmitter release via exocytosis (O'Connor et al., 1999). The role of several auto and heteroreceptors receptors on pre-synaptic nerve terminals has been identified including adrenergic, cholinergic, dopaminergic and GABAergic pre-synaptic autoreceptors. For example, adenosine receptors may have a role in the control of ATP release as a result of soluble nucleosidases released from the pre-synaptic nerve endings, which could potentially break down ATP to adenosine, which would then activate the autoreceptors (Todorov et al., 1997). Several types of pre-synaptic auto- and heteroreceptors are present in the pre-synaptic nerve terminals, including the ionotropic P2X receptor and metabotropic P2Y receptor. P2 receptors function as modulation sites for neurotransmitters release in response to ATP and other nucleotides produced by neuronal activity as well as by pathogenic signals. ATP influences synaptic transmission pre- and post-synaptically, in both positive and negative directions, by activating P2X and P2Y receptors, respectively (Sperlágh et al., 2007). Pre-synaptic metabotropic receptors regulate transmitter release in a negative feedback loop, but pre-synaptic ionotropic receptors can enhance synaptic transmission. Furthermore, activation of ligand-gated cation channels with high Ca^{2+} permeability could cause transmitter release to be triggered directly by Ca^{2+} influx through the receptor-ion channel complex (Sperlágh et al., 2007). Our project aimed to investigate the expression of pre-junctional P2 receptors (in the context of neurotransmission between sympathetic nerve and effector, e.g., blood vessel). There are many pre-junctional receptors yet to be uncovered, which might serve as auto- and/or heteroreceptors as well, and their physiological roles to be identified and utilized as targets for drug discovery. In this chapter, we will focus on P2 receptors which could be present on the pre-junctional nerve terminal of blood vessels. In addition, colocalisation studies of the P2 receptors with several markers were performed, these markers include PGP9.5 as a general marker of neurons, TH as an adrenergic sympathetic marker of neurons, VNUT as a marker of the vesicular storage of ATP, and NPY as a marker of vasomotor neurons.

Protein gene product 9.5 (PGP 9.5) is a neuron-specific protein and is part of the ubiquitin carboxyl-terminal hydrolase family that plays a role in the non-lysosomal proteolytic pathway. Antibodies against PGP9.5 are widely used in immunohistochemical studies as a nerve marker to investigate neuronal elements of the central and peripheral nervous systems, in addition to some non-neuronal cells (Kon et al., 1999). PGP 9.5 is prevalent in the neuron

cytoplasm and neuroendocrine cells, and is a pan-neuronal marker for nervous tissue. Antibodies against PGP 9.5 have been used to visualize different populations and subtypes of nerves in adult and developing peripheral tissues (Chou et al., 2001). This led us to use PGP 9.5 to visualize the innervation of whole arteries and visualize neuronal cells in the mouse superior cervical ganglion. In addition, the PGP9.5 antibody was used in colocalisation experiments with primary antibodies against P2 purinergic receptors to confirm the presence of the P2 receptors studied on positive neuronal cell bodies in the mouse superior cervical ganglion and positive nerves in the mouse superior mesenteric and carotid arteries. This was performed by the indirect immunofluorescence method using an antibody to PGP 9.5. It was demonstrated that PGP 9.5 immunoreactivity occurs in the guinea pig cardiovascular innervation and is present in more individual nerve fibres than other general neuronal markers. Thus, PGP 9.5 can be a useful neuronal marker when investigating cardiovascular innervation and for studying the relative proportions of nerve subpopulations (Gulbenkian et al., 1987).

Tyrosine hydroxylase (TH; tyrosine 3-monooxygenase) catalyzes the conversion of L-tyrosine to L-3,4-dihydroxyphenylalanine (L-DOPA), which is the initial and rate-limiting step in the biosynthetic pathway of catecholamines including dopamine, NA, and adrenaline. In all species, catecholamine synthesis is regulated by the interaction of TH with a cofactor, tetrahydrobiopterin (BH4). Tetrahydrobiopterin binds to the TH catalytic domain, resulting in enzymatic activity. TH is locally synthesized exclusively in the cell body and is subsequently transported to axons and pre-synaptic nerve terminals of noradrenergic neurons or the ultimate site of function (Gervasi et al., 2016). These catecholamines play vital roles in a variety of physiological adrenergic neurons and behavioural functions in the nervous and endocrine systems. TH and choline acetyltransferase function as enzyme markers for pre-ganglionic and post-ganglionic sympathetic nerves, respectively. Several studies reported that there is an increase in the activity of neuronal TH and β-hydroxylase associated with increasing the activity of the peripheral sympathetic nervous. Moreover, increased activity of these enzymes serves as an indicator of sympathetic neuronal activity (Lund et al., 1978). The role of TH in catecholamine neurotransmitter production suggests a link between the enzyme and a variety of neuropathogenic disorders, such as Parkinson's disease, Segawa syndrome, schizophrenia, and dystonia, as well as a variety of cardiovascular diseases. Thus, in this project polyclonal primary anti-TH antibody was used in colocalisation experiments with primary antibodies against P2 purinergic receptors to identify the presence of the P2 receptors studied on TH-positive sympathetic neuronal cell bodies in the mouse superior cervical ganglion. In addition, to investigate the presence of the P2 receptors on the perivascular nerves of the mouse superior mesenteric artery and carotid artery.

Vesicular nucleotide transporter (VNUT), the transporter encoded by the human and mouse SLC17A9 gene, which is responsible for the vesicular storage of ATP in synaptic vesicles and secretory granules in neurons and neuroendocrine cells. ATP is a key chemical transmitter in purinergic signal transmission. ATP is stored in secretory vesicles present in purinergic cells before secretion which results in the various purinergic responses, such as central control of autonomic functions, pain and mechanosensory transduction, neural-glial interactions, control of vessel tone and angiogenesis, and platelet aggregation through purinergic receptors (Sawada et al., 2008; Moriyama et al., 2017). VNUT transports various nucleotides (ATP, ADP, and GTP) across a membrane by using membrane potential as the driving force and is expressed in the various ATP-secreting cells (Moriyama et al., 2017). Despite the well-known features of the signalling pathway following secretion of ATP and activation of its purinergic receptors, the release mechanism of ATP through exocytosis, that is, vesicular ATP release, from the purinergic cells is poorly understood. Presently, it is thought that ATP is released from cells through at least three distinct pathways: exocytosis, channel-mediated release, and cell breakdown (Moriyama et al., 2017; Burnstock, 2007; Lazarowski, 2012). Briefly, neurotransmitters are packaged into vesicles and released via exocytosis. Different neurotransmitters have different vesicular transport mechanisms (e.g., vesicular monoamine transporter for monoamine transmitters like NA and dopamine). A proposed vesicular transporter for ATP is VNUT. In this chapter, colocalisation experiments of VNUT with P2 receptors were performed in the mouse superior cervical ganglion. Identifying VNUT-positive neurons will tell us which neurons are capable of vesicular storage of ATP and possible exocytotic release (Figure 4.1).

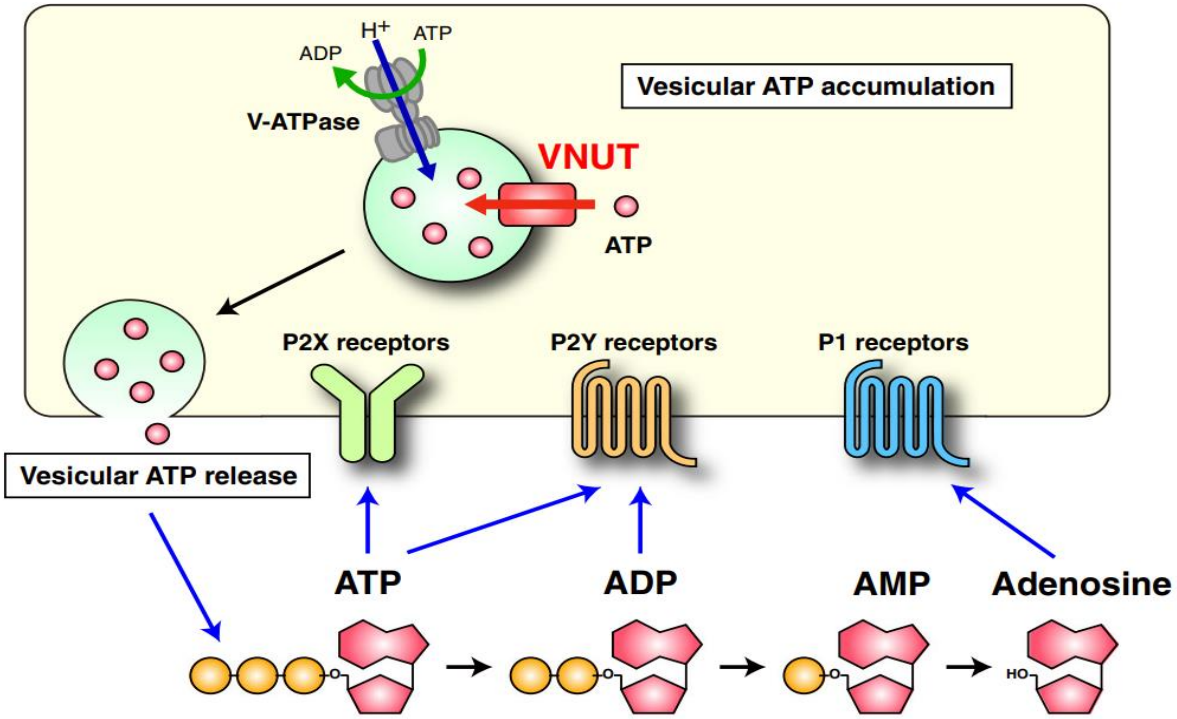

Figure 4.1: Vesicular storage and release of ATP from neurons and purinergic chemical transmission. Vesicular neurotransmitter transporters are responsible for the vesicular storage of neurotransmitters (ATP) in synaptic vesicles and secretory granules in neurons and neuroendocrine cells. The driving force ($\Delta\psi$) is provided by vacuolar H+ -ATPase (V-ATPase), which acts as a primary proton pump, at the expense of ATP hydrolysis. Then, the vesicular ATP is secreted through exocytosis from purinergic cells following stimulation. The released ATP and its hydrolysis metabolites, such as ADP, AMP, and adenosine, can subsequently bind to purinoceptors and convey signals in an autocrine or paracrine way (Moriyama et al., 2017).

Neuropeptide Y (NPY) often denotes those neurons that have vasomotor activity (innervate target tissue such as blood vessels and glands), as many neurons in the superior cervical ganglion will not have vasomotor activity. Approximately 90% of rat superior cervical ganglion neurons belong to one of three functional groups: vasomotor neurons that innervate and control blood flow in the head, pilomotor neurons that innervate arrector pili muscles and secretomotor neurons that serve the submandibular salivary glands (Headley et al., 2007). In the cells of paravertebral chain ganglia, NPY is a key cotransmitter in vasoconstrictor sympathetic neurons, which constitute 50–70% of the cells in paravertebral chain ganglia (Headley et al., 2007). The superior cervical ganglion is the primary source of sympathetic nerve fibres to cranial tissues, with small contributions from the lower sympathetic ganglia. Stimulation of these fibres leads to several responses including vasoconstriction, modulation of cerebrovascular autoregulation, control of intracranial pressure, blood volume and cerebrospinal fluid production. These responses are mediated via NA and NPY (Tajti et al., 1999). NPY-hrGFP transgenic reporter mice were used in this project to investigate NPY-positive neurons, which will tell us which neurons have vasomotor activities and could innervate blood vessels. To investigate this, immunohistochemical studies were performed with primary antibodies against P2 purinergic receptors to confirm the presence of the P2 receptors on NPY-positive neurons in the mouse superior cervical ganglion, superior mesenteric artery and carotid artery isolated from NPY-hrGFP transgenic reporter mice. In addition, an antibody to PGP9.5 was used in colocalisation studies in sections of the superior cervical ganglion of the NPY-GFP transgenic mice.

4.2 Aim

This study aimed to gain both a qualitative and quantitative understanding of the purinergic receptors (P2 receptors) present on the pre-junctional terminal of sympathetic nerves, focussing specifically on their expression in the cell bodies of the superior cervical ganglion and the pre-junctional terminal of sympathetic nerves in superior mesenteric arteries and carotid artery. Under physiological conditions, pre-junctional P2 receptors can regulate the release of various neurotransmitters via feedback loops, which could potentially provide a novel target for the therapeutic control of vascular tone and ultimately blood pressure. Frozen sections of mouse superior cervical ganglion, superior mesenteric artery and carotid artery, and whole-mount preparations of the superior mesenteric artery and carotid artery are used in immunohistochemical studies to colocalise all P2X receptors and P2Y1 with PGP9.5 and TH. In addition, immunohistochemistry studies were performed for P2 receptors (P2X2, P2X3 and

P2Y1) which were expressed by RT-PCR just in the mouse superior cervical ganglion but not in the superior mesenteric artery and carotid artery with, VNUT and NPY (using NPY/GFP reporter mice). Specific antibodies for P2X, P2Y receptors and the markers are used in these experiments shown in Table 2.14. When available, commercially available blocking peptides were used to test the specificity of primary polyclonal antibodies. In addition, Western blots were performed to confirm the specificity and functionality of the antibodies using the same mouse tissues, in addition to the mouse brain as a control. Confocal and apotome microscopes were used to visualise the tissues and the sections. The level of colocalisation of neuronal markers with receptors studied, was quantified using Image J software - to determine whether the expression of P2 receptors in neuronal cell bodies is significantly different.

4.3 Results

4.3.1 Protein expression of P2 purinergic receptors in the mouse superior cervical ganglion (coexpression of PGP9.5 with P2 receptors)

The protein expression of the P2 receptors consistently detected at the mRNA level using RT-PCR (section 3.3) were confirmed by immunohistochemistry staining in transverse sections (10 µm) of the superior cervical ganglion. In addition, the distribution of these receptors and the numbers of sympathetic neurons expressing P2 receptors were analysed. In this part of the chapter, the colocalisation of P2 purinergic receptors (P2X1, P2X2, P2X3, P2X4, P2X6, P2X7 and P2Y1) with PGP9.5 was explored to determine whether these receptors were coexpressed on autonomic superior cervical ganglion neurons. PGP9.5 and P2 receptor immunoreactivities were observed in the ganglionic cell bodies, except P2X6 receptor immunoreactivity which was absent. The ganglionic neuronal cell bodies showed intense immunoreactivity for PGP9.5 in the middle of the superior cervical ganglion. Immunocytochemistry not only confirmed that the mRNA expression profile was representative of the protein level expression of P2 receptors in the superior cervical ganglion, but it also provided an insight into the cellular localisation and distribution of each receptor. The staining was evenly distributed throughout the cytoplasm of these cells, and the immunocytochemical staining revealed that P2X1, P2X2, P2X3, P2X4, P2X7 and P2Y1 receptors (Figures 4.2 - 4.8) when they were detected, were distributed relatively uniformly throughout the superior cervical ganglion, although the staining was fainter for P2X3 receptor. Immunofluorescence doubling labelling for PGP9.5 (red) and P2 receptors revealed coexpression (yellow) of PGP9.5 with all receptors except P2X6 which was not expressed in the superior cervical ganglion (Figures 4.2 - 4.8). These results suggested that the receptors could be expressed by sympathetic post-ganglionic nerves that innervate arteries. Thus, these receptors could be present on perivascular nerves of the pre-junctional terminal of the tissues innervated by post-ganglionic nerves. These results also presented that the ganglion neurons showed variable levels of staining for PX1, P2X2, P2X3, P2X4, P2X7 and P2Y1 receptors. Differences in the expression level of each receptor subtype exist in subpopulations of neurons in the same ganglion, which indicates the diversity of receptor subtypes involved in the physiological functions of different neurons. Control sections are shown in which no primary antibodies were applied and where just the secondary antibody was applied, to see if there was any non-specific binding. None of the receptors showed significant immunoreactivity in the control sections (Figure 4.9). Staining was significantly reduced when using the control antigen peptide with the antibodies supplied with antigen peptide control (Figures 4.2, 4.3, 4.5 & 4.6).

The levels of staining were variable between neuronal cell bodies or between different receptors, but it could not be determined if this was an artefact from the antibody or the sectioning process. The expression levels of the receptors of each receptor on the ganglion neurons were quantified using Image J. although, different antibodies were used which makes the comparison of the relative protein expression level of each receptor less accurate due to differing antibody affinities and the efficacy of the antibody**.** The statistical analysis showed approximately 85% of neurons were labelled for P2X1, and P2X7 receptors, but the level of fluorescence was high for P2X1 and lower for P2X7. A low level of the expression of the P2X3 receptor was observed in superior cervical ganglion (~ 70%). The exception was that very strong P2X3 receptor immunoreactivity was detected in about 50% of neurons, while the remaining neurons showed weaker immunoreactivity. The anti-P2X4 antibodies gave a high percentage of coexpression with PGP9.5 (~ 95%). The labelling in these sections occurred in every cell, and the fluorescence was very bright and uniform for P2X4, however, the levels of fluorescence for P2X3 appeared to be low for this antibody. Most sections of the superior cervical ganglion neurons showed intense P2X2 and P2Y1 expression approximately 80% and 90% respectively (Figure 4.10). Moreover, there were significant differences in the coexpression of P2 receptors studied and PGP 9.5 in the superior cervical ganglion neurons (Figure 4.10). It was found that polyclonal antibodies for the seven P2X receptor subtypes (P2X6 receptor was absent) could label over 70-90% of neurons in the superior cervical ganglion neurons to different intensities. This study also suggested that many neurons could express numerous isoforms of P2 receptors in the same nerve cell body because over 70% of neurons were labelled by most of the antibodies. There was also considerable variation in the intensity of immunoreactivity in individual neurons within the ganglia. Few ganglionic cells did not show coexpression between PGP9.5 and P2 receptors (labelled for P2 receptor only) and that could indicate these receptors could have coexpression with other ganglionic cells such as glial or the PGP9.5 antibody did not bind well to the target epitope. Briefly, all of the anti-P2X antibodies (except P2X6) showed different levels of staining in the superior cervical ganglion neurons. The levels were variable and some receptors had a significantly different expression. We did not investigate the P2X5 receptor as some humans have a functional form and others do not (Bo et al., 2003). In mice, it is functional and can form heteromers in some cells however, there are no selective antagonists (Lalo et al., 2008). It is important to mention here that the comparison of high and low expression levels using any of the detection methods could be inaccurate. None of these methods evaluates the efficacy of the antibodies or primers being used. A low expression level may be just the result of using an antibody that did not bind well to the target epitope, which could be due to epitope masking caused by the protein's

structural folding. Moreover, immunohistochemistry results should be considered with care, unless the specificity of the antibody can be confirmed in the tissue being examined. Western blotting might be used to accomplish this, with the emergence of a single band of the correct molecular weight which would indicate specificity.

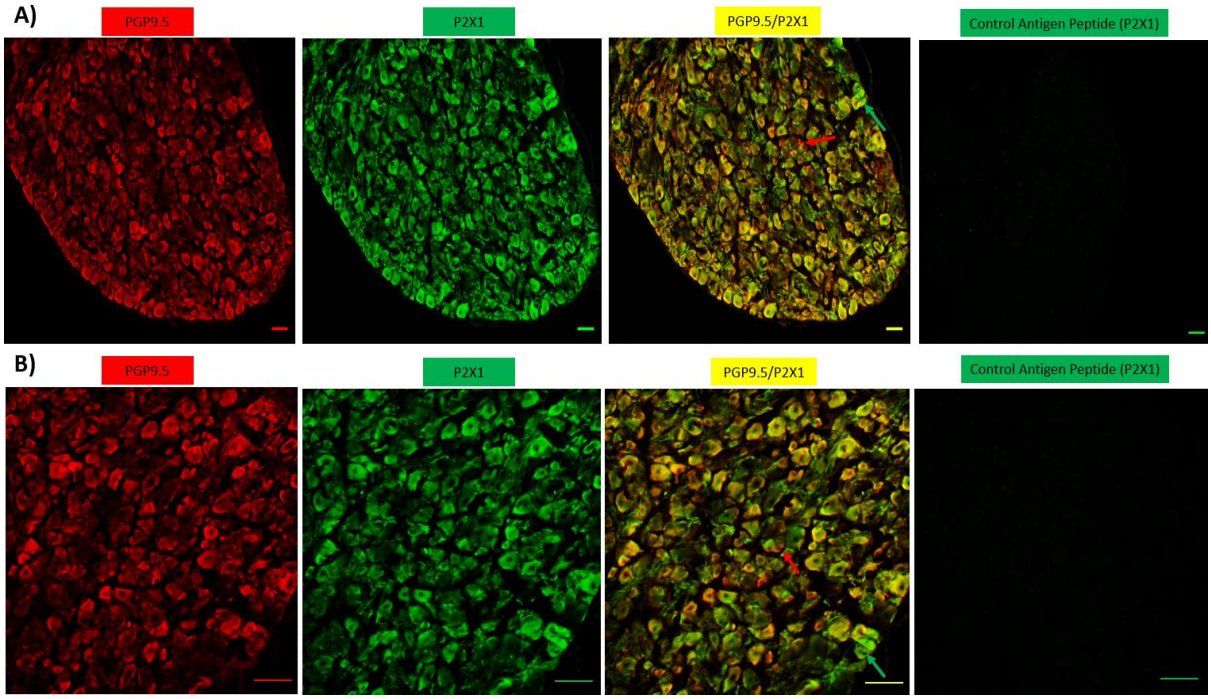

Figure 4.2: Coexpression of PGP 9.5 with P2X1 receptor in mouse superior cervical ganglion neurons. Immunocytochemical double staining for PGP9.5 (red) and P2X1 receptor (green) in transverse sections (10 µm) of mouse superior cervical ganglion. PGP 9.5 and P2X1 were colocalised in the same nerve cell body (yellow). Images were visualized using a Laser-scanning confocal microscope Zeiss LSM510 META (Zeiss), equipped with an excitation filter system of 458/488 nm for FITC and 467 for the red channel. Control sections are shown in which the control antigen peptide. The sections are seen at x10 (A) and x 20 (B) magnification. The exposure and camera settings remained consistent across all the images taken for each experiment. Scale bars represent 50 µm. The green arrow indicates neuronal cell bodies labelled for P2X1 receptor only. The red arrow indicates neuronal cell bodies labelled for PGP9.5 neuronal marker only. The results shown are representative from five independent experiments using five different mice.

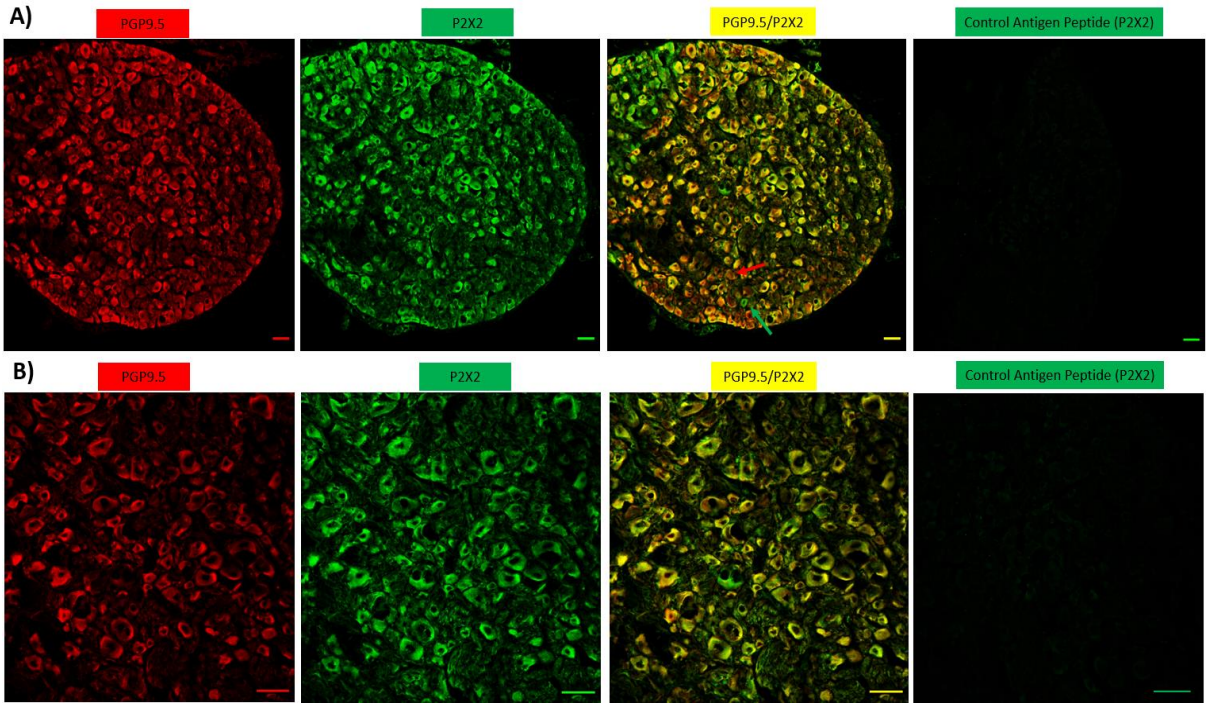

Figure 4.3: Coexpression of PGP 9.5 with P2X2 receptor in mouse superior cervical ganglion neurons. Immunocytochemical double staining for PGP9.5 (red) and P2X2 receptor (green) in transverse sections (10 µm) of mouse superior cervical ganglion. PGP 9.5 and P2X2 were colocalised in the same nerve cell body (yellow). Images were visualized using a Laser-scanning confocal microscope Zeiss LSM510 META (Zeiss), equipped with an excitation filter system of 458/488 nm for FITC and 467 for the red channel. Control sections are shown in which the control antigen peptide. The sections are seen at x10 (A) and x 20 (B) magnification. The exposure and camera settings remained consistent across all the images taken for each experiment. Scale bars represent 50 µm. The green arrow indicates neuronal cell bodies labelled for P2X2 receptor only. The red arrow indicates neuronal cell bodies labelled for PGP9.5 neuronal marker only. The results shown are representative from five independent experiments using five different mice.

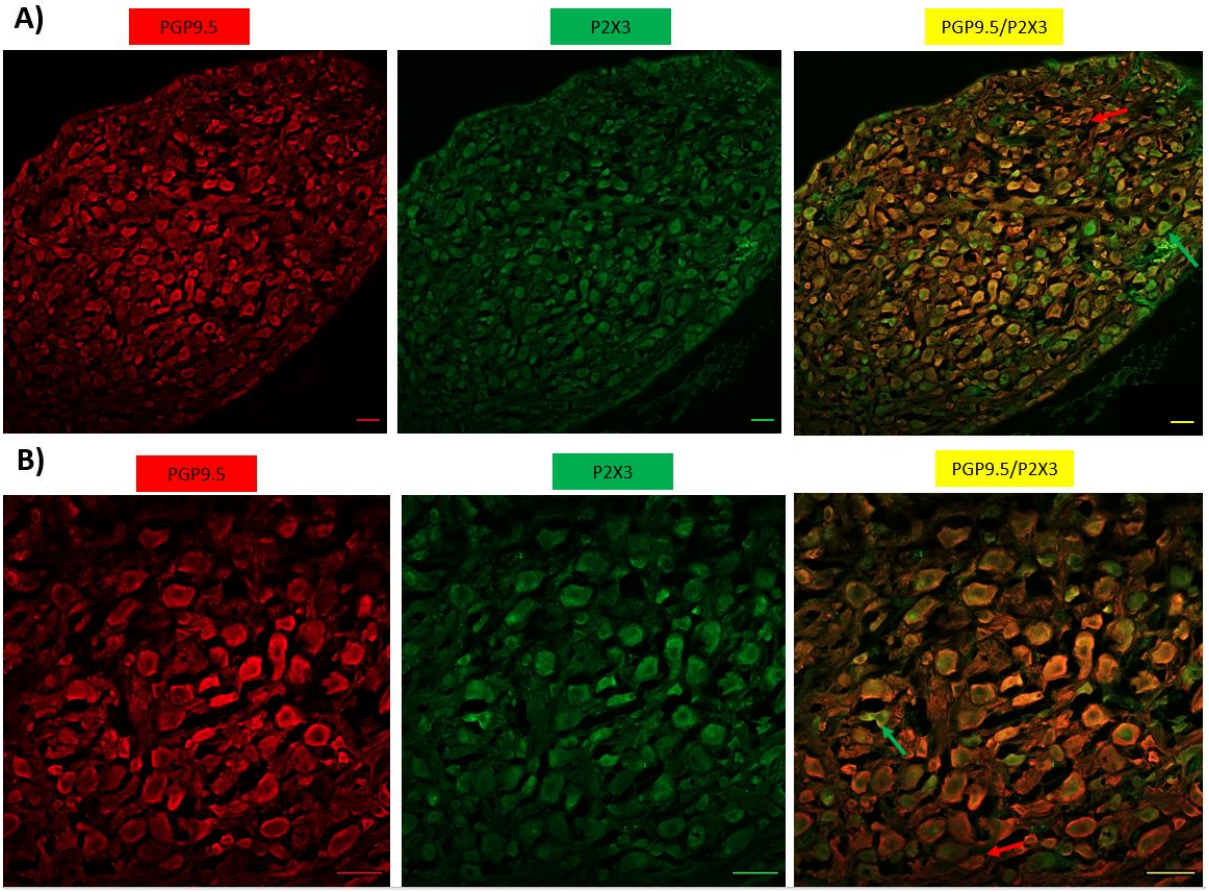

Figure 4.4: Coexpression of PGP 9.5 with P2X3 receptor in mouse superior cervical ganglion neurons. Immunocytochemical double staining for PGP9.5 (red) and P2X3 receptor (green) in transverse sections (10 µm) of mouse superior cervical ganglion. PGP 9.5 and P2X3 were colocalised in the same nerve cell body (yellow). Images were visualized using a Laser-scanning confocal microscope Zeiss LSM510 META (Zeiss), equipped with an excitation filter system of 458/488 nm for FITC and 467 for the red channel. The sections are seen at x10 (A) and x 20 (B) magnification. The exposure and camera settings remained consistent across all the images taken for each experiment. Scale bars represent 50 µm. The green arrow indicates neuronal cell bodies labelled for P2X3 receptor only. The red arrow indicates neuronal cell bodies labelled for PGP9.5 neuronal marker only. The results shown are representative from five independent experiments using five different mice.

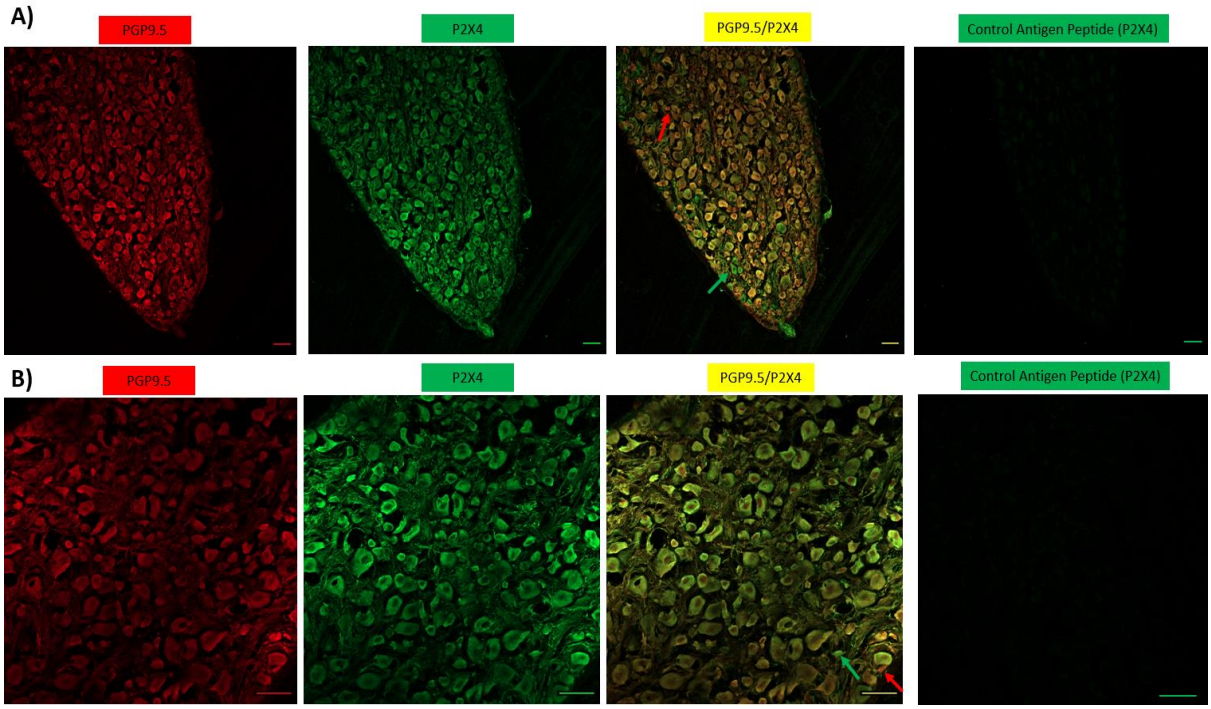

Figure 4.5: Coexpression of PGP 9.5 with P2X4 receptor in mouse superior cervical ganglion neurons. Immunocytochemical double staining for PGP9.5 (red) and P2X4 receptor (green) in transverse sections (10 µm) of mouse superior cervical ganglion. PGP 9.5 and P2X4 were colocalised in the same nerve cell body (yellow). Images were visualized using a Laser-scanning confocal microscope Zeiss LSM510 META (Zeiss), equipped with an excitation filter system of 458/488 nm for FITC and 467 for the red channel. Control sections are shown in which the control antigen peptide. The sections are seen at x10 (A) and x 20 (B) magnification. The exposure and camera settings remained consistent across all the images taken for each experiment. Scale bars represent 50 µm. The green arrow indicates neuronal cell bodies labelled for P2X4 receptor only. The red arrow indicates neuronal cell bodies labelled for PGP9.5 neuronal marker only. The results shown are representative from five independent experiments using five different mice.

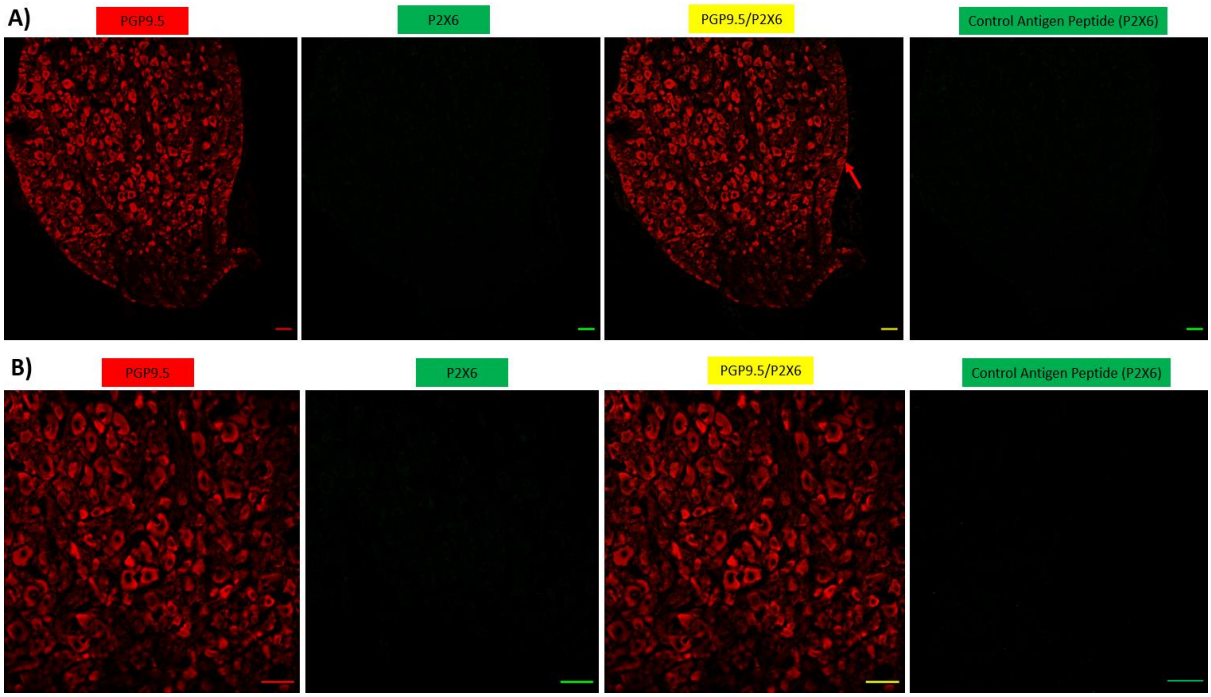

Figure 4.6: Coexpression of PGP 9.5 with P2X6 receptor in mouse superior cervical ganglion neurons. Immunocytochemical double staining for PGP9.5 (red) and P2X6 receptor (green) in transverse sections (10 µm) of mouse superior cervical ganglion. PGP 9.5 and P2X6 were not colocalised in the same nerve cell body (yellow). Images were visualized using a Laser-scanning confocal microscope Zeiss LSM510 META (Zeiss), equipped with an excitation filter system of 458/488 nm for FITC and 467 for the red channel. Control sections are shown in which the control antigen peptide. The sections are seen at x10 (A) and x 20 (B) magnification. The exposure and camera settings remained consistent across all the images taken for each experiment. Scale bars represent 50 µm. The red arrow indicates neuronal cell bodies labelled for PGP9.5 neuronal marker only. The results shown are representative from five independent experiments using five different mice.

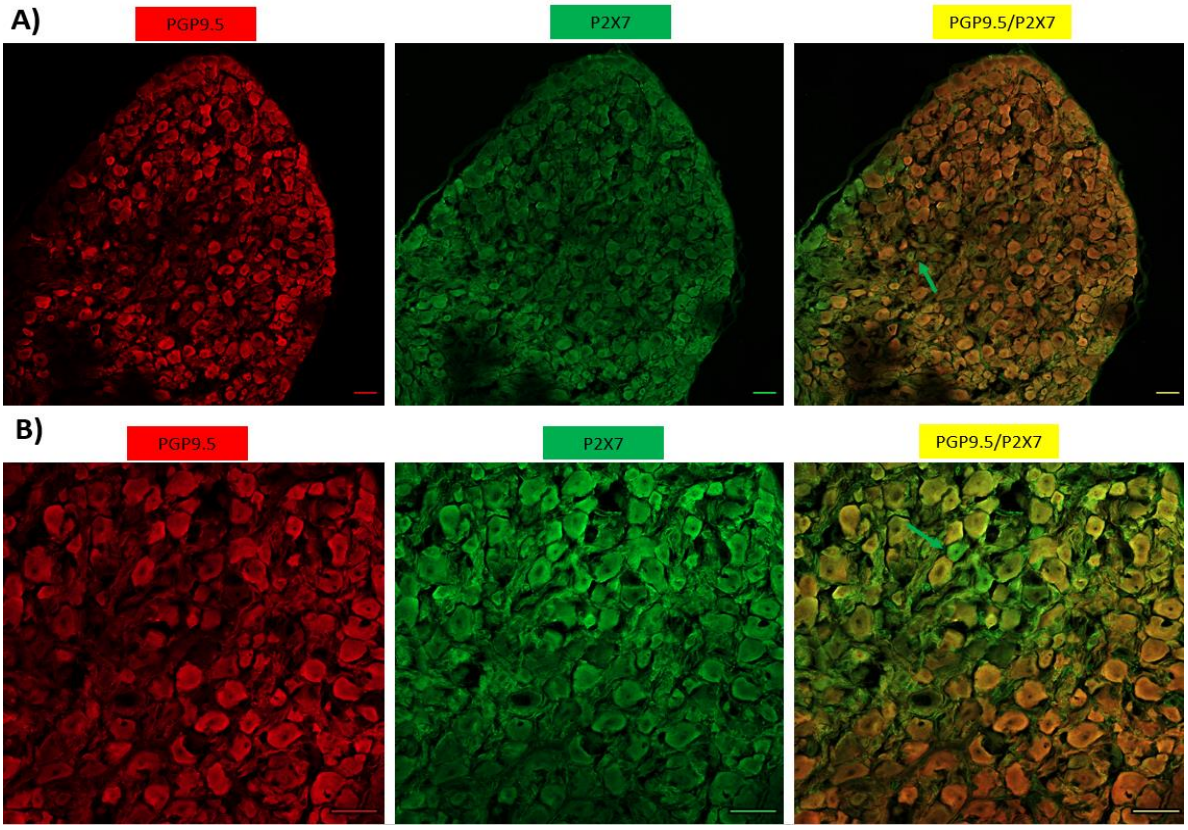

Figure 4.7: Coexpression of PGP 9.5 with P2X7 receptor in mouse superior cervical ganglion neurons. Immunocytochemical double staining for PGP9.5 (red) and P2X7 receptor (green) in transverse sections (10 µm) of mouse superior cervical ganglion isolated from five independent male mice. PGP 9.5 and P2X7 were colocalised in the same nerve cell body (yellow). Images were visualized using a Laser-scanning confocal microscope Zeiss LSM510 META (Zeiss), equipped with an excitation filter system of 458/488 nm for FITC and 467 for the red channel. Control sections are shown in which the control antigen peptide. The sections are seen at x10 (A) and x 20 (B) magnification. The exposure and camera settings remained consistent across all the images taken for each experiment. Scale bars represent 50 µm. The green arrow indicates neuronal cell bodies labelled for P2X7 receptor only. The results shown are representative from five independent experiments using five different mice.

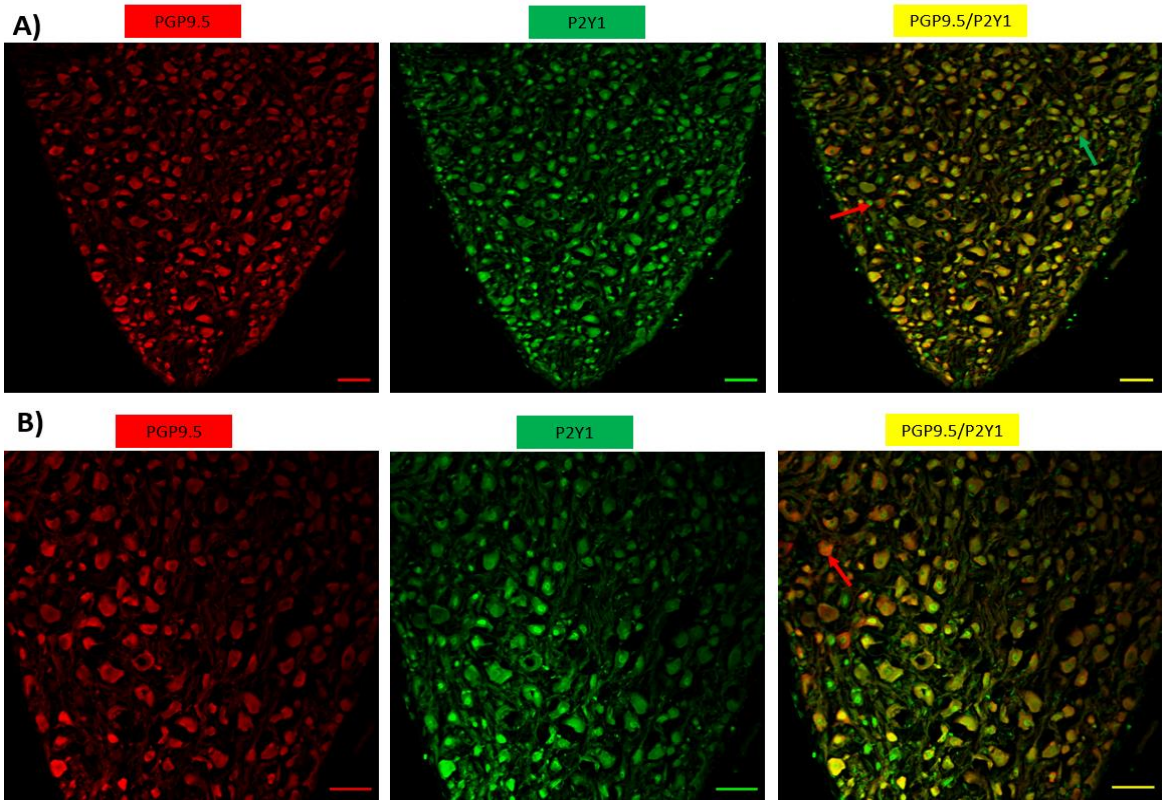

Figure 4.8: Coexpression of PGP 9.5 with P2Y1 receptor in mouse superior cervical ganglion neurons. Immunocytochemical double staining for PGP9.5 (red) and P2Y1 receptor (green) in transverse sections (10 µm) of mouse superior cervical ganglion. PGP 9.5 and P22Y1 were colocalised in the same nerve cell body (yellow). Images were visualized using a Laser-scanning confocal microscope Zeiss LSM510 META (Zeiss), equipped with an excitation filter system of 458/488 nm for FITC and 467 for the red channel. Control sections are shown in which the control antigen peptide. The sections are seen at x10 (A) and x 20 (B) magnification. The exposure and camera settings remained consistent across all the images taken for each experiment. Scale bars represent 50 µm. The green arrow indicates neuronal cell bodies labelled for P2Y1 receptor only. The red arrow indicates neuronal cell bodies labelled for PGP9.5 neuronal marker only. The results shown are representative from five independent experiments using five different mice.

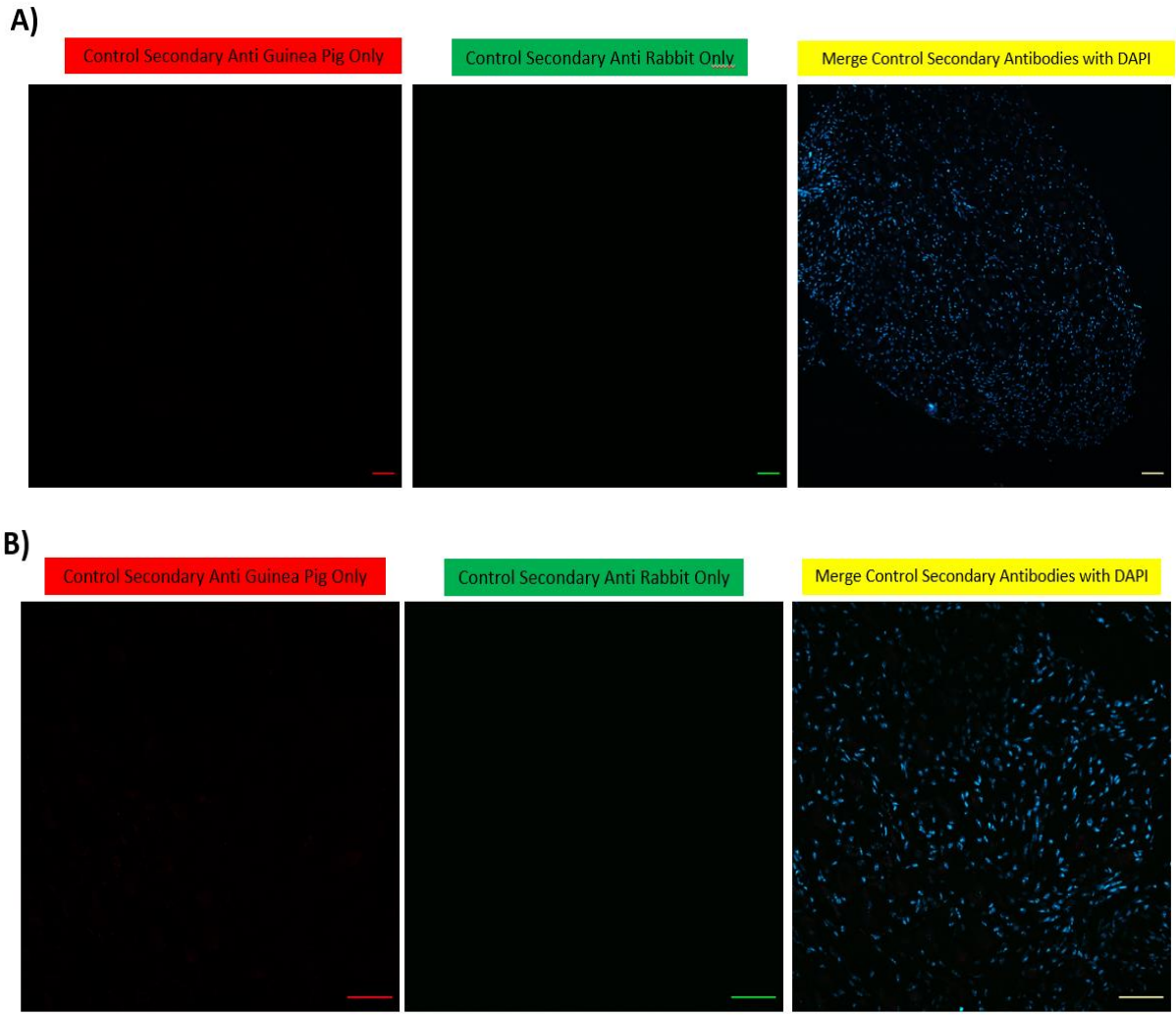

Figure 4.9: Control double immunofluorescence labelling for PGP9.5 and P2 receptors in mouse superior cervical ganglion neurons. Control sections are shown where just the secondary antibody was applied, to see if there was any non-specific binding and to determine the autofluorescence of the tissue. Immunocytochemical double staining for secondary anti guinea pig (red) and secondary anti rabbit (green) in transverse sections (10 µm) of the mouse superior cervical ganglion. Images were visualized using a Laser-scanning confocal microscope Zeiss LSM510 META (Zeiss), equipped with an excitation filter system of 458/488 nm for FITC and 467 for the red channel. In control sections, cells are counterstained with DAPI to visualise nuclei (blue). The sections are seen at x10 (A) and x 20 (B) magnification. The exposure and camera settings remained consistent across all the images taken for each experiment. Scale bars represent 50 µm. The results shown are representative from five independent experiments using five different mice.

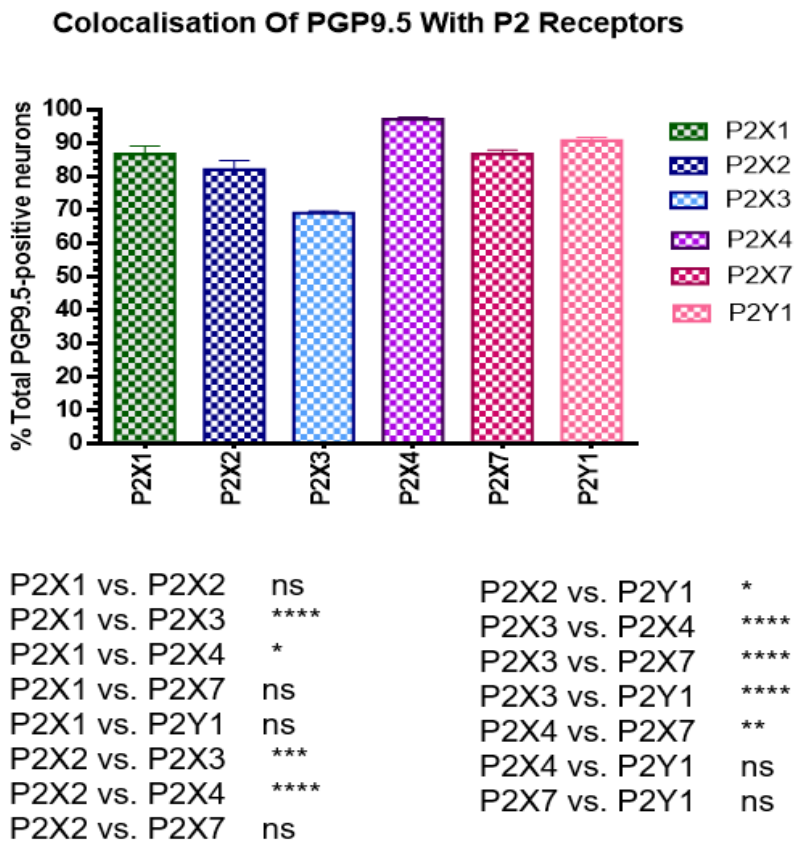

Figure 4.10: The percentage of PGP9.5-positive neurons expressing P2 receptors in the mouse superior cervical ganglion. Comparison of the percentage of superior cervical ganglion PGP9.5- positive neurons expressing the P2 receptors of interest. Experiments were compared by a one-way ANOVA followed by Brown-Forsythe multiple comparison test (GraphPad Prism 6), *p<0.05, **p<0.005, ***p<0.001, ****p<0.0001, ns indicates not significant (p>0.05), mean with SEM. The results shown are representative from five independent experiments using five different mice.

4.3.2 Protein expression of P2 purinergic receptors in the mouse superior cervical ganglion (coexpression of TH with P2 receptors)

The observation that the P2X2, P2X3 and P2Y1 mRNAs were expressed in the mouse superior cervical ganglion and not in the superior mesenteric artery and carotid artery led us to investigate the localization of the corresponding proteins in situ. To identify this, we identified sympathetic neurons by using TH (red) in colocalisation with PGP9.5 (green) using double-label immunofluorescence. Then, P2X2, P2X3 and P2Y1 subunits were involved in colocalisation with TH to determine whether these receptors were expressed by sympathetic superior cervical ganglion neurons. In addition, the study involved P2X1, P2X4 and P2X7 to investigate whether the receptors were expressed by sympathetic superior cervical ganglion neurons. We found many neurons in the superior cervical ganglion were strongly positive for TH as ~ 98% of the PGP9.5-positive cell bodies showed TH positivity (Figures 4.11 & 4.19.A). These results suggested the superior cervical ganglion neurons were mostly sympathetic, but other types of neurons could be placed in the superior cervical ganglion, such as sensory neurons, and that required further investigations using specific markers. It was reported by Getsy et al., (2004) that the small intensely fluorescent cells in the mouse superior cervical ganglion are also innervated by sensory afferent fibres of the glossopharyngeal nerve. Immunoreactivities for TH and the P2 receptors were observed in ganglionic cell bodies, again, P2X6 immunoreactivity was absent. Immunofluorescence doubling labelling for TH (red) and the P2 receptors (green) revealed colocalisation (yellow) of TH and the P2 receptors under investigation. The results from the present immunohistochemical study showed that the sympathetic neurons (TH-positive neurons) expressed a variety of P2 receptor subtypes. Moreover, the sympathetic ganglion neurons showed variable levels of staining for PX1, P2X2, P2X3, P2X4, P2X7 and P2Y1 (Figures 4.12 - 4.17). Thus, these receptors could be transferred during the neurotransmission process to perivascular sympathetic nerves of the pre-junctional terminal of the tissues innervated by sympathetic post-ganglionic nerves. However, few P2 nerve cell bodies were not colocalised with the sympathetic neurons and that may indicate that these receptors could be expressed by other types of neurons in the superior cervical ganglion. Control sections are shown in which no primary antibody was applied and where just the secondary antibody was applied, to see if there was any non-specific binding. None of the receptors showed significant immunoreactivity in the control sections (Figure 4.18). From the statistical analysis, approximately 85% of TH -positive neurons were labelled for P2X1, P2X4 and P2X7, but the coexpression of TH was higher with P2X2, and P2Y1 (~ 95 %). Low level expression of P2X3 receptor in the sympathetic ganglia (~ 70 %) indicates that this receptor subtype is not limited to the sensory ganglia where it was highly expressed (Xiang &

Burnstock, 1998). The coexpression of TH with P2X3 was significantly lesser than the coexpression of TH with the other five P2 receptors studied, P2X7 was significantly lesser than P2Y1 in the coexpression with TH. While the expression of P2X1, P2X2, P2X4, and P2X7 were not significantly different on TH-positive neurons (Figure 4.19.B). Briefly, all the anti-P2X antibodies (except P2X6) and P2Y1 showed coexpression with TH. The levels of P2 expression were variable and the expression of some receptors were significantly different in the sympathetic ganglia neurons. In addition, we suggest that receptor subtypes detected in sympathetic ganglia but not arteries could be expressed by sympathetic post-ganglionic nerves that innervate arteries.

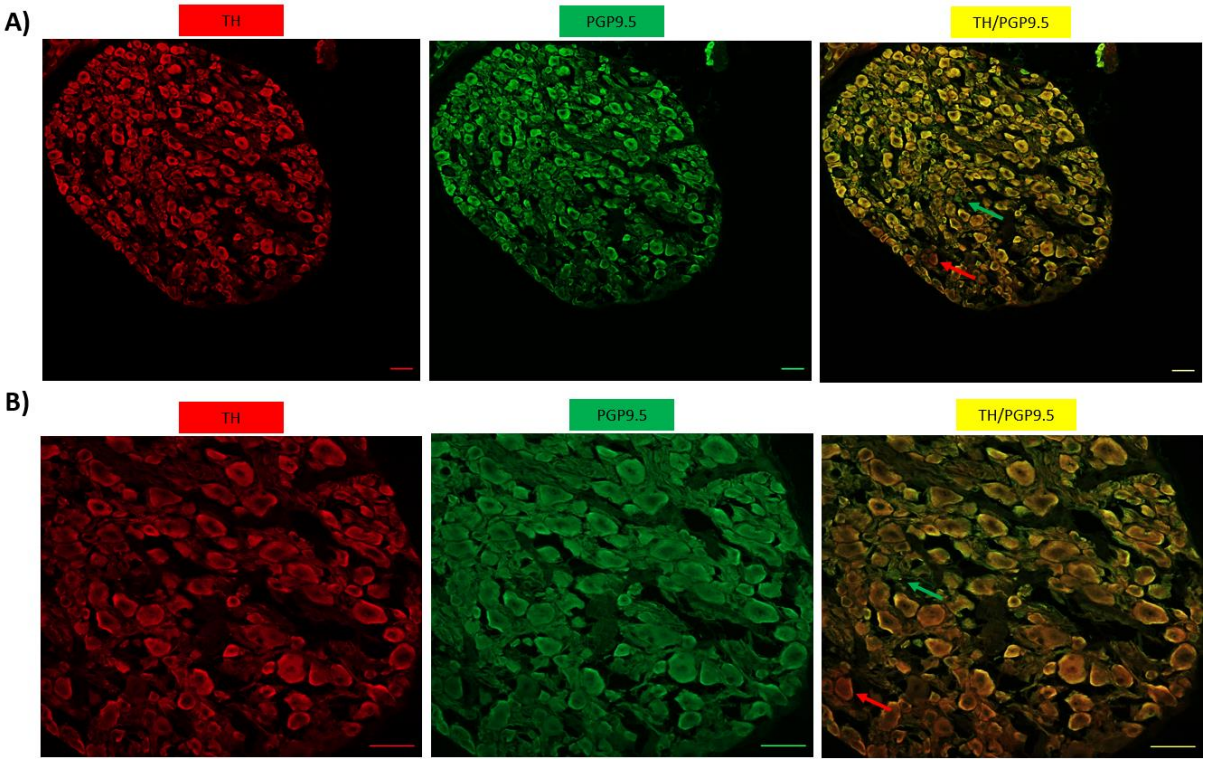

Figure 4.11: Coexpression of TH with PGP9.5 in mouse superior cervical ganglion neurons. Immunocytochemical double staining for TH (red) and PGP9.5 (green) in transverse sections (10 µm) of mouse superior cervical ganglion. TH and PGP9.5 were colocalised in the same nerve cell body (yellow). Images were visualized using a Laser-scanning confocal microscope Zeiss LSM510 META (Zeiss), equipped with an excitation filter system of 458/488 nm for FITC and 467 for the red channel. The sections are seen at x10 (A) and x 20 (B) magnification. The exposure and camera settings remained consistent across all the images taken for each experiment. Scale bars represent 50 µm. The green arrow indicates neuronal cell bodies labelled for the PGP9.5 general neuronal marker only. The red arrow indicates neuronal cell bodies labelled for TH adrenergic sympathetic neuronal marker only. The results shown are representative from five independent experiments using five different mice.

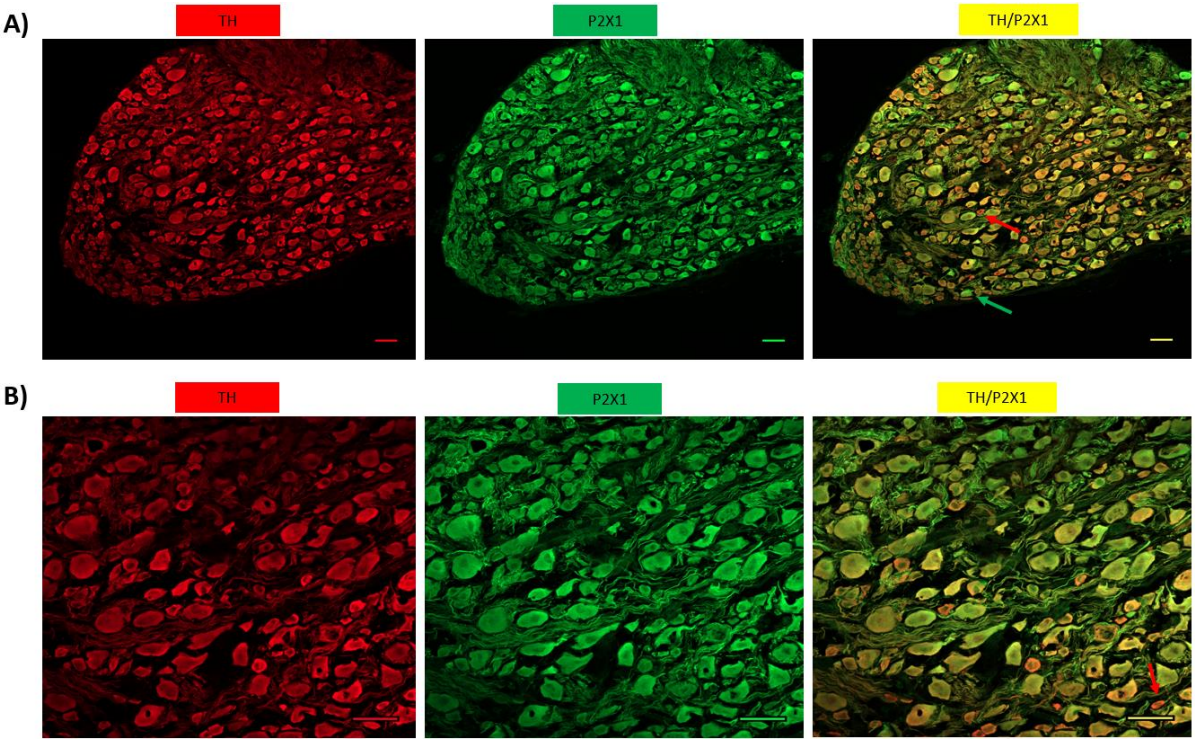

Figure 4.12: Coexpression of TH with P2X1 receptor in mouse superior cervical ganglion neurons. Immunocytochemical double staining for TH (red) and P2X1 receptor (green) in transverse sections (10 µm) of mouse superior cervical ganglion. TH and P2X1 receptor were colocalised in the same nerve cell body (yellow). Images were visualized using a Laser-scanning confocal microscope Zeiss LSM510 META (Zeiss), equipped with an excitation filter system of 458/488 nm for FITC and 467 for the red channel. The sections are seen at x10 (A) and x 20 (B) magnification. The exposure and camera settings remained consistent across all the images taken for each experiment. Scale bars represent 50 µm. The green arrow indicates neuronal cell bodies labelled for P2X1 receptor only. The red arrow indicates neuronal cell bodies labelled for TH neuronal marker only. The results shown are representative from five independent experiments using five different mice.

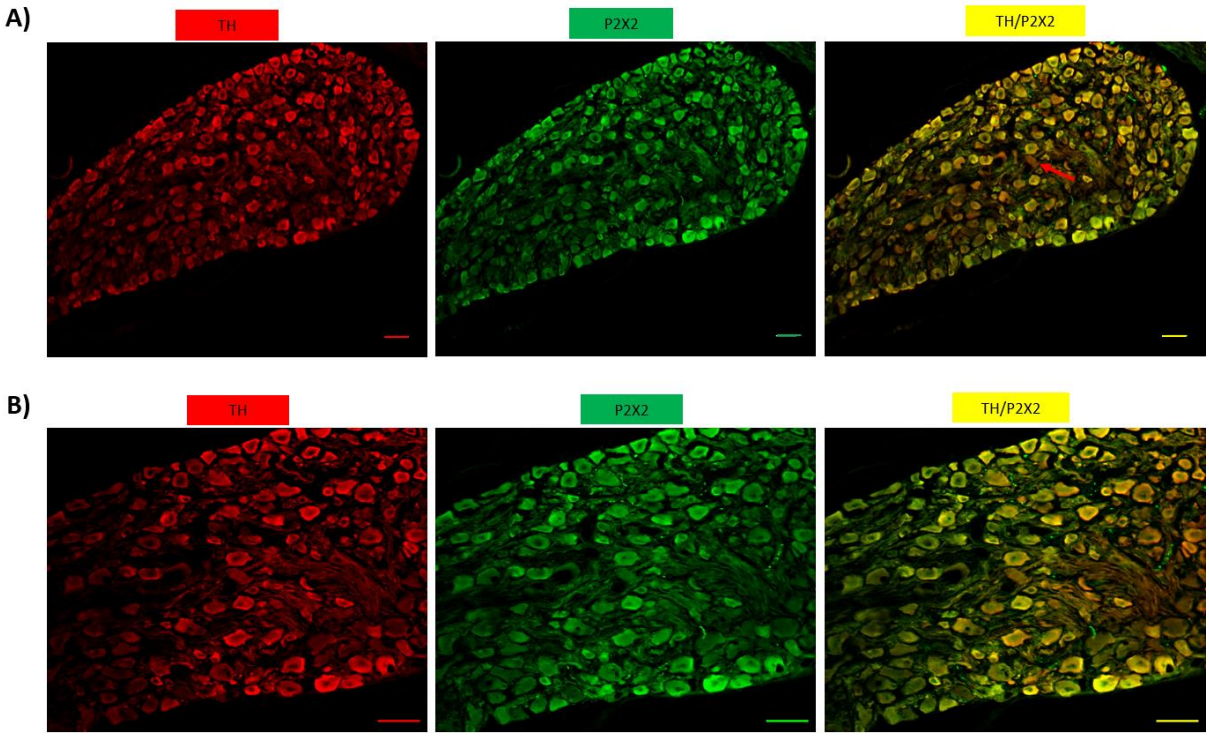

Figure 4.13: Coexpression of TH with P2X2 receptor in mouse superior cervical ganglion neurons. Immunocytochemical double staining for TH (red) and P2X2 receptor (green) in transverse sections (10 µm) of mouse superior cervical ganglion. TH and P2X2 receptor were colocalised in the same nerve cell body (yellow). Images were visualized using a Laser-scanning confocal microscope Zeiss LSM510 META (Zeiss), equipped with an excitation filter system of 458/488 nm for FITC and 467 for the red channel. The sections are seen at x10 (A) and x 20 (B) magnification. The exposure and camera settings remained consistent across all the images taken for each experiment. Scale bars represent 50 µm. The red arrow indicates neuronal cell bodies labelled for TH neuronal marker only. The results shown are representative from five independent experiments using five different mice.

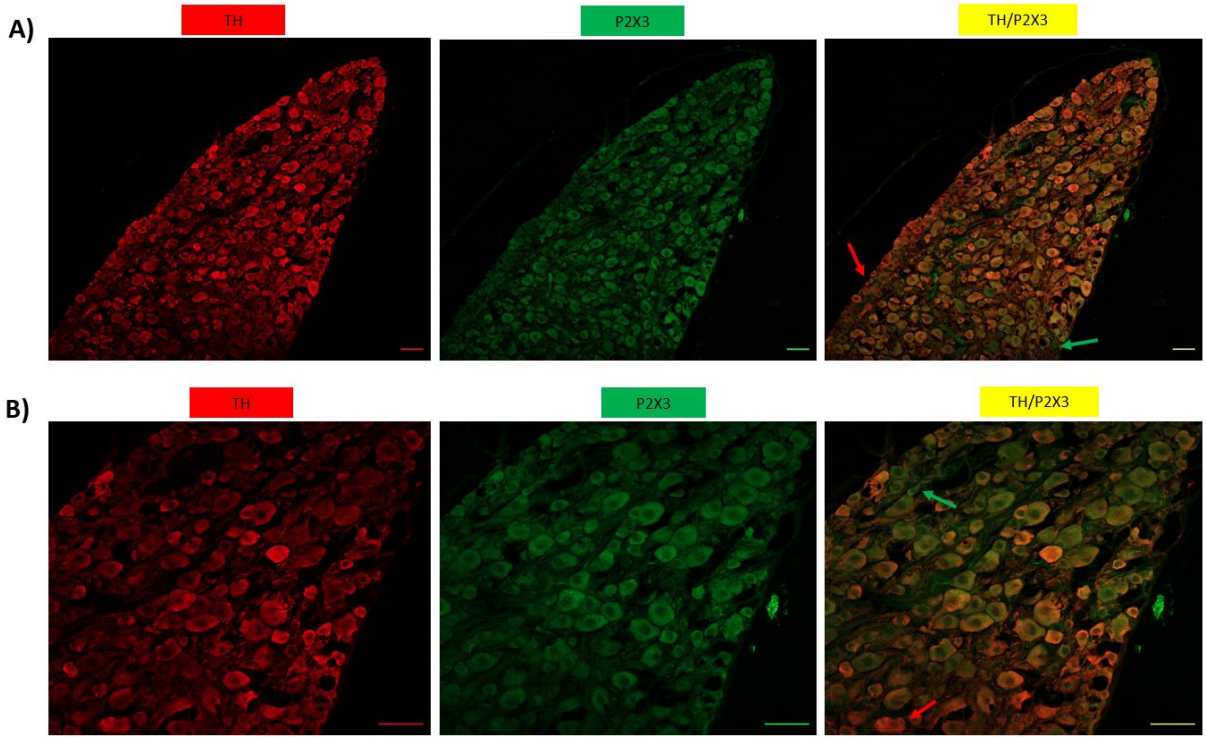

Figure 4.14: Coexpression of TH with P2X3 receptor in mouse superior cervical ganglion neurons. Immunocytochemical double staining for TH (red) and P2X3 receptor (green) in transverse sections (10 µm) of mouse superior cervical ganglion. TH and P2X3 receptor were colocalised in the same nerve cell body (yellow). Images were visualized using a Laser-scanning confocal microscope Zeiss LSM510 META (Zeiss), equipped with an excitation filter system of 458/488 nm for FITC and 467 for the red channel. The sections are seen at x10 (A) and x 20 (B) magnification. The exposure and camera settings remained consistent across all the images taken for each experiment. Scale bars represent 50 µm. The green arrow indicates neuronal cell bodies labelled for P2X3 receptor only. The red arrow indicates neuronal cell bodies labelled for TH neuronal marker only. The results shown are representative from five independent experiments using five different mice.

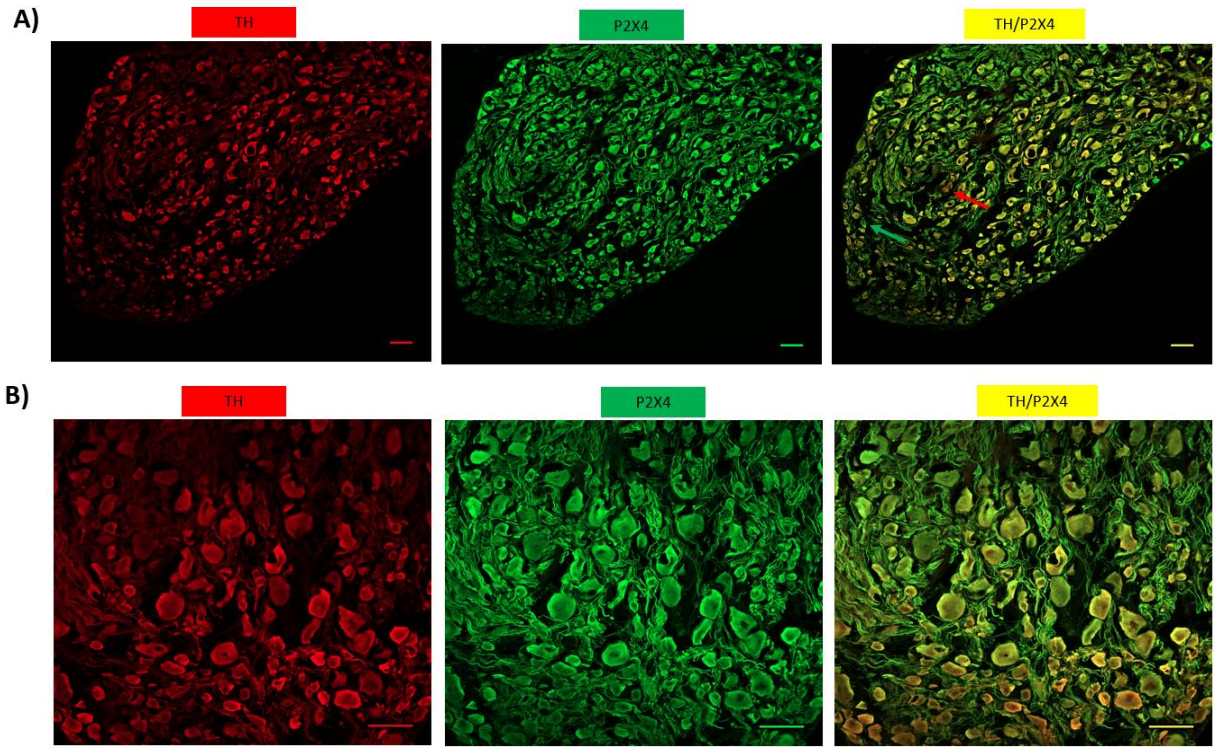

Figure 4.15: Coexpression of TH with P2X4 receptor in mouse superior cervical ganglion neurons. Immunocytochemical double staining for TH (red) and P2X4 receptor (green) in transverse sections (10 µm) of mouse superior cervical ganglion. TH and P2X4 receptor were colocalised in the same nerve cell body (yellow). Images were visualized using a Laser-scanning confocal microscope Zeiss LSM510 META (Zeiss), equipped with an excitation filter system of 458/488 nm for FITC and 467 for the red channel. The sections are seen at x10 (A) and x 20 (B) magnification. The exposure and camera settings remained consistent across all the images taken for each experiment. Scale bars represent 50 µm. The green arrow indicates neuronal cell bodies labelled for P2X4 receptor only. The red arrow indicates neuronal cell bodies labelled for TH neuronal marker only. The results shown are representative from five independent experiments using five different mice.

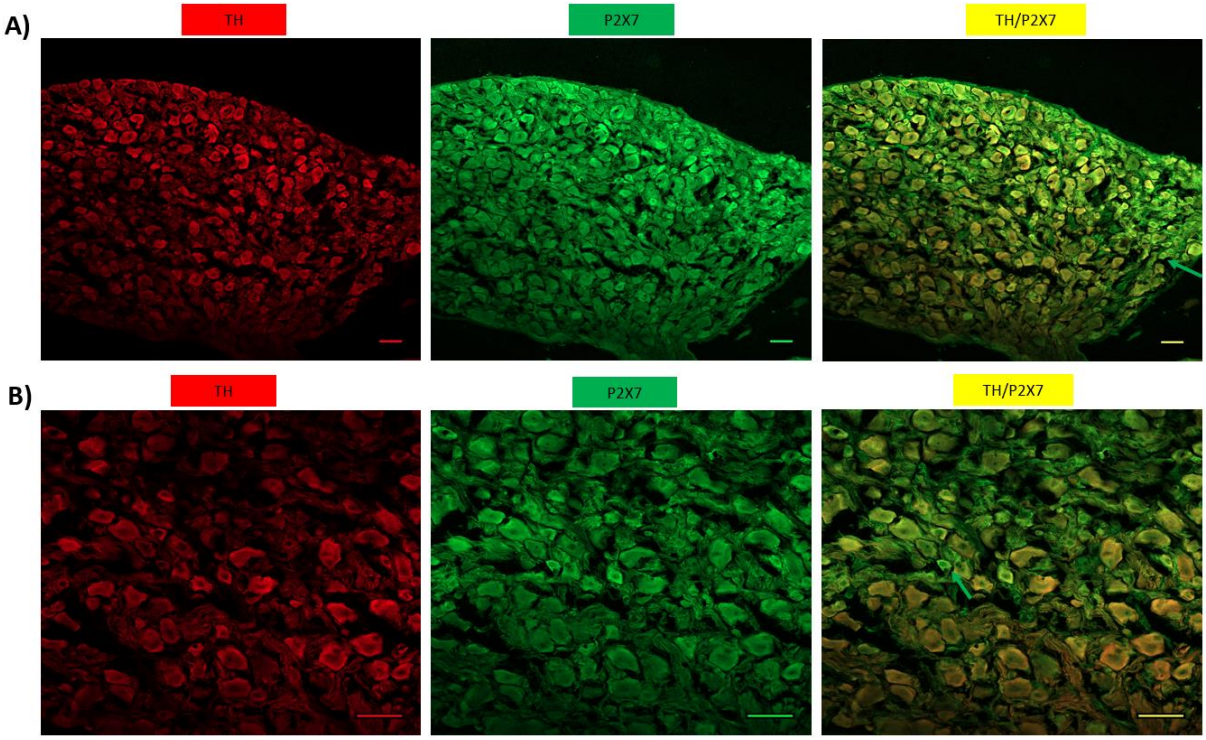

Figure 4.16: Coexpression of TH with P2X7 receptor in mouse superior cervical ganglion neurons. Immunocytochemical double staining for TH (red) and P2X7 receptor (green) in transverse sections (10 µm) of mouse superior cervical ganglion. TH and P2X7 receptor were colocalised in the same nerve cell body (yellow). Images were visualized using a Laser-scanning confocal microscope Zeiss LSM510 META (Zeiss), equipped with an excitation filter system of 458/488 nm for FITC and 467 for the red channel. The sections are seen at x10 (A) and x 20 (B) magnification. The exposure and camera settings remained consistent across all the images taken for each experiment. Scale bars represent 50 µm. The green arrow indicates neuronal cell bodies labelled for P2X7 receptor only. The results shown are representative from five independent experiments using five different mice.

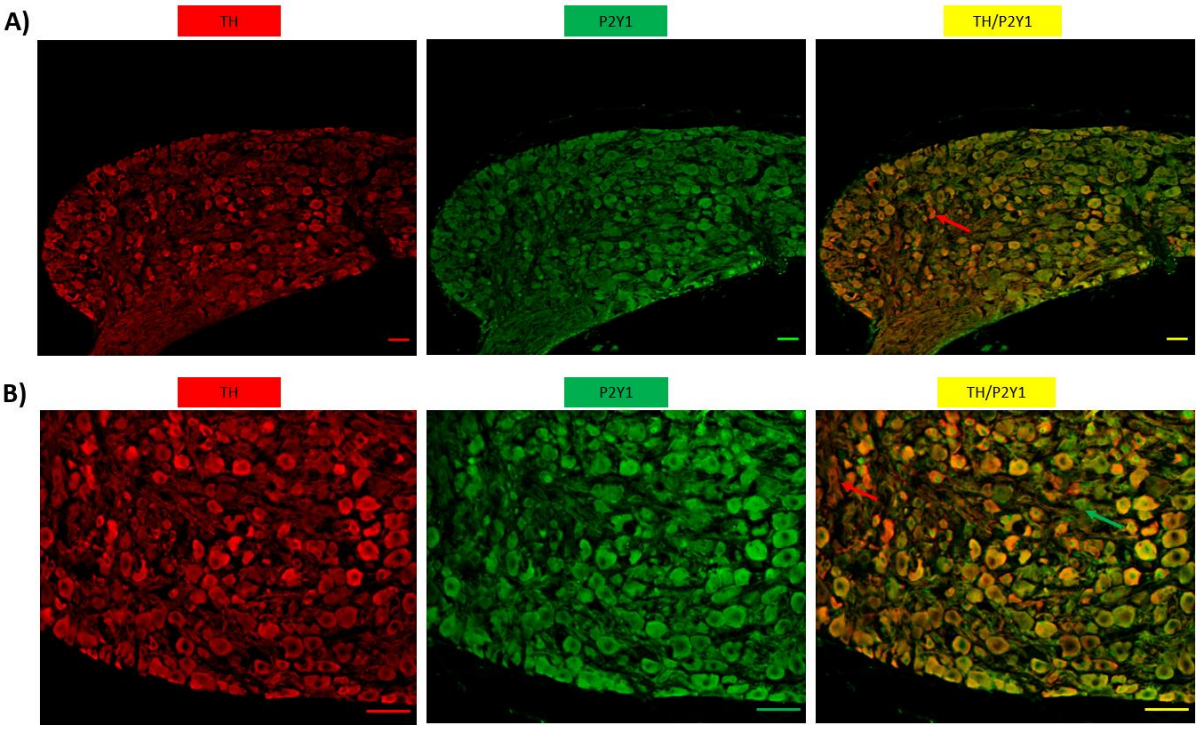

Figure 4.17: Coexpression of TH with P2Y1 receptor in mouse superior cervical ganglion neurons. Immunocytochemical double staining for TH (red) and P2Y1 receptor (green) in transverse sections (10 µm) of mouse superior cervical ganglion. TH and P2Y1 receptor were colocalised in the same nerve cell body (yellow). Images were visualized using a Laser-scanning confocal microscope Zeiss LSM510 META (Zeiss), equipped with an excitation filter system of 458/488 nm for FITC and 467 for the red channel. The sections are seen at x10 (A) and x 20 (B) magnification. The exposure and camera settings remained consistent across all the images taken for each experiment. Scale bars represent 50 µm. The green arrow indicates neuronal cell bodies labelled for P2Y1 receptor only. The red arrow indicates neuronal cell bodies labelled for TH neuronal marker only. The results shown are representative from five independent experiments using five different mice.

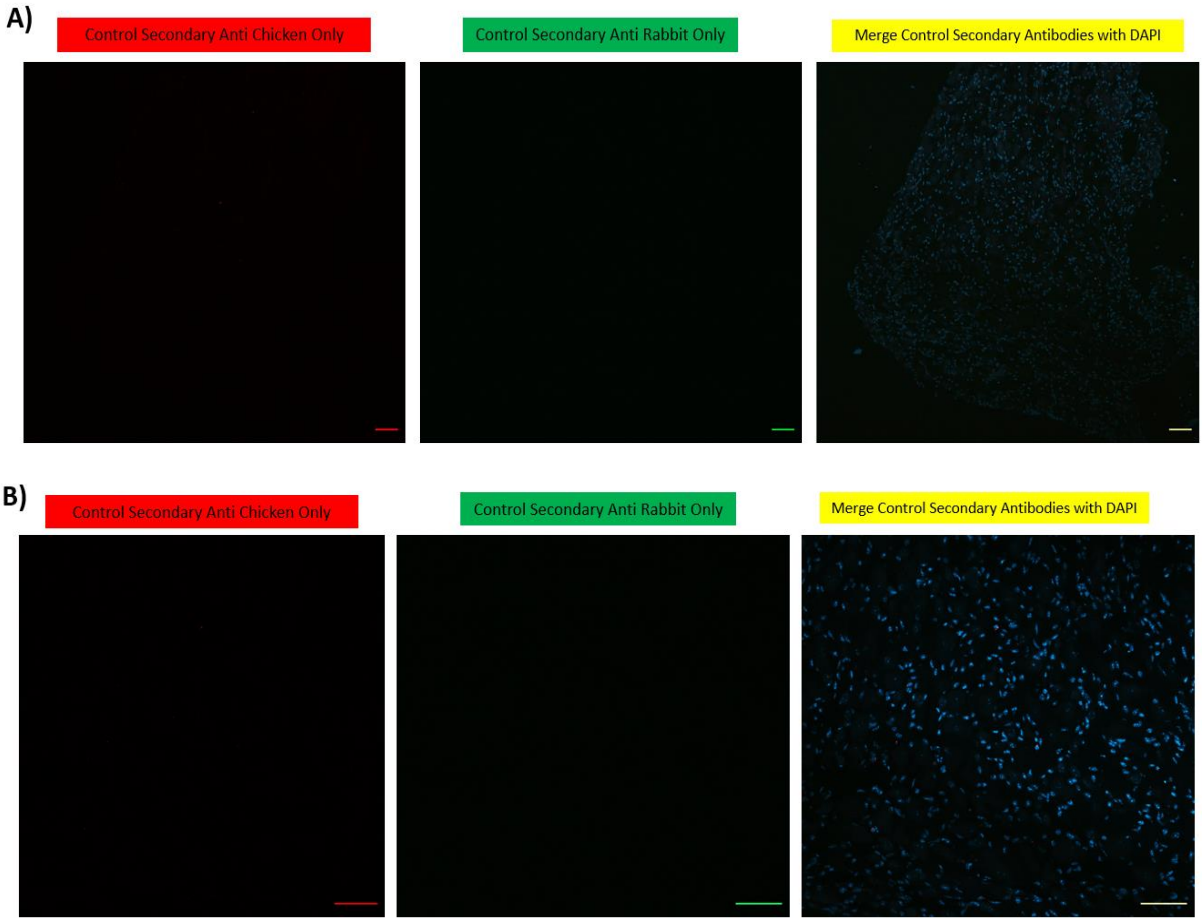

Figure 4.18: Control double immunofluorescence labelling for TH and P2 receptors in superior cervical ganglion neurons. Control sections are shown where just the secondary antibody was applied, to see if there was any non-specific binding and to determine the autofluorescence of the tissue. Immunocytochemical double staining for secondary anti chicken (red) and secondary anti rabbit (green) in transverse sections (10 µm) of the mouse superior cervical ganglion. Images were visualized using a Laser-scanning confocal microscope Zeiss LSM510 META (Zeiss), equipped with an excitation filter system of 458/488 nm for FITC and 467 for the red channel. In control sections, cells are counterstained with DAPI to visualise nuclei (blue). The sections are seen at x10 (A) and x 20 (B) magnification. The exposure and camera settings remained consistent across all the images taken for each experiment. Scale bars represent 50 µm. The results shown are representative from five independent experiments using five different mice.

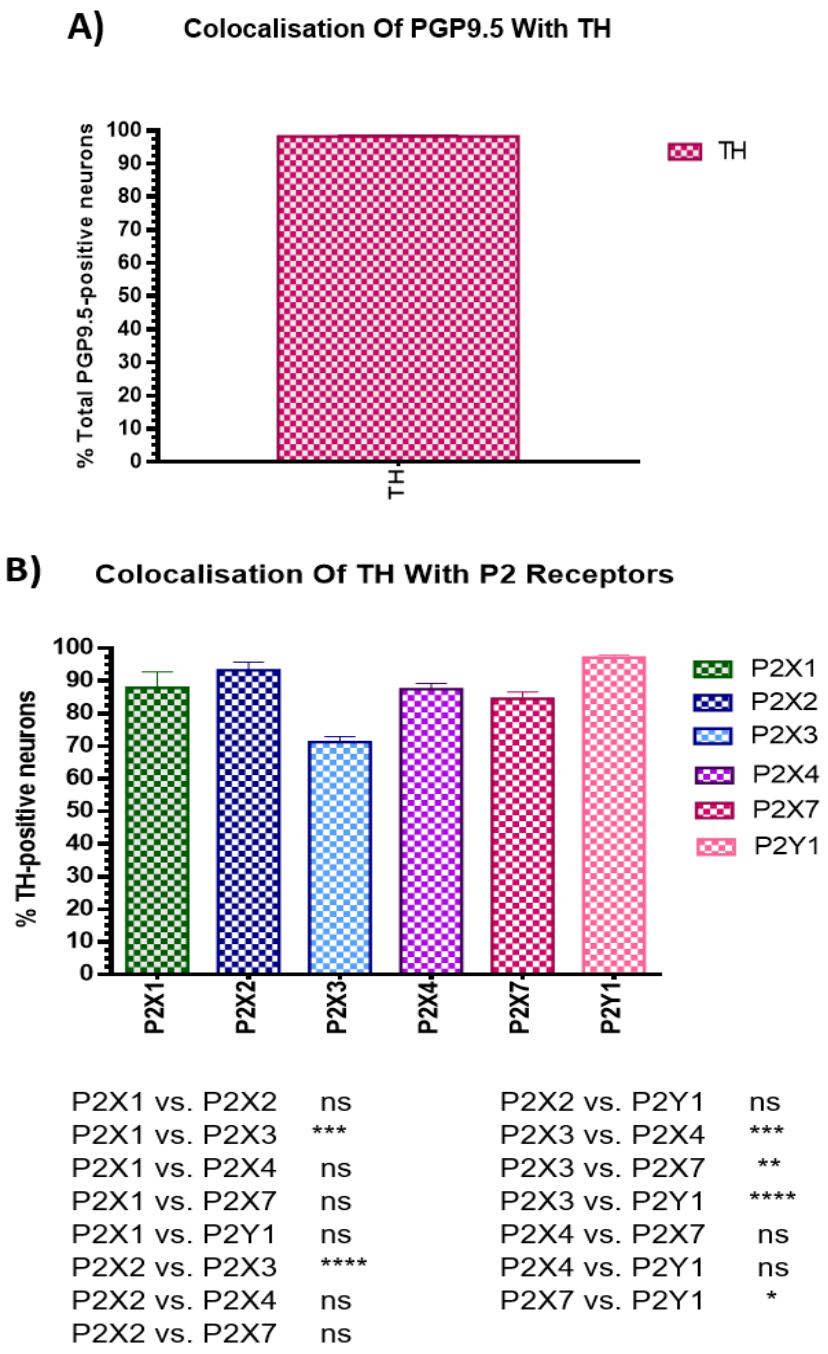

Figure 4.19: The percentage of TH-positive neurons expressing P2 receptors in mouse superior cervical ganglion. (A) The percentage of mouse superior cervical ganglion neurons showing TH-positive neurons. (**B)** Comparison of the expression of P2 receptors of interest in the superior cervical ganglion TH-positive neurons. Experiments were compared by a one-way ANOVA followed by Brown-Forsythe multiple comparison test (GraphPad Prism 6), *p<0.05, **p<0.005, ***p<0.001, ****p<0.0001, ns not significant (p>0.05), mean with SEM. The results shown are representative from five independent experiments using five different mice.

4.3.3 Protein expression of P2 purinergic receptors in the mouse superior cervical ganglion (coexpression of VNUT with P2 receptors)

In both the central and peripheral nervous systems, chemical transmission at the synapse is critical for cellular communication. In 2008, It was confirmed that SLC17A9 encoded the VNUT that is responsible for the vesicular storage of ATP and other nucleotides into secretory vesicles, playing an essential role in the vesicular release of nucleotides and the initiation of purinergic chemical transmission. VNUT may transport a wide variety of nucleotides in a vesicular membrane potential-dependent manner and is expressed in several ATP-secreting cells (Miras-Portugal et al., 2019). In this part of the project, by using antibodies against VNUT and PGP9.5 in double immunofluorescence using mouse superior cervical ganglion, we identified VNUT- positive neurons and quantified neurons that were capable of vesicular storage of ATP and possible exocytotic release. In addition, the colocalisation of P2X2, P2X3 and P2Y1 receptors with VNUT was quantified to identify the percentage of P2 positive neurons which were potentially capable of vesicular storage of ATP. Immunofluorescence doubling labelling for VNUT (red) and PGP9.5 (green) revealed most neurons in the superior cervical ganglion were strongly positive for VNUT as showed co-expression of PGP9.5 with VNUT, ~ 80% of the PGP9.5-positive nerve cell bodies showed VNUT positivity (Figure 4.20 & 4.25.A). The result suggested that 80% of neurons in the superior cervical ganglion are capable of vesicular storage of ATP. Furthermore, immunofluorescence doubling labelling for VNUT (red) with P2X2, P2X3 and P2Y1 receptors (green) showed coexpression (yellow) of VNUT with the P2 receptors studied. To show the distribution more clearly, the numbers per VNUT, P2-positive cells were calculated (Figure 4.21-4.23). From the statistical analysis, there was a significant difference in the expression level between P2X2, P2X3 and P2Y1 receptors for VNUT. We found ~75 % of P2X2 positive nerve cell bodies labelled for VNUT, ~ 85% of P2X3 labelled for VNUT and ~ 90 % of P2Y1 labelled for VNUT (Figure 4.25.B). Control sections are shown in which no primary antibody was applied and where just the secondary antibody was applied, to see if there was any non-specific binding (Figure 4.24). The percentage of P2-positive cells labelled for VNUT were variable and some receptors were significantly different in their coexpression. The coexpression of the P2X3 receptor with VNUT was significantly higher than for the P2X2 and P2Y1 subtypes. Thus, it was suggested that VNUT might play an important role in the regulation of ATP signalling in superior cervical ganglion through the accumulation of ATP in the neurons.

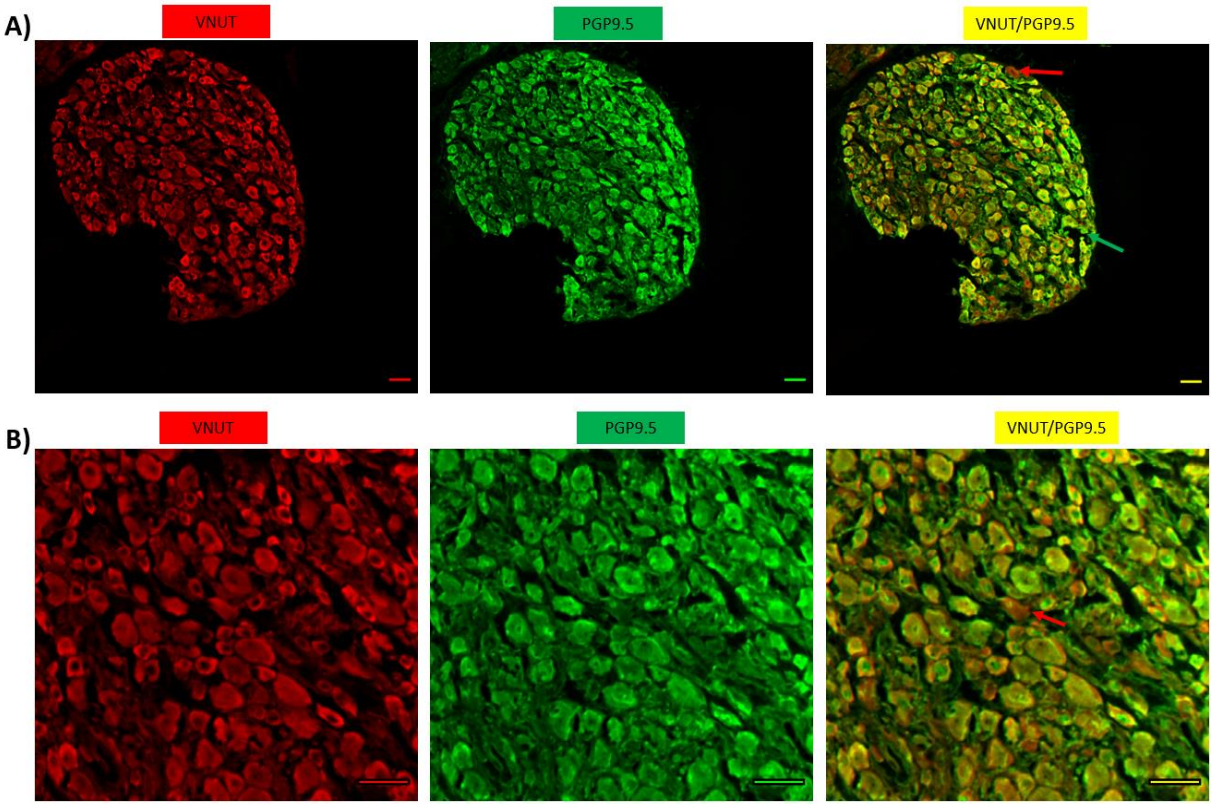

Figure 4.20: Coexpression of VNUT with PGP9.5 in mouse superior cervical ganglion neurons. Immunocytochemical double staining for VNUT (red) and PGP9.5 (green) in transverse sections (10 µm) of mouse superior cervical ganglion VNUT and PGP9.5 were colocalised in the same nerve cell body (yellow). Images were visualized using a Laser-scanning confocal microscope Zeiss LSM510 META (Zeiss), equipped with an excitation filter system of 458/488 nm for FITC and 467 for the red channel. The sections are seen at x10 (A) and x 20 (B) magnification. The exposure and camera settings remained consistent across all the images taken for each experiment. Scale bars represent 50 µm. The green arrow indicates neuronal cell bodies labelled for the PGP9.5 neuronal marker only. The red arrow indicates neuronal cell bodies labelled for VNUT only. The results shown are representative from five independent experiments using five different mice.

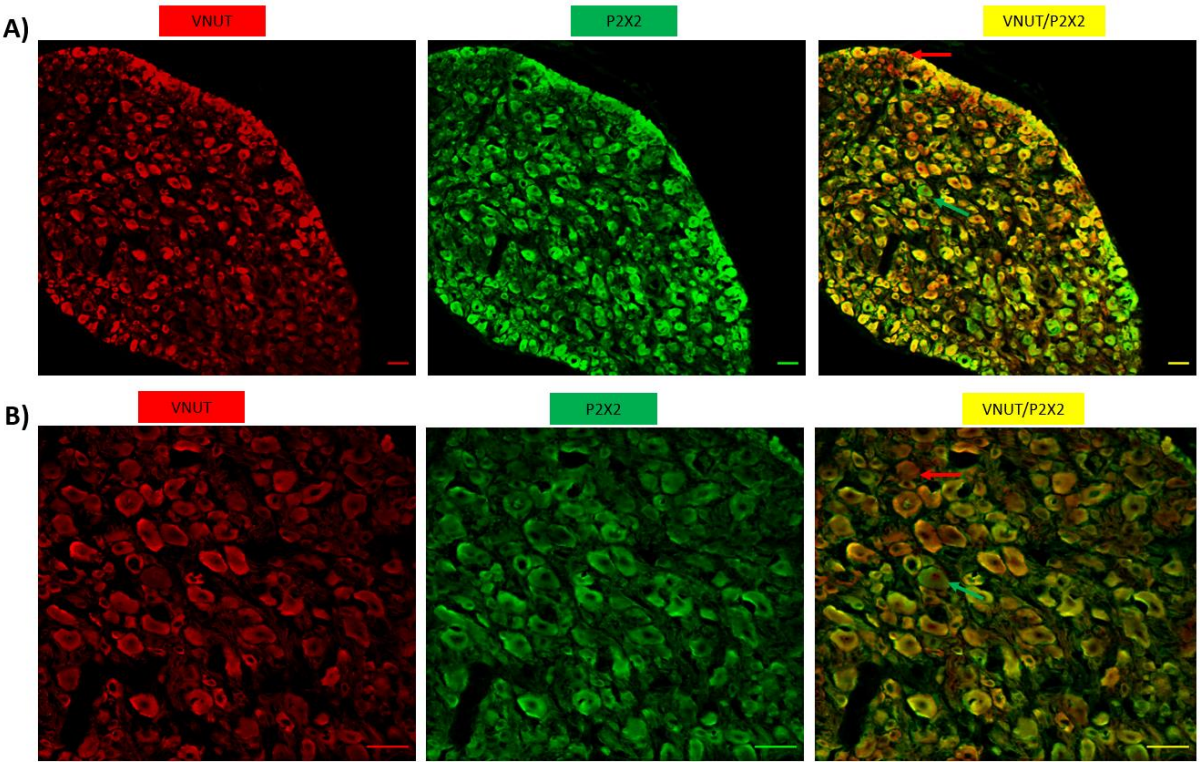

Figure 4.21: Coexpression of VNUT with P2X2 receptor in mouse superior cervical ganglion neurons. Immunocytochemical double staining for VNUT (red) and P2X2 receptor (green) in transverse sections (10 µm) of mouse superior cervical ganglion. VNUT and P2X2 receptor were colocalised in the same nerve cell body (yellow). Images were visualized using a Laser-scanning confocal microscope Zeiss LSM510 META (Zeiss), equipped with an excitation filter system of 458/488 nm for FITC and 467 for the red channel. The sections are seen at x10 (A) and x 20 (B) magnification. The exposure and camera settings remained consistent across all the images taken for each experiment. The green arrow indicates neuronal cell bodies labelled for P2X2 receptor only. The red arrow indicates neuronal cell bodies labelled for VNUT only. The results shown are representative from five independent experiments using five different mice.

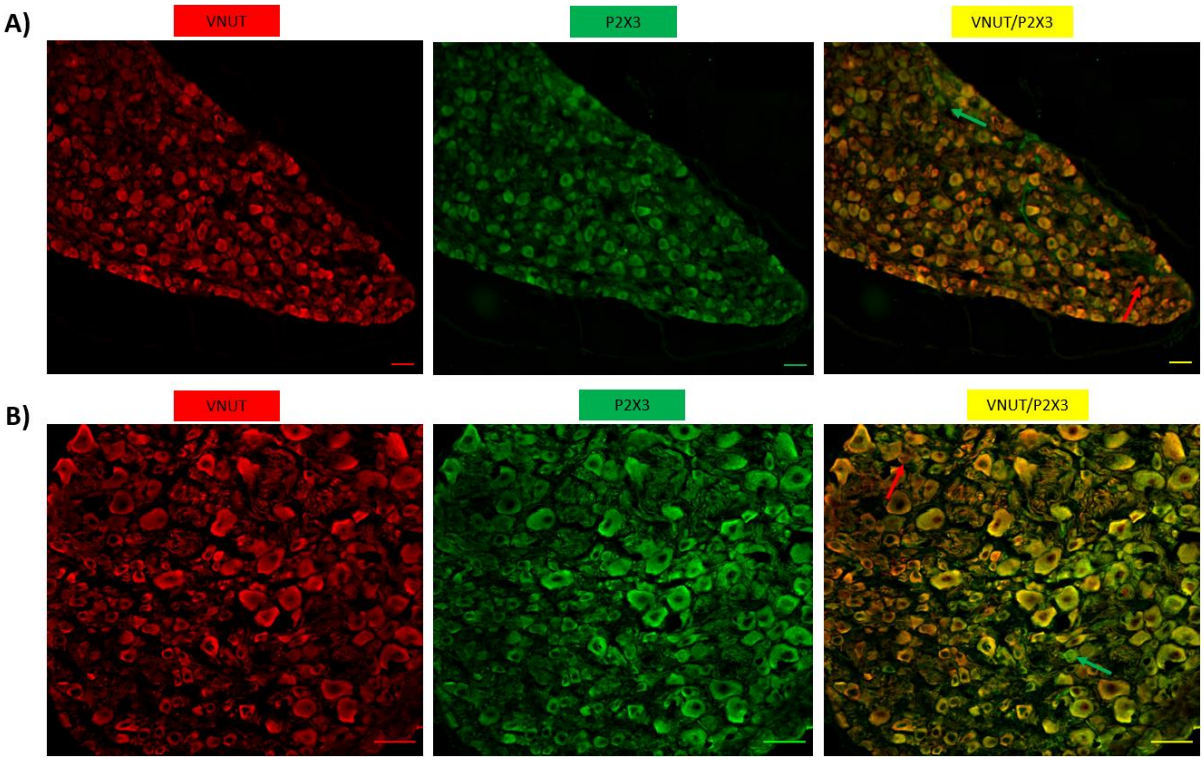

Figure 4.22: Coexpression of VNUT with P2X3 receptor in mouse superior cervical ganglion neurons. Immunocytochemical double staining for VNUT (red) and P2X3 receptor (green) in transverse sections (10 µm) of mouse superior cervical ganglion. VNUT and P2X3 receptor were colocalised in the same nerve cell body (yellow). Images were visualized using a Laser-scanning confocal microscope Zeiss LSM510 META (Zeiss), equipped with an excitation filter system of 458/488 nm for FITC and 467 for the red channel. The sections are seen at x10 (A) and x 20 (B) magnification. The exposure and camera settings remained consistent across all the images taken for each experiment. Scale bars represent 50 µm. The green arrow indicates neuronal cell bodies labelled for P2X3 receptor only. The red arrow indicates neuronal cell bodies labelled for VNUT only, The results shown are representative from five independent experiments using five different mice.

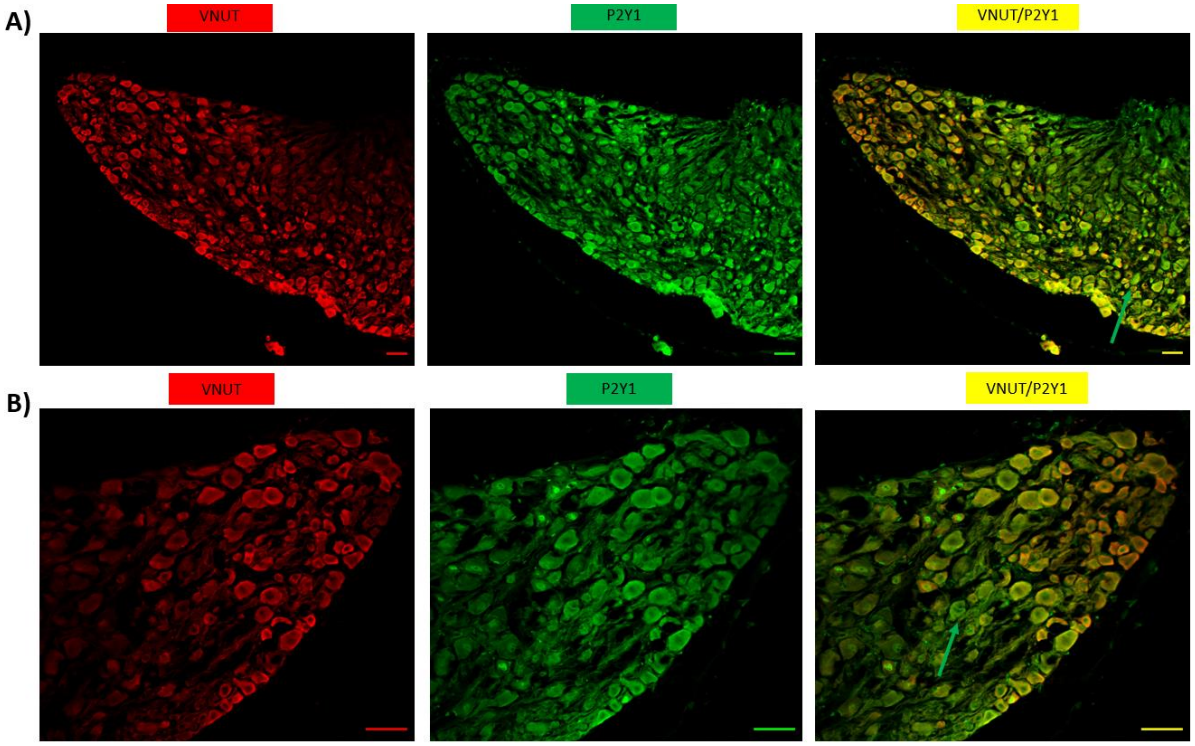

Figure 4.23: Coexpression of VNUT with P2Y1 receptor in mouse superior cervical ganglion neurons. Immunocytochemical double staining for VNUT (red) and P2Y1 receptor (green) in transverse sections (10 µm) of mouse superior cervical ganglion. VNUT and P2Y1 receptor were colocalised in the same nerve cell body (yellow). Images were visualized using a Laser-scanning confocal microscope Zeiss LSM510 META (Zeiss), equipped with an excitation filter system of 458/488 nm for FITC and 467 for the red channel. The sections are seen at x10 (A) and x 20 (B) magnification. The exposure and camera settings remained consistent across all the images taken for each experiment. Scale bars represent 50 µm. The green arrow indicates neuronal cell bodies labelled for P2Y1 receptor only. The results shown are representative from five independent experiments using five different mice.

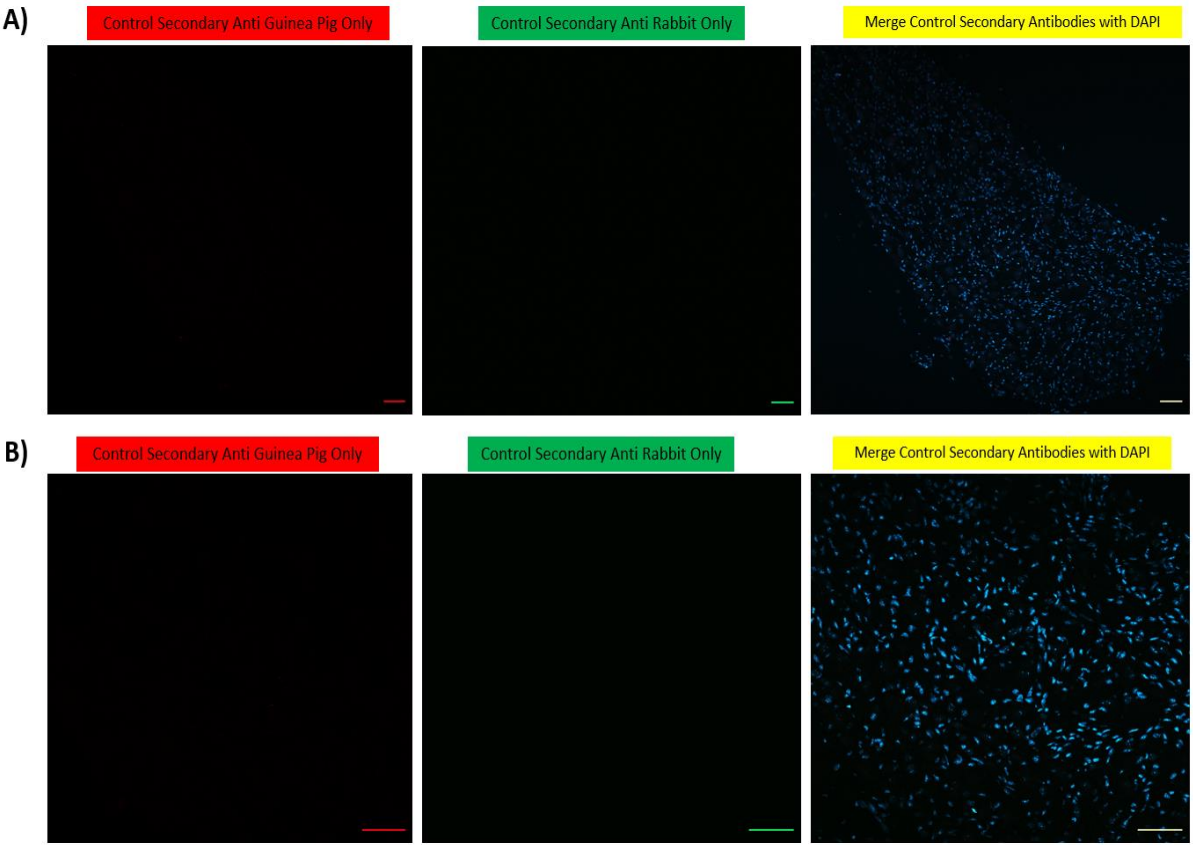

Figure 4.24: Control double immunofluorescence labelling for vesicular nucleotide transporter (VNUT) with P2 receptors in mouse superior cervical ganglion neurons. Control sections are shown where just the secondary antibody was applied, to see if there was any non-specific binding and to determine the autofluorescence of the tissue. Immunocytochemical double staining for secondary anti guinea pig (red) and secondary anti rabbit (green) in transverse sections (10 µm) of the mouse superior cervical ganglion. Images were visualized using a Laser-scanning confocal microscope Zeiss LSM510 META (Zeiss), equipped with an excitation filter system of 458/488 nm for FITC and 467 for the red channel. In control sections, cells are counterstained with DAPI to visualise nuclei (blue). The sections are seen at x10 (A) and x 20 (B) magnification. The exposure and camera settings remained consistent across all the images taken for each experiment. Scale bars represent 50 µm. The results shown are representative from five independent experiments using five different mice.

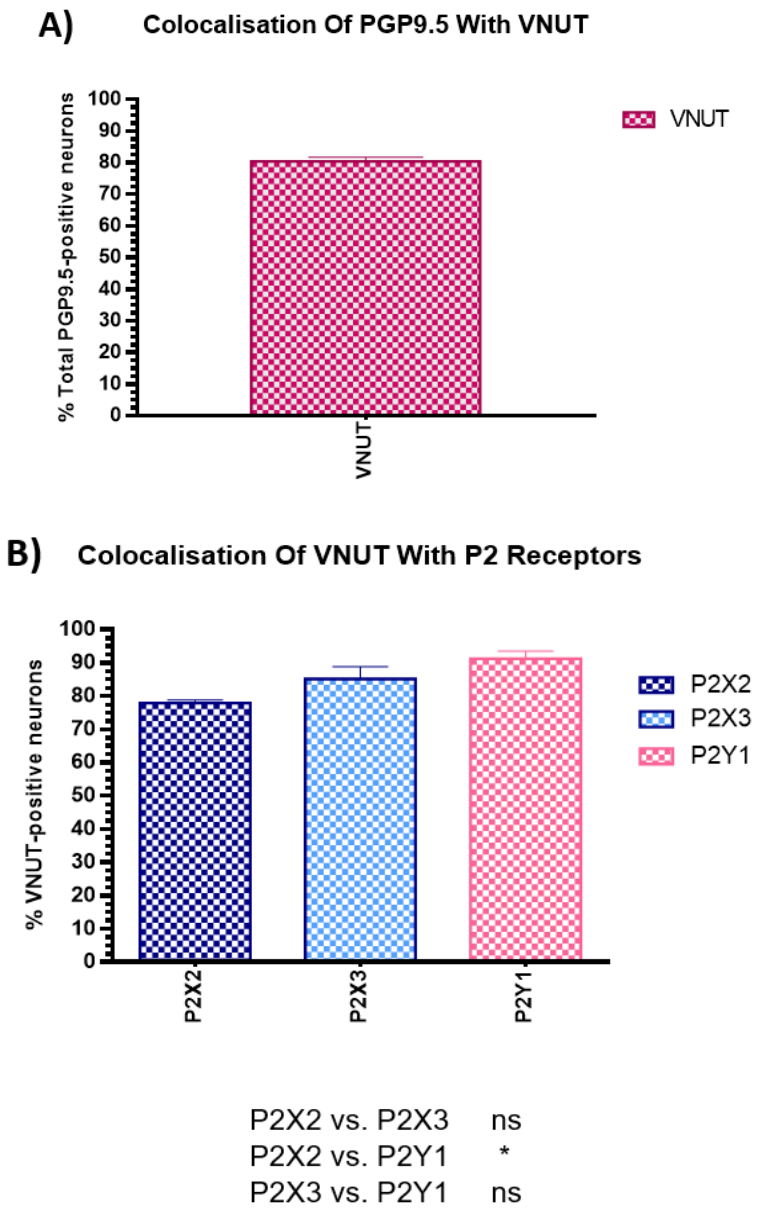

Figure 4.25: The percentage of P2-positive neurons which are capable of vesicular storage of ATP (positive for VNUT) in mouse superior cervical ganglion. (A) The percentage of mouse superior cervical ganglion neurons expressing VNUT. (**B)** Comparison of the P2 receptor subtypes expressing VNUT in the superior cervical ganglion neurons. Experiments were compared by a one-way ANOVA followed by Brown-Forsythe multiple comparison test (GraphPad Prism 6), *p<0.05, **p<0.005, ***p<0.001, ****p<0.0001, ns not significant (p>0.05), mean with SEM. The results shown are representative from five independent experiments using five different mice.

4.3.4 Expression of P2 purinergic receptor in pre-junctional nerves in the mouse superior mesenteric and carotid arteries

The distribution pattern of perivascular nerves and some subunits of P2 receptors in mouse superior mesenteric artery and common carotid artery were studied. Both right and left carotid arteries and 1st order of superior mesenteric artery were isolated from 15-20 weeks old mice and the distribution of perivascular nerves in each artery was immunohistochemically evaluated using antibodies against PGP9.5 and TH. Then, double immunohistochemical studies of PGP9.5 with purinergic receptors (P2X1, P2X2, P2X3, P2X4, P2X6, P2X7 and P2Y1) were performed to evaluate the presence of these receptors in perivascular nerves within the adventitia of the mouse superior mesenteric artery and carotid artery. Whole-mount preparations of the superior mesenteric artery and carotid artery stained for PGP 9.5 and the P2 receptors. In all studied segments of both superior mesenteric artery and carotid artery labelled for PGP 9.5 revealed a dense network of nerve fibres around outside of the mesenteric arteries or formed a plexus within the arterial wall of the carotid artery. Superior mesenteric arteries labelled for TH also revealed a network of neuronal fibres located within a dense layer at the level of the adventitia similar to PGP 9.5. Double immunolabelling for PGP 9.5 and TH revealed that most of the nerve fibres that contained PGP 9.5 also contained TH, however a small population of nerve fibres that contained PGP 9.5 did not contain TH (Figure 4.26.A). The results also demonstrated that the carotid artery did not show immunoreactivity for TH, suggesting that the carotid artery could not be innervated via the sympathetic nerves arising from sympathetic ganglia and other innervation phenotypes could be implicated such as sensory innervation (Figure 4.26.B). Double immunolabelling for PGP 9.5 and the P2 receptor of whole-mount preparations of the superior mesenteric artery revealed the majority of the nerve fibres showed colocalisation of PGP 9.5 with P2X2, P2X3, P2X4, P2X7 receptors and few of nerves were merged with P2X1 and P2Y1 (Figures 4.27.A - 4.33.A). Double immunolabelling for PGP 9.5 and the P2 receptor of whole-mount preparations of carotid artery revealed the majority of the nerve plexus showed colocalisation of PGP 9.5 and P2X2, P2X3, P2X4 and P2Y1 receptors, whilst P2X1, and P2X7 immunoreactivity were absent (Figure 4.27.B - 4.33 B). However, both the superior mesenteric artery and carotid artery did not show immunoreactivity for the P2X6 receptor (Figure 4.31 A & B). These findings suggested that mouse mesenteric arteries are primarily innervated with sympathetic nerves as a result of the high colocalisation nerves between PGP9.5 and TH. The results also suggested that the common carotid artery could not be innervated via sympathetic nerves due to the absence of TH nerves and other innervation types (such as sensory innervation) could be contributed. Moreover, our results revealed the presence of the P2X2, P2X3, and P2Y1 receptors in the

perivascular nerves within the adventitia of mouse superior mesenteric artery and carotid artery although they were not detected by RT-PCR (P2Y1 were expressed in the superior mesenteric artery but not carotid artery).

Confocal images of cryostat transverse sections (10 µm) of mouse superior mesenteric arteries showed immunoreactivities for P2X2, P2X3, P2X7 and P2Y1 receptors in the adventitia (Figure 4.36.A). Confocal images of cryostat transverse sections (10 µm) of the carotid arteries showed immunoreactivities for P2X2, P2X3 and P2Y1in the adventitia (Figure 4.36.B). The results showed the P2 receptors were distributed in cryostat sections was similar to that in whole mounts and was found in the adventitial side of the blood vessels and that confirmed that these receptors are located in the perivascular nerves layer only but not in smooth muscle and the endothelium. Control sections are shown in which no primary antibody was applied and where just the secondary antibody was applied, to see if there was any non-specific binding. None of the receptors showed significant immunoreactivity in the control sections (Figure 4.37).

As a result of both RT-PCR and immunohistochemistry studies, we could propose that P2X2, P2X3, P2X7 and P2Y1 could be present only in pre-junctional nerves within the adventitial layer but not in the smooth muscle cells and the endothelium. As previously reported in several studies, P2X1 and P2X4 can be present in the smooth muscle cells and the endothelium of the mouse mesenteric artery (Lewis & Evans, 2001), however, P2X7 was still controversial. Our present results indicated the presence of P2X7, in addition to P2X1, P2X4 and P2Y1, in the perivascular nerve of the superior mesenteric artery. Thus, these receptors (P2X2, P2X3, P2X7 and P2Y1) might serve as pre-junctional and could be able to regulate the release of various neurotransmitters via feedback loops, which could potentially provide a novel target for the therapeutic control of vascular tone and ultimately blood. Further functional experiments are required to investigate more about that. For that, in the rest of this chapter, we will focus more on pre-junctional P2X2, P2X3, P2X7 and P2Y1 receptors and discuss further the functional role of these receptors on perivascular nerves of blood vessels.

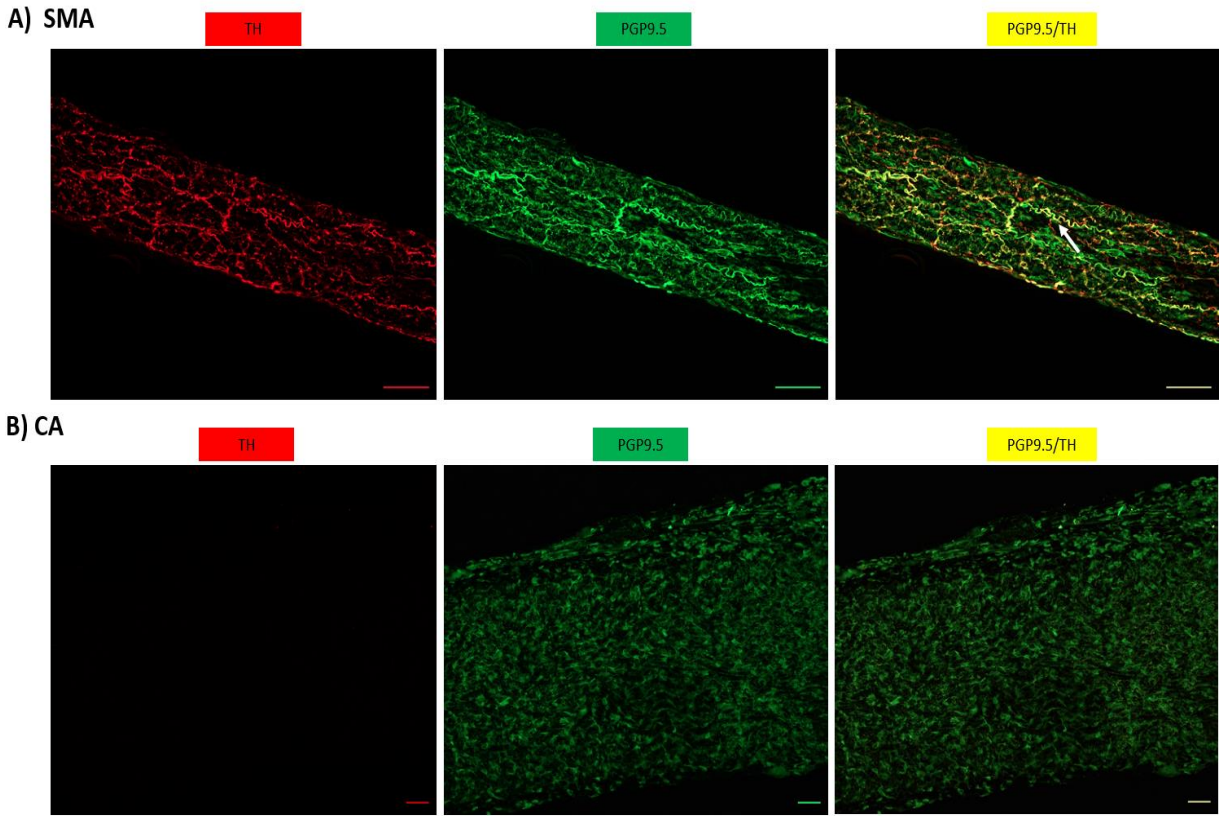

Figure 4.26: Coexpression of PGP9.5 and TH in whole-mount preparations of mouse superior mesenteric and carotid arteries. **(A)** Distribution of TH nerve fibres (red) and PGP9.5 (green) in whole-mount preparation of superior mesenteric artery. PGP 9.5 and TH were colocalised in the same nerve network (yellow). **(B)** Distribution of TH nerve plexus (red) and PGP9.5 (green) in whole-mount preparation of carotid artery. Images were visualized using a Laser-scanning confocal microscope Zeiss LSM510 META (Zeiss), equipped with an excitation filter system of 458/488 nm for FITC and 467 for the red channel. 7-10 optical images of the sections were scaled and overlapped together using Image J software, were magnified at x 20 for superior mesenteric artery and x 10 for carotid artery. The exposure and camera settings remained consistent across all the images taken for each experiment. Scale bars represent 50 μm. The white arrow indicates where nerves are colocalised. SMA indicates superior mesenteric artery, CA indicates carotid artery. The results shown are representative from five independent experiments using five different mice.

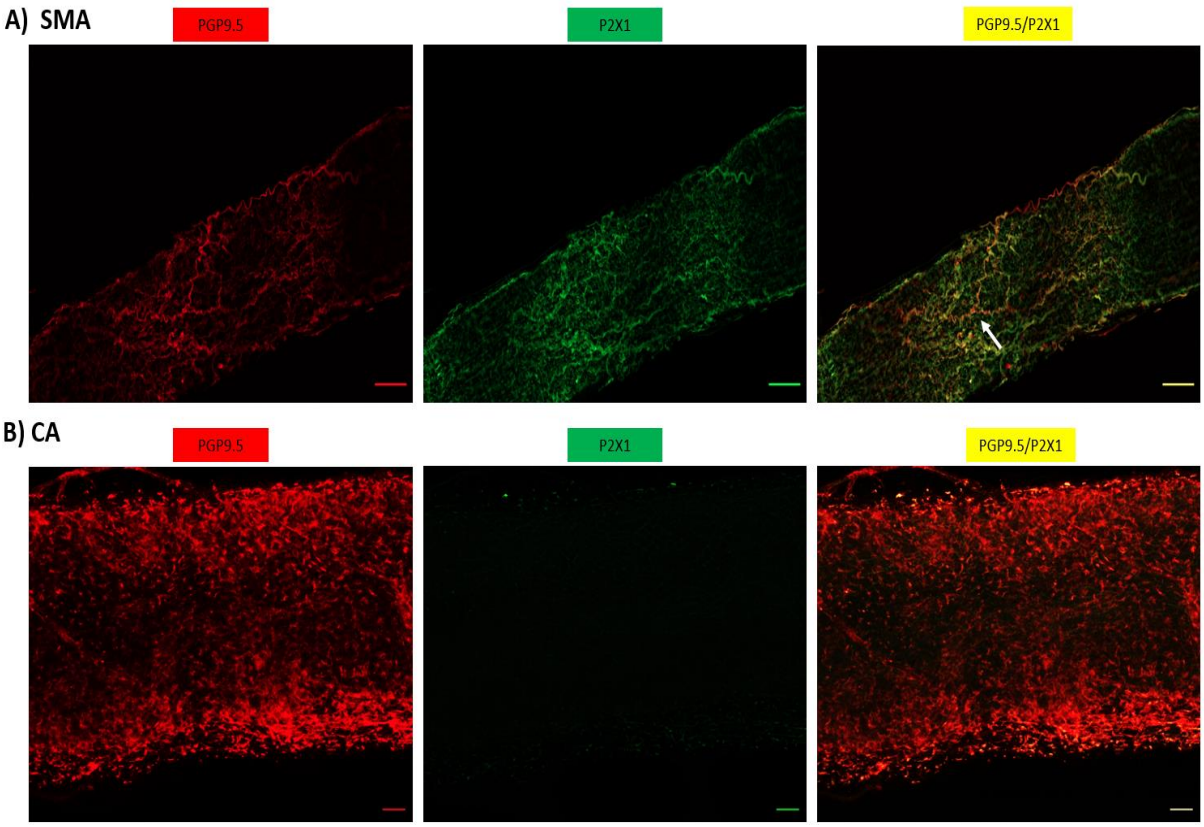

Figure 4.27: Coexpression of P2X1 and PGP9.5 in whole-mount preparations of mouse superior mesenteric and carotid arteries. **(A)** Distribution of PGP9.5 nerve fibres (red) and P2X1 (green) in whole-mount preparation of superior mesenteric artery. PGP 9.5 and P2X1 were colocalised in the same nerve network (yellow). **(B)** Distribution of PGP9.5 nerve plexus (red) and P2X1 (green) in whole-mount preparation of carotid artery. Images were visualized using a Laser-scanning confocal microscope Zeiss LSM510 META (Zeiss), equipped with an excitation filter system of 458/488 nm for FITC and 467 for the red channel. 7-10 optical images of the sections were scaled and overlapped together using Image J software, were magnified at x 20 for superior mesenteric artery and x 10 for carotid artery. The exposure and camera settings remained consistent across all the images taken for each experiment. Scale bars represent 50 μm. The white arrow indicates where nerves are colocalised. SMA indicates superior mesenteric artery, CA indicates carotid artery. The results shown are representative from five independent experiments using five different mice.

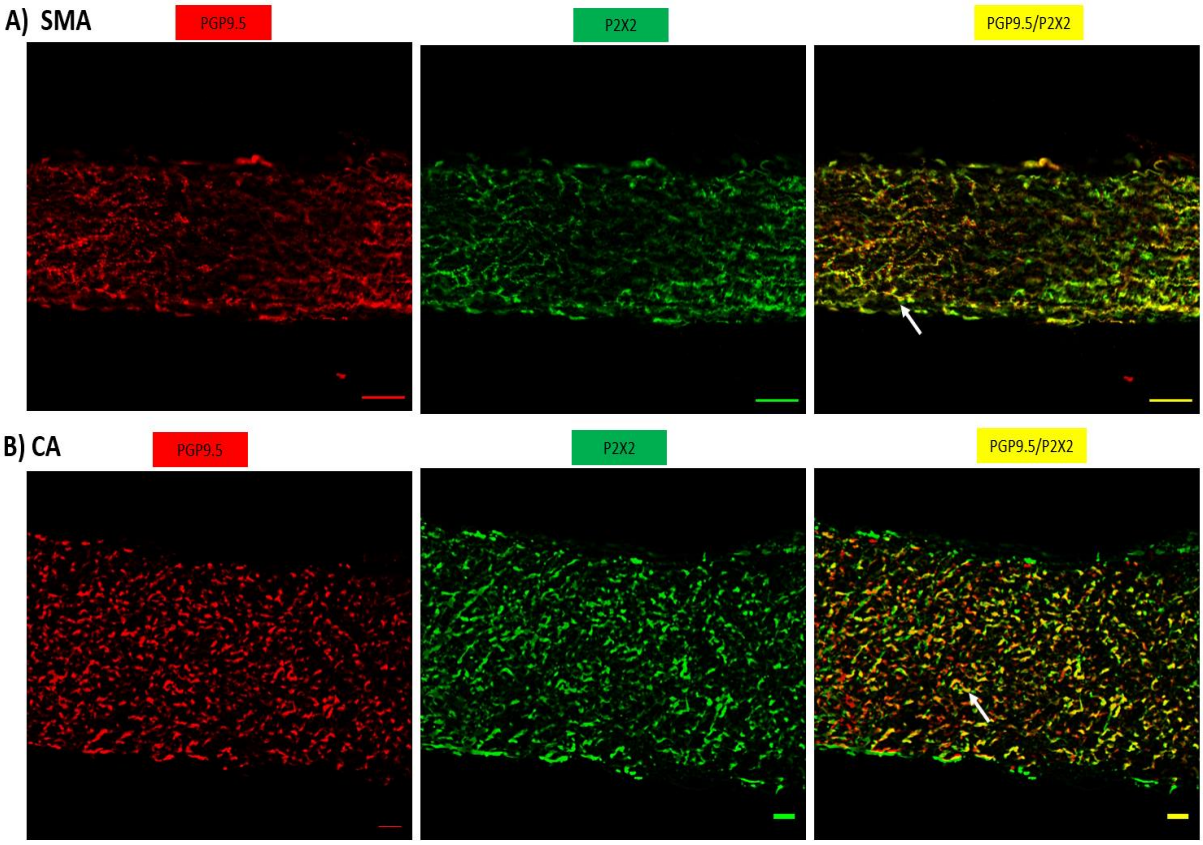

Figure 4.28: Coexpression of P2X2 and PGP9.5 in whole-mount preparations of mouse superior mesenteric and carotid arteries. **(A)** Distribution of PGP9.5 nerve fibres (red) and P2X2 (green) in whole-mount preparation of superior mesenteric artery. PGP 9.5 and P2X2 were colocalised in the same nerve network (yellow). **(B)** Distribution of PGP9.5 nerve plexus (red) and P2X2 (green) in whole-mount preparation of carotid artery. PGP9.5 and P2X2 were colocalised in the same nerve network (yellow). Images were visualized using a Laser-scanning confocal microscope Zeiss LSM510 META (Zeiss), equipped with an excitation filter system of 458/488 nm for FITC and 467 for the red channel. 7-10 optical images of the sections were scaled and overlapped together using Image J software, were magnified at x 20 for superior mesenteric artery and x 10 for carotid artery. The exposure and camera settings remained consistent across all the images taken for each experiment. Scale bars represent 50 μm. The white arrow indicates where nerves are colocalised. SMA indicates superior mesenteric artery, CA indicates carotid artery. The results shown are representative from five independent experiments using five different mice.

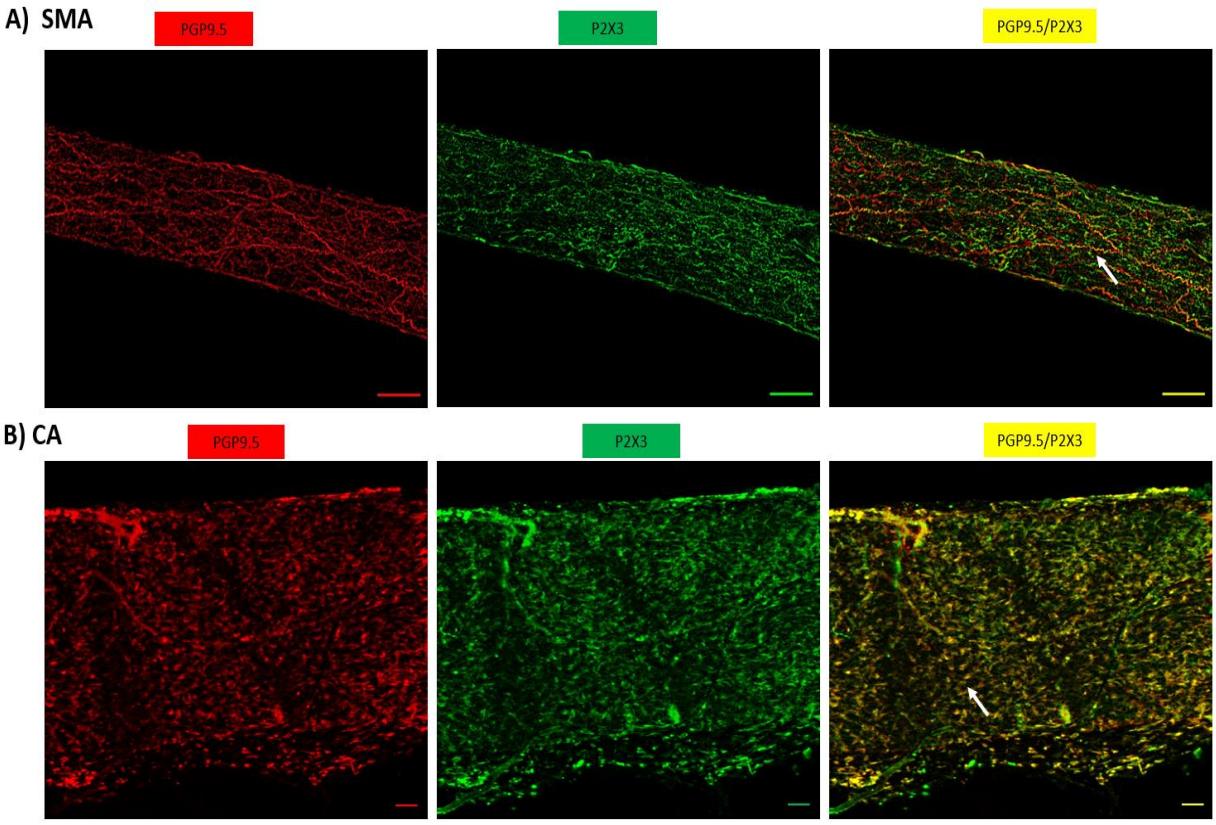

Figure 4.29: Coexpression of P2X3 and PGP9.5 in whole-mount preparations of mouse superior mesenteric and carotid arteries. **(A)** Distribution of PGP9.5 nerve fibres (red) and P2X3 (green) in whole-mount preparation of superior mesenteric artery. PGP 9.5 and P2X3 were colocalised in the same nerve network (yellow). **(B)** Distribution of PGP9.5 nerve plexus (red) and P2X3 (green) in whole-mount preparation of carotid artery. PGP9.5 and P2X3 were colocalised in the same nerve network (yellow). Images were visualized using a Laser-scanning confocal microscope Zeiss LSM510 META (Zeiss), equipped with an excitation filter system of 458/488 nm for FITC and 467 for the red channel. 7-10 optical images of the sections were scaled and overlapped together using Image J software, were magnified at x 20 for superior mesenteric artery and x 10 for carotid artery. The exposure and camera settings remained consistent across all the images taken for each experiment. Scale bars represent 50 μm. The white arrow indicates where nerves are colocalised. SMA indicates superior mesenteric artery, CA indicates carotid artery. The results shown are representative from five independent experiments using five different mice.

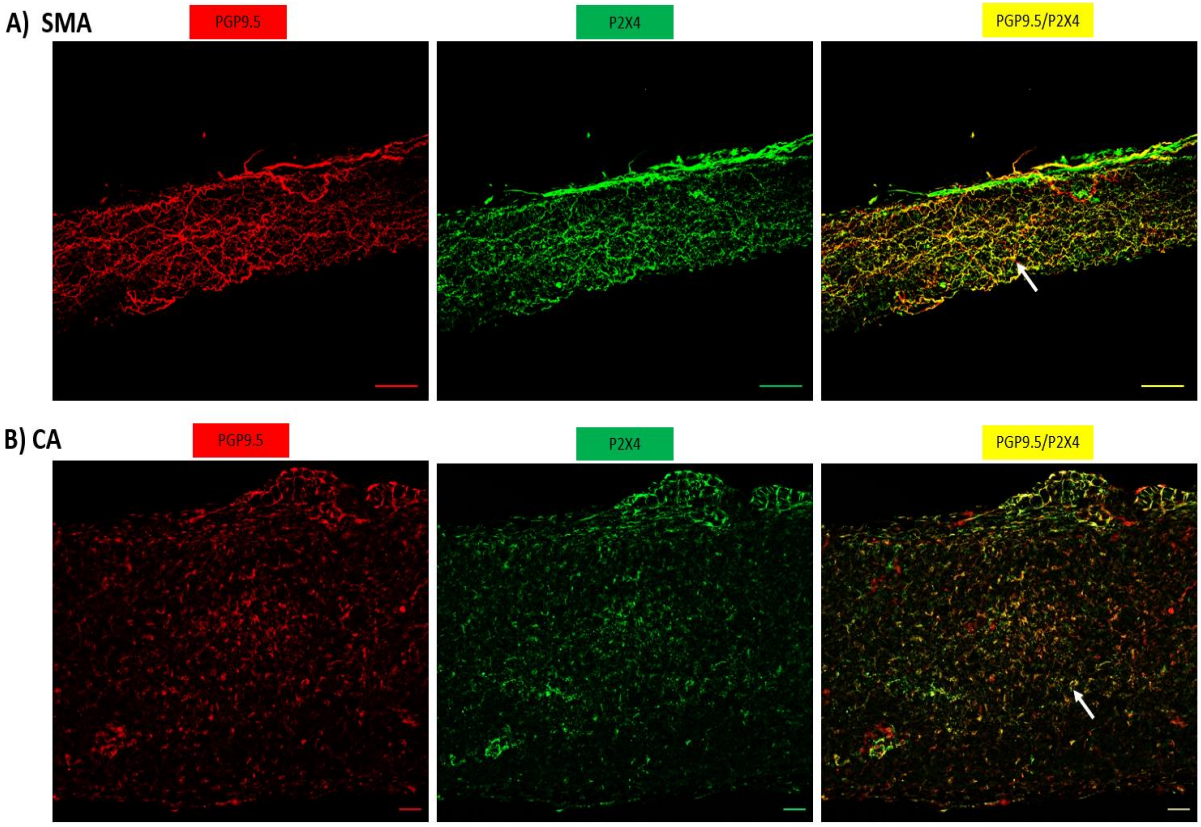

Figure 4.30: Coexpression of P2X4 and PGP9.5 in whole-mount preparations of mouse superior mesenteric and carotid arteries. **(A)** Distribution of PGP9.5 nerve fibres (red) and P2X4 (green) in whole-mount preparation of superior mesenteric artery. PGP 9.5 and P2X4 were colocalised in the same nerve network (yellow). **(B)** Distribution of PGP9.5 nerve plexus (red) and P2X4 (green) in whole-mount preparation of carotid artery. PGP9.5 and P2X4 were colocalised in the same nerve network (yellow). Images were visualized using a Laser-scanning confocal microscope Zeiss LSM510 META (Zeiss), equipped with an excitation filter system of 458/488 nm for FITC and 467 for the red channel. 7-10 optical images of the sections were scaled and overlapped together using Image J software, were magnified at x 20 for superior mesenteric artery and x 10 for carotid artery. The exposure and camera settings remained consistent across all the images taken for each experiment. Scale bars represent 50 μm. The white arrow indicates where nerves are colocalised. SMA indicates superior mesenteric artery, CA indicates carotid artery. The results shown are representative from five independent experiments using five different mice.

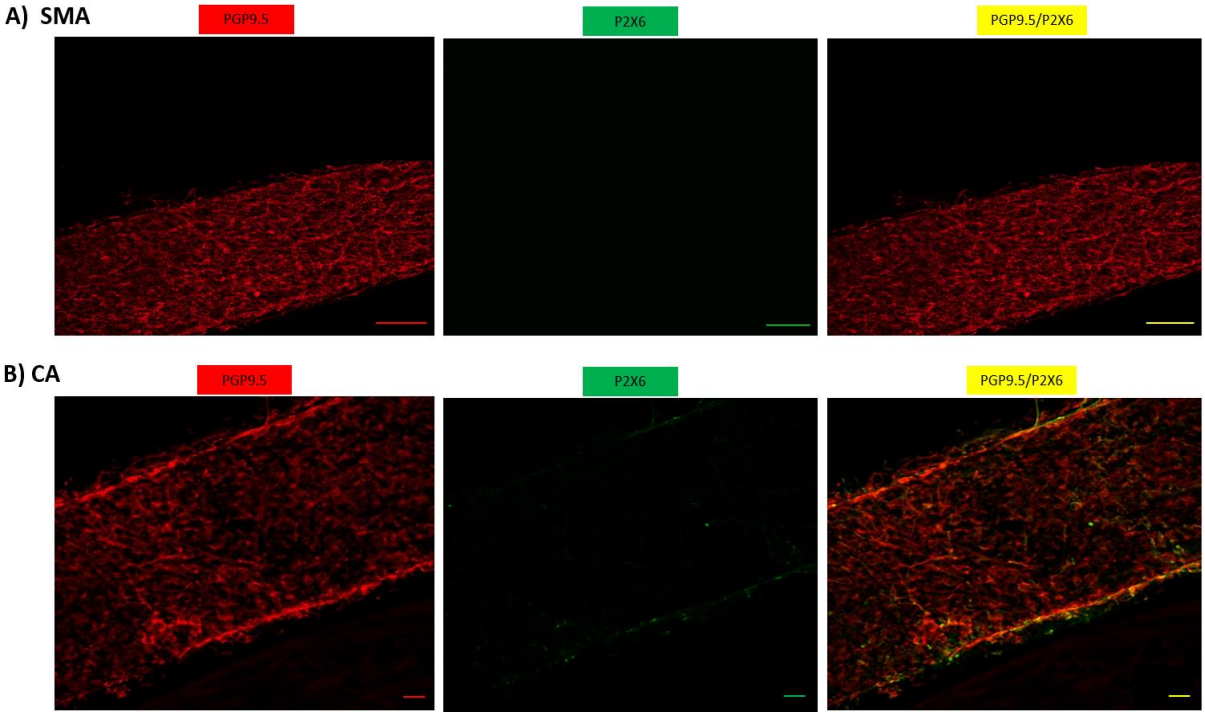

Figure 4.31: Coexpression of P2X6 and PGP9.5 in whole-mount preparations of mouse superior mesenteric and carotid arteries. **(A)** Distribution of PGP9.5 nerve fibres (red) and P2X6 (green) in whole-mount preparation of superior mesenteric artery. PGP 9.5 and P2X6 were colocalised in the same nerve network (yellow). **(B)** Distribution of PGP9.5 nerve plexus (red) and P2X6 (green) in whole-mount preparation of carotid artery. Images were visualized using a Laser-scanning confocal microscope Zeiss LSM510 META (Zeiss), equipped with an excitation filter system of 458/488 nm for FITC and 467 for the red channel. 7-10 optical images of the sections were scaled and overlapped together using Image J software, were magnified at x 20 for superior mesenteric artery and x 10 for carotid artery. The exposure and camera settings remained consistent across all the images taken for each experiment. Scale bars represent 50 μm. The white arrow indicates where nerves are colocalised. SMA indicates superior mesenteric artery, CA indicates carotid artery. The results shown are representative from five independent experiments using five different mice.

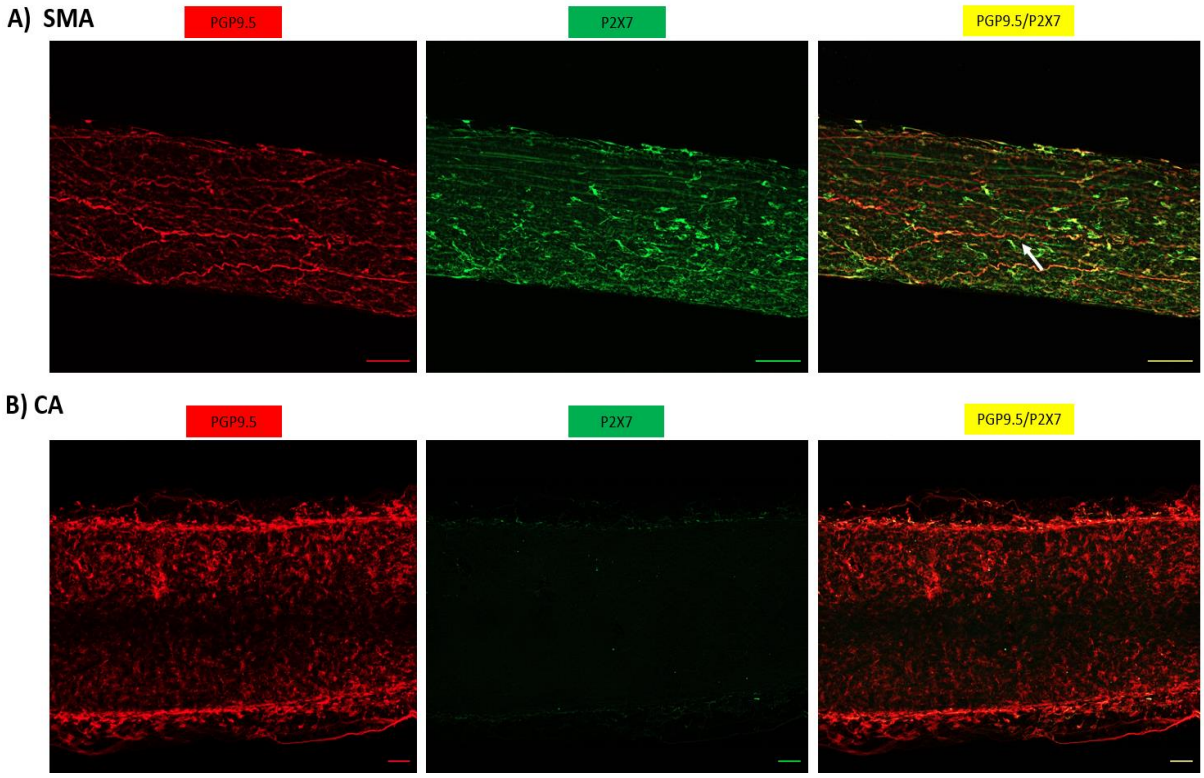

Figure 4.32: Coexpression of P2X7 and PGP9.5 in whole-mount preparations of mouse superior mesenteric and carotid arteries. **(A)** Distribution of PGP9.5 nerve fibres (red) and P2X7 (green) in whole-mount preparation of superior mesenteric artery. PGP 9.5 and P2X7 were colocalised in the same nerve network (yellow). **(B)** Distribution of PGP9.5 nerve plexus (red) and P2X7 (green) in whole-mount preparation of carotid artery. Images were visualized using a Laser-scanning confocal microscope Zeiss LSM510 META (Zeiss), equipped with an excitation filter system of 458/488 nm for FITC and 467 for the red channel. 7-10 optical images of the sections were scaled and overlapped together using Image J software, were magnified at x 20 for superior mesenteric artery and x 10 for carotid artery. The exposure and camera settings remained consistent across all the images taken for each experiment. Scale bars represent 50 μm. The white arrow indicates where nerves are colocalised. SMA indicates superior mesenteric artery, CA indicates carotid artery. The results shown are representative from five independent experiments using five different mice.

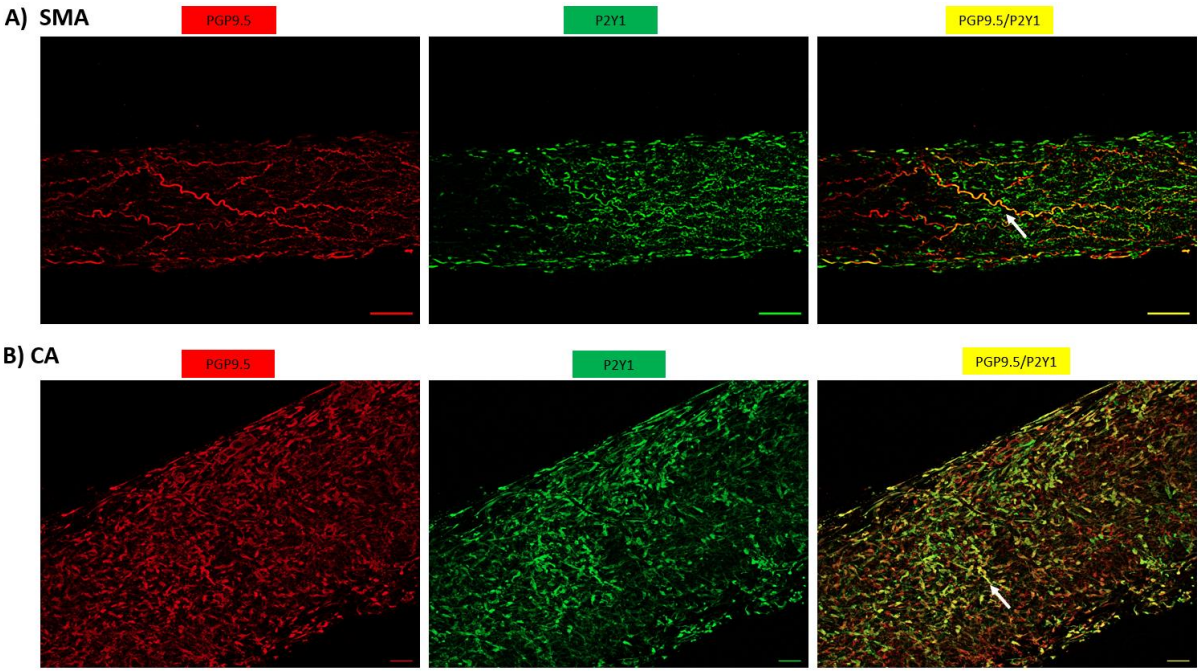

Figure 4.33: Coexpression of P2Y1 and PGP9.5 in whole-mount preparations of mouse superior mesenteric and carotid arteries. **(A)** Distribution of PGP9.5 nerve fibres (red) and P2Y1 (green) in whole-mount preparation of superior mesenteric artery. PGP 9.5 and P2Y1 were colocalised in the same nerve network (yellow). **(B)** Distribution of PGP9.5 nerve plexus (red) and P2Y1 (green) in whole-mount preparation of carotid artery. PGP9.5 and P2Y1 were colocalised in the same nerve network (yellow). Images were visualized using a Laser-scanning confocal microscope Zeiss LSM510 META (Zeiss), equipped with an excitation filter system of 458/488 nm for FITC and 467 for the red channel. 7-10 optical images of the sections were scaled and overlapped together using Image J software, were magnified at x 20 for superior mesenteric artery and x 10 for carotid artery. The exposure and camera settings remained consistent across all the images taken for each experiment. Scale bars represent 50 μm. The white arrow indicates where nerves are colocalised. SMA indicates superior mesenteric artery, CA indicates carotid artery. The results shown are representative from five independent experiments using five different mice.

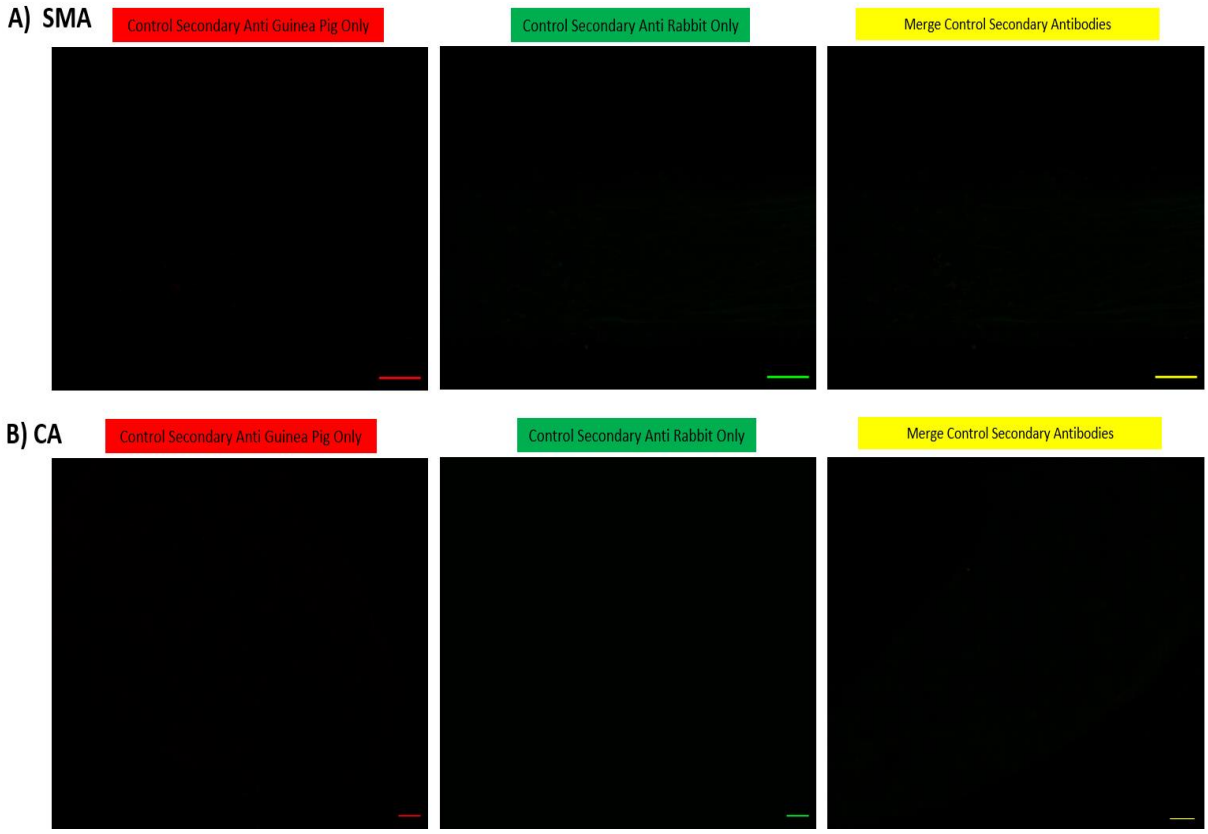

Figure 4.34: Control double immunofluorescence labelling of PGP9.5 and P2 receptors in mouse superior mesenteric artery and carotid artery. Control tissues are shown where just the secondary antibody was applied, to see if there was any non-specific binding and to determine the autofluorescence of the tissue. Immunocytochemical double staining for secondary anti guinea pig (red) and secondary anti rabbit (green) in the mouse superior mesenteric artery and carotid artery isolated from five independent male mice. Images were visualized using a Laser-scanning confocal microscope Zeiss LSM510 META (Zeiss), equipped with an excitation filter system of 458/488 nm for FITC and 467 for the red channel. 7-10 optical images of the sections were scaled and overlapped together using Image J software, were magnified at x 20 for superior mesenteric artery and x 10 for carotid artery. The exposure and camera settings remained consistent across all the images taken for each experiment. Scale bars represent 50 μm. SMA indicates superior mesenteric artery, CA indicates carotid artery. The results shown are representative from five independent experiments using five different mice.

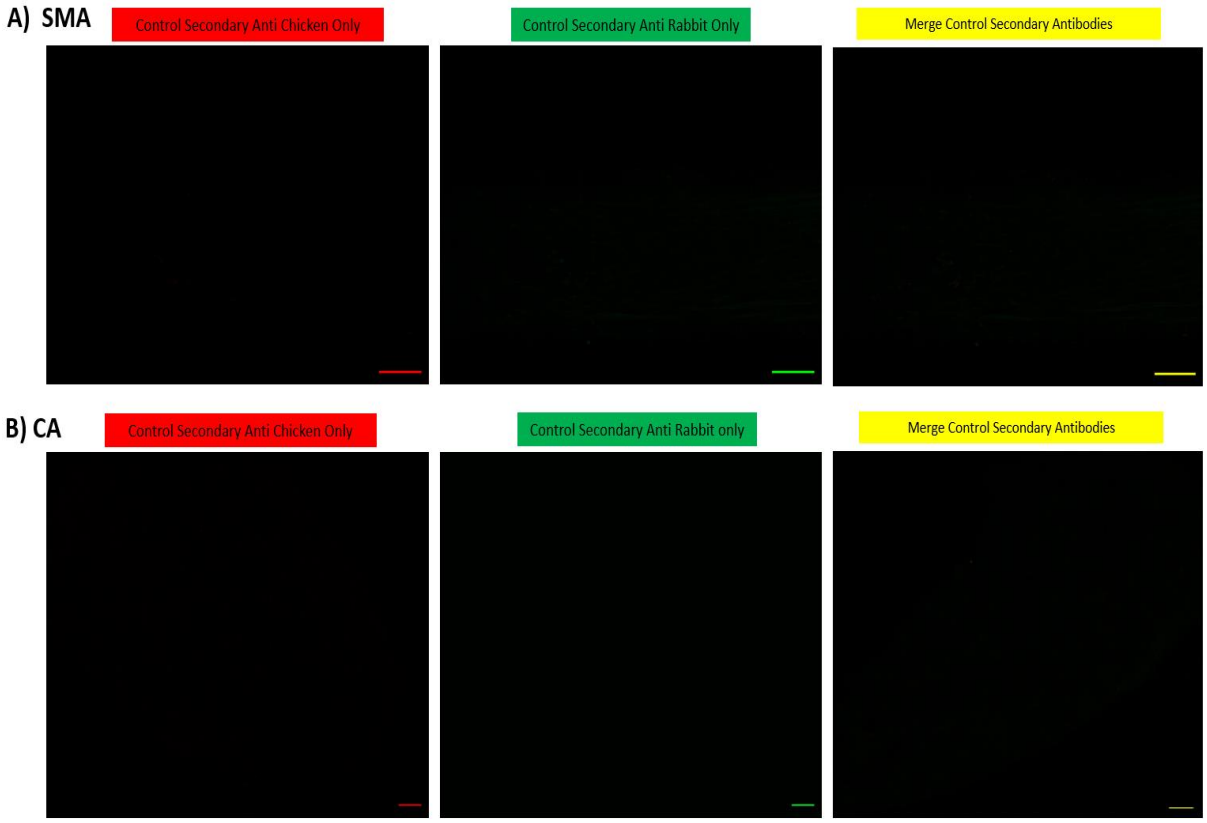

Figure 4.35: Control double immunofluorescence labelling of TH and PGP9.5 receptor in mouse superior mesenteric artery and carotid artery. Control tissues are shown where just the secondary antibody was applied, to see if there was any non-specific binding and to determine the autofluorescence of the tissue. Immunocytochemical double staining for secondary anti chicken (red) and secondary anti rabbit (green) in the mouse superior mesenteric artery (A) and carotid artery (B). Images were visualized using a Laser-scanning confocal microscope Zeiss LSM510 META (Zeiss), equipped with an excitation filter system of 458/488 nm for FITC and 467 for the red channel. 7-10 optical images of the sections were scaled and overlapped together using Image J software, were magnified at x 20 for superior mesenteric artery and x 10 for carotid artery. The exposure and camera settings remained consistent across all the images taken for each experiment. Scale bars represent 50 μm., CA indicates carotid artery, The results shown are representative from five independent experiments using five different mice.

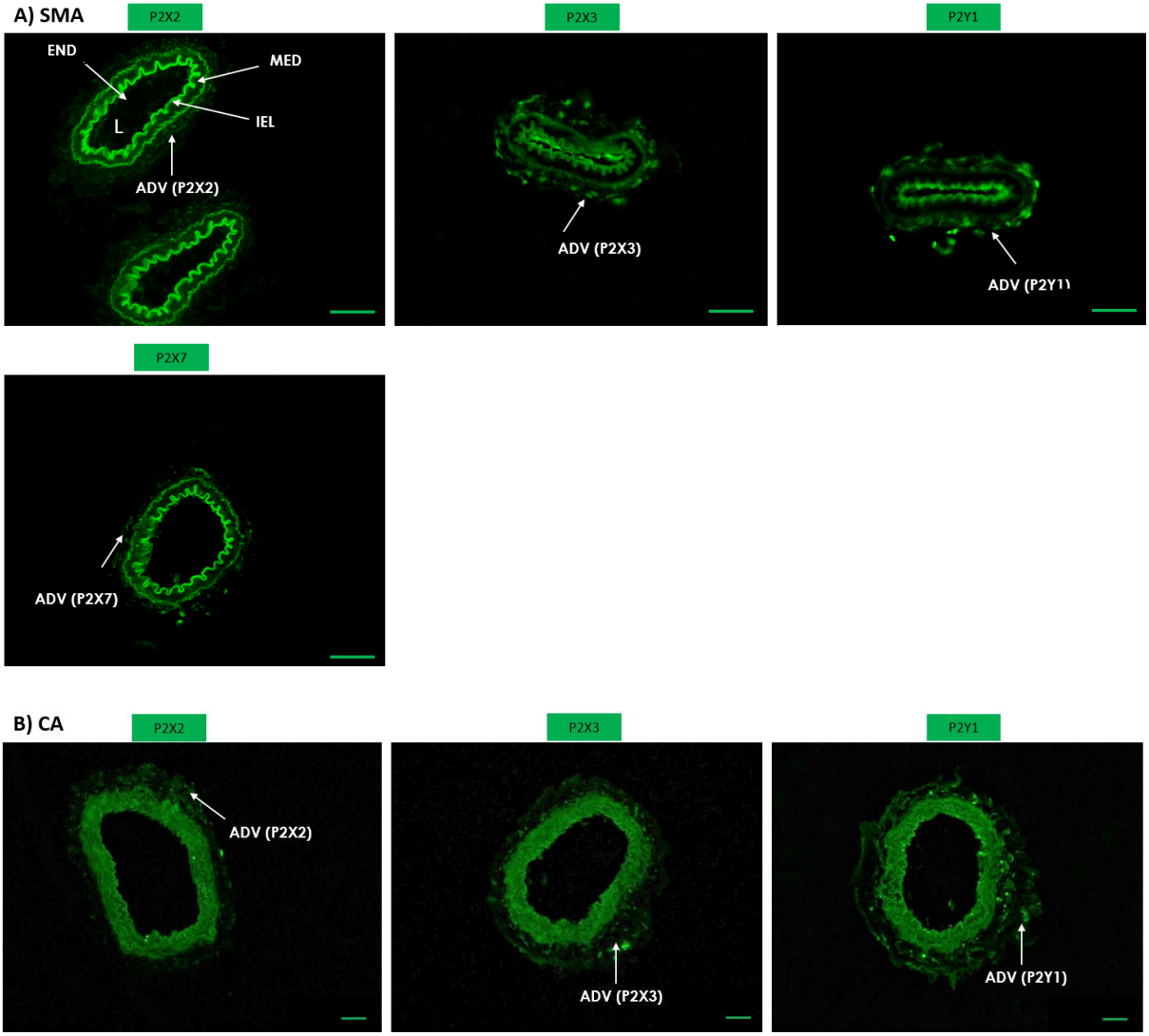

Figure 4.36. Immunofluorescence of cryostat sections of mouse superior mesenteric artery and carotid artery labelled with P2X2, P2X3, P2X7 and P2Y1. Immunostaining for P2X2, P2X3, P2X7 and P2Y1 receptor (green) of transverse sections (10 µm) of mouse superior mesenteric artery (A) and Immunostaining for P2X2, P2X3 and P2Y1 receptor of carotid artery (B). Images showed the distribution of P2X2, P2X3, P2X7 and P2Y1 receptors were found on the adventitial side of the vessel. Images were visualized using a Laser-scanning confocal microscope Zeiss LSM510 META (Zeiss), equipped with an excitation filter system of 458/488 nm for the FITC channel. Confocal images were magnified at x 20 for superior mesenteric artery and x 10 for carotid artery. The exposure and camera settings remained consistent across all the images taken for each experiment. Scale bars represent 50 µm. SMA indicates superior mesenteric artery, CA indicates carotid artery, END indicates the endothelium, ADV indicates the adventitia, MED indicates the media layer, L indicates lumen, IEL indicates internal elastic lamina. The results shown are representative from five independent experiments using five different mice

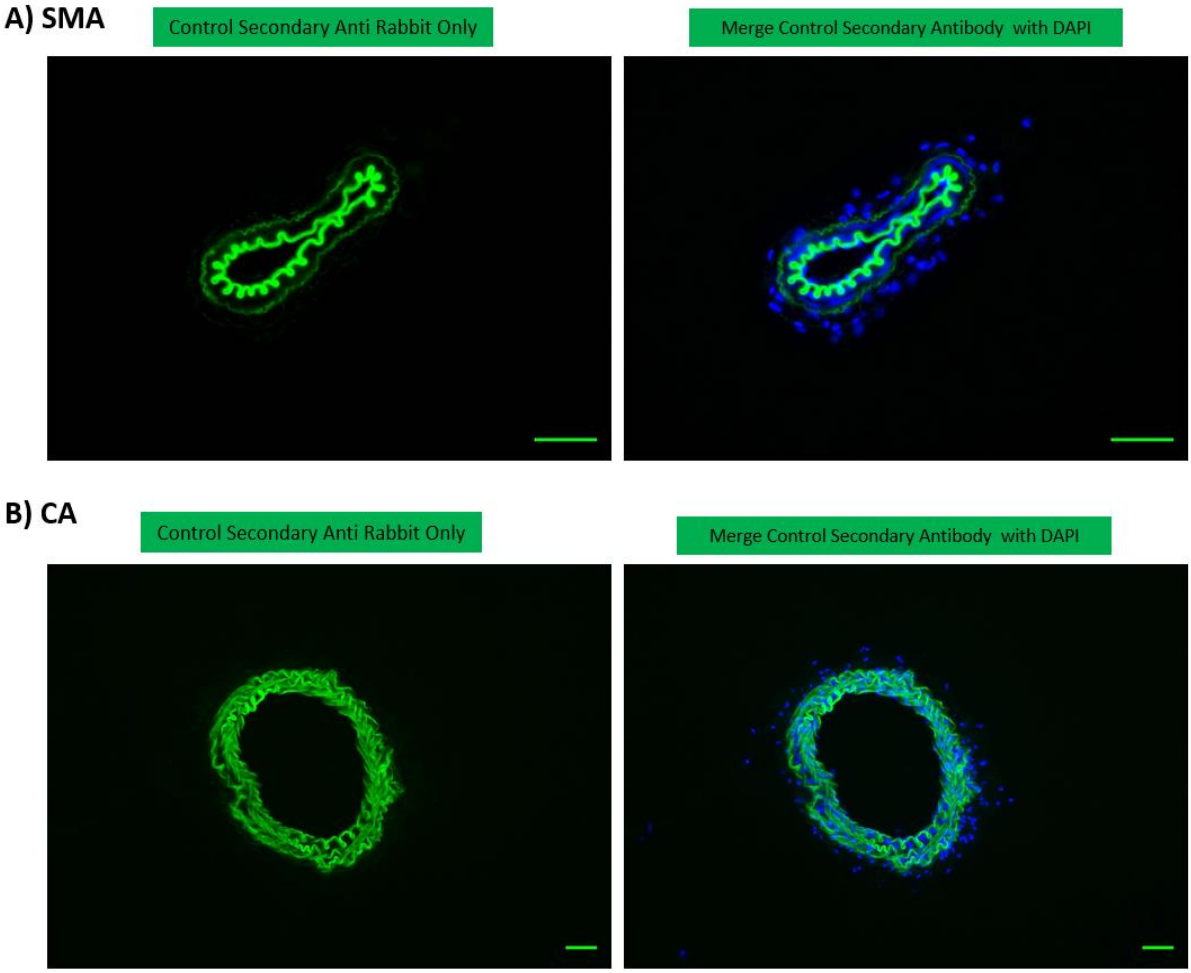

Figure 4.37: Control immunofluorescence of cryostat sections of mouse superior mesenteric artery and carotid artery labelling of P2 receptors. Control tissues are shown where just the secondary antibody was applied, to see if there was any non-specific binding and to determine the autofluorescence of the tissue. Immunocytochemical double staining for secondary anti rabbit (green) of transverse sections (10 µm) of mouse superior mesenteric artery **(A)** and carotid artery **(B)**. Images were visualized using a Laser-scanning confocal microscope Zeiss LSM510 META (Zeiss), equipped with an excitation filter system of 458/488 nm for the FITC channel. The tissues are seen at x10 for superior mesenteric artery (A) and x 20 for carotid artery (B) magnification. The exposure and camera settings remained consistent across all the images taken for each experiment. Scale bars represent 50 µm. The results shown are representative from five independent experiments using five different mice.

4.3.5 Mouse superior cervical ganglion neurons and P2-positive neurons have vasomotor activity by expressing NPY.

The NPY-hrGFP mice were used in this project to investigate NPY-positive neurons which may identify which neurons have vasomotor activities and could be able to innervate target tissues such as blood vessels and glands, as many neurons in the superior cervical ganglion do not have vasomotor activity. This approach is especially effective for NPY neurons, which despite their large number in some tissues such as the brain, they are not identifiable by morphological criteria alone such as NPY-immunostaining (Van den Pol et al, 2009). To quantify the superior cervical ganglion neurons and P2 positive nerve cell bodies which have positive immunoreactivity for NPY, the superior cervical ganglion sections from transgenic mice (NPY-hrGFP) were examined using antibodies against PGP9.5 and P2 receptors (P2X2, P2X3 and P2Y1). These targets were also investigated in whole-mount preparation of the superior mesenteric artery and carotid artery isolated from the same transgenic mice. In the superior cervical ganglion of transgenic NPY-GFP mice, the nerve cell bodies consistently displayed intense fluorescence for GFP expression in NPY-positive neurons. In sections immunohistochemically stained for PGP9.5, the NPY- positive cell bodies were seen enmeshed in dense PGP9.5-immunoreactive neurons, ~ 40% of nerve cell bodies were positive for both PGP9.5 and NPY-GFP (Figures 4.38 & 4.43.A). Many neurons appeared completely negative for NPY. That indicated that ~ 40% of superior cervical ganglion neurons had vasomotor activity resulting in innervating target tissues including blood vessels, thus controlling blood flow in the head. However, most NPY-negative neurons in the superior cervical ganglion are either secretomotor cells that control salivary glands or pilomotor neurons that innervate arrector pilli muscles. As it is shown in (Figures 4.44 - 4.46) The whole-mount preparations of superior mesenteric artery from transgenic NPY-GFP mice consistently displayed immunopositive nerves of NPY. The green fluorescence was apparent throughout the adventitia of the blood vessels. But the carotid artery stained negative for NPY. Moreover, few PGP9.5 positive nerves within the adventitia of the superior mesenteric artery (not carotid artery) nearly merged with NPY nerves. These results alongside carotid artery TH-negative nerves suggested that the NPY-positive neurons in the superior cervical ganglion were not involved in the sympathetic innervation of the carotid artery and the nerves through the carotid artery could arise from the carotid body and innervate other tissues such as the heart and saliva glands. As the superior cervical ganglion is a model of autonomic sympathetic ganglions and one of the sympathetic chains through the vertebrae, and superior mesenteric artery showed positive nerves for NPY, superior mesenteric artery could be innervated by the neurons raised from sympathetic superior mesenteric ganglions. In this study, the superior cervical ganglion

sections from the transgenic mice labelled for P2X2, P2X3 and P2Y1 (red) showed coexpression (yellow) with NPY (Figures 4.39 - 4.41). There was also considerable variation in the intensity of immunoreactivity of each receptor in individual neurons within the ganglion. The double immunostaining study showed numerous nerve cell bodies displaying colocalisation of P2X2, P2X3 and P2Y1 with NPY. From the statistical analysis, there was a significant difference between the colocalisation of P2X2, P2X3 and P2Y1 with NPY, P2X2 > P2Y1 > P2X3. We found that ~ 45% of P2X2-positive neuronal cell bodies showed colocalisation with NPY. However, the coexpression was less with P2X3 and P2Y1 ~ 40% and ~35% respectively (Figure 4.4.B). Whole-mount preparation of superior mesenteric artery and carotid artery labelled for P2X2, P2X3 and P2Y1 nerves (in red) formed plexuses in the external layer of all branches of the arteries. Positive correlations were observed between the P2X2, P2X3 and P2Y1 nerve fibres and numbers of NPY nerves in the superior mesenteric artery. This indicated that a small population of nerve fibres that contained P2X2, P2X3 and P2Y1 also contained NPY nerve fibres in the superior mesenteric artery but not the carotid artery (Figures 4.44 – 4.46). Control sections are shown in which no primary antibody was applied and where just the secondary antibody was applied, to see if there was any non-specific binding. None of the receptors showed significant immunoreactivity in the control sections (Figures 4.42 & 4.47). These results suggested that some of P2X2, P2X3 and P2Y1-positive neurons in the mouse superior cervical ganglion have vasomotor activity, thus could innervate specific tissues (but not carotid artery) via post-ganglionic nerves arising from their ganglia.

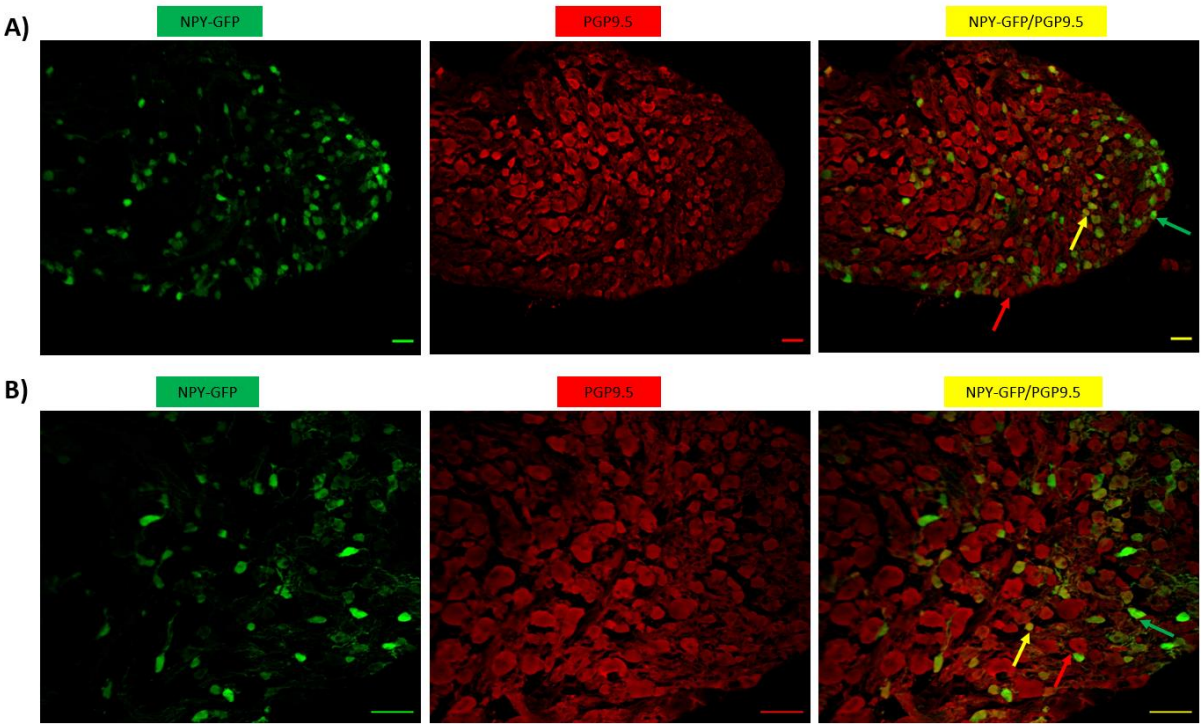

Figure 4.38: Immunofluorescence labelling for PGP 9.5 in superior cervical ganglion isolated from transgenic mice (NPY-hrGFP). NPY expression is green, and immunostaining for PGP9.5 is red in transverse superior cervical ganglion sections (10 µm). The merged image showed NPY-positive neurons and PGP9.5 were colocalised in the same nerve cell body (yellow). Images were visualized using a Laser-scanning confocal microscope Zeiss LSM510 META (Zeiss), equipped with an excitation filter system of 458/488 nm for FITC and 467 for the red channel. The sections are seen at x10 (A) and x 20 (B) magnification. The exposure and camera settings remained consistent across all the images taken for each experiment. Scale bars represent 50 µm. The green arrow indicates nerve cell bodies labelled for NPY only. The red arrow indicates nerve cell bodies labelled for PGP9.5 neuronal marker only. The yellow arrow indicates nerve cell bodies labelled for NPY and PGP9.5. The results shown are representative from three independent experiments using three different transgenic GFP-NPY male mice.

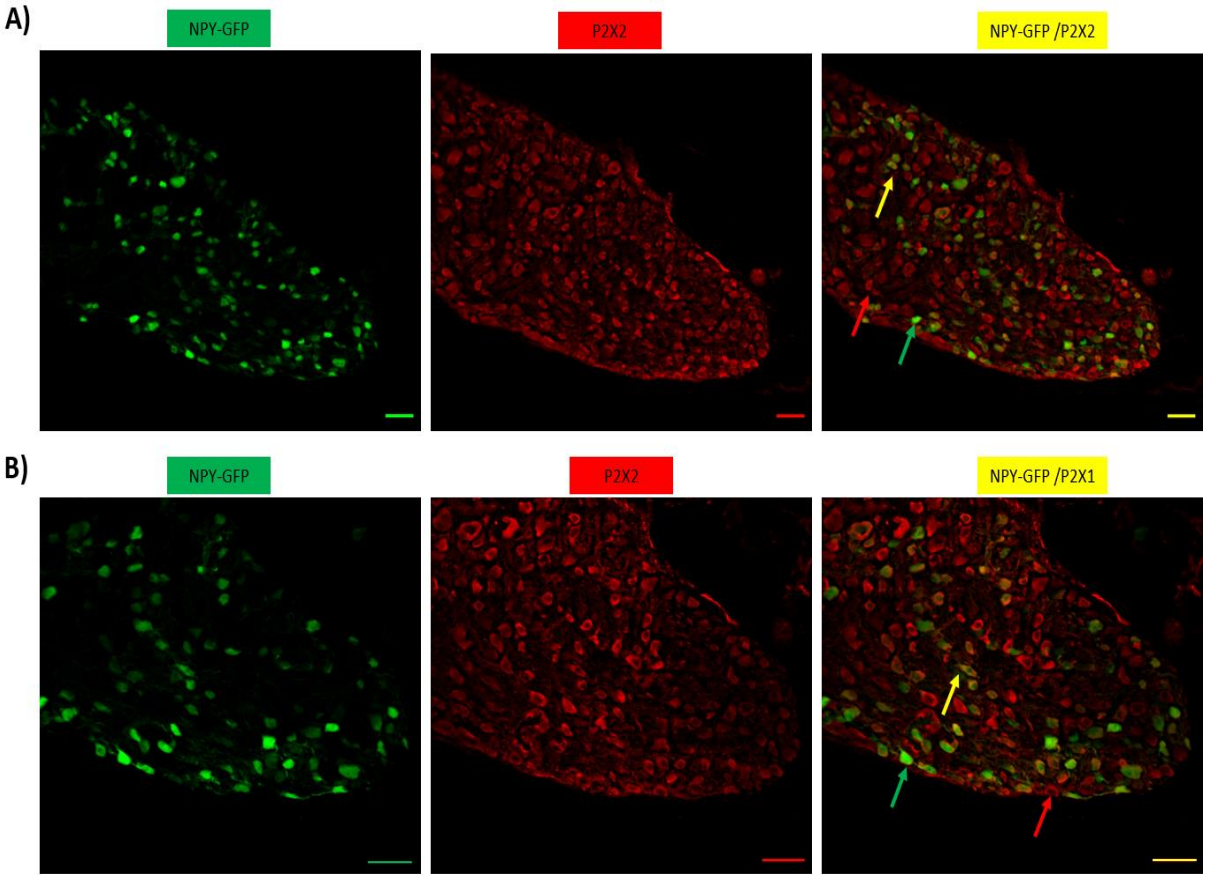

Figure 4.39: Immunofluorescence labelling for P2X2 in superior cervical ganglion isolated from transgenic mice (NPY-hrGFP). NPY expression is green, and immunostaining for P2X2 is red in transverse superior cervical ganglion sections (10 µm). The merged image showed NPY-positive neurons and P2X2 were colocalised in the same nerve cell body (yellow). Images were visualized using a Laser-scanning confocal microscope Zeiss LSM510 META (Zeiss), equipped with an excitation filter system of 458/488 nm for FITC and 467 for the red channel. The sections are seen at x10 (A) and x 20 (B) magnification. The exposure and camera settings remained consistent across all the images taken for each experiment. Scale bars represent 50 µm. The green arrow indicates nerve cell bodies labelled for NPY only. The red arrow indicates nerve cell bodies labelled for P2X2 receptor only. The yellow arrow indicates nerve cell bodies labelled for NPY and P2X2. The results shown are representative from three independent experiments using three different transgenic GFP-NPY male mice.

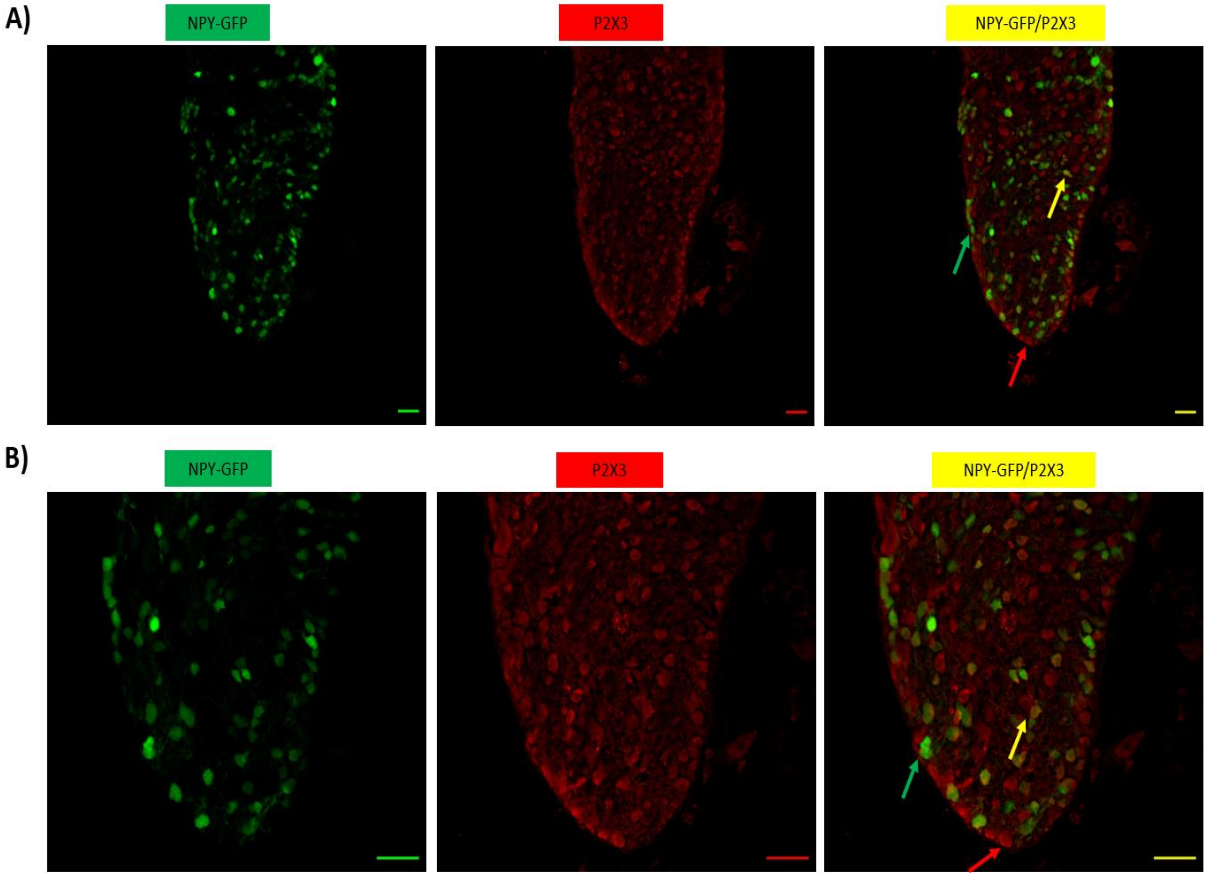

Figure 4.40: Immunofluorescence labelling for P2X3 in superior cervical ganglion isolated from transgenic mice (NPY-hrGFP). NPY expression is green, and immunostaining for P2X3 is red in transverse superior cervical ganglion sections (10 µm). The merged image showed NPY-positive neurons and P2X3 were colocalised in the same nerve cell body (yellow). Images were visualized using a Laser-scanning confocal microscope Zeiss LSM510 META (Zeiss), equipped with an excitation filter system of 458/488 nm for FITC and 467 for the red channel. The sections are seen at x10 (A) and x 20 (B) magnification. The exposure and camera settings remained consistent across all the images taken for each experiment. Scale bars represent 50 µm. The green arrow indicates nerve cell bodies labelled for NPY only. The red arrow indicates nerve cell bodies labelled for P2X3 receptor only,. The yellow arrow indicates nerve cell bodies labelled for NPY and P2X3. The results shown are representative from three independent experiments using three different transgenic GFP-NPY male mice.

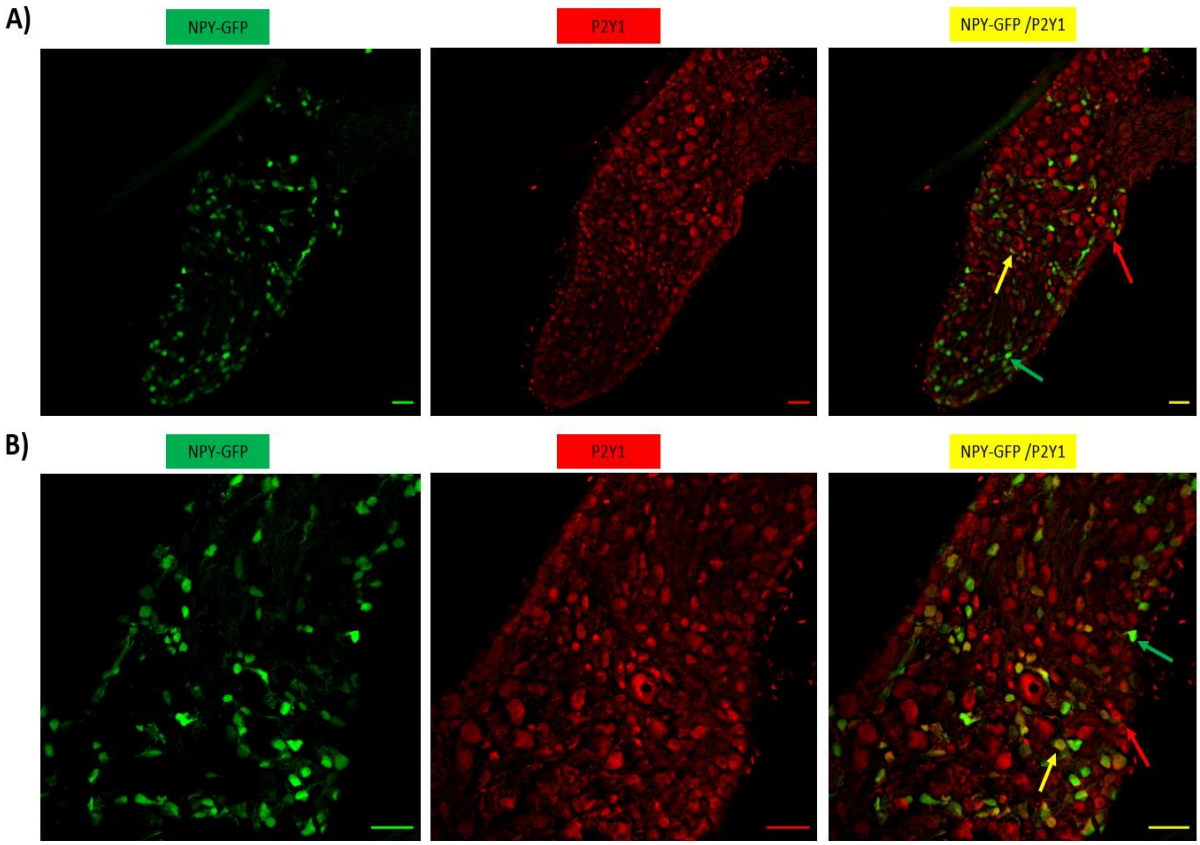

Figure 4.41: Immunofluorescence labelling for P2Y1 in superior cervical ganglion isolated from transgenic mice (NPY-hrGFP). NPY expression is green, and immunostaining for P2Y1 is red in transverse superior cervical ganglion sections (10 µm). The merged image showed NPY-positive neurons and P2Y1 were colocalised in the same nerve cell body (yellow). Images were visualized using a Laser-scanning confocal microscope Zeiss LSM510 META (Zeiss), equipped with an excitation filter system of 458/488 nm for FITC and 467 for the red channel. The sections are seen at x10 (A) and x 20 (B) magnification. The exposure and camera settings remained consistent across all the images taken for each experiment. Scale bars represent 50 µm. The green arrow indicates nerve cell bodies labelled for NPY only. The red arrow indicates nerve cell bodies labelled for P2Y1 receptor only. The yellow arrow indicates nerve cell bodies labelled for NPY and P2Y1. The results shown are representative from three independent experiments using three different transgenic GFP-NPY male mice.

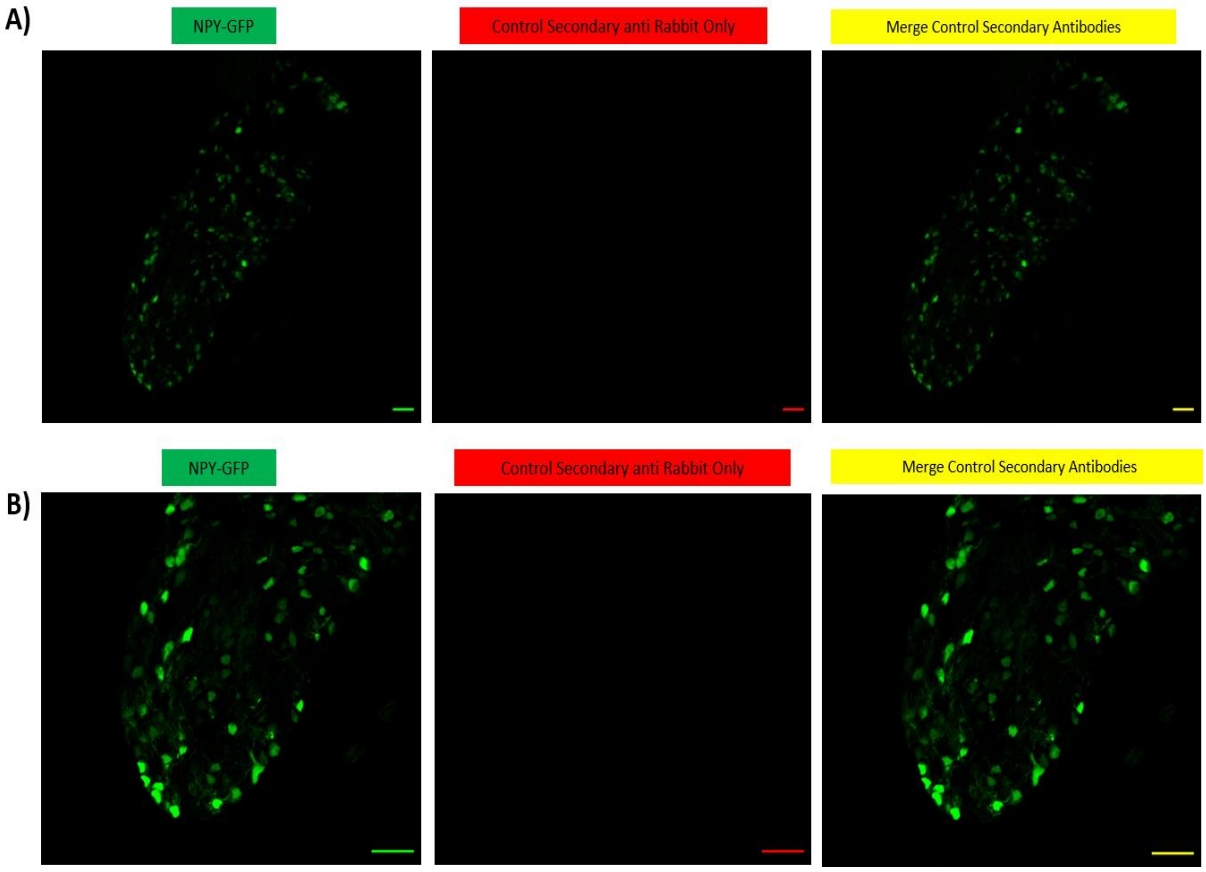

Figure 4.42: Control Immunofluorescence labelling for PGP9.5 and P2 receptor in superior cervical ganglion isolated from transgenic mice (NPY-hrGFP). Control sections are shown where just the secondary antibody was applied, to see if there was any non-specific binding and to determine the autofluorescence of the tissue. Immunostaining for secondary anti rabbit (red) in transverse superior cervical ganglion sections (10 µm). Images were visualized using a Laser-scanning confocal microscope Zeiss LSM510 META (Zeiss), equipped with an excitation filter system of 458/488 nm for FITC and 467 for the red channel. The sections are seen at x10 (A) and x 20 (B) magnification. The exposure and camera settings remained consistent across all the images taken for each experiment. Scale bars represent 50 µm. The results shown are representative from three independent experiments using three different transgenic GFP-NPY male mice.

.

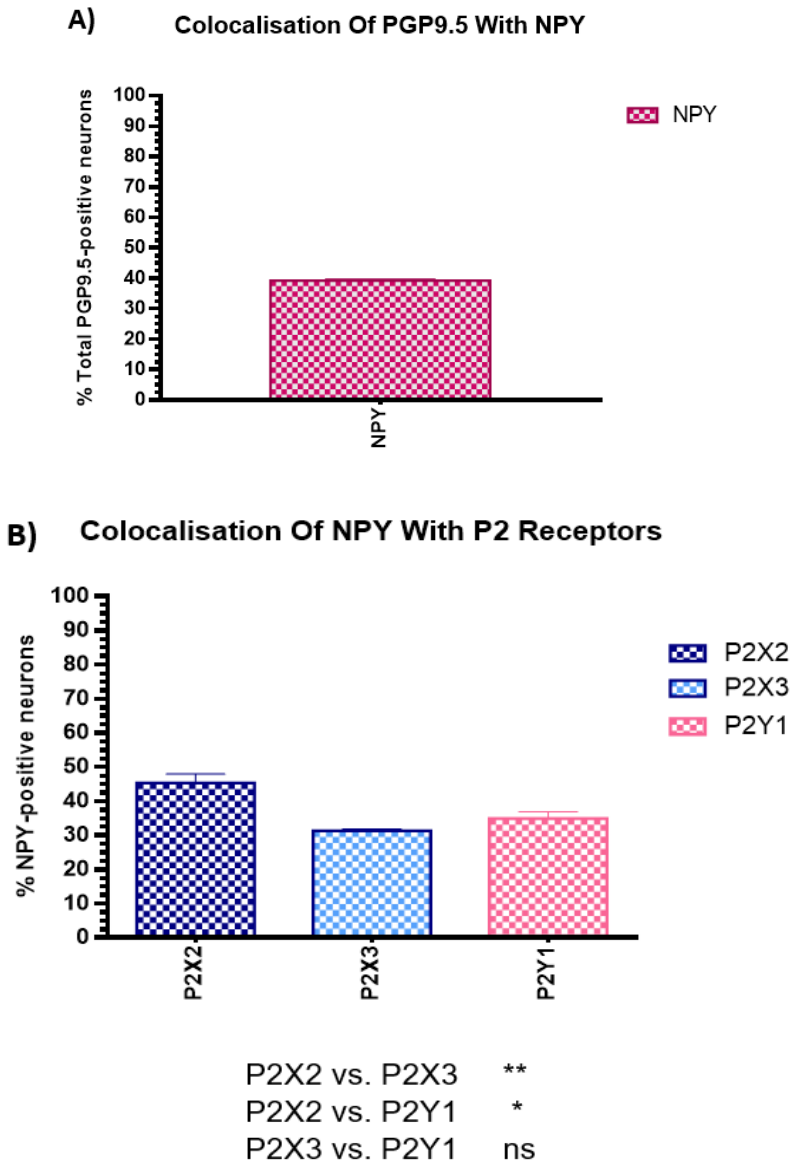

Figure 4.43: The percentage of P2-positive neurons have vasomotor activity (positive for NPY) in mouse superior cervical ganglion. (A) The percentage of NPY-positive superior cervical ganglion neurons. **(B)** Comparison of the percentage of P2X2, P2X3, and P2Y1-positive neurons expressing NPY in the superior cervical ganglion. Experiments were compared by a one-way ANOVA followed by (Brown-Forsythe multiple comparison test (GraphPad Prism 6), *p<0.05, **p<0.005, ***p<0.001, ****p<0.0001, ns not significant (p>0.05), mean with SEM. The results shown are representative from three independent experiments using three independent transgenic GFP-NPY male mice.

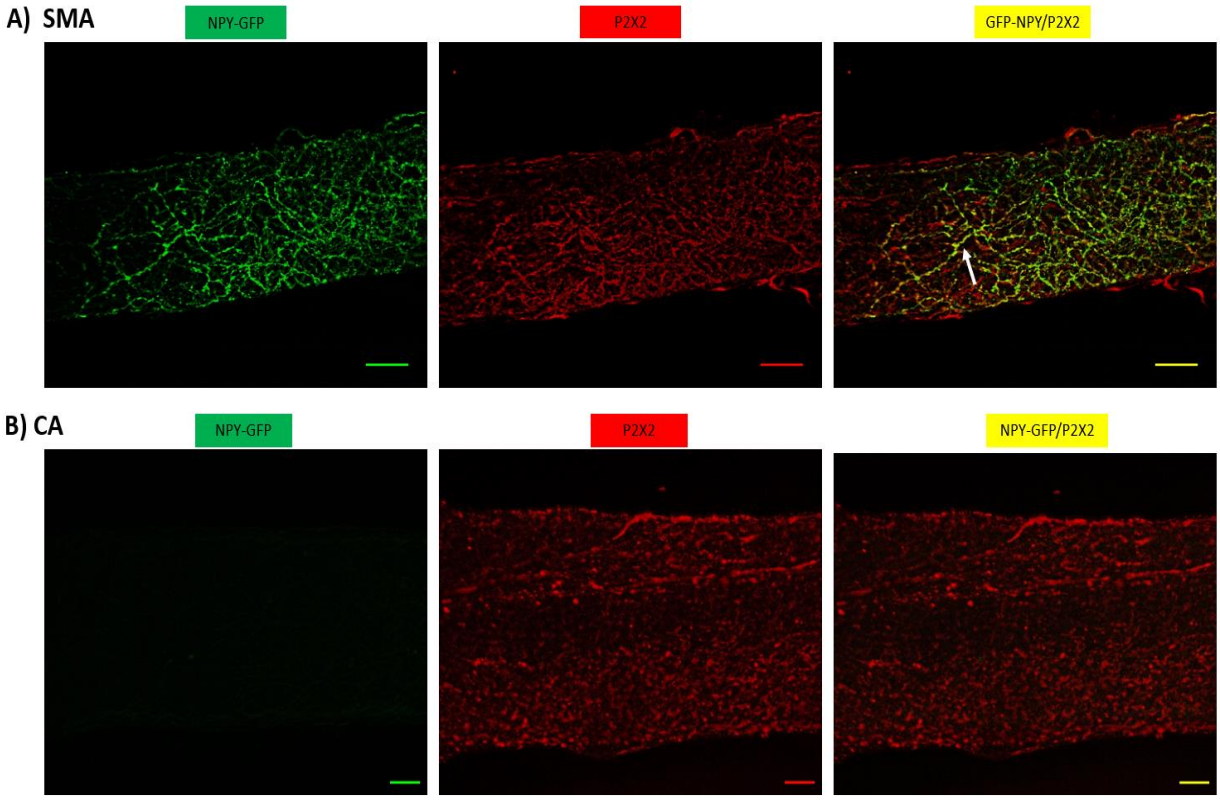

Figure 4.44: Immunofluorescence of whole-mount preparations of transgenic GFP-NPY mouse superior mesenteric artery and carotid artery labelled with P2X2. **(A)** Distribution of NPY nerve fibres (green) and P2X2 (red) in whole-mount preparations of superior mesenteric artery. Few nerves showed colocalisation for NPY and P2X2 (yellow). **(B)** Distribution of NPY nerve plexus (green not seen) and P2X2 (red) in whole-mount preparations of carotid artery. Images were visualized using a Laser-scanning confocal microscope Zeiss LSM510 META (Zeiss), equipped with an excitation filter system of 458/488 nm for FITC and 467 for the red channel. 7-10 optical images of the sections were scaled and overlapped together using Image J software, were magnified at x 20 for superior mesenteric artery and x 10 for carotid artery. The exposure and camera settings remained consistent across all the images taken for each experiment. Scale bars represent 50 μm. The white arrow indicates where nerves are colocalised. SMA indicates superior mesenteric artery, CA indicates carotid artery. The results shown are representative from three independent experiments using three different transgenic GFP-NPY male mice.

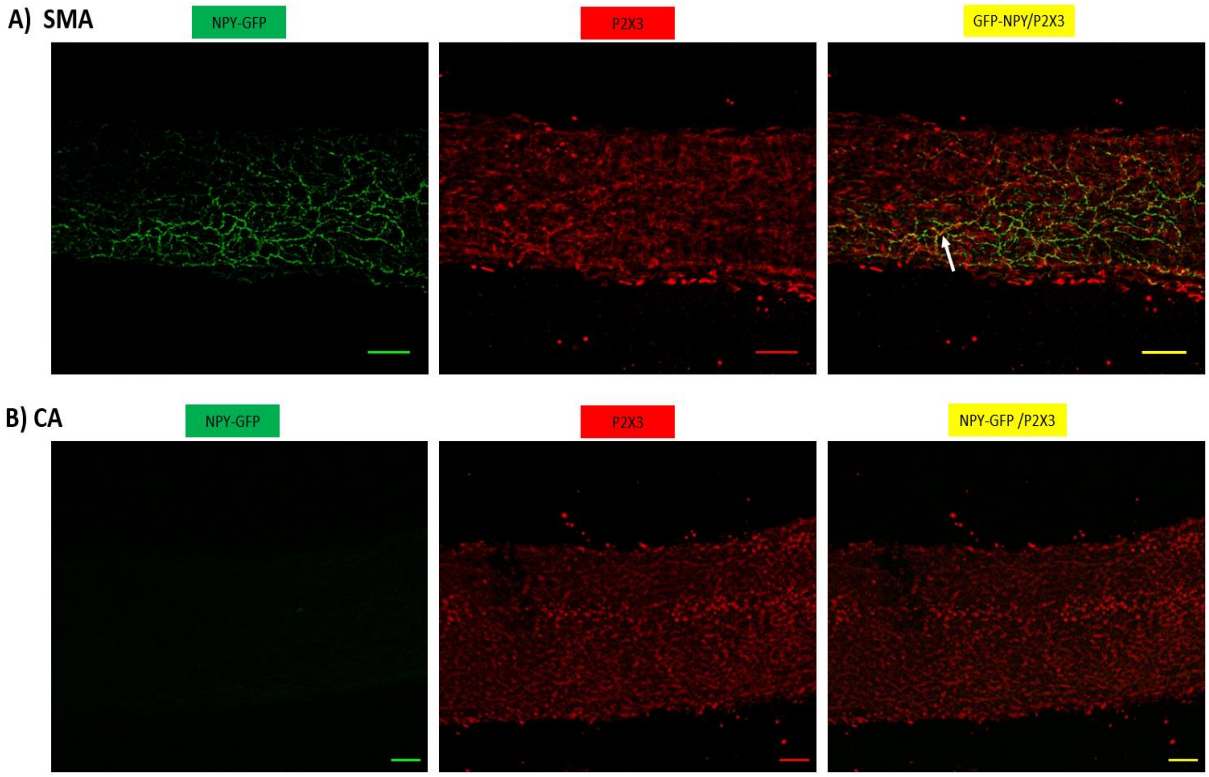

Figure 4.45: Immunofluorescence of whole-mount preparations of transgenic GFP-NPY mouse superior mesenteric artery and carotid artery labelled with P2X3. **(A)** Distribution of NPY nerve fibres (green) and P2X3 (red) in whole-mount preparations of superior mesenteric artery. Few nerves showed colocalisation for NPY and P2X3 (yellow). **(B)** Distribution of NPY nerve plexus (green-not seen) and P2X3 (red) in whole-mount preparations of carotid artery. Images were visualized using a Laser-scanning confocal microscope Zeiss LSM510 META (Zeiss), equipped with an excitation filter system of 458/488 nm for FITC and 467 for the red channel. 7-10 optical images of the sections were scaled and overlapped together using Image J software, were magnified at x 20 for superior mesenteric artery and x 10 for carotid artery. The exposure and camera settings remained consistent across all the images taken for each experiment. Scale bars represent 50 μm. The white arrow indicates where nerves are colocalised. SMA indicates superior mesenteric artery, CA indicates carotid artery. The results shown are representative from three independent experiments using three different transgenic GFP-NPY male mice.

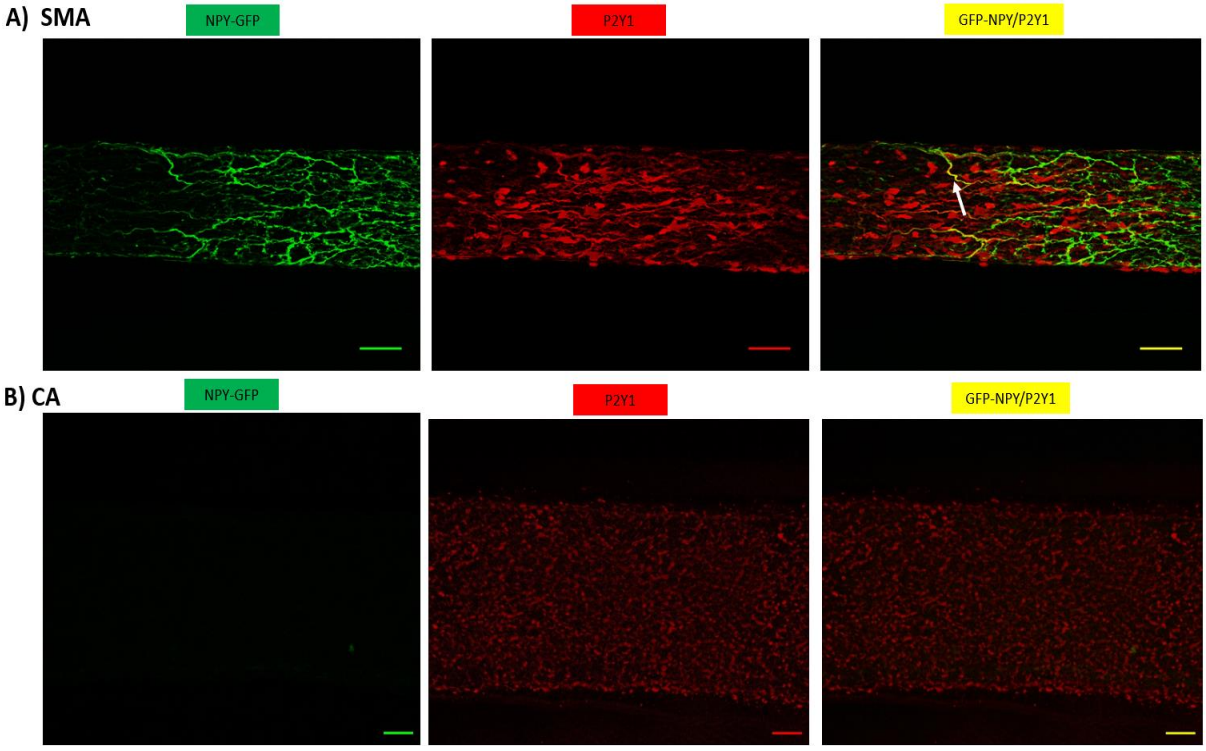

Figure 4.46: Immunofluorescence of whole-mount preparations of transgenic GFP-NPY mouse superior mesenteric artery and carotid artery labelled with P2Y1. **(A)** Distribution of NPY nerve fibres (green) and P2Y1 (red) in whole-mount preparations of superior mesenteric artery. Few nerves showed colocalisation for NPY and P2Y1 (yellow). **(B)** Distribution of NPY nerve plexus (green-not seen) and P2Y1 (red) in whole-mount preparations of carotid artery. Images were visualized using a Laser-scanning confocal microscope Zeiss LSM510 META (Zeiss), equipped with an excitation filter system of 458/488 nm for FITC and 467 for the red channel. 7-10 optical images of the sections were scaled and overlapped together using Image J software, were magnified at x 20 for superior mesenteric artery and x 10 for carotid artery. The exposure and camera settings remained consistent across all the images taken for each experiment. Scale bars represent 50 μm. The white arrow indicates where nerves are colocalised. SMA indicates superior mesenteric artery, CA indicates carotid artery. The results shown are representative from three independent experiments using three different transgenic GFP-NPY male mice.

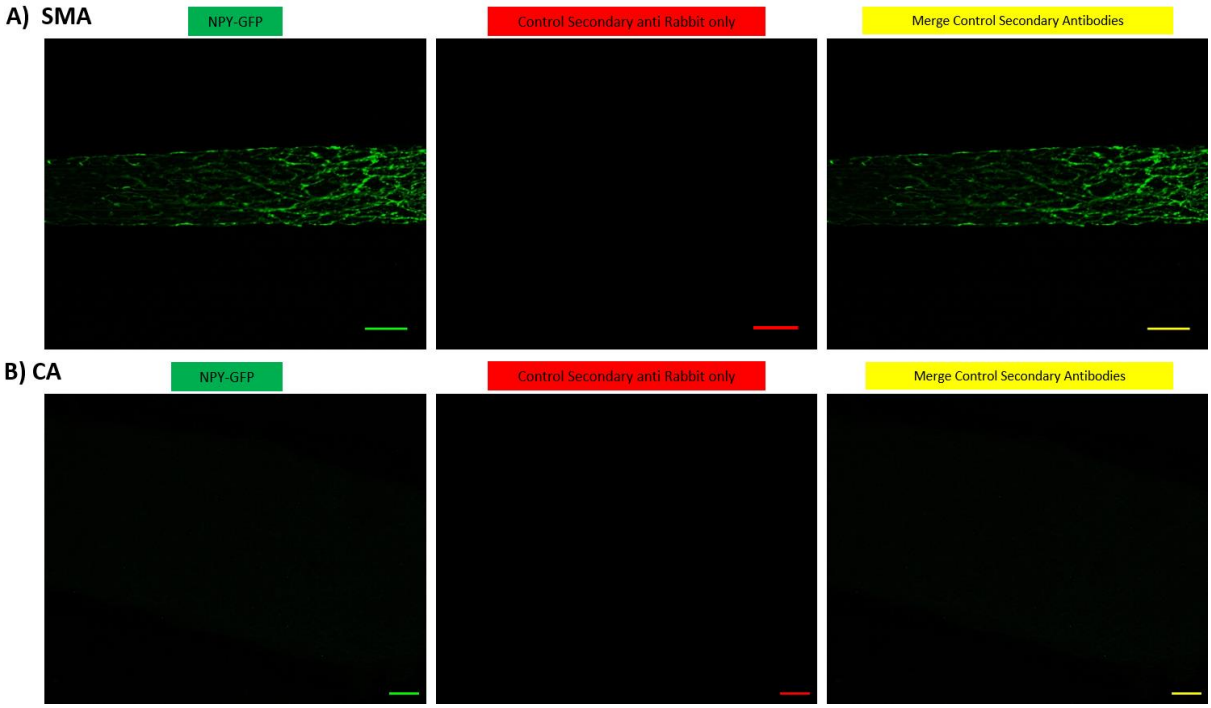

Figure 4.47: Control immunofluorescence of whole-mount preparations of transgenic GFP-NPY mouse superior mesenteric artery and carotid artery labelled with P2X2, P2X3 and P2Y1. Control tissues are shown where just the secondary antibody was applied, to see if there was any non-specific binding and to determine the autofluorescence of the tissue. Immunostaining for secondary anti rabbit (red) in the superior mesenteric artery (A) and carotid artery (B). Images were visualized using a Laser-scanning confocal microscope Zeiss LSM510 META (Zeiss), equipped with an excitation filter system of 458/488 nm for FITC and 467 for the red channel. 7-10 optical images of the sections were scaled and overlapped together using Image J software, were magnified at x 20 for superior mesenteric artery and x 10 for carotid artery. The exposure and camera settings remained consistent across all the images taken for each experiment. Scale bars represent 50 μm. SMA indicates superior mesenteric artery, CA indicates carotid artery. The results shown are representative from three independent experiments using three different transgenic GFP-NPY male mice.

4.3.6 Expression of total protein of P2 purinergic receptors in mouse superior cervical ganglion, superior mesenteric artery and carotid artery

Western blot analysis was performed to determine P2 purinergic receptor expression in total protein extracted from mouse superior cervical ganglion, superior mesenteric artery and carotid artery. We used the brain as a positive control. In addition, Western blot analysis confirmed the specificity of our antibodies. P2X2 (~ 55 kDa higher band, ~ 47 kDa lower band), P2X3 (~ 45 kDa), P2X4 (~ 49 kDa), P2X7 (~ 40 kDa lower band, ~ 68 higher band), and P2Y1 (~ 45 kDa) were detected at the expected product size in the mouse brain and superior cervical ganglion (Figure 4.48). However, no band was detected for antibody against P2X6. P2X1 showed a band larger than expected for the product size by sequence data (~ 60 kDa) in both the brain and the superior cervical ganglion. The P2X1 antibody was supplied by Alomone which is knockout validated in the mouse vas deferens. The explanation for these discrepancies is not clear. Certainly, posttranslational modifications such as glycosylation and/or receptor dimerization may be involved, but the exact explanation remains to be determined. Specific binding was detected at the expected product size for P2X3 and P2X4, but no band was detected for P2X2, P2X6 and P2Y1 in both superior mesenteric artery and carotid artery (Figure 4.48). P2X1 and P2X7 were not investigated in this project in the superior mesenteric artery and carotid artery. The presence of two bands for P2X2 and P2X7 receptor proteins was because of the six transcripts (splice variants) of the P2X2 gene and the five transcripts (splice variants) of the P2X7 gene detected by sequencing data. Recently, a new P2X7 splice variant (P2X7k) with an alternative first transmembrane domain was identified (Nicke et al., 2009). The specificity of the antibody binding was verified by preincubating the primary antibody with the respective control antigen for P2X2, P2X4 and P2X6. In each case, preincubation with the control antigen eliminated antibody staining consistent with specific banding under normal conditions. Preincubation with the control antigen also eliminated antibody staining for the positive control samples. The absence of P2X6 could be because of nonsense-mediated decay confirmed by sequence data. Nonsense-mediated decay is the pathway that the cells use to evolve various surveillance mechanisms to target mRNAs with mutations that would otherwise result in errors in protein synthesis. Nonsense-mediated decay is defined as a post-transcriptional mRNA quality control mechanism that removes premature termination codon-containing mRNAs that, if left intact, would result in the production of truncated proteins (Hug et al., 2016). These findings confirmed the RT-PCR results and the presence of P2X1, P2X2, P2X3, P2X4, P2X7 and P2Y1 in the superior cervical ganglion but not P2X6. The absence of P2X2 and P2Y1 protein in the superior mesenteric artery and carotid artery could be because of the low levels of these proteins in these blood vessels due to these receptors being located

in the perivascular nerves only. The marker on neurons (PGP9.5) showed a faint band by RT-PCR compared to smooth muscle and the endothelium markers. P2X3 proteins were detected in the superior mesenteric artery and carotid artery but immunohistochemical data showed the presence of this protein within the perivascular nerves within the adventitia only. Additionally, P2X3 and P2Y1 were tested using different antibodies, which detected bands at unexpected product sizes, previously to the ones shown in these results (see appendix).

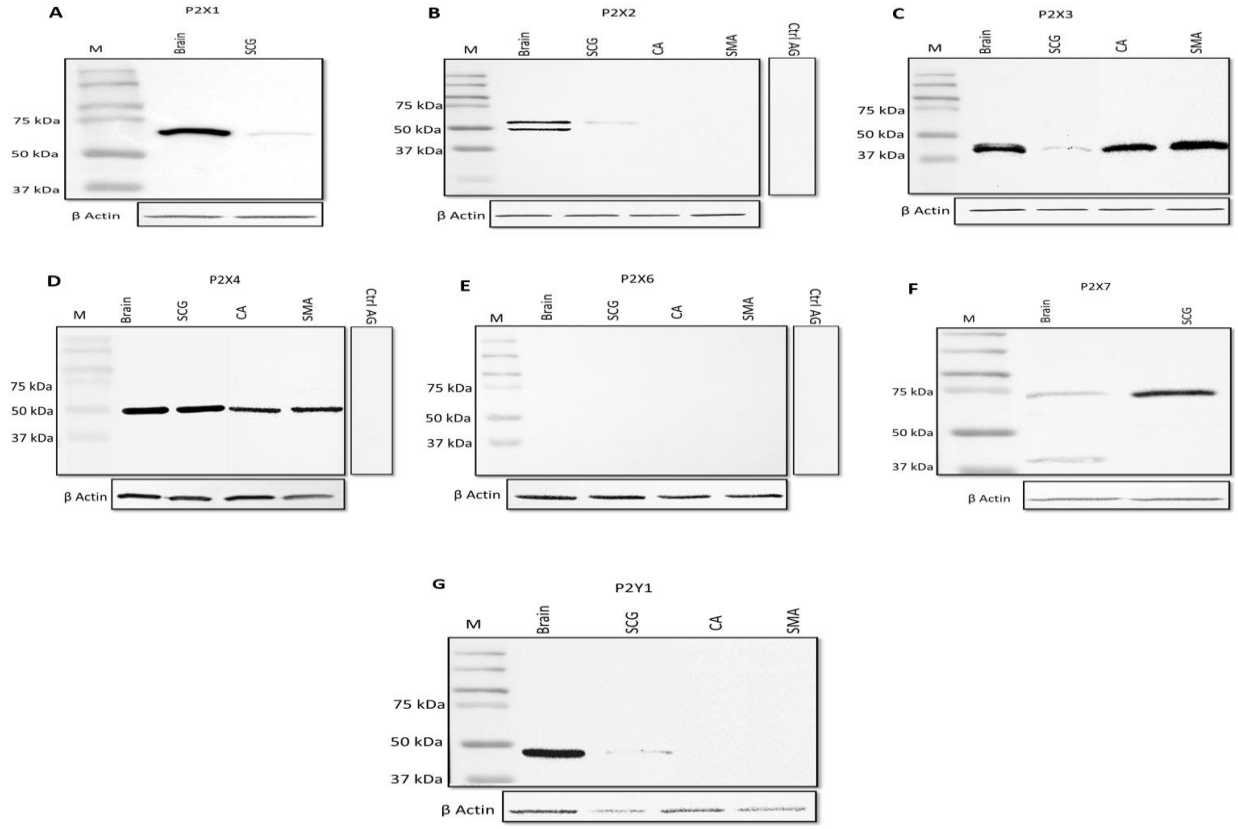

Figure 4.48: **Western blotting of P2 receptors in the mouse brain, superior cervical ganglion, superior mesenteric artery and carotid artery**. Lane 1 of each blot **(A-G)** contains the positive controls for each receptor protein and includes the mouse brain. The brain expressed all the receptors P2X1 (~ 60kDa), P2X2 (~ 55 kDa higher band, ~ 47 kDa lower band), P2X3 (~ 45 kDa), P2X4 (~ 49 kDa), P2X7 (~ 40 kDa lower band, ~ 68 higher band), and P2Y1 (~ 45 kDa) but not P2X6. **(A & F)** The Western immunoblots showing expression of P2X1 and P2X7 receptor protein in the superior cervical ganglion (second lane). **(B & G**) The Western immunoblots showed expression of P2X2 and P2Y1 receptors proteins in the superior cervical ganglion (second lane, ~ 55 kDa band only), but it was not expressed in the superior mesenteric artery (third lane) and carotid artery (fourth lane). **(C & D)** The Western immunoblots showing expression of P2X3 and P2X4 receptors proteins in the superior cervical ganglion (second lane), SMA (third lane) and carotid artery (fourth lane). **(E)** The immunoblot showed no expression of P2X6 in all tissues. β actin served as a loading control. M represents the molecular weight marker. Ctrl AG represents the primary antibody with the respective control antigen to verify specificity. SCG, superior cervical ganglion; SMA, superior mesenteric artery; CA, carotid artery 30 μg protein/lane. The results shown are representative from five independent experiments using five different mice. We obtained qualitatively similar results in three independent experiments from three independent male mice.

4.4 Discussion

4.4.1. Expression of P2 purinergic receptors at the protein level in mouse sympathetic superior cervical ganglion

This is the first study in which mouse superior cervical ganglion, superior mesenteric artery and carotid artery tissues have been examined for the expression of all P2X receptor isoforms, in addition to P2Y1 receptor at the protein level. It was previously reported that P2X receptors are expressed in both pre-synaptic and post-synaptic ganglia of sympathetic and parasympathetic nerves. Thus, the P2X receptors are involved in the regulation of neurotransmitter release during fast transmission (Abbracchio et al., 2009). However, similar studies have been performed for these tissues in rats, and the results shown here are predominantly in accordance with them. The distribution of P2X1, P2X2, P2X3, P2X4, P2X6, P2X7 and P2Y1 receptors, in mouse superior cervical ganglia, superior mesenteric artery and carotid artery was studied immunohistochemically. Our results illustrated that P2X1, P2X2, P2X3, P2X4, P2X7 and P2Y1 receptors were found on between 70-90 % of neurons in the superior cervical ganglia at different intensities. Moreover, it was found that the antibody for TH labelled over 98 % of the neurons in the superior cervical ganglia, which could confirm the sympathetic phenotype of the superior cervical ganglion. The level of immunostaining of each receptor in individual neurons within the ganglion also varied significantly. Previous studies reported high immunoreactivity for P2X2, P2X4 and P2X6 (labelled over 90% of the neurons), and low immunoreactivity for P2X1 and P2X3 in rat sympathetic superior cervical and coeliac ganglia. However, P2X5 was absent in the sympathetic ganglions. It was reported that approximately 98% of rat superior cervical ganglion neurons express TH and are functionally noradrenergic (Gibbins, 1995). Low level expression of the P2X3 receptor was found in the sympathetic ganglia, indicating that the P2X3 receptor subtype is not restricted to the sensory ganglia, where it is extensively expressed (Xiang & Burnstock, 1998). The same study reported that P2X1-6 were expressed in rat sensory trigeminal, dorsal root and nodose ganglions. However, the expression of P2X3 was higher than other receptors. In contrast to our results in mice, P2X6 was strongly expressed in the rat cervical ganglion and higher than P2X2 and P2X4 (Xiang & Burnstock, 1998). According to Takaki et al., (2015), small intensely fluorescent cells (interneurons), originating from the neural crest, and sympathetic neurons are found in the rat sympathetic ganglia and were shown to be immunoreactive for TH and/or dopamine β-hydroxylase. A previous study stated that most neurons in mouse sympathetic ganglion neurons had immunoreactivity for P2X2, but not P2X3 (Cockayne et al., 2005). This disagreed with our results that the sympathetic neurons expressed the P2X3 receptor. A previous functional study

using whole-cell voltage-clamp in mouse superior cervical ganglion reported that 62% of $P2X2^{+/+}$ neurons responded to 100 μM ATP, whereas only 3% of neurons showed a significant response to 100 μM ATP in the $P2X2^{-/-}$ mouse, confirming the presence and the functional role could P2X2 play (Cockayne et al., 2005). In contrast to Cockayne et al, Dunn et al reported that the sympathetic neurons in the rat superior cervical ganglion showed significant responses to ATP and α, β-meATP during the early post-natal period. This was due to the high level of the expression of P2X3 subtype giving rise to the presence of heteromeric P2X2/3 receptors, but these responses were decreased in mature rats due to few neurons were immunoreactive for the P2X3 subunit (Dunn et al., 2005). Studies using P2X1 knockout mice have shown that responsiveness to α, β-meATP in mouse superior cervical ganglion neurons is facilitated by P2X1, which confirmed the expression and functional role of P2X1 in the mouse sympathetic superior cervical ganglion (Dun et al., 2005; Calvert and Evans, 2004). In rat superior cervical ganglion, P2X2 was the most predominantly expressed, whereas few ganglionic cells were immunoreactive for P2X3, P2X4 and P2X5. P2X6 and P2X7 receptors displayed the next highest level of immunoreactivity after P2X2 in the rat superior cervical ganglion (Li et al., 2000). Immunoblots in the same study showed high expression of P2X2, P2X6 and P2X7, whilst the expression of P2X4 and P2X5 was lower. P2X3 immunolabelling was apparent even in one-day-old tissue, consistent with our study of P2X subtypes in the mouse superior cervical ganglion. A study in the rat superior cervical ganglion revealed positive immunoreactivities for all P2X receptors except P2X5 (Xiang et al., 1998). It has been reported by RT-PCR using total RNA extracted from adult mice superior cervical ganglion cell culture that P2Y1, P2Y2 and P2Y6 are expressed but not P2Y4 (Calvert et al., 2004). A previous study in guinea pig superior cervical ganglion showed positive immunoreactivity for P2X2 and P2X3 using antibodies raised against the corresponding rat receptor epitopes. However, P2X1, P2X4, P2X5 and P2X6 immunoreactivity were not detected in the guinea pig superior cervical ganglion (Dunn et al., 2001; Zhong et al, 2000). In addition to detection studies, electrophysiological studies have examined the pharmacology of P2X receptors which expressed immunohistochemically in the mouse superior cervical ganglion by using a model of sympathetic neurons differentiated from human SH-SY5Ycells. These are discussed in more detail in the next chapter (5). The current study revealed the presence of mRNA for P2X6 receptors, but no immunoreactivity was detected for this isoform when performing immunohistochemistry. There are several potential reasons for this inconsistency. It may be because of the nonsense-mediated decay transcripts detected by sequencing data (Supplementary S.3). Cells have evolved various surveillance mechanisms to target mRNAs with mutations that might otherwise result in errors in protein synthesis in both the cell nucleus and cytoplasm. The nonsense-mediated mRNA decay

pathway not only degrades mRNAs harbouring premature termination codons, but it also modulates the abundance of a huge number of cellular RNAs and is intimately linked to translation termination (Hug et al., 2016). Alternatively, the epitope that the antibody was targeted against may have defective protein folding, or interacted with other proteins (Calvert, 2003).

TH is locally synthesized in axons and pre-synaptic nerve terminals of noradrenergic neurons due to the presence of TH mRNA in distal superior cervical ganglion axons. This was confirmed by in situ hybridization histochemistry. This suggested that the biosynthesis of the catecholamine neurotransmitters (such as NA) is locally regulated in the axon and/or pre-synaptic nerve terminal. In addition, NPY mRNA was also expressed in axons using RT-PCR (Gervasi et al., 2016). Our results showed that over 98% of mouse superior cervical ganglion neurons expressed TH, it was found that polyclonal antibodies for P2X1, P2X2, P2X3, P2X4, P2X7 and P2Y1 receptor isoforms colocalised with over 90% of TH-positive neurons in this ganglion to different intensities. A previous study in adult Sprague-Dawley rats showed that the majority of sympathetic ganglion cells contain TH and dopamine β-hydroxylase and most of the neurons were double-labelled for both enzymes (Price., 1984). We hypothesised that receptor subtypes detected in sympathetic ganglia but not arteries "P2X2, P2X3, P2Y1 and "less likely P2X7" could be expressed by sympathetic post-ganglionic nerves that innervate arteries. Here they could serve as pre-junctional, regulating the release of neurotransmitters. It was previously suggested that P2X1, P2X2, P2X3, P2X2/3, P2X1/5, P2X4/6, and P2X7 receptors have been identified as being responsible for facilitatory regulation in various parts of the central nervous and perivascular nervous systems. P2Y1 and P2Y4 receptors may also mediate facilitation of transmitter release in certain areas of the nervous system. P2Y12 and P2Y13 receptor subunits mediate inhibition of neurotransmitter release (Sperlagh et al., 2007).

4.4.2 Mouse superior cervical ganglion neurons are capable of vesicular storage of ATP and possible exocytosis release by expressing VNUT

The colocalisation of P2X receptors and vesicles being mostly situated within cell bodies, indicates that the receptors are carried to the terminals of neurons in vesicles, where they may serve as auto- and/or heteroreceptors (Li et al., 2000). PGP9.5 colocalised with VNUT in transverse sections of the mouse superior cervical ganglion. In addition, the sections showed colocalisation of P2X2, P2X3 and P2Y1 with VNUT. The data showed that most of the PGP9.5-positive neurons were labelled for VNUT. Furthermore, approximately 75% - 90%

of the cell bodies expressing the receptors were positive for VNUT. The result indicated that 80% of neurons in the superior cervical ganglion were capable of vesicular storage of ATP. Moreover, the P2X2, P2X3 and P2Y1 neurons have ATP storage capability. In purinergic receptor-expressing cells, ATP is stored in secretory vesicles. It is reported that SLC17A9 protein is a vesicular nucleotide transporter and contributes to various purinergic responses, such as central control of autonomic functions, control of vessel tone and angiogenesis, pain and mechanosensory transduction, neural-glial interactions, and platelet aggregation through purine receptors (Sawada et al., 2008). VNUT-defective mice lose vesicular storage and release of ATP from neurons and neuroendocrine cells, leading to obstruction of the purinergic chemical transmission. As a result, VNUT plays a critical role in the vesicular storage and release of ATP (Moriyama et al., 2017). VNUT is widely found in cells all over the body where ATP is released. For instance, VNUT and TH were coexpressed on dopaminergic neurons of the substantia nigra and ventral tegmental area. VNUT was also mostly detected in IB4-positive dorsal root ganglion neurons in rats; IB4 is a marker of sensory neurons. This result suggested that VNUT was engaged in ATP accumulation in dorsal root ganglion neurons, particularly small and medium-sized ones, and could be implicated in ATP-mediated nociceptive signalling. (Ho et al., 2015; Nishida et al., 2014). Moreover, several previous results reported that VNUT was expressed in various tissues in different species, these tissues included vesicular acetylcholine-containing synaptic vesicles, the nerve terminals of enteric musculomotor neurons, cultured human corneal limbal and human conjunctival epithelial cells, platelets, T cells and macrophages. Thus, there is a wide distribution of nucleotide receptors and nucleotide signalling pathways in essentially all principal cell types except astrocytes and microglia of the brain, secretory lysosomes (for more details see reference Moriyama et al., 2017; Verkhratsky et al., 2020). The importance of the contribution of VNUT in vesicular ATP release was studied by Sakamoto et al (2014). They reported that vesicular storage of ATP, as well as depolarisation-evoked ATP release from isolated hippocampal neurons, was completely absent in VNUT-defective mice. This indicated that VNUT was a crucial factor for vesicular ATP release in various cells, including neurons and some neuroendocrine cells. Few studies have investigated the coexpression of VNUT with purinergic receptors in sympathetic neurons, thus, our study is the first study that showed the coexpression of VNUT and P2X2, P2X3 and P2Y1 in the mouse superior cervical ganglion. VNUT is a promising molecular target for decreasing vesicular ATP release, and it could lead to a novel pharmacological treatment for inhibiting purinergic chemical transmission with broad therapeutic potential.

4.4.3. Sympathetic innervation of mouse mesenteric and carotid arteries, and the expression of purinergic receptors in perivascular nerves of the superior mesenteric and carotid arteries

Our question was whether the sympathetic post-ganglionic neurons are involved in the innervation of the superior mesenteric and carotid arteries. In addition, whether the P2 purinergic receptors served as auto- and/or heteroreceptors to modulate transmitter release by ATP and other nucleotides released by neuronal activity and pathological signals. The smooth muscle of human mesenteric arteries is supplied by perivascular nerves which work with the endothelium to control blood flow to the organs. The nerves are mostly sympathetic and contain cotransmitters such as NA, ATP and NPY. They could also be sensory-motor nerves and nerve fibre extensions from the enteric nervous system (Birch et al., 2008). It was demonstrated that the carotid plexus, whose fibres travel alongside the carotid arteries and supply sympathetic innervation to the head and the neck, was formed by the superior cervical ganglion. It was noticed that the common and external carotid arteries were innervated via adrenergic nerves. However, the innervation of the internal carotid artery was minimal (Knoche & Kienecker, 1977). The superior cervical ganglion gives rise to the carotid plexus, the fibres of which travel alongside the carotid arteries and supply sympathetic innervation to the head. This includes the iris dilator muscles, lacrimal glands, salivary glands, levator palpebrae, erector pili muscles, and small blood vessels. (Ladd et al., 2014). Furthermore, a previous study in *Didelphis virginiana* showed that the carotid sinus was innervated via post-ganglionic fibres of the cervical sympathetic nerves from the superior cervical ganglion, indicating that these nerves had effects on the carotid baroreceptors (sense changes in systemic blood pressure and is situated in the adventitia of the carotid bulb of the internal carotid artery) and thus their possible role in blood pressure regulation (Porzionato et al., 2019). Efferent signals travel to the heart and blood vessels via the parasympathetic and sympathetic nerves. This reaction, known as the carotid sinus baroreflex, causes necessary modifications to maintain heart rate and blood pressure within normal physiological limits (Andani & Khan, 2020). Obviously, the available information about the innervation of mouse common carotid arteries is still incomplete and requires more investigation (Figure 4.49).

Our double immunostaining study of PGP9.5 with TH in the mouse superior mesenteric showed the nerves expressing both markers were around the outside of the mesenteric arteries (the adventitia). Most of the nerve fibres that contained PGP 9.5 also contained TH in the superior mesenteric arteries. However, a small population of nerve fibres that contained PGP 9.5 did not contain TH. Our results also demonstrated that the carotid artery labelled for PGP9.5

did not show immunoreactivity for TH. This suggested that the carotid artery could not be innervated via sympathetic adrenergic nerves arising from sympathetic ganglia and may be innervated via other types of neurons such as sensory neurons or nerves arise from the carotid body. These results differ from previous wok by Maklad et al., (2001) which the whole mount of the internal carotid and its branches showed the sympathetic plexus around them. The different results could be due to the specific location of artery segment used in each study, the common carotid artery were use in our study. It has been shown in a previous study in transverse sections of the human mesenteric artery labelled for PGP9.5, TH and NPY that nerves were distributed at the junction of the adventitia and the media, close to the external elastic lamina. The same study reported immunoreactivity for vasoactive intestinal peptide, SP and CGRP although at a lower density than PGP9.5, TH and NPY. This indicated the presence of sensory-motor nerves. In addition, the human artery did not label for NO synthase or choline acetyltransferase (Birch et al., 2008). Previous immunohistochemical findings in the rat mesenteric artery suggested that the density of immunoreactivity for TH, NPY, CGRP and SP nerve in the 1st order was significantly lower than in the 2nd and 3rd order This indicated a negative relationship between the diameter of the artery and the nerve density, except for TH nerves (Yokomizo et al., 2015). It was also reported that the densities of TH and SP nerves were similar to NPY and CGRP nerves in all branches, respectively. While the densities of NPY and TH nerves were markedly greater than those of NO synthase, CGRP, and SP nerves in the 2nd and 3rd orders (Yokomizo et al., 2015). Moreover, the previous study illustrated that vasoconstrictor nerves (TH and NPY) were colocalised in the sympathetic nerves innervating the mesenteric arteries, while TH nerves are close, they did not colocalise with vasodilator nerves (CGRP, SP and NO synthase), indicating both vasoconstrictor and vasodilator nerves lead to an axo-axonal interaction to control vascular tone (Yokomizo et al., 2015). According to Smyth et al (2006), cryostat sections of the canine mesenteric artery were most showed colocalisation for PGP 9.5 and TH and were distributed within a dense layer at the level of the adventitia. These results corroborated with the ones found in the current study.

Our study demonstrated that the majority of mouse superior mesenteric artery nerve fibres showed colocalisation of PGP9.5 with P2X2, P2X3, P2X4, P2X7 receptors, and a few nerves were found localised with P2X1 and P2Y1. Double immunolabelling for PGP 9.5 and the P2 receptor of whole-mount preparations of the carotid artery revealed the majority of the nerve plexus showed colocalisation of PGP 9.5 with P2X2, P2X3, P2X4 and P2Y1 receptors, whilst P2X1 and P2X7 immunoreactivity were absent. However, both the superior mesenteric and carotid arteries did not show immunoreactivity for the P2X6 receptor. It has been reported that P2X1, P2X4 and P2X5 receptors were immunohistochemically expressed in the rat

mesenteric artery in the smooth muscle layer. Conversely, immunoreactivity specific for P2X7 was observed in the outer adventitial layer, which contains collagen fibres and varicose sympathetic nerves (Lewis & Evans, 2000),), which is in close agreement with the current study. Others reported that P2X5 was barely expressed in rat mesenteric arteries, and the P2X7 receptor was poorly expressed in the smooth muscle layer of the large arteries and the outer adventitial layer of medium-sized arteries. A high level of expression was seen for the P2X1 receptor and a lower expression level for P2X4 on smooth muscle cells. Whereas no significant immunoreactivity was observed for P2X2, P2X3 and P2X6 in arterial tissues despite the positive labelling in sections of dorsal root ganglion and spinal cord (Lewis & Evans, 2001; Gitterman & Evans, 2000)

Regarding the expression of purinergic receptors on the mouse common carotid artery, the current study demonstrated the majority of the nerve plexus within the adventitia showed colocalisation of PGP 9.5 with P2X2, P2X3, P2X4 and P2Y1, whilst P2X1, P2X6 and P2X7 immunoreactivity were absent. It was previously reported that RT-PCR experiments in various arteries of rats (including mesenteric and caudal, the internal carotid, thoracic aorta and pulmonary arteries) revealed that P2X1, P2X4 and P2X7 receptors were expressed on all arteries, while P2X, P2X3, P2X5 and P2X6 were absent (Li et al., 2020). Another previous study in the mouse carotid body reported the expression of the P2X2 receptor which plays an essential role in carotid body function and contributes to ventilatory responses to hypoxia (Rong et al., 2003). It has been reported that in whole-mount preparations of the rat carotid artery, immunoreactivity for P2X3 nerve endings was detected in the internal carotid artery proximal to the carotid bifurcation, particularly in the region opposite the carotid body, but not in the external carotid artery. Moreover, in transverse cryostat sections of the internal carotid artery, P2X3-immunoreactive nerve endings were present in the adventitia near the media (smooth muscle cell) layer (Yokoyama et al., 2019). Minimal data is published on the expression of P2 receptors on the common carotid artery itself. Further studies on the electrophysiological and pharmacological properties are required to clarify the functional role of ATP in P2X2/P2X3-immunoreactive nerve endings in the rat common carotid artery and carotid sinus.

These immunolabeling results alongside RT-PCR results of both the sympathetic ganglion and the arteries suggested P2X2, P2X3, P2X7 and P2Y1 could be expressed by sympathetic post-ganglionic nerves that innervate arteries. Thus, they could be present only in perivascular nerves within the adventitial layer but not in smooth muscle cells and the endothelium. That was confirmed in our study by cryostat transverse sections of the superior

mesenteric and carotid arteries that showed P2X2, P2X3, P2X7 and P2Y1 receptors were distributed within the adventitial side. That led to suggest, that these receptors expressed in perivascular nerves could serve as pre-junctional receptors and could be able to modulate the release of various neurotransmitters via feedback loops. This could potentially provide a novel target for the therapeutic control of vascular tone and blood pressure.

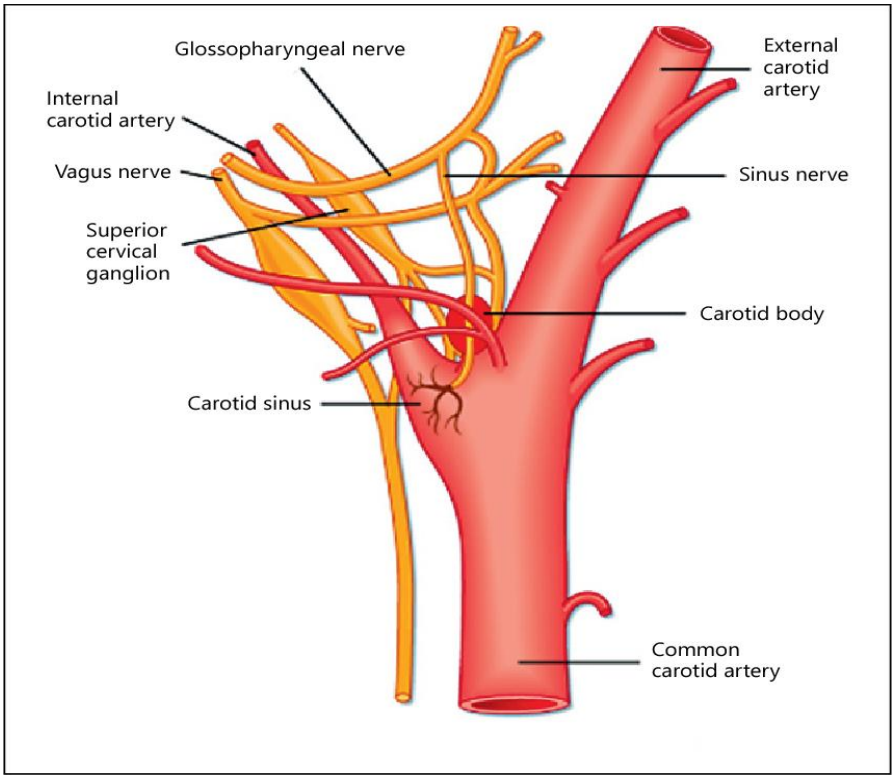

Figure 4.49: Anatomy of the common carotid artery, carotid sinus, carotid body and superior cervical ganglion. Afferent nerve fibres travel from baroreceptors in the carotid sinus wall and chemoreceptors in the carotid body to the solitary nucleus of the medulla in the brainstem via the glossopharyngeal nerve. NTS indicates the nucleus tractus solitarius (Yin et al., 2016)

As we were focused on the expression of purinergic receptors in the perivascular nerve site of the arteries (pre-junctional terminal), we will discuss the role of these receptors which could act as auto- and/or heteroreceptors and modulate neurotransmitter release. It has been reported that the activation of ionotropic P2X receptors on sympathetic nerve terminals directly provokes NA release mediated by nerve stimulation by a direct Ca^{2+} influx through the receptor-ion channel complex (Arthur et al., 2007). P2X2 is found in cultured superior cervical ganglion sympathetic neurons of the rat. It was reported that ATP elicits NA release from rat superior cervical ganglion neurons mediated by ionotropic receptors that are located on sympathetic nerve terminals or in proximity to the sites of transmitter release (Boehm et al., 1999). Conversely, it has been suggested that faciliatory ionotropic P2X receptors are not expressed in cultured mouse sympathetic nerve terminals. Our study showed the expression of P2X receptors in the mouse ganglion and the perivascular nerves of mesenteric arteries, but the functional role of these receptors requires further investigation (Nörenberg et al., 2001). It has been found that P2Y1, P2Y2, and P2Y6 receptors are expressed on neurons and astrocytes. Briefly, many studies reported the expression of P2Y receptor mRNA and protein in several different tissues, including sympathetic and parasympathetic sensory nerve terminals, basal ganglia, brainstem, cerebellum, cortex, hypothalamus, and hippocampus (Sperlágh et al., 2007; Hussl & Boehm, 2006). A comparable situation was defined for the neuromuscular junction where pre-synaptic nicotinic receptors mediated positive feedback and elicited neuromuscular transmission, and pre-synaptic muscarinic receptors mediated negative feedback and limited positive feedback to avoid overstimulation. Thus, pre-synaptic ionotropic P2X receptors and pre-synaptic metabotropic P2Y receptors at the sympathoeffector junctions could perform the same role as the pre-synaptic acetylcholine receptors at the neuromuscular junction (Boehm et al., 1999). It was previously suggested that P2X1, P2X2, P2X3, P2X2/3, P2X1/5, P2X4/6, and P2X7 receptors have been identified as being responsible for facilitatory regulation in various parts of the central nervous and perivascular nervous systems. P2Y1 and P2Y4 receptors may also mediate facilitation of transmitter release in certain areas of the nervous system. P2Y12 and P2Y13 receptor subunits mediate inhibition of neurotransmitter release (Sperlagh et al., 2007). It was reported that P2X receptors expressed in the sympathetic nerve terminals providing the heart seemed to be endogenously activated by ATP in myocardial ischemia. Thus, it might involve ischemia-induced arrhythmia and ischemic heart dysfunction. That could suggest that suppression of these facilitatory P2X receptors could be a target in the treatment of ischemic heart disease. Furthermore, it was suggested we use agonists of P2Y receptors to give the same effect as the inhibition of P2X receptors, as P2Y receptors are coexpressed on nerve terminals where P2X are present (Sesti et al., 2003). Previous findings

showed that P2Y1 and P2Y12 receptors form homo and heterooligomers at the membrane and mediate opposite effects at the rat sympathetic nerve terminals in response to agonist stimulation. P2Y1 receptors mediate the facilitation of NA release, most likely through inhibition of voltage-dependent K^+ channels, whereas P2Y12 receptors mediate an autoinhibition of NA release, most likely through an inhibition of voltage-gated K^+ channels (Chandaka et al., 2011). In conclusion, the release of different transmitters is employed to regulate both the central nervous system and the perivascular nervous system: inhibitory modulation is mediated by metabotropic P2Y receptors, while facilitatory modulation is facilitated by ionotropic P2X receptors, the of role P2X and P2Y receptors in the regulation of neurotransmitters is still investigating.

4.4.4 P2 purinergic receptors were positive for NPY in mouse superior cervical ganglion neurons and perivascular nerves of superior mesenteric artery but not carotid artery

In the present study, we examined the coexpression of NPY with PGP9.5 in the mouse sympathetic superior ganglion, superior mesenteric and carotid arteries to determine which neurons had vasomotor activity and thus play a role in innervating target tissues. In addition, we examined the coexpression of NPY and neurons positive for P2X2, P2X3 and P2Y1 in the superior ganglion, superior mesenteric and carotid arteries. Our results using transgenic NPY-hrGFP mice suggested that in the superior cervical ganglion, ~ 40% of neuronal cell bodies were positive for both markers PGP9.5 and NPY. Many neurons appeared completely negative for NPY. These results indicated that ~ 40% of superior cervical ganglion neurons may have vasomotor activity and innervate blood vessels or other tissue in the neck and the head. However, most NPY-negative neurons in the superior cervical ganglion might be either secretomotor cells that control salivary glands or pilomotor neurons that innervate arrector pilli muscles. The whole-mount preparation of superior mesenteric artery from transgenic NPY-GFP mice consistently displayed intense GFP fluorescence expressing NPY. This green fluorescence was apparent throughout the adventitia. However, the carotid artery did not show any fluorescence. Moreover, some PGP9.5 positive nerves within the adventitia of the superior mesenteric artery (not the carotid artery) were merged with NPY nerves. These results alongside the carotid artery TH-negative nerves suggested that the NPY-positive neurons in the superior cervical ganglion were not involved in the innervation of the carotid artery and the nerves thought the carotid artery could arise from the carotid body to innervate other tissues such as the heart and salivary glands (Potter et al, 1987). Moreover, other peptides could be involved in innervation patterns in the superior cervical ganglion and carotid artery such as

somatostatin, vasoactive intestinal polypeptide, dynorphin A and B and CGRP. Further investigations are required to identify which NPY could be involved in the innervation pattern. Furthermore, the double immunostaining study showed numerous nerve cell bodies displayed colocalisation between P2X2, P2X3 and P2Y1, and NPY. Whole-mount preparations of superior mesenteric arteries showed positive correlations between P2X2, P2X3 and P2Y1 expressing nerve fibres and the numbers of NPY nerves. This could indicate the ability of these P2-positive neurons to have vasomotor activity and they could be involved in the innervation pattern of the target tissue. NPY is a key cotransmitter in sympathetic vasoconstrictor neurons, which comprise about 50–70% of the cells in the paravertebral chain ganglia (Headley et al., 2007; Gibbins, 1995). The superior cervical ganglion is located at the rostral end of the paravertebral sympathetic chain and contains a mixture of neuronal cells that deliver sympathetic innervation to several tissues in the neck and the head. These neuronal cells innervate vascular beds in the brain, skin, muscle, choroid plexus, carotid body, piloerector hairs, salivary glands, the iris, and pineal gland (Li & Horn, 2006; Cardinali et al., 1981). Approximately 90% of rat superior cervical ganglion neurons are classified as secretomotor neurons, which project to the submandibular salivary glands, pilomotor neurons, which innervate the arrector pili muscle, or vasomotor neurons, which control blood flow in the head. In a previous study on Sprague-Dawley rat sympathetic ganglia, sympathetic axons in the submandibular gland showed immunoreactivity for TH and all axons showed colocalisation of TH with vesicular monoamine transporter (VMAT2), the vesicular transporter for catecholamines into vesicles for release at the synapse. Some axons showed coexpression of NPY with the vesicular monoamine transporter. According to this study, NPY-positive fibres were tightly packed and prominent near blood vessels. Vesicular monoamine transporter-positive, NPY-negative axons, on the other hand, were sparsely dispersed among the gland's secretory cells (Headley et al., 2007). Double immunostaining in rat mesenteric arteries showed coexpression of TH with NPY in different artery sizes with different densities (Yokomizo et al., 2015). It has been shown in various species including dogs, rabbits, pigs, guinea pigs, rats and cats that a dense network of NPY was found around arteries and arterioles of all species studied. In addition, the study revealed that NPY nerves were colocalised with TH and dopamine β-hydroxylase positive nerves, two markers for noradrenergic neurons (Pernowet al., 1987). Moreover, radioimmunoassay revealed the level of NPY in lumbosacral sympathetic ganglia is much higher than the level of NPY in skeletal muscle from guinea pigs, rabbits, dogs, pigs and humans (Pernowet al., 1987). A previous immunohistochemical study in the human superior cervical ganglion identified the expression of TH, dopamine-β-hydroxylase and various types of neuropeptides, including NPY, somatostatin, leu-enkephalin vasoactive

intestinal polypeptide and CGRP. In addition, 30% coexistence was observed between NPY and CGRP with TH in the human cervical ganglion. Other NPY such as dynorphin A and B, neuropeptides like SP, galanin, cholecystokinin, thyrotropin-releasing hormone, angiotensin II and neurotensin showed no immunoreactivity in the human superior cervical ganglion. (Baffi et al., 1992). Another previous study reported the expression of SP, dynorphin A and α-neo-endorphin in rat superior cervical ganglion (Folan & Heym,1989; Hökfelt et al., 1977). It was reported by Tajti et al (Tajti et al., 1999), that more than 75 % of neuronal cell bodies of the human superior cervical ganglion expressed NA and NPY and showed colocalisation. Although few of the neuronal cell bodies were immunoreactive for the vasoactive intestinal polypeptide, none of them expressed NO synthesis, CGRP and SP. The same study showed by RT-PCR the expression of other neuropeptides such as NPY Y1, NPY Y2 and vasoactive intestinal peptide receptor-1 in total RNA extracted from the human superior cervical ganglion. The innervation pattern of NPY in the mouse superior mesenteric artery in our study was confirmed by a previous functional study (Racchi et al., 1997). In the human inferior mesenteric artery and vein, they reported the involvement of ATP, NA and neuropeptide Y Y1 receptors in the vasoconstriction caused by human sympathetic nerve stimulation. This was abolished by using antagonists including 100 nM tetrodotoxin and 1 μM guanethidine, indicating the response was of neuronal origin. The previous study confirmed the NPY-dependent responses by using a selective neuropeptide Y Y1 receptor antagonist (BIBP 3226; N2-(Diphenylacetyl)-N-[(4-hydroxyphenyl)methyl]-D-arginine amide). Results were similar in a study using rat superior mesenteric artery and vein ring preparations (Racchi et al., 1997). It was suggested that most large distributing arteries were innervated via sympathetic noradrenergic neurons containing NPY, while smaller cutaneous arteries contained immunoreactivity to prodynorphin-derived peptides and NPY. However, immunoreactivity to prodynorphin-derived peptides was found in sympathetic neurons innervating the smallest arterioles and arteriovenous anastomoses, but no NPY was detected. Perivascular sympathetic neurons expressing prodynorphin-derived peptides but not NPY were thought to be important in the regulation of thermoregulatory cutaneous vascular circuits, according to Gibbins et al (Gibbins et al., 1990). It has been observed that NPY, which is generally produced in sympathetic neurons, is found in only a few trigeminal ganglion neurons. Thus, the role of NPY in trigeminal ganglion neurons was thought to be limited, but after mental nerve transection, NPY expression in the trigeminal ganglion neurons increases (Goto et al., 2017).

Few studies have investigated the coexpression of P2X, P2X3 and P2Y1 with NPY in the mouse sympathetic superior cervical ganglion and perivascular nerves in arteries. Our results revealed that approximately 30-40% of the P2X2, P2X3 P2Y1 positive neurons in the

mouse superior cervical ganglion showed coexpression with NPY. In addition, some P2X2, P2X3 and P2Y1 positive nerves in the superior mesenteric artery were positive for NPY, whereas the carotid artery showed no NPY expression. The results suggested that P2X2, P2X3 and P2Y1 positive neurons labelled for NPY could be involved in the innervation pattern of the superior mesenteric artery but not the carotid artery. It has been shown in a study in guinea pigs mesenteric ganglions of the stomach, small and large intestines that P2X2 was expressed in the nerve layer and colocalised with NO synthase. In addition, P2X2 coexpressed with vasoactive intestinal peptide in submucosal ganglia and gastric myenteric ganglia, while NPY immunoreactivity was absent in the submucosal ganglia (Castelucci et al., 2002). The absence of NPY in the carotid artery confirmed a previous study in the rat carotid artery. These results showed low NPY Y1 receptor expression by RT-PCR and Western blot. However, after 6-24 hours after angioplasty, the Y1, Y2, and Y5 NPY receptor mRNAs and proteins were upregulated. These results suggested that NPY expression could be a risk factor for atherosclerosis, and NPY receptor antagonists could be a novel therapeutic option for restenosis (Li et al., 2003). It has been found that NPY was colocalised with NA in several sympathetic nerves. Lately, it has been found in post-ganglionic sympathetic nerves running to blood vessels in the carotid body (Potter et al, 1987). This result could support that the sympathetic innervation of the blood vessels could be via the carotid body and not by the carotid artery. Finally, a very new functional study performed by our group in Samuel J. Fountain's lab (del Carmen Gonzalez-Montelongo & Fountain, 2021) revealed that in mouse small mesenteric arteries NPY facilitated P2X1 receptor-dependent vasoconstriction mediated by NPY Y1 receptor activation.

4.5 Summary

This project aimed to provide the first characterisation of the expression of all P2 purinergic receptors in the mouse sympathetic superior cervical ganglion and the perivascular nerves in the superior mesenteric and carotid arteries at the mRNA and protein level, focussing specifically on their expression in the cell bodies of the superior cervical ganglion and the pre-junctional terminal of sympathetic nerves in superior mesenteric arteries and carotid artery. In addition, the project aimed to investigate whether these receptors served as auto or heteroreceptors in the sympathetic neurons of the pre-junctional terminal of the superior mesenteric artery and carotid arteries by expressing the purinergic receptors in the nerves layer but not in smooth muscle and the endothelium. However, the functional role of these receptors requires further investigation. The present study demonstrated that the mouse superior cervical ganglion and superior mesenteric artery showed coexpression of P2X1, P2X2, P2X3, P2X4, P2X7 and P2Y1 receptors with the general neuronal marker PGP9.5 and the noradrenergic marker TH with different intensities. While the carotid artery showed coexistence of only P2X2, P2X3, P2X4, and P2Y1 with PGP 9.5. TH , P2X1 and P2X7 were absent in the carotid artery. All the tissues studied did not express P2X6, although it could be detected by RT-PCR in the superior cervical ganglion. These results confirmed the sympathetic phenotype of the superior cervical ganglion and the sympathetic nerves arising from the sympathetic ganglia could travel the post-ganglionic axon to innervate target tissues, such as the blood vessels. The results suggested that the mouse carotid artery could not be innervated via sympathetic nerves from the superior cervical ganglion and could be innervated via other types of nerves, such as sensory nerves via the carotid body. However, further studies are required to investigate the innervation pattern of the common carotid artery. Furthermore, the results showed that most of the neurons in the superior cervical ganglion (80%) and P2X2, P2X3, and P2Y1-positive neurons were labelled for VNUT. This indicated the capability of these neurons to accumulate ATP in the secretory vesicles and synaptic vesicles Thus, VNUT plays an important role in the vesicular storage and release of ATP initiating purinergic chemical transmission. The coexpression of PGP9.5 and the NPY indicated the vasomotor phenotype of the superior cervical ganglion neurons and the perivascular nerves of the superior mesenteric artery which ensure the innervation pattern of NPY-positive neurons once travel to the target tissue. However, the carotid artery did not express NPY and further studies are needed to investigate the innervation pattern of the carotid artery. Our RT-PCR results showed mRNA was present for all P2X receptors and P2Y receptors (except P2Y4) in the mouse superior cervical ganglion. Moreover, RT-PCR results showed the expression of P2X1, P2X4, P2X7, and all P2Y receptors (except P2Y1 and P2Y4) in the carotid artery. The superior mesenteric artery was similar to

the carotid artery in its expression pattern of P2X and P2Y receptors, but the P2Y1 was weakly expressed. These results led us to propose that P2X2, P2X3 and P2Y1 could be located in the perivascular nerves only in the blood vessels but not the smooth muscle cells or the endothelium. This was confirmed by our immunohistochemistry in whole-mount preparations and cryostat sections of the mouse superior mesenteric and carotid arteries. These results could suggest that P2X2, P2X3, P2X7 and P2Y1 (P2X7 also was suggested by previous studies to be expressed only in perivascular nerves) could be employed as pre-junctional receptors. Once the pre-junctional receptors are activated, they could dictate negative/positive feedback loops to inhibit/facilitate the release of neurotransmitters which play important physiological roles. The potential future application of this knowledge would be the discovery of a novel therapeutic target for the modulation of vascular tone. This has implications for the future treatment of hypertension.

Chapter 5: The expression and function of P2 purinergic receptors in the SH-SY5Y neuroblastoma cell line

5.1 Introduction

SH-SY5Y, neuroblast-like cells, are a subclone of the parental neuroblastoma cell line, SK-N-SH, and isolated from a metastatic bone tumour biopsy taken from a four-year-old female with neuroblastoma (Schneider et al., 2011). Neuroblastoma is identified as one of the most common extracranial solid malignant tumours of the sympathetic nervous system and mostly affects children in their early years (Johnsen et al., 2019). SH-SY5Ycells are sympathetic ganglionic cells with large dense-cored vesicles that contain NA, NPY, and have high dopamine-β-hydroxylase activity. These cells produce action potentials and contain voltage-dependent ion channels (Per Larsson et al., 2002). Because of its human origin, catecholaminergic neuronal characteristics, and ease of maintenance, this cell line is often used in research (Xicoy et al., 2017). By using a variety of methods, including the use of retinoic acid (the most commonly used for differentiation), phorbol esters, and brain-derived neurotrophic factor, these cells can be differentiated from a neuroblast-like state into mature human neuron-like phenotype characterized by neuronal markers. By using these methods, SH-SY5Y cells can be differentiated into specific neuron subtypes such as adrenergic, cholinergic, and dopaminergic neurons (Shipley et al., 2016). In this thesis, both undifferentiated and differentiated SH-SY5Y cells have been employed for *in vitro* experiments requiring neuronal-like cells.

The addition of retinoic acid to the cell culture media is one of the most widely used and well-studied strategies for inducing differentiation in SH-SY5Y cells. Retinoic acid is a vitamin A derivative with potent growth-inhibiting and cellular differentiation-promoting effects (Kovalevich & Langford, 2013; Melino et ac., 1997). Retinoic acid is an effective cell differentiating agent, which impacts a wide range of promoter sites in the neuronal and glial cells during embryonic and postnatal development. It has been demonstrated that retinoic acid-induced differentiation inhibits cell proliferation, promotes neurite outgrowth, changes cellular Na^+ conductance, increases acetylcholinesterase activity, and promotes synaptic vesicle recycling. To promote differentiation, retinoic acid is typically supplied at a concentration of 10 μM for a minimum of 3–5 days in serum-free or reduced serum media (Cheung et al., 2009). Following the treatment of SH-SY5Y cells with retinoic acid, a reported increase in the lifespan has been noted. This is achieved by activating the phosphatidylinositol 3-kinase/Akt signalling pathway and an increase in the antiapoptotic Bcl-2 protein. Moreover, some studies demonstrated that retinoic acid-induced differentiated cells are less susceptible to toxin-

mediated cell death caused by agents such as 6-hydroxydopamine (6-OHDA), 1-methyl-4-phenyl-1,2,3,6-tetrahydropyridine (MPTP), or its metabolite, 1-methyl-4-phenylpyridinium ion (MPP^+), compared to undifferentiated cells (Cheung et al., 2009). SH-SY5Y cells treated with retinoic acid can be differentiated to a cholinergic neuron phenotype; as confirmed by increasing the expression of choline acetyltransferase activity and vesicular monamine transporter (Lopes et al., 2010). Cells can be differentiated to a mature dopaminergic phenotype by retinoic acid and an additional agent such as phorbol esters. Furthermore, it was noticed that an increase in the expression of TH, dopamine receptor 2 and 3 isoforms, and dopamine transporter expression during retinoic acid-induced differentiation was followed by adding phorbol ester (Kovalevich & Langford, 2013). It was reported by Encinas et al., (2008) that following treatment with retinoic acid, SH-SY5Y cells responded to carbachol stimulation as a result of slight accumulation and increasing NA release, subsequently inducing SH-SY5Y cell differentiation to an adrenergic phenotype (Xie et al., 2010).

5.2 Aim

Purinergic receptors represent a very attractive pharmacological target, and they have been effectively addressed in other cell types for therapeutic purposes. Although undifferentiated SH-SY5Y cells have been used widely to study P2 purinergic receptor functions, the expression of P2 purinergic receptors in differentiated SH-SY5Y cells as a model of adrenergic neuronal cells remains a largely unexplored area of research. Therefore, mRNA and protein expression studies using RT-PCR and confocal microscopy, respectively, will be performed as an initial aim for this chapter. In this study, first, we used undifferentiated SH-SY5Y cells and differentiated SH-SY5Y cells to investigate the expression of P2 purinergic mRNA and protein by using RT-PCR and immunofluorescence, respectively. To confirm specificity and functionality, all primers were also tested using commercial human brain RNA. Next, a human SH-SY5Y cell line was employed as an *in vitro* model to investigate the contribution of P2 purinergic receptors to ATP-evoked Ca^{2+} response. To address this aim, several pharmacological tools such as receptor agonists and antagonists were employed to help characterize P2 purinergic receptors through quantification of intracellular Ca^{2+} release. In this chapter, we identified the molecular basis of nucleotide-evoked responses by intracellular Ca^{2+} release in undifferentiated SH-SY5Y cells and in vitro differentiated SH-SY5Y cells. The data generated from these experiments and previous studies led to focus on the purinergic P2X7 receptor to investigate the contribution of functional P2X7 receptor towards ATP-evoked Ca^{2+} response in both cells type using BzATP (target P2X7) and A2046321 (P2X7 antagonist). Very

little is currently known about the role of P2 receptors in both cell types and it is hoped that this study will provide a solid foundation to begin to understand the role of purinergic signalling in undifferentiated SH-SY5Y cells and differentiated SH-SY5Y cells.

5.3 Results

5.3.1 Differentiation of SH-SY5Y cells to a neuronal phenotype

Exposure of SH-SY5Y cells to retinoic acid induces differentiation to a more characteristically neuronal morphology (Schneider et al., 2011). Previous research has shown that retinoic acid-induced SH-SY5Y cells exhibit neuronal differentiation features such as cell growth elimination, extension of branched neurites, polarisation and decreased proliferation rate. In addition, differentiated cells have increased expression of neuron-specific markers such as enolase and associated protein-43. Conversely, undifferentiated SH-SY5Y cells are characterised morphologically by neuroblast-like, non-polarized cell bodies, with few shortened processes, and rapid proliferation. Our results showed that retinoic acid-treated SH-SY5Y cells (differentiated cells state or neuronal-like cells type) seemed smaller with thin cell bodies, the cells were more rounded and not clustered (Figures 5.1.C & D). One of the most important indicators of neuronal cell differentiation is the extensive network of neurites, with the formation of axons and dendrite-like projections that form longer processes that connect with neighbouring cells. In addition, differentiated SH-SY5Y cells showed a high expression level of NPY as a marker of neurons and differentiation (Farrelly et al., 2013) (Figure 5.2.C). Whereas undifferentiated SH-SY5Y cells appeared flat, larger, appeared to grow in clusters and formed clumps, as cells tend to grow on top of one another in the central region of a cell mass (Figures 5.1.A & B). In addition, undifferentiated SH-SY5Y cells showed a low level of NPY expression (Figure 5.2.A). When SH-SY5Y cells are unhealthy and start to die, cell bodies round up and processes degrade, resulting in a significant amount of debris. Control images are shown in which no primary antibodies were applied and where just the secondary anti-sheep antibody was applied, to see if there was any non-specific binding. No significant immunoreactivity for NPY was seen in the control (Figures 5.2.B & D) specimen. Based on these results we identified retinoic acid treatment of SH-SY5Y cells as optimal for neuronal differentiation of SH-SY5Y in an *in vitro* cell model. The differentiated cells could be adrenergic in phenotype but also might express dopaminergic markers. It was reported that retinoic or phorbol esters-induced differentiated SH-SY5Y cells can lead to an adrenergic phenotype. TH expression is essential because NA and adrenaline are generated from dopamine catalysed in a TH-dependent manner (Kovalevich & Langford, 2013). TH expression studies are shown in section 5.3.3.

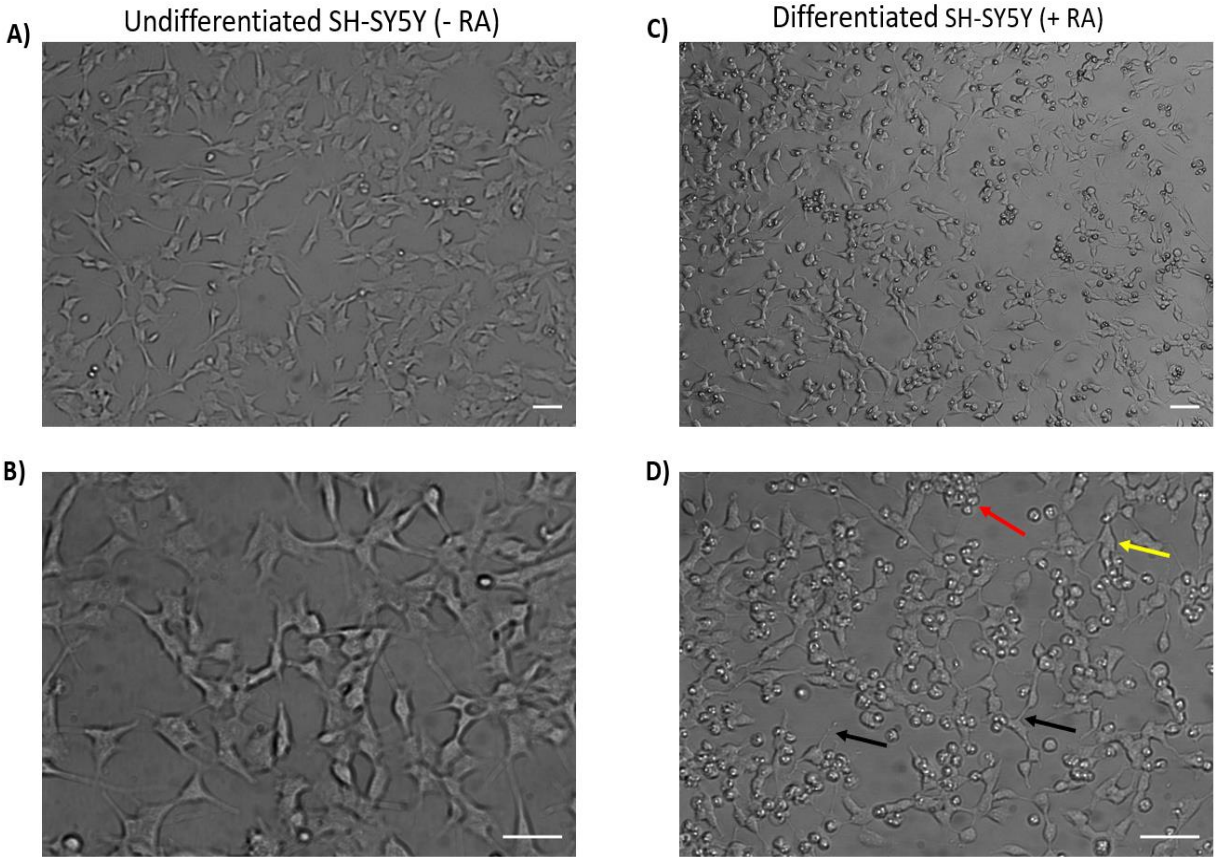

Figure 5.1: Retinoic acid-induced differentiated SH-SY5Y cells. (**A&B)** Brightfield images of SH-SY5Ycells before retinoic acid treatment. The cells seemed flat, large with few projections, grew in clusters, and formed clumps of cells on top of one another. (**C&D)** Brightfield images of SH-SY5Y cells after retinoic acid treatment for 5 days. The mature neuronal-like cells appeared smaller, more rounded, and neurite extension demonstrating diffuse axonal projections connecting to neighbouring cells was seen on day 5 (black arrows). The parental differentiated SH-SY5Y cells displayed an epithelial cell-like phenotype with no processes and the cells were flat and less rounded (yellow arrow). Phase contrast images were obtained at x10 (A-C) and x20 (B-D) magnification using an inverted epifluorescence microscope. The black arrow indicates a neuronal-like cell with elongated neuritic projections. The yellow arrow indicates an epithelial-like cell. The red arrow indicates unhealthy cells. - RA indicates SH-SY5Y cells before retinoic acid treatment, and + RA indicates SH-SY5Ycells after retinoic acid treatment. Scale bars represent 50 µm. The results shown are representative from five independent experiments.

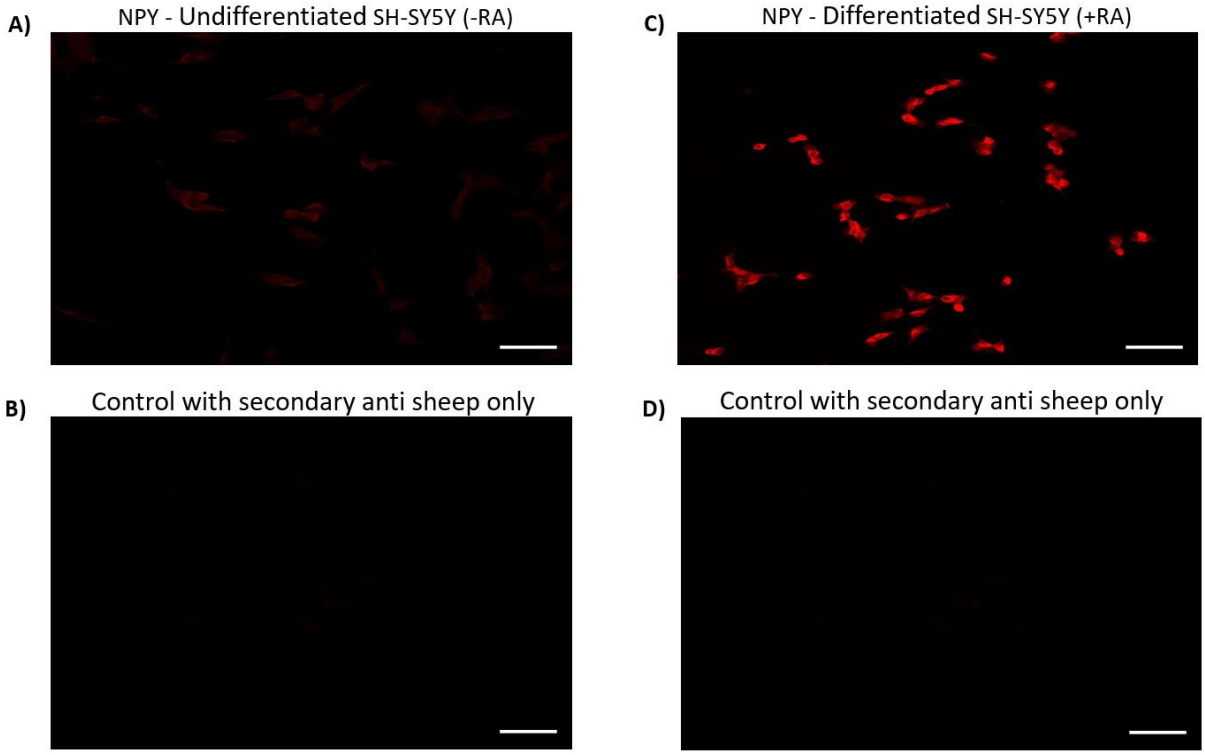

Figure 5.2: NPY expression in undifferentiated and differentiated SH-SY5Y cells. Immunofluorescence illuminates neuronal features of fully differentiated SH-SY5Y cells. (**A)** Undifferentiated SH-SY5Y cells showed a low level of NPY immunoreactivity. (**C)** Retinoic acid-treated SH-SY5Y cells showed a high level of NPY immunoreactivity. (**B &D)** Control sections are shown in which no primary antibodies were applied and where just the secondary anti sheep antibody was applied. Images were visualized using a Laser-scanning confocal microscope Zeiss LSM510 META (Zeiss), equipped with an excitation filter system of 467 for the red channel. The specimens were seen at x20 magnification. The exposure and camera settings remained consistent across all the images taken for each experiment. Scale bars represent 50 μm. The results shown are representative from five independent experiments.

5.3.2 Comparison of the mRNA expression of P2X and P2Y receptor subtypes in undifferentiated and differentiated SH-SY5Y cells

P2X7 and P2Y4 receptors are known to be expressed in SH-SY5Y cells (Per Larsson et al., 2002; Cavaliere et al., 2005). However, much uncertainty still exists about the expression of other P2X and P2Y receptors in these cells. This study, therefore, sought to investigate the expression of genes encoding P2 receptors in undifferentiated and differentiated SH-SY5Y neuroblastoma cells at the mRNA level. RT-PCR was employed to compare the expression of mRNA transcripts for P2 receptors between the undifferentiated and differentiated SH-SY5Y cells. To address this aim, the specificity and functionality of all primers (Tables 2.11 & 2.12) were first tested in commercial human brain mRNA. Following the validation of primers, the expression of mRNA transcripts for P2X and P2Y receptors in both cell types was examined. Tables 5.1 & 5.2 and Figures 5.3 & 5.4 give a summary of the results obtained from this study. Using the primers in Tables 2.11 & 2.12, mRNA transcripts for all P2X receptors (P2X1-7) and all P2Y receptors (with the exception of P2Y6 and P2Y11) were repeatedly found in the commercial human brain and showed a band at expected product size. As also shown in (Tables 5.1 & 5.2), non-quantitative analysis of mRNA transcripts revealed that undifferentiated SH-SY5Y cells expressed all of the P2X receptors at expected sizes (341 bp, 200 bp, 564bp, 250 bp, 263 bp, 405 bp and 414 bp, for P2X1-7, respectively). The undifferentiated SH-SY5Y cells also expressed all P2Y receptors except P2Y1 (fragment sizes of 243 bp, 427 bp, 391, 622 bp, 698 bp, 461bp and 370 bp, respectively). In comparison, the differentiated cells expressed all isoforms of P2X and P2Y receptors except P2X1 and P2Y6. It was also shown that P2X1, P2X2, and P2X6 primers produced other PCR amplificons of a lower (P2X1 and P2X6) and higher (P2X2) molecular weight in addition to the expected product. A similar PCR amplicon for P2X2 and P2X6 was also detected in the human brain, but not for P2X1 which showed only one variant in the human brain. An analysis of these primers using BLAST identified the second amplicons for P2X1 and P2X6, but it was not able to identify the alternative product produced during the amplification of P2X2. It was previously confirmed in human bladder the presence of P2X1 splice variants that is lacking part of the second transmembrane domain. Thus, the human bladder can express multiple subtypes of the P2X1 receptor which could be potential sites for modifying or regulating putative purinergic activation of the human bladder (Hardy et al., 2000). It was reported by Lynch et al., (1999) that genomic sequence indicated that these cDNAs represent alternatively spliced variants which could be detected in a variety of tissues. P2X2 alternative splice variants exhibit desensitisation differences from the normal receptor in the human bladder. These findings suggest that the splice variant could have a variety of functional outcomes (Hardy et al., 2000). The β-actin mRNA amplification product

was as expected (282 bp). The negative control (-RT) of mRNA transcripts for all P2X and P2Y receptors, mRNA did not have specific amplification bands in the corresponding lanes, indicating the obtained bands for expressed P2X receptors were synthesized cDNA rather than genomic DNA. (Figures 5.3 and 5.4). Taken together, the results of this study suggested that there were differences in the expression of P2X and P2Y receptors between undifferentiated and differentiated SH-SY5Y cells. We found P2X1 and P2Y6 were expressed in undifferentiated SH-SY5Y cells while they were absent in differentiated cells. Furthermore, P2Y1 was present in the differentiated SH-SY5Y cells, whilst was not expressed in undifferentiated SH-SY5Y cells. The results of this study indicated several novel findings with respect to the expression of P2X receptors in both cell types.

Table 5.1: An overview of mRNA expression for P2X receptors in the human brain, undifferentiated, and differentiated SH-SY5Y cells.

Receptor	Cells	Expressed	Cells	Expressed	Cells	Expressed
P2X1	Human Brain	+	Undifferentiated SH-SY5Y Cells	+	Differentiated SH-SY5Y Cells	-
P2X2		+		+		+
P2X3		+		+		+
P2X4		+		+		+
P2X5		+		+		+
P2X6		+		+		+
P2X7		+		+		+
β-actin		+		+		+

A (+) sign indicates that the gene was expressed and a (–) sign indicates that the gene was not expressed. The results shown are representative from five independent experiments.

Table 5.2: An overview of mRNA expression for P2Y receptors in the human brain, undifferentiated, and differentiated SH-SY5Y cells.

Receptor	Cells	Expressed	Cells	Expressed	Cells	Expressed
P2Y1	Human Brain	+	Undifferentiated SH-SY5Y Cells	-	Differentiated SH-SY5Y Cells	+
P2Y2		+		+		+
P2Y4		+		+		+
P2X4		+		+		+
P2Y6		-		+		-
P2Y11		-		+		+
P2Y12		+		+		+
P2Y13		+		+		+
P2Y14		+		+		+
β-actin		+		+		+

A (+) sign indicates that the gene was expressed and a (–) sign indicates that the gene was not expressed. The results shown are representative from five independent experiments.

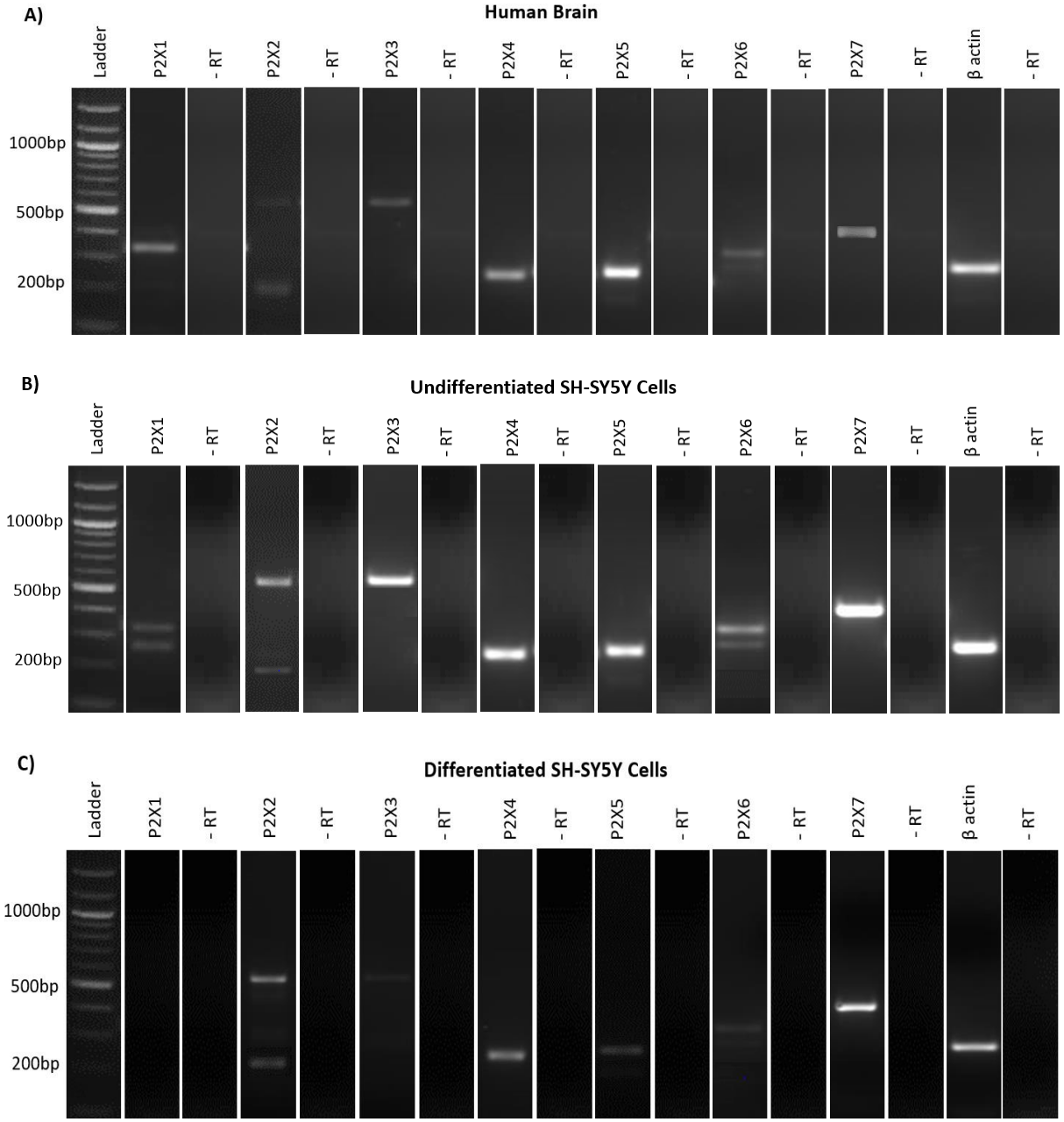

Figure 5.3: Expression of mRNA transcripts for P2X receptors in the human brain, undifferentiated and differentiated SH-SY5Y cells. (A) mRNAs for all P2X receptors were found in the human brain. (**B)** mRNAs for all P2X receptors were found in the undifferentiated SH-SY5Y cells. (**C)** mRNAs for all P2X receptors except P2X1 were found in the differentiated SH-SY5Y cells. β-actin mRNA (housekeeping gene) was expressed in all of the cells. No bands were present in the absence of reverse transcriptase showing there was no DNA contamination of the samples. Expression was detected at 341 bp (P2X1), 200 bp (P2X2), 564 bp (P2X3), 250 bp (P2X4), 263 bp (P2X5), 405 bp (P2X6), 414 bp (P2X7) and 282 bp (β-actin). - RT indicates the no reverse transcriptase control samples. The results shown are representative from five independent experiments.

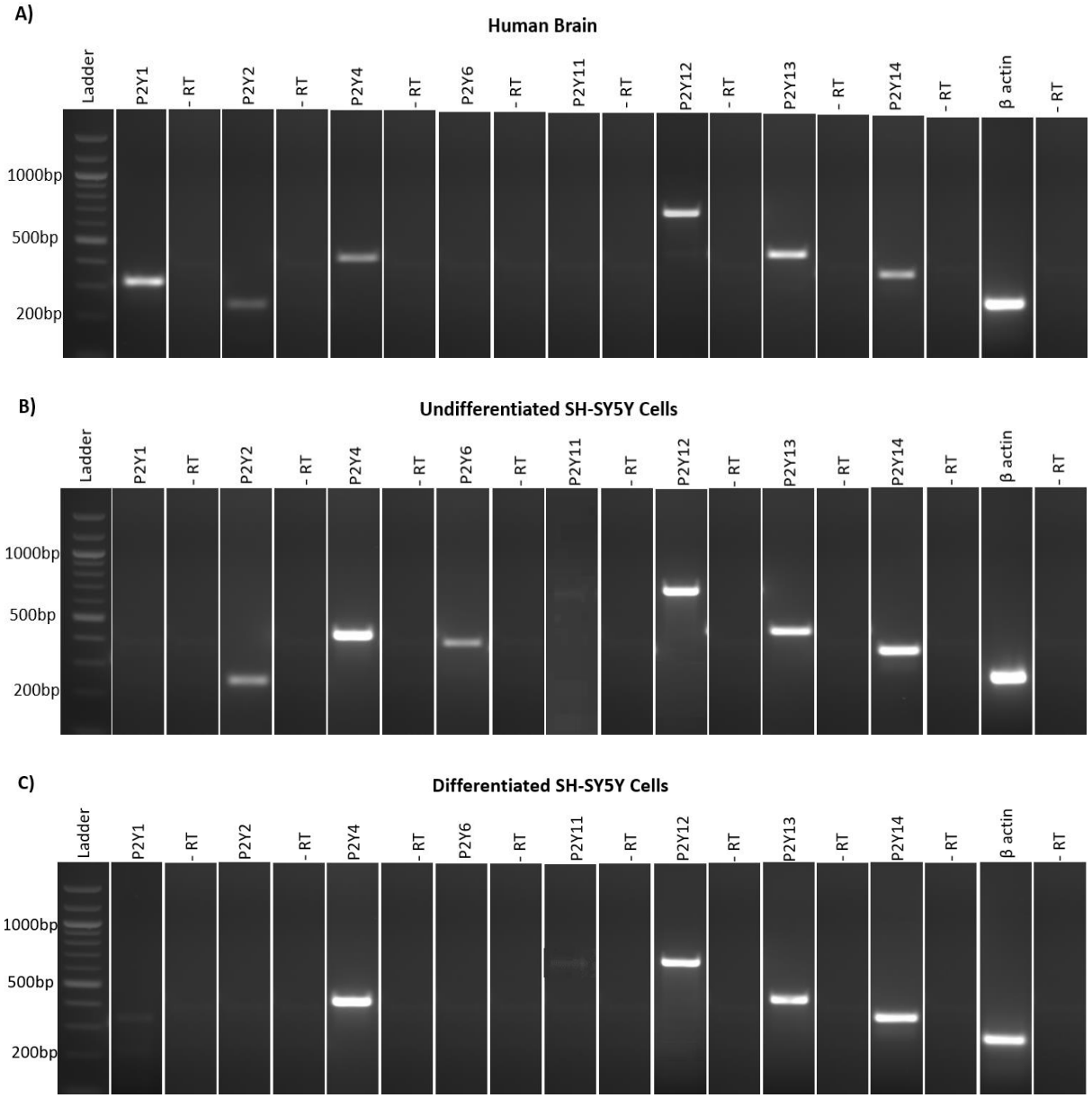

Figure 5.4: Expression of mRNA transcripts for P2Y receptors in the human brain, undifferentiated and differentiated SH-SY5Y cells. (A) mRNAs for all P2Y receptors except P2Y6 and P2Y11 were found in the human brain. **(B)** mRNAs for all P2Y receptors except P2Y1 were found in the undifferentiated SH-SY5Y cells. (**C)** mRNAs for all P2Y receptors except P2Y6 were found in the differentiated SH-SY5Y cells. β-actin mRNA (housekeeping gene) was expressed in all of the cells. No bands were present in the absence of reverse transcriptase showing there was no DNA contamination of the samples. Expression was detected at 326 bp (P2Y1), 243 bp (P2Y2), 427 bp (P2Y4), 391 bp (P2Y6), 622 bp (P2Y11), 698 bp (P2Y12), 461 bp (P2Y13), 370 bp (P2Y14) 282 bp (β-actin). - RT indicates the no reverse transcriptase control samples. The results shown are representative from five independent experiments.

5.3.3 Protein expression of P2 purinergic receptors in undifferentiated and differentiated SH-SY5Y cells

The protein expression of the P2 receptors consistently detected at the mRNA level using RT-PCR (section 5.3.2) was confirmed by immunostaining using confocal microscopy in undifferentiated and differentiated SH-SY5Y cells. All P2X antibodies used in this study target the intracellular epitope of each receptor, which required the cells to be fixed and permeabilized before staining with the antibodies. In line with the aim of our project to investigate the expression of P2 purinergic receptors in sympathetic neurons, and as our results suggested in section 4.3 that P2X2 and P2X3 were present only in perivascular sympathetic neurons of the mouse arteries (superior mesenteric artery and carotid artery), suggesting that receptor subtypes detected in sympathetic ganglia but not arteries could be expressed by sympathetic post-ganglionic nerves that innervate arteries. Here, we explore the coexpression of P2X2, P2X3, and P2X7 with the general neuronal marker PGP9.5 in undifferentiated and differentiated SH-SY5Y cells. As seen in (Figures 5.5 - 5.7), intense immunoreactivity was detected for all the receptors investigated (green) and the staining appears to be uniformly distributed throughout the cells. PGP9.5 immunoreactivity was highly expressed in both cell types also (red). Furthermore, axonal projections of the differentiated cells also showed positive immunoreactivity for the P2 receptors investigated and PGP9.5. P2X2, P2X3, and P2X7 in undifferentiated and differentiated SH-SY5Y cells were coexpressed with PGP9.5. Staining with secondary antibody (anti- guinea pig Alexa 647 and anti-rabbit Alexa 488) alone was performed as a negative control to ensure no false-positive staining was detected. None of the receptors showed significant immunoreactivity in the control cells (Figure 5.8). However, we were unable to determine whether the expression was mostly present on the cell surface, in the cytoplasm, perinuclear, or within the nucleus of the cells. Despite the inability to describe receptor localization within the two types of cells, these data collectively illustrate that P2X2, P2X3, and P2X7 receptors were expressed at the mRNA and protein levels in both cell types.

To confirm the adrenergic phenotype of differentiated cells compared with undifferentiated cells, coexpression of TH and P2X2, P2X3 and P2X7 was explored. As shown in (Figures 5.9 - 5.11) both undifferentiated and differentiated SH-SY5Y cells showed a moderate level of TH immunoreactivity and colocalisation with the P2X receptors studied. None of the receptors showed significant immunoreactivity in the control cells with the secondary anti-chicken antibody (Figure 5.12). Briefly, both undifferentiated and differentiated SH-SY5Y cells showed a high level of coexpression of PGP9.5 with P2X2, P2X3 and P2X7. We also observed an intermediate level of TH expression, which confirmed the adrenergic

phenotype in both cell types. Although the intensity of the staining varied slightly, inferences about the relative abundance of each receptor cannot be made due to differing antibody affinities. These results led us to investigate more about the functional role of these receptors using P2 receptors agonists including ATP, α, β-Me-ATP and BzATP to study nucleotide-evoked Ca^{2+} responses in undifferentiated and differentiated SH-SY5Y cells.

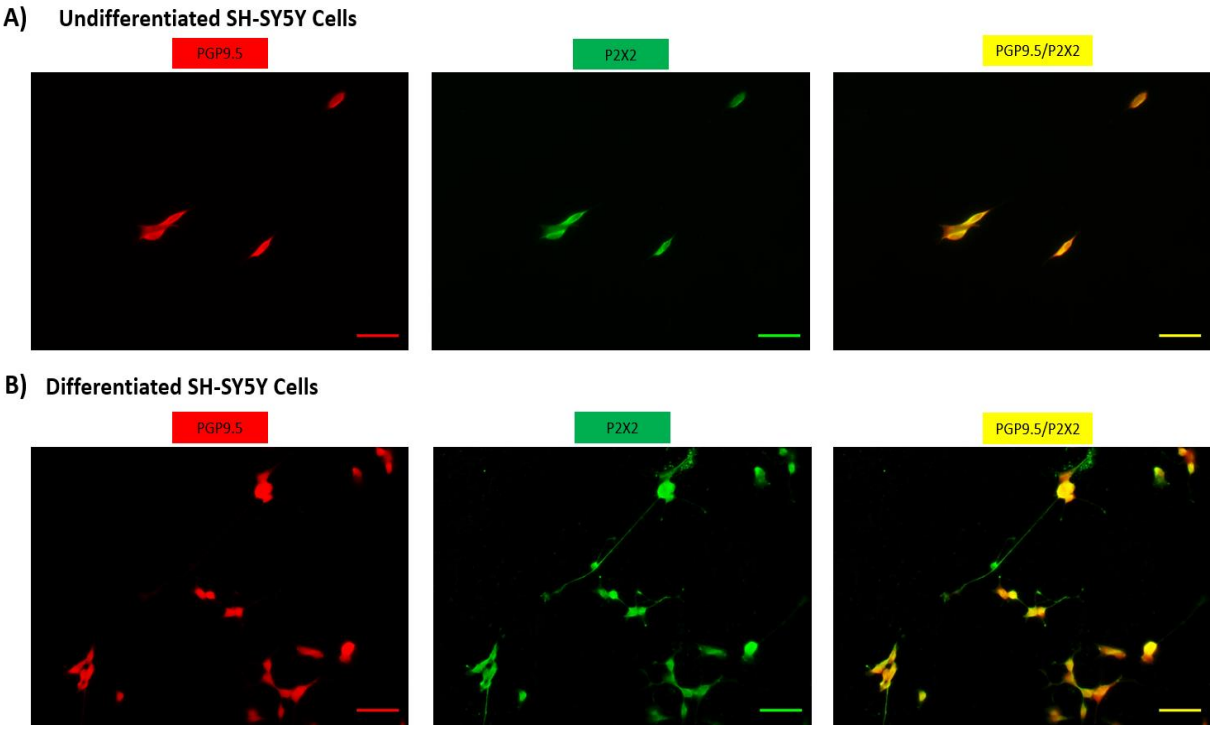

Figure 5.5: Colocalisation of PGP 9.5 with P2X2 receptor in undifferentiated and differentiated SH-SY5Y cells. (A) Colocalisation of PGP9.5 (red) and P2X2 receptor (green) in undifferentiated SH-SY5Y cells. **(B)** Colocalisation of PGP9.5 (red) and P2X2 receptor (green) in differentiated cells. Images were visualized using a Laser-scanning confocal microscope Zeiss LSM510 META (Zeiss), equipped with an excitation filter system of 458/488 nm for FITC and 647 for the red channel. The sections are seen at x20 magnification. The exposure and camera settings remained consistent across all the images taken for each experiment. Scale bars represent 50 μm. The results shown are representative from five independent experiments.

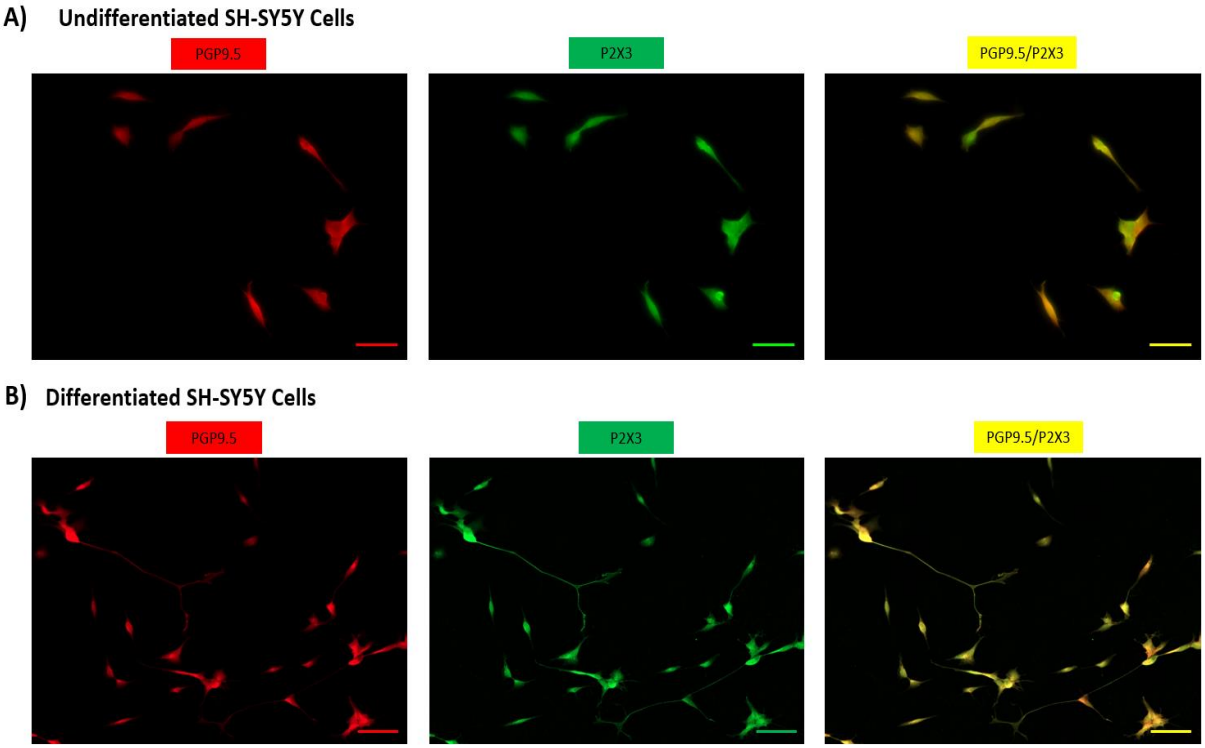

Figure 5.6: Colocalisation of PGP 9.5 with P2X3 receptor in undifferentiated and differentiated SH-SY5Y cells. (A) Colocalisation of PGP9.5 (red) and P2X3 receptor (green) in undifferentiated SH-SY5Y cells. **(B)** Colocalisation of PGP9.5 (red) and P2X3 receptor (green) in differentiated cells. Images were visualized using a Laser-scanning confocal microscope Zeiss LSM510 META (Zeiss), equipped with an excitation filter system of 458/488 nm for FITC and 647 for the red channel. The sections are seen at x20 magnification. The exposure and camera settings remained consistent across all the images taken for each experiment. Scale bars represent 50 μm. The results shown are representative from five independent experiments.

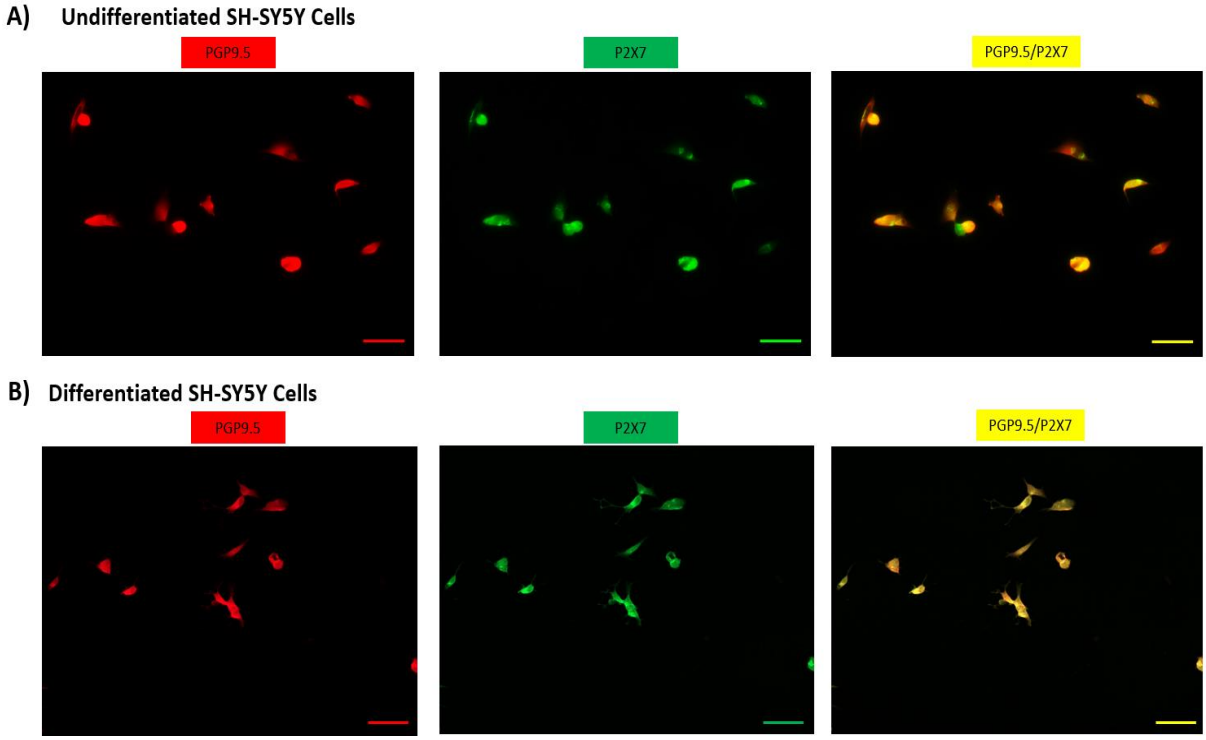

Figure 5.7: Colocalisation of PGP 9.5 with P2X7 receptor in undifferentiated and differentiated SH-SY5Y cells. (A) Colocalisation of PGP9.5 (red) and P2X7 receptor (green) in undifferentiated SH-SY5Y cells. **(B)** Colocalisation of PGP9.5 (red) and P2X7 receptor (green) in differentiated cells. Images were visualized using a Laser-scanning confocal microscope Zeiss LSM510 META (Zeiss), equipped with an excitation filter system of 458/488 nm for FITC and 647 for the red channel. The sections are seen at x20 magnification. The exposure and camera settings remained consistent across all the images taken for each experiment. Scale bars represent 50 μm. The results shown are representative from five independent experiments.

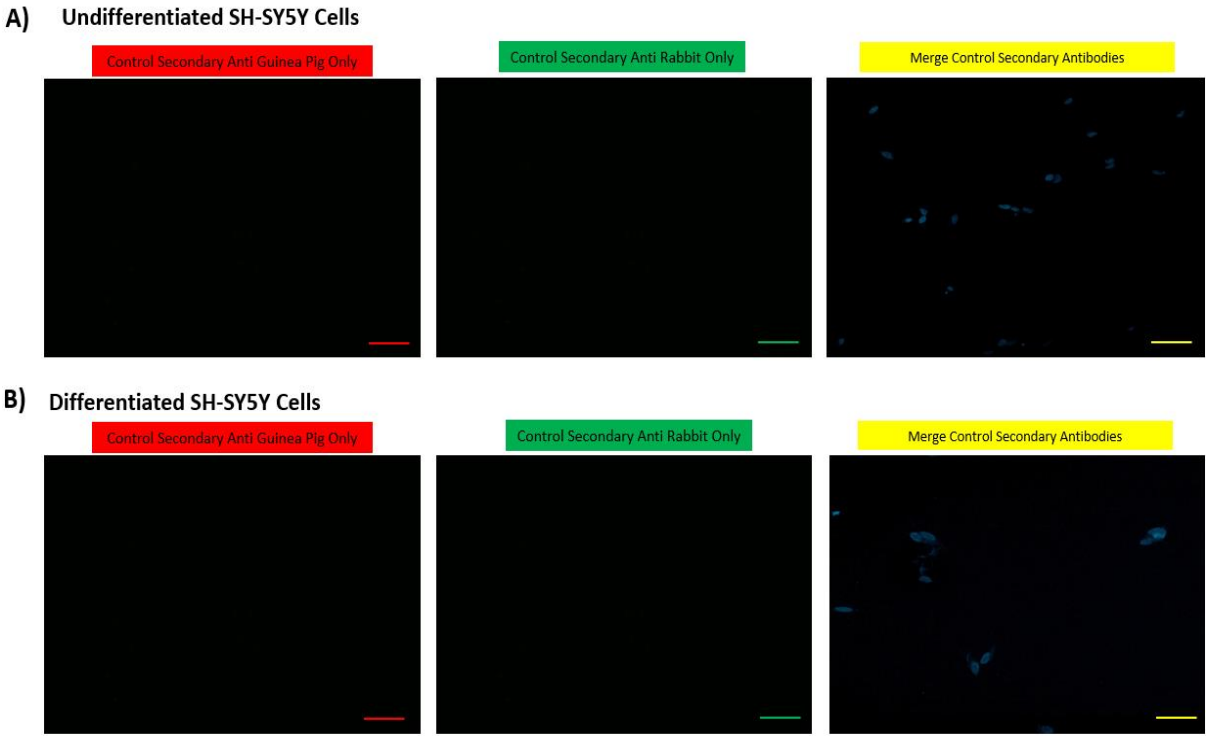

Figure 5.8: Control double immunofluorescence labelling for PGP9.5 and P2 receptors in undifferentiated SH-SY5Y cells and differentiated SH-SY5Y cells. Control sections are shown where just the secondary antibody was applied, to see if there was any non-specific binding and to determine the autofluorescence of the undifferentiated SH-SY5Y cells **(A)** and in vitro differentiated SH-SY5Y cells **(B)**. Immunocytochemical double staining for secondary anti guinea pig (red) and secondary anti rabbit (green). Images were visualized using a Laser-scanning confocal microscope Zeiss LSM510 META (Zeiss), equipped with an excitation filter system of 458/488 nm for FITC and 647 for the red channel. In control cells, cells are counterstained with DAPI to visualise nuclei (blue). The sections are seen at x20 magnification. The exposure and camera settings remained consistent across all the images taken for each experiment. Scale bars represent 50 μm. The results shown are representative from five independent experiments.

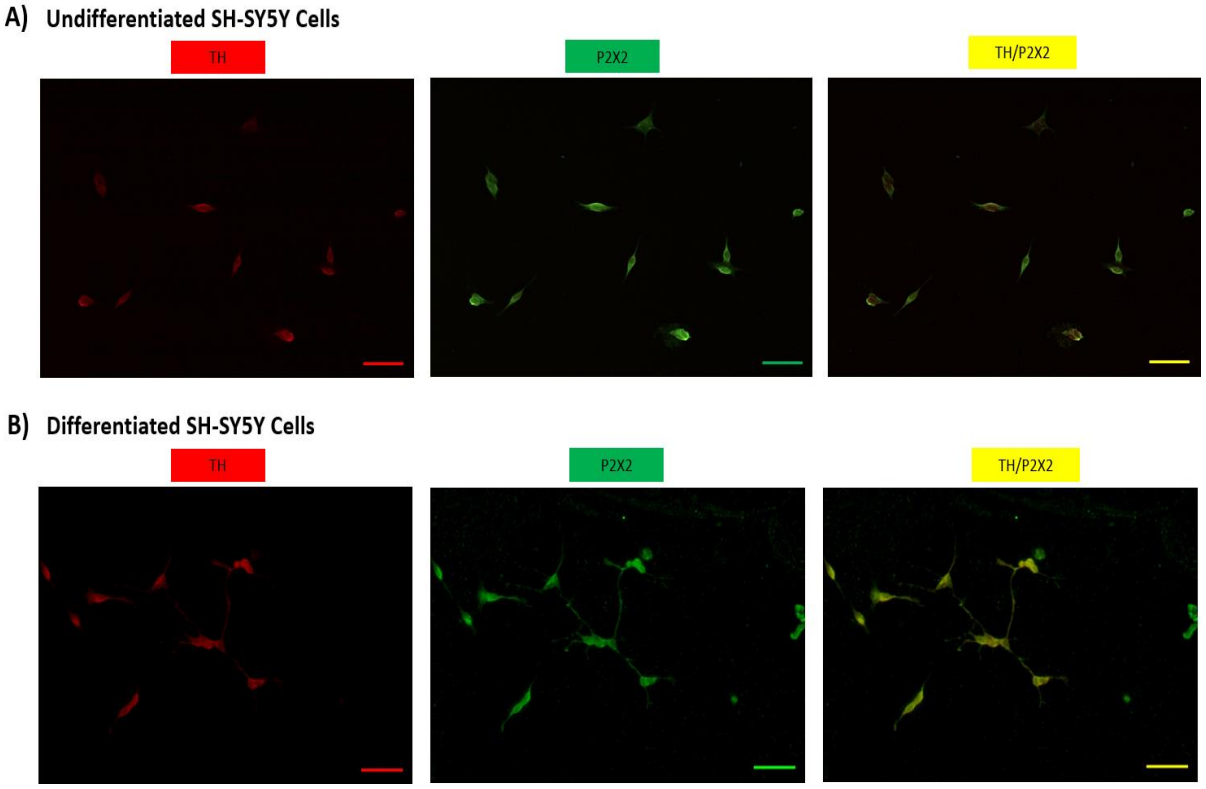

Figure 5.9: Colocalisation of TH with P2X2 receptor in undifferentiated and differentiated SH-SY5Y cells. (A) Colocalisation of TH (red) and P2X2 receptor (green) in undifferentiated SH-SY5Y cells. **(B)** Colocalisation of TH (red) and P2X2 receptor (green) in differentiated cells. Images were visualized using a Laser-scanning confocal microscope Zeiss LSM510 META (Zeiss), equipped with an excitation filter system of 458/488 nm for FITC and 647 for the red channel. The sections are seen at x20 magnification. The exposure and camera settings remained consistent across all the images taken for each experiment. Scale bars represent 50 μm. The results shown are representative from five independent experiments.

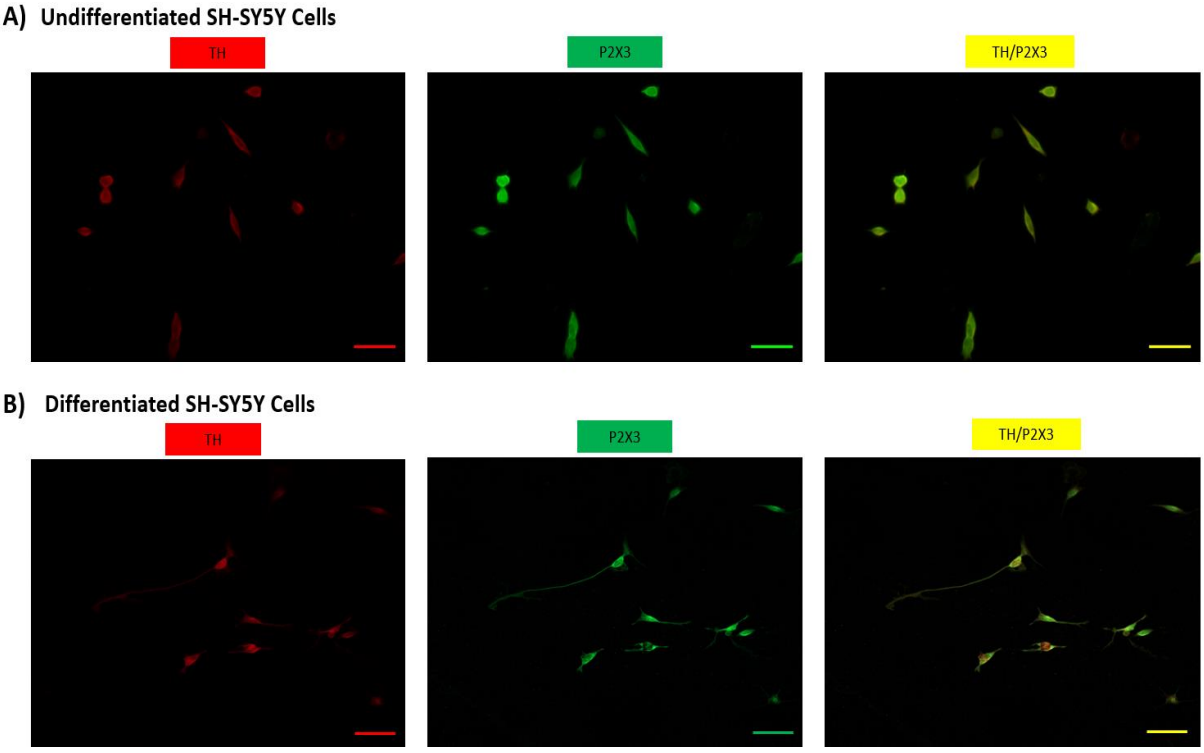

Figure 5.10: Colocalisation of TH with P2X3 receptor in undifferentiated and differentiated SH-SY5Y cells. (A) Colocalisation of TH (red) and P2X3 receptor (green) in undifferentiated SH-SY5Y cells. **(B)** Colocalisation of TH (red) and P2X3 receptor (green) in differentiated cells. Images were visualized using a Laser-scanning confocal microscope Zeiss LSM510 META (Zeiss), equipped with an excitation filter system of 458/488 nm for FITC and 647 for the red channel. The sections are seen at x20 magnification. The exposure and camera settings remained consistent across all the images taken for each experiment. Scale bars represent 50 μm. The results shown are representative from five independent experiments.

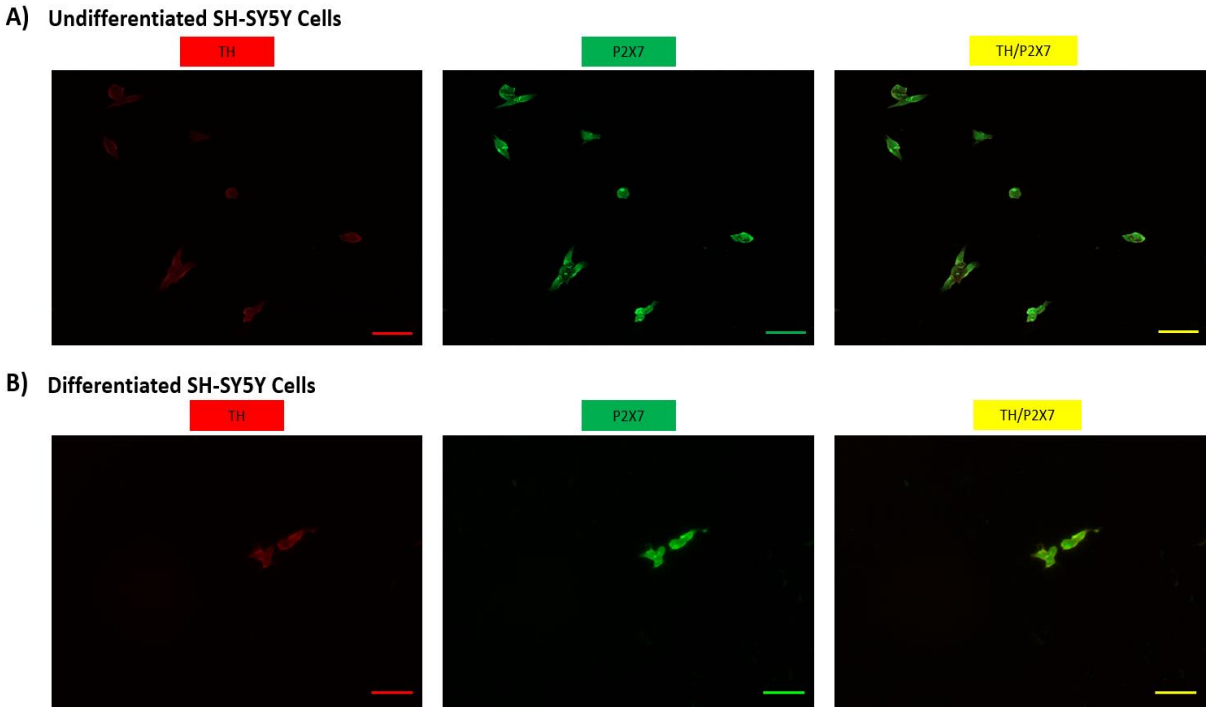

Figure 5.11: Colocalisation of TH with P2X7 receptor in undifferentiated and differentiated SH-SY5Y cells. (A) Colocalisation of TH (red) and P2X7 receptor (green) in undifferentiated SH-SY5Y cells. **(B)** Colocalisation of TH (red) and P2X7 receptor (green) in differentiated cells. Images were visualized using a Laser-scanning confocal microscope Zeiss LSM510 META (Zeiss), equipped with an excitation filter system of 458/488 nm for FITC and 647for the red channel. The sections are seen at x20 magnification. The exposure and camera settings remained consistent across all the images taken for each experiment. Scale bars represent 50 μm. The results shown are representative from five independent experiments.

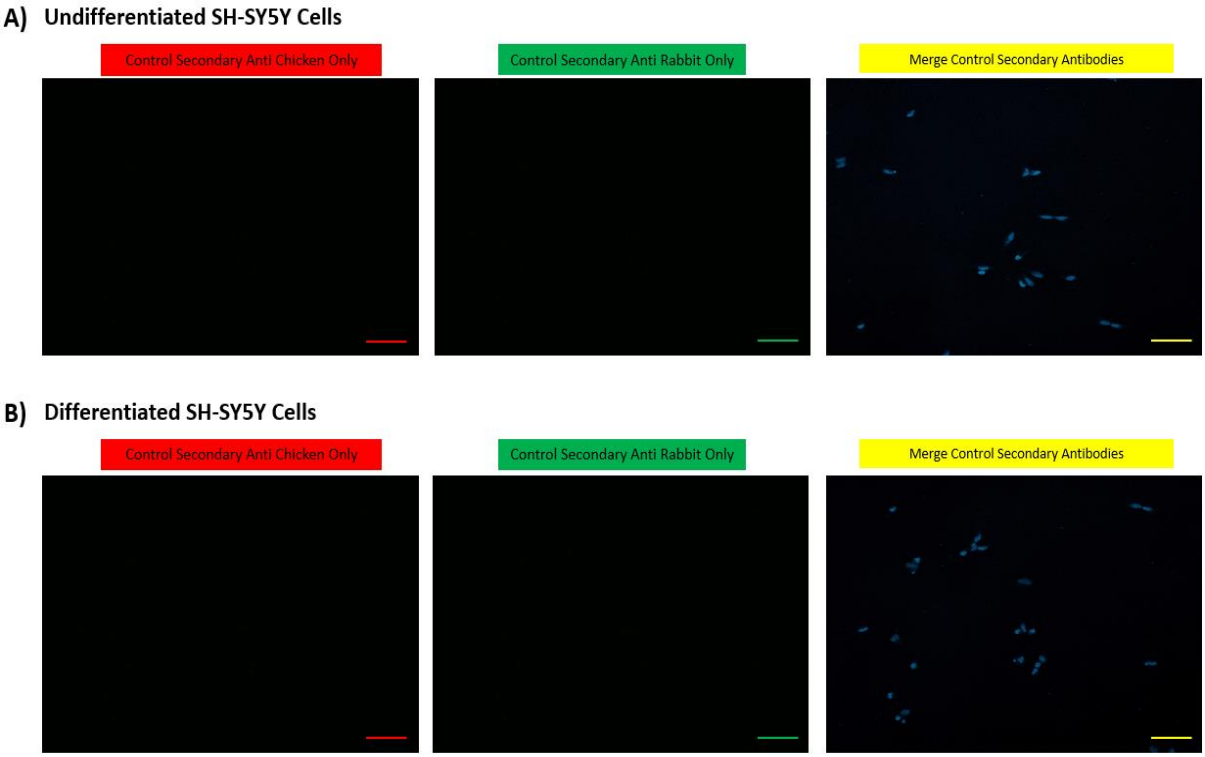

Figure 5.12: Control double immunofluorescence labelling for TH and P2 receptors in undifferentiated SH-SY5Y cells and differentiated SH-SY5Y cells. Control sections are shown where just the secondary antibody was applied, to see if there was any non-specific binding and to determine the autofluorescence of the undifferentiated SH-SY5Y cells **(A)** and in vitro differentiated SH-SY5Y cells **(B)** Immunocytochemical double staining for secondary anti chicken (red) and secondary anti rabbit (green). Images were visualized using a Laser-scanning confocal microscope Zeiss LSM510 META (Zeiss), equipped with an excitation filter system of 458/488 nm for FITC and 467 for the red channel. In control cells, cells are counterstained with DAPI to visualise nuclei (blue). The sections are seen x 20 magnification. The exposure and camera settings remained consistent across all the images taken for each experiment. TH indicates tyrosine hydroxylase. Scale bars represent 50 μm. The results shown are representative from five independent experiments.

5.3.4 Expression of total protein of P2 receptors in undifferentiated and differentiated SH-SY5Y cells

Western blot analysis was performed to determine purinergic P2 receptor expression in total protein extracted from undifferentiated and differentiated SH-SY5Y cells. In addition, Western blot analysis confirmed the specificity of our antibodies. Specific binding was detected at the expected product size for both undifferentiated and differentiated SH-SY5Y cells probed with antibodies against P2X2 (~ 45 kDa) (Figure 5.13.A). P2X7 was found at the expected molecular mass (~ 75 kDa) in undifferentiated SH-SY5Y cells. However, in differentiated cells, two bands were detected for P2X7: one faint band with a molecular mass of ~ 75 kDa and one strong band at ~ 50 kDa (Figure 5.13.C). The P2X7 antibodies used were knockout validated in the mouse vas deferens and the explanation for these discrepancies was not clear. Certainly, splice variants, different aggregation states, and posttranslational modifications such as glycosylation and/or receptor dimerization may be involved, but the exact explanation remains undetermined (Cavaliere et al., 2005). It was previously reported that human P2X7 has seven variants which result from alternative splicing. Two of these variations were compared to the full-length channel (one lacking the first transmembrane domain, the other lacking the entire cytoplasmic tail). Both variants were expressed in multiple tissues, and the cytoplasmic tail deletion variant was significantly expressed, according to RT-PCR analysis. Removal of the first transmembrane domain led to a non-functional channel. While Deletion of the cytoplasmic tail had no effects on ion movement but severely affected the ability to form a large pore and to promote activation of caspases (Cheewatrakoolpong et al., 2005). Finally, although P2X3 receptor protein was detected in the mouse brain, superior cervical ganglion and arteries, it was not detected in either the undifferentiated or differentiated SH-SY5Y cells (Figure 5.13.B). Although P2X3 protein was detected by immunofluorescence, the absence of P2X3 receptor protein by Western blot could be because of nonsense-mediated decay confirmed by sequence data (Supplementary S.4). Immunofluorescence and Western blot findings confirmed the RT-PCR results, the presence of P2X2 and P2X7 at protein levels, and confirmed the specificity of the antibodies. While immunofluorescence confirmed the presence of P2X3 at protein level.

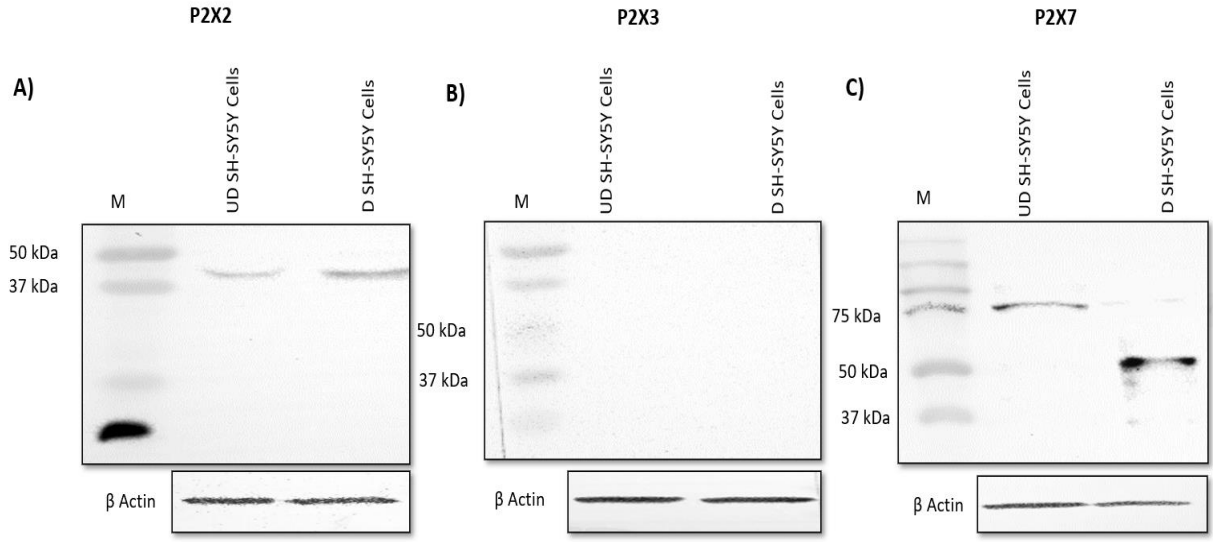

Figure 5.13: Western blot analysis of P2X2, P2X3 and P2X7 receptor expression in undifferentiated and differentiated SH-SY5Y cells. **(A)** The Western immunoblots showed expression of P2X2 receptor protein with a single band in both cell types at ~ 45 kDa. **(B)** The immunoblot showed no expression of P2X3 protein in either cell type. **(C)** P2X7 detected a single band at ~ 75 kDa in undifferentiated SH-SY5Y cells and two bands at ~ 75 kDa and ~50kDa in differentiated cells. β-actin served as a loading control. M represents the molecular weight marker. UD SH-SY5Y indicates undifferentiated SH-SY5Y cells. D SH-SY5Y indicates differentiated cells. 30 μg protein/lane. The results shown are representative from five independent experiments.

5.3.5 Nucleotide-evoked calcium responses in undifferentiated and differentiated SH-SY5Y cells

Activation of P2 receptors causes an elevation of intracellular Ca^{2+} levels due to direct Ca^{2+} entry from the extracellular space via ionotropic P2X receptors or release of Ca^{2+} from intracellular stores due to activation of metabotropic P2Y receptors. To determine whether the P2 receptors expressed in undifferentiated and differentiated SH-SY5Y cells were functionally active, exogenous nucleotides were applied and real-time monitoring of intracellular Ca^{2+} levels was performed. Administration of ATP, BzATP, α,β-Me-ATP or carbachol induced concentration-dependent increases in intracellular Ca^{2+} in both cell types in the presence of extracellular Ca^{2+}. The nucleotides had different potencies in undifferentiated and differentiated SH-SY5Y cells. The EC_{50} of ATP in undifferentiated and differentiated SH-SY5Y cells was 340.7 ± 39.6 μM and 840.7 ± 558 μM, respectively (N=5, P<0.01). The EC_{50} values for ATP in the differentiated cells and BzATP in the undifferentiated cells could not be accurately calculated as the responses had not plateaued within the range of concentrations tested. The EC_{50} of α, β-Me-ATP undifferentiated and differentiated SH-SY5Y cells was 113.1 ± 51.4 μM and 80.6 ± 29.4 μM, respectively (N=5) (Table 5.3). The response to BzATP was less potent in undifferentiated SH-SY5Y cells (EC_{50} 127.2 ± 20 μM, N=5) compared to differentiated cells (EC_{50} 116.6 ± 73 μM, N=5), P<0.01 (Figure 5.14 – 5.24).

Concentration-response experiments were performed at concentrations ranging from 0.3 μM to 2 mM ATP. In undifferentiated SH-SY5Y cells, significant increases in intracellular Ca^{2+} were detected upon application of 300 μM to 2 mM ATP, whilst significant increases in intracellular Ca^{2+} were detected following application of concentrations above 1 mM in the differentiated cells (Figure 5.14 and Figure 5.15). Maximal Ca^{2+} responses were consistently observed in response to the application of 2 mM ATP in both cell types, however, statistical analysis showed no significant difference in Ca^{2+} responses was seen between both cells following the application of ATP (Figure 5.16).

To examine the role of P2X receptors in nucleotide-evoked Ca^{2+} responses, α, β-Me-ATP (an agonist of heteromeric P2X2/3, and in particular P2X1) cells were stimulated with concentrations ranging from 0.3 μM to 1 mM. As shown in Figure 5.17, 1mM and 300 μM α, β-Me-ATP elicited a concentration-dependent increase in the intracellular Ca^{2+} level in undifferentiated SH-SY5Y cells. Maximal Ca^{2+} responses were obtained from the application of 1 mM α, β-Me-ATP in undifferentiated cells. Representative time-response traces are shown in Figure 5.17. However, although an increase in intracellular Ca^{2+}response was also observed in differentiated cells, these responses were comparable to the SBS control (Figure 5.18).

Moreover, no significant difference was seen between 1 mM and 300 μM in the differentiated cells in comparison to undifferentiated SH-SY5Y cells (Figure 5.19), suggesting P2X receptors are involved in the ATP-evoked Ca^{2+} responses in undifferentiated SH-SY5Y cells but not differentiated cells.

Cells were stimulated with concentrations of BzATP ranging from 1 μM to 300 μM. The application of BzATP concentrations ≥100 μM caused a significant increase in intracellular Ca^{2+} responses in undifferentiated (Figures 5.20 & 5.21) and differentiated cells (Figures 5.22 & 5.23). Maximal responses were observed at approximately 300 μM. However, no significant difference was seen between undifferentiated and differentiated cells (Figure 5.24). No changes in intracellular Ca^{2+} were observed in response to the application of 30 μM BzATP or below in both cell types (Figure 5.20 – 5.23). BzATP is not a selective agonist for P2X7 nucleotide receptors since it can also activate P2X1, P2X2, P2X3, P2X4 and P2X2/3 nucleotide receptors (Chen et al., 2018; Orellano et al, 2010).

5.3.6 P2X7 receptor was involved in nucleotide-evoked calcium responses in undifferentiated and differentiated SH-SY5Y cells

Our results (in section 5.3.2) showed almost all of the known P2X receptors were expressed in both undifferentiated and differentiated SH-SY5Y cells, excluding P2X1 which was not expressed in differentiated cells. However, only four P2X of the seven expressed P2X receptors are known to commonly form functional receptors in humans: P2X1, P2X2, P2X4 and P2X7 receptors. A previous study demonstrated that P2X5 and P2X6 receptors are non-functional in humans (Lynch et al., 1999; Torres et al., 1999; Ormond, 2006; Kotnis et al., 2010). Moreover, the response to the P2X1 receptor rapidly desensitises, so it is unlikely to be detected with the equipment used in this study. Our result suggested that heteromeric P2X2/3 didn't induce intracellular Ca^{2+}responses in differentiated cells. Our result using BzATP suggested P2X7 receptor was involved (alongside other P2X receptors such as P2X2 and P2X3) in nucleotide-evoked Ca^{2+} responses in undifferentiated SH-SY5Y cells and differentiated SH-SY5Y cells. To explore whether the BzATP-mediated Ca^{2+} response was elicited by activation of the P2X7 receptor, the selective P2X7 antagonist, A438079, was employed. Pre-incubation of both undifferentiated and differentiated SH-SY5Y cells with 10 μM A438079 could inhibit the magnitude of 300 μM BzATP-evoked Ca^{2+} responses in both cell types (0.29 ± 0.09 F ratio vs. 0.16 ± 0.01 F ratio in undifferentiated SH-SY5Y cells, 0.31 ± 0.02 F ratio vs. 0.13 ± 0.02 F ratio in differentiated SH-SY5Y cells, n=5, $P<0.01$) (Figures 5.21 & 5.23). However, A438079 could not significantly inhibit responses induced by 100 μM

BzATP (0.20 ± 0.09 F ratio vs. 0.14 ± 0.01 F ratio in undifferentiated SH-SY5Y cells, 0.22 ± 0.02 F ratio vs. 0.13 ± 0.02 F ratio in differentiated SH-SY5Y cells, n=5). These results suggested that the P2X7 receptor was involved in the nucleotide-evoked Ca^{2+} response. The P2X7 receptor could be a new promising therapeutic target for some cardiovascular disorders. Furthermore, several previous research demonstrated that P2X7 receptor activation accelerates the progression of cardiovascular diseases such as the hypertension, myocardial infarction, long-term heart transplant, dilated cardiomyopathy and autoimmune myocarditis, as well as atherosclerosis, diabetic retinopathy and thrombosis (Chen., 2018). The pathway is principally engaged in the inflammatory response caused by the P2X7 receptor. Therefore, more research on the role of P2X7 receptor in cardiovascular diseases such as hypertension are very necessary. Although more research on the role of P2X7 is required, there is no doubt that the P2X7 receptor is an emerging and essential therapeutic target in cardiovascular diseases.

Finally, carbachol was used as a positive control for Ca^{2+} release. Carbachol is an agonist for muscarinic acetylcholine receptors and facilitates extracellular Ca^{2+}influx via voltage-dependent Ca^{2+}channels as well as Ca^{2+}release from intracellular stores (Blackwood & Bolton, 1993). Interestingly, it was seen that carbachol-evoked Ca^{2+} response in differentiated SH-SY5Y cells was significantly higher than in undifferentiated SH-SY5Y cells (Figures 5.25 & 5.26), suggesting the cholinergic phenotype of neurons more than the undifferentiated cells. Cholinergic receptor activation raises Ca^{2+} cytosol by many processes including Ca^{2+} release from intracellular stores, and their activation as well increases the amplitude of intracellular Ca^{2+} transients induced by depolarisation. It was reported when the cholinergic agonist carbachol was present, activity-dependent increases in Ca^{2+} cytosol were increased and prolonged due to a slowing of Ca^{2+} clearance from the cytosol, rather than by increased Ca^{2+} entry during action potentials. Cholinergic stimulation could regulate the activation of Ca^{2+} dependent intracellular activities by modulating the temporal integration of Ca^{2+} signalling.

Table 5.3: Characteristics of the calcium responses evoked by maximal concentrations of nucleotides) in undifferentiated and differentiated SH-SY5Y cells. Mean ± SEM.

Cells	Nucleotide	Target	Peak magnitude (F ratio)	EC50 (μM)
Undifferentiated SH-SY5Y cells	ATP (2 mM)	P2X, P2Y	0.23 ± 0.05	340.7 μM
	ATP (1 mM)		0.22 ± 0.05	
	ATP (300 μM)		0.18 ± 0.05	
	α, β-Me-ATP (1 mM	P2X	0.15 ± 0.009	113.1 μM
	α, β-Me-ATP (300 μM)		0.14 ± 0.009	
	BzATP (300 μM)	P2X	0.29 ± 0.09	127.2 μM
	BzATP (100 μM)		0.20 ± 0.09	
	Carbachol	Muscarinic Receptor	0.99 ± 0.07	
Differentiated Neuronal Cells	ATP (2 mM)	P2X, P2Y	0.22 ± 0.02	840.7 μM
	ATP (1 mM)		0.16 ± 0.02	
	α, β-Me-ATP (1 mM)	P2X	0.11 ± 0.007	80.6 μM
	α, β-Me-ATP (300 μM)		0.11 ± 0.007	
	BzATP (300 μM)	P2X	0.31 ± 0.02	116.6 μM
	BzATP (100 μM)		0.22 ± 0.02	
	Carbachol	Muscarinic Receptors	1.53 ± 0.09	

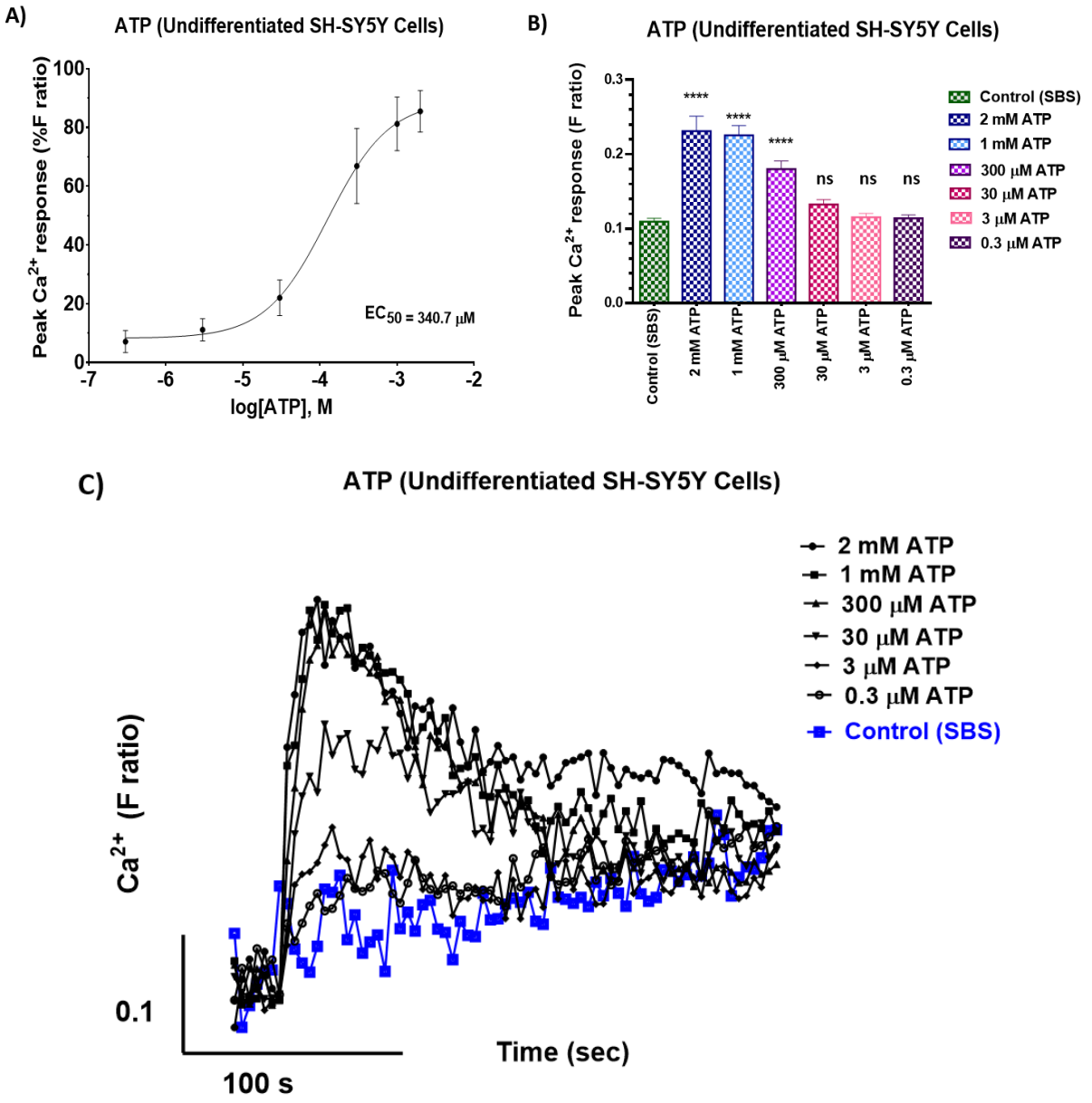

Figure 5.14: ATP elicited intracellular calcium responses in undifferentiated SH-SY5Y cells. (A) Concentration-response curves for intracellular Ca^{2+} responses elicited by ATP. Ca^{2+} responses were normalized to the maximal response observed in the cells, which was the response to 2 mM ATP. **(B)** Shows the peak response when the cells were stimulated with different concentrations of ATP ranging from 0.3 µM to 2 mM within a recording period of 250 seconds. **(C)** Shows the representative trace when the cells were stimulated with 0.3 µM to 2 mM ATP within a recording period of 250 seconds. The results shown are representative from five independent experiments. Experiments were compared by a one-way ANOVA followed by Brown-Forsythe multiple comparison test (GraphPad Prism 6), *p<0.05, **p<0.005, ***p<0.001, ****p<0.0001, ns not significant (p>0.05), mean with SEM.

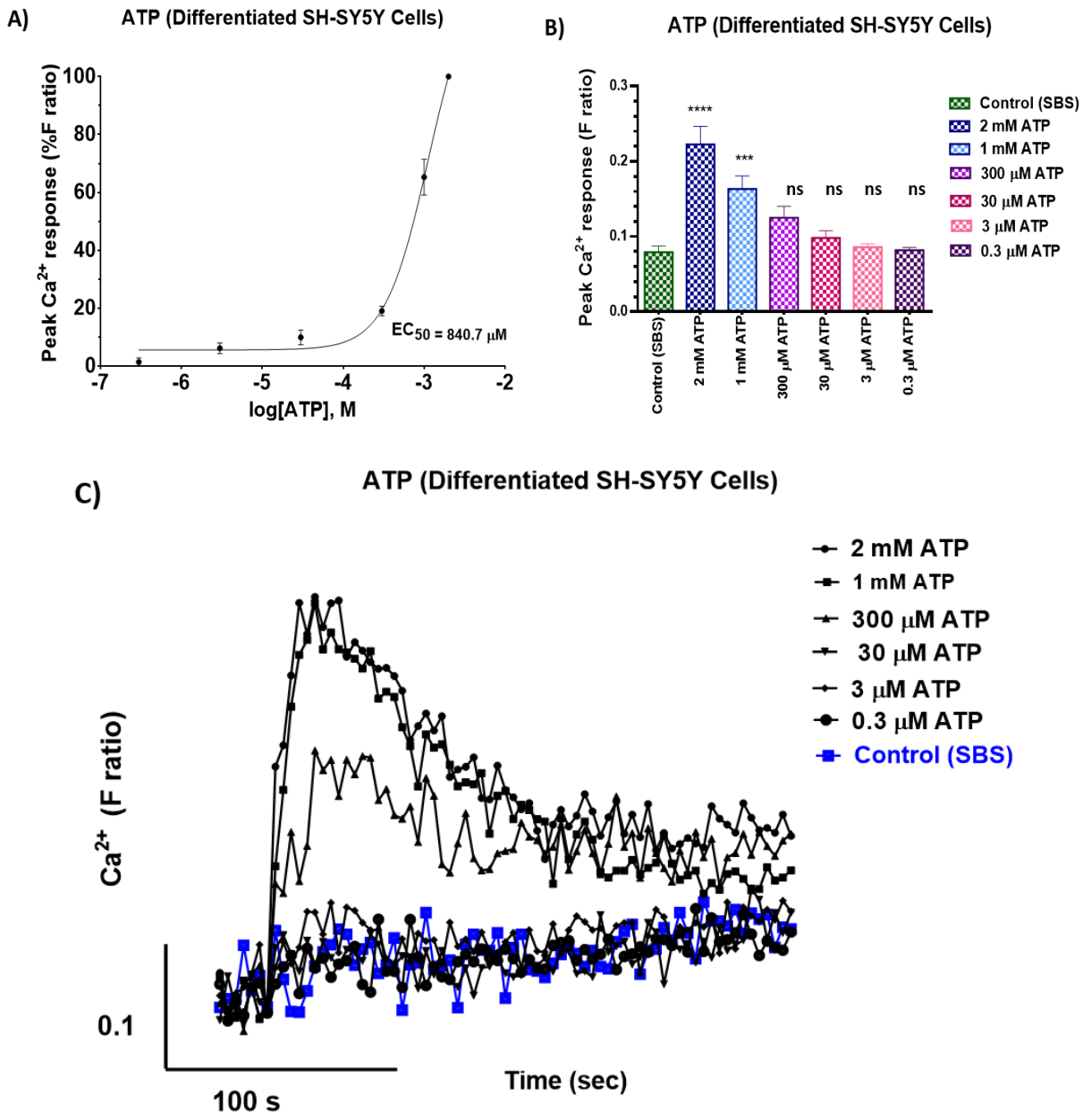

Figure 5.15: ATP elicited intracellular calcium responses in differentiated SH-SY5Y cells. **(A)** Concentration-response curves for intracellular Ca^{2+} responses elicited by ATP. Ca^{2+} responses were normalized to the maximal response observed in the cells, which was the response to 2 mM ATP. **(B)** Shows the peak response when the cells were stimulated with different concentrations of ATP ranging from 0.3 µM to 2 mM within a recording period of 250 seconds. **(C)** Shows the representative trace when the cells were stimulated with 0.3 µM to 2 mM of ATP within a recording period of 250 seconds. The results shown are representative from five independent experiments. Experiments were compared by a one-way ANOVA followed by Brown-Forsythe multiple comparison test (GraphPad Prism 6), *p<0.05, **p<0.005, ***p<0.001, ****p<0.0001, ns not significant (p>0.05), mean with SEM.

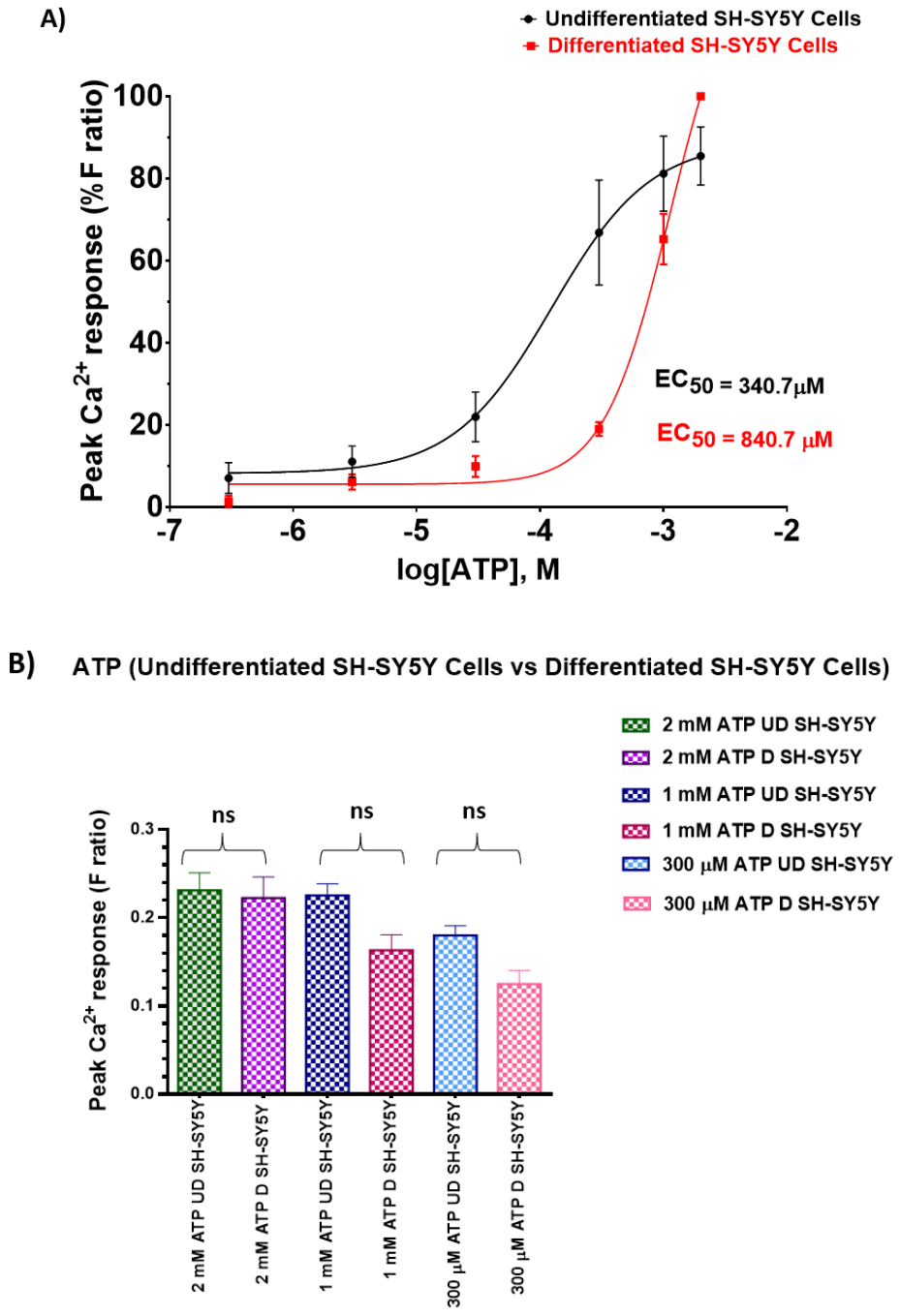

Figure 5.16: ATP elicited intracellular calcium responses in undifferentiated and differentiated SH-SY5Y cells. (A) Concentration-response curves for intracellular Ca^{2+} responses elicited by ATP in both cells. Ca^{2+} responses were normalized to the maximal response observed in the cells, which was the response to 2 mM ATP. **(B)** Shows the peak response when the cells were stimulated with different concentrations of ATP ranging from 300 µM to 2 mM within a recording period of 250 seconds. The results shown are representative from five independent experiments. Experiments were compared by a one-way ANOVA followed by Brown-Forsythe multiple comparison test (GraphPad Prism 6), *p<0.05, **p<0.005, ***p<0.001, ****p<0.0001, ns not significant (p>0.05), mean with SEM. UD indicates undifferentiated SH-SY5Y cells. D indicates differentiated SH-SY5Y cells.

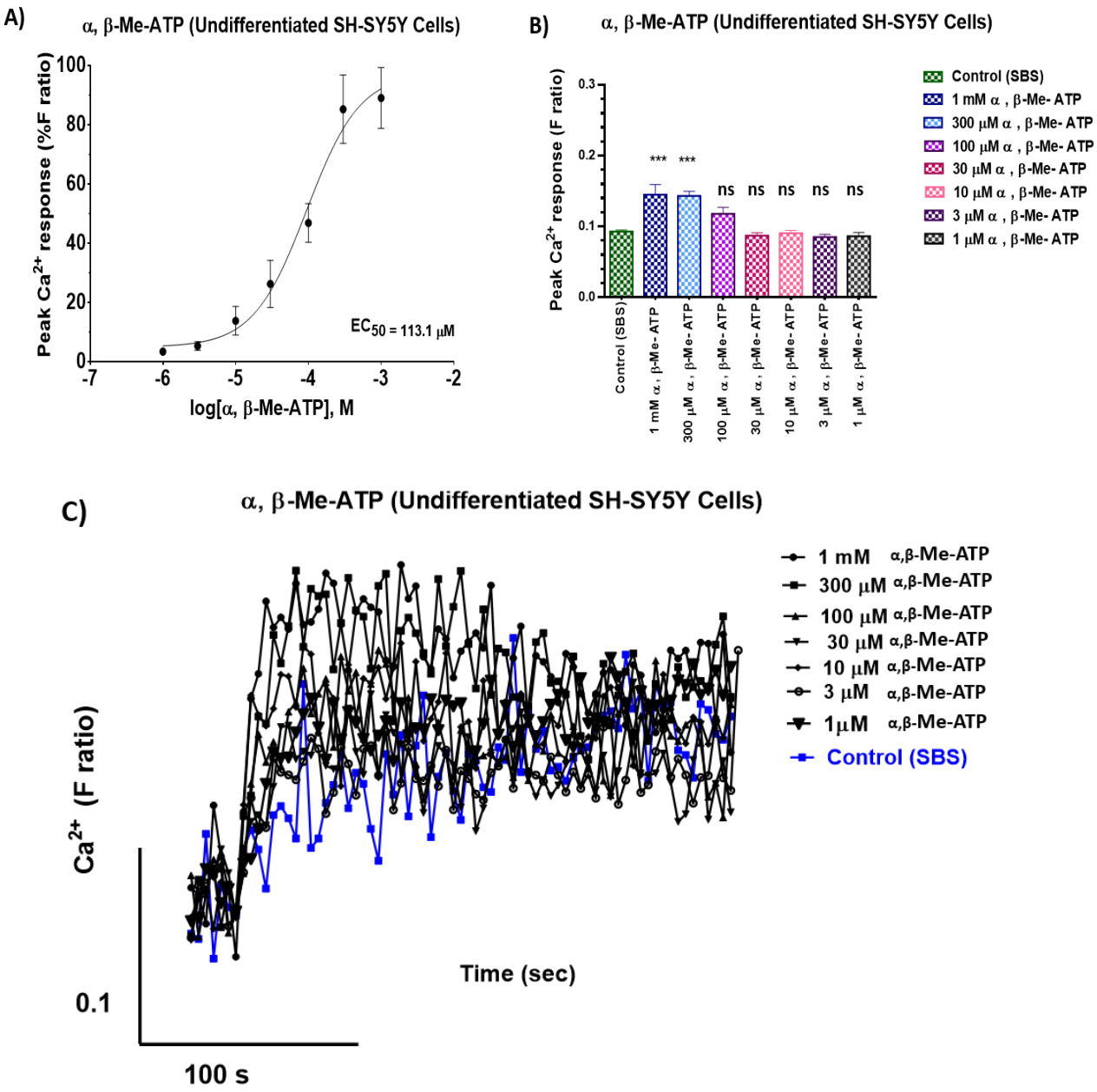

Figure 5.17: α,β-Me-ATP elicited intracellular calcium responses in undifferentiated SH-SY5Y cells. (A) Concentration-response curves for intracellular Ca^{2+} responses elicited by α,β-Me-ATP. Ca^{2+} responses were normalized to the maximal response observed in the cells, which was the response to 1 mM α,β-Me-ATP. **(B)** Shows the peak response when the cells were stimulated with different concentrations of α,β-Me-ATP ranging from 1 μM to 1mM within a recording period of 250 seconds. **(C)** Shows the representative trace when the cells were stimulated with 1 μM to 1mM of α,β-Me-ATP within a recording period of 250 seconds. The results shown are representative from five independent experiments. Experiments were compared by a one-way ANOVA followed by Brown-Forsythe multiple comparison test (GraphPad Prism 6), *p<0.05, **p<0.005, ***p<0.001, ****p<0.0001, ns not significant (p>0.05), mean with SEM.

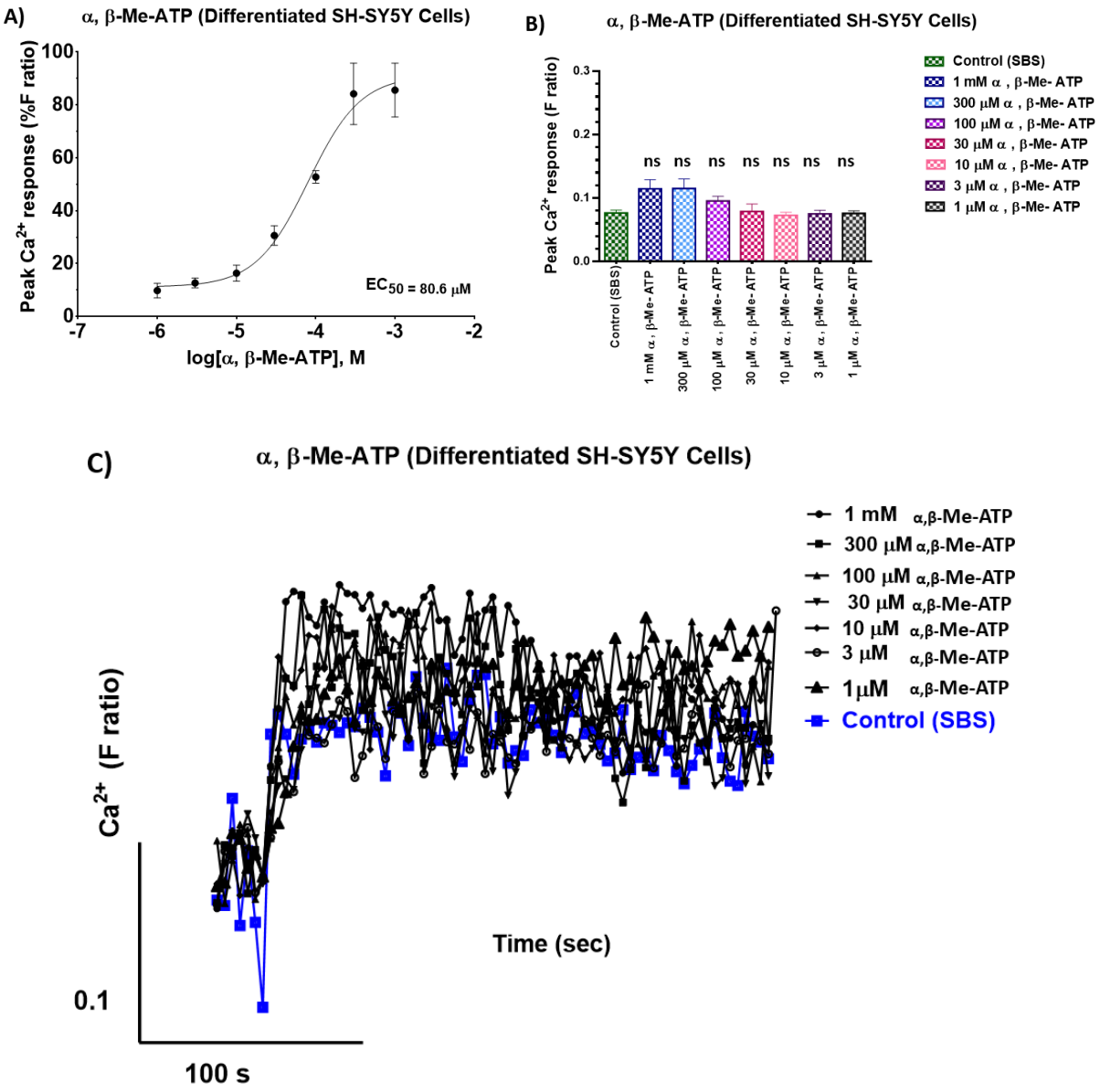

Figure 5.18: **α,β-Me-ATP did not significantly elicit intracellular calcium responses in differentiated SH-SY5Y cells. (A)** Concentration-response curves for intracellular Ca^{2+} responses elicited by α,β-Me-ATP. Ca^{2+} responses were normalized to the maximal response observed in the cells, which was the response to 1 mM α,β-Me-ATP. **(B)** Shows the peak response when the cells were stimulated with different concentrations of α,β-Me-ATP ranging from 1 μM to 1mM within a recording period of 250 seconds. **(C)** Shows the representative trace when the cells were stimulated with 1 μM to 1mM of α,β-Me-ATP within a recording period of 250 seconds. The results shown are representative from five independent experiments. Experiments were compared by a one-way ANOVA followed by Brown-Forsythe multiple comparison test (GraphPad Prism 6), *p<0.05, **p<0.005, ***p<0.001, ****p<0.0001, ns not significant (p>0.05), mean with SEM.

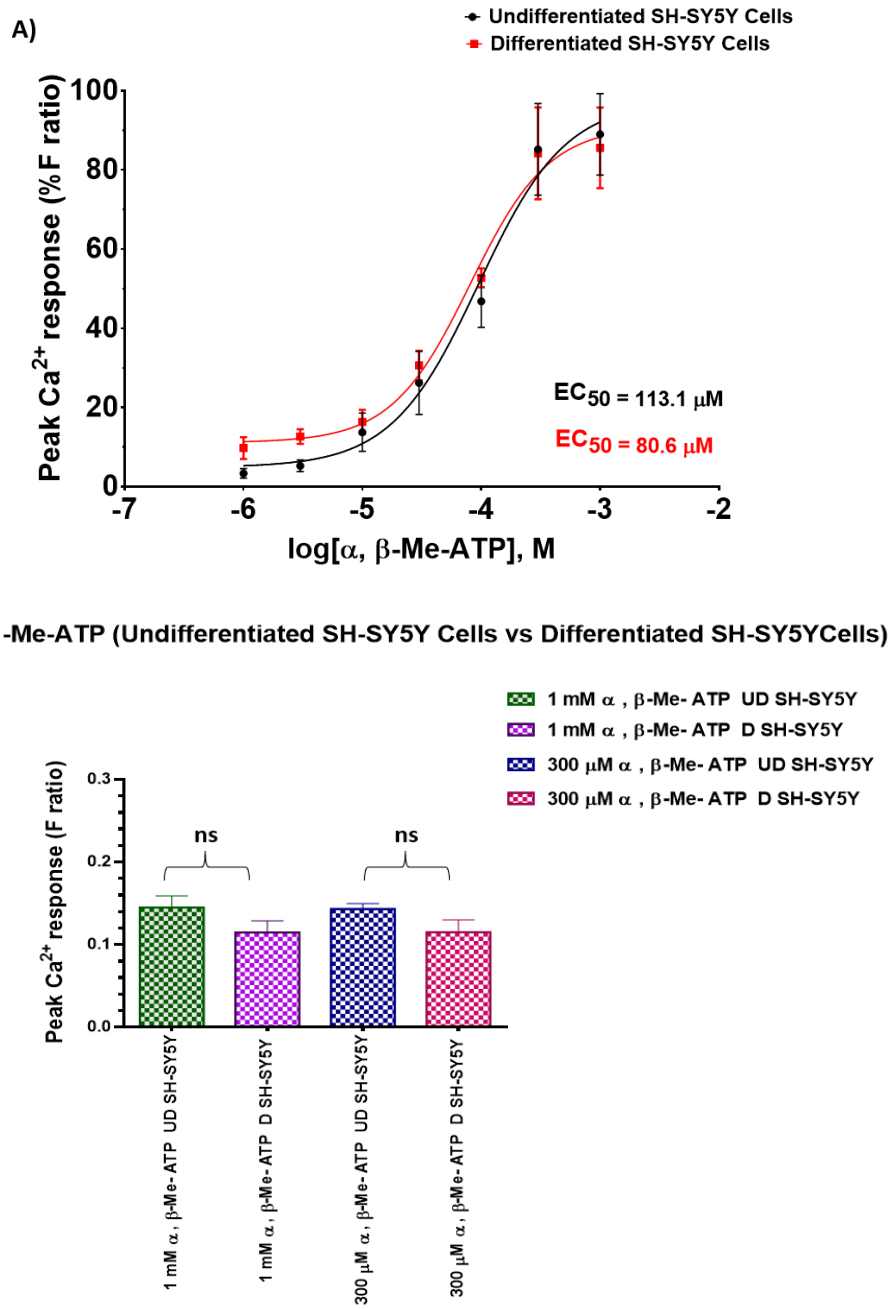

Figure 5.19: **α,β-Me-ATP elicited intracellular calcium responses in undifferentiated SH-SY5Y cells but not in SH-SY5Y cells. (A)** Concentration-response curves for intracellular Ca^{2+} responses elicited by α,β-Me-ATP. Ca^{2+} responses were normalized to the maximal response observed in the cells, which was the response to 1 mM α,β-Me-ATP. **(B)** Shows the peak response when the cells were stimulated with different concentrations of α,β-Me-ATP ranging from 300 μM to 1mM within a recording period of 250 seconds. The results shown are representative from five independent experiments. Experiments were compared by a one-way ANOVA followed by Brown-Forsythe multiple comparison test (GraphPad Prism 6), *p<0.05, **p<0.005, ***p<0.001, ****p<0.0001, ns not significant (p>0.05), mean with SEM. UD indicates undifferentiated SH-SY5Y cells. D indicates differentiated SH-SY5Y cells.

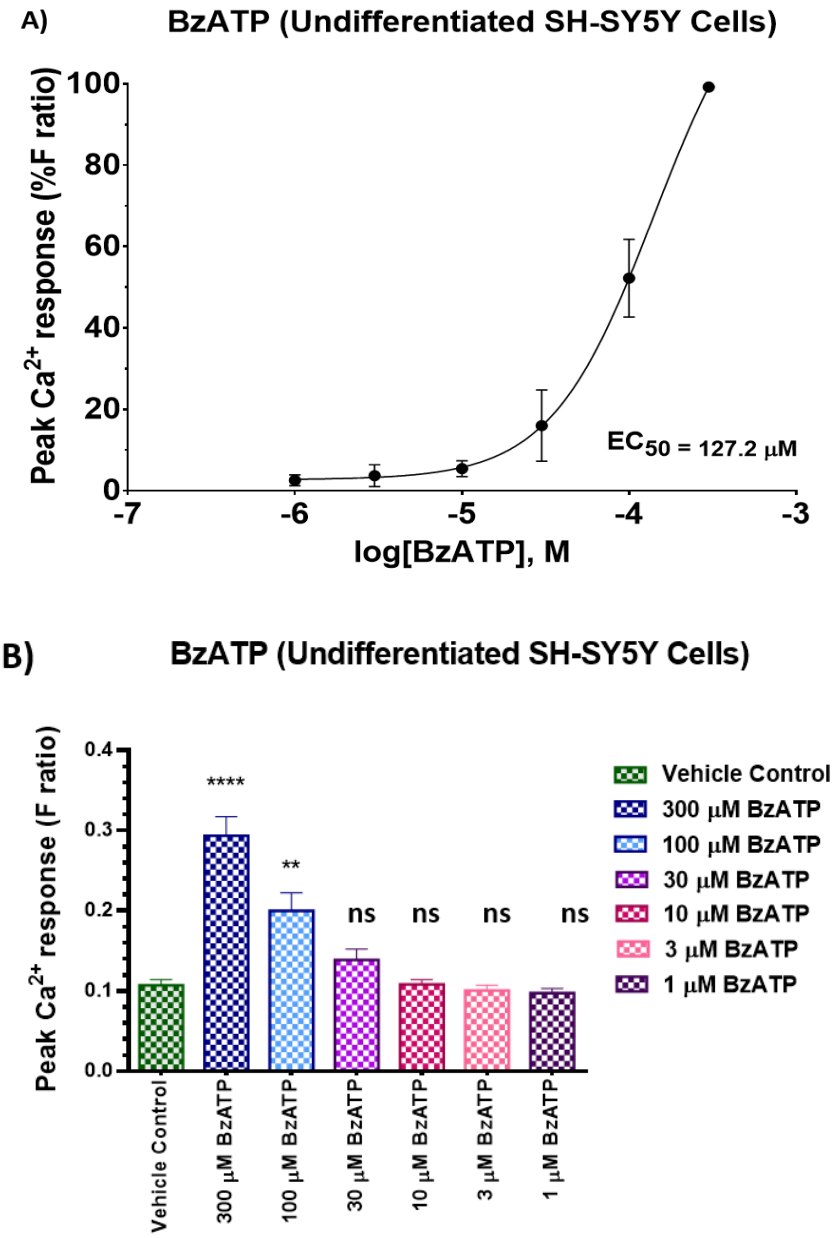

Figure 5.20: **BzATP (target P2X7) elicited intracellular calcium responses in undifferentiated SH-SY5Y cells. (A)** Concentration-response curves for intracellular Ca^{2+} responses elicited by BzATP. Ca^{2+} responses were normalized to the maximal response observed in the cells, which was the response to 300 µM BzATP. **(B)** shows the peak response when the cells were stimulated with different concentrations of BzATP ranging from 1 µM to 300 µM within a recording period of 250 seconds. The results shown are representative from five independent experiments. Experiments were compared by a one-way ANOVA followed by Brown-Forsythe multiple comparison test (GraphPad Prism 6), *p<0.05, **p<0.005, ***p<0.001, ****p<0.0001, ns not significant (p>0.05), mean with SEM. Vehicle control = SBS + DMSO

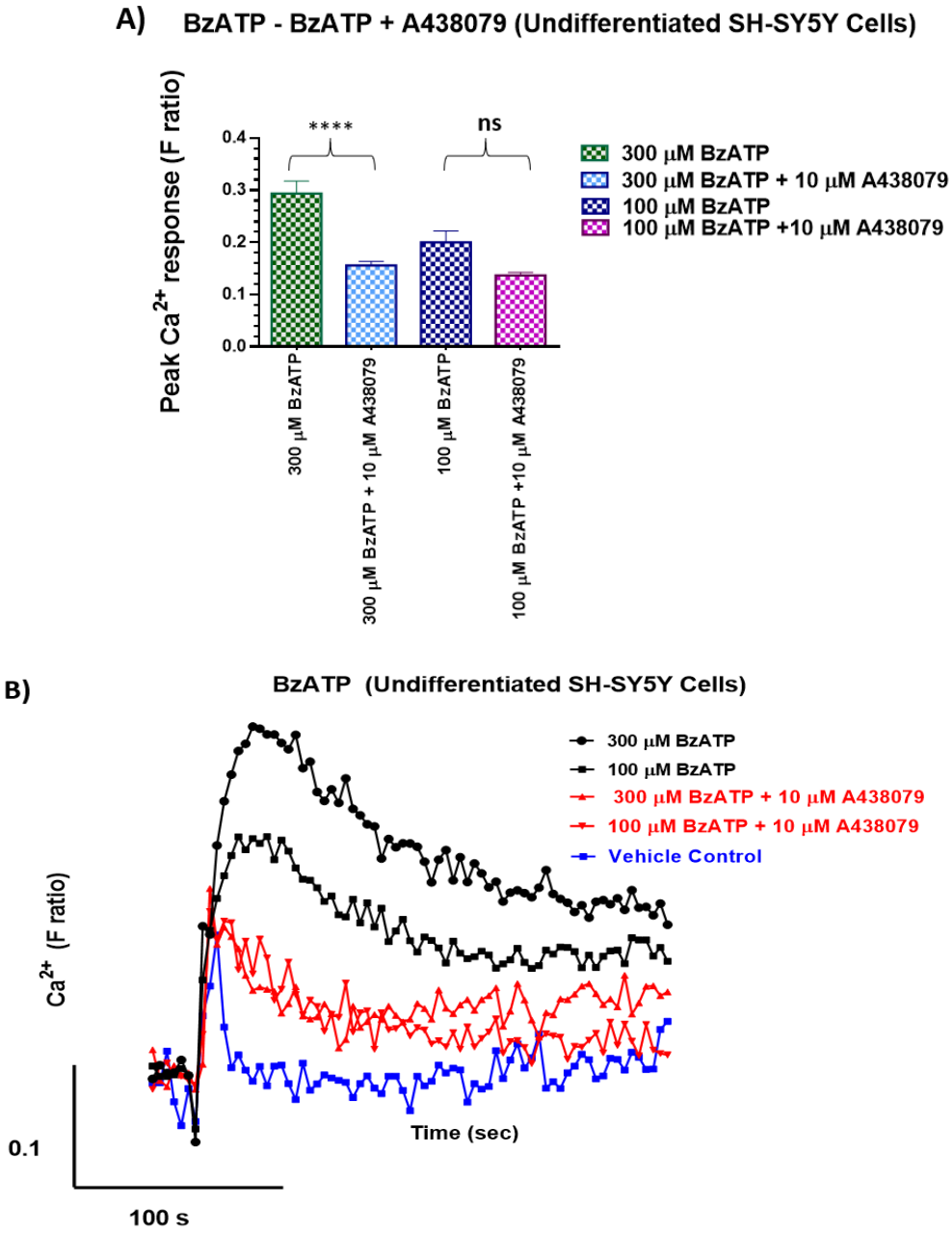

Figure 5.21: Selective antagonism of P2X7 receptors had an inhibitory effect on the BzATP-evoked calcium response in undifferentiated SH-SY5Y cells. (A) The bar chart shows the peak response when the cells were stimulated with 300 µM and100 µM BzATP followed by incubating with 10 µM A438079 antagonist of P2X7 within a recording period of 250 seconds. **(B)** shows the representative trace when the cells were stimulated with 300 µM and100 µM BzATP (Black), and the cells stimulated with 300 µM and100 µM BzATP treated with 10 µM A438079 within a recording period of 250 seconds (red). The results shown are representative from five independent experiments. Experiments were compared by a one-way ANOVA followed by Brown-Forsythe multiple comparison test (GraphPad Prism 6), *p<0.05, **p<0.005, ***p<0.001, ****p<0.0001, ns not significant (p>0.05), mean with SEM. Vehicle control = SBS + DMSO.

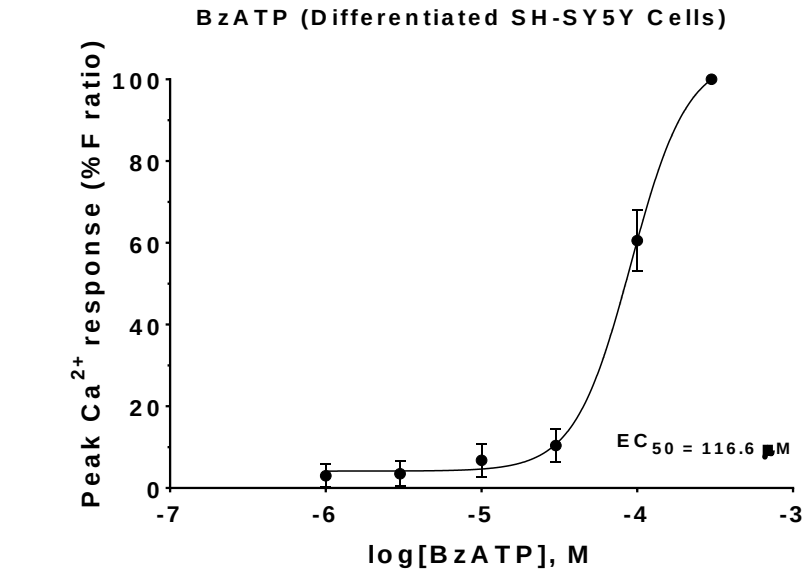

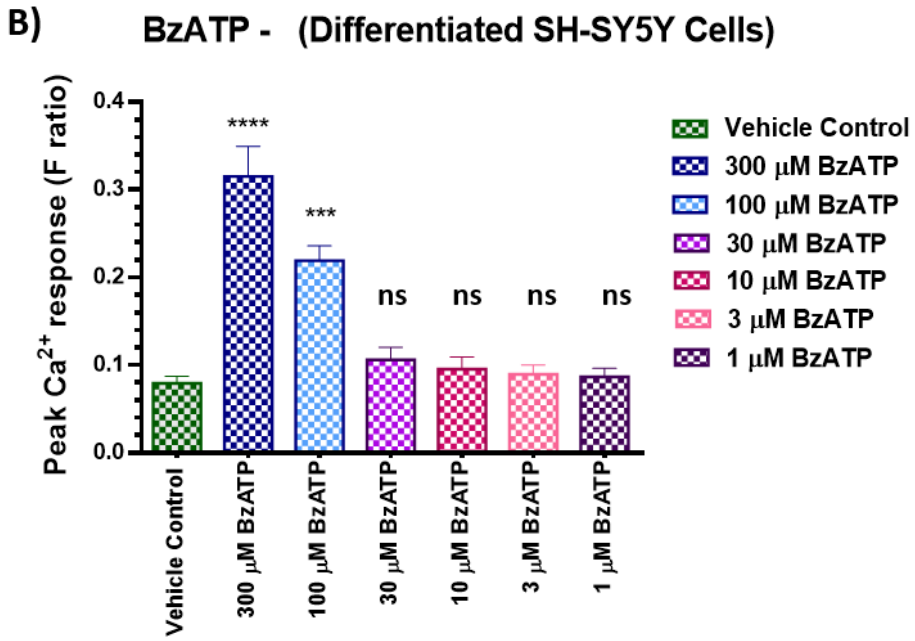

Figure 5.22: **BzATP (target P2X7) elicited intracellular calcium responses in differentiated SH-SY5Y cells. (A)** Concentration-response curves for intracellular Ca^{2+} responses elicited by BzATP. Ca^{2+} responses were normalized to the maximal response observed in the cells, which was the response to 300 µM BzATP. **(B)** shows the peak response when the cells were stimulated with different concentrations of BzATP ranging from 1 µM to 300 µM within a recording period of 250 seconds. The results shown are representative from five independent experiments. Experiments were compared by a one-way ANOVA followed by Brown-Forsythe multiple comparison test (GraphPad Prism 6), *p<0.05, **p<0.005, ***p<0.001, ****p<0.0001, ns not significant (p>0.05), mean with SEM. Vehicle control = SBS + DMSO.

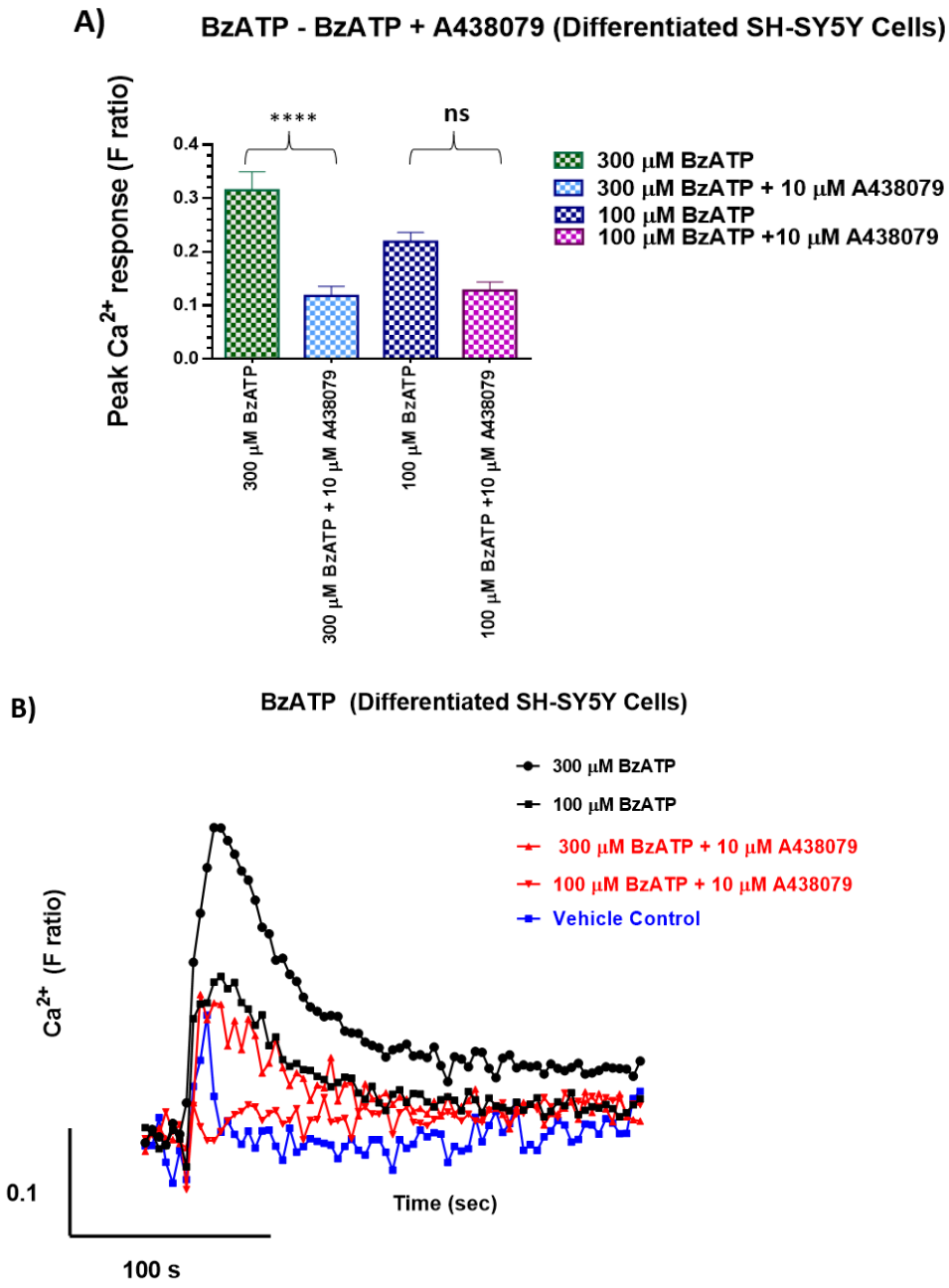

Figure 5.23: Selective antagonism of P2X7 receptors had an inhibitory effect on the BzATP-evoked calcium response in differentiated SH-SY5Y cells. (A) The bar chart shows the peak response when the cells were stimulated with 300 µM and100 µM BzATP followed by incubating with 10 µM A438079 antagonist of P2X7 within a recording period of 250 seconds. **(B)** shows the representative trace when the cells were stimulated with 300 µM and100 µM BzATP (Black), and the cells stimulated with 300 µM and100 µM BzATP treated with 10 µM A438079 within a recording period of 250 seconds (red). The results shown are representative from five independent experiments. Experiments were compared by a one-way ANOVA followed by Brown-Forsythe multiple comparison test (GraphPad Prism 6), *p<0.05, **p<0.005, ***p<0.001, ****p<0.0001, ns not significant (p>0.05), mean with SEM. Vehicle control = SBS + DMSO.

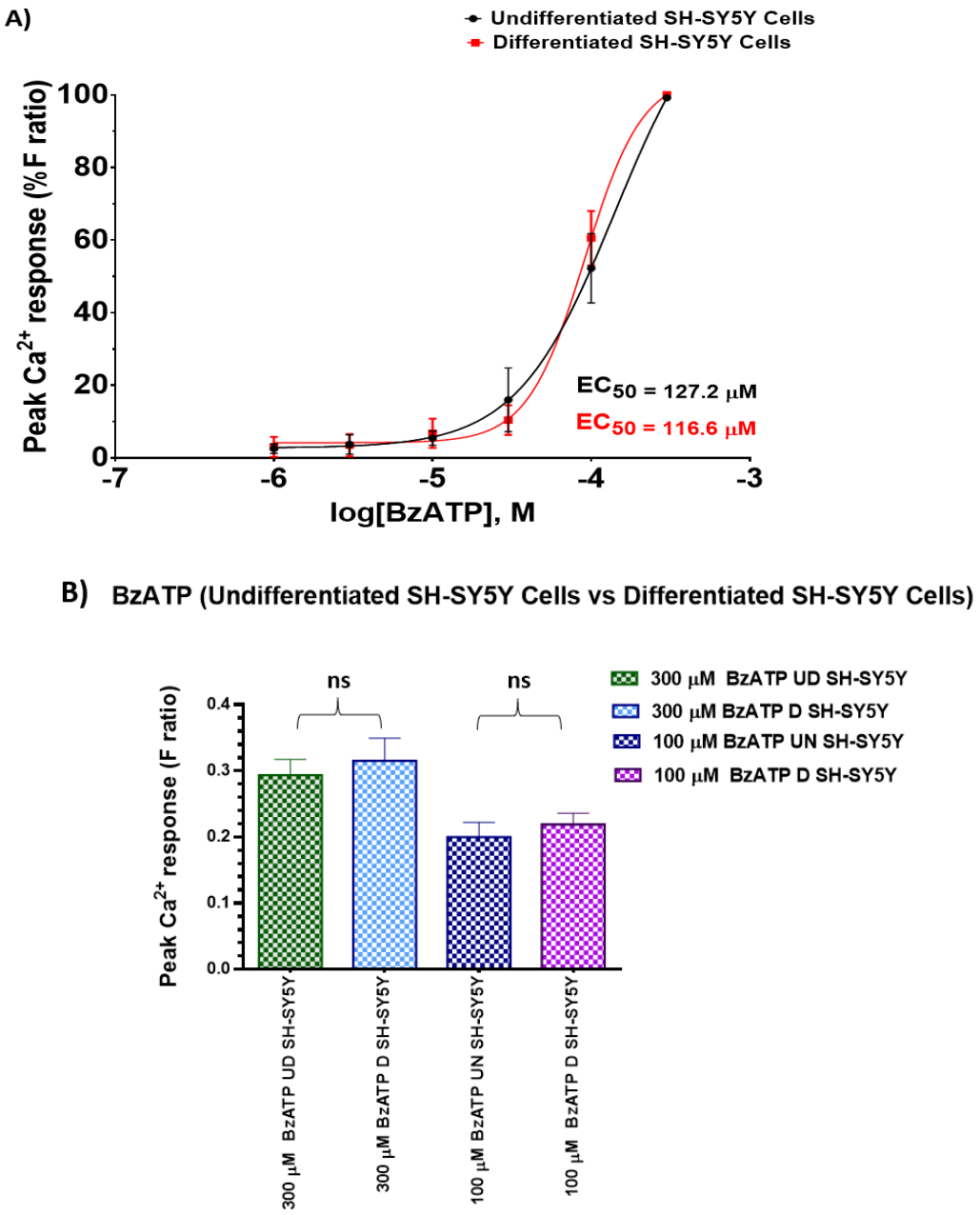

Figure 5.24: BzATP (target P2X7) elicited intracellular calcium responses in undifferentiated SH-SY5Y cells and differentiated SH-SY5Y cells. (A) Concentration-response curves for intracellular Ca^{2+} responses elicited by BzATP in both cells. Ca^{2+} responses were normalized to the maximal response observed in the cells, which was the response to 300 µM BzATP. **(B)** Shows the peak response when the cells were stimulated with 300 µM and 100 µM within a recording period of 250 seconds. The results shown are representative from five independent experiments. Experiments were compared by a one-way ANOVA followed by Brown-Forsythe multiple comparison test (GraphPad Prism 6), *p<0.05, **p<0.005, ***p<0.001, ****p<0.0001, ns not significant (p>0.05), mean with SEM. UD indicates undifferentiated SH-SY5Y cells. D indicates differentiated SH-SY5Y cells.

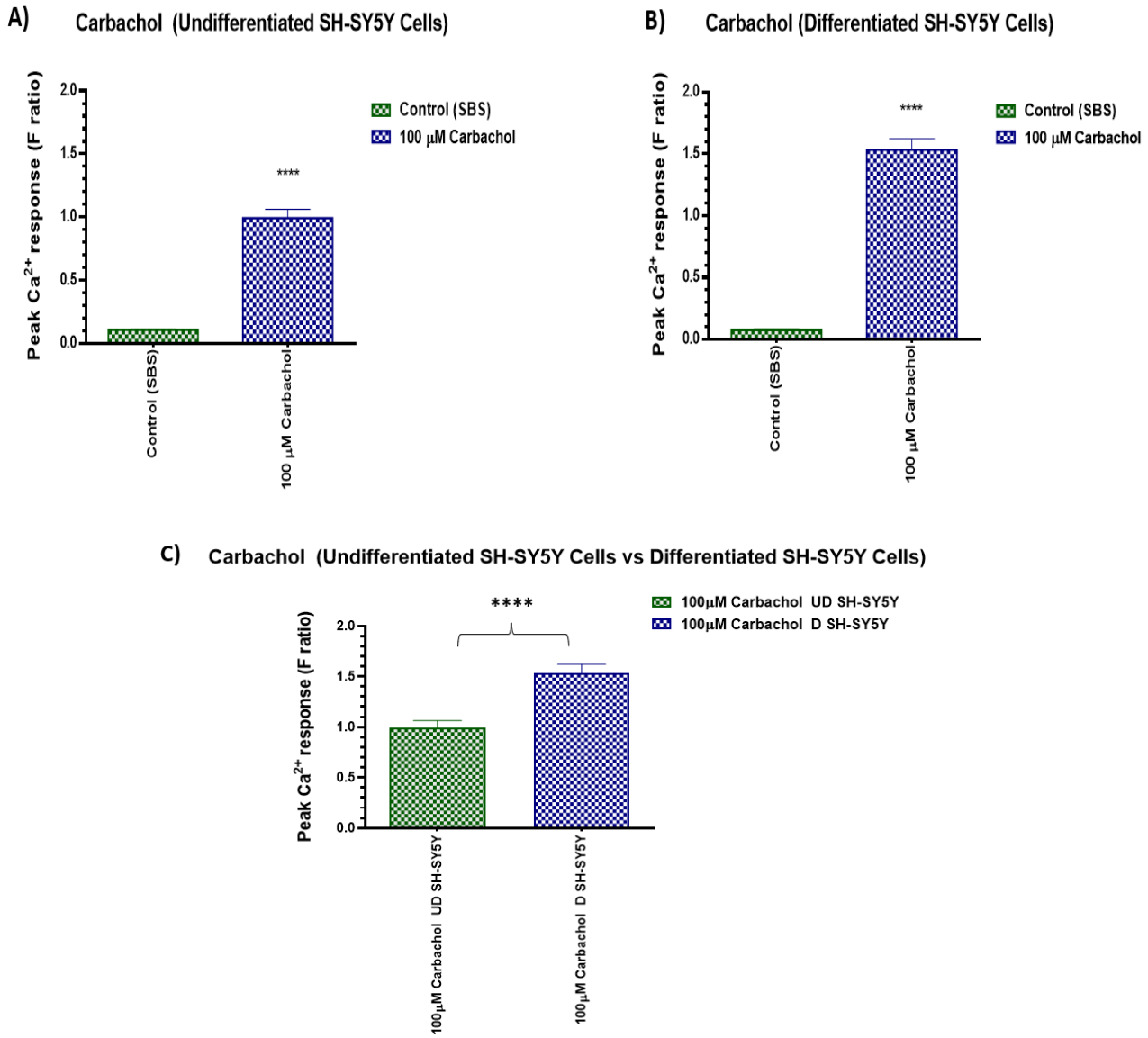

Figure 5.25: Carbachol elicited intracellular calcium responses in undifferentiated SH-SY5Y cells and differentiated SH-SY5Y cells. (A) Shows the peak response when the undifferentiated SH-SY5Y cells were stimulated with 100 µM carbachol within a recording period of 250 seconds. **(B)** Shows the peak response when the differentiated SH-SY5Y cells were stimulated with 100 µM carbachol within a recording period of 250 seconds. **(C)** carbachol-evoked Ca^{2+} response in differentiated SH-SY5Y cells was significantly higher than in undifferentiated SH-SY5Y cells. The results shown are representative from five independent experiments. Experiments were compared by a one-way ANOVA followed by Brown-Forsythe multiple comparison test (GraphPad Prism 6), *p<0.05, **p<0.005, ***p<0.001, ****p<0.0001, ns not significant (p>0.05), mean with SEM. UD indicates undifferentiated SH-SY5Y cells. D indicates differentiated SH-SY5Y cells.

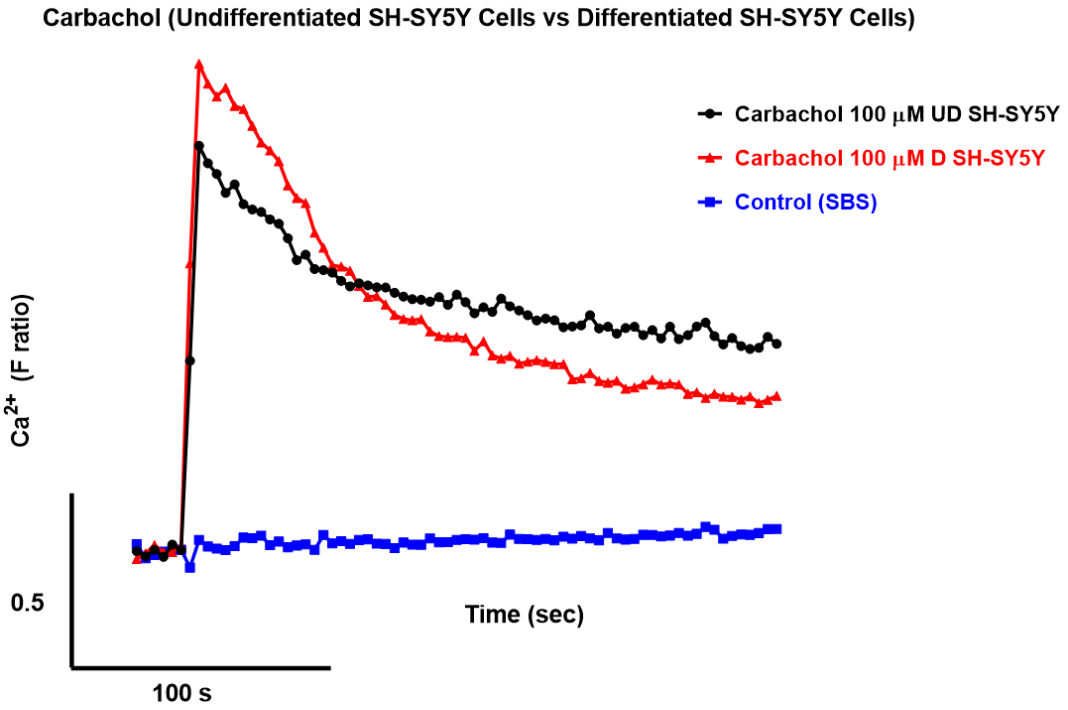

Figure 5.26: The representative trace of carbachol-evoked intracellular calcium responses in undifferentiated SH-SY5Y cells and differentiated SH-SY5Y cells. It shows the representative trace when both cells were stimulated with 100 µM of carbachol within a recording period of 250 seconds. The results shown are representative from five independent experiments. UD indicates undifferentiated SH-SY5Y cells. D indicates differentiated SH-SY-5Ycells.

5.4 Discussion

5.4.1 Differentiation of SH-SY5Y cells into an adrenergic neuron phenotype

SH-SY5Y cells can be differentiated into specific neuron subtypes such as adrenergic, cholinergic, and dopaminergic neurons by using the variety of methods described previously (Shipley et al., 2016). In our study, we used retinoic acid to differentiate SH-SY5Y cells into an adrenergic phenotype. We initially performed the differentiation experiments using phorbol esters PMA (20 nM) and retinoic acid (10 µM). However, when using PMA, the cells did not undergo growth arrest and begin to differentiate. Instead, the cells continued to proliferate as normal and differentiation was not achieved successfully. It would be useful to test the other markers of differentiation such as ChAT or VAChT to see if there is dual expression with TH and to investigate whether the cells could show cholinergic phenotype. Indeed, retinoic acid treatment altered the morphology of SH-SY5Y cells in culture. The differentiated neurons appeared smaller, more rounded and demonstrated extensive and elongated neuritic projections connecting to neighbouring cells was seen on day 5. Moreover, the differentiated neurons had a higher level of NPY expression compared to undifferentiated SH-SY5Y cells, which indicated the differentiation of retinoic acid-treated SH-SY5Y cells into a neuronal phenotype. Several previous investigations have found significant differences between undifferentiated and differentiated SH-SY5Y cells. Previous studies reported that the formation and elongation of neuritic processes, increased electrical excitability of the plasma membrane, production of synaptophysin-positive functional synapses, and induction of neuron-specific enzymes and neurotransmitters receptors are all part of neuronal differentiation. Whereas, SH-SY5Y cells are characterised morphologically by neuroblast-like, non-polarized cell bodies with few, shortened processes in their undifferentiated state. As cells appear to grow on top of one another in the middle part of a cell mass, they prefer to develop in clusters and may form clumps (Kovalevich, & Langford, 2013). which is in close agreement with the current study. Fully differentiated SH-SY5Y cells have previously been shown to express a variety of mature neuronal markers such as growth-associated protein (GAP-43), neuronal nuclei, synaptophysin, synaptic vesicle protein II, neuron-specific enolase, microtubule-associated protein and a lack of glial markers expression (Shipley et al., 2016). According to Qiao et al. (2012), neuroblastoma differentiation to neurons could be induced by retinoic acid; however, the molecular processes and signalling pathways that cause retinoic acid-mediated neuroblastoma cell differentiation are still unclear. Two morphologically distinct phenotypes were found in the parental differentiated SH-SY5Y cells: neuronal-like cells and epithelial-like cells. Cells with neuronal-like morphology express TH and dopamine-hydroxylase, which are

found in catecholaminergic neurons. While these enzymatic activities were absent from epithelial-like cells (Kovalevich & Langford, 2013).

Some studies have suggested that short exposure of SH-SY5Y cells to retinoic acid (up to 5 days) seemed to promote differentiation of neuronal-like cells phenotype (N-type cells), while longer treatment with retinoic acid (>10 days) promoted induction epithelial-like cells (S-type cell) (Encinas et al., 2000). These results corroborate with the ones found in the current study. Undifferentiated cells tend to be most similar to immature catecholaminergic neurons, while differentiated SH-SY5Y cells appear morphologically more similar to primary neurons with long, exquisite processes and are mostly polarized (Xie et al., 2010). In addition, differentiated SH-SY5Y cells showed increased activity of neuron-specific enolase, the dominant enolase-isoenzyme present in neuronal and neuroendocrine tissues and a lack in proliferation rate as cells are removed from the cell cycle (Kovalevich & Langford, 2013; Encinas et al., 2000). Depending on the differentiating agent, SH-SY5Y cells can be induced to a variety of mature neuronal phenotypes, including cholinergic, adrenergic, or dopaminergic (Xie et al., 2010).

Retinoic acid-treated SH-SY5Y cells can be differentiated into a cholinergic phenotype expressing choline acetyltransferase and vesicular monamine transporter (Lopes et al, 2010). SH-SY5Y cells exhibit a variety of mature neuronal markers after retinoic acid-mediated differentiation, including III-tubulin, microtubule-associated protein-2, synaptophysin, NeuN, synaptic-associated protein-97, and neuron-specific enolase. Furthermore, after retinoic acid application, the expression of the neurogenic differentiation genes NEUROD6 and NEUROD1 increases (Kovalevich & Langford, 2013). It has been demonstrated that both high-passage undifferentiated SH-SY5Y cells and differentiated SH-SY5Y cells express adequate levels of dopamine-β-hydroxylase, the enzyme that catalyzes the formation of NA from dopamine and can convert intracellular dopamine to NA. Furthermore, SH-SY5Y cells express the vesicular monoamine transporter and the norepinephrine transporter, characteristic of adrenergic neurons. It has been reported that neuroblastoma expresses neuropeptide Y (Y1, Y2, and Y5), a neurotransmitter released from mature sympathetic nerves, (Abualsaud et al., 2021). Another previous study has reported that SH-SY5Y cells could be differentiated into neuronal-like cells, which enhanced the expression of NPY through activation of protein kinase C (PKC) upon treatment with phorbol esters (Farrelly et al., 2013), which is in close agreement with the current study. Another study confirmed the adrenergic phenotype of differentiated SH-SY5Y cells reported by Pahlman et al., (1984), it has been shown that retinoic acid-treated SH-SY5Y cells induced a 4-fold increase in the concentration of NA, while phorbol esters caused a 200-

fold increase in NA concentration at the optimum concentration. This suggested that both agents are involved in SH-SY5Y differentiation into adrenergic neurons, resulting in increased neuron-specific enolase activity.

5.4.2 The expression of P2 receptors in undifferentiated and differentiated SH-SY5Y cells

Undifferentiated neuroblastoma SH-SY5Y cells are a well-established cell line used for *in vitro* differentiation of catecholaminergic neurons (Xicoy et al., 2017). The expression profile of P2X and P2Y receptors in undifferentiated or differentiated SH-SY5Y cells was investigated in this study. RT-PCR analysis detected mRNA expression of P2X2, P2X3, P2X4, P2X5, P2X6 and P2X7 in both cell types. While P2X1 mRNA was expressed only in undifferentiated SH-SY5Y cells. In addition, both cell types expressed P2Y2, P2Y4, P2Y11, P2Y12, P2Y13 and P2Y14. The mRNA of P2Y1 was detected only in differentiated cells and P2Y6 mRNA was found only in undifferentiated SH-SY5Y cells. Further, confocal microscopy identified that P2X2, P2X3, and P2X7 were all expressed in both cells and showed colocalisation with the neuronal marker PGP9.5. Additionally, TH showed moderate expression in both cell types and colocalised with the receptors investigated, highlighting the adrenergic phenotype of differentiated cells. This is in agreement with a previous study that showed that the SH-SY5Y cell line revealed modest dopamine-hydroxylase activity and low levels of choline acetyltransferase, acetylcholinesterase, and butyryl-cholinesterase, basal NA release and TH activity (Xicoy et al., 2017). It has been previously described that several dopaminergic neuronal markers are expressed in undifferentiated SH-SY5Y cells and differentiated states, these markers include TH, NA, and adrenaline (Kovalevich & Langford, 2013. The differential mRNA expression of P2X1, P2Y1, and P2Y6 in the two cell types, on the other hand, is a novel result that could help researchers decide which cell type to examine for each of these receptors.

The expression of P2X1, P2X, P2X4, P2X5, P2X6, P2X7, P2Y2, P2Y4, and P2Y6 mRNA in undifferentiated SH-SY5Y cells fits with previous reports described within the literature (Cavaliere et al., 2005). The Western blot in the Cavaliere study detected P2X3, unlike our study. A previous study confirmed the presence of P2X7 in SH-SY5Y cells via Western blot and 30 μM BzATP stimulation (Per Larsson et al., 2002). However, in contrast to a recent study performed by RT-PCR, Örçen et al., (2017) reported the expression of P2Y1 in undifferentiated SH-SY5Y cells alongside P2Y2, P2Y4 and P2Y6, P2Y12 and P2X7. Another study reported that SH-SY5Y cells expressed a high level of P2X7, P2Y4 and P2Y11, while P2Y1, P2Y2, P2Y6 and P2Y14 were not detected. It has been shown that P2X7

stimulation via ATP promotes neuroblastoma cell growth. Furthermore, because the SH-SY5Y neuroblastoma cell line has a high P2Y4 receptor expression, this receptor may be implicated in neuronal differentiation (Puchałowicz et al., 2014). Little is known about the expression of P2 receptors in the differentiated neuron. Our current results showed for the first time the expression of P2 receptors in differentiated SH-SY5Y cells. In the next section, we focused on P2X2, P2X3 and P2X7 and whether they have a functional role, especially in differentiated cells, as P2X7 has already been previously reported in the undifferentiated state. The P2X7 receptor is a particularly essential receptor isoform. It is activated by high ATP concentrations (>100 M), which are exclusively found in pathology (Puchałowicz et al., 2014; Carroll et al., 2009). P2X7 are present in several parts of the nervous system including microglia, astrocytes, oligodendrocytes and neurons. The presence of P2X7 receptors in neurons was previously unknown because of the poor specificity of antibodies and ligands used (Anderson & Nedergaard, 2006). However, later research employing new pharmacological and biomolecular methods revealed that P2X7 receptors are widely expressed in neurons in several brain areas (Puchałowicz et al., 2014; Engel et al., 2012). Previously a study identified the expression of the P2X7 receptor in neurons or neuron-like cells in rodents. Moreover, it has been demonstrated that P2X7 mRNA is found in neurons of the rat retina ganglion cell layer (Braendle et al., 1998). Since then, the P2X7 receptor has been demonstrated to play a key role in several aspects of neuronal physiology, including axonal elongation and branching, as well as neurotransmitter release (Miras-Portugal et al., 2017). Several studies reported that the P2X7 receptor plays a crucial role in nervous system diseases, immune response, osteoporosis and cancer. Recently, many studies indicated that the P2X7 receptor is also implicated in cardiovascular disease (Chen et al., 2018).

5.4.3 P2X7 receptor activation elicits intracellular calcium responses in undifferentiated and differentiated SH-SY5Y cells

Undifferentiated and differentiated SH-SY5Y cells expressed mRNA for almost all subtypes of P2X and P2Y receptors, excluding P2Y1, which was not expressed in undifferentiated SH-SY5Y cells, and P2X1 and P2Y6 which were not expressed in differentiated cells. To determine whether the P2 receptors expressed in undifferentiated and differentiated SH-SY5Y cells were functionally active, nucleotide-evoked Ca^{2+} responses were measured by applying exogenous nucleotides including ATP, BzATP, and α, β-Me-ATP. The mobilisation of intracellular Ca^{2+} in response to receptor activation is regarded as an important component of cellular signalling responsible for various cellular processes including

proliferation, apoptosis, differentiation and motility (Berridge et al., 2000; Berridge, 1997). The mobilization of Ca^{2+} in cells can be accomplished via the activation of P2X and P2Y receptors by nucleotides such as ATP (Puchalowicz et al., 2014). In agreement with others (Per Larsson et al., 2002), our results showed that ATP and BZATP significantly induced intracellular Ca^{2+} responses in both cell types with no difference between both cell types in response to these nucleotides. Only undifferentiated SH-SY5Y cells showed a significant increase in intracellular Ca^{2+} in a response to α, β-Me-ATP. Moreover, the P2X7 antagonist A438079 could inhibit BzATP-induced responses, suggesting the functional role of P2X7 in eliciting intracellular Ca^{2+} release. However, the role of the P2X7 receptor in the differentiated SH-SY5Y cells into neurons is less researched and still unclear. Regarding the undifferentiated SH-SY5Y cells, it was reported that the separate application of 300-100 µM of BzATP and 1-2 mM ATP resulted in a rapid promotion of intracellular Ca^{2+} release in undifferentiated neuronal SH-SY5Y cells by the opening of voltage-dependent Ca^{2+}channels of mainly the L-type, and transmitter release. These results corroborate with the ones found in the current study. Conversely, α, β-Me-ATP was ineffective, whilst the current study showed that α, β-Me-ATP led to a rapid elevation in intracellular Ca^{2+} (Per Larsson et al., 2002). In contrast to our current study, 300 µM BzATP prevented intracellular-free Ca^{2+} mobilization in SH-SY5Y cells differentiated by retinoic acid (Orellano et al., 2010). It was previously suggested that most neurons in rat and mouse sympathetic ganglia have responses to ATP, but not to α, β-Me-ATP (Dunn et al., 2001). Nevertheless, a few neurons in sympathetic ganglia responded to α, β-Me-ATP according to Calvert & Evans, (2004). A functional study in the rat superior cervical ganglion reported that the sympathetic neurons were more responsive to ATP and α, β-Me-ATP at birth and during the early postnatal period, due largely to the expression of the P2X3 receptor, but these responses were lower in mature rats (Dunn et al., 2005), which is in close agreement with the current study. Moreover, Orellano examined the effect of UTP, a potent P2Y nucleotide receptor agonist, on undifferentiated SH-SY5Y cells. The results showed that UTP did not induce intracellular-free Ca^{2+} mobilization of undifferentiated SH-SY5Y cells. Furthermore, it was reported by RT-PCR that the expression of P2X7 mRNA in undifferentiated SH-SY5Y cells and differentiated cells, was not changed after retinoic acid treatment. However, Western blot analysis described that the protein level of P2X7 was significantly reduced in retinoic acid-differentiated SH-SY5Y cells as a result of post-transcriptional mechanisms induction and that mediated the protection of retinoic acid-differentiated cells from cell death induced by exposure to extracellular nucleotides, while no changes were seen in the undifferentiated cells (Orellano et al., 2010). Another previous study in rat retinal ganglion cells showed that short exposure for the 2-minute duration of 10 µM

BzATP resulted in a large, continued increase in Ca^{2+} while sustained stimulation of the receptor could lead to cell death (Zhang et al., 2005). It has been reported that the exposure of the nerve endings of the cortex, striatum, midbrain, hippocampus and cerebellum to ATP and BzATP induced intrasynaptosomal Ca^{2+} increases that are sensitive to extracellular divalent cation concentration and specific P2X7 receptor antagonists including A438079 (Miras-Portugal et al., 2017). Another previous study used alpha-synuclein, a neuronal protein that regulates synaptic vesicle trafficking and subsequent neurotransmitter release, that interacts with neuronal P2X7 inducing intracellular free Ca^{2+} mobilization in neuronal cells (Wilkaniec et al., 2020). The application of 10 μM of extracellular ATP led to an increase in Ca^{2+} in glial cells and neurons of rat superior cervical ganglion (Kumagai& Saino,2000). In cerebellar granule neurons, 50 μM BzATP and 100 μM α, β-Me-ATP promoted intracellular Ca^{2+} upon to P2X7 receptor activation mediated by calcium⁄calmodulin-dependent protein kinase II (CaMKII) activation (León et al., 2006). Previously, it has been shown in the rat superior cervical ganglion that the exposure of 10 μM α, β-Me-ATP caused a Ca^{2+} increase in satellite cells but not in neurons (Kumagai& Saino,2000) which is in close agreement with the current study. A previous study in superior cervical ganglion neurons from P2X1 receptor-deficient mice showed that the changes in intracellular Ca^{2+} in response to 100 μM ATP were not significantly different from that of the WT. Moreover, 100 μM α, β-Me-ATP (an agonist at receptors containing P2X1, P2X3, or P2X6 receptor) caused an increase in intracellular Ca^{2+} in only 1.7% of the neurons that were responsive to ATP, indicating that there was no significant response of intracellular Ca^{2+} entrance upon the activation of P2X1 (Calvert & Evans, 2004). It has been demonstrated in a previous study in rat sympathetic superior cervical ganglion neurons are more responsive to ATP and α, β-Me-ATP at birth and during the early postnatal period, as a result of the P2X3 expression, however, these responses were significantly decreased in mature rats (Dunn et al., 2005). Taking this information into account, in addition to our results, P2X7 nucleotide receptors are primarily responsible for BzATP-induced responses during neuronal differentiation. Together, whether P2X7 abolished or induced intracellular Ca^{2+} responses, P2X7 receptors could be a significant therapeutic target for a wide range of neurological diseases.

Finally, the side-by-side comparison of carbachol-evoked intracellular Ca^{2+} responses showed a significant difference in Ca^{2+} profiles of the two cell types. The main was that undifferentiated SH-SY5Y cells had a smaller magnitude of carbachol-evoked Ca^{2+} response in comparison to the differentiated cells. According to Kovalevich & Langford. (Kovalevich & Langford, 2013) both muscarinic and nicotinic acetylcholine are expressed in SH-SY5Y cells. In addition, both undifferentiated and differentiated cells have G-protein coupled

muscarinic receptors on their membranes, although their levels and binding characteristics are regulated differently depending on the differentiation procedure. For example, the treatment of the cells with retinoic acid increased the number of muscarinic binding sites, whereas phorbol esters treatment reduced it. Moreover, both phorbol esters - and retinoic acid-treated cells induced a significant increase in acetylcholinesterase activity compared to undifferentiated cells, and this is in agreement with our previous study. It has been previously suggested that the release of NA by retinoic acid-differentiated SH-SY5Y cells increased in response to carbachol stimulation (Kovalevich & Langford, 2013). This explanation could support the enhancement of NA release in differentiated cells confirming the adrenergic phenotype of these cells.

5.5 Summary

Our results showed that retinoic acid-treated SH-SY5 cells differentiated into adrenergic neuron-like cells and induced morphological changes in SH-SY5Y cells such as branched neurites extending and rounded cells. Based on these findings we identified retinoic acid treatment under serum-free serum conditions as optimal conditions for adrenergic neuronal differentiation of the SH-SY5Y cells in our hands. A comparison for mRNA levels of all P2 purinergic receptors had never been performed in undifferentiated or differentiated SH-SY5Y cells. Almost all purinergic receptors were expressed at the transcriptional level in both cell types, excluding P2X1 and P2Y6 which were absent in differentiated cells, and P2Y1, which was not expressed in undifferentiated cells. Our results suggest that the BzATP promoted responses in differentiated cells are principally mediated by P2X7 nucleotide receptors. Based on such results and previous findings (Per Larsson et al., 2002), ATP is coreleased with other neurotransmitters, activation of the P2X7 receptor, in combination with other transmitter-activated receptors may serve a physiological role in altering Ca^{2+} signalling processes in neuronal tissues. The data outlined in this chapter identifies that P2X7 receptors are functionally active in differentiated SH-SY5Y cells.

Chapter 6

6.1 Key findings

6.1.1 mRNA expression of neuronal and vascular markers in mouse superior cervical ganglion, superior mesenteric artery and carotid artery

In this study, RT-PCR was performed to determine which type of perivascular nerves were predominant in mouse superior mesenteric artery and carotid artery. The superior cervical ganglion expressed PGP 9.5, TH, CGRP, α-SMA and vWF but VAChT, SP and nNOS were not expressed. These results indicated that the superior cervical ganglion has mostly sympathetic properties and could express sensory neurons. The superior mesenteric artery and carotid artery had a similar expression pattern, however, CGRP was not detected in the carotid artery. These results suggested that although the arteries were mostly innervated by sympathetic nerves, however, further investigations were required to confirm whether these blood vessels are innervated via sensory nerves. All tissues strongly expressed α-SMA and vWF as markers of the presence of smooth muscle cells and endothelial cells respectively. VAChT was absent in the three tissues studied, suggesting the absence of cholinergic properties in these tissues. Our results indicated the presence of the perivascular nerves in the arterial tissues. These nerves could be mostly sympathetic and arise from sympathetic ganglion via post-ganglionic axons. However, further immunohistochemical studies are required to confirm the presence of PGP9.5 and TH protein and the absence of parasympathetic phenotype in the tissues. The results showed that the tissues could also be innervated by sensory nerves due to the presence of CGRP, and Immunohistochemical studies could confirm that as well.

6.1.2 mRNA expression of P2X and P2Y receptor subtypes in mouse superior cervical ganglion, superior mesenteric artery and carotid artery

This project aimed to provide the first characterisation of the expression of all P2 purinergic receptors in the mouse sympathetic superior cervical ganglion and the perivascular nerves in superior mesenteric and carotid arteries at the mRNA and protein level, focussing specifically on their expression in the cell bodies of the superior cervical ganglion and the pre-junctional terminal of sympathetic nerves in the arteries. Our present result showed that amplified PCR products of the expected sizes were obtained for all P2X1-7 receptors in the superior cervical ganglion. In mouse mesenteric artery and carotid artery, P2X1, P2X4 and P2X7 mRNA revealed specific bands of the same size as the amplified target fragments. However, mRNAs for P2X2, P2X3, P2X5 and P2X6 were not detected the arteries. In addition,

the results showed mRNAs for all P2Y receptors (except P2Y11) were identified in the superior cervical ganglion. In mouse superior mesenteric artery, PCR products for P2Y1 (faint band), P2Y2, P2Y6, P2Y13 and P2Y14 receptors were amplified. Additionally, P2Y2, P2Y6, P2Y13 and P2Y14 could be expressed in the carotid artery, but not P2Y1 receptors. Perivascular sympathetic nerves arise from post-ganglionic efferent axons and form a plexus within the adventitia, with their cell bodies placed in the paravertebral ganglia (McLachlan, 2003). In addition, perivascular nerves are located in the adventitial layer of blood vessels and do not make direct contact with smooth muscle cells or endothelial cells (Westcott & Segal, 2013). Taken altogether, we suggested that receptor subtypes detected in sympathetic ganglia but not arteries (particularly P2X2, P2X3, P2Y1, and less likely P2X7) could be expressed by sympathetic post-ganglionic nerves that innervate arteries. Here they could serve as pre-junctional receptors, regulating the release of NA, ATP or NPY from sympathetic varicosities. Further investigations using immunohistochemical experiments were required to explore the colocalisation of P2X with neuronal markers such as PGP9.5 and TH to confirm the presence of these receptors on perivascular nerves of the blood vessels. Pre-junctional receptors could be able to regulate the release of various neurotransmitters via feedback loops, making them a useful therapeutic target.

6.1.3 Protein expression of P2 purinergic receptors on sympathetic neurons in mouse superior cervical ganglion and pre-junctional sympathetic nerves in superior mesenteric arteries and carotid arteries

Colocalisation studies of the P2 receptors with several markers were performed, these markers include PGP9.5 as a general marker of neurons, TH as an adrenergic sympathetic marker of neurons, VNUT as a marker of the vesicular storage of ATP, and NPY as a marker of vasomotor neurons. Immunofluorescence doubling labelling for PGP9.5 and P2 receptors revealed coexpression of PGP9.5 with all receptors studied (P2X1, P2X2, P2X3, P2X4, P2X7 and P2Y1) except P2X6 which was not expressed in the superior cervical ganglion. In addition, our results illustrated that six P2 receptor subtypes were found on between 70-90 % of neurons in the superior cervical ganglia at different intensities. These results also presented that the ganglion neurons showed variable levels of staining for PX1, P2X2, P2X3, P2X4, P2X7 and P2Y1 receptors, indicating the diversity of receptor subtypes involved in the physiological functions of different neurons. This study also suggested that many neurons could express numerous isoforms of P2 receptors in the same nerve cell body because over 70% of neurons were labelled by most of the antibodies. Few ganglionic cells did not show coexpression

between PGP9.5 and P2 receptors (labelled for P2 receptor only) and that could indicate these receptors could have coexpression with other ganglionic cells such as glial cells and small intensely fluorescent cells. Furthermore, we found many neurons in the superior cervical ganglion were strongly positive for TH as ~ 98% of the PGP9.5-positive cell bodies showed TH positivity. These results suggested the superior cervical ganglion neurons were mostly sympathetic, but other types of neurons could be placed in the superior cervical ganglion, such as sensory neurons, and that required further investigations using specific markers. We also found the sympathetic neurons (TH-positive neurons) expressed variable levels of staining for PX1, P2X2, P2X3, P2X4, P2X7 and P2Y1. However, few P2 nerve cell bodies did not appear colocalised with the sympathetic neurons and that may indicate that these receptors could be expressed by other types of neurons in the superior cervical ganglion.

Immunofluorescence doubling labelling for VNUT and PGP9.5 revealed most neurons in the superior cervical ganglion were strongly positive for VNUT (~ 80%) of the PGP9.5-positive nerve cell bodies showed VNUT positivity. The result suggested that 80% of neurons in the superior cervical ganglion are capable of vesicular storage of ATP. Moreover, immunofluorescence doubling labelling for VNUT with P2X2, P2X3 and P2Y1 receptors showed variable levels of the coexpression of VNUT with the P2 receptors studied. Thus, it was suggested that VNUT might play an important role in the regulation of ATP and purinergic signalling in superior cervical ganglion through the accumulation of ATP in the neurons. Taken together, we suggest that the receptor subtypes detected in sympathetic ganglia but not arteries could be expressed by sympathetic post-ganglionic nerves that innervate arteries. Thus, these receptors could be transferred during the neurotransmission process to perivascular sympathetic nerves of the pre-junctional terminal of the tissues, and that was confirmed by immunohistochemical studies in mouse superior mesenteric artery and carotid artery. Here they could serve as pre-junctional, regulating the release of neurotransmitters from sympathetic varicosities.

The innervation pattern of perivascular nerves in mouse superior mesenteric artery and common carotid artery, in addition to the presence of candidate P2 receptors on the pre-junctional nerves, was investigated. Superior mesenteric arteries labelled for TH also revealed a network of neuronal fibres located within a dense layer at the level of the adventitia similar to PGP 9.5. Double immunolabelling for PGP 9.5 and TH revealed that most of the nerve fibres that contained PGP 9.5 also contained TH, however a small population of nerve fibres that contained PGP 9.5 did not contain TH. The results also demonstrated that although the carotid artery was labelled for PGP 9.5, the carotid artery did not show immunoreactivity for TH,

suggesting that the carotid artery could not be innervated via the sympathetic nerves arising from sympathetic ganglia and other innervation phenotypes could be implicated such as sensory innervation. Thus, it would be useful to investigate more in future about innervation patterns of the blood vessels using other neurons markers such as markers of sensory neurons, parasympathetic neurons and cholinergic neurons. Double immunolabelling for PGP 9.5 and the P2 receptor of whole-mount preparations of the superior mesenteric artery revealed the majority of the nerve fibres showed colocalisation of PGP 9.5 with P2X2, P2X3, P2X4, P2X7 receptors, However, PGP9.5 nerves came into close contact, and few of nerves were merged with P2X1 and P2Y1. Double immunolabelling for PGP 9.5 and the P2 receptor of whole-mount preparations of the carotid artery revealed the majority of the nerve plexus showed colocalisation of PGP 9.5 and P2X2, P2X3, P2X4 and P2Y1 receptors, whilst P2X1, and P2X7 immunoreactivities were absent. However, both the superior mesenteric artery and carotid artery did not show immunoreactivity for the P2X6 receptor. Finally, to investigate NPY-positive neurons which may identify which neurons have vasomotor activities and could be able to innervate target tissues such as blood vessels and glands. The whole-mount preparations of superior mesenteric artery from transgenic NPY-GFP mice consistently displayed immunopositive nerves for NPY, but not the carotid artery. That suggested, that although 40 % of the superior cervical ganglion neurons stained positive for NPY, the NPY-positive neurons in the superior cervical ganglion were not involved in the sympathetic innervation of the carotid artery. Thus, the nerves through the carotid artery could arise from the carotid body and innervate other tissues such as the heart and saliva glands (Potter et al, 1987). Positive correlations were observed between the P2X2, P2X3 and P2Y1 nerve fibres and numbers of NPY nerves in the superior mesenteric artery.

As a result of both RT-PCR and immunohistochemistry studies in the superior cervical ganglion, superior mesenteric artery and carotid artery (Table 6.1), we could propose that P2X2, P2X3, P2X7 and could be expressed by sympathetic post-ganglionic nerves that innervate arteries. Thus, they might present in pre-junctional nerves within the adventitial layer of the arteries studied (except P2X7 was absent in the carotid artery) but not in the smooth muscle cells and the endothelium. As previously reported in several studies, P2X1 and P2X4 can be present in the smooth muscle cells and the endothelium of the mouse mesenteric artery (Lewis & Evans, 2001), however, P2X7 was still controversial. Our present results indicated the presence of P2X7, in addition to P2X1, P2X4 and P2Y1, in the perivascular nerve of the superior mesenteric artery. Thus, these receptors (P2X2, P2X3, P2X7 and P2Y1) might serve as pre-junctional and could be able to regulate the release of various neurotransmitters via

feedback loops, which could potentially provide a novel target for the therapeutic control of vascular tone and blood pressure.

Table 6.1: An overview of mRNA and protein expression for P2 receptors in the mouse superior cervical ganglion, superior mesenteric artery and carotid artery.

Receptor	Tissue	Expression by RT-PCR	Expression by IHC	Tissue	Expression by RT-PCR	Expression by IHC	Tissue	Expression by RT-PCR	Expression by IHC
P2X1	Superior cervical ganglion	+	+	Superior mesenteric artery	+	+	Carotid artery	+	-
P2X2		+	+		-	+		-	+
P2X3		+	+		-	-		-	+
P2X4		+	+		+	+		+	+
P2X5		+	Not Examined		-	Not Examined		-	Not Examined
P2X6		+	-		-	-		-	-
P2X7		+	+		+	+		+	-

Receptor	Tissue	Expression by RT-PCR	Expression by IHC	Tissue	Expression by RT-PCR	Expression by IHC	Tissue	Expression by RT-PCR	Expression by IHC
P2Y1	Superior cervical ganglion	+	+	Superior mesenteric artery	+	+	Carotid artery	+	-

A (+) sign indicates that the gene was detected and a (–) sign indicates that the gene was not detected. The results shown are representative from five independent experiments using five different mice. IHC; Imminhistochemistry

6.1.4 Expression of P2X and P2Y receptors in human undifferentiated SH-SY5Y and differentiated cells

Following the confirmation of differentiation of SH-SY5Y into neurons by morphological changes and by increased NPY expression, RT-PCR was employed to compare the expression of mRNA transcripts for P2 receptors between the undifferentiated and differentiated SH-SY5Y cells. The mRNA transcripts for all P2X receptors (P2X1-7) and all P2Y receptors (except P2Y1) were repeatedly expressed in undifferentiated SH-SY-5Ycells. While differentiated SH-SY5Y cells expressed all subtypes of P2X and P2Y receptors with the exception of P2X1 and P2Y6. Taken together, the results of this study indicated that there were differences in the expression of P2X and P2Y receptors between undifferentiated and differentiated SH-SY5Y cells. We found P2X1 and P2Y6 were expressed in undifferentiated SH-SY5Y cells while they were absent in differentiated cells. Furthermore, P2Y1 was present in the differentiated SH-SY5Y cells, whilst was not expressed in undifferentiated SH-SY5Y cells. The results of this study indicated several novel findings with respect to the expression of P2 receptors in both cell types. Moreover, immunofluorescence experiments revealed the coexpression of P2X2, P2X3, and P2X7 with TH in undifferentiated and differentiated SH-SY5Y cells. Both undifferentiated and differentiated SH-SY5Y cells showed a moderate level of TH immunoreactivity and colocalisation with the P2X receptors studied, which confirmed the adrenergic phenotype in both cell types. These results led us to investigate more about the functional role of these receptors using P2 receptors agonists including ATP, α, β-Me-ATP and BzATP to study nucleotide-evoked Ca^{2+} responses in undifferentiated and differentiated SH-SY5Y cells.

6.1.5 Nucleotide-evoked calcium responses in undifferentiated and differentiated SH-SY5Y cells

To determine whether the P2 receptors expressed in undifferentiated and differentiated SH-SY5Y cells were functionally active, exogenous nucleotides were applied and real-time monitoring of intracellular Ca^{2+} levels was performed. In undifferentiated SH-SY5Y cells, significant increases in intracellular Ca^{2+} were detected upon application of 300 μM to 2 mM ATP, whilst significant increases in intracellular Ca^{2+} were detected following application of concentrations above 1 mM in the differentiated cells. Statistical analysis showed no significant difference in Ca^{2+} responses was seen between both cells following the application of ATP. In undifferentiated SH-SY5Y cells, a significant concentration-dependent increase in the

intracellular Ca^{2+} level was observed upon the application of 1mM and 300 μM α, β-Me-ATP. Whereas no significant increases in intracellular Ca^{2+} were detected in differentiated SH-SY5Y cells, suggesting heteromeric P2X receptors are involved in the ATP-evoked Ca^{2+} responses in undifferentiated SH-SY5Y cells but not differentiated cells. The application of BzATP concentrations ≥100 μM caused a significant increase in intracellular Ca^{2+} responses in undifferentiated and differentiated cells. However, no significant difference was seen between undifferentiated and differentiated cells in the response of BzATP. Pre-incubation of both undifferentiated and differentiated SH-SY5Y cells with 10 μM A438079, the selective P2X7 antagonist, inhibited the magnitude of 300 μM BzATP-evoked Ca^{2+} responses in both cell types. However, A438079 could not significantly inhibit responses induced by 100 μM BzATP. These results suggested that the P2X7 receptor was involved in the ATP-evoked Ca^{2+} response. Interestingly, it was seen that carbachol-evoked Ca^{2+} response in differentiated neurons was significantly higher than in undifferentiated SH-SY5Y cells, suggesting the cholinergic phenotype of neurons more than the undifferentiated cells. Wire myography is a good method to investigate the functional role of P2 receptors but were unable to do and I would suggest that for future work.

6.2 Future work

A number of findings in this thesis have raised additional questions that could extend this research in several directions. The research presented in this thesis provides an excellent insight into the expression of P2 purinergic receptors in mouse sympathetic ganglia and perivascular nerves in superior mesenteric artery and carotid artery. However, the research presented here also exposes many potential avenues to pursue in the future. One of these potential areas of interest is determining the functional role of pre-junctional P2 receptors (P2X2, P2X3, P2X7 and P2Y1) in mouse mesenteric artery and carotid artery using wire myography. Perivascular nerves can be activated by electrical field stimulation of arterial ring preparations. Pharmacology can be used to block P2X and P2Y function and contraction and relaxation of arterial rings could be quantified by wire myography. In this study, I was able to identify the expression of many P2 receptors in human SH-SY5Y cells and differentiated SH-SY5Y cells, which appear to be involved in nucleotide-evoked Ca^{2+} responses. Further exploration of the possible functional roles of the other P2 receptors, in particular P2X7 receptors which appear to be involved in Ca^{2+} signalling, would be an excellent way to extend the findings presented here. Finally, data demonstrated here that sympathetic nerves might not be involved in the innervation of mouse carotid artery via superior cervical ganglion, thus it would be interesting to explore more about the innervation patterns of the carotid artery, using different neuron markers such as CGRP and SP, as markers of sensory neurons, and whether the carotid body is implicated in the innervation. In addition, it would be also interesting to investigate more about the expression and the function of purinergic receptors in the carotid body. It would also be good to consider potential experiments, such as proximity ligation assays or electron microscopy, to determine if the subunits form heteromeric channels. It would be also important to establish whether the presynaptic receptors are autoreceptors or heteroreceptors. The research presented in this thesis has hopefully served as a foundation for future research into the functional roles of purinergic transmission in sympathetic neurons.

6.3 Conclusion

P2 receptors are widely expressed throughout the cardiovascular system, and their effects include modulation of heart function, vascular tone, angiogenesis, and inflammation. Their widespread expression in the vasculature identifies purine receptors as potential targets for the development of novel drugs to treat cardiovascular disease. At the beginning of this project, I set out to meet three key aims: to characterise the P2 receptor profile in mouse superior cervical ganglion and perivascular nerves in arteries using RT-PCR, to confirm the presence of P2 receptors in perivascular sympathetic nerves in arteries using antibodies against P2 receptors in colocalisation studies with neuronal markers such as PGP9.g and TH, and to identify nucleotide-evoked responses in human undifferentiated SH-SY5Y cells and differentiated SH-SY5Y cells. During this study, I have determined by RT-PCR that almost all the known subtypes of P2 receptors are expressed in mouse superior cervical ganglion (except P2Y11). Moreover, I found that P2X2, P2X3, P2X7 and P2Y1 receptors were expressed on perivascular nerves of superior mesenteric arteries and carotid arteries. Using single- and double-labelling immunofluorescence techniques, the present study demonstrated that P2X2, P2X3, P2X7 and P2Y1-immunoreactive nerve fibre terminals are widely distributed in mouse superior mesenteric artery as well as in neurons in the superior cervical ganglion, suggesting they could be expressed by sympathetic post-ganglionic nerves that innervate arteries. Here they could serve as pre-junctional, regulating the release of NA, ATP or NPY from sympathetic varicosities. This will not only determine the function of the sympathetic nervous system in health and disease, but also the therapeutic and untoward effects of drugs that bind to the pre-junctional receptors in sympathetically innervated tissues. Although I was unable to uncover the physiological role of purinergic signalling in the pre-junctional nerve terminal of arteries, I believe that I have successfully met all of my initial aims. Furthermore, I found all P2X receptors (P2X1-7) and all P2Y receptors (except P2Y1) were expressed in undifferentiated SH-SY-5Ycells. While differentiated SH-SY5Y cells expressed all subtypes of P2X and P2Y receptors except P2X1 and P2Y6. Interestingly, I found only P2X7 receptors are involved in nucleotide-evoked Ca^{2+} responses in both cell types, whereas other P2X receptors could be functionally active in human SH-SY5Ycells however further investigations are required to identify which other P2X receptors subtypes are involved. The P2X7 receptor may be an emerging therapeutic target for some cardiovascular diseases such as hypertension. I hope that this finding will help in future efforts to manage the detrimental effects of P2 receptors in the treatment of hypertension.

Appendix

Western blot analysis was performed to determine P2 purinergic receptor expression in total protein extracted from mouse brain and superior cervical ganglion. In addition, Western blot analysis confirmed the specificity of our antibodies. P2X3 was tested using different antibodies. P2X3 antibodies (Alomone - APR-016, Abcam - AB-10269), both antibodies detected a band at (~ 100 kDa) and (~ 35 kDa) respectively, which are at unexpected product sizes of P2X3. These bands could be non-specific bands of P2X (Figure A1.A & A.1.B). The expected product size for P2X3 is (~ 45 kDa). The protein samples were treated with 1 µl PNGase F (New England Biolab, P0708), which is an improved reagent for the deglycosylation of different isotypes of antibodies and antibody-fusion proteins by removing almost all *N*-linked oligosaccharides from glycoproteins. The samples were then incubated at 37^{o}C for 1 hour. Then the Western blot protocol in chapter 2 (section 2.14) was performed. However, a band at the same unexpected product size was detected when the Anti P2X3 antibody (Alomone - APR-016) was used (Figure A1.A). Also, non-specific bands were detected for P2Y1 at (~25kDa, in the brain) and at (~75 kDa, in superior cervical ganglion) when the anti P2Y1 antibody (Alomone - APR-009) was applied. The expected product size for P2Y1 is (~ 45 kDa) (Figure A.1.C).

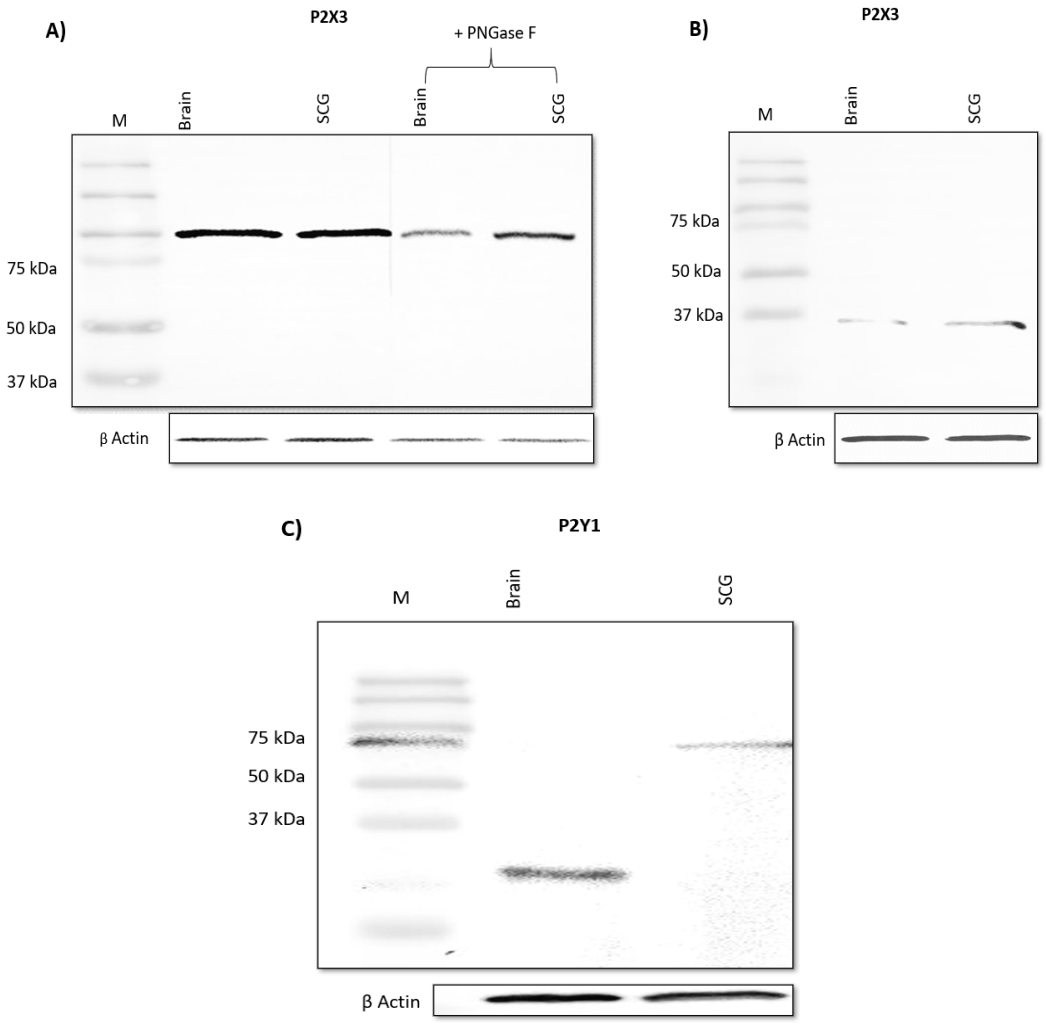

Figure A.1: **Western blotting of P2X3 and P2Y1 receptors in the mouse brain and superior cervical ganglion**. Lane 1 of the blots **(A-B)** contains the positive controls for each receptor protein and includes the mouse brain. The brain detected a non-specific band for the P2X3 receptor at (~100 kDa with APR 016, Fig A) and at (~35 kDa with AB-10269, Fig B). Lane 1 of the blot **(C),** the brain detected a non-specific band for P2Y1 receptors at (~25 kDa). Lane 2 of blots **(A-B)** showing a non-specific band for P2X3 at (~100 kDa with APR 016, Fig A) and at (~35 kDa with AB-10269, Fig B) in the superior cervical ganglion. Lane 2 of the blot **(C),** The superior cervical ganglion detected a non-specific band for P2Y1 receptors at (~75 kDa). Lane 3 and 4 of the blot **(A)** include the brain and the superior cervical ganglion protein treated with PNGase F, both brain and superior cervical ganglion detected a non-specific band for P2X3 receptor at (~100 kDa with APR 016). β actin served as a loading control. M represents the molecular weight marker. 30 μg protein/lane. Dilution used for P2X3 (1:500) for both antibodies; dilution used for P2Y1 (1:200). The results shown are representative from three independent experiments using three different mice.

References

Abbracchio, M. P. (2006). Update on the P2Y G protein-coupled nucleotide receptors: from molecular mechanisms and pathophysiology to therapy. *Pharmacol Rev*, *58*, 281-341.

Abbracchio, M. P., & Ceruti, S. (2006). Roles of P2 receptors in glial cells: focus on astrocytes. Purinergic signalling, 2(4), 595-604.

Abbracchio, M. P., Burnstock, G., Boeynaems, J. M., Barnard, E. A., Boyer, J. L., Kennedy, C., ... & Weisman, G. A. (2006). International Union of Pharmacology LVIII: update on the P2Y G protein-coupled nucleotide receptors: from molecular mechanisms and pathophysiology to therapy. Pharmacological reviews, 58(3), 281-341.

Abbracchio, M. P., Burnstock, G., Verkhratsky, A., & Zimmermann, H. (2009). Purinergic signalling in the nervous system: an overview. Trends in neurosciences, 32(1), 19-29.

Abualsaud, N., Caprio, L., Galli, S., Krawczyk, E., Alamri, L., Zhu, S., ... & Kitlinska, J. (2021). Neuropeptide Y/Y5 Receptor Pathway Stimulates Neuroblastoma Cell Motility Through RhoA Activation. *Frontiers in Cell and Developmental Biology*, 1849.

Agholme, L., Lindström, T., Kågedal, K., Marcusson, J., & Hallbeck, M. (2010). An in vitro model for neuroscience: differentiation of SH-SY5Y cells into cells with morphological and biochemical characteristics of mature neurons. *Journal of Alzheimer's disease*, *20*(4), 1069-1082.

Ali, S. (2019). Purinergic signalling in human adipose-derived mesenchymal stromal cells and in vitro differentiated adipocytes (*Doctoral dissertation, University of East Anglia*).

Andani, R., & Khan, Y. S. (2020). Anatomy, head and neck, carotid sinus.

Anderson, C. M., & Nedergaard, M. (2006). Emerging challenges of assigning P2X7 receptor function and immunoreactivity in neurons. *Trends in neurosciences*, *29*(5), 257-262.

Ansari, H. R., Nadeem, A., Tilley, S. L., & Mustafa, S. J. (2007). Involvement of COX-1 in A3 adenosine receptor-mediated contraction through endothelium in mice aorta. *American Journal of Physiology-Heart and Circulatory Physiology*, 293(6), H3448-H3455.

Antonio, L. S., Costa, R. R., Gomes, M. D., & Varanda, W. A. (2009). Mouse Leydig cells express multiple P2X receptor subunits. *Purinergic signalling*, *5*(3), 277-287.

Arthur, D. B., Taupenot, L., & Insel, P. A. (2007). Nerve growth factor-stimulated neuronal differentiation induces changes in P2 receptor expression and nucleotide-stimulated catecholamine release. *Journal of neurochemistry*, *100*(5), 1257-1264.

Atkinson, L., Batten, T. F. C., & Deuchars, J. (2000). P2X2 receptor immunoreactivity in the dorsal vagal complex and area postrema of the rat. *Neuroscience*, *99*(4), 683-696.

Babick, A., Elimban, V., Zieroth, S., & Dhalla, N. S. (2013). Reversal of cardiac dysfunction and subcellular alterations by metoprolol in heart failure due to myocardial infarction. Journal of cellular physiology, 228(10), 2063-2070.

Baffi, J., Go, T., Slowik, F., Horva, M., Lekka, N., Pa, E., & Palkovits, M. (1992). Neuropeptides in the human superior cervical ganglion. *Brain research*, *570*(1-2), 272-278.

Baffi, J., Go, T., Slowik, F., Horva, M., Lekka, N., Pa, E., & Palkovits, M. (1992). Neuropeptides in the human superior cervical ganglion. *Brain research*, *570*(1-2), 272-278.

Balashova, A., Pershin, V., Zaborskaya, O., Tkachenko, N., Mironov, A., Guryev, E., ... & Mukhina, I. (2019). Enzymatic digestion of hyaluronan-based brain extracellular matrix in vivo can induce seizures in neonatal mice. *Frontiers in neuroscience*, *13*, 1033.

Barja, F., Mathison, R., & Huggel, H. (1983). Substance P-containing nerve fibres in large peripheral blood vessels of the rat. *Cell and tissue research*, *229*(2), 411-422.

Barton, M., & Haudenschild, C. C. (2001). Endothelium and atherogenesis: endothelial therapy revisited. Journal of cardiovascular pharmacology, 38, S23-S25.

Bean, B. P. (1990). ATP-activated channels in rat and bullfrog sensory neurons: concentration dependence and kinetics. *Journal of Neuroscience*, *10*(1), 1-10.

Bell, M., & Zempel, H. (2021). SH-SY5Y-derived neurons: a human neuronal model system for investigating TAU sorting and neuronal subtype-specific TAU vulnerability. *Reviews in the Neurosciences*.

Bernier, L. P., Ase, A. R., & Séguéla, P. (2018). P2X receptor channels in chronic pain pathways. *British journal of pharmacology*, *175*(12), 2219-2230.

Berridge, M. J. (1997). Elementary and global aspects of calcium signalling. *The Journal of experimental biology*, *200*(2), 315-319.

Berridge, M. J. (2002). The endoplasmic reticulum: a multifunctional signaling organelle. *Cell calcium*, *32*(5-6), 235-249.

Berridge, M. J., Lipp, P., & Bootman, M. D. (2000). The versatility and universality of calcium signalling. *Nature reviews Molecular cell biology*, *1*(1), 11-21.

Berridge, MJ, Bootman, MD & Roderick, HL (2003). Calcium signalling: dynamics, homeostasis and remodelling. *Nat Rev Mol Cell Biol*, 4, 517-29

Biedler, J. L., Helson, L., & Spengler, B. A. (1973). Morphology and growth, tumorigenicity, and cytogenetics of human neuroblastoma cells in continuous culture. *Cancer research*, *33*(11), 2643-2652.

BioRender. (2022). Retrieved 9 June 2022, from https://app.biorender.com/gallery.

Birch, D. J., Turmaine, M., Boulos, P. B., & Burnstock, G. (2008). Sympathetic innervation of human mesenteric artery and vein. *Journal of vascular research*, *45*(4), 323-332.

Birch, D., Knight, G. E., Boulos, P. B., & Burnstock, G. (2008). Analysis of innervation of human mesenteric vessels in non-inflamed and inflamed bowel–a confocal and functional study. *Neurogastroenterology & Motility*, *20*(6), 660-670.

Birch, D., Knight, G. E., Boulos, P. B., & Burnstock, G. (2008). Analysis of innervation of human mesenteric vessels in non-inflamed and inflamed bowel–a confocal and functional study. *Neurogastroenterology & Motility*, *20*(6), 660-670.

Bisognano, J. D., Bakris, G., Nadim, M. K., Sanchez, L., Kroon, A. A., Schafer, J., ... & Sica, D. A. (2011). Baroreflex activation therapy lowers blood pressure in patients with resistant hypertension: results from the double-blind, randomized, placebo-controlled rheos pivotal trial. Journal of the American College of Cardiology, 58(7), 765-773.

Blackwood, A. M., & Bolton, T. B. (1993). Mechanism of carbachol-evoked contractions of guinea-pig ileal smooth muscle close to freezing point. *British journal of pharmacology*, *109*(4), 1029-1037.

Blocking Peptides - Controls for better results. (2021). Retrieved 16 December 2021, from https://www.alomone.com/info/blocking-peptides

Bo, X., Jiang, L. H., Wilson, H. L., Kim, M., Burnstock, G., Surprenant, A., & North, R. A. (2003). Pharmacological and biophysical properties of the human P2X5 receptor. *Molecular pharmacology*, *63*(6), 1407-1416.

Bobanovic, L. K., Royle, S. J., & Murrell-Lagnado, R. D. (2002). P2X receptor trafficking in neurons is subunit specific. *Journal of Neuroscience*, 22(12), 4814-4824.

Bodin, P., Milner, P., Winter, R., & Burnstock, G. (1992). Chronic hypoxia changes the ratio of endothelin to ATP release from rat aortic endothelial cells exposed to high flow. *Proceedings of the Royal Society of London. Series B: Biological Sciences*, *247*(1319), 131-135.

Boehm, S., & Kubista, H. (2002). Fine tuning of sympathetic transmitter release via ionotropic and metabotropic presynaptic receptors. *Pharmacological reviews*, *54*(1), 43-99.

Boeynaems, J. M., Communi, D., & Robaye, B. (2012). Overview of the pharmacology and physiological roles of P2Y receptors. *Wiley Interdisciplinary Reviews: Membrane Transport and Signaling*, *1*(5), 581-588.

Boison, D. (2008). Adenosine as a neuromodulator in neurological diseases. Current opinion in pharmacology, 8(1), 2-7.

Bolton, T. B., & Lim, S. P. (1991). Action of acetylcholine on smooth muscle. Zeitschrift fur Kardiologie, 80, 73-77.

Bootman, M. D., Collins, T. J., Peppiatt, C. M., Prothero, L. S., MacKenzie, L., De Smet, P., ... & Lipp, P. (2001, February). Calcium signalling—an overview. In *Seminars in cell & developmental biology* (Vol. 12, No. 1, pp. 3-10). Academic Press.

Brain, S. D., & Grant, A. D. (2004). Vascular actions of calcitonin gene-related peptide and adrenomedullin. Physiological reviews, 84(3), 903-934.

Brake, A. J., Wagenbach, M. J., & Julius, D. (1994). New structural motif for ligand-gated ion channels defined by an ionotropic ATP receptor. *Nature*, *371*(6497), 519-523.

Brändle, U., Spielmanns, P., Osteroth, R., Sim, J., Surprenant, A., Buell, G., ... & Glowatzki, E. (1997). Desensitization of the P2X2 receptor controlled by alternative splicing. *FEBS letters*, *404*(2-3), 294-298.

Brass, D., Grably, M. R., Bronstein-Sitton, N., Gohar, O., & Meir, A. (2012). Using antibodies against P2Y and P2X receptors in purinergic signaling research. *Purinergic signalling*, 8(1), 61-79.

Britannica, The Editors of Encyclopaedia. "autonomic nervous system". Encyclopedia Britannica, 18 Nov. 2022, https://www.britannica.com/science/autonomic-nervous-system. Accessed 13 January 2023.

Brizzolara, A. L., Crowe, R., & Burnstock, G. (1993). Evidence for the involvement of both ATP and nitric oxide in non-adrenergic, non-cholinergic inhibitory neurotransmission in the rabbit portal vein. British journal of pharmacology, 109(3), 606-608.

Brock, J. A., & Cunnane, T. C. (1999). Effects of Ca2+ concentration and Ca2+ channel blockers on noradrenaline release and purinergic neuroeffector transmission in rat tail artery. *British journal of pharmacology*, *126*(1), 11-18.

Brock, J. A., & Van Helden, D. F. (1995). Enhanced excitatory junction potentials in mesenteric arteries from spontaneously hypertensive rats. Pflügers Archiv, 430(6), 901-908.

Browne, L. E. (2012). Structure of P2X receptors. *Wiley Interdisciplinary Reviews: Membrane Transport and Signaling*, *1*(1), 56-69.

Browne, L. E., & North, R. A. (2013). P2X receptor intermediate activation states have altered nucleotide selectivity. *Journal of Neuroscience*, *33*(37), 14801-14808.

Burnstock, G. (1997). The past, present and future of purine nucleotides as signalling molecules. Neuropharmacology, 36(9), 1127-1139.

Burnstock, G. (1999). Release of vasoactive substances from endothelial cells by shear stress and purinergic mechanosensory transduction. *Journal of anatomy*, *194*(3), 335-342.

Burnstock, G. (2006). Vessel tone and remodelling. *Nature medicine*, *12*(1), 16-17.

Burnstock, G. (2007). Physiology and pathophysiology of purinergic neurotransmission. *Physiological reviews*.

Burnstock, G. (2008). Non-synaptic transmission at autonomic neuroeffector junctions. Neurochemistry international, 52(1-2), 14-25.

Burnstock, G. (2009). Autonomic neurotransmission: 60 years since sir Henry Dale. Annual Review of Pharmacology and Toxicology, 49, 1-30.

Burnstock, G. (2009). Purinergic regulation of vascular tone and remodelling. *Autonomic and Autacoid Pharmacology*, *29*(3), 63-72.

Burnstock, G. (2012). Discovery of purinergic signalling, the initial resistance and current explosion of interest. British journal of pharmacology, 167(2), 238-255.

Burnstock, G. (2015). Blood cells: an historical account of the roles of purinergic signalling. *Purinergic signalling*, *11*(4), 411-434.

Burnstock, G. (2017). Purinergic signaling in the cardiovascular system. *Circulation research*, *120*(1), 207-228.

Burnstock, G. (2018). Purine and purinergic receptors. *Brain and neuroscience advances*, *2*, 2398212818817494.

Burnstock, G. A. (1978). A basis for distinguishing two types of purinergic receptor. *Cell Membrane Receptors for Drugs and Hormone: A Multidisciplinary Approach*, 107-118.

Burnstock, G., & Knight, G. E. (2004). Cellular distribution and functions of P2 receptor subtypes in different systems. *Int Rev Cytol*, 240(1), 31-304.

Burnstock, G., & Ralevic, V. (2014). Purinergic signaling and blood vessels in health and disease. *Pharmacological reviews*, *66*(1), 102-192.

Burnstock, G., & Warland, J. J. (1987). A pharmacological study of the rabbit saphenous artery in vitro: a vessel with a large purinergic contractile response to sympathetic nerve stimulation. *British journal of pharmacology*, *90*(1), 111-120.

Buxton, I. L., Kaiser, R. A., Oxhorn, B. C., & Cheek, D. J. (2001). Evidence supporting the Nucleotide Axis Hypothesis: ATP release and metabolism by coronary endothelium. *American Journal of Physiology-Heart and Circulatory Physiology*, *281*(4), H1657-H1666.

Calkoen, E. E., Vicente-Steijn, R., Hahurij, N. D., van Munsteren, C. J., Roest, A. A., DeRuiter, M. C., ... & Jongbloed, M. R. (2015). Abnormal sinoatrial node development resulting from disturbed vascular endothelial growth factor signaling. *International journal of cardiology*, *183*, 249-257.

Calvert, J. (2003). *Characterisation of P2 receptors in mouse superior cervical ganglia*. University of Leicester (United Kingdom).

Calvert, J. A., & Evans, R. J. (2004). Heterogeneity of P2X receptors in sympathetic neurons: contribution of neuronal P2X1 receptors revealed using knockout mice. *Molecular pharmacology*, *65*(1), 139-148.

Calvert, J. A., Atterbury-Thomas, A. E., Leon, C., Forsythe, I. D., Gachet, C., & Evans, R. J. (2004). Evidence for P2Y1, P2Y2, P2Y6 and atypical UTP-sensitive receptors coupled to rises

in intracellular calcium in mouse cultured superior cervical ganglion neurons and glia. *British journal of pharmacology*, *143*(5), 525-532.

Cardinali, D. P., Vacas, M. I., & Gejman, P. V. (1981). The sympathetic superior cervical ganglia as peripheral neuroendocrine centers. *Journal of Neural Transmission*, *52*(1), 1-21.

Cario-Toumaniantz, C., Loirand, G., Ladoux, A., & Pacaud, P. (1998). P2X7 receptor activation–induced contraction and lysis in human saphenous vein smooth muscle. Circulation Research, 83(2), 196-203.

Carman, A. J., Mills, J. H., Krenz, A., Kim, D. G., & Bynoe, M. S. (2011). Adenosine receptor signaling modulates permeability of the blood–brain barrier. *Journal of Neuroscience*, 31(37), 13272-13280.

Carroll, W. A., Donnelly-Roberts, D., & Jarvis, M. F. (2009). Selective P2X7 receptor antagonists for chronic inflammation and pain. *Purinergic signalling*, *5*(1), 63-73.

Castelucci, P., Robbins, H. L., Poole, D. P., & Furness, J. B. (2002). The distribution of purine P2X2 receptors in the guinea-pig enteric nervous system. *Histochemistry and cell biology*, *117*(5), 415-422.

Catterall, W. A. (2000). Structure and regulation of voltage-gated Ca2+ channels. *Annual review of cell and developmental biology*, *16*(1), 521-555.

Cavaliere, F., Nestola, V., Amadio, S., D'Ambrosi, N., Angelini, D. F., Sancesario, G., ... & Volonté, C. (2005). The metabotropic P2Y4 receptor participates in the commitment to differentiation and cell death of human neuroblastoma SH-SY5Y cells. *Neurobiology of disease*, *18*(1), 100-109.

Chambers, J. K., Macdonald, L. E., Sarau, H. M., Ames, R. S., Freeman, K., Foley, J. J., ... & Trill, J. (2000). AG protein-coupled receptor for UDP-glucose. Journal of Biological Chemistry, 275(15), 10767-10771.

Chandaka, G. K., Salzer, I., Drobny, H., Boehm, S., & Schicker, K. W. (2011). Facilitation of transmitter release from rat sympathetic neurons via presynaptic P2Y1 receptors. *British journal of pharmacology*, *164*(5), 1522-1533.

Chang, Z., Huangfu, C., Grainger, A. T., Zhang, J., Guo, Q., & Shi, W. (2017). Accelerated atherogenesis in completely ligated common carotid artery of apolipoprotein E-deficient mice. *Oncotarget*, *8*(66), 110289.

Cheewatrakoolpong, B., Gilchrest, H., Anthes, J. C., & Greenfeder, S. (2005). Identification and characterization of splice variants of the human P2X7 ATP channel. *Biochemical and biophysical research communications*, *332*(1), 17-27.

Chen, Z., He, L., Li, L., & Chen, L. (2018). The P2X7 purinergic receptor: an emerging therapeutic target in cardiovascular diseases. *Clinica Chimica Acta*, *479*, 196-207.

Cheung, Y. T., Lau, W. K. W., Yu, M. S., Lai, C. S. W., Yeung, S. C., So, K. F., & Chang, R. C. C. (2009). Effects of all-trans-retinoic acid on human SH-SY5Y neuroblastoma as in vitro model in neurotoxicity research. *Neurotoxicology*, *30*(1), 127-135.

Chinen, T., Yamamoto, S., Takeda, Y., Watanabe, K., Kuroki, K., Hashimoto, K., ... & Kitagawa, D. (2020). Nu MA assemblies organize microtubule asters to establish spindle bipolarity in acentrosomal human cells. *The EMBO journal*, *39*(2), e102378.

Christofi, F. L., Wunderlich, J., Yu, J. G., Wang, Y. Z., Xue, J., Guzman, J., ... & Cooke, H. (2004). Mechanically evoked reflex electrogenic chloride secretion in rat distal colon is triggered by endogenous nucleotides acting at P2Y1, P2Y2, and P2Y4 receptors. *Journal of Comparative Neurology*, *469*(1), 16-36.

Clapham, D. E. (2007). Calcium signaling. *Cell*, *131*(6), 1047-1058.

Claxson, A., Morris, C., Blake, D., Siren, M., Halliwell, B., Gustafsson, T., ... & Bergelin, I. (1990). The anti-inflammatory effects of D-myo-inositol-1.2. 6-trisphosphate (PP56) on animal models of inflammation. Agents and actions, 29(1-2), 68-70.

Cockayne, D. A., Dunn, P. M., Zhong, Y., Rong, W., Hamilton, S. G., Knight, G. E., ... & Ford, A. P. (2005). P2X2 knockout mice and P2X2/P2X3 double knockout mice reveal a role for the P2X2 receptor subunit in mediating multiple sensory effects of ATP. *The Journal of physiology*, *567*(2), 621-639.

Coddou, C., Yan, Z., Obsil, T., Huidobro-Toro, J. P., & Stojilkovic, S. S. (2011). Activation and regulation of purinergic P2X receptor channels. *Pharmacological reviews*, *63*(3), 641-683.

Collo, G., North, R. A., Kawashima, E., Merlo-Pich, E., Neidhart, S., Surprenant, A., & Buell, G. (1996). Cloning of P2X5 and P2X6 receptors and the distribution and properties of an extended family of ATP-gated ion channels. Journal of Neuroscience, 16(8), 2495-2507.

Conti, F. F., de Oliveira Brito, J., Bernardes, N., da Silva Dias, D., Sanches, I. C., Malfitano, C., ... & De Angelis, K. (2014). Cardiovascular autonomic dysfunction and oxidative stress induced by fructose overload in an experimental model of hypertension and menopause. BMC cardiovascular disorders, 14(1), 185.

Corr, L., & Burnstock, G. (1994). Analysis of P2-purinoceptor subtypes on the smooth muscle and endothelium of rabbit coronary artery. *Journal of cardiovascular pharmacology*, *23*(5), 709-715.

Corti, F., Olson, K. E., Marcus, A. J., & Levi, R. (2011). The exprgitteression level of ecto-NTP diphosphohydrolase1/CD39 modulates exocytotic and ischemic release of neurotransmitters in a cellular model of sympathetic neurons. Journal of Pharmacology and Experimental Therapeutics, 337(2), 524-532.

Crecelius, A. R., Kirby, B. S., Luckasen, G. J., Larson, D. G., & Dinenno, F. A. (2012). ATP-mediated vasodilatation occurs via activation of inwardly rectifying potassium channels in humans. *The Journal of physiology*, 590(21), 5349-5359.

Da Silva, R. L., Resende, R. R., & Ulrich, H. (2007). Alternative splicing of P2X6 receptors in developing mouse brain and during in vitro neuronal differentiation. *Experimental physiology*, *92*(1), 139-145.

Dalziel, H. H., Machaly, M., & Sneddon, P. (1989). Comparison of the purinergic contribution to sympathetic vascular responses in SHR and WKY rats in vitro and in vivo. European journal of pharmacology, 173(1), 19-26.

Damon, D. H. (2005). Sympathetic innervation promotes vascular smooth muscle differentiation. *American Journal of Physiology-Heart and Circulatory Physiology*, *288*(6), H2785-H2791.

Danilova, T., Galli, E., Pakarinen, E., Palm, E., Lindholm, P., Saarma, M., & Lindahl, M. (2019). Mesencephalic astrocyte-derived neurotrophic factor (MANF) is highly expressed in mouse tissues with metabolic function. *Frontiers in endocrinology*, *10*, 765.

Davenport, A. P., Hyndman, K. A., Dhaun, N., Southan, C., Kohan, D. E., Pollock, J. S., ... & Maguire, J. J. (2016). Endothelin. Pharmacological reviews, 68(2), 357-418.

De Fontgalland, D., Wattchow, D. A., Costa, M., & Brookes, S. J. H. (2008). Immunohistochemical characterization of the innervation of human colonic mesenteric and submucosal blood vessels. *Neurogastroenterology & Motility*, *20*(11), 1212-1226.

De Lorenzo, S., Veggetti, M., Muchnik, S., & Losavio, A. (2006). Presynaptic inhibition of spontaneous acetylcholine release mediated by P2Y receptors at the mouse neuromuscular junction. *Neuroscience*, *142*(1), 71-85.

del Carmen Gonzalez-Montelongo, M., & Fountain, S. J. (2021). Neuropeptide Y facilitates P2X1 receptor-dependent vasoconstriction via Y1 receptor activation in small mesenteric arteries during sympathetic neurogenic responses. *Vascular Pharmacology*, *136*, 106810.

Depace, D. M. (1982). Evidence for a blood-ganglion barrier in the superior cervical ganglion of the rat. *The Anatomical Record*, *204*(4), 357-363.

Dixon, A. K., Gubitz, A. K., Sirinathsinghji, D. J., Richardson, P. J., & Freeman, T. C. (1996). Tissue distribution of adenosine receptor mRNAs in the rat. *British journal of pharmacology*, *118*(6), 1461-1468.

Donnelly-Roberts, D. L., Namovic, M. T., Han, P., & Jarvis, M. F. (2009). Mammalian P2X7 receptor pharmacology: comparison of recombinant mouse, rat and human P2X7 receptors. *British journal of pharmacology*, *157*(7), 1203-1214.

Draid, M., Shiina, T., El-Mahmoudy, A., Boudaka, A., Shimizu, Y., & Takewaki, T. (2005). Neurally released ATP mediates endothelium-dependent hyperpolarization in the circular smooth muscle cells of chicken anterior mesenteric artery. British journal of pharmacology, 146(7), 983-989.

Draid, M., Shiina, T., El-Mahmoudy, A., Boudaka, A., Shimizu, Y., & Takewaki, T. (2005). Neurally released ATP mediates endothelium-dependent hyperpolarization in the circular

smooth muscle cells of chicken anterior mesenteric artery. British journal of pharmacology, 146(7), 983-989.

Drosopoulos, J. H., Kraemer, R., Shen, H., Upmacis, R. K., Marcus, A. J., & Musi, E. (2010). Human solCD39 inhibits injury-induced development of neointimal hyperplasia. *Thrombosis and haemostasis*, 103(02), 426-435.

Dunn, P. M., Gever, J., Ruan, H. Z., & Burnstock, G. (2005). Developmental changes in heteromeric P2X2/3 receptor expression in rat sympathetic ganglion neurons. *Developmental dynamics*, *234*(3), 505-511.

Dunn, P. M., Gever, J., Ruan, H. Z., & Burnstock, G. (2005). Developmental changes in heteromeric P2X2/3 receptor expression in rat sympathetic ganglion neurons. *Developmental dynamics*, *234*(3), 505-511.

Dunn, P. M., Zhong, Y., & Burnstock, G. (2001). P2X receptors in peripheral neurons. *Progress in neurobiology*, *65*(2), 107-134.

Dunn, P. M., Zhong, Y., & Burnstock, G. (2001). P2X receptors in peripheral neurons. *Progress in neurobiology*, *65*(2), 107-134.

Ecke, D., Hanck, T., Tulapurkar, M. E., Schäfer, R., Kassack, M., Stricker, R., & Reiser, G. (2008). Hetero-oligomerization of the P2Y11 receptor with the P2Y1 receptor controls the internalization and ligand selectivity of the P2Y11 receptor. *Biochemical Journal*, *409*(1), 107-116.

Ellis, J. L., & Burnstock, G. (1989). Modulation of neurotransmission in the guinea-pig vas deferens by capsaicin: involvement of calcitonin gene-related peptide and substance P. British journal of pharmacology, 98(2), 707-713.

Emerson, G. G., & Segal, S. S. (2000). Electrical coupling between endothelial cells and smooth muscle cells in hamster feed arteries: role in vasomotor control. *Circulation research*, *87*(6), 474-479.

Encinas, M., Iglesias, M., Liu, Y., Wang, H., Muhaisen, A., Cena, V., ... & Comella, J. X. (2000). Sequential treatment of SH-SY5Y cells with retinoic acid and brain-derived neurotrophic factor gives rise to fully differentiated, neurotrophic factor-dependent, human neuron-like cells. *Journal of neurochemistry*, *75*(3), 991-1003.

Encinas, M., Iglesias, M., Liu, Y., Wang, H., Muhaisen, A., Cena, V., ... & Comella, J. X. (2000). Sequential treatment of SH-SY5Y cells with retinoic acid and brain-derived neurotrophic factor gives rise to fully differentiated, neurotrophic factor-dependent, human neuron-like cells. *Journal of neurochemistry*, *75*(3), 991-1003.

Engel, T., Gomez-Villafuertes, R., Tanaka, K., Mesuret, G., Sanz-Rodriguez, A., Garcia-Huerta, P., ... & Diaz-Hernandez, M. (2012). Seizure suppression and neuroprotection by targeting the purinergic P2X7 receptor during status epilepticus in mice. *The FASEB journal*, *26*(4), 1616-1628.

Erlinge, D., & Burnstock, G. (2008). P2 receptors in cardiovascular regulation and disease. Purinergic signalling, 4(1), 1-20.

Evans, R. J., & Surprenant, A. (1992). Vasoconstriction of guinea-pig submucosal arterioles following sympathetic nerve stimulation is mediated by the release of ATP. British journal of pharmacology, 106(2), 242-249.

Farrelly, L. A., Savage, N. T., O'Callaghan, C., Toulouse, A., & Yilmazer-Hanke, D. M. (2013). Therapeutic concentrations of valproate but not amitriptyline increase neuropeptide Y (NPY) expression in the human SH-SY5Y neuroblastoma cell line. *Regulatory Peptides*, *186*, 123-130.

Feldman-Goriachnik, R., Wu, B., & Hanani, M. (2018). Cholinergic responses of satellite glial cells in the superior cervical ganglia. *Neuroscience letters*, *671*, 19-24.

Ferrari, M. F., Coelho, E. F., Farizatto, K. L., Chadi, G., & Fior-Chadi, D. R. (2011). Modulation of tyrosine hydroxylase, neuropeptide Y, glutamate, and substance P in ganglia and brain areas involved in cardiovascular control after chronic exposure to nicotine. *International journal of hypertension*, *2011*.

Fields, R. D., & Burnstock, G. (2006). Purinergic signalling in neuron–glia interactions. Nature Reviews Neuroscience, 7(6), 423-436.

Fioretto, E. T., Rahal, S. C., Borges, A. S., Mayhew, T. M., Nyengaard, J. R., Marcondes, J. S., ... & Coppi, A. A. (2011). Hypertrophy and neuron loss: structural changes in sheep SCG induced by unilateral sympathectomy. *International Journal of Developmental Neuroscience*, *29*(4), 475-481.

Fischer, W., & Krugel, U. (2007). P2Y receptors: focus on structural, pharmacological and functional aspects in the brain. Current medicinal chemistry, 14(23), 2429-2455.

Florea, V. G., & Cohn, J. N. (2014). The autonomic nervous system and heart failure. Circulation research, 114(11), 1815-1826.

Folan, J. C., & Heym, C. (1989). Immunohistochemical evidence for different opioid systems in the rat superior cervical ganglion as revealed by imipramine treatment and receptor blockade. *Journal of Chemical Neuroanatomy*, *2*(2), 107-118.

Forstermann, U., & Munzel, T. (2006). Endothelial nitric oxide synthase in vascular disease: from marvel to menace. Circulation, 113(13), 1708-1714.

Freddo, T. F., & Chaum, E. (2017). *Anatomy of the eye and orbit: the clinical essentials*. Lippincott Williams & Wilkins.

Fredholm, B. B., IJzerman, A. P., Jacobson, K. A., Klotz, K. N., & Linden, J. (2001). International Union of Pharmacology. XXV. Nomenclature and classification of adenosine receptors. *Pharmacological reviews*, *53*(4), 527-552.

Fredholm, B. B., IJzerman, A. P., Jacobson, K. A., Linden, J., & Müller, C. E. (2011). International Union of Basic and Clinical Pharmacology. LXXXI. Nomenclature and classification of adenosine receptors—an update. *Pharmacological reviews*, *63*(1), 1-34.

Fredriksson, R., Lagerström, M. C., Lundin, L. G., & Schiöth, H. B. (2003). The G-protein-coupled receptors in the human genome form five main families. Phylogenetic analysis, paralogon groups, and fingerprints. Molecular pharmacology, 63(6), 1256-1272.

Gaete, P. S., Lillo, M. A., Puebla, M., Poblete, I., & Figueroa, X. F. (2019). CGRP signalling inhibits NO production through pannexin-1 channel activation in endothelial cells. *Scientific reports*, *9*(1), 1-17.

Geddawy, A., Shimosato, T., Tawa, M., Imamura, T., & Okamura, T. (2010). Mechanism underlying endothelium-dependent relaxation by 2-methylthio-ADP in monkey cerebral artery. *Journal of pharmacological sciences*, 1009090448-1009090448.

Gerevich, Z., & Illes, P. (2004). P2Y receptors and pain transmission. Purinergic Signalling, 1(1), 3-10.

Gervasi, N. M., Scott, S. S., Aschrafi, A., Gale, J., Vohra, S. N., MacGibeny, M. A., ... & Kaplan, B. B. (2016). The local expression and trafficking of tyrosine hydroxylase mRNA in the axons of sympathetic neurons. *Rna*, *22*(6), 883-895.

Getsy, P. M., Coffee, G. A., Hsieh, Y. H., & Lewis, S. J. (2021). The superior cervical ganglia modulate ventilatory responses to hypoxia independently of preganglionic drive from the cervical sympathetic chain. *Journal of Applied Physiology*, *131*(2), 836-857.

Gever, J. R., Cockayne, D. A., Dillon, M. P., Burnstock, G., & Ford, A. P. (2006). Pharmacology of P2X channels. *Pflügers Archiv*, *452*(5), 513-537.

Gever, J. R., Cockayne, D. A., Dillon, M. P., Burnstock, G., & Ford, A. P. (2006). Pharmacology of P2X channels. Pflügers Archiv, 452(5), 513-537.

Gibbins, I. L. (1995). Chemical neuroanatomy of sympathetic ganglia. *Autonomic ganglia*, *6*, 73-122.

Gibbins, I. L., & Morris, J. L. (1990). Sympathetic noradrenergic neurons containing dynorphin but not neuropeptide Y innervate small cutaneous blood vessels of guinea-pigs. *Journal of the autonomic nervous system*, *29*(2), 137-149.

Giniatullin, R., & Nistri, A. (2013). Desensitization properties of P2X3 receptors shaping pain signaling. *Frontiers in cellular neuroscience*, 7, 245.

Gitterman, D. P., & Evans, R. J. (2000). Properties of P2X and P2Y receptors are dependent on artery diameter in the rat mesenteric bed. British journal of pharmacology, 131(8), 1561-1568.

Gitterman, D. P., & Evans, R. J. (2001). Nerve evoked P2X receptor contractions of rat mesenteric arteries; dependence on vessel size and lack of role of L-type calcium channels and calcium induced calcium release. British journal of pharmacology, 132(6), 1201-1208.

Glass, R., & Burnstock, G. (2001). Immunohistochemical identification of cells expressing ATP-gated cation channels (P2X receptors) in the adult rat thyroid. The Journal of Anatomy, 198(5), 569-579.

Glass, R., Townsend-Nicholson, A., & Burnstock, G. (2000). P2 receptors in the thymus: expression of P2X and P2Y receptors in adult rats, an immunohistochemical and in situ hybridisation study. Cell and tissue research, 300(2), 295-306.

Goetz, U., Da Prada, M., & Pletscher, A. (1971). Adenine-, guanine-and uridine-5'-phosphonucleotides in blood platelets and storage organelles of various species. *Journal of Pharmacology and Experimental Therapeutics*, *178*(1), 210-215.

Golovina, V. A., & Blaustein, M. P. (2006). Preparation of primary cultured mesenteric artery smooth muscle cells for fluorescent imaging and physiological studies. *Nature protocols*, *1*(6), 2681-2687.

Goto, T., Iwai, H., Kuramoto, E., & Yamanaka, A. (2017). Neuropeptides and ATP signaling in the trigeminal ganglion. *Japanese Dental Science Review*, *53*(4), 117-124.

Gourine, A. V., Wood, J. D., & Burnstock, G. (2009). Purinergic signalling in autonomic control. *Trends in neurosciences*, *32*(5), 241-248.

Grynkiewicz, G., Poenie, M., & Tsien, R. Y. (1985). A new generation of Ca2+ indicators with greatly improved fluorescence properties. *Journal of biological chemistry*, *260*(6), 3440-3450.

Guidry, G., & Landis, S. C. (2000). Absence of cholinergic sympathetic innervation from limb muscle vasculature in rats and mice. *Autonomic Neuroscience*, *82*(3), 97-108.

Guimarães, S., & Moura, D. (2001). Vascular adrenoceptors: an update. *Pharmacological reviews*, *53*(2), 319-356.

Guns, P. J. D., Korda, A., Crauwels, H. M., Van Assche, T., Robaye, B., Boeynaems, J. M., & Bult, H. (2005). Pharmacological characterization of nucleotide P2Y receptors on endothelial cells of the mouse aorta. *British journal of pharmacology*, *146*(2), 288-295.

Guns, P. J. D., Van Assche, T., Fransen, P., Robaye, B., Boeynaems, J. M., & Bult, H. (2006). Endothelium-dependent relaxation evoked by ATP and UTP in the aorta of P2Y2-deficient mice. *British journal of pharmacology*, 147(5), 569-574.

Guo, C., Masin, M., Qureshi, O. S., & Murrell-Lagnado, R. D. (2007). Evidence for functional P2X4/P2X7 heteromeric receptors. *Molecular pharmacology*, *72*(6), 1447-1456.

Guo, C., Rudolph, S., Neuwirth, M. E., & Regehr, W. G. (2021). Purkinje cell outputs selectively inhibit a subset of unipolar brush cells in the input layer of the cerebellar cortex. *bioRxiv*.

Guo, C., Rudolph, S., Neuwirth, M. E., & Regehr, W. G. (2021). Purkinje cell outputs selectively inhibit a subset of unipolar brush cells in the input layer of the cerebellar cortex. *Elife*, *10*, e68802.

Guyenet, P. G. (2006). The sympathetic control of blood pressure. Nature Reviews Neuroscience, 7(5), 335.

Hajnoczky, G. (2003). Davies E, and Madesh M. *Calcium signaling and apoptosis. Biochem Biophys Res Commun*, *304*, 445-454.

Hamel, E. (2006). Perivascular nerves and the regulation of cerebrovascular tone. *Journal of applied physiology*, *100*(3), 1059-1064.

Hamilton, N., Vayro, S., Kirchhoff, F., Verkhratsky, A., Robbins, J., Gorecki, D. C., & Butt, A. M. (2008). Mechanisms of ATP-and glutamate-mediated calcium signaling in white matter astrocytes. Glia, 56(7), 734-749.

Hansen, M. A., Bennett, M. R., & Barden, J. A. (1999). Distribution of purinergic P2X receptors in the rat heart. Journal of the autonomic nervous system, 78(1), 1-9.

Hardy, L. A., Harvey, I. J., Chambers, P., & Gillespie, J. I. (2000). A putative alternatively spliced variant of the P2X1 purinoreceptor in human bladder. *Experimental physiology*, *85*(4), 461-463.

Hargitai, D., Pataki, Á., Raffai, G., Füzi, M., Dankó, T., Csernoch, L., ... & Zsembery, Á. (2010). Calcium entry is regulated by Zn2+ in relation to extracellular ionic environment in human airway epithelial cells. *Respiratory physiology & neurobiology*, *170*(1), 67-75.

Harhun, M. I., Povstyan, O. V., & Gordienko, D. V. (2010). Purinoreceptor-mediated current in myocytes from renal resistance arteries. British journal of pharmacology, 160(4), 987-997.

Harrington, L. S., & Mitchell, J. A. (2004). Novel role for P2X receptor activation in endothelium-dependent vasodilation. *British journal of pharmacology*, *143*(5), 611-617.

Harrington, L. S., & Mitchell, J. A. (2005). P2X1 receptors and the endothelium. *Memórias do Instituto Oswaldo Cruz*, *100*, 111-112.

Harrington, L. S., Evans, R. J., Wray, J., Norling, L., Swales, K. E., Vial, C., ... & Mitchell, J. A. (2007). Purinergic 2X1 receptors mediate endothelial dependent vasodilation to ATP. *Molecular pharmacology*, *72*(5), 1132-1136.

Hatanaka, Y., Hobara, N., Honghua, J., Akiyama, S., Nawa, H., Kobayashi, Y., ... & Kawasaki, H. (2006). Neuronal nitric-oxide synthase inhibition facilitates adrenergic neurotransmission in rat mesenteric resistance arteries. *Journal of Pharmacology and Experimental Therapeutics*, *316*(2), 490-497.

Headley, D. B., Suhan, N. M., & Horn, J. P. (2007). Different subcellular distributions of the vesicular monoamine transporter, VMAT2, in subclasses of sympathetic neurons. *Brain research*, *1129*, 156-160.

Heym, C., Common, B., Yin, S., Klima-schewski, L., Couraud, J. Y., & Bachmann, S. (1993). Neurochemistry, connectivity and plasticity of small intensely fluorescent (SIF) cells in the rat superior cervical ganglion. *Annals of Anatomy-Anatomischer Anzeiger*, *175*(4), 309-319.

Hill, C. E., Phillips, J. K., & Sandow, S. L. (2001). Heterogeneous control of blood flow amongst different vascular beds. *Medicinal research reviews*, *21*(1), 1-60.

Hirst, R. A., Harrison, C., Hirota, K., & Lambert, D. G. (1999). Measurement of [Ca 2+] i in whole cell suspensions using fura-2. *Calcium Signaling Protocols*, 31-39.

Ho, T., Jobling, A. I., Greferath, U., Chuang, T., Ramesh, A., Fletcher, E. L., & Vessey, K. A. (2015). Vesicular expression and release of ATP from dopaminergic neurons of the mouse retina and midbrain. *Frontiers in cellular neuroscience*, *9*, 389.

Hoard, J. L., Hoover, D. B., Mabe, A. M., Blakely, R. D., Feng, N., & Paolocci, N. (2008). Cholinergic neurons of mouse intrinsic cardiac ganglia contain noradrenergic enzymes, norepinephrine transporters, and the neurotrophin receptors tropomyosin-related kinase A and p75. *Neuroscience*, *156*(1), 129-142.

Hobara, N., Goda, M., Kitamura, Y., Takayama, F., & Kawasaki, H. (2006). Innervation and functional changes in mesenteric perivascular calcitonin gene-related peptide-and neuropeptide Y-containing nerves following topical phenol treatment. *Neuroscience*, *141*(2), 1087-1099.

Hodges, G. J., Jackson, D. N., Mattar, L., Johnson, J. M., & Shoemaker, J. K. (2009). Neuropeptide Y and neurovascular control in skeletal muscle and skin. *American Journal of Physiology-Regulatory, Integrative and Comparative Physiology*, *297*(3), R546-R555.

Hofmann, T., Obukhov, A. G., Schaefer, M., Harteneck, C., Gudermann, T., & Schultz, G. (1999). Direct activation of human TRPC6 and TRPC3 channels by diacylglycerol. *Nature*, *397*(6716), 259-263.

Hökfelt, T., Elfvin, L. G., Schultzberg, M., Goldstein, M., & Nilsson, G. (1977). On the occurrence of substance P-containing fibers in sympathetic ganglia: immunohistochemical evidence. *Brain Research*, *132*(1), 29-41.

Holton, P. (1959). The liberation of adenosine triphosphate on antidromic stimulation of sensory nerves. *The Journal of physiology*, *145*(3), 494.

Hong, S. J., & Chang, C. C. (1998). Evaluation of intrinsic modulation of synaptic transmission by ATP in mouse fast twitch muscle. *Journal of neurophysiology*, *80*(5), 2550-2558.

Honore, P., Donnelly-Roberts, D., Namovic, M. T., Hsieh, G., Zhu, C. Z., Mikusa, J. P., ... & Jarvis, M. F. (2006). A-740003 [N-(1-{[(cyanoimino)(5-quinolinylamino) methyl] amino}-2, 2-dimethylpropyl)-2-(3, 4-dimethoxyphenyl) acetamide], a novel and selective P2X7 receptor

antagonist, dose-dependently reduces neuropathic pain in the rat. *Journal of Pharmacology and Experimental Therapeutics*, *319*(3), 1376-1385.

Hug, N., Longman, D., & Cáceres, J. F. (2016). Mechanism and regulation of the nonsense-mediated decay pathway. *Nucleic acids research*, *44*(4), 1483-1495.

Hussl, S., & Boehm, S. (2006). Functions of neuronal P2Y receptors. *Pflügers Archiv*, *452*(5), 538-551.

Inscho, E. W., Cook, A. K., Imig, J. D., Vial, C., & Evans, R. J. (2004). Renal autoregulation in P2X1 knockout mice. *Acta physiologica Scandinavica*, *181*(4), 445-453.

Ishida, K., Matsumoto, T., Taguchi, K., Kamata, K., & Kobayashi, T. (2013). Mechanisms underlying reduced P 2 Y 1-receptor-mediated relaxation in superior mesenteric arteries from long-term streptozotocin-induced diabetic rats. *Acta Physiologica*, *207*(1), 130-141.

Ito, T., Iino, S., & Nojyo, Y. (2005). A part of cholinergic fibers in mouse superior cervical ganglia contain GABA or glutamate. *Brain research*, *1046*(1-2), 234-238.

Jackson, E. K., Cheng, D., Mi, Z., Verrier, J. D., Janesko-Feldman, K., & Kochanek, P. M. (2012). Role of A1 receptors in renal sympathetic neurotransmission in the mouse kidney. *American Journal of Physiology-Renal Physiology*, *303*(7), F1000-F1005.

Jackson, E. K., Cheng, D., Mi, Z., Verrier, J. D., Janesko-Feldman, K., & Kochanek, P. M. (2012). Role of A1 receptors in renal sympathetic neurotransmission in the mouse kidney. *American Journal of Physiology-Renal Physiology*, *303*(7), F1000-F1005.

Jacobson, K. A., Balasubramanian, R., Deflorian, F. and Gao, Z.-G. (2012) ‘G protein-coupled adenosine (P1) and P2Y receptors: ligand design and receptor interactions.’, *Purinergic signalling*, 241 8(3), pp. 419–36. doi: 10.1007/s11302-012-9294-7.

Jacobson, K. A., Jarvis, M. F., & Williams, M. (2002). Purine and pyrimidine (P2) receptors as drug targets. *Journal of medicinal chemistry*, *45*(19), 4057-4093.

Jarvis, M. F., & Khakh, B. S. (2009). ATP-gated P2X cation-channels. *Neuropharmacology*, *56*(1), 208-215.

Ji, X., Naito, Y., Hirokawa, G., Weng, H., Hiura, Y., Takahashi, R., & Iwai, N. (2012). P2X7 receptor antagonism attenuates the hypertension and renal injury in Dahl salt-sensitive rats. *Hypertension Research*, *35*(2), 173-179.

Jin, X., Shepherd, R. K., Duling, B. R., & Linden, J. (1997). Inosine binds to A3 adenosine receptors and stimulates mast cell degranulation. *The Journal of clinical investigation*, *100*(11), 2849-2857.

Johnsen, J. I., Dyberg, C., & Wickström, M. (2019). Neuroblastoma—A neural crest derived embryonal malignancy. *Frontiers in molecular neuroscience*, 9.

Joseph, S. M., Pifer, M. A., Przybylski, R. J., & Dubyak, G. R. (2004). Methylene ATP analogs as modulators of extracellular ATP metabolism and accumulation. *British journal of pharmacology*, *142*(6), 1002-1014.

Kaley, G. (2000). Regulation of vascular tone: role of 20-HETE in the modulation of myogenic reactivity. *Circulation research*, *87*(1), 4-5.

Kauffenstein, G., Tamareille, S., Prunier, F., Roy, C., Ayer, A., Toutain, B., ... & Henrion, D. (2016). Central role of P2Y6 UDP receptor in arteriolar myogenic tone. *Arteriosclerosis, thrombosis, and vascular biology*, *36*(8), 1598-1606.

Kawai, Y., Yokoyama, Y., Kaidoh, M., & Ohhashi, T. (2010). Shear stress-induced ATP-mediated endothelial constitutive nitric oxide synthase expression in human lymphatic endothelial cells. *American Journal of Physiology-Cell Physiology*, 298(3), C647-C655.

Kawasaki, H., Takasaki, K., Saito, A., & Goto, K. (1988). Calcitonin gene-related peptide acts as a novel vasodilator neurotransmitter in mesenteric resistance vessels of the rat. *Nature*, *335*(6186), 164-167.

Kawate, T., Michel, J. C., Birdsong, W. T., & Gouaux, E. (2009). Crystal structure of the ATP-gated P2X4 ion channel in the closed state. *Nature*, *460*(7255), 592-598.

Kelm, M., Feelisch, M., Deussen, A., Strauer, B. E., & Schrader, J. (1991). Release of endothelium derived nitric oxide in relation to pressure and flow. *Cardiovascular research*, 25(10), 831-836.

Khakh, B. S., Bao, X. R., Labarca, C., & Lester, H. A. (1999). Neuronal P2X transmitter-gated cation channels change their ion selectivity in seconds. *Nature neuroscience*, *2*(4), 322-330.

Khakh, B. S., Burnstock, G., Kennedy, C., King, B. F., North, R. A., Séguéla, P., ... & Humphrey, P. P. (2001). International union of pharmacology. XXIV. Current status of the nomenclature and properties of P2X receptors and their subunits. *Pharmacological reviews*, *53*(1), 107-118.

Khmyz, V., Maximyuk, O., Teslenko, V., Verkhratsky, A., & Krishtal, O. (2008). P2X 3 receptor gating near normal body temperature. Pflügers Archiv-European Journal of Physiology, 456(2), 339-347.

Kim, G. D., Das, R., Goduni, L., McClellan, S., Hazlett, L. D., & Mahabeleshwar, G. H. (2016). Kruppel-like factor 6 promotes macrophage-mediated inflammation by suppressing B cell leukemia/lymphoma 6 expression. *Journal of Biological Chemistry*, *291*(40), 21271-21282.

King, A. J., Osborn, J. W., & Fink, G. D. (2007). Splanchnic circulation is a critical neural target in angiotensin II salt hypertension in rats. *Hypertension*, *50*(3), 547-556.

King, B. (2001). International Union of Pharmacology. XXIV. Current Status of the Nomenclature and Properties of P2X Receptors an... *PHARMACOLOGICAL REVIEWS*, *53*(1), 107-118.

Knoche, H., & Kienecker, E. W. (1977). Sympathetic innervation of the carotid bifurcation in the rabbit and cat: Blood vessels, carotid body and carotid sinus. *Cell and Tissue Research*, *184*(1), 103-112.

Koltsova, S. V., Maximov, G. V., Kotelevtsev, S. V., Lavoie, J. L., Tremblay, J., Grygorczyk, R., ... & Orlov, S. N. (2009). Myogenic tone in mouse mesenteric arteries: evidence for P2Y receptor-mediated, Na+, K+, 2Cl− cotransport-dependent signaling. *Purinergic signalling*, *5*(3), 343-349.

Kotnis, S., Bingham, B., Vasilyev, D. V., Miller, S. W., Bai, Y., Yeola, S., ... & Whiteside, G. T. (2010). Genetic and functional analysis of human P2X5 reveals a distinct pattern of exon 10 polymorphism with predominant expression of the nonfunctional receptor isoform. *Molecular pharmacology*, *77*(6), 953-960.

Kovalevich, J., & Langford, D. (2013). Considerations for the use of SH-SY5Y neuroblastoma cells in neurobiology. In *Neuronal Cell Culture* (pp. 9-21). Humana Press, Totowa, NJ.

Kovalevich, J., & Langford, D. (2013). Considerations for the use of SH-SY5Y neuroblastoma cells in neurobiology. In *Neuronal Cell Culture* (pp. 9-21). Humana Press, Totowa, NJ.

Kumagai, M., & Saino, T. (2001). Effects of ATP on intracellular calcium dynamics of neurons and satellite cells in rat superior cervical ganglia. *Histochemistry and Cell Biology*, *115*(4), 285-292.

Labs, J. (2021). How to Determine Protein Molecular Weight. Retrieved 16 December 2021, from https://www.azom.com/article.aspx?ArticleID=19609

Ladd, F. V. L., Ladd, A. A. L., da Silva, A. A., & Coppi, A. A. (2014). Stereological and allometric studies on neurons and axo-dendritic synapses in superior cervical ganglia. *International Review of Cell and Molecular Biology*, *311*, 123-155.

Lalo, U., Pankratov, Y., Wichert, S. P., Rossner, M. J., North, R. A., Kirchhoff, F., & Verkhratsky, A. (2008). P2X1 and P2X5 subunits form the functional P2X receptor in mouse cortical astrocytes. *Journal of Neuroscience*, *28*(21), 5473-5480.

Larsson, C., Thomas, A. P., & Hoek, J. B. (1998). Carbachol-stimulated Ca2+ increase in single neuroblastoma SH-SY5Y cells: effects of ethanol. *Alcoholism: Clinical and Experimental Research*, *22*(3), 637-645.

Layhadi, J. (2017). *P2X4 receptor in human macrophages: role in ATP-evoked calcium responses and cytokine production* (Doctoral dissertation, University of East Anglia).

Layhadi, J. (2017). P2X4 receptor in human macrophages: role in ATP-evoked calcium responses and cytokine production (*Doctoral dissertation, University of East Anglia*).

Lazarowski, E. R. (2012). Vesicular and conductive mechanisms of nucleotide release. *Purinergic signalling*, *8*(3), 359-373.

León, D., Hervás, C., & Miras-Portugal, M. T. (2006). P2Y1 and P2X7 receptors induce calcium/calmodulin-dependent protein kinase II phosphorylation in cerebellar granule neurons. *European Journal of Neuroscience*, *23*(11), 2999-3013.

Lewis, C. J., & Evans, R. J. (2000). Lack of run-down of smooth muscle P2X receptor currents recorded with the amphotericin permeabilized patch technique, physiological and pharmacological characterization of the properties of mesenteric artery P2X receptor ion channels. *British journal of pharmacology*, *131*(8), 1659-1666.

Lewis, C. J., & Evans, R. J. (2001). P2X receptor immunoreactivity in different arteries from the femoral, pulmonary, cerebral, coronary and renal circulations. *Journal of vascular research*, *38*(4), 332-340.

Lewis, C. J., & Evans, R. J. (2001). P2X receptor immunoreactivity in different arteries from the femoral, pulmonary, cerebral, coronary and renal circulations. *Journal of vascular research*, *38*(4), 332-340.

Lewis, C. J., Surprenant, A., & Evans, R. J. (1998). 2′, 3′-O-(2, 4, 6-trinitrophenyl) adenosine 5′-triphosphate (TNP-ATP)–a nanomolar affinity antagonist at rat mesenteric artery P2X receptor ion channels. *British journal of pharmacology*, *124*(7), 1463.

Li, C., & Horn, J. P. (2006). Physiological classification of sympathetic neurons in the rat superior cervical ganglion. *Journal of neurophysiology*, *95*(1), 187-195.

Li, G. H., Lee, E. M., Blair, D., Holding, C., Poronnik, P., Cook, D. I., ... & Bennett, M. R. (2000). The distribution of P2X receptor clusters on individual neurons in sympathetic ganglia and their redistribution on agonist activation. *Journal of Biological Chemistry*, *275*(37), 29107-29112.

Li, L. Z., Yue, L. H., Zhang, Z. M., Zhao, J., Ren, L. M., Wang, H. J., & Li, L. (2020). Comparison of mRNA expression of P2X receptor subtypes in different arterial tissues of rats. *Biochemical genetics*, *58*(5), 677-690.

Li, L., Lee, E. W., Ji, H., & Zukowska, Z. (2003). Neuropeptide Y–induced acceleration of postangioplasty occlusion of rat carotid artery. *Arteriosclerosis, thrombosis, and vascular biology*, *23*(7), 1204-1210.

Li, M., Kawate, T., Silberberg, S. D., & Swartz, K. J. (2010). Pore-opening mechanism in trimeric P2X receptor channels. Nature communications, 1, 44.

Li, X., Zhu, L. J., Lv, J., & Cao, X. (2022). Purinoceptor: a novel target for hypertension. *Purinergic Signalling*, 1-13.

Liu, S. F., Crawley, D. E., Rohde, J. A., Evans, T. W., & Barnes, P. J. (1992). Role of nitric oxide and guanosine 3', 5'-cyclic monophosphate in mediating nonadrenergic, noncholinergic relaxation in guinea-pig pulmonary arteries. *British journal of pharmacology*, *107*(3), 861.

Liu, X., Jiang, F., Wang, Z., Tang, L., Zou, B., Xu, P., & Yu, T. (2021). Hypoxic bone marrow mesenchymal cell-extracellular vesicles containing miR-328-3p promote lung cancer

progression via the NF2-mediated Hippo axis. *Journal of Cellular and Molecular Medicine*, *25*(1), 96-109.

Liu, X., Wang, Q., Yang, Y., Stewart, T., Shi, M., Soltys, D., ... & Zhang, J. (2021). Reduced erythrocytic CHCHD2 mRNA is associated with brain pathology of Parkinson's disease. *Acta neuropathologica communications*, *9*(1), 1-16.

Loesch, A., & Burnstock, G. (2000). Ultrastructural localisation of ATP-gated P2X2 receptor immunoreactivity in vascular endothelial cells in rat brain. *Endothelium*, 7(2), 93-98.

Loesch, A., Mayhew, T. M., Tang, H., Ladd, F. V. L., Ladd, A. A. L., de Melo, M. P., ... & Coppi, A. A. (2010). Stereological and allometric studies on neurons and axo-dendritic synapses in the superior cervical ganglia of rats, capybaras and horses. *Cell and tissue research*, *341*(2), 223-237.

Lopes, F. M., Schröder, R., da Frota Júnior, M. L. C., Zanotto-Filho, A., Müller, C. B., Pires, A. S., ... & Klamt, F. (2010). Comparison between proliferative and neuron-like SH-SY5Y cells as an in vitro model for Parkinson disease studies. *Brain research*, *1337*, 85-94.

Lund, D. D., Knuepfer, M. M., Brody, M. J., Bhatnagar, R. K., Schmid, P. G., & Roskoski Jr, R. (1978). Comparison of tyrosine hydroxylase and choline acetyltransferase activity in response to sympathetic nervous system activation. *Brain research*, *156*(1), 192-197.

Lundberg, J. M. (1996). Pharmacology of cotransmission in the autonomic nervous system: integrative aspects on amines, neuropeptides, adenosine triphosphate, amino acids and nitric oxide. *Pharmacological reviews*, 48(1), 113-178.

Lundberg, J. M., Franco-Cereceda, A., Hua, X., Hökfelt, T., & Fischer, J. A. (1985). Co-existence of substance P and calcitonin gene-related peptide-like immunoreactivities in sensory nerves in relation to cardiovascular and bronchoconstrictor effects of capsaicin. *European journal of pharmacology*, 108(3), 315-319.

Lundberg, L. M., Alm, P., Wharton, J., & Polak, J. M. (1988). Protein gene product 9.5 (PGP 9.5). *Histochemistry*, *90*(1), 9-17.

Lynch, K. J., Touma, E., Niforatos, W., Kage, K. L., Burgard, E. C., van Biesen, T., ... & Jarvis, M. F. (1999). Molecular and functional characterization of human P2X2 receptors. *Molecular pharmacology*, *56*(6), 1171-1181.

Lynge, J., & Hellsten, Y. (2000). Distribution of adenosine A1, A2A and A2B receptors in human skeletal muscle. *Acta Physiologica Scandinavica*, *169*(4), 283-290.

MacDermott, A. B., Role, L. W., & Siegelbaum, S. A. (1999). Presynaptic ionotropic receptors and the control of transmitter release. *Annual review of neuroscience*, *22*(1), 443-485.

Maklad, A., Quinn, T., & Fritzsch, B. (2001). Intracranial distribution of the sympathetic system in mice: DiI tracing and immunocytochemical labeling. *The Anatomical Record: An Official Publication of the American Association of Anatomists*, *263*(1), 99-111.

Malmsjö, M., Hou, M., Pendergast, W., Erlinge, D., & Edvinsson, L. (2003). The stable pyrimidines UDPβS and UTPγS discriminate between contractile cerebrovascular P2 receptors. *European journal of pharmacology*, 458(3), 305-311.

Mancia, G., Grassi, G., Giannattasio, C., & Seravalle, G. (1999). Sympathetic activation in the pathogenesis of hypertension and progression of organ damage. Hypertension, 34(4), 724-728.

Mangiarua, E. I., & Lee, R. M. (1990). Increased sympathetic innervation in the cerebral and mesenteric arteries of hypertensive rats. Canadian journal of physiology and pharmacology, 68(4), 492-499.

Maningat, A. L., & Munakomi, S. (2021). Neuroanatomy, Superior Cervical Ganglion. *StatPearls [Internet]*.

Marina, N., Ang, R., Machhada, A., Kasymov, V., Karagiannis, A., Hosford, P. S., ... & Kasparov, S. (2015). Brainstem hypoxia contributes to the development of hypertension in the spontaneously hypertensive rat. *Hypertension*, *65*(4), 775-783.

Martin-Aragon Baudel, M., Espinosa-Tanguma, R., Nieves-Cintron, M., & Navedo, M. F. (2020). Purinergic signaling during hyperglycemia in vascular smooth muscle cells. *Frontiers in Endocrinology*, *11*, 329.

Mayerhofer, A., Föhr, K. J., Sterzik, K., & Gratzl, M. (1992). Carbachol increases intracellular free calcium concentrations in human granulosa-lutein cells. *Journal of endocrinology*, *135*(1), 153-159.

McGehee, D. S., & Role, L. W. (1996). Presynaptic ionotropic receptors. *Current opinion in neurobiology*, *6*(3), 342-349.

Melikian, N., Seddon, M. D., Casadei, B., Chowienczyk, P. J., & Shah, A. M. (2009). Neuronal nitric oxide synthase and human vascular regulation. *Trends in cardiovascular medicine*, *19*(8), 256-262.

Melino, G., Thiele, C. J., Knight, R. A., & Piacentini, M. (1997). Retinoids and the control of growth/death decisions in human neuroblastoma cell lines. *Journal of neuro-oncology*, *31*(1), 65-83.

Merino-Jiménez, C., Miguel, F., Feria Pliego, J. A., Zetina Rosales, M. E., Cifuentes, F., & Morales, M. A. (2018). Sympathetic hyperactivity and age affect segregation and expression of neurotransmitters. *Frontiers in cellular neuroscience*, *12*, 411.

Metcalfe, M. J., Baker, D. M., Turmaine, M., & Burnstock, G. (2007). Alterations in purinoceptor expression in human long saphenous vein during varicose disease. European journal of vascular and endovascular surgery, 33(2), 239-250.

Metcalfe, M. J., Baker, D. M., Turmaine, M., & Burnstock, G. (2007). Alterations in purinoceptor expression in human long saphenous vein during varicose disease. *European journal of vascular and endovascular surgery*, *33*(2), 239-250.

MGI-Mouse Genome Informatics-The international database resource for the laboratory mouse. (2022). Retrieved 6 January 2022, from http://www.informatics.jax.org/.

MGI-Mouse Genome Informatics-The international database resource for the laboratory mouse. 2022. *Informatics.jax.org*. http://www.informatics.jax.org/, January 15, 2022.

Miao, F. J. P., & Lee, T. J. F. (1990). Cholinergic and VIPergic innervation in cerebral arteries: a sequential double-labeling immunohistochemical study. *Journal of Cerebral Blood Flow & Metabolism*, *10*(1), 32-37.

Miller, R. J. (1998). Presynaptic receptors. *Annual review of pharmacology and toxicology*, *38*(1), 201-227.

Milner, P., & Burnstock, G. (1996). Chronic sensory denervation reduces thrombin-stimulated endothelin release from aortic endothelial cells. *Experientia*, *52*(3), 242-244.

Milner, P., Bodin, P., Loesch, A., & Burnstock, G. (1990). Rapid release of endothelin and ATP from isolated aortic endothelial cells exposed to increased flow. *Biochemical and biophysical research communications*, *170*(2), 649-656.

Miras-Portugal, M. T., Menéndez-Méndez, A., Gómez-Villafuertes, R., Ortega, F., Delicado, E. G., Pérez-Sen, R., & Gualix, J. (2019). Physiopathological role of the vesicular nucleotide transporter (VNUT) in the central nervous system: relevance of the vesicular nucleotide release as a potential therapeutic target. *Frontiers in Cellular Neuroscience*, *13*, 224.

Miras-Portugal, M. T., Sebastián-Serrano, Á., de Diego García, L., & Díaz-Hernández, M. (2017). Neuronal P2X7 receptor: involvement in neuronal physiology and pathology. *Journal of Neuroscience*, *37*(30), 7063-7072.

Mitsuoka, K., Miwa, Y., Kikutani, T., & Sato, I. (2018). Localization of CGRP and VEGF mRNAs in the mouse superior cervical ganglion during pre-and postnatal development. *European journal of histochemistry: EJH*, *62*(4).

Mizuno, K., Shiozawa, K., Katoh, T. A., Minegishi, K., Ide, T., Ikawa, Y., ... & Hamada, H. (2020). Role of Ca2+ transients at the node of the mouse embryo in breaking of left-right symmetry. *Science advances*, *6*(30).

Molliver, D. C., S. P. Cook, J. A. Carlsten, D. E. Wright, and E. W. McCleskey, 2002: ATP and UTP excite sensory neurons and induce CREB phosphorylation through the metabotropic receptor, P2Y2. Eur J Neurosci, 16,1850-60.

Moores, T. S., Hasdemir, B., Vega-Riveroll, L., Deuchars, J., & Parson, S. H. (2005). Properties of presynaptic P2X7-like receptors at the neuromuscular junction. *Brain research*, *1034*(1-2), 40-50.

Moriyama, Y., Hiasa, M., Sakamoto, S., Omote, H., & Nomura, M. (2017). Vesicular nucleotide transporter (VNUT): appearance of an actress on the stage of purinergic signaling. *Purinergic signalling*, *13*(3), 387-404.

Mulderry, P. K., Ghatei, M. A., Rodrigo, J., Allen, J. M., Rosenfeld, M. G., Polak, J. M., & Bloom, S. R. (1985). Calcitonin gene-related peptide in cardiovascular tissues of the rat. *Neuroscience*, *14*(3), 947-954.

Mulryan, K., Gitterman, D. P., Lewis, C. J., Vial, C., Leckie, B. J., Cobb, A. L., ... & Evans, R. J. (2000). Reduced vas deferens contraction and male infertility in mice lacking P2X1 receptors. *Nature*, *403*(6765), 86-89.

Murchison, D., & Griffith, W. H. (2000). Mitochondria buffer non-toxic calcium loads and release calcium through the mitochondrial permeability transition pore and sodium/calcium exchanger in rat basal forebrain neurons. *Brain research*, *854*(1-2), 139-151.

Navar, L. G. (2014). Physiology: hemodynamics, endothelial function, renin–angiotensin–aldosterone system, sympathetic nervous system. Journal of the American Society of Hypertension: JASH, 8(7), 519.

Nelson, D. W., Gregg, R. J., Kort, M. E., Perez-Medrano, A., Voight, E. A., Wang, Y., ... & Carroll, W. A. (2006). Structure− activity relationship studies on a series of novel, substituted 1-benzyl-5-phenyltetrazole P2X7 antagonists. *Journal of medicinal chemistry*, *49*(12), 3659-3666.

Nicke, A., Kuan, Y. H., Masin, M., Rettinger, J., Marquez-Klaka, B., Bender, O., ... & Soto, F. (2009). A functional P2X7 splice variant with an alternative transmembrane domain 1 escapes gene inactivation in P2X7 knock-out mice. *Journal of Biological Chemistry*, *284*(38), 25813-25822.

Nishanthi, A., & Vimal, M. (2017). Role of Presynaptic receptors in health and disease. *Indian Journal of Research in Pharmacy and Biotechnology*, *5*(3), 194-200.

Nishanthi, A., & Vimal, M. (2017). Role of Presynaptic receptors in health and disease. *Indian Journal of Research in Pharmacy and Biotechnology*, *5*(3), 194-200.

Nishida, K., Nomura, Y., Kawamori, K., Moriyama, Y., & Nagasawa, K. (2014). Expression profile of vesicular nucleotide transporter (VNUT, SLC17A9) in subpopulations of rat dorsal root ganglion neurons. *Neuroscience Letters*, *579*, 75-79.

Nörenberg, W., Göbel, I., Meyer, A., Cox, S. L., Starke, K., & Trendelenburg, A. U. (2001). Stimulation of mouse cultured sympathetic neurons by uracil but not adenine nucleotides. *Neuroscience*, *103*(1), 227-236.

Nori, S., Fumagalli, L., Bo, X., Bogdanov, Y., & Burnstock, G. (1998). Coexpression of mRNAs for P2X1, P2X2 and P2X4 receptors in rat vascular smooth muscle: an in situ hybridization and RT-PCR study. *Journal of vascular research*, *35*(3), 179-185.

Nori, S., Fumagalli, L., Bo, X., Bogdanov, Y., & Burnstock, G. (1998). Coexpression of mRNAs for P2X1, P2X2 and P2X4 receptors in rat vascular smooth muscle: an in situ hybridization and RT-PCR study. *Journal of vascular research*, *35*(3), 179-185.

North, R. A. (2002). Molecular physiology of P2X receptors. *Physiological reviews*, *82*(4), 1013-1067.

North, R. A. (2016). P2X receptors. *Philosophical Transactions of the Royal Society B: Biological Sciences*, *371*(1700), 20150427.

North, R. A., & Surprenant, A. (2000). Pharmacology of cloned P2X receptors. *Annual review of pharmacology and toxicology*, *40*(1), 563-580.

O'Connor, S. C., Brain, K. L., & Bennett, M. R. (1999). Individual sympathetic varicosities possess different sensitivities to alpha 2 and P2 receptor agonists and antagonists in mouse vas deferens. *British journal of pharmacology*, *128*(8), 1739-1753.

Opgaard, O. S., Gulbenkian, S., Bergdahl, A., Barroso, C. P., Andrade, N. C., Polak, J. M., ... & Edvinsson, L. (1995). Innervation of human epicardial coronary veins: immunohistochemistry and vasomotility. Cardiovascular research, 29(4), 463-468.

Örçen, A., YılmAz, V., Akcan, U., Tüzün, E., & Erten, G. (2017). Viability of SH-SY5Y cells is associated with purinergic P2 receptor expression alterations. *Acta Biologica Hungarica*, *68*(1), 22-34.

Orellano, E. A., Rivera, O. J., Chevres, M., Chorna, N. E., & González, F. A. (2010). Inhibition of neuronal cell death after retinoic acid-induced down-regulation of P2X7 nucleotide receptor expression. *Molecular and cellular biochemistry*, *337*(1), 83-99.

Ormond, S. J., Barrera, N. P., Qureshi, O. S., Henderson, R. M., Edwardson, J. M., & Murrell-Lagnado, R. D. (2006). An uncharged region within the N terminus of the P2X6 receptor inhibits its assembly and exit from the endoplasmic reticulum. *Molecular pharmacology*, *69*(5), 1692-1700.

Ouyang, J., Chen, X., Su, S., Li, X., Xu, X., Yu, X., ... & Zhu, X. (2021). Neuroligin1 Contributes to Neuropathic Pain by Promoting Phosphorylation of Cofilin in Excitatory Neurons. *Frontiers in Molecular Neuroscience*, *14*, 22.

Påhlman, S., Ruusala, A. I., Abrahamsson, L., Mattsson, M. E., & Esscher, T. (1984). Retinoic acid-induced differentiation of cultured human neuroblastoma cells: a comparison with phorbolester-induced differentiation. *Cell differentiation*, *14*(2), 135-144.

Pakdeechote, P., Rummery, N. M., Ralevic, V., & Dunn, W. R. (2007). Raised tone reveals purinergic-mediated responses to sympathetic nerve stimulation in the rat perfused mesenteric vascular bed. *European journal of pharmacology*, *563*(1-3), 180-186.

Pankratov, Y., Lalo, U., Krishtal, O. A., & Verkhratsky, A. (2009). P2X receptors and synaptic plasticity. *Neuroscience*, 158(1), 137-148.

Pankratov, Y., Lalo, U., Krishtal, O., & Verkhratsky, A. (2002). Ionotropic P2X purinoreceptors mediate synaptic transmission in rat pyramidal neurones of layer II/III of somato-sensory cortex. *The Journal of physiology*, 542(2), 529-536.

Pankratov, Y., Lalo, U., Krishtal, O., & Verkhratsky, A. (2003). P2X receptor-mediated excitatory synaptic currents in somatosensory cortex. *Molecular and Cellular Neuroscience*, 24(3), 842-849.

Pankratov, Y., Lalo, U., Verkhratsky, A., & North, R. A. (2007). Quantal release of ATP in mouse cortex. *The Journal of general physiology*, 129(3), 257-265.

Parravicini, C., Ranghino, G., Abbracchio, M. P., & Fantucci, P. (2008). GPR17: molecular modeling and dynamics studies of the 3-D structure and purinergic ligand binding features in comparison with P2Y receptors. *BMC bioinformatics*, 9(1), 263.

Parvathenani, L. K., Tertyshnikova, S., Greco, C. R., Roberts, S. B., Robertson, B., & Posmantur, R. (2003). P2X7 mediates superoxide production in primary microglia and is up-regulated in a transgenic mouse model of Alzheimer's disease. *Journal of Biological Chemistry*, *278*(15), 13309-13317.

Patoary, M. N. I., Tropper, C., McDougal, R. A., Lin, Z., & Lytton, W. W. (2017). Parallel stochastic discrete event simulation of calcium dynamics in neuron. *IEEE/ACM transactions on computational biology and bioinformatics*, *16*(3), 1007-1019.

Pavlov, V. A., & Tracey, K. J. (2012). The vagus nerve and the inflammatory reflex—linking immunity and metabolism. *Nature Reviews Endocrinology*, 8(12), 743.

Per Larsson, K., Jon Hansen, A., & Dissing, S. (2002). The human SH-SY5Y neuroblastoma cell-line expresses a functional P2X7 purinoceptor that modulates voltage-dependent Ca2+ channel function. *Journal of neurochemistry*, *83*(2), 285-298.

Pernow, J., Öhlén, A., Hökfelt, T., Nilsson, O., & Lundberg, J. M. (1987). Neuropeptide Y: presence in perivascular noradrenergic neurons and vasoconstrictor effects on skeletal muscle blood vessels in experimental animals and man. *Regulatory peptides*, *19*(5-6), 313-324.

Piirainen, H., Ashok, Y., Nanekar, R. T., & Jaakola, V. P. (2011). Structural features of adenosine receptors: from crystal to function. *Biochimica et Biophysica Acta (BBA)-Biomembranes*, *1808*(5), 1233-1244.

Plater, M. E., Ford, I., Dent, M. T., Preston, F. E., & Ward, J. D. (1996). Elevated von Willebrand factor antigen predicts deterioration in diabetic peripheral nerve function. Diabetologia, 39(3), 336-343.

Pocock, J. M., & Kettenmann, H. (2007). Neurotransmitter receptors on microglia. *Trends in neurosciences*, 30(10), 527-535.

Porzionato, A., Macchi, V., Stecco, C., & De Caro, R. (2019). The carotid sinus nerve—structure, function, and clinical implications. *The Anatomical Record*, *302*(4), 575-587.

Potter, E. K., & McCloskey, D. I. (1987). Excitation of carotid body chemoreceptors by neuropeptide-Y. *Respiration physiology*, *67*(3), 357-365.

Price, J. (1984). Immunohistochemical evidence for dopaminergic neurons in the rat superior cervical ganglion. *Proceedings of the Royal society of London. Series B. Biological sciences*, *222*(1228), 357-362.

Puchałowicz, K., Tarnowski, M., Baranowska-Bosiacka, I., Chlubek, D., & Dziedziejko, V. (2014). P2X and P2Y receptors—role in the pathophysiology of the nervous system. *International journal of molecular sciences*, *15*(12), 23672-23704.

Puledda, F., & Goadsby, P. J. (2016). Current approaches to neuromodulation in primary headaches: focus on vagal nerve and sphenopalatine ganglion stimulation. Current pain and headache reports, 20(7), 47.

Putney Jr, J. W., Broad, L. M., Braun, F. J., Lievremont, J. P., & Bird, G. S. J. (2001). Mechanisms of capacitative calcium entry. *Journal of cell science*, *114*(12), 2223-2229.

Qiao, J., Paul, P., Lee, S., Qiao, L., Josifi, E., Tiao, J. R., & Chung, D. H. (2012). PI3K/AKT and ERK regulate retinoic acid-induced neuroblastoma cellular differentiation. *Biochemical and biophysical research communications*, *424*(3), 421-426.

Queiroz, G., Talaia, C., & Gonçalves, J. (2003). ATP modulates noradrenaline release by activation of inhibitory P2Y receptors and facilitatory P2X receptors in the rat vas deferens. *Journal of Pharmacology and Experimental Therapeutics*, *307*(2), 809-815.

Racchi, H., Irarrázabal, M. J., Howard, M., Morán, S., Zalaquett, R., & Huidobro-Toro, J. P. (1999). Adenosine 5′-triphosphate and neuropeptide Y are co-transmitters in conjunction with noradrenaline in the human saphenous vein. *British journal of pharmacology*, 126(5), 1175-1185.

Racchi, H., Schliem, A. J., Donoso, M. V., Rahmer, A., Zúñiga, Á., Guzmán, S., ... & Huidobro-Toro, J. P. (1997). Neuropeptide Y Y1 receptors are involved in the vasoconstriction caused by human sympathetic nerve stimulation. *European journal of pharmacology*, *329*(1), 79-83.

Racchi, H., Schliem, A. J., Donoso, M. V., Rahmer, A., Zúñiga, Á., Guzmán, S., ... & Huidobro-Toro, J. P. (1997). Neuropeptide Y Y1 receptors are involved in the vasoconstriction caused by human sympathetic nerve stimulation. *European journal of pharmacology*, *329*(1), 79-83.

Ralevic, V. (2001). Roles of purines and pyrimidines in endothelium. In *Purinergic and Pyrimidinergic Signalling II* (pp. 101-120). Springer, Berlin, Heidelberg.

Ralevic, V. (2009). Purines as neurotransmitters and neuromodulators in blood vessels. *Current vascular pharmacology*, *7*(1), 3-14.

Ralevic, V. (2012). P2X receptors in the cardiovascular system. Wiley Interdisciplinary Reviews: *Membrane Transport and Signaling*, 1(5), 663-674.

Ralevic, V. (2021). Purinergic signalling in the cardiovascular system—a tribute to Geoffrey Burnstock. *Purinergic Signalling*, *17*(1), 63-69.

Ralevic, V., & Burnstock, G. (1990). Postjunctional synergism of noradrenaline and adenosine 5′-triphosphate in the mesenteric arterial bed of the rat. *European journal of pharmacology*, 175(3), 291-299.

Ralevic, V., & Burnstock, G. (1998). Receptors for purines and pyrimidines. *Pharmacological reviews*, 50(3), 413-492.

Ralevic, V., & Dunn, W. R. (2015). Purinergic transmission in blood vessels. *Autonomic Neuroscience*, 191, 48-66.

Ralevic, V., Karoon, P., & Burnstock, G. (1995). Long-term sensory denervation by neonatal capsaicin treatment augments sympathetic neurotransmission in rat mesenteric arteries by increasing levels of norepinephrine and selectively enhancing postjunctional actions. *Journal of Pharmacology and Experimental Therapeutics*, *274*(1), 64-71.

Ramirez, A. N., & Kunze, D. L. (2002). P2X purinergic receptor channel expression and function in bovine aortic endothelium. American Journal of Physiology-Heart and Circulatory Physiology, 282(6), H2106-H2116.

Ramme, D., Regenold, J. T., Starke, K., Busse, R., & Illes, P. (1987). Identification of the neuroeffector transmitter in jejunal branches of the rabbit mesenteric artery. *Naunyn-Schmiedeberg's archives of pharmacology*, 336(3), 267-273.

Ray, F. R., Huang, W., Slater, M., & Barden, J. A. (2002). Purinergic receptor distribution in endothelial cells in blood vessels: a basis for selection of coronary artery grafts. *Atherosclerosis*, *162*(1), 55-61.

Rayment, S. J., Latif, M. L., Ralevic, V., & Alexander, S. P. H. (2007). Evidence for the expression of multiple uracil nucleotide-stimulated P2 receptors coupled to smooth muscle contraction in porcine isolated arteries. *British journal of pharmacology*, *150*(5), 604-612.

Retrieved 11 June 2022, from https://teachmeanatomy.info/head/nerves/sympathetic/.

Rivera, I., Zhang, S., Fuller, B., Edwards, B., Seki, T., & Wang, M. et al. 2007. P2 receptor regulation of [Ca2+]iin cultured mouse mesangial cells. *American Journal of Physiology-Renal Physiology*, 292(5): F1380-F1389.

Roberts, J. A., Vial, C., Digby, H. R., Agboh, K. C., Wen, H., Atterbury-Thomas, A., & Evans, R. J. (2006). Molecular properties of P2X receptors. *Pflügers Archiv*, *452*(5), 486-500.

Robinson, S. E., Schwartz, J., & Costa, E. (1980). Substance P in the superior cervical ganglion and the submaxillary gland of the rat. *Brain research*, *182*(1), 11-17.

Rodrigues, J. Q. D., da Silva Jr, E. D., de Magalhães Galvão, K., Miranda-Ferreira, R., Caricati-Neto, A., Jurkiewicz, N. H., ... & Jurkiewicz, A. (2014). Differential regulation of atrial contraction by P1 and P2 purinoceptors in normotensive and spontaneously hypertensive rats. *Hypertension Research*, *37*(3), 210-219.

Rodrigues, R. J., Almeida, T., Richardson, P. J., Oliveira, C. R., & Cunha, R. A. (2005). Dual presynaptic control by ATP of glutamate release via facilitatory P2X1, P2X2/3, and P2X3 and

inhibitory P2Y1, P2Y2, and/or P2Y4 receptors in the rat hippocampus. *Journal of Neuroscience*, *25*(27), 6286-6295.

Rong, W., Gourine, A. V., Cockayne, D. A., Xiang, Z., Ford, A. P., Spyer, K. M., & Burnstock, G. (2003). Pivotal role of nucleotide P2X2 receptor subunit of the ATP-gated ion channel mediating ventilatory responses to hypoxia. *Journal of Neuroscience*, *23*(36), 11315-11321.

Roth, G. A., Abate, D., Abate, K. H., Abay, S. M., Abbafati, C., Abbasi, N., ... & Borschmann, R. (2018). Global, regional, and national age-sex-specific mortality for 282 causes of death in 195 countries and territories, 1980–2017: a systematic analysis for the Global Burden of Disease Study 2017. *The Lancet*, *392*(10159), 1736-1788.

Ruan, H. Z., & Burnstock, G. (2005). The distribution of P2X5 purinergic receptors in the enteric nervous system of mouse. *Cell and tissue research*, *319*(2), 191-200.

Rubino, A., Ralevic, V., & Burnstock, G. (1993). The P1-purinoceptors that mediate the prejunctional inhibitory effect of adenosine on capsaicin-sensitive nonadrenergic noncholinergic neurotransmission in the rat mesenteric arterial bed are of the A1 subtype. *Journal of Pharmacology and Experimental Therapeutics*, *267*(3), 1100-1104.

Rudnitskaya, E. A., Kozlova, T. A., Burnyasheva, A. O., Tarasova, A. E., Pankova, T. M., Starostina, M. V., ... & Kolosova, N. G. (2020). Features of postnatal hippocampal development in a rat model of sporadic Alzheimer's disease. *Frontiers in Neuroscience*, *14*, 533.

Ruffolo, R. R., Nichols, A. J., Stadel, J. M., & Hieble, J. P. (1991). Structure and function of alpha-adrenoceptors. *Pharmacological Reviews*, 43(4), 475-505.

Rummery, N. M., Brock, J. A., Pakdeechote, P., Ralevic, V., & Dunn, W. R. (2007). ATP is the predominant sympathetic neurotransmitter in rat mesenteric arteries at high pressure. *The Journal of physiology*, 582(2), 745-754.

Sakamoto, S., Miyaji, T., Hiasa, M., Ichikawa, R., Uematsu, A., Iwatsuki, K., ... & Moriyama, Y. (2014). Impairment of vesicular ATP release affects glucose metabolism and increases insulin sensitivity. *Scientific reports*, *4*(1), 1-10.

Sánchez-Nogueiro, J., Marín-García, P., & Miras-Portugal, M. T. (2005). Characterization of a functional P2X7-like receptor in cerebellar granule neurons from P2X7 knockout mice. *FEBS letters*, *579*(17), 3783-3788.

Sawada, K., Echigo, N., Juge, N., Miyaji, T., Otsuka, M., Omote, H., ... & Moriyama, Y. (2008). Identification of a vesicular nucleotide transporter. *Proceedings of the National Academy of Sciences*, 105(15), 5683-5686.

Schmidt, M., & Löffler, G. (1998). Induction of aromatase activity in human adipose tissue stromal cells by extracellular nucleotides: Evidence for P2-purinoceptors in adipose tissue. *European journal of biochemistry*, *252*(1), 147-154.

Schneider, L., Giordano, S., Zelickson, B. R., Johnson, M. S., Benavides, G. A., Ouyang, X., ... & Zhang, J. (2011). Differentiation of SH-SY5Y cells to a neuronal phenotype changes cellular bioenergetics and the response to oxidative stress. *Free Radical Biology and Medicine*, *51*(11), 2007-2017.

Schneider, L., Giordano, S., Zelickson, B. R., Johnson, M. S., Benavides, G. A., Ouyang, X., ... & Zhang, J. (2011). Differentiation of SH-SY5Y cells to a neuronal phenotype changes cellular bioenergetics and the response to oxidative stress. *Free Radical Biology and Medicine*, *51*(11), 2007-2017.

Schuller, H. M. (2007). Neurotransmitter receptor-mediated signaling pathways as modulators of carcinogenesis. *Neuronal Activity in Tumor Tissue*, *39*, 45-63.

Schwiebert, L. M., Rice, W. C., Kudlow, B. A., Taylor, A. L., & Schwiebert, E. M. (2002). Extracellular ATP signaling and P2X nucleotide receptors in monolayers of primary human vascular endothelial cells. *American Journal of Physiology-Cell Physiology*, *282*(2), C289-C301.

Sedaa, K. O., Bjur, R. A., Shinozuka, K. A. Z. U. M. A. S. A., & Westfall, D. P. (1990). Nerve and drug-induced release of adenine nucleosides and nucleotides from rabbit aorta. *Journal of Pharmacology and Experimental Therapeutics*, *252*(3), 1060-1067.

Segal, S. S., Brett, S. E., & Sessa, W. C. (1999). Codistribution of NOS and caveolin throughout peripheral vasculature and skeletal muscle of hamsters. *American Journal of Physiology-Heart and Circulatory Physiology*, *277*(3), H1167-H1177.

Seref-Ferlengez, Z., Maung, S., Schaffler, M. B., Spray, D. C., Suadicani, S. O., & Thi, M. M. (2016). P2X7R-Panx1 complex impairs bone mechanosignaling under high glucose levels associated with type-1 diabetes. *PLoS One*, *11*(5), e0155107.

Sesti, C., Koyama, M., Broekman, M. J., Marcus, A. J., & Levi, R. (2003). Ectonucleotidase in sympathetic nerve endings modulates ATP and norepinephrine exocytosis in myocardial ischemia. *Journal of Pharmacology and Experimental Therapeutics*, *306*(1), 238-244.

Sévigny, J., Sundberg, C., Braun, N., Guckelberger, O., Csizmadia, E., Qawi, I., ... & Robson, S. C. (2002). Differential catalytic properties and vascular topography of murine nucleoside triphosphate diphosphohydrolase 1 (NTPDase1) and NTPDase2 have implications for thromboregulation. Blood, *The Journal of the American Society of Hematology*, 99(8), 2801-2809.

Sheng, Y., & Zhu, L. (2018). The crosstalk between autonomic nervous system and blood vessels. *International journal of physiology, pathophysiology and pharmacology*, *10*(1), 17.

Shipley, M. M., Mangold, C. A., & Szpara, M. L. (2016). Differentiation of the SH-SY5Y human neuroblastoma cell line. *JoVE (Journal of Visualized Experiments)*, (108), e53193.

Shipley, Mackenzie M., Colleen A. Mangold, and Moriah L. Szpara. "Differentiation of the SH-SY5Y human neuroblastoma cell line." *Journal of visualized experiments: JoVE* 108 (2016).

Silva, C. L. M., Tamura, E. K., Macedo, S. M. D., Cecon, E., Bueno-Alves, L., Farsky, S. H. P., ... & Markus, R. P. (2007). Melatonin inhibits nitric oxide production by microvascular endothelial cells in vivo and in vitro. *British journal of pharmacology,* 151(2), 195-205.

Simon, J., Kidd, E. J., Smith, F. M., Chessell, I. P., Murrell-Lagnado, R., Humphrey, P. P., & Barnard, E. A. (1997). Localization and functional expression of splice variants of the P2X2 receptor. *Molecular Pharmacology*, *52*(2), 237-248.

Simonsen, U., Garcia-Sacristán, A., & Prieto, D. (1997). Involvement of ATP in the non-adrenergic non-cholinergic inhibitory neurotransmission of lamb isolated coronary small arteries. British journal of pharmacology, 120(3), 411-420.

Skalli, O., Pelte, M. F., Peclet, M. C., Gabbiani, G., Gugliotta, P., Bussolati, G., ... & Orci, L. (1989). Alpha-smooth muscle actin, a differentiation marker of smooth muscle cells, is present in microfilamentous bundles of pericytes. *Journal of Histochemistry & Cytochemistry*, *37*(3), 315-321.

Smith, C., Merchant, M., Fekete, A., Nyugen, H. L., Oh, P., Tain, Y. L., ... & Baylis, C. (2009). Splice variants of neuronal nitric oxide synthase are present in the rat kidney. *Nephrology Dialysis Transplantation*, *24*(5), 1422-1428.

Smyth, L. M., Breen, L. T., & Mutafova-Yambolieva, V. N. (2006). Nicotinamide adenine dinucleotide is released from sympathetic nerve terminals via a botulinum neurotoxin A-mediated mechanism in canine mesenteric artery. *American Journal of Physiology-Heart and Circulatory Physiology*, *290*(5), H1818-H1825.

Smyth, L., Bobalova, J., Ward, S. M., Keef, K. D., & Mutafova-Yambolieva, V. N. (2000). Cotransmission from sympathetic vasoconstrictor neurons: differences in guinea-pig mesenteric artery and vein. *Autonomic Neuroscience*, *86*(1-2), 18-29.

Sobey, C. G., Sozzi, V., & Woodman, O. L. (1994). Ischaemia/reperfusion enhances phenylephrine-induced contraction of rabbit aorta due to impairment of neuronal uptake. *Journal of cardiovascular pharmacology,* 23(4), 562-568.

Song, L., McMackin, M., Nguyen, A., & Cortopassi, G. (2017). Parkin deficiency accelerates consequences of mitochondrial DNA deletions and Parkinsonism. *Neurobiology of disease*, *100*, 30-38.

Song, X., Gao, X., Guo, D., Yu, Q., Guo, W., He, C., ... & Xiang, Z. (2012). Expression of P2X2 and P2X3 receptors in the rat carotid sinus, aortic arch, vena cava, and heart, as well as petrosal and nodose ganglia. *Purinergic signalling*, *8*(1), 15-22.

Sperlágh, B., Heinrich, A., & Csölle, C. (2007). P2 receptor-mediated modulation of neurotransmitter release—an update. *Purinergic signalling*, *3*(4), 269-284.

Spitsbergen, J. M., Stewart, J. S., & Tuttle, J. B. (1995). Altered regulation of nerve growth factor secretion by cultured VSMCs from hypertensive rats. *American Journal of Physiology-Heart and Circulatory Physiology*, *269*(2), H621-H628.

Sprague, R. S., Ellsworth, M. L., & Detrich, H. H. (2003). Nucleotide release and purinergic signaling in the vasculature driven by the red blood cell. *Current Topics in Membranes*, 243-269.

Sprague, R. S., Ellsworth, M. L., Stephenson, A. H., & Lonigro, A. J. (1996). ATP: the red blood cell link to NO and local control of the pulmonary circulation. *American Journal of Physiology-Heart and Circulatory Physiology*, *271*(6), H2717-H2722.

Stamboulian, S., Choi, J. S., Ahn, H. S., Chang, Y. W., Tyrrell, L., Black, J. A., ... & Dib-Hajj, S. D. (2010). ERK1/2 mitogen-activated protein kinase phosphorylates sodium channel Nav1. 7 and alters its gating properties. *Journal of Neuroscience*, *30*(5), 1637-1647.

Starke, K., Gothert, M., & Kilbinger, H. (1989). Modulation of neurotransmitter release by presynaptic autoreceptors. *Physiological reviews*, *69*(3), 864-989.

Stevenson, C. (2015). *Unravelling the role of α2-adrenoceptors and P2X purinoceptors in vascular sympathetic neurotransmission using a mouse lacking α1-adrenoceptors* (Doctoral dissertation, University of Glasgow).

Sun, Q., Zhen, G., Li, T. P., Guo, Q., Li, Y., Su, W., ... & Cao, X. (2021). Parathyroid hormone attenuates osteoarthritis pain by remodeling subchondral bone in mice. *Elife*, *10*, e66532.

Sun, X. P., & Stanley, E. F. (1996). An ATP-activated, ligand-gated ion channel on a cholinergic presynaptic nerve terminal. *Proceedings of the National Academy of Sciences*, *93*(5), 1859-1863.

Sung, C. P., Arleth, A. J., & Feuerstein, G. Z. (1991). Neuropeptide Y upregulates the adhesiveness of human endothelial cells for leukocytes. *Circulation research*, 68(1), 314-318.

Supłat-Wypych, D., Dygas, A., & Barańska, J. (2010). 2′, 3′-O-(4-benzoylbenzoyl)–ATP-mediated calcium signaling in rat glioma C6 cells: role of the P2Y 2 nucleotide receptor. *Purinergic signalling*, *6*(3), 317-325.

Surprenant, A., Rassendren, F., Kawashima, E., North, R. A., & Buell, G. (1996). The cytolytic P2Z receptor for extracellular ATP identified as a P2X receptor (P2X7). *Science*, *272*(5262), 735-738.

Suzuki, Y., Inoue, T., & Ra, C. (2010). L-type Ca2+ channels: a new player in the regulation of Ca2+ signaling, cell activation and cell survival in immune cells. *Molecular immunology*, *47*(4), 640-648.

Syed, N. I. H., & Kennedy, C. (2012). Pharmacology of P2X receptors. *Wiley Interdisciplinary Reviews: Membrane Transport and Signaling*, *1*(1), 16-30.

Tajti, J., Möller, S., Uddman, R., Bodi, I., & Edvinsson, L. (1999). The human superior cervical ganglion: neuropeptides and peptide receptors. *Neuroscience letters*, *263*(2-3), 121-124.

Takaki, F., Nakamuta, N., Kusakabe, T., & Yamamoto, Y. (2015). Sympathetic and sensory innervation of small intensely fluorescent (SIF) cells in rat superior cervical ganglion. *Cell and tissue research*, *359*(2), 441-451.

Taylor, B. K., Abhyankar, S. S., Vo, N. T. T., Kriedt, C. L., Churi, S. B., & Urban, J. H. (2007). Neuropeptide Y acts at Y1 receptors in the rostral ventral medulla to inhibit neuropathic pain. *Pain*, *131*(1-2), 83-95.

The Basis of Western Blot - Creative Diagnostics. (2021). Retrieved 16 December 2021, from https://www.creative-diagnostics.com/The-Basis-of-Western-Blot.htm

Todd, K. J., & Robitaille, R. (2006). Purinergic modulation of synaptic signalling at the neuromuscular junction. *Pflügers Archiv*, *452*(5), 608-614.

Todorov, L. D., Mihaylova-Todorova, S., Craviso, G. L., Bjur, R. A., & Westfall, D. P. (1996). Evidence for the differential release of the cotransmitters ATP and noradrenaline from sympathetic nerves of the guinea-pig vas deferens. *The Journal of physiology*, 496(3), 731-748.

Todorov, L. D., Mihaylova-Todorova, S., Westfall, T. D., Sneddon, P., Kennedy, C., Bjur, R. A., & Westfall, D. P. (1997). Neuronal release of soluble nucleotidases and their role in neurotransmitter inactivation. *Nature*, *387*(6628), 76-79.

Todorov, L. D., Mihaylova-Todorova, S., Westfall, T. D., Sneddon, P., Kennedy, C., Bjur, R. A., & Westfall, D. P. (1997). Neuronal release of soluble nucleotidases and their role in neurotransmitter inactivation. *Nature*, *387*(6628), 76-79.

Torres, G. E., Egan, T. M., & Voigt, M. M. (1999). Hetero-oligomeric assembly of P2X receptor subunits: specificities exist with regard to possible partners. *Journal of Biological Chemistry*, *274*(10), 6653-6659.

Torres, G. E., Haines, W. R., Egan, T. M., & Voigt, M. M. (1998). Co-expression of P2X1 and P2X5 receptor subunits reveals a novel ATP-gated ion channel. *Molecular Pharmacology*, *54*(6), 989-993.

Toulme, E., Garcia, A., Samways, D., Egan, T. M., Carson, M. J., & Khakh, B. S. (2010). P2X4 receptors in activated C8-B4 cells of cerebellar microglial origin. *Journal of General Physiology*, *135*(4), 333-353.

Tracey, K. J. (2007). Physiology and immunology of the cholinergic antiinflammatory pathway. The Journal of clinical investigation, 117(2), 289-296.

Trzebski, A. (1992). Arterial chemoreceptor reflex and hypertension. *Hypertension*, *19*(6_pt_1), 562-566.

Tsien, R. Y. (1981). A non-disruptive technique for loading calcium buffers and indicators into cells. *Nature*, *290*(5806), 527-528.

Tsuda, M., Shigemoto-Mogami, Y., Koizumi, S., Mizokoshi, A., Kohsaka, S., Salter, M. W., & Inoue, K. (2003). P2X 4 receptors induced in spinal microglia gate tactile allodynia after nerve injury. *Nature*, 424(6950), 778-783.

Umapathy, N. S., Kaczmarek, E., Fatteh, N., Burns, N., Lucas, R., Stenmark, K. R., ... & Gerasimovskaya, E. V. (2013). Adenosine A1 receptors promote vasa vasorum endothelial cell barrier integrity via Gi and Akt-dependent actin cytoskeleton remodeling. *PloS one*, 8(4).

Valdecantos, P., Briones, R., Moya, P., Germain, A., & Huidobro-Toro, J. P. (2003). Pharmacological identification of P2X1, P2X4 and P2X7 nucleotide receptors in the smooth muscles of human umbilical cord and chorionic blood vessels. *Placenta*, *24*(1), 17-26.

Van den Pol, A. N., Yao, Y., Fu, L. Y., Foo, K., Huang, H., Coppari, R., ... & Broberger, C. (2009). Neuromedin B and gastrin-releasing peptide excite arcuate nucleus neuropeptide Y neurons in a novel transgenic mouse expressing strong Renilla green fluorescent protein in NPY neurons. *Journal of Neuroscience*, *29*(14), 4622-4639.

Vanoevelen, J., Raeymaekers, L., Dode, L., Parys, J. B., De Smedt, H., Callewaert, G., ... & Missiaen, L. (2005). Cytosolic Ca2+ signals depending on the functional state of the Golgi in HeLa cells. *Cell calcium*, *38*(5), 489-495.

Vartian, N., Moskvina, E., Scholze, T., Unterberger, U., Allgaier, C., & Boehm, S. (2001). UTP evokes noradrenaline release from rat sympathetic neurons by activation of protein kinase C. *Journal of neurochemistry*, *77*(3), 876-885.

Vázquez-Villoldo, N., Domercq, M., Martín, A., Llop, J., Gómez-Vallejo, V., & Matute, C. (2014). P2X4 receptors control the fate and survival of activated microglia. *Glia*, *62*(2), 171-184.

Verbeuren, T. J., Simonet, S., & Herman, A. G. (1994). Diet-induced atherosclerosis inhibits release of noradrenaline from sympathetic nerves in rabbit arteries. *European Journal of Pharmacology: Environmental Toxicology and Pharmacology*, 270(1), 27-34.

Verkhratsky, A., Zimmermann, H., Abbracchio, M. P., Illes, P., & DiVirgilio, F. (2020). In memoriam Geoffrey Burnstock: creator of purinergic signaling. *Function*, *1*(1), zqaa006.

Vial, C., & Evans, R. J. (2000). P2X receptor expression in mouse urinary bladder and the requirement of P2X1 receptors for functional P2X receptor responses in the mouse urinary bladder smooth muscle. *British journal of pharmacology*, *131*(7), 1489-1495.

Vial, C., & Evans, R. J. (2002). P2X1 receptor-deficient mice establish the native P2X receptor and a P2Y6-like receptor in arteries. *Molecular pharmacology*, *62*(6), 1438-1445.

Vidal, M., Hicks, P. E., & Langer, S. Z. (1986). Differential effects of α-β-methylene ATP on responses to nerve stimulation in SHR and WKY tail arteries. *Naunyn-Schmiedeberg's archives of pharmacology*, *332*(4), 384-390.

von Kügelgen, I. (2006). Pharmacological profiles of cloned mammalian P2Y-receptor subtypes. *Pharmacology & therapeutics*, *110*(3), 415-432.

von Kügelgen, I., & Hoffmann, K. (2016). Pharmacology and structure of P2Y receptors. *Neuropharmacology*, *104*, 50-61.

von Kügelgen, I., & Starke, K. (1991). Noradrenaline-ATP co-transmission in the sympathetic nervous system. Trends in pharmacological sciences, 12, 319-324.

von Kügelgen, I., Schöffel, E., & Starke, K. (1989). Inhibition by nucleotides acting at presynaptic P 2-receptors of sympathetic neuro-effector transmission in the mouse isolated vas deferens. *Naunyn-Schmiedeberg's archives of pharmacology*, *340*(5), 522-532.

Von Kügelgen, I., Stoffel, D., Schobert, A., & Starke, K. (1996). P2-purinoceptors on postganglionic sympathetic neurones. *Journal of autonomic pharmacology*, *16*(6), 413-416.

Vonend, O., Okonek, A., Stegbauer, J., Habbel, S., Quack, I., & Rump, L. C. (2005). Renovascular effects of sympathetic cotransmitters ATP and NPY are age-dependent in spontaneoulsy hypertensive rats. *Cardiovascular research*, 66(2), 345-352.

Vulchanova, L., Arvidsson, U., Riedl, M., Wang, J., Buell, G., Surprenant, A., ... & Elde, R. (1996). Differential distribution of two ATP-gated channels (P2X receptors) determined by immunocytochemistry. *Proceedings of the National Academy of Sciences*, *93*(15), 8063-8067.

Wang, L., Karlsson, L., Moses, S., Hultgårdh-Nilsson, A., Andersson, M., Borna, C., ... & Erlinge, D. (2002). P2 receptor expression profiles in human vascular smooth muscle and endothelial cells. *Journal of cardiovascular pharmacology*, *40*(6), 841-853.

Wang, R., Cao, L., Shen, Z., & Cao, Y. (2018). Up-regulation of contractile endothelin receptors by airborne fine particulate matter in rat mesenteric arteries via activation of MAPK pathway. *Environmental Science and Pollution Research*, *25*(15), 14713-14725.

Wang, S., Iring, A., Strilic, B., Juárez, J. A., Kaur, H., Troidl, K., ... & Lundberg, J. O. (2015). P2Y 2 and G q/G 11 control blood pressure by mediating endothelial mechanotransduction. *The Journal of clinical investigation*, *125*(8), 3077-3086.

Webb, T. E., Simon, J., Krishek, B. J., Bateson, A. N., Smart, T. G., King, B. F., ... & Barnard, E. A. (1993). Cloning and functional expression of a brain G-protein-coupled ATP receptor. *FEBS letters*, *324*(2), 219-225.

Webb, T. E., Simon, J., Krishek, B. J., Bateson, A. N., Smart, T. G., King, B. F., ... & Barnard, E. A. (1993). Cloning and functional expression of a brain G-protein-coupled ATP receptor. *FEBS letters*, *324*(2), 219-225.

Wenker, I. C., Sobrinho, C. R., Takakura, A. C., Mulkey, D. K., & Moreira, T. S. (2013). P2Y1 receptors expressed by C1 neurons determine peripheral chemoreceptor modulation of breathing, sympathetic activity, and blood pressure. *Hypertension*, *62*(2), 263-273.

Westcott, E. B., & Segal, S. S. (2013). Perivascular innervation: a multiplicity of roles in vasomotor control and myoendothelial signaling. *Microcirculation*, 20(3), 217-238.

White, J. D., Stewart, K. D., Krause, J. E., & McKelvy, J. F. (1985). Biochemistry of peptide-secreting neurons. *Physiological reviews*, 65(3), 553-606.

White, P. J., Webb, T. E., & Boarder, M. R. (2003). Characterization of a Ca2+ response to both UTP and ATP at human P2Y11 receptors: evidence for agonist-specific signaling. *Molecular pharmacology*, 63(6), 1356-1363.

Wihlborg, A. K., Wang, L., Braun, O. O., Eyjolfsson, A., Gustafsson, R., Gudbjartsson, T., & Erlinge, D. (2004). ADP receptor P2Y12 is expressed in vascular smooth muscle cells and stimulates contraction in human blood vessels. *Arteriosclerosis, thrombosis, and vascular biology*, 24(10), 1810-1815.

Wilkaniec, A., Cieślik, M., Murawska, E., Babiec, L., Gąssowska-Dobrowolska, M., Pałasz, E., ... & Adamczyk, A. (2020). P2X7 receptor is involved in mitochondrial dysfunction induced by extracellular alpha synuclein in neuroblastoma SH-SY5Y cells. *International Journal of Molecular Sciences*, *21*(11), 3959.

Wilson, H. L., Varcoe, R. W., Stokes, L., Holland, K. L., Francis, S. E., Dower, S. K., ... & Crossman, D. C. (2007). P2X receptor characterization and IL-1/IL-1Ra release from human endothelial cells. British journal of pharmacology, 151(1), 96-108.

Wu, Q., Boyle, M. P., & Palmiter, R. D. (2009). Loss of GABAergic signaling by AgRP neurons to the parabrachial nucleus leads to starvation. *Cell*, *137*(7), 1225-1234.

Wu, T., Dai, M., Shi, X. R., Jiang, Z. G., & Nuttall, A. L. (2011). Functional expression of P2X4 receptor in capillary endothelial cells of the cochlear spiral ligament and its role in regulating the capillary diameter. American Journal of Physiology-Heart and Circulatory Physiology, 301(1), H69-H78.

Xiang, Z., & Burnstock, G. (2005). Distribution of P2Y2 receptors in the guinea pig enteric nervous system and its coexistence with P2X2 and P2X3 receptors, neuropeptide Y, nitric oxide synthase and calretinin. *Histochemistry and cell biology*, *124*(5), 379-390.

Xiang, Z., Bo, X., & Burnstock, G. (1998). Localization of ATP-gated P2X receptor immunoreactivity in rat sensory and sympathetic ganglia. *Neuroscience letters*, *256*(2), 105-108.

Xicoy, H., Wieringa, B., & Martens, G. J. (2017). The SH-SY5Y cell line in Parkinson's disease research: a systematic review. *Molecular neurodegeneration*, *12*(1), 1-11.

Xie, H. R., Hu, L. S., & Li, G. Y. (2010). SH-SY5Y human neuroblastoma cell line: in vitro cell model of dopaminergic neurons in Parkinson's disease. *Chinese medical journal*, *123*(08), 1086-1092.

Yamamoto, K., de Waard, V., Fearns, C., & Loskutoff, D. J. (1998). Tissue distribution and regulation of murine von Willebrand factor gene expression in vivo. *Blood, The Journal of the American Society of Hematology*, *92*(8), 2791-2801.

Yamamoto, K., Korenaga, R., Kamiya, A., & Ando, J. (2000). Fluid shear stress activates Ca2+ influx into human endothelial cells via P2X4 purinoceptors. Circulation Research, 87(5), 385-391.

Yamamoto, K., Sokabe, T., Matsumoto, T., Yoshimura, K., Shibata, M., Ohura, N., ... & Ando, J. (2006). Impaired flow-dependent control of vascular tone and remodeling in P2X4-deficient mice. *Nature medicine*, *12*(1), 133-137.

Yang, S., Cheek, D. J., Westfall, D. P., & Buxton, I. L. (1994). Purinergic axis in cardiac blood vessels. Agonist-mediated release of ATP from cardiac endothelial cells. *Circulation research*, *74*(3), 401-407.

Yegutkin, G. G. (2014). Enzymes involved in metabolism of extracellular nucleotides and nucleosides: functional implications and measurement of activities. *Critical reviews in biochemistry and molecular biology*, *49*(6), 473-497.

Yin, D., & Slavin, K. V. (2016). Carotid sinus/nerve stimulation for treatment of resistant hypertension and heart failure. *Stimulation of the Peripheral Nervous System*, *29*, 83-93.

Yokomizo, A., Takatori, S., Hashikawa-Hobara, N., Goda, M., & Kawasaki, H. (2015). Characterization of perivascular nerve distribution in rat mesenteric small arteries. *Biological and Pharmaceutical Bulletin*, *38*(11), 1757-1764.

Yokota, H., Mukai, H., Hattori, S., Yamada, K., Anzai, Y., & Uno, T. (2018). MR imaging of the superior cervical ganglion and inferior ganglion of the vagus nerve: structures that can mimic pathologic retropharyngeal lymph nodes. *American Journal of Neuroradiology*, *39*(1), 170-176.

Yokoyama, T., Settai, K., Nakamuta, N., & Yamamoto, Y. (2019). Distribution and morphology of baroreceptors in the rat carotid sinus as revealed by immunohistochemistry for P2X3 purinoceptors. *Histochemistry and Cell Biology*, *151*(2), 161-173.

Yoshioka, K., Saitoh, O., & Nakata, H. (2002). Agonist-promoted heteromeric oligomerization between adenosine A1 and P2Y1 receptors in living cells. FEBS letters, 523(1-3), 147-151.

Zettler, C., & Rush, R. A. (1993). Elevated concentrations of nerve growth factor in heart and mesenteric arteries of spontaneously hypertensive rats. *Brain research*, *614*(1-2), 15-20.

Zhang, X., Zhang, M., Laties, A. M., & Mitchell, C. H. (2005). Stimulation of P2X7 receptors elevates Ca2+ and kills retinal ganglion cells. *Investigative ophthalmology & visual science*, *46*(6), 2183-2191.

Zhong, Y., Dunn, P. M., & Burnstock, G. (2000). Guinea-pig sympathetic neurons express varying proportions of two distinct P2X receptors. *The Journal of Physiology*, *523*(2), 391-402.

Zimmermann, H. (2006). Nucleotide signaling in nervous system development. *Pflügers Archiv*, *452*(5), 573-588.

Zimmermann, H. (2006, April). Ectonucleotidases in the nervous system. In *Purinergic Signalling in Neuron–Glia Interactions: Novartis Foundation Symposium 276* (pp. 113-130). Chichester, UK: John Wiley & Sons, Ltd.

Zou, Q., Leung, S. W., & Vanhoutte, P. M. (2012). Activation of nicotinic receptors can contribute to endothelium-dependent relaxations to acetylcholine in the rat aorta. *Journal of Pharmacology and Experimental Therapeutics*, 341(3), 756-763.

Supplementary

S.1 Nucleotide and amino acid sequences of the mouse P2X2 gene including the DNA and cDNA.

Gene: P2rx2 ENSMUSG00000029503

Description	purinergic receptor P2X, ligand-gated ion channel, 2 [Source:MGI Symbol;Acc:MGI:2665170]
Gene Synonyms	P2X2a, P2x2
Location	Chromosome 5: 110,487,678-110,491,078 reverse strand. GRCm39:CM000998.3
About this gene	This gene has 6 transcripts (splice variants), 189 orthologues, 6 paralogues and is associated with 7 phenotypes.
Transcripts	Hide transcript table

Show/hide columns (1 hidden) Filter

Transcript ID	Name	bp	Protein	Biotype	CCDS	UniProt Match	Flags
ENSMUST00000058016.16	P2rx2-201	1895	497aa	Protein coding	CCDS80363	Q8K3P1-5	Ensembl Canonical, GENCODE basic, TSL:1
ENSMUST00000195985.5	P2rx2-203	2096	485aa	Protein coding	CCDS51607	Q8K3P1-1	GENCODE basic, APPRIS ALT2, TSL:1
ENSMUST00000112478.8	P2rx2-202	1632	416aa	Protein coding	CCDS51608	Q8K3P1-2	GENCODE basic, APPRIS P2, TSL:1
ENSMUST00000200037.5	P2rx2-205	1569	395aa	Protein coding	CCDS80362	Q8K3P1-3	GENCODE basic, TSL:1
ENSMUST00000200214.2	P2rx2-206	1568	398aa	Protein coding	CCDS80361	Q8K3P1-4	GENCODE basic, TSL:1
ENSMUST00000199165.5	P2rx2-204	2010	No protein	Retained intron		-	TSL:2

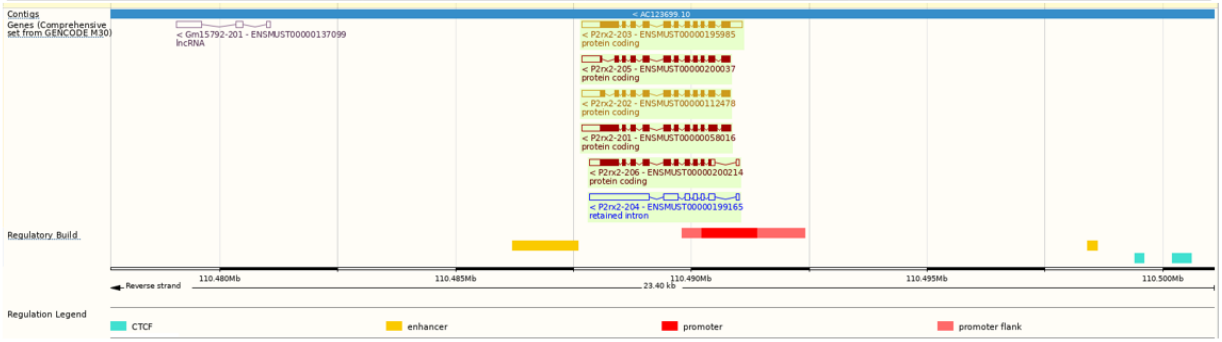

>ENSMUST00000112478.8 ENSMUSG00000029503:ENSMUST00000112478.8 cdna:protein_coding (292 bp)

ATGGCCGCTGCACAGCCCCGGCTTCCCGCGGGGGCGGCCATGGTCCGGCGCTTGGCCCGGGGCTGCTGGTCCGCGTTCT
GGGACTACGAGACGCCCAAGGTGATCGTGGTGCGGAATCGGCGCCTGGGATTCGTGCACCGCATGGTGCAGCTGCTCAT
TCTGCTTTACTTCGTGTGGTACGTCTTCATCGTGCAGAAAAGCTACCAGGATAGCGAAACCGGTCCGGAGAGCTCCATC
ATCACCAAAGTCAAGGGGATCACCATGTCGGAACACAAAGTGTGGGACGTGGAGGAATACGTAAAGCCCCCGGAGGGGG
GCAGTGTAGTCAGCATCATCACCAGGATCGAGGTTACTCCTTCCCAGACCCTGGGAACATGCCCAGAGAGCATGAGGGT
TCACAGCTCTACCTGCCATTTAGATGACGACTGTGTGGCCGGACAGCTGGACATGCAGGGCAATGGGATTCGGACAGGA
CGCTGTGTACCCTATTACCATGGGGACTCCAAGACCTGCGAGGTGTCAGCCTGGTGCCCGGTGGAGGATGGGACTTCTG
AAAACCATTTTCTGGGTAAAATGGCCCCAAATTTCACCATCCTCATCAAGAACAGCATCCACTATCCCAAGTTCAAGTT
CTCCAAGGGCAACATTGCAAGCCAGAAGAGTGACTACCTGAAGCACTGCACGTTTGATCAGGACTCTGATCCATACTGT
CCCATCTTCAGGCTGGGCTTCATTGTAGAGCAAGCAGGAGAGAACTTCACAGAACTGGCACACAAGGGCGGTGTCATTG
GGGTCATCATCAACTGGAACTGTGACCTGGACTTGTCTGAATCAGAGTGCAACCCCAAATATTCTTTCCGGAGGCTCGA
CCCCAAGTATGACCCTGCCTCTTCAGGCTACAACTTCAGGTTTGCCAAATATTACAAGATAAACGGCACCACCACCACT
CGAACTCTCATCAAAGCCTATGGGATTCGAATTGACGTTATTGTGCATGGACAGGCAGGGAAATTCAGTCTCATTCCCA
CCATCATCAATCTGGCCACTGCTCTGACCTCCATCGGGGGTGGGCTCCTTTCTGTGTGACTGGATTTTGTTAACGTTCAT
GAACAAAAACAAGCTCTACAGCCATAAGAAGTTCGACAAGGTGGTGGACACTCTTGACCAGCATATGGGACAAAGGCCT
CCTGTCCCTGAGCCTTCCCAACAGGACTCCACATCCACGGACCCCAAAGGTTTGGCCCAACTTTGATCTCATCCTCACT
AAGCTACAGACCTGGATCTGGGAGGGCAGAGACAGCTTCTGCTGCTAGGCAGCCCTAGGGAAGATCTGCGCTCTTCAGT
AACCATGTCCACGTGACTGGGAAACAGACACCTGTGCAAGAAGATAGGCATCTTGCTCTGGGCCAGGCTTACATTCTTC
CTCTCCCTAAGGCTTCTGGGGAGAAGTGGGTCCCTGCCATTTCCTTTCCCAACAGAACTCCTCATAGGATCCCCTGTCC
TTTCCCTGCCCACCTTTTGTACTCTCACACAGCACTCTGGGACCCCAAATTAGAGCTGTCTTCCGGTTGTATTTTAAGC
CCCCCTTTAGAAGTCACACAGCGTGCTGAGTCCAATAAACCAGTGATGAGCT

>ENSMUST00000200037.5 ENSMUSG00000029503:ENSMUST00000200037.5
cdna:protein_coding (229 bp)
ATGGCCGCTGCACAGCCCCGGCTTCCCGCGGGGGCGGCCATGGTCCGGCGCTTGGCCCGGGGCTGCTGGTCCGCGTTCT
GGGACTACGAGACGCCCAAGGTGATCGTGGTGCGGAATCGGCGCCTGGGATTCGTGCACCGCATGGTGCAGCTGCTCAT
TCTGCTTTACTTCGTGTGGTACGTCTTCATCGTGCAGAAAAGCTACCAGGATAGCGAAACCGGTCCGGAGAGCTCCATC
ATCACCAAAGTCAAGGGGATCACCATGTCGGAACACAAAGTGTGGGACGTGGAGGAATACGTAAAGCCCCCGGAGGGGG
GCAGTGTAGTCAGCATCATCACCAGGATCGAGGTTACTCCTTCCCAGACCCTGGGAACATGCCCAGAGAGCATGAGGGT
TCACAGCTCTACCTGCCATTTAGATGACGACTGTGTGGCCGGACAGCTGGACATGCAGGGCAATGGGATTCGGACAGGA
CGCTGTGTACCCTATTACCATGGGGACTCCAAGACCTGCGAGGTGTCAGCCTGGTGCCCGGTGGAGGATGGGACTTCTG
AAAACCATTTTCTGGGTAAAATGGCCCCAAATTTCACCATCCTCATCAAGAACAGCATCCACTATCCCAAGTTCAAGTT
CTCCAAGGGCAACATTGCAAGCCAGAAGAGTGACTACCTGAAGCACTGCACGTTTGATCAGGACTCTGATCCATACTGT
CCCATCTTCAGGCTGGGCTTCATTGTAGAGCAAGCAGGAGAGAACTTCACAGAACTGGCACACAAGGGCGGTGTCATTG
GGGTCATCATCAACTGGAACTGTGACCTGGACTTGTCTGAATCAGAGTGCAACCCCAAATATTCTTTCCGGAGGCTCGA
CCCCAAGTATGACCCTGCCTCTTCAGGCTACAACTTCAGGTTTGCCAAATATTACAAGATAAACGGCACCACCACCACT
CGAACTCTCATCAAAGCCTATGGGATTCGAATTGACGTTATTGTGCATGGACAGGCAGGGAAATTCAGTCTCATTCCCA
CCATCATCAATCTGGCCACTGCTCTGACCTCCATCGGGGGTGGGCTCCTTTCTGTGTGACTGGATTTTGTTAACGTTCAT
GAACAAAAACAAGCTCTACAGCCATAAGAAGTTCGACAAGGACTCCACATCCACGGACCCCAAAGGTTTGGCCCAACTT
TGATCTCATCCTCACTAAGCTACAGACCTGGATCTGGGAGGGCAGAGACAGCTTCTGCTGCTAGGCAGCCCTAGGGAAG
ATCTGCGCTCTTCAGTAACCATGTCCACGTGACTGGGAAACAGACACCTGTGCAAGAAGATAGGCATCTTGCTCTGGGC
CAGGCTTACATTCTTCCTCTCCCTAAGGCTTCTGGGGAGAAGTGGGTCCCTGCCATTTCCTTTCCCAACAGAACTCCTC
ATAGGATCCCCTGTCCTTTCCCTGCCCACCTTTTGTACTCTCACACAGCACTCTGGGACCCCAAATTAGAGCTGTCTTC
CGGTTGTATTTTAAGCCCCCCTTTAGAAGTCACACAGCGTGCTGAGTCCAATAAACCAGTGATGAGCT

>ENSMUST00000195985.5 ENSMUSG00000029503:ENSMUST00000195985.5
cdna:protein_coding (499 bp)
CCTCCCGGGGCTCTCCGGGCTGGCCTGGCCTCTCCGCTCTTCTTGTCACCAAACTGGAGTTGTGATCCACCAACTGCAC
CACCAGGCTGCACTCTGAGCCGCACCCCGCCGCACCTGCAGTCTTCAGTAAGACTGGAAAGGGACTAGATTGCTACTGT
CACAAAGGGCGGGGAGCGAGGCCACACCCCCAGCCTGCCCACGAGAGGCCGAGAGTGTGAGGCGCTCCAGCAGCTCTTG
TGGACCGAGCTCCTTGGGCCATGGCCGCTGCACAGCCCCGGCTTCCCGCGGGGGCGGCCATGGTCCGGCGCTTGGCCCG
GGGCTGCTGGTCCGCGTTCTGGGACTACGAGACGCCCAAGGTGATCGTGGTGCGGAATCGGCGCCTGGGATTCGTGCAC
CGCATGGTGCAGCTGCTCATTCTGCTTTACTTCGTGTGGTACGTCTTCATCGTGCAGAAAAGCTACCAGGATAGCGAAA
CCGGTCCGGAGAGCTCCATCATCACCAAAGTCAAGGGGATCACCATGTCGGAACACAAAGTGTGGGACGTGGAGGAATA
CGTAAAGCCCCCGGAGGGGGGCAGTGTAGTCAGCATCATCACCAGGATCGAGGTTACTCCTTCCCAGACCCTGGGAACA
TGCCCAGAGAGCATGAGGGTTCACAGCTCTACCTGCCATTTAGATGACGACTGTGTGGCCGGACAGCTGGACATGCAGG
GCAATGGGATTCGGACAGGACGCTGTGTACCCTATTACCATGGGGACTCCAAGACCTGCGAGGTGTCAGCCTGGTGCCC
GGTGGAGGATGGGACTTCTGAAAACCATTTTCTGGGTAAAATGGCCCCAAATTTCACCATCCTCATCAAGAACAGCATC
CACTATCCCAAGTTCAAGTTCTCCAAGGGCAACATTGCAAGCCAGAAGAGTGACTACCTGAAGCACTGCACGTTTGATC
AGGACTCTGATCCATACTGTCCCATCTTCAGGCTGGGCTTCATTGTAGAGCAAGCAGGAGAGAACTTCACAGAACTGGC
ACACAAGGGCGGTGTCATTGGGGTCATCATCAACTGGAACTGTGACCTGGACTTGTCTGAATCAGAGTGCAACCCCAAA
TATTCTTTCCGGAGGCTCGACCCCAAGTATGACCCTGCCTCTTCAGGCTACAACTTCAGGTTTGCCAAATATTACAAGA
TAAACGGCACCACCACCACTCGAACTCTCATCAAAGCCTATGGGATTCGAATTGACGTTATTGTGCATGGACAGGCAGG
GAAATTCAGTCTCATTCCCACCATCATCAATCTGGCCACTGCTCTGACCTCCATCGGGGGTGGGCTCCTTTCTGTGTGAC
TGGATTTTGTTAACGTTCATGAACAAAAACAAGCTCTACAGCCATAAGAAGTTCGACAAGGTGCGTACCCCAAGGCACC
CCTCAAGTAGATGGCCTGTGACCCTTGCCCTTGTCTTGGGCCAGATCCCTCCCCCACCTAGTCACTACTCCCAGGACCA
GCCACCCAGCCTTCCATCAGGTGAAGGACCAGCTTTGGGAGAAGGGGCAGAGCTACCACTGGCTGTCCAGCCTCCTCGG
TCTTGCTCCAGCTCTGCTCTGACTGAGCAGGTGGTGGACACTCTTGACCAGCATATGGGACAAAGGCCTCCTGTCCCTG
AGCCTTCCCAACAGGACTCCACATCCACGGACCCCAAAGGTTTGGCCCAACTTTGATCTCATCCTCACTAAGCTACAGA
CCTGGATCTGGGAGGGCAGAGACAGCTTCTGCTGCTAGGCAGCCCTAGGGAAGATCTGCGCTCTTCAGTAACCATGTCC
ACGTGACTGGGAAACAGACACCTGTGCAAGAAGATAGGCATCTTGCTCTGGGCCAGGCTTACATTCTTCCTCTCCCTAA
GGCTTCTGGGGAGAAGTGGGTCCCTGCCATTTCCTTTCCCAACAGAACTCCTCATAGGATCCCCTGTCCTTTCCCTGCC
CACCTTTTGTACTCTCACACAGCACTCTGGGACCCCAAATTAGAGCTGTCTTCCGGTTGTATTTTAAGCCCCCCTTTAG
AAGTCACACAGCGTGCTGAGTCCAATAAACCAGTGATGAGCT

>ENSMUST00000058016.16 ENSMUSG00000029503:ENSMUST00000058016.16
cdna:protein_coding (499 bp)
GTGGACCGAGCTCCTTGGGCCATGGCCGCTGCACAGCCCCGGCTTCCCGCGGGGGCGGCCATGGTCCGGCGCTTGGCCC
GGGGCTGCTGGTCCGCGTTCTGGGACTACGAGACGCCCAAGGTGATCGTGGTGCGGAATCGGCGCCTGGGATTCGTGCA
CCGCATGGTGCAGCTGCTCATTCTGCTTTACTTCGTGTGGGTTGCCTCCGGAGCCGGCACCGCCCTATCCCACAGGTAC
GTCTTCATCGTGCAGAAAAGCTACCAGGATAGCGAAACCGGTCCGGAGAGCTCCATCATCACCAAAGTCAAGGGGATCA
CCATGTCGGAACACAAAGTGTGGGACGTGGAGGAATACGTAAAGCCCCCGGAGGGGGGCAGTGTAGTCAGCATCATCAC
CAGGATCGAGGTTACTCCTTCCCAGACCCTGGGAACATGCCCAGAGAGCATGAGGGTTCACAGCTCTACCTGCCATTTA
GATGACGACTGTGTGGCCGGACAGCTGGACATGCAGGGCAATGGGATTCGGACAGGACGCTGTGTACCCTATTACCATG
GGGACTCCAAGACCTGCGAGGTGTCAGCCTGGTGCCCGGTGGAGGATGGGACTTCTGAAAACCATTTTCTGGGTAAAAT
GGCCCCAAATTTCACCATCCTCATCAAGAACAGCATCCACTATCCCAAGTTCAAGTTCTCCAAGGGCAACATTGCAAGC
CAGAAGAGTGACTACCTGAAGCACTGCACGTTTGATCAGGACTCTGATCCATACTGTCCCATCTTCAGGCTGGGCTTCA
TTGTAGAGCAAGCAGGAGAGAACTTCACAGAACTGGCACACAAGGGCGGTGTCATTGGGGTCATCATCAACTGGAACTG
TGACCTGGACTTGTCTGAATCAGAGTGCAACCCCAAATATTCTTTCCGGAGGCTCGACCCCAAGTATGACCCTGCCTCT

TCAGGCTACAACTTCAGGTTTGCCAAATATTACAAGATAAACGGCACCACCACCACTCGAACTCTCATCAAAGCCTATG
GGATTCGAATTGACGTTATTGTGCATGGACAGGCAGGGAAATTCAGTCTCATTCCCACCATCATCAATCTGGCCACTGC
TCTGACCTCCATCGGGGGTGGGCTCCTTTCTGTGTGACTGGATTTTGTTAACGTTCATGAACAAAAACAAGCTCTACAGC
CATAAGAAGTTCGACAAGGTGCGTACCCCAAGGCACCCCTCAAGTAGATGGCCTGTGACCCTTGCCCTTGTCTTGGGCC
AGATCCCTCCCCCACCTAGTCACTACTCCCAGGACCAGCCACCCAGCCTTCCATCAGGTGAAGGACCAGCTTTGGGAGA
AGGGGCAGAGCTACCACTGGCTGTCCAGCCTCCTCGGTCTTGCTCCAGCTCTGCTCTGACTGAGCAGGTGGTGGACACT
CTTGACCAGCATATGGGACAAAGGCCTCCTGTCCCTGAGCCTTCCCAACAGGACTCCACATCCACGGACCCCAAAGGTT
TGGCCCAACTTTGATCTCATCCTCACTAAGCTACAGACCTGGATCTGGGAGGGCAGAGACAGCTTCTGCTGCTAGGCAG
CCCTAGGGAAGATCTGCGCTCTTCAGTAACCATGTCCACGTGACTGGGAAACAGACACCTGTGCAAGAAGATAGGCATC
TTGCTCTGGGCCAGGCTTACATTCTTCCTCTCCCTAAGGCTTCTGGGGAGAAGTGGGTCCCTGCCATTTCCTTTCCCAA
CAGAACTCCTCATAGGATCCCCTGTCCTTTCCCTGCCCACCTTTTGTACTCTCACACAGCACTCTGGGACCCCAAATTA
GAGCTGTCTTCCGGTTGTATTTTAAGCCCCCCTTTAGAAGTCACACAGCGTGCTGAGTCCAATAAACCAGTGATGAGC

>ENSMUST00000199165.5 ENSMUSG00000029503:ENSMUST00000199165.5
cdna:retained_intron
GATCCACCAACTGCACCACCAGGCTGCACTCTGAGCCGCACCCCGCCGCACCTGCAGTCTTCAGTACGTCTTCATCGTG
CAGAAAAGCTACCAGGATAGCGAAACCGGTCCGGAGAGCTCCATCATCACCAAAGTCAAGGGGATCACCATGTCGGAAC
ACAAAGTGTGGGACGTGGAGGAATACGTAAAGCCCCCGGAGGGGGGCAGTGTAGTCAGCATCATCACCAGGATCGAGGT
TACTCCTTCCCAGACCCTGGGAACATGCCCAGAGAGCATGAGGGTTCACAGCTCTACCTGCCATTTAGATGACGACTGT
GTGGCCGGACAGCTGGACATGCAGGGCAATGGGATTCGGACAGGACGCTGTGTACCCTATTACCATGGGGACTCCAAGA
CCTGCGAGGTGTCAGCCTGGTGCCCGGTGGAGGATGGGACTTCTGAAAACCATTTTCTGGGTAAAATGGCCCCAAATTT
CACCATCCTCATCAAGAACAGCATCCACTATCCCAAGTTCAAGTTCTCCAAGTGAGTCTGAGGAGTAATTGCAAATGCC
CGACCAGTATGTAGGCATGTGCTGGGAGCAGGTGTTTGTTTTCTGCTTCTCCTTAGGGGCAACATTGCAAGCCAGAAGA
GTGACTACCTGAAGCACTGCACGTTTGATCAGGACTCTGATCCATACTGTCCCATCTTCAGGCTGGGCTTCATTGTAGA
GCAAGCAGGAGAGAACTTCACAGAACTGGCACACAAGGGCGGTGTCATTGGGGTCATCATCAACTGGAACTGTGACCTG
GACTTGTCTGAATCAGAGTGCAACCCCAAATATTCTTTCCGGAGGCTCGACCCCAAGTATGACCCTGCCTCTTCAGGCT
ACAACTTCAGGTACCTTGTTCTGGATCCATGACAGACAGTGGTGGCTGTGTTGACTATAGTCCCACCAGAAGAAGTCCT
AAAGAGAGGAAGATGGGTGTGTTCGAGTGCCACAGTCCTCAGACTGACAGCTTTGACATTACTTTGGTTCCCTCGACCC
TAGGTTTGCCAAATATTACAAGATAAACGGCACCACCACCACTCGAACTCTCATCAAAGCCTATGGGATTCGAATTGAC
GTTATTGTGCATGGACAGGTACGCACGGCTGAAGGGTTCCACCTAGGCCTGTGCTGGGCTAGCTCCATGCCCCTTATAG
CATCCCATCCTCAAGCAGCCTGTGTTGAAGGTCTAACTAAATGCATGTCTGTTGTCTACAGGCAGGGAAATTCAGTCTC
ATTCCCACCATCATCAATCTGGCCACTGCTCTGACCTCCATCGGGGTGGTAAGAAATCCAGATCCCCTTAGGGGTCTGA
GTCAGGTAGGGAGTGCTTGGTATGCCTTTACCCACTCGCACCTGCTGATTTCAGGGCTCCTTTCTGTGTGACTGGATTT
TGTTAACGTTCATGAACAAAAACAAGCTCTACAGCCATAAGAAGTTCGACAAGGTGCGTACCCCAAGGCACCCCTCAAG
TAGATGGCCTGTGACCCTTGCCCTTGTCTTGGGCCAGATCCCTCCCCCACCTAGTCACTACTCCCAGGACCAGCCACCC
AGCCTTCCATCAGGTGAAGGACCAGCTTTGGGAGAAGGGGCAGAGCTACCACTGGCTGTCCAGCCTCCTCGGTCTTGCT
CCAGCTCTGCTCTGACTGAGCAGGTGGTGGACACTCTTGACCAGCATATGGGACAAAGGCCTCCTGTCCCTGAGCCTTC
CCAACAGGACTCCACATCCACGGACCCCAAAGGTTTGGCCCAACTTTGATCTCATCCTCACTAAGCTACAGACCTGGAT
CTGGGAGGGCAGAGACAGCTTCTGCTGCTAGGCAGCCCTAGGGAAGATCTGCGCTCTTCAGTAACCATGTCCACGTGAC
TGGGAAACAGACACCTGTGCAAGAAGATAGGCATCTTGCTCTGGGCCAGGCTTACATTCTTCCTCTCCCTAAGGCTTCT
GGGGAGAAGTGGGTCCCTGCCATTTCCTTTCCCAA

>ENSMUST00000200214.2 ENSMUSG00000029503:ENSMUST00000200214.2
cdna:protein_coding (499 bp)
GATCCACCAACTGCACCACCAGGCTGCACTCTGAGCCGCACCCCGCCGCACCTGCAGTCTTCAGTACGTCTTCATCGTG
CAGAAAAGCTACCAGGATAGCGAAACCGGTCCGGAGAGCTCCATCATCACCAAAGTCAAGGGGATCACCATGTCGGAAC
ACAAAGTGTGGGACGTGGAGGAATACGTAAAGCCCCCGGAGGGGGGCAGTGTAGTCAGCATCATCACCAGGATCGAGGT
TACTCCTTCCCAGACCCTGGGAACATGCCCAGAGAGCATGAGGGTTCACAGCTCTACCTGCCATTTAGATGACGACTGT
GTGGCCGGACAGCTGGACATGCAGGGCAATGGGATTCGGACAGGACGCTGTGTACCCTATTACCATGGGGACTCCAAGA
CCTGCGAGGTGTCAGCCTGGTGCCCGGTGGAGGATGGGACTTCTGAAAACCATTTTCTGGGTAAAATGGCCCCAAATTT
CACCATCCTCATCAAGAACAGCATCCACTATCCCAAGTTCAAGTTCTCCAAGGGCAACATTGCAAGCCAGAAGAGTGAC
TACCTGAAGCACTGCACGTTTGATCAGGACTCTGATCCATACTGTCCCATCTTCAGGCTGGGCTTCATTGTAGAGCAAG
CAGGAGAGAACTTCACAGAACTGGCACACAAGGGCGGTGTCATTGGGGTCATCATCAACTGGAACTGTGACCTGGACTT
GTCTGAATCAGAGTGCAACCCCAAATATTCTTTCCGGAGGCTCGACCCCAAGTATGACCCTGCCTCTTCAGGCTACAAC
TTCAGGTTTGCCAAATATTACAAGATAAACGGCACCACCACCACTCGAACTCTCATCAAAGCCTATGGGATTCGAATTG
ACGTTATTGTGCATGGACAGGCAGGGAAATTCAGTCTCATTCCCACCATCATCAATCTGGCCACTGCTCTGACCTCCAT
CGGGGTGGGCTCCTTTCTGTGTGACTGGATTTTGTTAACGTTCATGAACAAAAACAAGCTCTACAGCCATAAGAAGTTC
GACAAGGTGCGTACCCCAAGGCACCCCTCAAGTAGATGGCCTGTGACCCTTGCCCTTGTCTTGGGCCAGATCCCTCCCC
CACCTAGTCACTACTCCCAGGACCAGCCACCCAGCCTTCCATCAGGTGAAGGACCAGCTTTGGGAGAAGGGGCAGAGCT
ACCACTGGCTGTCCAGCCTCCTCGGTCTTGCTCCAGCTCTGCTCTGACTGAGCAGGTGGTGGACACTCTTGACCAGCAT
ATGGGACAAAGGCCTCCTGTCCCTGAGCCTTCCCAACAGGACTCCACATCCACGGACCCCAAAGGTTTGGCCCAACTTT
GATCTCATCCTCACTAAGCTACAGACCTGGATCTGGGAGGGCAGAGACAGCTTCTGCTGCTAGGCAGCCCTAGGGAAGA
TCTGCGCTCTTCAGTAACCATGTCCACGTGACTGGGAAACAGACACCTGTGCAAGAAGATAGGCATCTTGCTCTGGGCC
AGGCTTACATTCTTCCTCTCCCTAAGGCTTCTGGGGAGAAGTGGGTCCCTGCCATTTCCTTTCCCAA

>5 dna:chromosome chromosome:GRCm39:5:110487678:110491078:-1

CCTCCCGGGGCTCTCCGGGCTGGCCTGGCCTCTCCGCTCTTCTTGTCACCAAACTGGAGTTGTGATCCACCAACTGCAC
CACCAGGCTGCACTCTGAGCCGCACCCCGCCGCACCTGCAGTCTTCAGTAAGACTGGAAAGGGACTAGATTGCTACTGT
CACAAAGGGCGGGGAGCGAGGCCACACCCCCAGCCTGCCCACGAGAGGCCGAGAGTGTGAGGCGCTCCAGCAGCTCTTG
TGGACCGAGCTCCTTGGGCCATGGCCGCTGCACAGCCCCGGCTTCCCGCGGGGGCGGCCATGGTCCGGCGCTTGGCCCG
GGGCTGCTGGTCCGCGTTCTGGGACTACGAGACGCCCAAGGTGATCGTGGTGCGGAATCGGCGCCTGGGATTCGTGCAC
CGCATGGTGCAGCTGCTCATTCTGCTTTACTTCGTGTGGTGCGCCGGCCGGGGCACAGTGGGCAATCGGGCGGGAGGGG
ATACTCAGCCCTGGGCTTGTGCGGGCGCCCTTAGGGCTTTAGGAGAGGGATATCCTGGTCTCTCCAGGGTTGCCTCCGG
AGCCGGCACCGCCCTATCCCACAGGTACGTCTTCATCGTGCAGAAAAGCTACCAGGATAGCGAAACCGGTCCGGAGAGC
TCCATCATCACCAAAGTCAAGGGGATCACCATGTCGGAACACAAAGTGTGGGACGTGGAGGAATACGTAAAGCCCCCGG
AGGTGCGGCGCTTCCTGCCCCAGGCCCGATGCTCCTCCGCGGTGTGACCCGTCTGAGTGAGCTGACAGGCCCACCGCGC
CTTTATTTCTGCACCCAGGGGGGCAGTGTAGTCAGCATCATCACCAGGATCGAGGTTACTCCTTCCCAGACCCTGGGAA
CATGCCCAGAGGTGAGGCCGGTCAAGGGTGGTCTGGGAAAACCTAGGCCAGTTGCAGAGTCTACCCTCTAACCTACAAT
CTCCACCCTAGAGCATGAGGGTTCACAGCTCTACCTGCCATTTAGATGACGACTGTGTGGCCGGACAGCTGGACATGCA
GGGCAATGGTCAGTGTGCATCAGGGACAGTGGGGAAGGCAGGGTTAGCCTGACCTCAGTAGATTAACCAGTGTGTGTCC
TGTAGGGATTCGGACAGGACGCTGTGTACCCTATTACCATGGGGACTCCAAGACCTGCGAGGTGTCAGCCTGGTGCCCG
GTGGAGGATGGGACTTCTGAAAAGTATGCAGGATCTACAGACCCCATCGGCAGTCTCCTTTCTCCTTACTGATGAAGAT
CAGATTAACTGGGAGGAGGAGGGAGACCATGTCCTCCTTCCTGCCCTTGGGATTTGGGGGAAAGGAGACTAAACCACTG
TCTGTAACTTTGCAGCCATTTTCTGGGTAAAATGGCCCCAAATTTCACCATCCTCATCAAGAACAGCATCCACTATCCC
AAGTTCAAGTTCTCCAAGTGAGTCTGAGGAGTAATTGCAAATGCCCGACCAGTATGTAGGCATGTGCTGGGAGCAGGTG
TTTGTTTTCTGCTTCTCCTTAGGGGCAACATTGCAAGCCAGAAGAGTGACTACCTGAAGCACTGCACGTTTGATCAGGA
CTCTGATCCATACTGTCCCATCTTCAGGCTGGGCTTCATTGTAGAGCAAGCAGGAGAGAACTTCACAGAACTGGCACAC
AAGGTAAGGATCAGAGGGCATGGGGACAGAGAAGCTGGGTGTCAGCATTTGCTGCCTAGGAAGGGTTTTACTGCATCTA
GATGTACCTTCTTTGTCTTGGTTAGCTTTAGCTGTGTTTAGGCAGAGGGGAGAAATGTGATCACGGTCTGTGCAGGCAC
CCGCTCAATTATTGACACCTGGTCCCATGACTGGTGCTAGTACCTCACTGCCTCCAAAACCAGAAATGACTAGCTCTCT
GGACCTTTGGCTCTGAGCTGAACCCTATTCCTTGAGGTTTTTCTGCTTTATGTTCTTCAGCCCTCCTTGGCTCACTTCT
CTGCAGGGCGGTGTCATTGGGGTCATCATCAACTGGAACTGTGACCTGGACTTGTCTGAATCAGAGTGCAACCCCAAAT
ATTCTTTCCGGAGGCTCGACCCCAAGTATGACCCTGCCTCTTCAGGCTACAACTTCAGGTACCTTGTTCTGGATCCATG
ACAGACAGTGGTGGCTGTGTTGACTATAGTCCCACCAGAAGAAGTCCTAAAGAGAGGAAGATGGGTGTGTTCGAGTGCC
ACAGTCCTCAGACTGACAGCTTTGACATTACTTTGGTTCCCTCGACCCTAGGTTTGCCAAATATTACAAGATAAACGGC
ACCACCACCACTCGAACTCTCATCAAAGCCTATGGGATTCGAATTGACGTTATTGTGCATGGACAGGTACGCACGGCTG
AAGGGTTCCACCTAGGCCTGTGCTGGGCTAGCTCCATGCCCCTTATAGCATCCCATCCTCAAGCAGCCTGTGTTGAAGG
TCTAACTAAATGCATGTCTGTTGTCTACAGGCAGGGAAATTCAGTCTCATTCCCACCATCATCAATCTGGCCACTGCTC
TGACCTCCATCGGGGTGGTAAGAAATCCAGATCCCCTTAGGGGTCTGAGTCAGGTAGGGAGTGCTTGGTATGCCTTTAC
CCACTCGCACCTGCTGATTTCAGGGCTCCTTTCTGTGTGACTGGATTTTGTTAACGTTCATGAACAAAAACAAGCTCTA
CAGCCATAAGAAGTTCGACAAGGTGCGTACCCCAAGGCACCCCTCAAGTAGATGGCCTGTGACCCTTGCCCTTGTCTTG
GGCCAGATCCCTCCCCCACCTAGTCACTACTCCCAGGACCAGCCACCCAGCCTTCCATCAGGTGAAGGACCAGCTTTGG
GAGAAGGGGCAGAGCTACCACTGGCTGTCCAGCCTCCTCGGTCTTGCTCCAGCTCTGCTCTGACTGAGCAGGTGGTGGA
CACTCTTGACCAGCATATGGGACAAAGGCCTCCTGTCCCTGAGCCTTCCCAACAGGACTCCACATCCACGGACCCCAAA
GGTTTGGCCCAACTTTGATCTCATCCTCACTAAGCTACAGACCTGGATCTGGGAGGGCAGAGACAGCTTCTGCTGCTAG
GCAGCCCTAGGGAAGATCTG**CGCTCTTCAGTAACCATGTCC**ACGTGACTGGGAAACAGACACCTGTGCAAGAAGATAGG
CATCTTGCTCTGGGCCAGGCTTACATTCTTCCTCTCCCTAAGGCTTCTGGGGAGAAGTGGGTCCCTGCCATTTCCTTTC
CCAACAGAACTCCTCATAGGATCCCCTGTCCTTTCCCTGCCCACCTTTTGTACTCTCACACAGCACTCTGGGACCCCAA
ATTAGAGCTGTCTTCCGGTTGTATTTTAAGCCCCCCTTTAGAAGTCACACAGCGTGCTGAGTCCAATAAACCAGTGATG
AGCT

S2. Multiple sequence alignment of the different P2X2 transcripts and the DNA sequence.

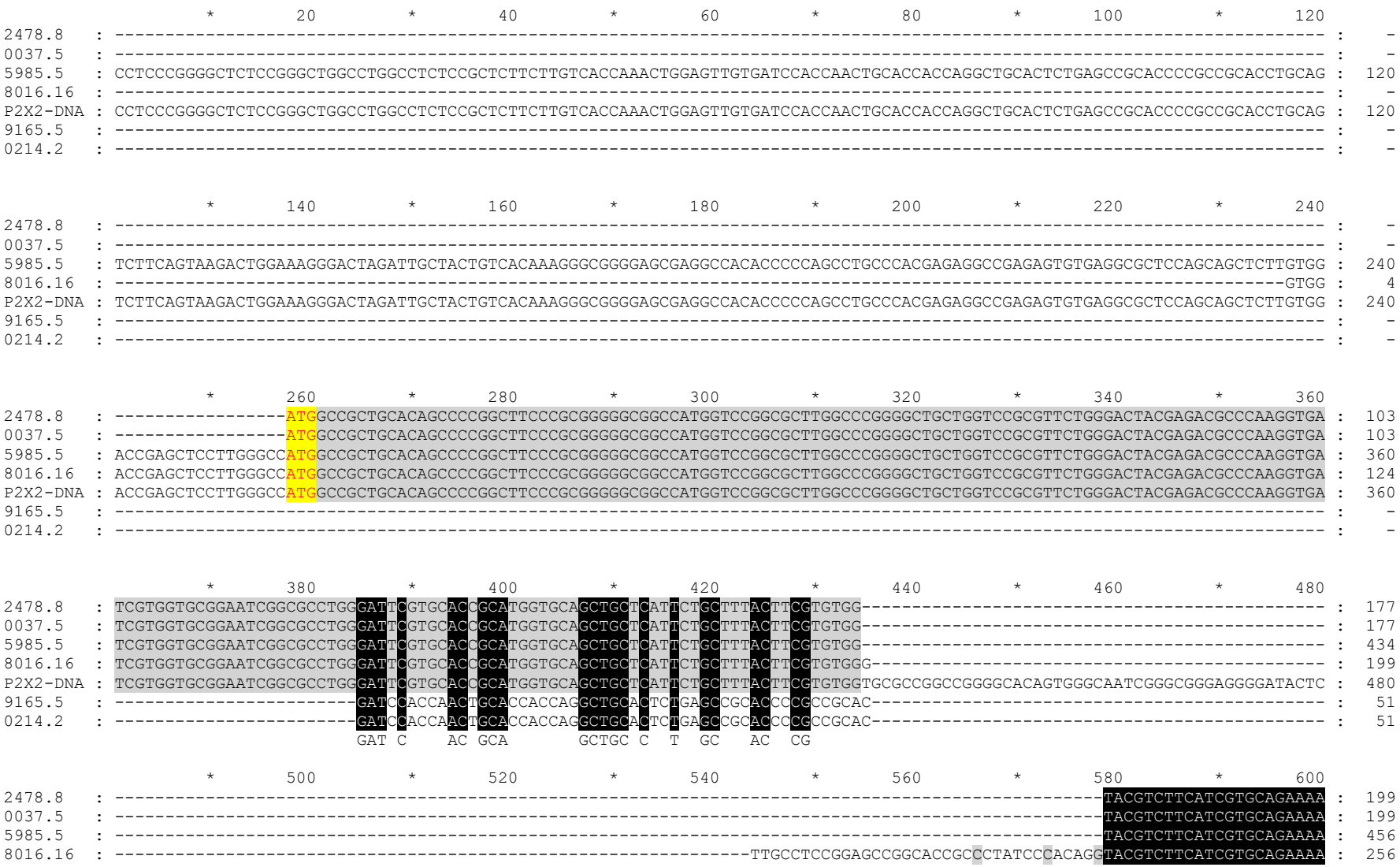

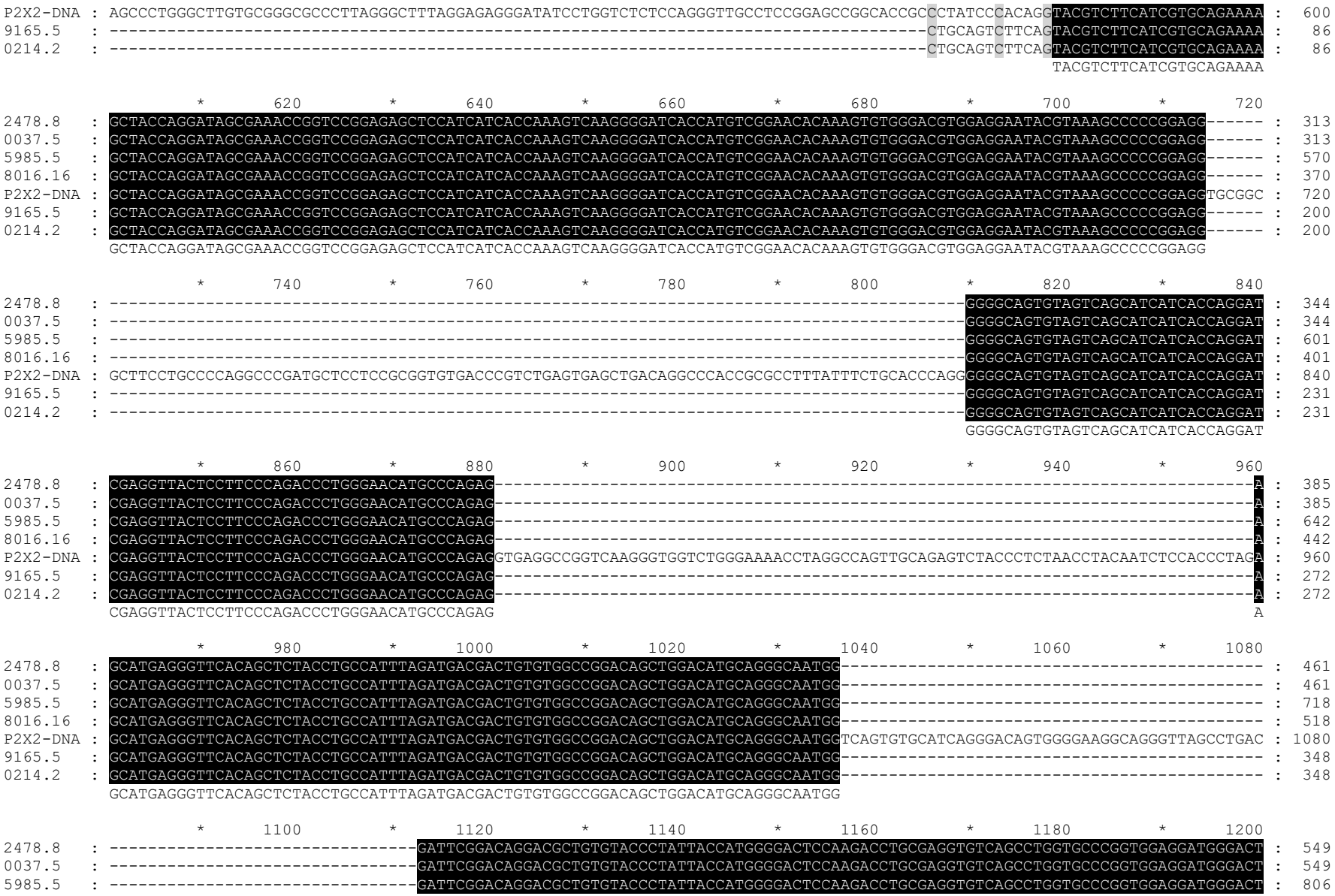

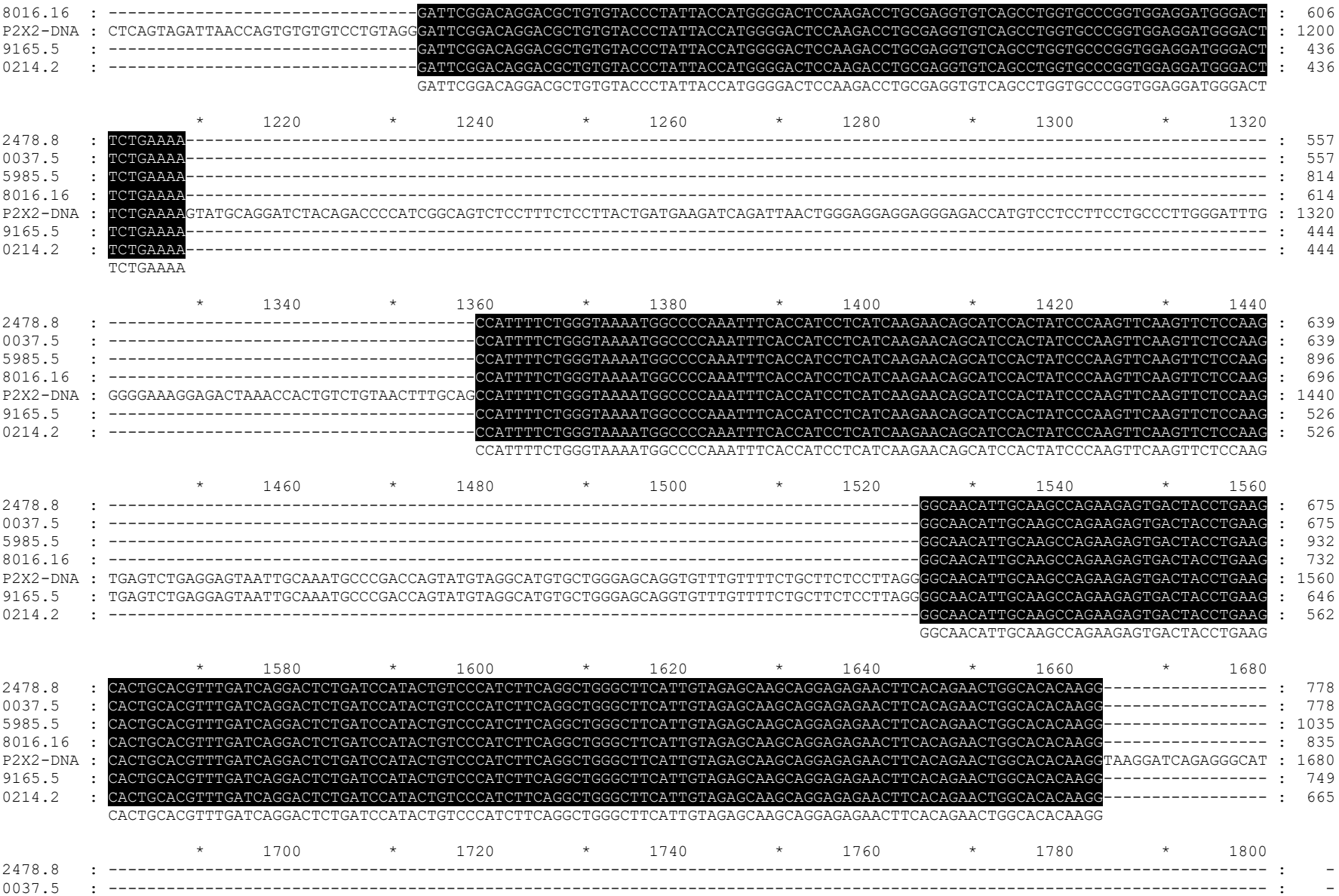

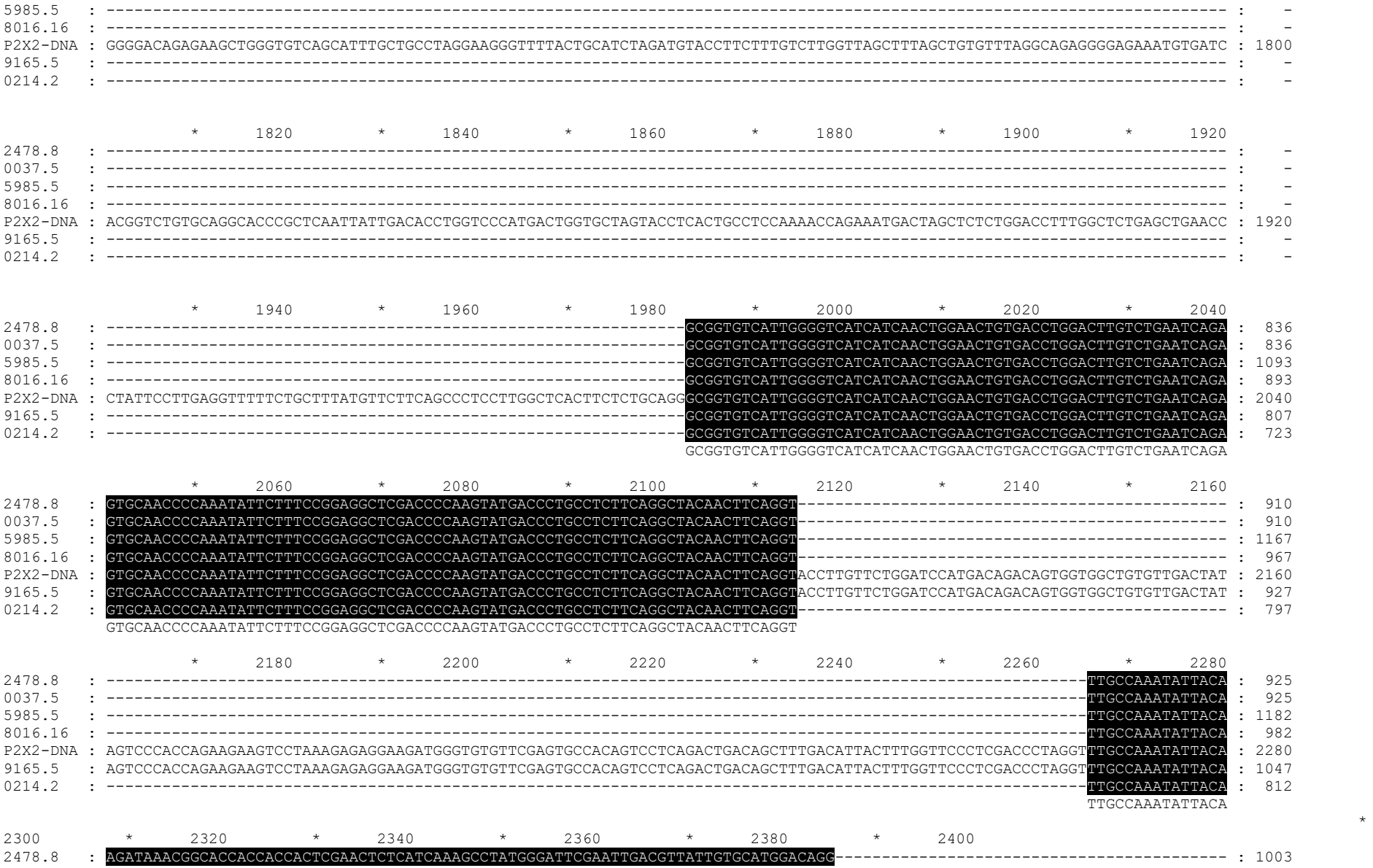
5985.5 : - : -
8016.16 : - : -
P2X2-DNA : GGGGACAGAGAAGCTGGGTGTCAGCATTTGCTGCCTAGGAAGGGTTTTACTGCATCTAGATGTACCTTCTTTGTCTTGGTTAGCTTTAGCTGTGTTTAGGCAGAGGGGAGAAATGTGATC : 1800
9165.5 : - : -
0214.2 : - : -
* 1820 * 1840 * 1860 * 1880 * 1900 * 1920
2478.8 : - : -
0037.5 : - : -
5985.5 : - : -
8016.16 : - : -
P2X2-DNA : ACGGTCTGTGCAGGCACCCGCTCAATTATTGACACCTGGTCCCATGACTGGTGCTAGTACCTCACTGCCTCCAAAACCAGAAATGACTAGCTCTCTGGACCTTTGGCTCTGAGCTGAACC : 1920
9165.5 : - : -
0214.2 : - : -
* 1940 * 1960 * 1980 * 2000 * 2020 * 2040
2478.8 : GCGGTGTCATTGGGGTCATCATCAACTGGAACTGTGACCTGGACTTGTCTGAATCAGA : 836
0037.5 : GCGGTGTCATTGGGGTCATCATCAACTGGAACTGTGACCTGGACTTGTCTGAATCAGA : 836
5985.5 : GCGGTGTCATTGGGGTCATCATCAACTGGAACTGTGACCTGGACTTGTCTGAATCAGA : 1093
8016.16 : GCGGTGTCATTGGGGTCATCATCAACTGGAACTGTGACCTGGACTTGTCTGAATCAGA : 893
P2X2-DNA : CTATTCCTTGAGGTTTTTCTGCTTTATGTTCTTCAGCCCTCCTTGGCTCACTTCTCTGCAGGGCGGTGTCATTGGGGTCATCATCAACTGGAACTGTGACCTGGACTTGTCTGAATCAGA : 2040
9165.5 : GCGGTGTCATTGGGGTCATCATCAACTGGAACTGTGACCTGGACTTGTCTGAATCAGA : 807
0214.2 : GCGGTGTCATTGGGGTCATCATCAACTGGAACTGTGACCTGGACTTGTCTGAATCAGA : 723
GCGGTGTCATTGGGGTCATCATCAACTGGAACTGTGACCTGGACTTGTCTGAATCAGA
* 2060 * 2080 * 2100 * 2120 * 2140 * 2160
2478.8 : GTGCAACCCCAAATATTCTTTCCGGAGGCTCGACCCCAAGTATGACCCTGCCTCTTCAGGCTACAACTTCAGGT : 910
0037.5 : GTGCAACCCCAAATATTCTTTCCGGAGGCTCGACCCCAAGTATGACCCTGCCTCTTCAGGCTACAACTTCAGGT : 910
5985.5 : GTGCAACCCCAAATATTCTTTCCGGAGGCTCGACCCCAAGTATGACCCTGCCTCTTCAGGCTACAACTTCAGGT : 1167
8016.16 : GTGCAACCCCAAATATTCTTTCCGGAGGCTCGACCCCAAGTATGACCCTGCCTCTTCAGGCTACAACTTCAGGT : 967
P2X2-DNA : GTGCAACCCCAAATATTCTTTCCGGAGGCTCGACCCCAAGTATGACCCTGCCTCTTCAGGCTACAACTTCAGGTACCTTGTTCTGGATCCATGACAGACAGTGGTGGCTGTGTTGACTAT : 2160
9165.5 : GTGCAACCCCAAATATTCTTTCCGGAGGCTCGACCCCAAGTATGACCCTGCCTCTTCAGGCTACAACTTCAGGTACCTTGTTCTGGATCCATGACAGACAGTGGTGGCTGTGTTGACTAT : 927
0214.2 : GTGCAACCCCAAATATTCTTTCCGGAGGCTCGACCCCAAGTATGACCCTGCCTCTTCAGGCTACAACTTCAGGT : 797
GTGCAACCCCAAATATTCTTTCCGGAGGCTCGACCCCAAGTATGACCCTGCCTCTTCAGGCTACAACTTCAGGT
* 2180 * 2200 * 2220 * 2240 * 2260 * 2280
2478.8 : TTGCCAAATATTACA : 925
0037.5 : TTGCCAAATATTACA : 925
5985.5 : TTGCCAAATATTACA : 1182
8016.16 : TTGCCAAATATTACA : 982
P2X2-DNA : AGTCCCACCAGAAGAAGTCCTAAAGAGAGGAAGATGGGTGTGTTCGAGTGCCACAGTCCTCAGACTGACAGCTTTGACATTACTTTGGTTCCCTCGACCCTAGGTTTGCCAAATATTACA : 2280
9165.5 : AGTCCCACCAGAAGAAGTCCTAAAGAGAGGAAGATGGGTGTGTTCGAGTGCCACAGTCCTCAGACTGACAGCTTTGACATTACTTTGGTTCCCTCGACCCTAGGTTTGCCAAATATTACA : 1047
0214.2 : TTGCCAAATATTACA : 812
TTGCCAAATATTACA
*
2300 * 2320 * 2340 * 2360 * 2380 * 2400
2478.8 : AGATAAACGGCACCACCACCACTCGAACTCTCATCAAAGCCTATGGGATTCGAATTGACGTTATTGTGCATGGACAGG : 1003

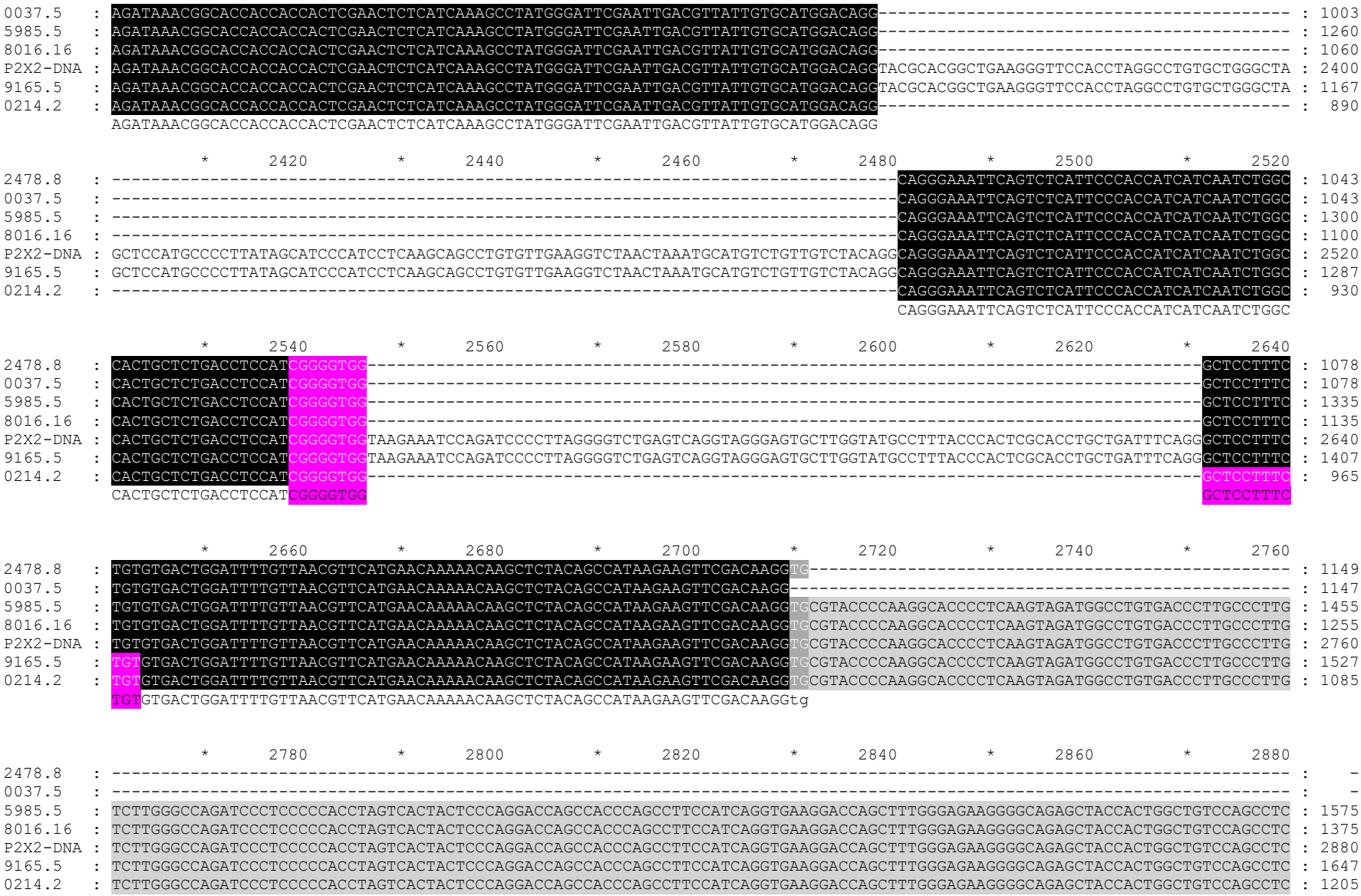

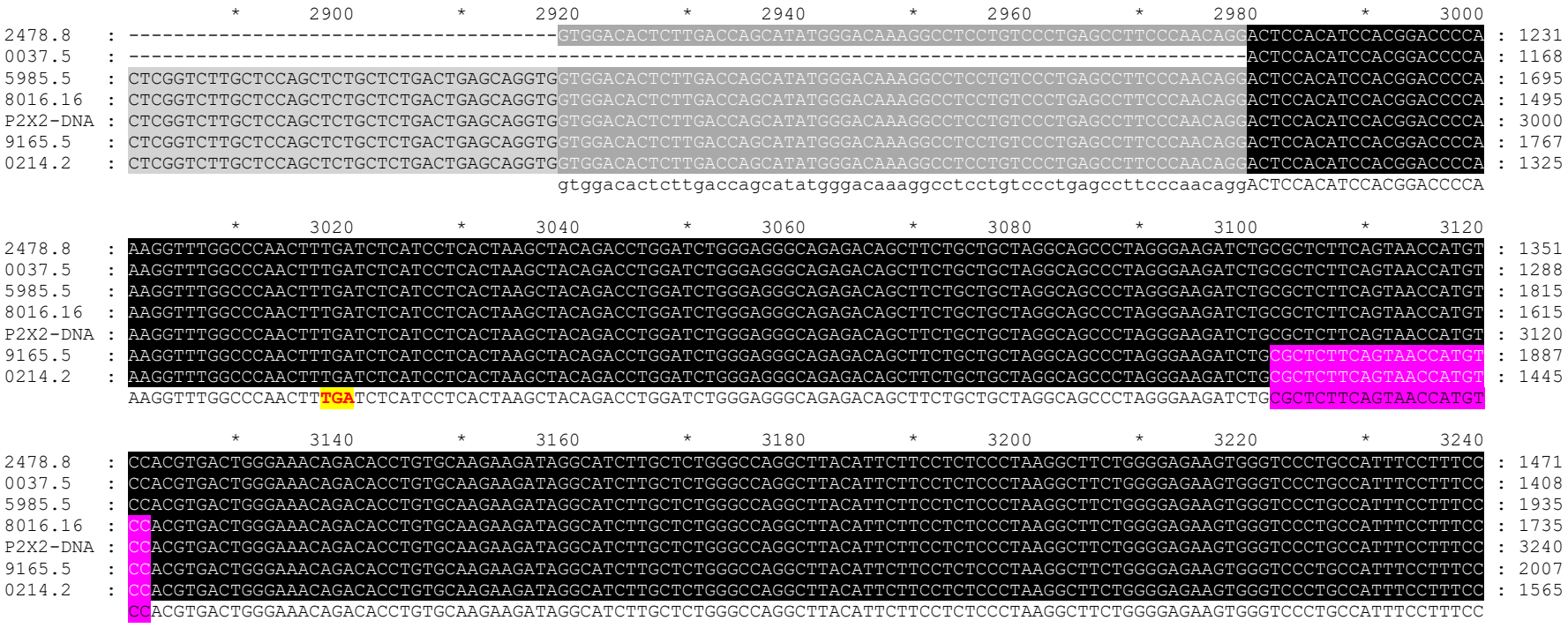
2478.8 : ----------GTGGACACTCTTGACCAGCATATGGGACAAAGGCCTCCTGTCCCTGAGCCTTCCCAACAGGACTCCACATCCACGGACCCCA : 1231
0037.5 : ----------ACTCCACATCCACGGACCCCA : 1168
5985.5 : CTCGGTCTTGCTCCAGCTCTGCTCTGACTGAGCAGGTGGTGGACACTCTTGACCAGCATATGGGACAAAGGCCTCCTGTCCCTGAGCCTTCCCAACAGGACTCCACATCCACGGACCCCA : 1695
8016.16 : CTCGGTCTTGCTCCAGCTCTGCTCTGACTGAGCAGGTGGTGGACACTCTTGACCAGCATATGGGACAAAGGCCTCCTGTCCCTGAGCCTTCCCAACAGGACTCCACATCCACGGACCCCA : 1495
P2X2-DNA : CTCGGTCTTGCTCCAGCTCTGCTCTGACTGAGCAGGTGGTGGACACTCTTGACCAGCATATGGGACAAAGGCCTCCTGTCCCTGAGCCTTCCCAACAGGACTCCACATCCACGGACCCCA : 3000
9165.5 : CTCGGTCTTGCTCCAGCTCTGCTCTGACTGAGCAGGTGGTGGACACTCTTGACCAGCATATGGGACAAAGGCCTCCTGTCCCTGAGCCTTCCCAACAGGACTCCACATCCACGGACCCCA : 1767
0214.2 : CTCGGTCTTGCTCCAGCTCTGCTCTGACTGAGCAGGTGGTGGACACTCTTGACCAGCATATGGGACAAAGGCCTCCTGTCCCTGAGCCTTCCCAACAGGACTCCACATCCACGGACCCCA : 1325
gtggacactcttgaccagcatatgggacaaaggcctcctgtccctgagccttcccaacaggACTCCACATCCACGGACCCCA
2478.8 : AAGGTTTGGCCCAACTTTGATCTCATCCTCACTAAGCTACAGACCTGGATCTGGGAGGGCAGAGACAGCTTCTGCTGCTAGGCAGCCCTAGGGAAGATCTGCGCTCTTCAGTAACCATGT : 1351
0037.5 : AAGGTTTGGCCCAACTTTGATCTCATCCTCACTAAGCTACAGACCTGGATCTGGGAGGGCAGAGACAGCTTCTGCTGCTAGGCAGCCCTAGGGAAGATCTGCGCTCTTCAGTAACCATGT : 1288
5985.5 : AAGGTTTGGCCCAACTTTGATCTCATCCTCACTAAGCTACAGACCTGGATCTGGGAGGGCAGAGACAGCTTCTGCTGCTAGGCAGCCCTAGGGAAGATCTGCGCTCTTCAGTAACCATGT : 1815
8016.16 : AAGGTTTGGCCCAACTTTGATCTCATCCTCACTAAGCTACAGACCTGGATCTGGGAGGGCAGAGACAGCTTCTGCTGCTAGGCAGCCCTAGGGAAGATCTGCGCTCTTCAGTAACCATGT : 1615
P2X2-DNA : AAGGTTTGGCCCAACTTTGATCTCATCCTCACTAAGCTACAGACCTGGATCTGGGAGGGCAGAGACAGCTTCTGCTGCTAGGCAGCCCTAGGGAAGATCTGCGCTCTTCAGTAACCATGT : 3120
9165.5 : AAGGTTTGGCCCAACTTTGATCTCATCCTCACTAAGCTACAGACCTGGATCTGGGAGGGCAGAGACAGCTTCTGCTGCTAGGCAGCCCTAGGGAAGATCTGCGCTCTTCAGTAACCATGT : 1887
0214.2 : AAGGTTTGGCCCAACTTTGATCTCATCCTCACTAAGCTACAGACCTGGATCTGGGAGGGCAGAGACAGCTTCTGCTGCTAGGCAGCCCTAGGGAAGATCTGCGCTCTTCAGTAACCATGT : 1445
AAGGTTTGGCCCAACTTTGATCTCATCCTCACTAAGCTACAGACCTGGATCTGGGAGGGCAGAGACAGCTTCTGCTGCTAGGCAGCCCTAGGGAAGATCTGCGCTCTTCAGTAACCATGT
2478.8 : CCACGTGACTGGGAAACAGACACCTGTGCAAGAAGATAGGCATCTTGCTCTGGGCCAGGCTTACATTCTTCCTCTCCCTAAGGCTTCTGGGGAGAAGTGGGTCCCTGCCATTTCCTTTCC : 1471
0037.5 : CCACGTGACTGGGAAACAGACACCTGTGCAAGAAGATAGGCATCTTGCTCTGGGCCAGGCTTACATTCTTCCTCTCCCTAAGGCTTCTGGGGAGAAGTGGGTCCCTGCCATTTCCTTTCC : 1408
5985.5 : CCACGTGACTGGGAAACAGACACCTGTGCAAGAAGATAGGCATCTTGCTCTGGGCCAGGCTTACATTCTTCCTCTCCCTAAGGCTTCTGGGGAGAAGTGGGTCCCTGCCATTTCCTTTCC : 1935
8016.16 : CCACGTGACTGGGAAACAGACACCTGTGCAAGAAGATAGGCATCTTGCTCTGGGCCAGGCTTACATTCTTCCTCTCCCTAAGGCTTCTGGGGAGAAGTGGGTCCCTGCCATTTCCTTTCC : 1735
P2X2-DNA : CCACGTGACTGGGAAACAGACACCTGTGCAAGAAGATAGGCATCTTGCTCTGGGCCAGGCTTACATTCTTCCTCTCCCTAAGGCTTCTGGGGAGAAGTGGGTCCCTGCCATTTCCTTTCC : 3240
9165.5 : CCACGTGACTGGGAAACAGACACCTGTGCAAGAAGATAGGCATCTTGCTCTGGGCCAGGCTTACATTCTTCCTCTCCCTAAGGCTTCTGGGGAGAAGTGGGTCCCTGCCATTTCCTTTCC : 2007
0214.2 : CCACGTGACTGGGAAACAGACACCTGTGCAAGAAGATAGGCATCTTGCTCTGGGCCAGGCTTACATTCTTCCTCTCCCTAAGGCTTCTGGGGAGAAGTGGGTCCCTGCCATTTCCTTTCC : 1565
CCACGTGACTGGGAAACAGACACCTGTGCAAGAAGATAGGCATCTTGCTCTGGGCCAGGCTTACATTCTTCCTCTCCCTAAGGCTTCTGGGGAGAAGTGGGTCCCTGCCATTTCCTTTCC

```
                    *      3260         *      3280         *      3300         *      3320         *      3340         *      3360
2478.8    : CAACAGAACTCCTCATAGGATCCCCTGTCCTTTCCCTGCCCACCTTTTGTACTCTCACACAGCACTCTGGGACCCCAAATTAGAGCTGTCTTCCGGTTGTATTTTAAGCCCCCCTTTAGA : 1591
0037.5    : CAACAGAACTCCTCATAGGATCCCCTGTCCTTTCCCTGCCCACCTTTTGTACTCTCACACAGCACTCTGGGACCCCAAATTAGAGCTGTCTTCCGGTTGTATTTTAAGCCCCCCTTTAGA : 1528
5985.5    : CAACAGAACTCCTCATAGGATCCCCTGTCCTTTCCCTGCCCACCTTTTGTACTCTCACACAGCACTCTGGGACCCCAAATTAGAGCTGTCTTCCGGTTGTATTTTAAGCCCCCCTTTAGA : 2055
8016.16   : CAACAGAACTCCTCATAGGATCCCCTGTCCTTTCCCTGCCCACCTTTTGTACTCTCACACAGCACTCTGGGACCCCAAATTAGAGCTGTCTTCCGGTTGTATTTTAAGCCCCCCTTTAGA : 1855
P2X2-DNA  : CAACAGAACTCCTCATAGGATCCCCTGTCCTTTCCCTGCCCACCTTTTGTACTCTCACACAGCACTCTGGGACCCCAAATTAGAGCTGTCTTCCGGTTGTATTTTAAGCCCCCCTTTAGA : 3360
9165.5    : CAA------------------------------------------------------------------------------------------------------------------ : 2010
0214.2    : CAA------------------------------------------------------------------------------------------------------------------ : 1568
            CAA

                    *      3380         *      3400
2478.8    : AGTCACACAGCGTGCTGAGTCCAATAAACCAGTGATGAGCT : 1632
0037.5    : AGTCACACAGCGTGCTGAGTCCAATAAACCAGTGATGAGCT : 1569
5985.5    : AGTCACACAGCGTGCTGAGTCCAATAAACCAGTGATGAGCT : 2096
8016.16   : AGTCACACAGCGTGCTGAGTCCAATAAACCAGTGATGAGC- : 1895
P2X2-DNA  : AGTCACACAGCGTGCTGAGTCCAATAAACCAGTGATGAGCT : 3401
9165.5    : ---------------------------------------- :    -
0214.2    : ---------------------------------------- :    -
```

S.3 Nucleotide and amino acid sequences of the mouse P2X6 gene including the DNA, cDNA and non-sense-mediated decay RNA.

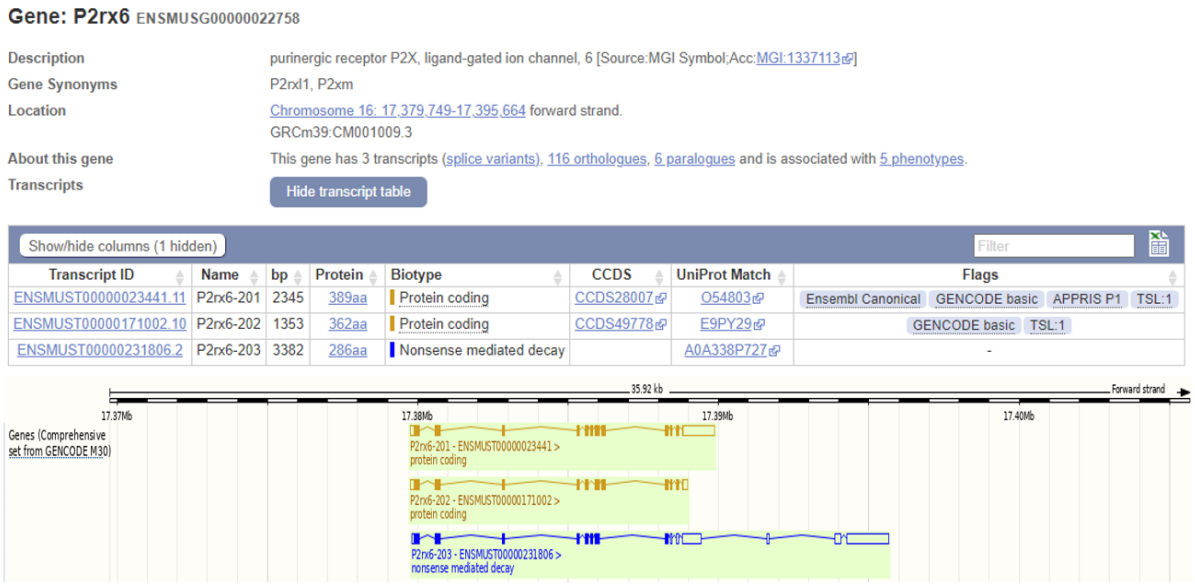

>ENSMUST00000171002.10 ENSMUSG00000022758:ENSMUST00000171002.10 cdna:protein_coding
(No amplification.. forward primer is missing in this cDNA sequence)

GGGGTTTGGGAATGAGGCAGGAGCCAGCTCCTACTGAATTTGAGATGTCCCTTTAACAACACTGGCCTGAATCCCATGC
ATGGCTTCTTGGCCTCCAGTTCAGCTGCGGCTAAAGTTGCCTGCTGACTCATGCAGTTGCAGCCAGCAGGAACTGGGAA
CATGGCTTCTGCAGCCGCAGCAGCACTCGTGAGCTGGGGGTTTCTGGATTACAAGACGGAGAAATATGTGCTAACCAGG
AACTGTCGGGTGGGCGTCTCCCAGAGGCTGCTGCAGCTGGCAGTGGTAGTCTACGTGATAGGGTGGGCCCTCTTGGCCA
AAAAAGGCTACCAGGAACGGGACTTGGCCCCTCAGACTTCTGTCATCACCAAACTCAAGGGGGTTTCTGTAACCCAGGT
TAAGGAGCTGGAGAACCGGCTGTGGGACGTGGCTGACTTTGTGAAGCCATCACAGGGAGAGAACGTGTTCTTCCTGGTA
ACCAACTTCCTCGTGACACCAGCTCAAGTCCAGGGCAGATGTCCAGAGCATCCTTCCGTTCCTCTGGCTAACTGCTGGG
CTGATGAAGACTGCCCCGAAGGGGAGACGGGGACATACAGCCATGGCATAAAAACTGGTCAGTGTGTGGTGTTCAACGG
AACCCACAGGACCTGTGAGATCTGGAGCTGGTGCCCAGTGGAGAGTGGTGCTGTGCCCAGATCCAATGCCTTATTAACC
TGGGACAACACATATTTCAAGCATTGTCTCTATGATCCACTCTCCAGTCCGTACTGCCCAGTGTTCCGCATCGGGGACC
TTGTGGCCATGGCTGGAGGGGACTTTGAGGACCTGGCCTTGCTGGGTGGTGCTGTGGGCATCAGCATTCACTGGGATTG
CAACCTGGACACGAAAGGCTCTGACTGCTGTCCCCAGTACTCCTTCCAGCTGCAGCAGAAAGGGTACAACTTCAGGACA
GCCAATCACTGGTGGGCAGCCTCAGGCGTGGAGACCCGGAGCCTGCTCAAGCTCTATGGAATCCGTTTTGACATTCTTG
TCACTGGGCAGGCAGGGAAGTTCGCGCTCATCCCTACGGCCATCACAGTGGGCACAGGAGCGGCTTGGCTGGGCATGGT
CACCTTCCTCTGTGACCTGCTGCTACTGTATGTGGATAGAGAGGCCGGTTTCTACTGGAGAACCAAATATGAAGAGGCA
AGAGCCCCAAAGACGACTACCAACAGTTCATAGACCGAGCCAGCCTTCTCACCCGCTAACCCTGTTACCCAAGTGTCCT
AGGAGTGGTTTGCACCTGCCCCATGTCTGCTGCTGCTGGGATCCAGGCATCCACGCACCGCACCGCACCGATGGCCTGT
CTGGATGGCT

>ENSMUST00000023441.11 ENSMUSG00000022758:ENSMUST00000023441.11
cdna:protein_coding
(Expected PCR product size = 566 bp)
GGGGTTTGGGAATGAGGCAGGAGCCAGCTCCTACTGAATTTGAGATGTCCCTTTAACAACACTGGCCTGAATCCCATGC
ATGGCTTCTTGGCCTCCAGTTCAGCTGCGGCTAAAGTTGCCTGCTGACTCATGCAGTTGCAGCCAGCAGGAACTGGGAA
CATGGCTTCTGCAGCCGCAGCAGCACTCGTGAGCTGGGGGTTTCTGGATTACAAGACGGAGAAATATGTGCTAACCAGG
AACTGTCGGGTGGGCGTCTCCCAGAGGCTGCTGCAGCTGGCAGTGGTAGTCTACGTGATAGGGTGGGCCCTCTTGGCCA
AAAAAGGCTACCAGGAACGGGACTTGGCCCCTCAGACTTCTGTCATCACCAAACTCAAGGGGGTTTCTGTAACCCAGGT
TAAGGAGCTGGAGAACCGGCTGTGGGACGTGGCTGACTTTGTGAAGCCATCACAGGGAGAGAACGTGTTCTTCCTGGTA
ACCAACTTCCTCGTGACACCAGCTCAAGTCCAGGGCAGATGTCCAGAGCATCCTTCCGTTCCTCTGGCTAACTGCTGGG
CTGATGAAGACTGCCCCGAAGGGGAGACGGGGACATACAGCCATGGCATAAAAACTGGTCAGTGTGTGGTGTTCAACGG

AACCCACAGGACCTGTGAGATCTGGAGCTGGTGCCCAGTGGAGAGTGGTGCTGTGCCCAGGAAGCCCCTGCTAGCTCAG
GCCAAGAACTTCACACTCTTCATCAAAAATACTGTAACCTTCAGCAAGTTCAACTTCTCCAGATCCAATGCCTTATTAA
CCTGGGACAACACATATTTCAAGCATTGTCTCTATGATCCACTCTCCAGTCCGTACTGCCCAGTGTTCCGCATCGGGGA
CCTTGTGGCCATGGCTGGAGGGGACTTTGAGGACCTGGCCTTGCTGGGTGGTGCTGTGGGCATCAGCATTCACTGGGAT
TGCAACCTGGACACGAAAGGCTCTGACTGCTGTCCCCAGTACTCCTTCCAGCTGCAGCAGAAAGGGTACAACTTCAGGA
CAGCCAATCACTGGTGGGCAGCCTCAGGCGTGGAGACCCGGAGCCTGCTCAAGCTCTATGGAATCCGTTTTGACATTCT
TGTCACTGGGCAGGCAGGGAAGTTCGCGCTCATCCCTACGGCCATCACAGTGGGCACAGGAGCGGCTTGGCTGGGCATG
GTCACCTTCCTCTGTGACCTGCTGCTACTGTATGTGGATAGAGAGGCCGGTTTCTACTGGAGAACCAAATATGAAGAGG
CAAGAGCCCCAAAGACGACTACCAACAGTTCATAGACCGAGCCAGCCTTCTCACCCGCTAACCCTGTTACCCAAGTGTC
CTAGGAGTGGTTTGCACCTGCCCCATGTCTGCTGCTGCTGGGATCCAGGCATCCACGCACCGCACCGCACCGATGGCCT
GTCTGGATGGCTGCCACCCACTGGCCTATTCATTCCTGAGGCTTACACCCTCTCCCTGCTGGTTAAAGTTTAGGGCTTG
GGAAGGAAGAGGGTTCTGGCTTGGGAAAATGGAGGACAAAGCTTCAGCGGGACTAGAGGGGAGTTGGGATAATTCCGAC
AGACTCCGAATGCAGATTCCCTCCTGGGTTCAGTCAGAGGGGTGGGGTGGGGGGCGATGTGGCTGAATAAGTGGTGGCT
GGTATCCTTGGAACTTTCTATATGTCTGCTGGGGGACTCTGCCATCCAGTTCATGCCCTCCATCCCTGCCCTGGCCCTG
GTTACCAAGGTTTCTCAGGAGCCTAAGGTGTGAGAAATTGCATGTCTGGGATTCACTGCCATCAAGTCAGTCCTGGAAG
CCTCAACCTACTCTGAAACACCTGCCTGCCAGAACCTTAACTCTGGCTCCAGCCAGAGCGCCATAGTTTCAAGGTATAA
TCTCTAATGAAGCGCACTAAGGTTCCTTAGGACTGGCTGGTTCTGGATCTATAACCATGTGAGGCCTCGATCCTTCCCT
CAGTGAGACTTTCCCCACGCACCAGAGCCCATAGAAAGGATAGCAAGGACGGGCTGCAGAGACGATCCTGGTCCAAGTG
TAGGGCATAGTTTAGGAAGTACAGAGGCAGTTTTGTTGTGCATGTGTGGTCACCGAGAGAGAACCAAGGCTGAGGTGAA
AACAGCAGCAACAGCTGGGATCTCCAGGCTTCCACAGCCTCCAAAAACCCTTGGAGTTCCTGGTGCCACTCAGCTCTCA
GGACTGTGGCCTGCAAAGGGCTATGATGGGAAGGCGCGGCTCCTGGAGGTGGTTCATGTGGACACTGTAGTCCTGGGGG
TAGGGGGACCCAAAGAACCCTGATATCACTGCTGAAGTAAAGCTTGCCAAAGCC

>ENSMUST00000231806.2 ENSMUSG00000022758:ENSMUST00000231806.2
cdna:nonsense_mediated_decay
(Expected PCR product size = 456 bp)
CCCTTTAACAACACTGGCCTGAATCCCATGCATGGCTTCTTGGCCTCCAGTTCAGCTGCGGCTAAAGTTGCCTGCTGAC
TCATGCAGTTGCAGCCAGCAGGAACTGGGAACATGGCTTCTGCAGCCGCAGCAGCACTCGTGAGCTGGGGGTTTCTGGA
TTACAAGACGGAGAAATATGTGCTAACCAGGAACTGTCGGGTGGGCGTCTCCCAGAGGCTGCTGCAGCTGGCAGTGGTA
GTCTACGTGATAGGGTGGGCCCTCTTGGCCAAAAAAGGCTACCAGGAACGGGACTTGGCCCCTCAGACTTCTGTCATCA
CCAAACTCAAGGGGGTTTCTGTAACCCAGGTTAAGGAGCTGGAGAACCGGCTGTGGGACGTGGCTGACTTTGTGAAGCC
ATCACAGGGAGAGAACGTGTTCTTCCTGGTAACCAACTTCCTCGTGACACCAGCTCAAGTCCAGGGCAGATGTCCAGAG
CATCCTTCCGTTCCTCTGGCTAACTGCTGGGCTGATGAAGACTGCCCCGAAGGGGAGACGGGGACATACAGCCATGGCA
TAAAAACTGGTCAGTGTGTGGTGTTCAACGGAACCCACAGGACCTGTGAGATCTGGAGCTGGTGCCCAGTGGAGAGTGG
TGCTGTGCCCAGGAAGCCCCTGCTAGCTCAGGCCAAGAACTTCACACTCTTCATCAAAAATACTGTAACCTTCAGCAAG
TTCAACTTCTCCAGATCCAATGCCTTATTAACCTGGGACAACACATATTTCAAGCATTGTCTCTATGATCCACTCTCCA
GTCCGTACTGCCCAGTGTTCCGCATCGGGGACCTTGTGGCCATGGCTGGAGGGGACTTTGAGGACCTGGCCTTGCTGGA
CAGCCAATCACTGGTGGGCAGCCTCAGGCGTGGAGACCCGGAGCCTGCTCAAGCTCTATGGAATCCGTTTTGACATTCT
TGTCACTGGGCAGGCAGGGAAGTTCGCGCTCATCCCTACGGCCATCACAGTGGGCACAGGAGCGGCTTGGCTGGGCATG
GTCACCTTCCTCTGTGACCTGCTGCTACTGTATGTGGATAGAGAGGCCGGTTTCTACTGGAGAACCAAATATGAAGAGG
CAAGAGCCCCAAAGACGACTACCAACAGTTCATAGACCGAGCCAGCCTTCTCACCCGCTAACCCTGTTACCCAAGTGTC
CTAGGAGTGGTTTGCACCTGCCCCATGTCTGCTGCTGCTGGGATCCAGGCATCCACGCACCGCACCGCACCGATGGCCT
GTCTGGATGGCTGCCACCCACTGGCCTATTCATTCCTGAGGCTTACACCCTCTCCCTGCTGGTTAAAGTTTAGGGCTTG
GGAAGGAAGAGGGTTCTGGCTTGGGAAAATGGAGGACAAAGCTTCAGCGGGACTAGAGGGGAGTTGGGATAATTCCGAC
AGACTCCGAATGCAGATTCCCTCCTGGGTTCAGTCAGAGGGGTGGGGTGGGGGGCGATGTGGCTGAATAAGTGGTGGCT
GGTATCCTTGGAACTTTCTATATGTCTGCTGGGGGACTCTGCCATCCAGTTCATGCCCTCCATCCCTGCCCTGGCCCTG
GTTACCAAGGTTTCTCAGGAGCCTAAGGTGTGAGAAATTGCATGTCTGGGATTCACTGCCATCAAGTCAGTCCTGGAAG
CCTCAACCTACTCTGAAACACCTGCCTGCCAGAACCTTAACTCTGGCTCCAGCCAGAGCGCCATAGTTTCAAGAACCCT
TCCTCACCTCTGGAGAGTTGGAGCCATGTGTACCCACACCACGCAGAAAGCTGGAGCAAACAGCCCACCCCAGTCCTCG
CCTCCTCTCCTTAGGAGCCCAGGTCAGCTGCACCATGGACCTACTTTAGAAGGCTTGAATGGGACGCGTGTCAGGGACT
GTGGGCAGAGGGATAGAACGCATGGAAGTCCTTCCTGTCAGCTTTCAGGGCAGTGGAACTGGCAGAGAGAAGCAGACCT
GCAGCGGACCTGCGAACCAGGTTGGAGGAACAGCTCACCTGAAGCCAGGAGGCCAGAGCTGCAAGGGCCCCGATTCCCG
ATTCCCGGATGTGAAAGCTGTGGTGCACCTCCCCTCGCCATATGCTCCGCAGCCACAGCTGCTGAGGCTAGCTGCCTCC
GCCATGTCCCTGTGCCCCTAGACGCCCAAGCCTTCTCTTGCATTTACGTTCCCGCAGCAGCGGTCCCTCCAGACCCGCT
ATGACCCACCTGCTGTCGCCGTCGCTGCCACCGTGCGCACTGCGCCTGCCCCACTAGTTTACAACGCCTGCGTGCAGGG
CCCGCCCCTCGCTGCCAGGCGCCAGATAAACCCGAGCCTCACGACTCACATCACTGGTTGGGTTCTGTACAGGGTCCCC
GCACCGCACCACGTCACGTATCAGAATAACCCTCTAAGCGAGTAAACTTCCAACATCGAGACTAGAGCTGACCTGGGTC
CTAGGGCTTACTCCACATTTCATCCACCTCCCTAGGTGAGGAAGCCTGCTCGACTAACCTGCTGAGCCCCTTCTCTGGG
TCCAGGTTGGGGGTAGAGCCAAGCCTGATACCGCCCCAGAGCAATTACTCTCCTTGATCTCCCTCCACCCCAACACAAC
TACAATTGGAAAACGTCCAGGTCCCCACCACGGAGCCTGCAAATGTCCAGCACAGTGAGATGAAGACAGGGGTCTGGCA
GAGTGACCCTGGCACTCTAAACCTCAGTGGAGTGGCAGTAAGCACCTTGCACACTAGGCTAGAGAGGGCAGCCTTCCGG
ACGTGTTCTGTGAATTGGCAGAATTTACAAAGCTATTGTCTGTCTGGTAGTGTCCCATAAAAGGACAGTAGCCAGCATC
AGAAGACAGCTTGCAACTCTACAGCAGGACTGCCACTTAGGCCCTCAAATATCAGTGACAGCCTCAGAGCACCTGACAG
GACCTGGACATTCTTAAAGGACTCTCCATTCATGATAGCCAGCAGCTCTCCGCATTTGTCACCAGCGTTCCCGCCATCA
GGGTGCCTGGGTCAGCTACGGCATAAAATCTCCAGAGTCCGCTTATGCTTAGCTCTGAGGAATCTTTTCTCTCTCTCTT
CTTCTCAGATTGAAAACAAAGGTGGCAGCTAGGTAGGGTGACCTATGCCTGTAATTCTGGCACTTGGAGGATCAAAAGA
TTGAAGACCATGTATAAGTATGTATACATAGTTTTCATATATGTATGTGTGGCAATACATATGTGGTGAGGTGCTGACT

TGTTGACAGCAAGACAATAGCCCAGCAAAGCCAAGTCGGGCAAAACCGAGGTAGGCATGTTTCTCCCAGAACTTTATAT
ATTTGACCTACAATACATATCTAATGTAGTTAGTATGTATATGCAATAAAATAAACATACAACT

>16 dna:chromosome chromosome:GRCm39:16:17379749:17395664:1
(No amplification.. reverse primer is designed on a splicing site, so it cannot anneal on the DNA sequence)
GGGGTTTGGGAATGAGGCAGGAGCCAGCTCCTACTGAATTTGAGATGTCCCTTTAACAACACTGGCCTGAATCCCATGC
ATGGCTTCTTGGCCTCCAGTTCAGCTGCGGCTAAAGTTGCCTGCTGACTCATGCAGTTGCAGCCAGCAGGAACTGGGAA
CATGGCTTCTGCAGCCGCAGCAGCACTCGTGAGCTGGGGGTTTCTGGATTACAAGACGGAGAAATATGTGCTAACCAGG
AACTGTCGGGTGGGCGTCTCCCAGAGGCTGCTGCAGCTGGCAGTGGTAGTCTACGTGATAGGGTAAGAACCGCTCCTGG
CCAGACTGCAGAGTCTGCTGTGGGGGGTCTTGCTTGCCGAGGGATAAAAGTTGGCTTTTTAGAACCCCAGCTGGTGGGA
AAGTGGGAATGGGGGTGAGAGGTAGTCAGAAGGGATTTTAGTCCATTCAGAGAACAGTGGAAGATCCATTCGCCCACGT
AAGGGGCTTTGTCTCCAGCGTCTTCTCGGTCTCTGTTAGCGTCTGCAGTTCTCCTGCCCTAAGGTACCCTGATGCAGCA
GGAGGCAGTAATTCTCTGAGCAACACAGCACTAAGCCTCTCAGAGAGACCACCAGCTGGATGTCCGAAAAGTCTTTGAG
AAGGGAGCTGGGTTTGCTGAGTGTGTGAAGGCACTGGCTGTGAAAAGTGACCATCGTCATCTGAGAGCTCCACCTACTC
AGGGGTATAGAGCAAGAGGCGCAGCTAGACAGAAGGTGGAGGCCTCCATGCTGGTCTGGGAGCCTAGTGTGTGAGCACT
GCTACTCCTTATCTAGACATTACACTATCCATCATCCTTTCCCTAGGTGGGCCCTCTTGGCCAAAAAAGGCTACCAGGA
ACGGGACTTGGCCCCTCAGACTTCTGTCATCACCAAACTCAAGGGGGTTTCTGTAACCCAGGTTAAGGAGCTGGAGAAC
CGGCTGTGGGACGTGGCTGACTTTGTGAAGCCATCACAGGTAGGTCCCCAGCGCTGCTGCAGGAAGTCAGAATTCTTCA
GCCACCACCACCAACCACACCTGCCGTGCATGAGAGACATAGGATGCAGGAGGAAGGGTTCTGAGTCAGTGTGAGAAAA
CAGCTTTCAGGGATGTGGAGCTTCCCAAGCCAAGAAGCCAGGGCCTGCGGAACTTCCTTTAAAGGAAGGTTATCGATGC
AACTCAGTGGCAGAGAGCTTGCCTGGCATTCATAGCTTCCGAGCTTCAATGCTAGAACCACCAAACAAACAAGCAAAAA
CAAAAATACCATCCACCCCACCCATCCAGCACCCATGTGGTGGAGAGATACATGTGAGAAGGAATGAAATATCTTCGGT
TCATGATTTATGCTTGGAAGTGAAATGTAGGGGATGGGAACCCAGGGCTTGAGCTTGCTGAAGTCCCCTTGCTATCATT
TAGGGATCTTGGATCAAGTTCATTTTTTTTTCTTCCCAATGATGAAAGAATTAAAAGGCAGAGGCTGGAGAGATGGCTC
AGTTGTTGAGAACACTGGCTGTTCTTGCAGAAAATACAGCTTCTGTTCCTAGAACCCACATAGTAGCTCATAGCTTTCT
GTCATTTCAGTTCCAGGGGATTCTATGCTGTCTTCTGGCCTCTGAGGGCCTCAGGCAGGCACACACACACACACACACA
CACACACACACACACACACTAATTAAATAAAACAACTCGGCTGGATGCTCAGCATATGCCTGTAATCCCAGCACTCTAG
AGGCAGATGCAAGTAGAGCTCTGAGTTTCAAGACCAGGCTGGGTCTACACAGCAAGTTCCAGGATAGCCAAGGCTACAC
AGAGAAAGCCTGTCTTGAAATAAAACAAAGCCAAAAAAAAAAAAATACCCTGCTCAAAAATAGAGTGAAAAGGCAAGAAA
TAAGTCACAGTCACAGCAAATACATGTCTCATTAAAAGTGAGAGTGCACACATCCCACACACAAAAGAGACAGGCTTCC
CACCAGAGGGAAGGGAATTTAGAAACCAAAATCCATTCTCCCATGGAGGGCTGCTGGTTTTAAATATCTGTGGTGGGAT
AGGATGGGTGCCTCTGTCCTGAATTTTGGATTATCAACTTGAAAGAAGAAGCTGATAAGTCCAGAGGTTCATGCAAGCT
GAGACATGCCCAGGACCAGCCTTGAATATAGCTGGACTAGTCTAGACCATTCATCCAGAAGGGGGTCCTTCTGGCAGGG
AAAAAAAAAAAAGTTCACCAAGCCTTTGTCTTGGAAGGAGGTGGTGAGGAAGAGTCTGGGAGTTGACGGATCTGTGATG
TATACACCACCCCTTCCCCATCCTTGCCTGTCACAGTACAGTCTGACTCCTTTCATGTCACTCACATGCCCCTCTTTGT
CTCTTTTAGGGAACATCTTCTCTTCTCCCTCCACCTAGCCCCAGTTACCAGCTGTTACGGGACATTTCCTGAGGAGACA
TAAACAAATGTCTGTATACCTCAGATAGGGCACCAACGATGAACCAATTCCATTCCAAATAAGTTCTGTGAACCAGTGA
CTAATTGTGGTTCCCTGTAGGCATAAGTGAGGGGTACTTACAGGAGCACCAGTGACTCAGGCAGCTATCATCTGTTGGC
TCCAGGTGGTAGTAGCTTTCTATATGGGAGCATGCTCTCTCTCTCTCTCTCTCTCTCTCTCTCTCTCTCTCCCTC
TCACACACACCCACACACACACATCAGCAGGCTCCCTCTGTCCCCACTTTGGGTGAGTGCATGAGAATTTGAAATGACA
CTTGTATGGAAGATACGGATAGAGGCATGACACTTTCTGAGCTCAGGGGAGGCCGTAAACCTAGTCAGCTTCACCTGCT
TCACTGGACGCCATTTTCTGCAGGACAAATTGGCAACTAGATGGGACCAAAAACTATTCCCACAAAATCCAGGCTACCC
AGGCTGGGCTCTACCTCAGAGGGTGCTGGCCTAGCCTGTCTGAGATCCGGAGTTCCATTCCCAGCACTGAGAGCAACAA
AAAGCAAACAAACCAGGCTGTCAGCTTCTATCTTCTCAGTTGAGACCAACCTTCAGCCTTGCCTTCTAGGGAGAGAACG
TGTTCTTCCTGGTAACCAACTTCCTCGTGACACCAGCTCAAGTCCAGGGCAGATGTCCAGAGGTAAGCTTGTCCAGAGC
CTCTAACACACACCCACCCCTTTTTTTCTCATCAGCCCTGTCTCCTTTCTCCTTCACTCATGGCTCAAAGCTCAGTCCC
AGCTTGGTATGTCTATCCCAGGCAAAGGGCTACACTTTTCTAGAAGTCATTTCACCAAGTCTTTACATCTGCTGTTCAC
GAGGAATACTTTAATTCCCATTAAACAGGTGATTAGGGCTCCATATGTCCAATCACTTTTCCAAGGGTACCCCAAGTAT
GGGTTACCGGCACAGTATCTGAGGACACCCCTTGGGGTCTCCAACCTTTACAACACCAGACCTTGATGTGGGACAGTTT
CATTGAGATGTCCAGCGTTTTTTCCATGCTGGTCCTGCCTCTGGGTTACAGCCAGGCACACACTCACCTGAGCATTAAT
GGCAAGAAGCAGGCTAGAAGATCACCTCTTCTCTTGGCCAGCTTTTATTAGTGTACTCAGAGTCCGATGTCATCTGGGG
GACTGGCTAGCACACTCTGCTTTGCCTTCTGGTAATATGTGATCTCTGGGTGTTTTTCAGCCCAACTGTGTTCCTGTTT
CAGCTTTCTCCCCCATTCTTAGATTCTGACACAGCCATGGGGGCATCCACACACCCACTCCCAATCTCACCTTTTCCCC
TTGTTTGGGAATATTCCAGAAAATCTTTCAAAGAGCATATTAGCTCTCACCAACCAAGGCTTCTGTGTGAACAGTCAGG
ATCCATCCCATATATATGCACCACATTCAAAGCCAACTTCTGCTCAGCAGGACTCCAGGCTCTGGTATTTGGTCACATT
ACAGTTCCAGGGGCTGTCACATGTCTATGGTTGACACCTATCCACAAAGGAGGTGACATATGTGTACAAAGGATGATTC
TCCCTCAGGGAACCTAGACAATATTCACACCTCTAGATGCTAAGAAGACATCGATTTCAGGTTCAGCATGTAGACAGCT
CCAAAACGTCATCAAGCCTATGTGTCAACTTCTTAAAAAGCACATGGTCCTTCCTCTTTCCCTGTCTGAGGCTCTTGAT
TCTTCTTGTGAACTTCTAGTGACTGAGCAGTTGTTCACCAGACCTGATGACCAGGTTTCCTGAGAATAACCAGAGTTCT
TGCAGGATTTTTCTTGGAAGATTAGTGACCGGGTTCCTCCAAGCACATGCTCAATGATCCCAAGTGTCATATCCCTCTG
CAAACCTTTCTTGACACTCCCCCTCCCCTGCACGACATCTAGGATAGGCCCTGTGCTGGGCTGGCAGAGAGCTCCAAAC
CCCTGTACTTCAAGTTGCAGTTACTGTCCAGCCAAGGCAGCAGGTTCCACGATGCTCACACAAGGCAGAGGCCACAGTG
TGGAAACTCAGGGAAGTGCACGGGCTAAATCTTAAAGGAGCTGGCGATGTGGATCAGTGTGGCTGCAGCAGAATGCCAA
GGCAGAAGGAGCCTCATGGGCAGAGACCATGTTTAAGAGGATGAAGTGTCTCAGGATACATTCCTGCTGCTCAGTGTGA
CTGGAGCATAGATCTGGGTTAGGTTACAGAAAGGACAGCCCAAGATAACATGGGCCCTCTGAATTCTGCTAAGAATCTG
GACTTAATGTATGAGCAGAATGAGTGCGTGGAAGAGACTCTCAGCCTCTCATCTTTCAGGCTGCTGGGTAGAGGCGCCC

ACCTCTCATCTCAGAGTCTGAAGGATTTGGAGACATAGACACAGGTTGGGACAGCAGAACAGAGAAGGTACCTGTCCTC
TGACCTTGGATCCTAGGCCACCCTTCACAAAAGTCCTAAGTCTCCTGGCTTTTCAATCCCTCAGCCATTCTTGCTTCCA
TGGTATTGTGGTCCTCCTGGAGTTCCCTATGAACTGAACCCCCATAAGGGTCCTGAAACTCAAGGCTGCTTCCTCTCTT
AGGTCAGGGACCCCCAGGAAGCTCACCCACATTTTCCTTGACGTGCTCCCCCCATGACTCTTTGACCTTATGTAGACAT
AATGTCCATCCATGTATGGCAGAAAAGATTGGCCCTGGGGGGAGGGGGCTTTCCACCCTGTATAGGTCCCTCTTTGATA
GCTACACCTACCACATACTGAGCATCACCAGTTTGTCCTTCTGTGGTTCTTTAGCACCCCACCCCCACTCTGTTATCCC
AGCTAGACTGGACAGAAGAGCTGAGCCTCAGGAACAGAGCTGAACAGAGAGCTCTGGGCACACAGCCCTGTACCAGCAT
TTCACCATGTTGCTGATGGCTTTTCCCTCCTAGGTTGTAGTTTTCATCTTCCCTGTGCTTCCAGACCCAGGCTGCCTGG
GAGGAAGCTGGGGTTCTTGTCTTTGCAGTCTGTGATGCTGAGTCACAAACTGGAGGCATCCTCTGCGCTATTGGTGACT
AGGGTCTCTCTTACCTACCTCAGCATCCTTCCGTTCCTCTGGCTAACTGCTGGGCTGATGAAGACTGCCCCGAAGGGGA
GACGGGGACATACAGCCATGGTAACTGTGGCCTTGGACCTCTCCTGTCTCTGCTAGAATAAGGGAAGGGGAGGGAATAC
TTGGGGGTCCCTGAATGCAGGCCCCGCTGAGCTTGTCTGTGCAGCATCCCATTCTGCCAACAAGCCCATACTCCACAGC
CTCCTCAGGATCCATGGAGATGAGAGGACTTGGAGCTCATTTTGTGTTTTCAAGGCATAAAAACTGGTCAGTGTGTGGT
GTTCAACGGAACCCACAGGACCTGTGAGATCTGGAGCTGGTGCCCAGTGGAGAGTGGTGCTGTGCCCAGGTAAGCTTCC
TCTCTCTCCCAGGGCAGGGTCCCAGAATAAGCAAAATGATGCCAGCATACTGTCTATCTTCAGGAAGCCCCTGCTAGCT
CAGGCCAAGAACTTCACACTCTTCATCAAAAATACTGTAACCTTCAGCAAGTTCAACTTCTCCAGGTAGCTTGGGCAGG
TCTTGGCTGAGCCCATATCCTTCATGCTTCTTGAGTCATCTGATCGCTATCAATCTCCTTTCTAGATCCAATGCCTTAT
TAACCTGGGACAACACATATTTCAAGCATTGTCTCTATGATCCACTCTCCAGTCCGTACTGCCCAGTGTTCCGCATCGG
GGACCTTGTGGCCATGGCTGGAGGGGACTTTGAGGACCTGGCCTTGCTGGTAAGTTATTTGGGGCAGTGTCCTGTGCAG
CTCAGGGGCAGGTTCTCAGGACCATACACCAGTGGAACAGGCTGTGTTGTGTGCAGGGTGGTGCTGTGGGCATCAGCAT
TCACTGGGATTGCAACCTGGACACGAAAGGCTCTGACTGCTGTCCCCAGTACTCCTTCCAGCTGCAGCAGAAAGGGTAC
AACTTCAGGTATGGCCCTAACTGCTCGAATGCTGGCTGCTGTTCCTGGTTCAGGGCCTCCTCCACCTAGTTCCGTAGGA
GCACACCCAGCTTGGACTCAGGGTCTCTGCTGTGTGTACAAGGATTCTGGGTGTTCCCGGTCCCCGGGCTCCACCTTGC
TTCCCTCACTTGCCTGCCCCCCACCTGCAGATCTTCTCATGGCCTCTCCCAGGTGACCCTGTGTCCCTAGAGCAAAGAC
ACTTTTCATTTTTAAAAAAGTTTTATTTATCTATTATTTATATGAGTACACTGTAGCTGTCTTCAGACACACCAAAAGA
GGGCATCGGATTCCATTACAGATGGTTATGAGCCACCGTGTGGTTGCTGGAAATTGAACTCAGGACCTCTGTAAGAGTA
GTCACTACTCTTAACCATTGAGCCAACTTTCCAGCCCAACACTTTACATTTTTAATTCCCCTGTAGGACTTTATCTTAA
AATTTTCCCCAAAAATTCTGTGGGAAAATTCAGACTAGTAAAACAAATATTCATGTACTTCTGACCTGGTTTCTTCCTT
GCTGTGAAGGGGCATAATGACCATGGCAGCTCTTAAAAGGAAACATTTCATAGGGGCTGGCTTCAGTTTCAGAGATTTA
GCCTATTATTATCATCATGGAAGGAAGCATGGTGGAGTGCAGGCAGACATGGTACTGGAGGAGCCTAAAGTTCTACATC
TCTGTGTTCCACACTGGGCATAGCTTGAACATAGGAGACCTCAAAGTCCCACCTCCACAGTGACACACTTCATCCAACA
AAGCTACACCCACTCCAGCAAGGCCATACCTCTTAATAAGTAGTGCCAGTCCTTATGGGCCAAGCATTCACACACATGA
GTCTATGGGGCCTTTCCTAGTCAAACCACCATACCTGGTTTGCTAGTGTTGCCTTTTCTTTCCTTGGCAGCACTAGGGA
TTAGACCTGTGGCCTCAGAACTATTTGAGAGTAAATATTAGATAGTGTGTGCTCACCCTTCTCAATACTGTCATGGAAT
GCTTCCACTACTGTCCCATTGTCACAGACAACTCTGGACTTGGATAGGCAGTCATAGTACATGCTATGATCCCTAATCC
CAGCCCTCAGGAGGCAGAGAAGGATTAGGAGCTCAGAGTCATCCTTTGCTTTGTAGCCAGTCTGAGGCAACCTGGTGAA
GGAGAGGAGGAGGAGGGAGGGAAGAATGGAGGAAGGGAGGGAGGAAGGGGACAACAGAGGCGGGAGGAGAAAGAAGGAA
GTAGGGAAAGGCTATTGGTAGATTAAGTCTAACATTTTATATTTACCCCACTGTGTTATTAGTGTTCCTGAGTTTTTTT
ATTTTCTGACCCCAGAAGCACCCAGAAATCTTAAATTACAAATATTGTCATATCTTTTAGTTTCCTAAGAGAATCTTGG
GCTCCTCCTGCCATGTAATATCATTTTATTACACGTAGTAGCAGGTGTGCACAGGTGGCCATAGGTCTAATGGCGGTGA
CTCATTGTGCTTGGCTCCCCACCTTGTACAACCTTCTGCGGGAGGCTTCTCGGCCTTAGGGCCCTTGCTGGCACCTCTC
TGTTGGGATGCCTCTTCTGAAGCCTGCCACAGCACCCACATCAGCACCTGCATCGGTACCCTCATCAGCACCCTCATCA
GCACCCTCATCAGCACCCGCGTCAGCACCCGCATCGCTTTCTTCCCTGGTTCTGTGCTGCAGGACTTCCTTGCCTCAGA
GTTCCTCCAGCCCTCACGGCTATTCCCCTTCCTTCTCTCAGACCTGTGCTGCCAAGATCTAGATCAGCATGCTTCCTGC
CTCTCTGACTCTCAGAGCAGGGCTCTCCCTTCAGTCAGGCCCTGCTCAGGTTCTGATTTGCTTCCGCTGTCCTTAAAAA
CCTATGTGGAGCCTTAGGACTCAGGACCAGGTAGAGTCCATGGATAAGCTTGCCTGGAACACAGTATGCAAGCACTGGA
GTCTTCTCTGCTATCCCCAGGACAGCCAATCACTGGTGGGCAGCCTCAGGCGTGGAGACCCGGAGCCTGCTCAAGCTCT
ATGGAATCCGTTTTGACATTCTTGTCACTGGGCAGGTAAAGTTCAGACCAGGGGAAGGATTTGTGGAGGTTTGGGAGGA
CAACCACAGTCCGAGAGCTTCATCCCAGGTCTCTTAGGCAGGGAAGTTCGCGCTCATCCCTACGGCCATCACAGTGGGC
ACAGGAGCGGCTTGGCTGGGCATGGTGAGTTTAATCACCTAAGGTTCTCTTGGGCTGCAGTAACCACCAGCCAGGGCCT
GCTGGCACCTGCTGGATCTGCATGTTGTTTCCGGAGGGTGGGCAAGTTGAGAACTCTGGAACATGGTAGGTCCTGCCTC
TTCCAGGTCACCTTCCTCTGTGACCTGCTGCTACTGTATGTGGATAGAGAGGCCGGTTTCTACTGGAGAACCAAATATG
AAGAGGTGAGTTGTGGGCCTGCTTGTGTCCCAGAGCTGAGGTCACTTTGCTGAGAACACTGGGTTCTGCCTCACTCAGG
GGGAATGTTAGCTTGATTCCTAATCTGTTTCTTTTTTAGGCAAGAGCCCCAAAGACGACTACCAACAGTTCATAGACCG
AGCCAGCCTTCTCACCCGCTAACCCTGTTACCCAAGTGTCCTAGGAGTGGTTTGCACCTGCCCCATGTCTGCTGCTGCT
GGGATCCAGGCATCCACGCACCGCACCGCACCGATGGCCTGTCTGGATGGCTGCCACCCACTGGCCTATTCATTCCTGA
GGCTTACACCCTCTCCCTGCTGGTTAAAGTTTAGGGCTTGGGAAGGAAGAGGGTTCTGGCTTGGGAAAATGGAGGACAA
AGCTTCAGCGGGACTAGAGGGGAGTTGGGATAATTCCGACAGACTCCGAATGCAGATTCCCTCCTGGGTTCAGTCAGAG
GGGTGGGGTGGGGGGCGATGTGGCTGAATAAGTGGTGGCTGGTATCCTTGGAACTTTCTATATGTCTGCTGGGGGACTC
TGCCATCCAGTTCATGCCCTCCATCCCTGCCCTGGCCCTGGTTACCAAGGTTTCTCAGGAGCCTAAGGTGTGAGAAATT
GCATGTCTGGGATTCACTGCCATCAAGTCAGTCCTGGAAGCCTCAACCTACTCTGAAACACCTGCCTGCCAGAACCTTA
ACTCTGGCTCCAGCCAGAGCGCCATAGTTTCAAGGTATAATCTCTAATGAAGCGCACTAAGGTTCCTTAGGACTGGCTG
GTTCTGGATCTATAACCATGTGAGGCCTCGATCCTTCCCTCAGTGAGACTTTCCCCACGCACCAGAGCCCATAGAAAGG
ATAGCAAGGACGGGCTGCAGAGACGATCCTGGTCCAAGTGTAGGGCATAGTTTAGGAAGTACAGAGGCAGTTTTGTTGT
GCATGTGTGGTCACCGAGAGAGAACCAAGGCTGAGGTGAAAACAGCAGCAACAGCTGGGATCTCCAGGCTTCCACAGCC
TCCAAAAACCCTTGGAGTTCCTGGTGCCACTCAGCTCTCAGGACTGTGGCCTGCAAAGGGCTATGATGGGAAGGCGCGG
CTCCTGGAGGTGGTTCATGTGGACACTGTAGTCCTGGGGGTAGGGGGACCCAAAGAACCCTGATATCACTGCTGAAGTA

AAGCTTGCCAAAGCCAGAAGTAGTAGTAGTCCTGTGTAGTCCTTAAAGGGAGAAACAAGGAAAGGGAGATGGTCCAGCC
ATGGGAACCCCAGCAGGAGGTTCAGAGTAGACCTAGGGCTTTCTCCTTCTCTGAACTGTAGCCGTAGGCTAGAAGTAGT
GGCTGCAAGTCCAAGTACCTGTGCATACCCAAGTGTATCACTCATGCACTAATCCAAGCCCACCTTCCAGGGACACTGT
TGCCCTGGAGATTACTAGGTAGCAGAGAACCCAAGGGATCCATCTGAAAACATTTCCAGGGGATACGGAGGCAATAAGA
GCTGTGGCCAGGAGCCTGAATTTGGAAACATCAGTCAATTCACTCTGTACATAGTGTGTACTGCAAGGGTGGCTGCCCT
GAGCGTGCAAGAATGTGCTGGGGAGAGTGTCTTGGGGGCATTGCTTGTTCAGTGCATTTCAGTGGCCCTAAGCAGACCT
TGGGCACATGTTTCCTGGAAGCCCAGGAAAATCAAAAGATCCTGACATCCAATGTCTTTTTGAGTTACCCATTTTAAAT
CCAGATTGTGATAGATATTCCCTGCTAGAGAACATGTCAGGGATCTGGGGGAGGGGGGTGTATATGTCAGTAGTGGAAT
GCTTGTCTAACAATCTCAAGGCCCTGGCTCCCACCTCAAGTACCACATGTGCATATGCGTGTGCGCACACCACACACGT
ACTCACACACTCACATATGAACATACATGTGTGCACACACGCATGCACATGCACACGCTGCTGAGAACATGTCAGAAAT
CTGTTCCTGTCTTGTCATATAACCCTCTTCACATCATGCATGGAACTTTCCTCCTCAGAAAGTCTTTGACAGGCCTTCT
GTGTCTCTGCTGTGGACTAGGAACAACTGCTTGGTTCTCCAGGCAGGTGAGAACTCAGAGCTATGAAGAATACCACAGT
GTACATGACAGCTGGTCACAACACTAGCTGATTAGTTATTATTCTGGGTCTCAGGGGCTGAAGCCACTTCCCTGCCCAC
TCTGCCCCACCTGCCCAGGTATCCAGAGTTAATCATAAACAGGAAGACAGTGGGCAACGAGTCCACACCAGCACTAGCC
TCAGCCTAGTCCATGATAGCCGAAGACTCCGTTCCTGTGTTGAGACTCTGAGAACACTCCCAGCCCAGTCTGGGCAGGC
TTCAAACCCAAGCTTCCTTAAGTAGGCAGCTGCCAATTCTTCTGGCCTCTGGATGTTGGGGATGGAGACCTCCATGAGC
AAGCCTCCGTGGCCAGCTACTCAGTACAACCTGACTCCCGGACTGGTGATTGACTAGAGGGCTGCACAGCTTGCACAGT
TTCCTCCAGGCTACCGCTGGGGAATACCACGTAGTGTGCTGTAGTCAGCTCCAATGGCTCCCTCTGGTTCTCCTTGCTG
TGCCAGATGCCATAGCCAAAATACACGACAAGTCCTGCAGGAGTGGGTGAGAGTGTGAGGGCCAGGTTCCAACCCCACC
TGACCTCTTTGATCTTCCCATTGTAATACACTTGAGTCCAAGCCCAGGCCCCACTCACCGACCAGCAGCCAGAAGATAA
AGCGTAGCCAGGTCAGGTAGCTCAGCTTCAGCATGAGGCAAGTGTTGAGAAGGATGCTCAGGGCTGGAGTCAGGGGCAC
CAAAGGGATCTGGGGGTATAAGGGTGAGTCTGAGCGTGGCTATAGGATCTATACACCAGCCCAGAGCCTGACTGTGGAA
ATTCCACAGAACCCTTCCTCACCTCTGGAGAGTTGGAGCCATGTGTACCCACACCACGCAGAAAGCTGGAGCAAGTAAG
AACGGACAAACCTATCTCCCCAGCCCCATGAGCCCTGTGCATTCTCAGGTAGGCTAAGAGGCTAGGCAGAGGGAACAGG
GAGGACTGAGAAGGAACAGGATCAATGAGGCATGGGGGAGGAGGGAGGTGTACCTGGAAAGTGTCTTGCTTCTTTTGCT
GCTGATGAGCCCCCAGGACCAGGAGGCTGGACAGAAAGACAGCACCACTGATGACCAGCAGCAAGACATAGCCCCACTG
TGGGAGGTGCAGGTCTGAGTTCCCGAAGACCAGCACACACGCCAGAGAGATAGCCGAGGCTACCAAGATGCCAAGCGCC
CAGGCCACGGCGGTTCCAGGGCTGCATCCATCCAGGAAGCCCAGGAAGGGCTTCAGGGCTGGCCGCAGCTGCCCAGGCT
CAGACATTGAGGTCTGCTCAGCACCCACTAGCTGTATATGGTCCGAAAAGGAGTCATATTTCTTAGCTGTGGGGCCAGG
GCTGGCTAGGCAAGGGGAGCTGGGTGGAGAAGCTTTTTGGAAACGCAGCACAATGATGCTGGTGGCTACAAAGGTATAG
GCCAGCAGGGTGCCGATGGATAGGAACTGGACCAGTGCCTCAAGGTCCAGCAGCAGTGCCAGGAGGGCCATGAGGACCC
CAAACACCAGGATTCCTACCACAGGCACCTGTGTCCGGGGGTGTACACGGGCAAACACCTGGAAGAAGAGCCCATCGGC
AGCCATGGCGTAGACAATGCGCGGCAGGGAGAAGAGGTTGCTGAGCAGGACGGTGTTCATGGCTGCAGCAGAGCACAGG
GAGCAGTCAGCACAGCAGATAAGCTCAGAGCGGGCCACTGCTAGGCTCACAGATAGAATGTGTACTGAGGGTGTCAGCT
TCTCACCTCCCACCCAGGACTGGGGCACTTCTGTTCAGGCCAATTAATGAACCTTTTGAAAGCTCGCCGTCTGCCTGTA
AGCAGAACCTGTGCCACCAGACTGATATTCTGTGTACAATTTGTGGGGAGAGGGTCTGCCAGCAAGTCTGTGTTTTCAT
GAACTCATTATACAAGTAGTAAAGCTGGAGCATGGATAGAAGTATTTTGAGAGGTTTGGGGCAGGGCCCTCTACCTTGT
CCCCTCCCACCCTGCCCAGAAGGGACCCTTACCACAGATAGAGCCAACTGCCACAATGAAGCCAGCCCAGCTGTAACCC
CGCCTGTAGAAAGCATCAGCAAGCGCCGAGTCAGGGTCTAGGCTGTGCCAAGGTACCATGAGGGTTAACACAGTGGAGA
CCAGAATATAGGCACCAGCTGCCAGGCTGAGGGAGATGGCGATGGCCATGGGCACCGCCCACCGTGGGTTTTTGGCCTC
CTCACTGGAGGCAGCAATAACATCAAATCCCACGAAGGCATAGAAACAGGTGGCTGTGCCAGCCAGGATGCCAGAGAAG
CCGAAGGGTGCGAAACCACCTTCTTCTGCACTCCAGTTGTGAGGACGGGCCAGGATGAAACCCAGGACAATGATGAAGA
GGATCACAATCAGACTGATGGCTGAGAACGTGTGATTAAGCCAGGAGGAGACTCGGGCTCCGCAGGAGACAAAGGCAGA
AGCCACGAGTAAAATGCCAGCGGCCAGAAAATCTGGATAGTGAGCTAGGAAGGGCACCTGCCAGACGCCCAGGTGAGAC
TCCGTGAAGTTGCGAATGCTGTGGTTAAAGATGGCATCCAAATAGCCACTCCAGGCACGGGCTACAGCGGCACCTCCAA
TGAGGTATTCTAGAAGCACATTCCAGCCTATGAGGAATGCCCATATCTCCCCCATGGACACGTACGTGAATAGGTATGC
TGAGCCAGTACGGGGCACACGGGCTCCAAACTCTGCATAGCATAGGGCCGCCAGCAGGGAGGCTACAGCGGCCACCAAA
AAGGACAAGAGCACAGCGGGGCCAGCCATGTCCTTGGCCACTGTGCCTGTGAGCACATAGAGCCCAGATCCCACCATGC
CACCCACACCCAGTAGAGTCAAGTCCAGTGTGGACAGGCAGCGCCGCAGTGATGTCTCCATGCTAGACTCTTCCAGTGG
CTTCAGACGGTTCAGTTTCTGGCAGAAGCGTGCCAAACAGGCAGTACTGGGCAGTCCCCGGGCCATGGCAGACGGAGTA
CTGAACCAGTTTCTGGAACCTACTGGGGACAGACAGCGGGAATAACCAACCATCCTCCATTCTTTCATAGACAGCCCAC
CCCAGTCCTCGCCTCCTCTCCTTAGGAGCCCAGGTCAGCTGCACCATGGACCTACTTTAGAAGGCTTGAATGGGACGCG
TGTCAGGGACTGTGGGCAGAGGGATAGAACGCATGGAAGTCCTTCCTGTCAGCTTTCAGGGCAGTGGAACTGGCAGAGA
GAAGCAGACCTGCAGCGGACCTGCGAACCAGGTAGGTGGTTCTGTGAGTGAGTGGGAGGTTGCTTAAGAACAGGCTTGG
AACAGGCTGCACCACGAGCAAGAAGAAATGGGAGGCTTCCCTGGAGCAGTGCCAGGTTGTCAGGACCCGGAACAGGAGC
CGCTCCTGCAGCCGGGAACGTGGCCAAAGGGACATGGCCTCAGAGAAAAGCGATCACCCCCTCTTCTGCCAGGTTGGAG
GAACAGCTCACCTGAAGCCAGGAGGCCAGAGCTGCAAGGGCCCCGATTCCCGATTCCCGGATGTGAAAGCTGTGGTGCA
CCTCCCCTCGCCATATGCTCCGCAGCCACAGCTGCTGAGGCTAGCTGCCTCCGCCATGTCCCTGTGCCCCTAGACGCCC
AAGCCTTCTCTTGCATTTACGTTCCCGCAGCAGCGGTCCCTCCAGACCCGCTATGACCCACCTGCTGTCGCCGTCGCTG
CCACCGTGCGCACTGCGCCTGCCCCACTAGTTTACAACGCCTGCGTGCAGGGCCCGCCCCTCGCTGCCAGGCGCCAGAT
AAACCCGAGCCTCACGACTCACATCACTGGTTGGGTTCTGTACAGGGTCCCCGCACCGCACCACGTCACGTATCAGAAT
AACCCTCTAAGCGAGTAAACTTCCAACATCGAGACTAGAGCTGACCTGGGTCCTAGGGCTTACTCCACATTTCATCCAC
CTCCCTAGGTGAGGAAGCCTGCTCGACTAACCTGCTGAGCCCCTTCTCTGGGTCCAGGTTGGGGGTAGAGCCAAGCCTG
ATACCGCCCCAGAGCAATTACTCTCCTTGATCTCCCTCCACCCCAACACAACTACAATTGGAAAACGTCCAGGTCCCCA
CCACGGAGCCTGCAAATGTCCAGCACAGTGAGATGAAGACAGGGGTCTGGCAGAGTGACCCTGGCACTCTAAACCTCAG
TGGAGTGGCAGTAAGCACCTTGCACACTAGGCTAGAGAGGGCAGCCTTCCGGACGTGTTCTGTGAATTGGCAGAATTTA
CAAAGCTATTGTCTGTCTGGTAGTGTCCCATAAAAGGACAGTAGCCAGCATCAGAAGACAGCTTGCAACTCTACAGCAG

GACTGCCACTTAGGCCCTCAAATATCAGTGACAGCCTCAGAGCACCTGACAGGACCTGGACATTCTTAAAGGACTCTCC
ATTCATGATAGCCAGCAGCTCTCCGCATTTGTCACCAGCGTTCCCGCCATCAGGGTGCCTGGGTCAGCTACGGCATAAA
ATCTCCAGAGTCCGCTTATGCTTAGCTCTGAGGAATCTTTTCTCTCTCTCTTCTTCTCAGATTGAAAACAAAGGTGGCA
GCTAGGTAGGGTGACCTATGCCTGTAATTCTGGCACTTGGAGGATCAAAAGATTGAAGACCATGTATAAGTATGTATAC
ATAGTTTTCATATATGTATGTGTGGCAATACATATGTGGTGAGGTGCTGACTTGTTGACAGCAAGACAATAGCCCAGCA
AAGCCAAGTCGGGCAAAACCGAGGTAGGCATGTTTCTCCCAGAACTTTATATATTTGACCTACAATACATATCTAATGT
AGTTAGTATGTATATGCAATAAAATAAACATACAACT

S4. Nucleotide and amino acid sequences of the P2X3 gene including the DNA, cDNA and non-sense-mediated decay RNA.

Gene: P2RX3 ENSG00000109991

Description	purinergic receptor P2X 3 [Source:HGNC Symbol;Acc:HGNC:8534]
Gene Synonyms	P2X3
Location	Chromosome 11: 57,338,352-57,372,396 forward strand. GRCh38:CM000673.2
About this gene	This gene has 3 transcripts (splice variants), 272 orthologues and 7 paralogues.
Transcripts	Hide transcript table

Show/hide columns (1 hidden)

Transcript ID	Name	bp	Protein	Biotype	CCDS	UniProt Match	RefSeq Match
ENST00000263314.3	P2RX3-201	3792	397aa	Protein coding	CCDS7953	P56373	NM_002559.5
ENST00000534820.1	P2RX3-203	837	50aa	Nonsense mediated decay		H0YDR6	-
ENST00000533436.1	P2RX3-202	468	No protein	Processed transcript		-	-

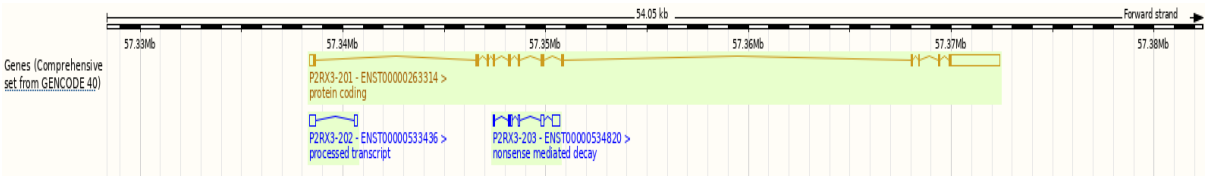

>ENST00000263314.3 ENSG00000109991:ENST00000263314.3 cdna:protein_coding

GGCCTCTTGGAAGCCAGAGTATCAAGAGCAGAGAATCTCACTAGGATTGCATGGCTTAAAGGGACAGGCTCCCCATTCCTCCA
ACCCCTCTAAGCTGCCCCCTCCAGGTCGTGATCTCGTCTCCCTGTCCTGTAGGACCTCCCTCTCCTGAGGCCACCACTGGGCC
CCCTTCTGAGTGTCCCCTGAGCACTCTCTCAGCATGAACTGCATATCCGACTTCTTCACCTATGAGACCACCAAGTCGGTGGT
TGTGAAGAGCTGGACCATCGGGATCATCAACCGAGTAGTTCAGCTTCTGATCATCTCCTACTTTGTAGGGTGGGTTTTCTTGC
ACGAGAAGGCTTACCAGGTACGGGACACAGCCATTGAGTCCTCGGTGGTAACCAAGGTGAAGGGCTCCGGACTCTACGCCAAC
AGAGTCATGGATGTGTCTGATTACGTGACGCCACCTCAGGGCACCTCGGTCTTTGTCATCATCACCAAGATGATTGTTACTGA
AAATCAGATGCAAGGATTCTGCCCAGAGAGTGAGGAGAAATACCGCTGTGTATCAGACAGCCAGTGCGGGCCTGAGCGCTTGC
CAGGTGGGGGGATCCTCACTGGCCGCTGCGTGAACTACAGCTCTGTGCTCCGGACCTGTGAGATCCAGGGCTGGTGCCCCACG
GAGGTGGACACAGTGGAAACGCCCATCATGATGGAAGCTGAGAACTTCACTATTTTCATCAAGAACAGCATCCGTTTCCCCCT
CTTCAACTTTGAGAAGGGAAACCTCCTTCCCAACCTGACAGCCAGGGACATGAAGACCTGCCGCTTCCACCCGGACAAGGACC
CTTTCTGCCCCATCTTGCGGGTAGGGGACGTGGTCAAGTTTGCGGGGCAGGATTTTGCCAAACTGGCGCGCACGGGGGGAGTT
CTGGGCATTAAGATCGGCTGGGTGTGCGACTTGGACAAGGCCTGGGACCAGTGCATCCCCAAATACTCCTTCACCCGGCTCGA
CAGCGTTTCTGAGAAAAGCAGCGTGTCCCCAGGCTACAACTTCAGGTTTGCCAAGTACTACAAAATGGAAAATGGCAGTGAGT
ACCGCACCCTCCTGAAGGCTTTTGGCATCCGCTTCGACGTGCTGGTATACGGGAATGCTGGCAAGTTCAACATCATCCCCACC
ATCATCAGCTCTGTGGCGGCCTTTACTTCTGTGGGAGTGGGAACTGTTCTCTGTGACATCATCCTGCTCAACTTCCTCAAGGG
GGCCGACCAGTACAAAGCCAAGAAGTTTGAGGAGGTGAATGAGACTACGCTGAAAATCGCGGCTTTGACCAACCCAGTGTACC
CCAGCGACCAGACCACAGCGGAGAAGCAGTCCACCGATTCGGGGGCCTTCTCCATAGGCCACTAGGGCCTCTTTCCAGGGCCC
CACACTCACAAAGGCTCCAGGCCTCCCCACAGAGGACCCTGCCTGAGCAAGGGGCATGGGAGGGAAGAGGGGCTCTCATTTCT
GCTGCTCATTCCATGAGCATAGCTGGGACCCAAGTGTCTGGGCCTCCGACTGCTCCAGCAGACAGGCAGTGCTCCCTGCTGAG
ACCCCAATCTCACCTTCACTCCTTGCCTGGCCCCATCTGCTTCCTAGGACCCCTGGGGCAGGAGCACCTGAGCCATCCCCTTC
CCAAAGAGTAGAGATTATAATGTAGGACAGATGGCCACAAGGGCCTACCAAGTGCCAGGCACTTTCACACACGTTATCTCATT
TAATCCTTAGAATAATCCTATGAGGTAGATATTAGTTTCCCTTGTTTTGAAGATAAACCAAGGCTCAGAGAGACTGAGTCATT
TGCCCCAGGCCAGATAGCCAGGATGTGAGAGAGCTGGGATTTGAACGTCCGTCTGACTAACTCCATCGCCCACACCCCATGAG
AGAAGAATGAACTCCCAGGGTCCATCAGCCCTGCTGCTTCAGCCGCCTCCACCCTGACGGTGATTCGGTTAATAAAGAGTAAG
CCCCATGCCTTTCCCAGCAACAAAGTTTGCATTTTAGGGAGACTGGTTAGACAGTGGTGAGGGACCCCATCTCTGACTTGGGT
GCATCCCAAATTTAGAAGGAAACAGAAGGCATGGCTGTCAGTGAATTTTTCCTCATCACTCCCCATAGCTCTCTCCCCAAACC
AGGGAAGGGGTCATTCTTGTTCTTCTCTGGGACCCCACACCCACACACATCTGGGCCCCCTCACTCTGGGGATTTGATTCCCG
GACCTGGGATCCTGTCGTAGGCTGGGACCCTGTTCCAGGAGTTCAGCAGTCCTCATTTACAACAACAGTGAAAATGCTCCAGT
AAGGCCTGGTGCCTTGTGAGCTGCTCAGCTGGGTTGGCCAGGCCTGTCCCCATAGGGTCTTAATAAGGTGCCCCATTTTCTAA
GGTTAGAAGCTAAAGGGGCCTTTTAAACCATCTTATCTAACCCTCTTGCTTACAGATGAGCAAACTGAGGCCAGAAAGGGAAA
ATGACTGGTTCAGTGCCACAGTTCATGGCCAAAAAGGAACCCACATGTCCTGGCCCTTCAGGGAAGGAGGCAAGAACAGGAAG
CTGGATCCATTGACCCAGACATCCTCTATCCCCTTTCTGTCCTCTCCTACAGTGAGAGGCCCAGAAATTGCCCCAGGGCAGGG
CTCTGGGGCAGAACCAGGTTTTGTGAATCCTAAGCATATACAATTTGGGGGCATCTCTTTAGAAAGAATACAAAATTAGGTAT
TAGAAGGGGCTCATGCAAGTGAATGAGCCTAAAGAATGTTTCAATAGCTTCATGATAAATCTGCATCTGGCAGTCAGAGTGGG
CATGATCATGAGGTCTTAGCTGCACCAGCTCAACTGTAGATGGAGGGCGGCCCCTCAACACACGGCACAGGAAGTGGGGAAGG
GACAGCTTCAGGAGTAGTTCAGGAGGCTCAAATGGTGGGTACTTGCAAAGGCCTTGCCCAATGACCCCCCGCTCCAGGGGGAG

AAGGGGTAAGACCCACCCCACATAAAGCTCAACACCCCTTCCCTCACTCTGCCCTAACCCACAGCCCCATGCCCAGGATGGTG
GGGCATATCTCCCCAGGGTCAGCCTTGGGAATTGGGCAGTGCCTGGAGATCTGACCAGACTATGCTTCTCCAGCAGAGACATC
AGTGAAGGCAGCACCACATTCTCCACCTGGGACTCCCCCAGGCATCCCTGGGGAATTCAGCTCTTGGGAGGCTGGGGTCACAG
GGATTCTCTCTAATGGGGAGATGGAGGCAGTGGTGTCCTGAAGGGACCCTCCCCCCCAACCCCTCCCTTTTACCCAGATGGAG
GTGGTCCTCCTGTAGGTGCCTCCGCCCCTCTGGAGCCGGCCAGCAAGTGTGTGTGAGCCTGAGGTTGTCCTCCGCATATCTGA
ACTAAGTTACCACTTCTGTGTGCTAGATGTAGGGTTAATATCAGTAGTGATAAAAACAGCTACCTTGTCTCTGTTGCATTATG
GTTTACTCAGCACAATCACCAACATAATCACATGGACCCTCACACCAACGCTGGTGAGTCCGCTATGGTTTGTCATTAATCCT
ATTTGATAGAAAAAGAAATTTACAGTACGTGGAAATGAGATCTGGAACCTATGCCCATTCCTAACACTACATTGCCTCTTTAA
TCATTCAACATAAAAGCCAACACTGATTACTTACTATTGGCAGGCAATGGACCAAATGAGTGACAGGGATTGTCTAACTCAAC
CCCCACTTTACAGAAGAAGAAACAGATGCATACTAAAATAAAGAAACTGAAATAGAA

>ENSG00000109991:ENST00000263314.3 peptide: ENSP00000263314 pep:protein_coding
MNCISDFFTYETTKSVVVKSWTIGIINRVVQLLIISYFVGWVFLHEKAYQVRDTAIESSVVTKVKGSGLYANRVMDVSDYVTP
PQGTSVFVIITKMIVTENQMQGFCPESEEKYRCVSDSQCGPERLPGGGILTGRCVNYSSVLRTCEIQGWCPTEVDTVETPIMM
EAENFTIFIKNSIRFPLFNFEKGNLLPNLTARDMKTCRFHPDKDPFCPILRVGDVVKFAGQDFAKLARTGGVLGIKIGWVCDL
DKAWDQCIPKYSFTRLDSVSEKSSVSPGYNFRFAKYYKMENGSEYRTLLKAFGIRFDVLVYGNAGKFNIIPTIISSVAAFTSV
GVGTVLCDIILLNFLKGADQYKAKKFEEVNETTLKIAALTNPVYPSDQTTAEKQSTDSGAFSIGH

>ENST00000533436.1 ENSG00000109991:ENST00000533436.1 cdna:processed_transcript
CAAGAGCAGAGAATCTCACTAGGATTGCATGGCTTAAAGGGACAGGCTCCCCATTCCTCCAACCCCTCTAAGCTGCCCCCTCC
AGGTCGTGATCTCGTCTCCCTGTCCTGTAGGACCTCCCTCTCCTGAGGCCACCACTGGGCCCCCTTCTGAGTGTCCCCTGAGC
ACTCTCTCAGCATGAACTGCATATCCGACTTCTTCACCTATGAGACCACCAAGTCGGTGGTTGTGAAGAGCTGGACCATCGGG
ATCATCAACCGAGTAGTTCAGCTTCTGATCATCTCCTACTTTGTAGGCAAAAATGTACCAGCATCTCTGCATGCCAGGCACTG
TGGATTGAGGACGGAATGGTGGGCAAAAGCAGACAGGGTCCTCGCCCTCCTGGGGCTTACAGCGGAAGGCAAGAGATGGCATT
CATCTGATGATCTCCACAAACGTGAAATGTCAACTGTGGCTTAGAGGTGCACA

>ENST00000534820.1 ENSG00000109991:ENST00000534820.1 cdna:nonsense_mediated_decay
AAATACCGCTGTGTATCAGACAGCCAGTGCGGGCCTGAGCGCTTGCCAGGTGGGGGGATCCTCACTGGCCGCTGCGTGAACTA
CAGCTCTGTGCTCCGGACCTGTGAGATCCAGGGCTGGTGCCCCACGGAGGTGGACACAGTGGAAACGTAAGGCTCCAAGCCAG
ACAGGAGGAGACAGGCCCCCACCTCAGCTCCCCTTTGCCCATGTGGGAGCCGTGCGTCTCTGAGCTTGAGGAGGGCCCATCAT
GATGGAAGCTGAGAACTTCACTATTTTCATCAAGAACAGCATCCGTTTCCCCCTCTTCAACTTTGAGAAGGGAAACCTCCTTC
CCAACCTGACAGCCAGGGACATGAAGACCTGCCGCTTCCACCCGGACAAGGACCCTTTCTGCCCCATCTTGCGGGTAGGGGAC
GTGGTCAAGTTTGCGGGGCAGGATTTTGCCAAACTGGCGCGCACGAGTCTCGATCTGTCTCCCAGGCTAGAGTGCATGGCGCG
ATTTCGGCTCACTGCAACCTCCGCCTCCCAGGTTCACGCCATTCTCCTGCCTCAGCTTCCGGAGTAGCTGGGACCAAGCCCGG
CTAATTTTTGGTATTTTTAGTAGAGTCAGGGGTTCGCCGTGTTAGCCAGGATGGTCTCGATCTCCTGACCTCGTGATCCGCCC
GCCTCGGCCTCCCAAAGTGCTGGGATTACAGGCGTGAATCACCGCACCCGGCCACCACAGCACTTCTTTACTGAGCAGTATAT
GACATGTCACTTTCCGTTCTCCCTGCCTCCGTCTCCCACCTGGAGGATGGGAGGAAATCATTTGTCACCACCTCCACCCCACC
CCCACCC

>ENSG00000109991:ENST00000534820.1 peptide: ENSP00000434166 pep:
nonsense_mediated_decay
KYRCVSDSQCGPERLPGGGILTGRCVNYSSVLRTCEIQGWCPTEVDTVET

>11 dna:chromosome chromosome:GRCh38:11:57338352:57372396:1
GGCCTCTTGGAAGCCAGAGTATCAAGAGCAGAGAATCTCACTAGGATTGCATGGCTTAAAGGGACAGGCTCCCCATTCCTCCA
ACCCCTCTAAGCTGCCCCCTCCAGGTCGTGATCTCGTCTCCCTGTCCTGTAGGACCTCCCTCTCCTGAGGCCACCACTGGGCC
CCCTTCTGAGTGTCCCCTGAGCACTCTCTCAGCATGAACTGCATATCCGACTTCTTCACCTATGAGACCACCAAGTCGGTGGT
TGTGAAGAGCTGGACCATCGGGATCATCAACCGAGTAGTTCAGCTTCTGATCATCTCCTACTTTGTAGGGTGAGTCTGTGGCC
TTTCAGGTTCCTGGCGGGGTGGGCTGCCTGGTATCCCGTCTTCACCCTCCTGCCTCGGTGCTACCATCCAGCTTCCTGAGCTC
CTCTGCTCCTGGGGGAAACAGTTTCTTCTGTGGAGCCGAGTCTTAAAGACTGGCCTCTGCCACCCCCACCTAGGGCCTAAATT
CACCCAGGTGAATTCTTTTCCCAGTTCGTCCTCCAGGGTTGAGATTGGTTTCAAGACACACGCTCGGAGTAGTAGGGTCCCTG
CCCCGGCACTGCCCTCCACCGAGGGAGGGCTCAGGAGCTCCATCTCCACCCTCCCTGCTCTCATCTCCCCAACAAGAGAACAG
GCAGACCCCCTCCCACATCTTCGAATTCCCCTCAGTCAAGTCTTCGGGGTCTCAAAAAGACAAGACAGCACAGGAATAGGGAA
GGGAAGGCACTGAGACAAGGGGGTGGTGGCAGGTTGATCAAGTTGGTGGCCGGGAGGGAAAGAGAGAACTGGATCTGTTTTAG
AATGAGGAATTTCCTTCTGGCATGGATGGGTGAGATGGTGAGAGAGAGAAGGGCAAGGGAGAAGCCCTCTGCTCTTGAAGGGG
AGGACAAAGAGGGAACTGCCCCTTGATGAGGAAACAAACAGAGGCCCAAGGGAAGAGTGGCCAAGGAGAAAAGGAGCTTTTCT
GAACATAGTGCCGCTCCCTCCCCAGGAATCCAGAAATGCTCCCCTTTGTCAAAAAGTGTAAGTTCCCTACCTCTCCCTGACCC
TGTGCCATGTAACCCATCCTAGGAGTTGCTTAAGAGCCAGGAAGGTGCAACCATCCCCTCAGCCCCCACCGCCTGCAAGCACA
CACCTACACACACACACACACGCACACAAAGGGCTGTGGAGCAGACAATGGCTGGGGAAGAATGCAGGTCCTGTCCTTCTT
GTGGTCATTTCCACACACTGGTGGGCACCAGGAAATACAGGCAGAAACCTCGAAGGTTTTCTTTCCTGGCATGCGGGTCTCCA
ATCTTATGCTGTTCTTTCAGACAATGGGTCTTTGCATTTGAGGCAGCAATCCACTGACTGTCAGGAGTTAGTTCAAGCAGGTC
AAAGGAGAATCCTGTGTGCCTGTGGGCTGAAGCTGCATGCAAACCTGCTTGCTTGAAATGTTGAAGTTTATGCGAGGGTGTGG
AGGGAAAGGTGGCTAGATGTGACTTTTTAGGTGATTTTTTGCTCTGTGTGCTGGGCAAGCCCTGGTAGGCTTCAGTGGGCAGG
TATTGTAAAAAGGCTGTACCATCCAGTGCTCCTTTGGGAGATTTTAGAAAAGGGATTCAAGCTTTGGAATAGCATTAAATGGC
CACAAAGTTCCCTTCCAATGTTGAGGTTTTGTGAGATACGAGGTTTGCAAATGTTCGCTGTCTGCATCTCTAGAGCTTGGCTC
AAAGTTGGTTCCTAAATGTTCTGTGTTCACGTGTATATTCAATGCTGTGGTTGTTTATAGCCACAAGATGGTATGTTGGCCCA
GGTGAGTGCAAAATCTGGCTCAGCACATTCCCCTTCTGGCCTGGCTCCACTGGCTCCAGGCAGAGATTGATGGGGGAGAGAGT
GGGCTCCTAGACCAGCCCGCTCAGCCCCCACTGCCCTTGTCTCTGTCTCATCATGATCAGATAGAATCCTCCAGTCCTCAGGG
CTGGAGCCCAGCCTGCTGGAGCGAGTGTGCGAAGCTCTTTAGCATCTTAATTTCCAACCCCATCCATCTCCTAGCCTGACAGC
TCCCCACGGGACACTGCCTTCCAGTTACATCAGCGCCCTCTGCAGCCCAGCCCCCTGACCTGAGTCCCATCTCCGTGTATGTG
AACCCATGCACGTTGTGACTTCATGAGTCCACCGTCATTAATTTAGCAAAAATGTACCAGCATCTCTGCATGCCAGGCACTGT

GGATTGAGGACGGAATGGTGGGCAAAAGCAGACAGGGTCCTCGCCCTCCTGGGGCTTACAGCGGAAGGCAAGAGATGGCATTC
ATCTGATGATCTCCACAAACGTGAAATGTCAACTGTGGCTTAGAGGTGCACAGTTATAGAGAGCCGCTTCTGTGAAGGTGTTT
GGCCCAGTCAGGGAGTAAGGGAAGGTTTTCTGGAGATGTGACATTTTAGCCAAGACCCGAAGGATGAGTAAGAGCAGCCCAGG
TGAAAGAGGGAAGGAAGAGAGTTCAGGGCAGAGAAACCCACCTCTGCAAAGGGAAGGAGGCTGGCAAACAGGGGAAAGAAAAG
AAGGTCATTGTGGCTGGAGCCGAGGGAGCAGAGATGAGTGAGGGTGGTGTACGGTGGATGGGAACACACACAGAGGCCGGACC
TCAGACACCCTTAGAGAGCTTTTGTTTTTACAGGAGATGAATAAACAGAAGCCATGGAAGCATTTTAACCCGTGTGTCTGTGT
GCACTTTTGTGTGTGTGTGCACGTGAGTTTGAGAGAGAGAGAGACAGACACGATGAGATCTGAGTTGGGAAGAGCACCTGGGC
TGATTCCCTGGAAGTGGAAGGAGTAGGAGTGGGTGCAGGAAAACCTGCTAAGAGGCAGTTTATGCAGAGAGGTGACAGTGGCT
TGGACCCAATCGAATTTGAAGGGATTTTTAAGGCTATAGTGTTAATATTTCACTGATACTTCAATCTCTTCCCCATCATCCCA
ACCAGGTCAACAACCTAGACTCTGCCTAACATGAGTCCATCATTTCTCTGAGAACTTCTCAGCAACACACCACCTGGTCATCT
CACATACGCTCTCACCCCCGCCCCTGGCCTCAGCTGCTTGTCTGTGGTTGACACCATTTCATCACTATTTTCCTTTACCCACT
CCAGGGCACACAGAGAGGCCTGGACTTACCTGATGTTTCTCACATCTTTTCTGGGTCCACGTGGTAATCCCCACTCACCTCTG
TGGAGTGGGACTTCCCGAGAGCCCATCCCCGTTCTGGATCCTTTGGGGACCTGAGAAGTTGAAGGAAATCCCTAGGATCTGAG
TCCCTGGAAGCAATAGCCTGTGCTTGGCCTGAGGTTGATTTCCAGGGCCTTCCTGGAGGAAGCTGCCTCCTTGCAAACTAGGA
GGCCAGGGACTTCCCAGGCCTTTGATGCCCCATTGTGCTGAAGGGTCACTGGTGGCTGCTGGAGCCTCTGACCCCACCACAGC
CCTGCCCTACCTGCCCTGTTCCTCCCCCATACAAGACCCAGTCCACAAACTTGCCATCTGTACAGCCCCATGCTTTGGTTCAT
AAAATTCAGCCTCATTTCAGATCTTAGGTGGGAGTTCAATACATAAAGCAGGTGAAAGGGAGGAGCTGCTCTGGTTTAAAGAG
AAGGGTCTAGAATCCTGCCTTCTTGGCTCTCCACTCCATCCTCTCAGCCCAGGGTATCACTGTGAGGCACCTTGTCAGCACAA
TTAAGTGACAGATATGGTGGAAAGAGCTGTTATGGTGGGAAGAACTGTTGGGCTGCCCCATCTTTTTTTTTTTTTTTTTTTT
TTTTTTTTGAGACGGAGCCTTGCTCTGTCCCTCAGGCCGGAGTGCAGTGGTGCAATCTCGACTCACTGCAACCTCCGCCTCCT
GGGTTGAAGCGACTCTCCTGCCTCAGCCTCCCCGGTAGCTGGGATTACAGGCCTGTGCCACGACGCCCGGCTAATTTTTGTAT
TTTTAGTAGAGATGGGGTTTCACCATGTTGGCCAGGCTGGTCTCGAACTCCTGACCTCAAGTGATCCACCTGCCTCGGCCTCC
CAAAGTGCAGGGATTACAACATGAGTCACCATGCCTGGCTGGATGCCCCATCTGGACCAGTCATCCTGGTCCAGAGAGAGGAG
TGACTCTCATTCCTGCCTGCCCTCTCCCCCAATATGGAACGTAGAGCACTTGGTTAGAAGCCTGGCTCTGACACCAACTAGGA
GAGGGCCTCCTAAGAGTGACTTTACATCTCTAAGTCTCAGTCCCCATATCTGGAAAATGGATTTAGGAATACCTCCTCCCTGG
GAGTTATAGGGAGGGGAGGTAACATATGTCAAGTGCCTTGCGGAGATGGTGACTCAGTAATAGATGGCAACTGCGACTACTTC
ACAAAGACCCCCCCATCACCCCTCCCCCTTTCCCTCTGCCCAGCTCACACCTTCCTAAGAGACCCCTCTCCTCCTCCCACACA
CACAGCGTGCACTCTTCACACCCACTCCCCAGCCTCCTCCTTGGCTCCCTGGGGGCGGATGGGAGGGTGCTGGGGCGCGGCTC
TGGCCTCTCTCCTGCACATCCCACCTGCCAAGGAGCTGCCACACGCCTTCCGCTCTATAAATAATAAACCATGAATGCGAGAA
GAAAATAGTCAGAGCAGCAGAGTAAATGCCAAGAATCGAAGGCTCAGGCCTGCCCTAGCTCCTGAGCCCTGGCCTCCAGAGAC
AGCCTCAGCCCCTCCGTTCTGGAAATGAAGCATCCCCTTCTTTCTAGCTGCCTTGATGACATCCCGAGGCCCTGTGAGGCCAT
TGAAATTCTTCCACTTGTTATTTAAGTCAGAGAGAGAATTCTAATGTGGCCTCTCCACCCCACTGGGCACAAGAAGGAGCCTT
GAAGGAGGAGGAGGAGGAGGTAGGAGATTGGTTGATTGTTCCTTGGAGTCCTCGGCCCTTTCCTCCTGAGACTTTCCTAAGCC
AGGAGATGCTTTCACTGGTGATGGAGCAGGAGCTGGTAGGAAAAGCACAGGGTCCGGTTCAGGGGGCCAGCATGGCCTGGCTT
TGAGCTGGGACACAGCTAGAGACCTTCGAGTGAAGAGGCTGTGAGTGGTCTGGAGCACGTTGTCTGGTTAGAGCTGACATACC
AGCTTTGCAATCCTGGGCAAGTTAGCACCCTCTCTGTGCCTCAGTTTCCTCATTCATGACATGAAGGTAATAACGAAGCTGTC
TCAGTAAGAATGTAGTGAAAGATTCGGCTTAGCAAGTGCCGCATTGGTTATATAATACTAGTCTGAACTCTGCATCTCCAAAT
GTTCCTGGACTTTAAGGACGCAGGGCAGGGGCCTCAGAAAACCATTTCCTTAGGTCGACACTGAGAAATATGTCTATTCTGTG
GCTAGGCACATTGAAGCTCGGTTCCAGAAGGGTGTGTTTAGACCACAGTTTGCACTCTGCGAATGTACAGCCAACAGCCATCT
TAGCTGGAAGCAGAGAGCCTAGGCCCCAGACCTCACTCCCTTCACTCTGCAGGGCCCCAGGCTGTGAGCTAATAATGCTCATT
TGGGTTTCCTGTGACAGGGAGGCTCCCTTCTCTTCTTCAAGGACGTAATTTGGCAGATGGGATTTCTACGTGAGGCATACTTC
CTTGTGAAATCTGAATGAAACCCCTCCCCTTCCAAAAAAAGAAGAAAAGAAAAGTGCTGGGAGATAAAGCAGCACCACAAAGC
CCCATAGAAGGCGGTATGCATGAGAGCATTTTACAAGCACGCAAGTCACTCTAAGTGGTGCGTTAATCAGGATGCCGCCTGCC
TGCTCTAAAGGAGCAATAGGAAAGCAGGTAACGGGTTTGAAGCCATATGCTGGTGCTTTGACTACACCCTTTCTCTCCTGCTC
AAGAAATCATTCAGAATTCAAGCCAGTAATACTACTGAAAAAATGATAAATATGTGAGGTAGTAAATATGATCATTAGCATGA
CATAATCATTCCACAAGGTATAGGCATATCAAAACACCCACATTGTGCCCCATGAATACGTACAATTATTACTTATCAATAAT
AAATAGGGCTGGGCATGGTGGATCCCGCCTGTAATCCCAGCACTTTGGGAGGCCAAGGCAGGCAGATCACTTGAGGCCAGGAG
TTTGAGACCAGCCTGGCCAACATGGGAAAACCCCGTCTCTACTAAAAACAAAAAAGTTAGCCAGGCGTGGTTGTGCATGCCTG
TAGTCCCAGCTACTCAGGAGGCTGAGGCACGAGAATCACTTGAGCCCGGGAGGCAGAGGTTGCAGTGAGCCGAGATGGCGCCA
GTGCCTGGGTAACAGAGTGACACTCTGTCTCAAATAATAATAATAAATAGTATTTATTTATCAAAAATTTAAACTTAAATTAG
AATAAAAAGAAAAAAAGATTCCAGTGAGCAAAGGAAGACCCATGATGGGGATAACACCAAACCCTCTCACTGAAAACCGAACG
AAGAGCCACTTGCAAATATCCGCTGGGGTTTGCAGTAAATAGGATTGTGGTGTCCAAACTATAAGTGGCTGGGACCCCCGGTA
CGTTCTGGGAGCTGCTGCTGTTTGCATGTTCCAACAGTAGGTGACCCCAGAGATCATTCAGTCCAGCCTCCACCTGAGGAAGG
GGCCTCCTCTCAGCACACCTGCCAGGTGAGCAACATGCTGTCCTGGAGTCTTCCCAGACGTGTGGCACGCGTGTGGTGACTTT
CCGCAGCAGGCGGTTCTGGGATTGAAGTCCTCGCCCACCTCCTTATAGAATCCTCAGGTCAGCCCAGCTCCTGGCTCTGCAGC
TTCCCAGCCTCTAACTCCTACGGCTTTGTCTTCTCTGGGCTACACAGTCTCAAATTCCTTCCACTCACCTTCATCTGGTGTGG
TTTTCCAACCTCGTGCCACCCTGGTTAGAAGCAGAAAATGCCCTCACCCAGCATTTCCAAAAGTGTGCTCCTCTGTTCCATGA
GACGTCACCAGTATTTCTCCAAGACTGGCTTCTGTGGTCAAATAAGATTGGGAGACAGTGAGGTTAACAAAATGTAACAGATG
TATTTGTTTGTTTACATCGTATGTTTCTCGGGGAGGGAGGAGGGTTGCATGGCATTTTCTAAACGTATTTGATGAGGTTTTCT
CATCTGTCGAATGGGAATGGTGGCAGCATCTACCTCCCAGTGTGCCATCAGGAATAAAGGCAATCTTGCCAAAGGCTGGAAGT
GTGGGATTAAGTGAGGCTGAGCGGGGACTTCAGCCTTGAGGGCTGTGATTGGCGATTTCAAATGGAAAGGCAGGCACTTTATA
GGAAAGCAGAGGCACGAGTTGCCAGCAGGTATTTGCAGGCCCTTTTGCTCGAGGCCAGGAAAGTCTGAGAAGGAAGATAGGGA
TGGAAAAAGGGAAGGCCTCATCCACGTGGTCCCATTATGGCTTAAAGCTGTAGGAAGGCGCCAGTACAGGTAAATGACCACTG
GGTGGCAGCACAATCCAGGGAATAAGATCAGACTCTTCCCTCCCTCCTCCCCCAGCCCCCCCACCTTCAACCGAGCTCCTTTA
CCTGCCAGGTAAAAGCTCAGCCGCTGTCCCCCGCTTCCTCCTCTGTTCTCATCTGACACCTGGGCAGATAGATTCTGCCAAGC
ACCGAGCTCCCAAGGACCTTTATTGATTTGTTTACTGAGCTACTTTGTGTTGGACACTTAGGGTACAGCCGTGGGCCAAGGCT
GGAATGCATGGGAGCAGAGGCCTGGGATCCTCTGTCCTTCTGTCTCCTGGGTGCCTGCCAGAGAAGTGGCCCCCATCAGCAGC
ATGGAATGACTTTGAGCCATGCATTCTCAATGGGGCCATATGGCCCCCAAGGAGGTGAAAATTGGTTCTCACTCTTTTTATGC
ATAAAGCACAAATTTGCATACAGTACATAAACAGATATCTGTGATATCAAAGTTTCATGGAGGGGGGGACCACTAGGGGAGAA
AATGTCTAGAAAGGCACCTGAGGGGCAGTAATGGGACAAAAGGTGGAGAAACGCTATTCTAAGTCAACCAAGGGCTCACTCTA
GGTCTCACGCCTCTGGAAGGAACCATCCGCACACCCTGCCAGGCATGGCCAAGTGTTGGCAGGAAGGTGACCTCTCCCAGCTT

CTGTCTGCTGGGTCTATGGACTCCTCTCTTTCTCTTCATTTATGCTCTCCTGCCCCAGGTGGGTTTTCTTGCACGAGAAGGCT
TACCAGGTACGGGACACAGCCATTGAGTCCTCGGTGGTAACCAAGGTGAAGGGCTCCGGACTCTACGCCAACAGAGTCATGGA
TGTGTCTGATTACGTGACGCCACCTCAGGTATGGTACCCCTACCCAGAGAGGCATGTGGATGTCCAGACACTGGGCAGGTTGG
AAGGGAGAAAGCGAGCAAAGAGTGCCAATGGGATTCCCAAACTAGAATCCATGATGTCACTGATCCAGAGGACCTCTCCCCCA
GCAGCTGAGAGCTGTGTGAGAGCTTGGGCCTGCGGTGCTGGGCATCAGGAAAGCTGGGTTCCTCTCCAGGCTCTGCCACAACT
TGTAATGCAATCAAGGACAACACACATGGGAGAAGGGGGCCATGTGGGTGGCTGCAAAGAGCCAGCTCTGCCCCTCACCAGCC
CTGTGACCTTGGCCAAGTCACTAGACACAAGCCTTGCTTTCCTCATCTGTAGAGTGGGGATAATCAGTTATAGTCCCTGTCTC
ACTGATTGGGACTGTTGGATGTTTTTCTCTCCCTTCTTCTCCTCCCAAGGGCACCTCGGTCTTTGTCATCATCACCAAGATGA
TTGTTACTGAAAATCAGATGCAAGGATTCTGCCCAGAGGTGAGGGGAGGACAGAGGTTGGGTGAAGCAGGTCAAGGCTGAAAA
TGTTGGTGGGAGTGGGAGCAGTGGCAGGGAGGTATGAGCAGAGGCCCCAAGTCTGACCTTGCAACTGGGACCTGGGACCTCCA
CCCTCCTGAGGCTGTTGGTTATGGGGAGGTCGAGGGAGTCGCGGAGCTCACCAGGCCAGGACAGTGTCCTTCACCAACCTGTG
ACCCGTCTGCCCACAGAGTGAGGAGAAATACCGCTGTGTATCAGACAGCCAGTGCGGGCCTGAGCGCTTGCCAGGTGGGGGTG
AGTCCAGCCCCTTACCCACCCCACAATCCCAAGTGTTAGTGGGACCCATGGGGGAGAGCCCGTCGTTGGAGAGGGAGTGGGAA
CCAGCCTGTTCCATGTCATTCTGCTGGCATTTACAGTTGCTCCCTGGGTGCCACACCCAGTGGGTGCTACAAAGGTGGCATGG
CCCCTGCCCCCAGAGGAGTTCCCAGTCTAGGATGGTGGTGACAGACAGGGGTGCTTGAAGTGGCCTGTGCTGTCCAGGAGGTA
CAAAAGACTGTTGAGCCTGGGGGAGGGGGAGAGATTGCTTCTGGGTGAGCAGTACCCAAAGGCTTCCTTGAGGTGGTGACATT
TGGGATGGTCCCTGAAGATGAATAGGATTTGGCAGGACAGAGGGGGCTTCAAAAAGTTCATTCCAGACAGAAGGAACAGCTGC
AGCACAGACTCAGAGGCAAGGAAGGAAGCACAAGAAGAAGAGGTGTCCTCAGGGTTGCTGGGGCTCGGAGCACATGAAAGGAA
GGCTGTCACCTCCCTTTGGCTGGGTCTGGGGCTCAGGAGAAGCAGCAGGAGAGAAGTCAGCTCCCTTTTCCCTGCCTGCTCTT
TTCCCCCACTTGCCAGGGTCCCTGATGGGGGGAAGGGAAGAGGGAGGAAGGAAAGGGAGAGGAGCAAAGGGCAGGCAGCCACC
CAGCAGCTGTGGCTCTCACTTTAGGGATCCTCACTGGCCGCTGCGTGAACTACAGCTCTGTGCTCCGGACCTGTGAGATCCAG
GGCTGGTGCCCCACGGAGGTGGACACAGTGGAAACGTAAGGCTCCAAGCCAGACAGGAGGAGACAGGCCCCCACCTCAGCTCC
CCTTTGCCCATGTGGGAGCCGTGCGTCTCTGAGCTTGAGGAGGGTCTGTGGCTTTCTCCAGTGTTGTCCCTTCCTGGTGTGGG
GGGTGGCCTCAGGCCCAGGGTATCATCTTCCCCAGCCCACCCACCTGCCTCCTCCTCCTGCTGTGACACTCAGGCACAGACAG
CCCCTTCCTATAGCCCACTCTCAAAGTGCCCTTTATCTATAAGAGGTCTCCCTTTGGAGGCATCCACCAGGAAAGGTCGCCCT
CAGGTGAAAGCCTTCATTTCCCCCTCTTCTTCCTGGAAAGCTAAGGCCTCCTGTGCTCACCCACAGGCCCATCATGATGGAAG
CTGAGAACTTCACTATTTTCATCAAGAACAGCATCCGTTTCCCCCTCTTCAACTTTGAGAAGTGAGTCCCCACTCCTTCCCTA
AAGCCAAGATGCAGGCACCCCCGGCCCTGCCAACCTGTTTTCAGGGAAGTGGAGATGCCCCCTCGCCACAGTTCTTCCCACTT
TCGCTCCACTGACCCATCTCCCTGGGCCTACCATTCCCAATCTCCCAGCGGGCCTTGGCCACTGAGGATCAGGTGAACTTTGG
GGTCAGTTTCTCTGCCAGCCTCCCCACCTTGGGGCTCAGACCCAAACGGGAGTTTTGCTTGGGGTAGGAGAGGGACAACTTAG
GCCTAGTCGTGGGTCAAGGATGCCTTCAACGGTTGAAACCCTTTCGGTCTCGTCCCATTCTTTTTCCCCACATCTAGCCCATG
TGTGGAAATCCCTTTTCTCTTAGTCAGTTCAGCCCCCCTTCATTGACTTACTCATTCCACAGCTACTCAGTGGGCATTGGCCA
TGTGCAGAGGGCAATGCCAGTCACTACAGAAGTGCACTAGGCCAGGCGCAGTGACAAATGCCTGTAATCCCTGCACTTTGGGA
GGCCGAGAAGGGTGGATCACGAGGTCAGGAGTTTGCGACCAGCCTGGCCAACATGGTGAAACCCTGTCTGTACCAAAAAAAAA
AAAAAAAAATTAGCCAGGCGCCGTGGCACACCCCTGTAATCCCAGCTACTTGGGAGACTGAGGCAGGAGAATCGCTTGAACCT
GGGAGGCAGAGGTTGCAGTGAGCCGAGATCATGCCACCGCGCTCCAGCCTGGGCAACAGACCGAGACTCCGTCTCAAAAAAAA
AAAAATGCACAGAGTAACCAAGAATGATTCCTGCCCTCTCGAACTCCCAGCCTGGCAGCTGGAGATTAGTCACCGACATACAT
CACCCTGATACACAGGGAAGGCGGTGATGGGGCACCAGAAAGATGCAGGGAAAGGAAAGAGGGGAGGGAGATGGCGAGGTCCA
GATGAAGGCTGAGGGCTCAGATCCCCCCTAGGCCTGGGCTCCGGAAGGCGGGGAGAGATTGCACAAGACGATCTTCCCATGAA
CCCTGGGCTGACCTCTCTCTCTGCTCCTCCCCAGGGGAAACCTCCTTCCCAACCTGACAGCCAGGGACATGAAGACCTGCCGC
TTCCACCCGGACAAGGACCCTTTCTGCCCCATCTTGCGGGTAGGGGACGTGGTCAAGTTTGCGGGGCAGGATTTTGCCAAACT
GGCGCGCACGGTGAGGACCTAGCCATTCTTCCGCGACCCCAAACTCCCCACCTTCAGCCCTTTCCCAGATTTCAGGGCCCTTT
GGCCGGCACTGGCCAGGAGCCGCCGCGAGACAGCGCCACCTGGTGGAAGCATCCCAGGCCGCCACTGGCTTTGTGCCTGAATC
CTTTCTGCTTTCCCCGCGCAGAGCGATCTTGCCCCCCGCCTCCGCCGAGTCCACCTTCCTCAAGCCTCAGTTTCCCACTCCCA
TCTTCACACTTCACCTCAGGCAAAGGCCTTAGATCTGTAATAAGCCCCAAACGACGGGAAAGTAGACCTGTGGCCACTTTCTC
CTGTGTTGTAGCTAAAGCACTGAAGATCCCAAAATTAGGACTCAGAGGCTCCAATGTTCGCATCCGAGCCACAACCTTTTTTT
TTTTTTTTTTTTTTGAGACAGAGTCTCGATCTGTCTCCCAGGCTAGAGTGCATGGCGCGATTTCGGCTCACTGCAACCTCCGC
CTCCCAGGTTCACGCCATTCTCCTGCCTCAGCTTCCGGAGTAGCTGGGACCAAGCCCGGCTAATTTTTGGTATTTTTAGTAGA
GTCAGGGGTTCGCCGTGTTAGCCAGGATGGTCTCGATCTCCTGACCTCGTGATCCGCCCGCCTCGGCCTCCCAAAGTGCTGGG
ATTACAGGCGTGAATCACCGCACCCGGCCACCACAGCACTTCTTTACTGAGCAGTATATGACATGTCACTTTCCGTTCTCCCT
GCCTCCGTCTCCCACCTGGAGGATGGGAGGAAATCATTTGTCACCACCTCCACCCCACCCCCACCCTGGCCCAGAGCAGGGAG
TCAGAGGGCGAGGGGAAAGCTCATACCCGGCCCGTTTCTTCAGGGGGGAGTTCTGGGCATTAAGATCGGCTGGGTGTGCGACT
TGGACAAGGCCTGGGACCAGTGCATCCCCAAATACTCCTTCACCCGGCTCGACAGCGTTTCTGAGAAAAGCAGCGTGTCCCCA
GGCTACAACTTCAGGTAATTCCCTGTCTCCTGGGACACCAGGAGAAGAAGGTGCGGGCTGTTAACGGCAATGTTTATTGGGGA
GACAAGATCCCACATCCATCCACCCACCCCTGGCCCCAAGTCCCACCTCAGGTTTCATTTCAAATCAGGAAGGACTCTCTAAC
AGCCATTAGGATCTAGCTGGTTGTCCTGGGAGACAGTGTCTCCTTATCACTGAAGGGGACCACGCCAAGGATTCCTGCTGCAG
GTCAGTAGTTAGAAGAGAGGGCCAAGGTCTCTTGAAATGCTAGGGTTCTGCGATTCTTTGCCTGTTCCTAACACTGGCCTGAA
ACTGTGACGTGCTTAAGTGACTTCCAGATAGGCCCATTCCCTGCCCTGGGCCTGAATTTTCTAAGGTTTCTCGCTCTACAAAG
TAAGGGTGATAACTGGTATCATTTTACATTTTACAAGATGGCAACTTTGCATTTCTCTCCGCAAACGTGTGTCACCAGTAGCA
ATTATAATTGTCTCTGGTTCTTCAATGCCTCTCCAAACAAGAACTCAGACCAGTCTTTAAATATCATCCCAATGGCTTTGAGA
CTTCAGGGATCTTTTCGGGTTTTGTTTTGTTTTGTTTTTCCATTTTGAAGAAAGGGAGAGAGGAATTAGAGGACAAACTGTTT
GGAAGCAACTGAAAGCGCTTGAACAAGCCATTTGTCTTCTCCCATCCTAATTTCCCCACCTATGAAATTGTGATAGTACCACT
GTGATCTTCAGGATTCAATTAACCAATGTGTGAAAAGCTTCAGCTTTCTGTTTTGTTTCTCTCTTCTTTTTTTTCTGAATCAT
TCATTTATTGATTCATCCATTAAACACATACCAATTGTCTACTACGTGCTGAGGACCGTACTCAGTTATCTTAGGTTAGCAGT
TCTCAAAGTGTAGACTACAAGGTCAACACTACTTATTAAAGGTTTTGTTTTCTTTTTAATTGATAAATAACAATTGCATATAT
ATGGGATACAATGTGATGTTTTGATACATGTATACATTGTGGATTTCCCCCAGTTTTTGAAGATCCTGAAGTTTCTGGCAGGG
CCCTGTTTAAGTACACAGCATTATACACTAAACAGCTTAAATAGAACAAATAGGGAGTGACCAGGGGAAAAAAATACATAAGA
ATATATTTCATTTACATTTGAACATAAGAATGTATATTTGAATATATTCAAATAAATGTTACTCAAATTTCCTTTGTTGAGGT
GGTATTCTCTGATACAATGGCATACGTAAGCCAAAAATAATCATTTCACCTTTTAAAATTGTTAATTTATAACTTAAAAAAAT
AATCACCCACCCCATTAAGCTTTATATTTAATAGTTTAAAATATACATGTATATTCTCTGGAAAGAAGAATCTTTAAAAATTG
AAGTACTTTCATCATCAACTCCAAACTTTAAAAAAACCATAGGAAACAACACATATTTTAAAGTAGGTTAAAAATACTGTGCG

GCTCACTGGCAGAAATTGGCATATTTATTCAGTTGGTATATCACACTGAGATCAATACAAAGGATATTTGTATGGTGGCTTAA
AATAGTAACATATTAATAAAATTCTCATGATCTAAAATGCAAGTTTTCATCTTCATAACTTCCCTTTGGCCATTGGGAATTCT
TTAATCCTCCAAATAACTCATTTGGCAGAAAAGCTTATGAAGAATGTGAATATTATAAAGACCCCCAACTACTGATATCGTAC
AGTTTTAGAACAGCATCTCTCATCTAAATAAGAATTGGTCTGGAGTTCTTTATCTCCAATTTATTGCACTGTGGCTGCCTTCC
CTCCCTCCCCACCTGAGCACAGAAGGATGCGGGATAGACCTGGTCCTAAATAAGCTTGGAGGGTATTTGGGGAGGCAGGACGG
AATATCCCCAAAGACCCTGCCTGCATAATTCCCAGAGGCCTAAGAGAAACCACCCCCTCTTAGGATCTCAGATAATTGACTCC
CCCAACAAAGTCCCCCAGGCCAGAGAAGAAGGAGGCAAAGCTGCTTAGTTTGACCCTTGTGATTTAAAAGTTTCCAGAGGGCC
CAAGTAATAGCCCTGACATTGGGGGACATCTGATATCAGTGGCAAGCAGAGGGCTCTGCCCAAGCCCCTTCCCATCCCTTCAC
CTGGGTGCCCACCCACCACCCTCATGCAACCTCAAACTACTGGCACCCAAGGCTAAGCTAAGAGCCCACGTGTGGGAGGCTGC
AAAGCTGTCTTTCTGAATGCTTGAATAAGAGAGAAAGGGTCACAAAGCCAGGTTCAGTGCGGGTCACAGTGCACTTTCTATGA
TATGGTAAGATGTACGCTGTTTTTTAGAATCTCACCAAGCTACTTATCAGTAGAAACCATACTAGTCACCCTGTGTGCAAAAC
GTTTTGTGTGCTTCAGCTCAGCATTCCTTGCATGCCCTACGAAGTAGATGCTACAATATCCCCCCCAACTTTATAAAGGAGAA
GATGGAGTCTCACTGTTAAATAACATTCTCAAAGTCACAAAGCAAGCAAGAGGGGGAGCCTGGATTCAAAACATATTTCTTTG
GATGATCTCCACCCCAGCCAGGAAGACTAGGGACATTTGTACTTGTTAATCCTCAGAAAAAAAAGCATGCCTATGTGGTTGAC
ACTTTCATCCCAGCTTAAAAACAAAGAATCTAAGTTCCAAGGAGATTTCAAGACTAGCAGATGCTGGCAGCACAATTCATAGC
CCGGCCTTTTGTCTCCCAAACAATTCATTTGCTGCTCCCTCCAACAGAGGCAGATTTTTCAACACCCCTACTGTTGCCATTTG
CTCTGGAGGGAATGGAATTATTCAGCCAAGATTCGGCCGTGTTTGAATCTGCTAACTAAGACATCCAGAGGCAGCTAGAGATT
CACATTTCCATCACTAATTACATTCGCAGCTCCCTTCCAAATGTCACTCCCCCCCCCCCGCCCCTATTTTTTGTAGCTCTTTG
CCTGCAGAATCAGAGATTTTGAGAATTTATAGCTGTTGAAGTTCCCCTTGCAGTCACCCAGAGTAAGGCGGTCACTTTACAGA
TGAGGAAGCGGAAGTTCCAAAGGGGGCATCTTAGAGTAGCCTCAAAGGTCATTGGATCTCAACTCCTAATGTGACCCTTGTGA
TTTAAAGGAGTTTACGGACCCATGTAAGAGATTACAGGCCCATGTAATCACCCTGACACTGGGGGATATCTGATCTCCGTGGC
AAGCAAAGTGGCCTGCTCCATTCATTGGAAAGGTGACCTCAAATTGAGCCAAAATGTGCCTCCCTTTAAATCCTCTCCAGTGT
ACTTGGTGCTGTCCATGCAAGTTAATCTTTATTTTTGTGATCCCCTAAAGATTCTGTTCTTCCCCTACCTGAAATTTAGTGGA
GACATTTTATTTTTACTCCTTGGTCTGTTCTGCGTGGCTAAAGACTCCGTGGGCCGCTTTAACTTAGTATTTTTATGAAGCCT
CTTTCTAAGCACACTGAGATTGCAGTTGGTGGGGTCATCTGGATTTCTAGCAGACAAAATGCAGCAATTTCTAAAAATAAGAA
CTGTTGAGAGTCACCAGTTCAGTGCTGCACAAGTGAAAGGCGCCCTCAGCAGAGCCCTGCAGTTCTTCAGGAGGCTCTCTTCT
CTGTTGGCAAGGTTTCTGAGGCCCAGGTAGACCCTCAATTCACAGGAGCAGGATTTTAACAAGAGTACTATATTTCCCAAAGT
CCTGGGAACAGGTGATGTTGTGTGTGTGTGTGAGTGTGTGTGCACATGCGAGTTCGTGAGAGTGGGTGTATTTGTTAGTGGGT
GAATGTGTGAGGCTGAGAGTGAGTGTGTCAGTGTGTGTGTGTGTGCGTGAGTGTATAGGCATTGATGGTGCAATGACAGATTA
AAAATACTGTATCCGTCAGGGTCCCCGCAGGAAACAGATGGCACATTCTAACTGGGTAATCTGAGGAGAGTTTAATAAAGGGA
CTGTTTCAAAGGTGTGGGCAGGGTGTACGGAAACCACACAGATAGTGCAGTGCCAGGGCCAGAAACAGGACACTGGTTACCAC
CCAGGTCTGAAGAGGCGAGGAGAGGAAGCAGTGACAGGAACATGGAGACGGACAGAGCTGTGAGCAGAGGACAGCCTGACATG
TGGCTGTGACTCAGGAGAGCCCCACCAGAAGCCAGAGCTGAGGCAAAGTGGCCCACTGAGGCAGCCCAGGGCAGGGCGAGGAA
GGGAGGAGCACGGACCTGAGGGGCACCTGCAGAGATGTCCAGGACAAGTCCTGACAACTTTCATCTGTGAAATTACAGCCCTT
CCTTAACTTTCAGAGGTCTCTAACTGCTTTATGCCCCCGATGAAAATGGGGACCATTGTCCAAGGAAGATGCATGTATTCATA
GACATGAGAAAATTCACAGGCAAGTTCTCTTCTTAAAGGATATTTTATTTCTTTTTTTTTTTTTTTTTTTTGAGACAGAGTT
TTGCTCTGTTGCCCAGGCTGGAATGCAGTAGTGCAGTAGTCTCGGCTCACTGCAACCTCTACCTCCCGGGTTGATGCAATTCC
CCTGCCTCAGCCTCCCCAGTAGCTGGGATTACAGGTGCCCGCCACCACGCCCAGCTAATTTTTGTATTTTTAGTAGAGACGGG
ATTTCAACATGTTGGCCAGGCTGGTCTCGAACTCCTAACTTCAAGTAATCCACCCACCTTGGTCTCCCAAAGTGCTGGGATTA
TACGCGTGAGCTACCACGCCTAGCCAGGTTATTTCATTTCTACAAATAAGATACAAATACATTCTCAGAGTAATAAATCCAAC
CAATACTGATATATACAAAGTAATGACATGGGAAGTCCCCTTCATTCCCCCAGGCCTGCACCCTTTGCAGGGAATTAACATCT
GGGACGGTTTAATGAGTTTCTTTCCAGTTCTTATTCTATGCATTTATATTTATGCAGCATAAAATTCCAAGACTTTGAGGCCC
TCTAAAAGCCTATCCCGTAGCCAGGTGTGGAAGCTCCTGCCTGTAATCCCAGCACTTTGGGAGGCTGAGGCGGGAGGATCCCT
TGAAGCCAGGAGTTTGAGACCAGCCTGGGCAGCAATAGCAAGACTCCTTCTCTACAAAAATAAGATTAAAAATTCTAAAAAAT
AAATAATAAATGAAAGCCTATCCCTGCACCTCAGATTAAGAGCCCTAGAGTTAAGTTTGCAAAGCCCTTTCACACCTATTTTT
GACAGATCACAGCTCACCATCTTCCCCCACCCCCAAGGTAGGCTCAGAAAGATTTCAAAACTTGCCTGAGATTATACAGCCTA
ATTAAGAGGCACATCAGGACTCAAACCCAGGGATTTGATCTATATCCATTGCTTCCAGCATGCCTTGCGCCATCACATGGCCT
GCAAAAAAGGGGAAAAAAAAATAGCTCTAAGAGATATACCTGGTAGTGATGGCTGGTGTGATTGACGGGAGAGAATCGAAACT
GCATTTCAAAATGCCTGATTTCTTGTTTCTCCTCTGAGAGTTCCTAAGACAGCTTTGCTACTAAAAGGCAACGCAGTTTTGGA
TTTCCTCTTTTGGTGTCTGGGACAAAAAAACATTTGTTCAGCTGCTAGATGTTCCTGGTGCGGTAGGTGTTTCTAGTGATCGT
TTTATGTTGGAAATGTACCCACAGCAGCTTTCATGAAGCTCGGAGATTTGGCGCCTGTCCTGCTTCCAGGCAGAAACGTGTGG
ATCAGCAAGATCTTAGGCCAATTGACAGAGACAGAATCGAAGTGCACCCTTGGCTTTGATCATTCTCTCTACAATCTGGATTT
TTCTCTTTCCAAAAGCCATAGAATATGCGTTAAAAGCAGCCAGCACCGTCATTTCCACAGAAACACTTGAAGGCCCTCTTCCA
TGGGAAGTGTACTTGCTTGAATTCTCCATAATCCATTTTCTTCATCATTTTTAGGTTTCAGTGGAAGTGATGCAATTAGAGTG
ATCTTGGATTTAGATAGCCCTTTATCATGTTCATGTCTACCCTATTCTCACAGCAACCAGTATTATTCATAGAAAATATTAGC
TAACACTCATTGAACACTTACCAGTGAGCCAGAGAATTAGCAGGTTCTCTGTGTGATTATCTTGTTGACCCTGAAGAGAGAAC
ATTTTAGAGCCAGGTGTGGTGGCTCACACCTGTAATAATCCCAGCACTTTGGGAGGCCAAGGCGGGCAGATCACGAGTTCAGG
AGTTCAAGACTGTCCTGGCCAACATAATGAAACCCTGTCTCTATTAAAAATTTTTTTAAAAATCAGCCAGGCGTGGTGGCACG
CACCTGTAATCCCAGTTACTCAGGAGGCTGAGGCAGGAGAATTGCTTGAACCCAGAGACGGAGGTTGTAGTGAGCTGAGATCT
CACCACTGCACTCCAGCCTGGGTGACAGAGTGAGACTGTCAAAAAAATAAAAAAAGATATAACAACTCAAGAGAACATTTTAG
AACTGGATACCTGAGCTCAGGGGTTTCATCTACCTGTCCAAGGCCACACAGCTCCTACTGCTGGAGCCAGAATTCAAACCCTA
GCAGTCTGGCTCCAGAACCTGTGCTTGCAACCACAAGTAGGACCAGTATGGTAACGCCCATTCTACAGATGAGGAAACTGAGG
CCAAAAAGATCCCTCTCAGGAGCAGAGAGCGAGTAAACTGGCTCTCAGGTACATCTTCTGGCTCCAGGTCCATTGATCTTTCC
CTACCTTATTAATTAAAGATAAATTAATAGTAATGCATTTTTAAAGATCAACAAGAAGCGTTTTTTTTTAATGCCTGCCTTTGA
GGTTGATTTGGTGCCTGGAATATGAATAAATAAGTATGGCTTTGGGCCCTTCTCTAAGGAGAAGAGTTCCAGCCTGTTCTAAG
GATGTTGCCCCACCCTGAAGCAAAGAGTCTGCCAGGAGATATTTTCCTATCAGTATAAAATCAACTGTAAAAGTGTATTTCAG
CTGGCAAAATTACTTCCCACCAGGCAAAGCTTTGCTGAGAACACCACCACTTTCACTTAGAAACCCAAATTCCAGGCCCAAGT
TTTCCCTTGCAAGTCAAACCCGGCTCCGGCAAGTTTGTTGCTGTTTTTCCTGCTGCTGTAACAGTTACGTGTCCCTGCTTTAA
GAAGGAATTTCCACCACTCGATGAGAGGATGGATCATTTCTAAACAGATGTCTGAGAGCTTCCAAGGGATTTGTACATCGTGA
TAAAAAAACCCTTCTCCATTCAGCAAACGTTTATTGACTGCTGACTACTGCAAATGTCAGCTCAGCATGGGGAAGTACTTCTA
ACAGTTAGAGCTATCCAAAGCTAAATTTGGGCTGCTCCTACAGGTAGTGAGTTTCCTTGCACTGAATGTATTCAGGCATCGGC

AGGGAAACCCTTTGTAGATAATGTAGGGAGAACTTTGAAGGTCTCTTTCAACTTCCAGATTATATCACATGCTGGGCTTTGTG
GCGAATACAGAGATGAACAAGACCAGTTCCTAGAATCAAGCAAGTTTTAATATAGTGATGATAAATTTGAATCCAAATAACGA
AAAATGCTTATACAAAAGAAATATATATATGTTATGCTGGGGCAAGCCAAGGATGGTCAGGATGAAGCAGAAGTAAAGCAGAA
GGATGTGGGCTACAGTTCAGGCCTTGCTGTTAATCCTGGATGTGATGTTAAGCACGTCTCATTGCCTCTGTGGGCCTCAGTTT
CCTCCTCTGTAAAATGGGCTGGTTAAAGATGATGATCTTTTAGGCTCCTTCAAGCCCTAAAAGTCTGAATCAACATGTGTGGG
TGTCTGAGGAAGGGCTGTGGAAATTTGGGCTGCTGAAGCATGCACTATTATTTATAGACCTATCACAATCACGTTGGAATGGA
GCTCCAGCCCTGCCCTGCAGAAGCGCATCTGACAAATGATTTATTATGGTAATTGACGTTTGTACTTACTCATTCTTTATCTC
TTGCTGGTAATGCCACAAGGGAGCGCACGCACACTCACACACACACGCACTCACACGCACAACATCCCAGCACTATTAGGCCT
CAGAATCATTCGATTGAGTCCTGTGTTAGAGGTGTCCTGTCTGGTCACAGCTAGGGGTGTCTCAGTGAAGGCCCCGGAGGCAA
AGCACATTCAGCTGGGGTTTGTGAAGAAATTTACACAACAGGAACCAGCATGGGAGTCGAGGCACACAGGGATGAACAAAGTG
GGAAGCCGTCACCACTGTAGACCTGCCGCCCCCGCGGGAGGAATGGGAGCCTGGTTTTGAGCTGGGGTGCCTGACAGGAGCAG
CAGTCAAAGTGACACAGCCACAGGCAAAATCAAGGCAGAGCAGGGAAGCAGCGAGCAGATACATACCCCATCCCCTCCTTCCC
ACCCTCGGGTCCCCTGCCAGTGCCGCCCATTGACCAAATTCCCCAGAAACCAGGGGGGAGGAAGCCAGGGAATGTGGGCTGCA
GAGGTCCACCTGCAGGGCTGCCCAGACCAGAGACTGGCTCCTGGGGCAAGTGCAGAGTCTCTGGCCCACCAGGTAACCATCCC
CGCTGCCCTTCAAGTGTCTGGGCTCCAGTGGCCCTTCCAGCCACGCCTGTCAGAGGAGCCCCCGACCCTGAAAACTCTGGCCC
TGCCTGTGCCTCTGGGCTGCTTTCCCCTTTTCCAGCTCAGCGCTGGCAGCTGTTCGGGCTCTGTTCTTTCCTCTGATGCCTAT
GGCATCATTGCAGTCACAGCCATGCTGTGCTTTCTCCACAGCTGAGGTGTTTTCACAGACACCAGCTTAGCAAGCTCCCTGCC
CACTGAGGCTGCAAGGAACTCCTTTTGGCTCCTCTCTTAGGGAGGCAGTAGGGGTAGGCAAGGGCTTTGGAGTCAAGCAGCCA
GATTTCAGATCCCAGCTGTGCCCCTTGCAGGCAGAGTAGCCTATGGAGCATGTCTGTGCCTTTCCCCAACCTGTAAAATCAGG
CATGTTGCCTGATGACCAGTACCCAATATTAAGAGAAAGCTGTGTGCTAGGTACTATGTTCAGCCTTCACATTCCATAGTCAT
TTAATCCTCTAGGCAACCCTAGAGCTACTGCTCTCATCTCCATTTTACAGATGGAAAAACAGACTCAGAGAGGTAATTCACCC
AAGGTCATATAAACTAGGTGGCACAGCCGGGATTCAGGCCCAGGACTATCTCATTTCAAAGTGCGTAAGCCGCCAGCTAACTC
ATTCAGCTGTTGTGAGGCCTAAATGAAACAACAGGTGTGGAAGCCTCTAGCCTAGTGCTTAGCAGGAGTAACTGTCCCACATA
TATTTTCCTACTCTTTCCCGCATTGCCCCTATCGAGAGGCTGGCTCCCACAAGTGGCACCCACTTTCCCACCTAGCTAGCTGC
CAAATCTAACTGTGTTCTGCTGGGGAGAGAAGCAGCCTGTTGTTACTACCTTATACTAGCTCCACCTGCAGAATCAGGAGCAT
TTGGAGAAACCAGTGGCAGCAGGAGGGAGCCCTGAGGACAACCTACCTAAACTCAATCTTTGAGATGTCAAGAATCTCAGAAA
TTATTTATTCTTCTAGCAAGCATTTACTCAACCCCCTACTGTGAGCATTAGGCCTTTGGGCAAACAGAAACAGTGAGATATGA
GGCCAGGCGCGGTGGCTCATTCCTGTAATTCCAGCACTTTGGGAGGTCGAGGTGAGCGGTTCACAAGGTCAGGATGGAGACCA
TCCTGGCCAACATGGTGAACCCCTGTCTCTACTAAAAAAAATACAAAAAATTAGCTGGGCATGGTGGTGCACACCTGTAATCC
CAGCTACTTGGGAGGCTGAGGCAGGAGATGCACTTGAACCCAGCAGGCAGAGGATGCAGTGAGCCGAGATCGCTCCACTGTGT
ACTCCAGCCTGGTGACAGAGCGAGACTCTGTCTCAAAAAAAAAAAGAAAAAAAGAAAGAAAAAGAAACAGCGAGATATGGCTC
ATAGTCCGTAGTCCAAATTATTAGCTATAGTCTGGTGTGGCAGATACTGTAGTAGAGGCCTGAATCCTAATGGAGAGAGAAAA
GGCAGCCCTGGGGGATGTCCCAACCCCAGCTCATGCCCCTGGTTTGTAGCATTGGCTGGATTTCTGTGAGGTAAATACTCCAG
GATGGTCAATTTCAAGCTACCAAGGTGAAGTCACTAAACATGGAATTGGGAAGAGATGCACACAATTGGCTGCCAGCTGGGAT
GTGTGGACCCAGCTGCTGCCACTTCCATCTGCCTCTACCCACCAGCCCACCAACCCTCTTCCAGCTGCTTCAGAAACACCACG
TTCTTTCCCGTGAGAGGGCCTGCAGATCCCTCAGCCAGGAAAGCGGCCCCTGCCTCTGGCCTTCTTGCCCTTTTAACTCTCCA
TCCTTCAAGCCCCAGCTTGAGGGTCACTTTTTTTTTTTTTAAGTTTAAGTTCTGGGATACATGTGCAGGACGTGCAGGTTTGT
TACGTAGGTAAACGTGTGCCGTGGTAGTTTGCCGCACAATAAACCCATCACTTAGGTATTAAGCCCCACATGCATTAGCTATT
TATCCTGATGCTCTCCTTCCCCCTGCACCCCCAACAGGCACCAGTGTGTGTTGTTCCCCTCCCTGTATCCATGTGTTCTCATT
GTTCAGCTCCCACTTATGAATGATAACATGCAATGTTTGGTTTTCTGTTCTTGTGTTAGTTTGCTGAGGATGATGGCTTCCAG
CTTCATCTATATCCCTGCAAAGATCATGATCTCATTCCTTTTCATGGCTGCATAGTATTCCATGGTATATATACCACATTTTC
TTTATCCAGTCTATCATTGATGGGCATTTGAGTTGATTCCATGTGTTTGCTATTGTGAACAGTGCTGCAATAAACATGCATGC
ATGTATCTTTATAATAGAATGATTTATATTCCTTTGGGTATATACCCAGTAAGGGGATTGCTGGGTTAAATGGTATTGCCGGT
TTCAGGGTCACTTTCACATGAAGCCTTGCCTAACCCCCAGCCTAGGTTAGACATCTAACTGTGCTCATAGAATGGCACTCCTC
TCCTTCCCAACCCTTCCTTATGTCCGATTTTAGCTACTTATGGGCTTGTGTGGTTAATTAGTATTTCTCTCCCTCTCATGACA
GCAGAGCTTGGCAAGGTATCAGCAGTACCTAGAACAGTATCTGGCACAGAGCAGGTGTGCTCCAAATGTTTGTTGAATGCTGA
AAGAACAAGAGGTCATCTGAGCTGGGCTCTAATGGATGAATAGGAGTCTGCAAGGTGGAAAAGGGAGGCAAGAGGAACAGCAT
GGGCAAAAGCATAGACATCTGTGTCTGTGGGATGTGTTCAGGAAATGCAGGAAGGCAGGTAGTCTGGTGTGGCTGGAACTTGA
GCGTGTGGCAGGGAGAAGAGCTTGCAGATAAGGCAGGTGGACTGGGCCAGGTCGGGAGGAGTCAAGGTATCGAATGGTCCTGT
CATTCTCACCAACCCCAATCCTAACCAAAAAAATAAAAATGATCTGGTAAGAACCAGAGGACTTGGGGAAAATCAAGGCTTGG
GCATGGTGTATGTAGCTGAGCCATTCCCCTTTTTAGATGAGGAGGCTACAGGGTCCTTCTGTCCTGACACTGCATGGCCCCCC
AGGCTTCCTGTTCTGCTCCCAGCCAGTGACTCTGGGTATGGAGACCCACCTAGCAAATGCAAAAAGATGCACCAGCTGGAGAA
CGAAATTAGTTATGACCCAACAGAAATCAAGCAACAAAAGAACAGTGTAGAATGCTGGCTAAGAGTGTGGGTCCGACAGCTGG
ACTGCCTGGGTTCGAATCCCAGCTTCACTCACTGTTGGTTTTGTGACCTTAGACAAGTTGCTTCACCTCTCTGATCTTGATTC
CTCAGCTGTGACATGGGAATAGCAACAGTACTTAAATGCAATGGGGTGGTTGTGAGCATTAAATGAGCTAATAAGCATAAGCA
CTTAGCACAGTGTCGGGTCACAGAGGAGTACTCAGTAGATGTTGGCTGTTATTATTACTAATATCATTATCTACAGGAGCCAG
GAGAGTGTAATGATTAAAGTAAATGTAGATATTGTTTCATTTTATCTTTATGCTAGGATAAGGGATGTGTTTTAAGCACGGAC
TATATATGGACACTCTCTCAACTCATCCTCCTCAGAGCTCTTTTTCCTCCAATTTTTCAGTTGAAGTAAAAAGCTCAGAGAAG
TCGAATGACCTTCCCAAGATCAAGAAGCTAATTCACAACAGCCATAGCACCACACCCAGATCCCCTAGGGCCTCCTTAGAGGG
TTTACTCCTGGGATATAGCATCATGGGACTGTGCCCTCTGTCTAATCCTGAGTAACTCCCCAACTTCAGCTCTTTCTTTGTCC
CTTGGCAAATTACATCTCTCAGCCATGAAATTCTGAGAGTTTGCAACAGTCAGGGTTAGCATTGCTAGTTGCTATAACAAACA
AACCCCTCATTTCAGTGGCTTAATGTGAAGGTTGATTTCTTACCTATGGCACAGTGCACTGTGGGCCAGTGGGGGTGGGGAGC
GCCATGCAGTCATTCAGGGATCTAGGCTCCTGCCATCTTGACTCAGTCTCTCTAGAGCCTCAGAGTCCTCTCCTGACTCCTGA
GCAACTGGCCATCAGGTGAGGAAAGGGAAGACATAGAAGGTACACTGCTCTAAACTACCTCAGTCCAGAGGTAACAAACCTCA
CGGCCATTCATATTTCATCAGCAAAAACTAGTCATGGGGCCCCAGCTAAATGCAGGGGACTGGGAAATGTGGTCTAATCATCT
GCAAAGAGAGGAGATAACCAGACCCTGGTGACCAATGAGCTGTCTCTGTCACAGGGGTGGGCAGATTCTGTGATCCCCATCGG
CCACAGGAGAGTGCAGAAGCTGGGACTTCTGGGTTACCCCCTCTGTCTGCAGCCTGGGCCCACACTCCCTGAGCTCTGTTCCT
CCTCCCTCCACCCGGGAAGAGAACCAGTCCCTGCCAACCCTCCTCAGAGGGTGGGTGGTTGGTGAGATAATGATCTTACCATG
CTTATTGCCTCTTGGAAGGCAGGTGCTGGAGAAAAACCAAGTCCGCTTTGATTTTTCTCCCTGTTCCCTTCACATTCCTTCCC
AGGATAAATTTAGCCAGCCCTCACTTTGAACGGCAGTGCCCAGGATACGACTTTTTGTTCTCCAAGTTGATGTCACTGTCAGA
GCCGTTTTCATGGTTGCAGCCTTTGGCCAGCAGTAAAGATTTCCGGATGACAGGCCCAGCCTCTGCCCTGCCCCAAACCTCTG

TGATCCACCCTCTCACCCCTGCCCACTACCCATGGGCATGAGGAACCACATCTCTGAGACAAGGGCCTTAAATTCTCCAGTGA
TGTGAGACAGGACACAGTATTTAGAAGGCTTTGATATCTTGCACAAGGGCTGCGTTATCCTTAACAGCCTCCAAGAGCTCAGA
GGCAGGATGGTTCAAGGGGTATGAGCATGAACTTTGGAGGCATCGGTATGGATTAGAATCCCAGCTCTGGCAAGTTATCTTCT
CACCTGTCTCCTCATCTGTACAATGACTCAACAACAGTATAGTCTTCATGAGATTAGTGGAGATGCTTATATTAAGGAACTTC
CTATATTGTTGGTGCTCTATAAACAGTGGGCATGGAGACAGTGATGGTCTATAAGGACCTCCTGGAGCCTTCTGCCCATTCCA
GATACTTCTTTTGCAGACTTCTTTAAAATATCCCGAGAGTCCTCCTTGGAGAATTATGTTCTTAGGCCCTGTCATCTTTATAG
AAATGACGCCCTCTCTTGTGTCCATCCTATTATCCTCCTTTTGCTGCACCTTGAATTCATTCTGTTTTGCCTTGGTTGTGAGG
CTGTCTTCCTCCACCACCTAGACTTGAACTTAGCATCATTTTAAAGCTGGTTTAGCCCCTCCCCTCTTTCCTTGACCTCCAAG
CCCTCTTCCGGATAAGTGGTTGCACTTCTTTCTGCTGCCTTCCAAGGTCCACTCTCATTCTTACTCTGGGTCTTACTCTTTCT
TGGGATCCCCTTGCCTCCCCTGCCCCTCCCTCAGCTGCACAGCCCACAAGGAAACACCTTCCCAGGTCAGGCTGCCCTGGAAA
CCTTTTTTTCACTGAGTCGTTCTCAGCCTTACTCGAGCAACAGGTACATCACTCAGGCACACCAGCTCTGCTTGTGCCCACGC
ATAGGCAGAGACAGAAAATGTGTCACCCATTCTCCAGTGCTCCCTCCTGACCCAGATAAAGCTCTCTAGGACTGAGCTTGCTC
CTCTGTAAAGTGGGAGTGGTCAGGGTAGGTAACCTGAGGGGAAACAGTGGGTGGTCTCACAGGGGTGACTGAATAAAGAGACT
ATACACAAAGGTGCATTCCAGGTAAAGGGAAGGGAACTAACCAGGCCAGTGAAGGGCCTCTGTGCTGGCAGTGAGGCCAAGCT
GCTACCGCCTAGGCTGGCGGGAGTGAGGGGAGGAGCAATTCCCAGAACCTGAACAAAAGCTGAGGCTGCCCAGCCACCTCAGT
GCCCTGGCCTCTCTTTTTCCCTGCCCTCTGATCTCCTCTCAGCGCCTTCCATTGGCTGAACCCACCTGGAAACGGAGGCCAAA
GCGGTCTTTGCAGATCAGGCTCTCAGGGCCCAGAGCTGGGCACAGAAGGGACAGAGAATGGCTGTGGAGGAGCAGACAGAATC
TCTAACACAAGAATCTCAATGGTGTTCGCATTTACCCTGTCTCACCAACAGACCTTCTAGCAGGGCATGAGCACACCTGTGCT
TATAGACATGGAAATGGACACCCTGAAGGCTAAGGAACACCAGAGGCCACATTAACAAGTGGGGGAGCCAGGATTTAGATTCA
TTTCTGCCTAATTCCAGAATGCCCCACTGCCAGATGGCAGCCAGAGCAGATAGTGGCATACGTTCTCCTTCCCCATCACAAGT
TATCTTCCTCCCATGCCTGTAATCCCTCAATGACTGATTCACTGGGGCTGAGCATTTCCTTCTCTCTGTTGTACAGGTTCAAA
TGCAAATATCCCTGTCAGGAGCATCACGTCAATCACTGAACACTTTCAGGGAATCAGTTTCTCAGGCCCCTGGTGGGAGAGGC
CTGGGAATCTGTGGGGACTGGAGACACTGAGAGGGAACAATGTGGACCCCACACGGCTAAGGAGTTTTCTGGGCCCTTTCACT
CCTGTGATTTCACTTAATCCTCACCACTTTCCAAAGTTACTGGCATCAGGAACCCATTTTACAGCTGTAGGACAGTAGCCCAA
AGAGATGACACTTTCCTAATGTTAGAGTTTGGCCCGTGATGAGCAGAGCCACGCAGCAGGAAGTGCACTGGCTTTAGAAGCTG
AAAGACTGATGCGATTTGAATCCCAAATCCAGCACTTCACTAACTGCGAAACCACAGGCAAATCTCCTCCCCACCATAGGCAT
CTACAAAATGGGGGTCTGAACACTCACGTCTCTGTGTTGAACACTAACCCCTGTTTGTGGTGAGAATGAAATGGGATCATTTT
CCTGAGTCCCCGGCATGGTTCATGGCACCCAGAAGCCAAGGCAGAGAAGGTGCAGGGGTCAAAATCTTGGACTTGGGCAAATC
TAGTGCTGAGCTCACCAGCTGGTGAACTCAGCACCAGCTCTGGGTAACCCCAGACAAGTCTCCTTACCCTCTCAGAACCTCAT
TTGAAAAACAGAGCAATCACATGCCTATCTATAATTGTCCGCTTTCCGTTGCTTCTACAAAATACCTGAATCTGGGTAATTGA
CAAAGAAAAGGAATTTATTTCTTCATGTATAGAGGCTGAGAAGTCCAAGGCTGTGGAGCCAGACGCATCTGGTGAGTCTTCCT
ACTGGTGGGGACTGCAGTCTCGGGCGCAGGGTGTCACATGGAGAGGGGGCTGGGTGTGCTAACGTGCTAGCTCAGATCTCTCT
TCCTCTTCTTACAAACCCACCAGTTCCCCTCCCATGATAGCCCATTAATCCATTAATCCATGAATGGATTAATCCATCCATGA
GGGCAGAGCCCGCAGGGTCCAATCGCCTCTTAAAGGCCCCACCTGTCAATACTGCCACATTGGGGATGAAGTTTCGACATGAG
TTTTGGATGAGGACATTCAAACCATAGCACTATCCCAAAGGTTTGTTGCAAGGGTGAAATGAGACGAATAGTCTGAAAGCACC
TTTCAAAACTGCTCTATAAATGTAAACAACAACAATGGGTTTCCTGAGTGCTTAATGTATTCCAGGCACTGTCTACACCCCTG
ACGTGTGTGGTTTCACTCAATGCTCATGGCAGCCTTATGAAGCAGGACTTTTGTATAGTATTCCCACCCACAAATGAGGAAAT
TGAGTCTCAGAGATGTTAAGTAACTGGCCCAACGTTGCACAGTCAGTAAGCGGCAGAGCCAGGCTTTGAGCCCAAATAAGCAG
AGTGAGCTGGGCTCTGGGAGACCCAGACAAATGGAACTGAAGAAGCTTGGAGTCTAGCAGTGGCTCAAACTTTCTAGCACATC
AGAATCACTGATGGAAATTATTTAAAAGGCAAGTTCTGGCCGGACGCGGTGGCTCACCCCTATAATCCCAGCACTTTTGGAGG
CCGAGGCGGGTGGATCACTTGAGGTCAGGAGTTCGAGACCAGACTGGCCAACATGGTGAAACCCTGTCTCTACTAAAAATACA
AAAATTAGCCAGGGATGGTGGCGCGTGCCTGTAATCCCAGCTACTCGGGAAGCTGAGGCAGGAGAATCACTTGAACCCAGAAG
GCAGAGGTTTCAGTGAGCCAAGATCGCACCACTGCACTGCAATGTGGGCGACAGAATGAGACTCTGTCTCAAAAATATAAAAA
TAAATAAAAGGCAAGTTCTTGGGCTGCACCCACAGAGATGCTGATTCTGTGGGTTCAGGGTGGAGCTCAGGAATCTGCTTTTA
TAACAAGCCCCCAAGATGATGCTTGTGTGAGGGGTCAGCTAACCACACAGGGAGGAGCGTGGCAGTTGTCTCAGCAAACCGTA
AGTAAGGGTTGCTCAGTGAGCCAAGACACAGGGCTCTGGAGGACCCAGAAGGTTCAGGCAGGAGAGACAGGATCCCACAGAGG
GACCCATCTCTGCCTCTGACCTCCAGGTTTGCCAAGTACTACAAAATGGAAAATGGCAGTGAGTACCGCACCCTCCTGAAGGC
TTTTGGCATCCGCTTCGACGTGCTGGTATACGGGAATGTGAGTCCATGGGCCAGGCAGATGGGGTGGACAGGGGAGGCAGCCC
AGACCACCTCTCGGGTTCTGAAAAAGCTCCTCTGGGGGGCAGGGGTCTGCTGCTGGCCAGCTTTGACACCCTCAGTGGGTCAC
TCTCCCATCAATTCACCTGTCCCGTGAAGGGGAGGGATCTGCTGATCCACCAAGAACCCTTCTGGCGCCACGTGCAGCCTCGG
GCCTCACCCCCATCCCATGGGCCCTCTGCCCACTTGCCTTGGTCTTTGTGCACACAGGCTGGCAAGTTCAACATCATCCCCAC
CATCATCAGCTCTGTGGCGGCCTTTACTTCTGTGGGAGTGGTGAGTTCAGCCCCTCCACGCTCTGACGGGCCAGTCAGAGTGG
GGCCCGGACTGGTACCAGCAGGCAGGGGAGTGACGGCGGCAAAACTCTGCCTCTGCCTGGAATGTAAAACCCCTACCCCCACT
TGCTAGGTGCTTCAGTCTCCTTGGCCACCACCCTGCTGCGTCAGCCCTGGCTGGAACGTCTCCAGTCATGGAGAGCTCATTAC
CTCCGGAAGCAGCCTTCCCGTTTTCAGGAGACTCCACCTGTTATAGAGTTCCCGTTTCTCACCGTATAGCTGGGGGAGGAGGC
TCTGGGTTTCTGCAGACCTGAGATGCCTTAATGAGGAACAGAGCCCACGTGGCATGGTGGGCACATAGCCTGCCTTCAGGGAC
TTCCACCCTTCCACCCCACGCAGTCCTCTCTCTGTGCAGCTGTGGTCTGGGTCACCCCTAGGAGCTGGGAAGGCAGCCCTGAA
ACATCCTGCAAAGTCCCTGGGCATTTTTCTAAGAGGGAACATCATTCAGTCCTCCCTGGAGGACTGGTCCCCACCCTGGCCTG
CAATCTGCTAACATGCTAGCTCGGATCTCTCTTCCTCATCTTATAAAGCCACCAGCTCCCCTCCCATGATAGCCCATTAATCC
ATTAATCCATGCATCCATGAACGGATTAATCCATCCATGAGGGCAGAGCCCGCAGGGTCCAATCACCTCTTAAAGGCCCCACT
TGTCAATACTGCCACGCTGGGGATTAAGTTTCAGCACGAGTTTGGATGAGGACATTCAAACCATAGCACTATCCCAAAAGTTT
GTTGCAAGGGTGAAATGTCCTGCCCACTGTTTAGGCAGCTTGGGGGTGCTGCCCGAGCCCAGCACTTCCTGCCACCCTGATCC
CACCCAACCCAGGGCACCCCTCGGAGCCCGCCCTGCCTCTCCTCCTCCAGGGAACTGTTCTCTGTGACATCATCCTGCTCAAC
TTCCTCAAGGGGGCCGACCAGTACAAAGCCAAGAAGTTTGAGGAGGTGAGTTGGGGAAGGGGCACCCTTGGATAAAAGGGAGA
GGGGGCAGGGCAGGCAGGGGCAGGGACTCTCAGTGGCTCCCCTTCTGAGGCCTTCTGAAGGGGGGTTCACCAGGCCTCAATGA
ATATTTGGGGTCCAGACAAGGGAAGGCTTGGCCAAGACTGGGCTCTGCAGAGAATCTTGGGGGTTCTGTGGGTCATCTCTGTC
ATGGTCCCCACCCCGTCACCTCCCCTCTCCATTTCTGGGGCAGGACTAGGGGAGGCCATGGGATGAATGGGGTTTCTGTTTGC
CCTCGGGGTACATGGGAGGGGCCTTGGGATCACACAGATGTCCTGGCTCCCCTCATGACTAGGTCATGGGCGCCCACTGCTGA
GTCTGTCAAATGGGGTCACAAAAGAGGACATTGCCCATAGTCAGAACTTGACAACACCAGCTCTTTCGCCTGCAGGTGAATGA
GACTACGCTGAAAATCGCGGCTTTGACCAACCCAGTGTACCCCAGCGACCAGACCACAGCGGAGAAGCAGTCCACCGATTCGG
GGGCCTTCTCCATAGGCCACTAGGGCCTCTTTCCAGGGCCCCACACTCACAAAGGCTCCAGGCCTCCCCACAGAGGACCCTGC

CTGAGCAAGGGGCATGGGAGGGAAGAGGGGCTCTCATTTCTGCTGCTCATTCCATGAGCATAGCTGGGACCCAAGTGTCTGGG
CCTCCGACTGCTCCAGCAGACAGGCAGTGCTCCCTGCTGAGACCCCAATCTCACCTTCACTCCTTGCCTGGCCCCATCTGCTT
CCTAGGACCCCTGGGGCAGGAGCACCTGAGCCATCCCCTTCCCAAAGAGTAGAGATTATAATGTAGGACAGATGGCCACAAGG
GCCTACCAAGTGCCAGGCACTTTCACACACGTTATCTCATTTAATCCTTAGAATAATCCTATGAGGTAGATATTAGTTTCCCT
TGTTTTGAAGATAAACCAAGGCTCAGAGAGACTGAGTCATTTGCCCCAGGCCAGATAGCCAGGATGTGAGAGAGCTGGGATTT
GAACGTCCGTCTGACTAACTCCATCGCCCACACCCCATGAGAGAAGAATGAACTCCCAGGGTCCATCAGCCCTGCTGCTTCAG
CCGCCTCCACCCTGACGGTGATTCGGTTAATAAAGAGTAAGCCCCATGCCTTTCCCAGCAACAAAGTTTGCATTTTAGGGAGA
CTGGTTAGACAGTGGTGAGGGACCCCATCTCTGACTTGGGTGCATCCCAAATTTAGAAGGAAACAGAAGGCATGGCTGTCAGT
GAATTTTTCCTCATCACTCCCCATAGCTCTCTCCCCAAACCAGGGAAGGGGTCATTCTTGTTCTTCTCTGGGACCCCACACCC
ACACACATCTGGGCCCCCTCACTCTGGGGATTTGATTCCCGGACCTGGGATCCTGTCGTAGGCTGGGACCCTGTTCCAGGAGT
TCAGCAGTCCTCATTTACAACAACAGTGAAAATGCTCCAGTAAGGCCTGGTGCCTTGTGAGCTGCTCAGCTGGGTTGGCCAGG
CCTGTCCCCATAGGGTCTTAATAAGGTGCCCCATTTTCTAAGGTTAGAAGCTAAAGGGGCCTTTTAAACCATCTTATCTAACC
CTCTTGCTTACAGATGAGCAAACTGAGGCCAGAAAGGGAAAATGACTGGTTCAGTGCCACAGTTCATGGCCAAAAAGGAACCC
ACATGTCCTGGCCCTTCAGGGAAGGAGGCAAGAACAGGAAGCTGGATCCATTGACCCAGACATCCTCTATCCCCTTTCTGTCC
TCTCCTACAGTGAGAGGCCCAGAAATTGCCCCAGGGCAGGGCTCTGGGGCAGAACCAGGTTTTGTGAATCCTAAGCATATACA
ATTTGGGGGCATCTCTTTAGAAAGAATACAAAATTAGGTATTAGAAGGGGCTCATGCAAGTGAATGAGCCTAAAGAATGTTTC
AATAGCTTCATGATAAATCTGCATCTGGCAGTCAGAGTGGGCATGATCATGAGGTCTTAGCTGCACCAGCTCAACTGTAGATG
GAGGGCGGCCCCTCAACACACGGCACAGGAAGTGGGGAAGGGACAGCTTCAGGAGTAGTTCAGGAGGCTCAAATGGTGGGTAC
TTGCAAAGGCCTTGCCCAATGACCCCCCGCTCCAGGGGGAGAAGGGGTAAGACCCACCCCACATAAAGCTCAACACCCCTTCC
CTCACTCTGCCCTAACCCACAGCCCCATGCCCAGGATGGTGGGGCATATCTCCCCAGGGTCAGCCTTGGGAATTGGGCAGTGC
CTGGAGATCTGACCAGACTATGCTTCTCCAGCAGAGACATCAGTGAAGGCAGCACCACATTCTCCACCTGGGACTCCCCCAGG
CATCCCTGGGGAATTCAGCTCTTGGGAGGCTGGGGTCACAGGGATTCTCTCTAATGGGGAGATGGAGGCAGTGGTGTCCTGAA
GGGACCCTCCCCCCCAACCCCTCCCTTTTACCCAGATGGAGGTGGTCCTCCTGTAGGTGCCTCCGCCCCTCTGGAGCCGGCCA
GCAAGTGTGTGTGAGCCTGAGGTTGTCCTCCGCATATCTGAACTAAGTTACCACTTCTGTGTGCTAGATGTAGGGTTAATATC
AGTAGTGATAAAAACAGCTACCTTGTCTCTGTTGCATTATGGTTTACTCAGCACAATCACCAACATAATCACATGGACCCTCA
CACCAACGCTGGTGAGTCCGCTATGGTTTGTCATTAATCCTATTTGATAGAAAAAGAAATTTACAGTACGTGGAAATGAGATC
TGGAACCTATGCCCATTCCTAACACTACATTGCCTCTTTAATCATTCAACATAAAAGCCAACACTGATTACTTACTATTGGCA
GGCAATGGACCAAATGAGTGACAGGGATTGTCTAACTCAACCCCCACTTTACAGAAGAAGAAACAGATGCATACTAAAATAAA
GAAACTGAAATAGAA